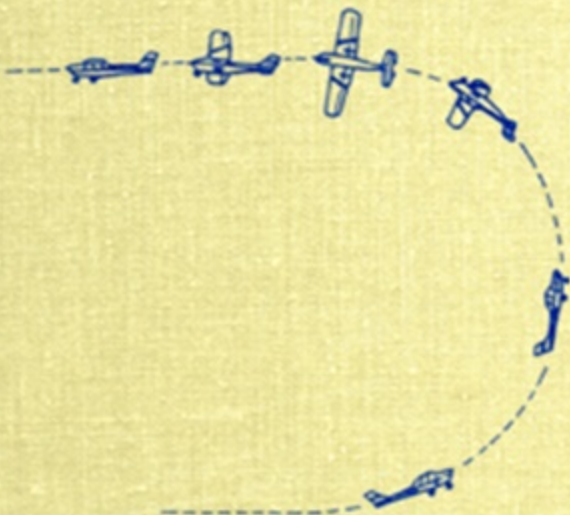


S. K. OJHA



Flight Performance of Aircraft

AIAA
Education Series

J. S. PRZEMIENIECKI/SERIES EDITOR-IN-CHIEF

Flight Performance of Aircraft

S. K. Ojha

Indian Institute of Technology
Bombay, India



EDUCATION SERIES

J. S. Przemieniecki

Series Editor-in-Chief

Air Force Institute of Technology

Wright-Patterson Air Force Base, Ohio

Published by

American Institute of Aeronautics and Astronautics, Inc.

370 L'Enfant Promenade, SW, Washington, DC 20024-2518

American Institute of Aeronautics and Astronautics, Inc., Washington, DC

Library of Congress Cataloging-in-Publication Data

Ojha, S. K. (Shiva Kumar), 1934—

Flight performance of aircraft/S. K. Ojha
p. cm.—(AIAA education series)

Includes bibliographical references and index.

1. Airplanes—Performance. I. Title. II. Series

TL671.4.037 1995 629132'52—dc20

95-4456

ISBN 1-56347-113-2

Copyright © 1995 by the American Institute of Aeronautics and Astronautics, Inc. All rights reserved.
Printed in the United States. No part of this publication may be reproduced, distributed, or transmitted,
in any form or by any means, or stored in a database or retrieval system, without the prior written
permission of the publisher.

Data and information appearing in this book are for informational purposes only. AIAA is not re-
sponsible for any injury or damage resulting from use or reliance, nor does AIAA warrant that use or
reliance will be free from privately owned rights.

Dedicated to My Parents,

Satyavati Devi

and

Krishna Swaroop Ojha

Texts Published in the AIAA Education Series

- Flight Performance of Aircraft
S. K. Ojha, 1995
- Operations Research Analysis in Test and Evaluation
Donald L. Giadrosich, 1995
- Radar and Laser Cross Section Engineering
David C. Jenn, 1995
- Introduction to the Control of Dynamic Systems
Frederick O. Smetana, 1994
- Tailless Aircraft in Theory and Practice
Karl Nickel and Michael Wohlfahrt, 1994
- Mathematical Methods in Defense Analyses
Second Edition
J. S. Przemieniecki, 1994
- Hypersonic Aerothermodynamics
John J. Bertin, 1994
- Hypersonic Airbreathing Propulsion
William H. Heiser and David T. Pratt, 1994
- Practical Intake Aerodynamic Design
E. L. Goldsmith and J. Seddon, Editors, 1993
- Acquisition of Defense Systems
J. S. Przemieniecki, Editor, 1993
- Dynamics of Atmospheric Re-Entry
Frank J. Regan and Satya M. Anandakrishnan, 1993
- Introduction to Dynamics and Control of Flexible Structures
John L. Junkins and Youdan Kim, 1993
- Spacecraft Mission Design
Charles D. Brown, 1992
- Rotary Wing Structural Dynamics and Aeroelasticity
Richard L. Bielawa, 1992
- Aircraft Design: A Conceptual Approach
Second Edition
Daniel P. Raymer, 1992
- Optimization of Observation and Control Processes
Veniamin V. Malyshev, Mihkail N. Krasilshikov, and Valeri I. Karlov, 1992
- Nonlinear Analysis of Shell Structures
Anthony N. Palazotto and Scott T. Dennis, 1992
- Orbital Mechanics
Vladimir A. Chobotov, 1991
- Critical Technologies for National Defense
Air Force Institute of Technology, 1991
- Defense Analyses Software
J. S. Przemieniecki, 1991
- Inlets for Supersonic Missiles
John J. Mahoney, 1991
- Space Vehicle Design
Michael D. Griffin and James R. French, 1991
- Introduction to Mathematical Methods in Defense Analyses
J. S. Przemieniecki, 1990
- Basic Helicopter Aerodynamics
J. Seddon, 1990
- Aircraft Propulsion Systems Technology and Design
Gordon C. Oates, Editor, 1989

(Continued on next page.)

Texts Published in the AIAA Education Series (continued)

Boundary Layers

A. D. Young, 1989

Aircraft Design: A Conceptual Approach

Daniel P. Raymer, 1989

Gust Loads on Aircraft: Concepts and Applications

Frederic M. Hoblit, 1988

Aircraft Landing Gear Design: Principles and Practices

Norman S. Currey, 1988

Mechanical Reliability: Theory, Models and Applications

B. S. Dhillon, 1988

Re-Entry Aerodynamics

Wilbur L. Hankey, 1988

Aerothermodynamics of Gas Turbine and Rocket Propulsion,

Revised and Enlarged

Gordon C. Oates, 1988

Advanced Classical Thermodynamics

George Emanuel, 1988

Radar Electronic Warfare

August Golden Jr., 1988

An Introduction to the Mathematics and Methods of Astrodynamics

Richard H. Battin, 1987

Aircraft Engine Design

Jack D. Mattingly, William H. Heiser, and Daniel H. Daley, 1987

Gasdynamics: Theory and Applications

George Emanuel, 1986

Composite Materials for Aircraft Structures

Brian C. Hoskins and Alan A. Baker, Editors, 1986

Intake Aerodynamics

J. Seddon and E. L. Goldsmith, 1985

Fundamentals of Aircraft Combat Survivability Analysis and Design

Robert E. Ball, 1985

Aerothermodynamics of Aircraft Engine Components

Gordon C. Oates, Editor, 1985

Aerothermodynamics of Gas Turbine and Rocket Propulsion

Gordon C. Oates, 1984

Re-Entry Vehicle Dynamics

Frank J. Regan, 1984

Published by

American Institute of Aeronautics and Astronautics, Inc., Washington, DC

Foreword

Flight Performance of Aircraft, by Shiva Kumar Ojha of the Indian Institute of Technology, Bombay, is a welcome addition to aerospace literature. Its comprehensive coverage of the subject of aircraft performance is particularly noteworthy. The text goes beyond the typical topics found in recent textbooks. It pays special attention to the atmosphere and weather conditions that are integral parts of flying. Although this volume was developed as an introductory textbook for undergraduate students in aeronautical engineering, it also will be of interest to pilots and flight test engineers by providing them with the underlying principles behind their operating manuals and procedures.

Performance analyses are discussed for all phases of flight, starting from take-off, and including climb, cruise, turn, descent, and finally landing. Other topics include engine failure, unpowered flight, and gliding flight for glider aircraft. The mathematical tools needed for the understanding of the subject materials covered in this text do not go beyond solving quadratic equations or first or second derivatives and completing simple integrations sufficient to calculate some of the most important flight parameters, such as liftoff speed, steepest climb angle, fastest climb, tightest turn, or maximum range. Performance analyses are presented for two types of propulsion systems: piston-prop and turbojet. Thus, the performance of both low-speed and high-speed aircraft is covered.

The AIAA Education Series embraces a broad spectrum of theory and application of different disciplines in aerospace, including aerospace design practice. Recently the Series has been expanded to encompass defense science and technology. The Series has been in existence for over 10 years, and its fundamental philosophy to develop texts that serve both as teaching tools for students and reference materials for practicing engineers and scientists remains unchanged.

J. S. Przemieniecki
Editor-in-Chief
AIAA Education Series

Preface

The subject of aircraft performance is a relatively modern discipline. Performance problems can be viewed only after the science and technology of keeping aircraft airborne have been perfected. After the first successful powered flight in December 1903, the problems of aircraft performance started getting attention from the second decade of this century onward. There has been spectacular improvement in the performance of aircraft in the last few decades. Until recently, the subject matter of aircraft performance was dealt with in one or two chapters in books devoted to aerodynamics, aircraft design, flight mechanics, or aircraft stability and control. At the time I was collecting topics for this book and assembling its contents, there was no book devoted solely to the subject of aircraft performance in the English language, or probably in any other language. By the time this book is written, a few books on the subject of aircraft performance will have already appeared. The present book is, however, different from these recent books on aircraft performance, as explained below.

This is an introductory textbook for undergraduate students of aeronautical or aerospace engineering. It is written to appeal to several other groups of readers. Graduate students having no background in aeronautics can use it as a textbook, and they will be able to appreciate different disciplines of aeronautics and learn their relative importance. This book will also serve the purpose of pilots and flight test engineers who are searching for the underlying principles behind their operating manuals and procedures. The mathematics used is minimal as it does not go beyond solving quadratic equations, first or second derivatives, and simple integrations. This aspect makes the book attractive to all those who desire to know how an airplane flies and how to calculate some of the most important flight parameters, such as liftoff airspeed, steepest climb angle, fastest climb, tightest turn, best range, maximum endurance, etc.

The performance analysis is carried out for almost all phases of flight, starting from takeoff, and including climb, cruise, turn, descent, and finally landing. Engine failure, unpowered flight, and gliding flights are also discussed. The principles of soaring are discussed, as well as the locations used during the aerial sports of soaring and gliding.

Sufficient importance is given to optimization of the various performance parameters, and the results are presented analytically. The mathematical treatment developed is concerned primarily with the conceptual and preliminary design phases of aircraft.

The performance analysis depends on the type of propulsive unit used with the specific types of aircraft. In a book of this size it is not possible to include performance calculations for all the different types of engines used as aircraft propulsion units. This book undertakes performance analysis for two different types of aircraft, namely, piston-prop and turbojet. The piston-prop engine is representative of reciprocating engines and it is used in low-speed aircraft. The turbojet engine can be considered representative of gas turbine engines and is used

in high-speed aircraft. Thus, the performances of both low-speed and high-speed aircraft is covered here.

A comprehensive treatment of a subject requires that it be presented in full perspective. Subject matter that includes mathematically elegant discussions sometimes is given much more coverage in certain books, which may even go to the extent of neglecting some nonmathematical portions of a given subject. This book adopts a balanced view and provides due importance to the nonmathematical aspects of a subject.

The uniqueness of a book can be assessed through its contents, their arrangement, and the way the subject matter is treated. Some important aspects that make this book unique are indicated below.

1) The performance analysis developed theoretically in Chapters 7–16 has resulted in presenting the results for most of the cases in analytic form. Many of these analytic solutions, to the best of my information, appear for the first time in this book. These results have also been applied to different aircraft.

2) The book pays sufficient attention to the atmosphere and weather conditions, which are integral parts of flying. Chapter 2 familiarizes readers with the nature of the atmosphere and weather in the context of flying. Chapter 19 explains the different types of weather hazards and mentions the precautionary measures that need to be adopted by the pilot while flying through them. Chapter 20, the last chapter in the book, discusses how the worldwide network of meteorological information is synthesized, reported, and forecasted for the benefit of pilots and to ensure flying safety.

3) The book includes two chapters (Chapters 11 and 15) on steady horizontal turns and one (Chapter 17) on aerial maneuvers. Thus, this book provides significantly more coverage on aircraft maneuvers than has hitherto appeared in other books on aircraft performance.

4) The book informs its readers not only on performance calculation procedures, but it also goes further to explain performance testing methods, in Chapter 18. The introduction of this chapter helps those concerned with understanding the contents of an aircraft performance manual and the pilot's views on performance. In order for the reader to better understand Chapter 18, Chapter 6 explains the different ways of measuring altitudes, airspeeds, and wind speeds that are generally used by pilots and meteorologists.

5) The book gives sufficient importance to the basic forces that dictate and decide the performance of an aircraft. Aerodynamic forces are discussed in Chapter 3, propulsive thrust by jet engines in Chapter 4, and the propulsive power of reciprocating engines in Chapter 5. These chapters have been written so that they allow the book to be self-contained, they eliminate the need for previous study before reading this book, and allow the reader to make a smooth transition to further aerodynamics and propulsion courses in later semesters.

6) Chapter 1 begins by providing relevant and useful information about aircraft, flight instruments, and basic aerodynamic forces. This familiarizes those interested in aircraft performance calculation with the quantities that can be measured in practice. It helps make the book understandable to beginners and to nonaeronautical engineering and science students. The meanings of aircraft performance and its scope are also explained here.

A book is usually intended to stimulate its readers, apart from the satisfaction it may provide to its author. I have attempted to put forth various ideas in unambiguous and clear terms. I have kept in mind that the book will be read by many

non-English-speaking readers whose second or third language may be English. The dictionary meanings of many scientific and technical words are explained, which helps the reader understand the use of such words. At certain places, very brief background information is mentioned to explain the genesis of certain scientific or technical concepts. The book incorporates the International System (SI) of units because it is the most modern system and all future literature will adopt it. As the conversion to SI units is yet to be completed in certain countries, this book also provides units of the English and American system in many instances. I have tried to enhance the readers' confidence in theory by applying it to different aircraft and solving many numerical questions and examples. Problems are provided at the end of each chapter to help readers reinforce their understanding of the topics presented.

A preface would be regarded as complete if readers are clearly informed about 1) the author's motivation of writing the book, 2) the readers for whom the book is meant, 3) the subject matter of the book, and 4) its scope. Clarity on these points can enhance the way the book's subject matter is presented. The first two items have already been explained, but discussion of the last two items is only begun in the preface; more will be said in the last section of Chapter 1, where the author explains the question, "What is aircraft performance?"

This book covers more material than can possibly be dealt with in one semester. If a teacher desires, he can limit himself to teaching the performance analysis of either turbojet or piston-prop aircraft, leaving the rest of the book for self-study by students. The teacher can also omit the chapters on aerodynamics and propulsion if students have already taken courses of these subjects.

Writing a book of this nature requires seeking help from various sources. I am thankful to the Indian Institute of Technology, Bombay, and to the Aeronautical Research and Development Board, New Delhi, for providing assistance at different periods during the writing of this book. I am also thankful to the Aircraft and Systems Testing Establishment, Bangalore, and to the Regional Meteorological Center, Bombay, for their help when I was writing Chapters 18, 19, and 20. I remain grateful to many of my colleagues who have always helped me in various ways to complete the manuscript of this book.

Shiva Kumar Ojha

July 1995

Table of Contents

Foreword

Preface

Chapter 1. Aircraft, Basic Forces, and Performance	1
1.1 Introduction	1
1.2 Components of Aircraft Configuration	2
1.3 Different Types of Aircraft	4
1.4 Basic Motions and Attitudes of Aircraft	6
1.5 Control Surfaces of Aircraft	7
1.6 Cockpit Controls	8
1.7 Powered Flight Controls and Fly-by-Wire System	9
1.8 Flight Instruments	10
1.9 Navigational Aids and Avionics	13
1.10 Aircraft Weight	15
1.11 Forces Acting on Aircraft	17
1.12 What Is Aircraft Performance?	19
References	25
Problems	26
Chapter 2. The Atmosphere and Flying Weather	29
2.1 Introduction	29
2.2 Principles of Atmospheric Changes	30
2.3 Temperature, Pressure, and Density of the Atmosphere	32
2.4 Winds	40
2.5 Vertical Air Currents	45
2.6 Water Vapor, Humidity, and Saturation of the Atmosphere	46
2.7 Processes of Evaporation, Condensation, Sublimation, and Freezing	48
2.8 Moisture and Precipitation	49
2.9 Dew, Frost, Fog, and Mist	50
2.10 Clouds	51
2.11 Rain and Drizzle	56
2.12 Hail and Snow	57
2.13 Air Masses and Air Fronts	58
2.14 Atmospheric Pollution	60
2.15 Visibility	64

2.16	Classification of Atmosphere into Zones	65
2.17	Standard Atmosphere	67
	References	75
	Problems	76
Chapter 3. Aerodynamic Forces on Aircraft		81
3.1	Introduction	81
3.2	Air Flow Characteristics	81
3.3	Flow Parameters	86
3.4	Airfoils	87
3.5	Wings	93
3.6	High-Lift Devices for Wings	98
3.7	Fuselage	104
3.8	Aircraft Configuration	104
3.9	Flight Control by Aerodynamic Surfaces	109
3.10	Aerodynamic Interference Effects	111
3.11	Experimental Methods in Aerodynamics	115
3.12	Pressure, Velocity, and Density Relationships	116
	References	119
	Problems	121
Chapter 4. Propulsive Thrust by Jet Engines		125
4.1	Introduction	125
4.2	Jet Propulsion and Gas Turbine Engines	125
4.3	Turbojet Engine	128
4.4	Turboprop Engine	139
4.5	Turbofan Engine	141
4.6	Comparative Study of Different Gas Turbine Engines	143
4.7	Ramjet and Rocket Engines	145
	References	147
	Problems	147
Chapter 5. Propulsive Power by Piston-Prop Engines		151
5.1	Introduction	151
5.2	Piston Engine	151
5.3	Carburetor	153
5.4	Fuel Injection System	155
5.5	Aspirated Engine, Supercharging, and Critical Altitude	155
5.6	Engine Power and Engine Ratings	156
5.7	Power Variations with Altitude, Airspeed, Temperature, and Humidity	157
5.8	Engine Instruments	158
5.9	Propeller	160
5.10	Thrust and Torque Calculations of a Propeller	163
5.11	Propeller Parameters	166
5.12	Propeller Efficiency	167

5.13	Types of Propellers	169
5.14	Different Propeller States	170
5.15	Trends in Propeller Design	171
	References	171
	Problems	171
Chapter 6. Altitudes, Airspeeds, and Wind Speeds		175
6.1	Introduction	175
6.2	Altitude	175
6.3	Airspeed	178
6.4	Wind Speeds	186
	References	190
	Problems	190
Chapter 7. Gliding and Unpowered Flights		193
7.1	Introduction	193
7.2	Equations of Motion	193
7.3	Gliding Flight Parameters	194
7.4	Best- (Maximum-) Range Glides	198
7.5	Best- (Maximum-) Endurance Glides	203
7.6	Soaring	209
	References	210
	Problems	211
Chapter 8. Cruising Flights of Turbojet Aircraft		215
8.1	Introduction	215
8.2	Cruise, Cruising Range, and Endurance	215
8.3	Equations of Motion of Cruising Flight	216
8.4	Airspeed	217
8.5	Necessary Condition of Flight	218
8.6	Thrust Required and Thrust Available	218
8.7	Range and Its Flight Parameters	221
8.8	Endurance of Cruising Flight	229
8.9	Engine-Inoperative Cruise	230
8.10	Application to an Aircraft	231
	Reference	233
	Problems	233
Chapter 9. Optimization of Cruising Flights of Turbojet Aircraft		237
9.1	Introduction	237
9.2	Minimum-Thrust (or Minimum-Drag) Flight	237
9.3	Maximum-Range Flights	239
9.4	Maximum-Endurance Flights	251
9.5	Application to an Aircraft	254
	References	256
	Problems	256

Chapter 10. Climbing Flights of Turbojet Aircraft	259
10.1 Introduction	259
10.2 Basic Equations of Climb	259
10.3 Climbing Flight Parameters	261
10.4 Steepest Climb	266
10.5 Fastest Climb	271
10.6 Most Economical Climb	278
10.7 Climb with Allowance for Acceleration	278
10.8 Energy Method of Optimal Climb	280
10.9 Application to an Aircraft	289
References	290
Problems	290
Chapter 11. Turning Flights of Turbojet Aircraft	293
11.1 Introduction	293
11.2 Equations of Motion of the Coordinated Turn	293
11.3 Turning Flight Parameters	295
11.4 Maximum Load Factor and Maximum Bank Angle	298
11.5 Fastest Turn (Maximum Turning Rate)	301
11.6 Tightest Turn (Minimum Turning Radius)	303
11.7 Turning at Stalling Airspeed	304
11.8 Turning in Vertical Plane	305
11.9 Application to an Aircraft	308
Reference	309
Problems	309
Chapter 12. Cruising Flights of Piston-Prop Aircraft	313
12.1 Introduction	313
12.2 Equations of Motion of a Steady Level Flight	313
12.3 Airspeed	314
12.4 Power Required	315
12.5 Range and Its Flight Parameters	317
12.6 Endurance	321
12.7 Effects of Wind	323
12.8 Application to an Aircraft	324
Problems	325
Chapter 13. Optimization of Cruising Flights of Piston-Prop Aircraft	329
13.1 Introduction	329
13.2 Minimum-Power Flight	329
13.3 Maximum-Range Flights	330
13.4 Maximum-Endurance Flights	336
13.5 Application to an Aircraft	340
Reference	341
Problems	341

Chapter 14. Climbing Flights of Piston-Prop Aircraft	345
14.1 Introduction	345
14.2 Basic Equations of Climb Performance	345
14.3 Climbing Flight Parameters	346
14.4 Steepest Climb	348
14.5 Fastest Climb	352
14.6 Application to an Aircraft	358
References	360
Problems	360
Chapter 15. Coordinated Turning Flights of Piston-Prop Aircraft	363
15.1 Introduction	363
15.2 Equations of Motion of a Coordinated Turn	363
15.3 Turning Flight Parameters	364
15.4 Turning Flight at Maximum Load Factor	366
15.5 Fastest Turn	367
15.6 Tightest Turn	369
15.7 Turning Flight at Stalling Airspeed	371
15.8 Application to an Aircraft	372
Reference	373
Problems	373
Chapter 16. Takeoff and Landing Performance	377
16.1 Introduction	377
16.2 Characteristic Distances Along Runway	377
16.3 Characteristic Airspeeds During Takeoff and Landing	380
16.4 Braking Friction During Takeoff and Landing	382
16.5 Analysis of the Takeoff Phase of an Aircraft	383
16.6 Analysis of Landing Phase of Aircraft	389
16.7 Aircraft Retardation Devices	392
16.8 Performance with Engine Failure	393
16.9 Effects of Wind, Runway Slope, Temperature, and Altitude	397
References	399
Problems	399
Chapter 17. Aerobatic Maneuvers and Flight Boundaries	403
17.1 Introduction	403
17.2 Proficiency Flight Maneuvers	404
17.3 Basic Aerobatics	407
17.4 Flight Boundaries	413
17.5 Sustained Turn Performance and Agility	415
References	416
Problems	416
Chapter 18. Performance Evaluation by Flight Tests	419
18.1 Introduction	419
18.2 Airspeed, Temperature, and Angle of Attack Calibrations	420

18.3	Lift Coefficient Curve and Drag Polar by Flight Tests	422
18.4	Stall Tests	423
18.5	Takeoff and Landing Tests	426
18.6	Climb Performance Tests	429
18.7	Descent Performance Tests	440
18.8	Cruise Performance Tests	442
18.9	Turning Performance Tests	450
	References	458
	Problems	458
Chapter 19. Weather Hazards and Flying		463
19.1	Introduction	463
19.2	Fog and Flying	463
19.3	Turbulence and Flying	465
19.4	Thunderstorm Clouds and Flying	467
19.5	Ice and Flying	471
19.6	High-Altitude Jet Stream and Flying	476
19.7	Windshear and Flying	477
19.8	Bird-Strike Hazard and Flying	480
	References	482
	Problems	482
Chapter 20. Weather Observations, Reports, and Forecasts to Flying		485
20.1	Introduction	485
20.2	Means for Measuring Weather Elements	486
20.3	Weather Symbols, Abbreviations, and Codes	489
20.4	Weather Reports	494
20.5	Weather Forecasts to Aviation	498
	References	500
	Problems	500
Appendix A. Basic Conversion Factors		503
Appendix B. Useful Data for Solving Numerical Problems		505
Index		507

Aircraft, Basic Forces, and Performance

1.1 Introduction

The subject of aircraft performance attracted attention only after the art and technology of flying had been perfected by the disciplines of aerodynamics, aircraft structure, and aircraft propulsion. Historically, the first powered flight could not succeed until these disciplines had advanced considerably. Before the relevant fundamentals of these disciplines and the problems of aircraft performance are undertaken in the subsequent chapters, it is pertinent to become familiar with the important components and instruments of the aircraft whose performance one intends to study. These preliminary discussions are useful to the performance calculator who may want to know the performance parameters that can be actually measured during flight. The information presented here will also increase his level of confidence in the subject, as it is not necessary for him to know the design details of the aircraft and how it is piloted. Words like *aircraft* and *performance* are very general in their dictionary meaning and it is essential to understand them clearly here.

An *aircraft* is a structural body that makes a skillful way or crafts through the air. It can be an airplane, glider, helicopter, or any other structure or machine navigating in the air. An *airplane* is a powered heavier-than-air flying vehicle with fixed or variable sweep wings. A *glider* is a similar vehicle with fixed wings, but it has no engine. A *helicopter* obtains lift and propulsion from overhead revolving blades or rotors (also called rotary wings), in the horizontal or inclined plane, and it moves both vertically and horizontally. The word *aircraft*, which is both singular and plural, is often interchanged in common usage for *airplane*, and this practice has been adopted throughout this book.

An aircraft configuration, or *airframe*, has many basic structural components exposed to the atmosphere that can be recognized by a nearby person looking at the aircraft when it is standing still or moving slowly on the ground. These components are explained here with the help of figures and charts. These aircraft (airplanes) can be of different types which are classified here. Aircraft can have different types of motions and orientations during flight. Control and navigation of the aircraft require certain control surfaces, control panels, and instruments.

Aircraft performance is the result of aerodynamic, gravitational, and propulsive forces acting on the aircraft. Certain simplifying assumptions are discussed here to represent these forces. Application of Newton's laws of motion to these forces yields the equations of motion that form a theoretical basis for the subject of aircraft performance.

The exact meaning of the term *aircraft performance*, and its unique meaning in the context of the classical and interrelated disciplines of aerodynamics, aircraft structure, and propulsion, are explained toward the end of this chapter. The meaning of the solutions of the aircraft performance problems, and the conceptual scheme according to which the different chapters of this book are organized and

introduced, are also dealt with here. This chapter concludes by emphasizing the scope of the subject of aircraft performance.

1.2 Components of Aircraft Configuration

Aircraft share some common features in their structural and aerodynamic design. The structural design attempts to minimize the weight of the aircraft without losing the strength of its structure. The aerodynamic design tries to maximize the lift force without increasing the drag force on the aircraft. The aircraft components exposed to the atmosphere determine the aerodynamic forces of its performance. Some of these components are movable and are used to generate desirable aerodynamic forces to control the linear and angular motions of the aircraft during flight. A line diagram of the three different views of a typical simple turbojet aircraft is shown in Fig. 1.1, and its components are further explained through a chart in Fig. 1.2. The main parts of the aircraft configuration are the fuselage, the wing unit, the tail unit or empennage, and the air intake or air inlet.

1.2.1 Fuselage Unit

The central large cylindrical body around the center line of the aircraft is the fuselage. The fuselage houses passengers, crew members, cargo, baggage, equipment, part of the aviation fuel if necessary, and other items that may be required for the safety and comfort of the passengers. The front portion of the fuselage generally contains the control room, known as the cockpit, of the aircraft where the pilot, copilot, and flight engineers work. A number of flight, navigational, and control instruments are installed in the cockpit at suitable places. Landing gears which support the weight of the aircraft when it is at rest or rolling on

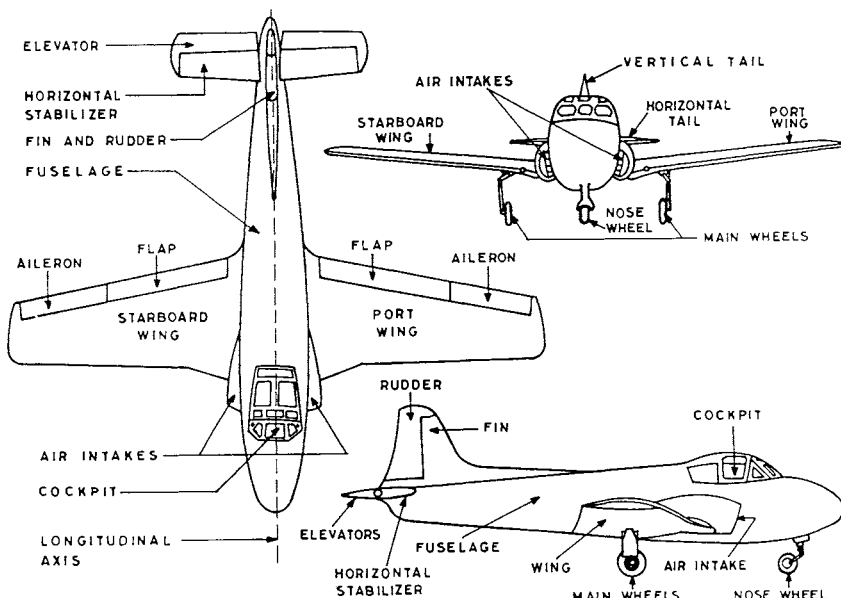


Fig. 1.1 Three views of turbojet aircraft.

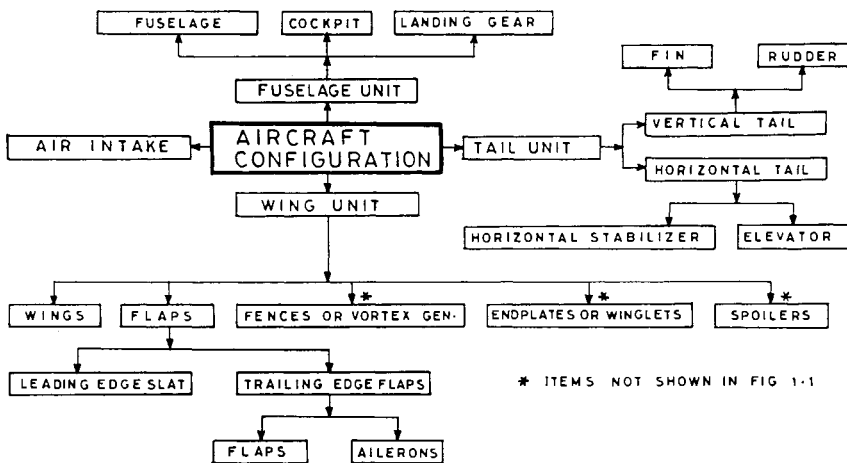


Fig. 1.2 Components of aircraft configuration.

the ground are located at the bottom of the fuselage. The wheels of the landing gears ensure that the aircraft will roll smoothly on the ground during takeoff and landing. The landing gears are generally retractable and are placed in the body of the fuselage when the aircraft is airborne.

1.2.2 Wing Unit

The two wings are the main lifting surfaces of the aircraft and are generally situated on the opposite sides of the fuselage, as shown in Fig. 1.1. The wing on the right-hand side of the aircraft, as seen by its pilot, is called the *starboard* wing whereas the wing on the left-hand side is called the *port* wing. The two words starboard and port are commonly used to mean the right-hand side and the left-hand side, respectively. The origin of these words is not clear but they were commonly used in sea navigation, much before the inception of air flights. The action of the wings can be sufficiently enhanced by attaching some movable and fixed surfaces to the wings. A detailed discussion of these surfaces will be given in Chapter 3, but their locations and purpose are mentioned below.

A wing may have a slat near its leading edge and a flap near its trailing edge. The leading-edge slat is not shown in Fig. 1.1, but it provides smooth flow of air near the leading edge of the wing. The trailing-edge flaps have two basic purposes, depending on whether they are located inboard (near the fuselage) or outboard (away from the fuselage). The inboard trailing-edge flaps are simply called *flaps* and the outboard trailing-edge flaps are called *ailerons*. The purpose of the flaps near the fuselage is to obtain additional lift whenever required, usually during takeoff, climb, and landing. A flap can be a single flap (Fig. 1.1), a double flap, or a multiple flap. The double and multiple flaps can be extended backward and placed one behind the other; these are not shown in Fig. 1.1. An aileron is a control surface that is used to turn and control the aircraft about its longitudinal axis (center line). The ailerons on the two sides of the fuselage are generally deflected in opposite directions to enhance the rolling moment of the aircraft. For example, if the aileron on the right-hand side is deflected down, the aileron on the left-hand side would simultaneously be deflected up.

The boundary-layer fences and vortex generators (not shown in Fig. 1.1) are situated on the upper surface of the wings to avoid boundary-layer drift toward the tips of the wings. The *fences* are long thin plates of small height, placed along the chord but normal to the wing surface at different spanwise stations. The *vortex generators* are small, thin triangular or rectangular plates that are placed at a small distance above and parallel to the upper surface.

The end-plates, or winglets, are used to minimize induced drag, which arises due to vortices arising from the tips of the wings. The end-plates (not shown in Fig. 1.1) are located at the wingtips, but normal to the plane of the wings, to eliminate the presence of the tip vortices. The end-plate is just a thin circular plate placed normal to the wing at the wingtip. The latest development in the field of induced drag reduction is the winglet, which is a miniature wing placed normal to the wing at the tip.

An aircraft wing may also have spoilers to act as control surfaces, as explained in Sec. 1.5.

1.2.3 Tail Unit (*Empennage*)

The tail unit of the aircraft, sometimes called the empennage, consists of horizontal and vertical tails. Both tails are streamlined bodies like symmetric wings, consisting of fixed and movable surfaces. The fixed surface stabilizes the motion, i.e., tends to bring back the aircraft to its original equilibrium condition of the flight after a small disturbance. The movable surface at the back of the fixed surface is like a flap that controls the motion. The fixed surface of the horizontal tail is called the *horizontal stabilizer* and the movable surface at its back is referred to as the *elevator*. The horizontal tail stabilizes and controls the rotation of the aircraft about its lateral axis which passes through the center of gravity of the aircraft. In some modern aircraft, the complete horizontal stabilizer is rotated instead of just the elevator (this is called a flying tail). The fixed surface of the vertical tail is called the *vertical stabilizer* or *fin* and the movable surface at its back is commonly referred to as the *rudder*. The vertical tail stabilizes and controls the rotation of aircraft about the normal axis (or vertical axis) passing through the center of gravity of the aircraft.

1.2.4 Air Intake

An *air intake* is generally a diffuser duct provided to ensure that the aircraft engine is properly supplied with air under all conditions of flight operation, without unduly interfering with the smooth flow of air over the surface of the aircraft. The purpose of the diffuser is to efficiently slow down the motion of the air in order to meet the air flow requirement at the compression face. Air intakes exist both for *podded* and *integrated* installations of the engine. In the integrated installations, the engine is an integral part of either the fuselage or the wing. The air at the mouth of the intake is divided into two parts: one part is breathed by the engine and becomes internal flow, and the other part is the external flow moving over the airframe with the task of preserving the proper aerodynamics of the airframe.

1.3 Different Types of Aircraft

Aircraft are used for a multitude of activities and there are different types of aircraft which are classified in different ways. An aircraft can be microlight, light,

or large. Aircraft of take off weight less than 12,500 lb (or 5700 kg) are called *light* or *small aircraft*,¹ whereas *large aircraft* have takeoff weights greater than 12,500 lb. The classification can also be based on its functional use, the Mach number range it flies, the type of power plant being used for propulsion, and the special design features of the aircraft configuration.

1.3.1 Functional Uses

The functional uses of aircraft can be broadly classified into civil and military. There are also special-purpose aircraft that can be put to both civil or military use. The civil applications of aircraft are passenger travel and cargo transport. The main types of military aircraft are fighters and bombers. Fighters can be classified as strategic, escort, and interceptors. Bombers can be tactical and strategic. There are also ground attack planes and multipurpose planes like fighter-bomber aircraft. The types of special-purpose aircraft include executive, ambulance, agriculture, weather research reconnaissance, training, sport, and aerobatic. There are also aircraft that can take off and land in lakes, on the sea, or on the deck of a ship. The size, speed, cruising altitude, maneuverability, range, and endurance of aircraft have considerably increased during the last four decades, out of both desire and necessity.

1.3.2 Mach Number Ranges

The classification based on speed is commonly expressed in terms of Mach number $M (= V/a)$, which is the ratio of flight airspeed V to the speed of the sound a in the ambient atmosphere. The Mach number of the flight represents the airspeed of the aircraft in relation to the speed of sound. For example, $M = 2$ means that the aircraft is flying at twice the speed of sound in the ambient atmosphere. Thus there are low-speed ($M < 0.3$), low-subsonic ($0.3 < M < 0.6$), high-subsonic ($0.6 < M < 0.8$), transonic ($0.8 < M < 1.2$), supersonic ($1.2 < M < 5$), and hypersonic ($M > 5$) aircraft; the numerical values indicated here are approximate values. The design features of wing, tail, and other components of the aircraft depend considerably on the Mach number range in which the aircraft primarily flies.

1.3.3 Types of Power Plants

The type of power plant and the number of engines used also distinguish an aircraft. An aircraft may have a piston-prop engine or a gas turbine engine. The gas turbine engine may be a turbojet, turboprop, or turbofan type. The number of engines installed in an aircraft may be one (single engine), two (twin-engine), or three or more (multiengine). Low-speed and low-subsonic aircraft use piston-prop engines whereas high-speed aircraft employ gas turbine engines. For safety reasons, twin-engine or multiengine aircraft are preferred, but the greater number of engines also increases the weight of these aircraft.

1.3.4 Types of Aircraft Configurations

There are many design features of aircraft configuration that differ among various models. Some of these include the shape, size, and location of different aircraft components like the fuselage, wing, stabilizer and elevator; fin and rudder; landing gear; and power plant. An aircraft may be a conventional single-fuselage, twin-fuselage design, or a pod-and-boom construction. The wing may be rectangular,

tapered, swept back, or delta. The wing may be low-wing, mid-wing, or high-wing, depending on whether it is located below the fuselage, in the middle of it, or above it, respectively. Conflicting requirements at different speeds have also resulted in variable-geometry and variable-sweep wings for high-speed aircraft. The stabilizer of an aircraft may be located ahead of the wing, as in canard design, instead of conventionally at the tail end of the fuselage. The power plant may be submerged in the wings or fuselage, installed below the wings, or located on both sides of the fuselage. The exact size, shape, and location of all of the aforementioned components are major problems for an aircraft designer. A logical discussion of the solutions to these problems can be found in books of aircraft design.

1.4 Basic Motions and Attitudes of Aircraft

An aircraft has different kinds of motions and it can be oriented in different attitudes, which are described below.

1.4.1 Choice of Aircraft Axes

An aircraft is generally a symmetrical body, and the plane of symmetry passes through the center line of the fuselage. Although some asymmetrical aircraft have been designed on an experimental basis, they are exceptions to the rule. The most commonly chosen axes are the longitudinal axis, the lateral axis, and the normal (or vertical) axis; these axes are orthogonal to each other and pass through the center of gravity (CG) of the aircraft. The longitudinal axis is along the center line of the fuselage, the lateral axis is along the spanwise direction of the wing, and the normal axis is perpendicular to the plane containing the first two axes. The longitudinal and normal axes lie in the plane of symmetry of the aircraft. The rotation of the aircraft about the longitudinal, lateral, and normal axes is called *roll*, *pitch*, and *yaw*, respectively.

A mathematical formulation of flight dynamics of an aircraft, like any other dynamics (especially those associated with stability and control problems²) would require a proper selection of the coordinate axes. It is common to select a right-handed Cartesian coordinate system comprising three orthogonal straight lines whose origin (common point) coincides with the CG of the aircraft. It is further left to our choice to select these axes. The three types of systems that are common in flight mechanics are the wind-axis system, the principal inertia-axes system, and the ground-axes system. In all the three systems, the lateral axis is the same. For the wind-axis system, the direction of the flight path (or the relative wind direction) is the *x*-axis and the origin moves with the CG of the aircraft. In the principal inertia-axes system, the axes are the principal axes of the aircraft and the origin coincides with the CG of the aircraft. In the ground-axes system, the origin is fixed on the ground, and the *x* and *y* coordinates are parallel to the Earth.

1.4.2 Translational Motion

In translational mode, the aircraft has linear motions (translations) with three degrees of freedom. It can move forward or backward, up or down, and sideways. An airplane generally requires certain minimum forward airspeed to become airborne. Therefore, any other translational motion such as up, down, or sideways must be

superimposed on the forward motion of the aircraft. The climb and descent of aircraft are generally nothing but the vertical motion superimposed on the horizontal motion of the aircraft. All transport aircraft fly mostly in translational mode.

1.4.3 ***Rotational Motion***

In rotational mode, the aircraft has three additional degrees of freedom comprising rotation about the three orthogonal axes. Thus the aircraft can roll, pitch, and yaw. The requirement of the airplane to remain airborne dictates that any such rotation must be superimposed on the forward motion of the airplane. All aerobatics or other maneuvers are combinations of both translational and rotational motions of the aircraft. An aircraft can also make oscillatory motions such as short-period and long-period (phugoid) motions, Dutch roll, and snaking; these belong to the domain of aircraft stability and control.

1.5 **Control Surfaces of Aircraft**

Certain movable surfaces, called *control surfaces*, are attached at different locations of the aircraft configuration. Each control surface generates aerodynamic force sufficient to perform a specific task. The aerodynamics of these control surfaces is explained in Chapter 3, but their locations and importance are presented here.

1.5.1 ***Elevators***

The *elevators* control the pitching movement of aircraft by rotating it about the lateral axis passing through the center of gravity of the aircraft. The elevators are used to cause the aircraft's nose to move up (or down), which is required for increasing (or decreasing) drag, or for climbing (or descending). The elevators are flaps at the trailing edge of the tail plane. The upward angular deflection produces downward force to the elevator and, therefore, nose-up moment about the center of gravity of the aircraft is established. Similarly, downward angular deflection of the elevators results in nose-down moment of the aircraft.

1.5.2 ***Ailerons***

The *ailerons* control the rolling movement of the aircraft by rotating it about the longitudinal axis. They are used to bank (or roll) the aircraft, either clockwise or anticlockwise. The ailerons are generally situated near the wingtips as trailing-edge flaps of the wing. The deflections of these flaps are synchronized such that if the aileron on the right-hand side deflects down or up, the aileron on the left-hand side deflects in the opposite direction. This makes the rolling moment more effective. For example, if the right-hand-side aileron is deflected down and the left-hand-side aileron is deflected up, this causes positive lift to the right-hand-side aileron and negative lift to the left-hand-side aileron. This makes the aircraft roll anticlockwise, as observed by the pilot.

1.5.3 ***Rudder***

The *rudder* controls yaw by rotating the aircraft about its normal axis, which passes through the CG of the aircraft. The rudder is located as the trailing-edge flap of the fin in the normal (or vertical) plane. The angular deflection of the rudder

to the right produces leftward force on the rudder, causing the aircraft to show yaw movement. Similarly, angular deflection of the rudder to the left causes yaw toward the left. The rudder is used during asymmetrical flight caused by engine inoperation on any one side of the aircraft. The rudder also acts as a yaw damper by suppressing involuntary movement of the aircraft in roll and yaw.

1.5.4 **Spoilers**

The *spoilers* are used to spoil the smooth flow of air by causing separation of the flow over the wings; this produces loss of lift and increase in drag. They are used as airspeed brakes and can also be used to control the roll response of the aircraft. The spoilers are rectangular flat plates; when in use, they protrude normal to the surface of the wings by deflecting them about their hingeline. When not in use, they remain flush with the surface of the wing. They can be located on both the upper and lower surfaces of both wings. When all of the spoilers are used simultaneously on both wings, they considerably increase drag and reduce lift. They are therefore used as airspeed brakes. When they are used only on the upper surface of one wing, the lift of that wing is reduced, causing the aircraft to roll. Therefore, the spoilers are also used to enhance the roll response of the aircraft, as in the Airbus A320.³

Before proceeding to the next section, we note that in certain applications the control surfaces mentioned in the above paragraphs are required to do more than one job. They are used as combined control surfaces because their activities have been conjoined. This has given rise to names like flaperons, elevons, etc., which are explained in Chapter 3.

1.6 Cockpit Controls

All control surfaces are operated by the pilots in the cockpit with the help of control devices called *cockpit controls*. The cockpit controls of a large aircraft are generally hydraulically operated because the force required to operate them is so great (see Sec. 1.7). The movement of the cockpit controls is proportional to the aerodynamic loads acting on the control surfaces, thus giving the pilot a feel for such forces. The higher the load on a control surface, the more the pilot will have to move the control device. Some important cockpit controls and their actions are described here.

1.6.1 **Control Column**

The control column, which can be moved backward and forward in the cockpit, is connected to the elevators. When the control column is moved backward, the elevators are raised up; this causes nose-up attitude of the aircraft. Similarly, forward movement of the control column lowers the elevators; this causes nose-down attitude of the aircraft.

1.6.2 **Control Wheel**

The ailerons are generally operated by a control wheel pivoted on the control column. The ailerons of the wings are linked so that they move in the opposite direction, assisting each other in producing a roll displacement. Thus, when the

control wheel is turned to the left, the left-wing aileron is raised, and the right-wing aileron is lowered, which causes a roll displacement to the left of the pilot. Similarly, the opposite effect is created when the control wheel is turned to the right.

1.6.3 Rudder Pedals

The rudder is operated by a pair of *rudder pedals*. When the left pedal is pushed forward, the rudder is turned to the left, which displaces the aircraft nose to the left of the pilot. Similarly, pushing the right pedal forward causes the aircraft nose to displace to the right.

1.6.4 Toe Brakes

Braking of landing wheels is applied by *toe brakes* that are situated on each side, just above the rudder pedals. The left-hand-side toe brakes provide brakes to the left-hand-side wheels whereas the right-hand-side toe brakes provide brakes to the right-hand-side wheels.

1.6.5 Sidestick

The introduction of a completely electronically operated fly-by-wire (FBW) system provides no direct mechanical operation of the control surfaces. This has led to the development of a new form of control called the *sidestick*. It is a miniature form of joystick (control column) designed for one-handed operation.⁴ It is mounted at the side of the pilot's seat. The use of a sidestick produces a less cluttered flight deck.

1.6.6 Trim Controller

The *trim controller* in the cockpit is a separate trim wheel that operates the tabs. The tabs are located at the trailing edge, as flaps of the control surfaces, and are commonly used for trimming the control surfaces. This allows the aircraft to be flown nearly hands-off much of the time. Tabs can be used as a trimming device, a balancing device, or, in some cases, as primary control surfaces.⁵

1.7 Powered Flight Controls and Fly-by-Wire System

On very small, slow airplanes the pilot can deflect a control surface about its hingeline against the air forces. On larger airplanes, however, the aerodynamic forces on a control surface are large and it is beyond the strength of the pilot to move such a control surface. The control force required for a given control surface increases with the increase in deflection at constant airspeed, and also with the increase in airspeed at constant deflection. The control forces can be made lighter by balancing the control surface in many different ways,⁶ such as setback hinge, horn balance, trailing edge balance tabs, etc.; in this way, only a portion of the force required is supplied by the pilot and the rest is supplied by balancing the control surface.

Airplane sizes have increased enormously in the past few decades. Thus, airspeeds and altitudes have also increased, and this in turn causes Mach number effects, which change the pitch of the aircraft and upset the pressure distribution over the control surfaces, leading to unwanted changes in the hinge moments. On

large airplanes the balancing itself becomes a problem because the balance required varies with the deflections, airspeeds, and configuration changes. Thus, the aerodynamic controls become difficult, costly, and time consuming. The answer to this problem lies in powered control surfaces.

A powered flight control basically has a hydraulically operated servo-control unit, consisting of a control valve and an actuating jack, connected between the pilot's controls and the relevant control surfaces. A good powered control system is so good that a pilot has no indication that there is a servo system between him and the control surface. There are many types of powered control units, which differ in their design.⁶ Some aircraft may have power control units on all of the primary control surfaces, whereas the other control surfaces may be manually operated. For safety reasons, each control surface is generally provided with more than one device for its operation.

A power-operated flying control surface, by its very nature, is irreversible and the aerodynamic forces are not transmitted back to the pilot. The pilot has no information about the aerodynamic forces acting on the control surfaces. It is therefore necessary to incorporate an artificial means allowing the pilot to "sense" or feel these forces, located at a point between the pilot's controls and their connection to the servo-unit control levers.

A fly-by-wire (FBW) system is a particular type of powered flight control which is incorporated these days in some highly sophisticated aircraft. The FBW system, as the name suggests, has wires carrying electrical signals from the pilot's controls, replacing mechanical linkages entirely. In operation, the moments and forces exerted by the pilot on the cockpit controls are measured by electrical pickups in the cockpit, and the signals produced are thus amplified and relayed to operate the hydraulic actuator units that are directly connected to the flight control surfaces.

The FBW system improves the performance, efficiency, and even the safety of the aircraft. It may even coordinate control surface movements that would be too complex for a pilot to manage unaided. The FBW system is now increasingly used by modern aircraft. Concorde was the first supersonic civil aircraft to employ FBW controls, but it has also retained mechanical control linkages as a standby. Among a number of technologic firsts in the Airbus A320, it is the first subsonic commercial aircraft to incorporate a FBW control system throughout its normal flight.³

1.8 Flight Instruments

During flight, certain instruments are required to determine the airspeed of the aircraft, its altitude, attitude, rate of climb, acceleration, rate of turn, and bank angle. These instruments and their functions are described here.

1.8.1 Airspeed Indicator

The *airspeed indicator* (ASI) records the indicated airspeed of the aircraft with respect to the wind which may be moving parallel to the flight path. The sensing element is the pitot-static tube consisting of pitot and static tubes. The pitot tube senses the total pressure p_0 , and the static pressure tube senses the static pressure p_s of the relative wind. These pressures are converted into airspeed shown on the dial. The markings on the dial of the ASI are color coded to indicate safe operating

ranges in various flight configurations of the aircraft. The ASI does not give the true airspeed which is obtained after applying certain corrections and calculations (see Sec. 6.2 of Chapter 6) to the readings of the airspeed indicator.

1.8.2 Altimeter

Depending on its type the *altimeter* can measure either pressure altitude or true height. The altimeter measuring pressure altitude is quite common; this is essentially an aneroid barometer. Its sensing element is the static pressure hole of the pitot-static tube. If properly located on the aircraft, this hole senses the ambient atmospheric pressure. The scale of the altimeter is graduated to indicate directly the altitude in feet or meters. Note that this altimeter measures the pressure altitude of the standard atmosphere for which the instrument has been designed. It does not read the true altitude or height.

The true height is measured by radar altimeter, also known as absolute altimeter or the radio altimeter. This type of altimeter is generally used within about 2500 ft (762 m) of the ground. The instrument transmits radio signals toward the Earth. The reflected signals are also picked up by the instrument which combines them with the transmitting signals and produces a “beat.” The beat frequency is directly proportional to the height of the aircraft above the ground, and hence the instrument can be calibrated to give the height.

1.8.3 Vertical Speed Indicator

The *vertical speed indicator* (VSI) shows the vertical velocity or the rate of climb of the aircraft when it is ascending or descending. The sensing element is the same as that for the altimeter which measures pressure altitude. It is based on the principle that the change in barometric pressure is associated with the change in altitude. The instrument usually has the lag of 6–9 s so that the rapid changes in the rate of climb cannot be read correctly at any moment.

Instantaneous VSIs that do not have time lag are also available now. They operate on a more complicated principle but provide an instantaneous indication of the vertical airspeed.

1.8.4 Machmeter

The *Machmeter* is an instrument that measures the Mach number of flight. In compressible flow range, the Mach number is an important nondimensional parameter. A pilot can recognize the nature of aerodynamic forces if he knows the Mach number during flight. The Machmeter requires the sensing of the differential pressure $p_0 - p$, as in ASI, and the static pressure p , as used in altimeter. Thus the Machmeter combines the principles of the airspeed indicator and the altimeter. The airspeed and altimeter capsules supply signals simultaneously to a series of gears and levers to produce the Machmeter. It is a complex instrument, difficult to calibrate, and often slightly inaccurate. It is not used in test flight work except as a reference instrument.

1.8.5 Turn-and-Slip Indicator

The *turn-and-slip indicator* combines two instruments in one. This device is also called turn-and-bank indicator, or the needle-and-ball instrument. The needle

indicates the direction and rate of turn (not the amount of turn) of the aircraft. The ball indicates whether there is any slipping or skidding in the turn. The needle is actuated by a rate gyroscope, which senses rate of turn. The ball is simply an agate or steel ball in a liquid-filled curved glass tube. During a slip or skid, the ball moves away from the center of the tube in the direction of excessive force. In a balanced turn the ball remains in the center because the centrifugal force balances a component of gravity.

Many modern aircraft use a new type of instrument called the *turn coordinator*. This instrument replaces the needle of the turn-and-slip indicator with a miniature aircraft, which is displayed on the instrument. The miniature aircraft banks in the direction of the turn. The movement of the miniature aircraft, actuated by a gyroscope, is proportional to the roll rate of the aircraft. The ball indicator here has the same purpose as in the turn-and-slip indicator.

1.8.6 Accelerometer

The *accelerometer* measures acceleration parallel to the vertical axis of the aircraft. It is essentially a spring balance device that measures forces due to acceleration and is mounted near the center line of the fuselage. It has three pointers displayed on the dial. One pointer gives an instantaneous display of the force being applied at any time. The second pointer gives the maximum positive g , and the third pointer gives the maximum negative g being applied; these two pointers remain at the corresponding maximum values until they are reset. An accelerometer is a very useful instrument in aerobatic maneuvers as it warns the pilot to avoid overstressing the aircraft.

1.8.7 Attitude Indicator (Artificial Horizon)

The *attitude indicator* works on a gyroscopic principle; it consists of a horizon bar, a miniature aircraft, and a pointer.⁷ The horizon bar provides a mechanical horizon as a means of reference to the pilot when the natural horizon cannot be seen due to clouds, fog, rain, or other obstructions to visibility. This is achieved by connecting the horizon bar, with suitable linkages, to a gyro wheel. The attitude indicator is, therefore, also called the *artificial horizon* or the *gyro horizon*. The attitude indicator, with its miniature aircraft and horizon bar, displays a picture of the attitude of the aircraft. The relationship of the miniature aircraft to the horizon bar is the same as the relationship of the real aircraft to the natural horizon. The instrument gives an instantaneous indication of even the small changes in attitude. A pointer at the top indicates the bank angle in degrees on the index scale graduated 0–90 deg right or left.

In a case where the aircraft is flying level, the miniature aircraft is lined up level with the horizon bar. When the aircraft noses up, the horizon bar sinks below the miniature aircraft, and reverse is the case with the nose down condition. When the aircraft banks, the miniature aircraft also banks and the pointer at the top indicates the bank angle on the index scale.

Many modern aircraft use a more versatile piece of equipment called the *attitude director indicator* (ADI). This is a self-contained gyro indicator with flight director bars (one bar for roll and another for pitch), rate of turn and slip indicators, and rudder stabilization and flight control functions.⁸

1.8.8 Primary Flight Display

The *primary flight display* (PFD) is a display unit giving attitude and guidance information, airspeed, vertical and lateral deviation, auto flight system (AFS) modes, and radio altitude in separated zones.

1.9 Navigational Aids and Avionics

A dictionary meaning of the word navigate is “to manage or direct the course of a ship, boat, aircraft, etc.” Navigation deals with the methods of determining or planning a ship’s or aircraft’s position and course during the journey. It is important for a ship or aircraft to be able to locate and control its position in space at any specified time. Various methods for navigation are employed, e.g., geometry, astronomy, lights, compass, gyroscope, radio signals, and video signals. Computer-based systems are being increasingly introduced in civil aircraft.^{9,10} Flight control and guidance systems, in particular, incorporate a large number of computers and microprocessors that make flight operations more efficient. Certain important navigational aids and equipment are mentioned here.

1.9.1 Radio Navigation Aids

Most aircraft of the present generation are equipped with radios that provide a means of navigation and communication with ground stations. There are a variety of radio navigation systems available for use but some of the most commonly used include the very-high-frequency omnidirectional range–radio magnetic indicator (VOR-RMI), automatic direction finder–radio magnetic indicator (ADF-RMI), instrumental landing system (ILS), distance measuring equipment (DME), etc.

The VOR is the transmitting facility at the ground station that projects signals in straight lines (radials) in all directions; the word *omni* means all. These signals are received and indicated by the RMI; thus the instrument on the aircraft is called the VOR-RMI.

Many general aviation-type aircraft are equipped with the ADF radio receiving equipment called ADF-RMI. The pilot tunes the receiving equipment to a ground station known as a nondirectional radio beacon (NDB). The NDB stations normally operate in a low or medium frequency band of 200–415 kHz. The NDB has one advantage over the VOR in that the low or medium frequencies are not affected by the line of sight. The signals follow the curvature of the Earth; therefore, if the aircraft is within the power range of the station, the signals can be received regardless of the altitude. The navigational display consists of a dial on which the azimuth is printed, and a needle that rotates around the dial pointing to the station to which the receiver is tuned.

The ILS consists of very-high-frequency electromagnetic beams to guide the aircraft in both the horizontal and vertical planes on to the runway. It consists of an ILS beam in the form of lobes, which have to be captured by the aircraft antenna. This provides guidance in the azimuth. Another beam called a glide slope beam gives vertical guidance to the aircraft enabling it to touch down at the threshold; the aircraft’s angle of glide is approximately 3–4 deg.

The DME measures the slant range distance and not the actual horizontal distance. In the operation of the DME, paired pulses at a specific spacing are sent out from the aircraft that are received at the ground station which in turn transmits paired pulses back to the aircraft at the same pulse spacing but on a

different frequency. The time required for the round trip of this signal exchange is measured by the DME of the aircraft and is translated into distance from the aircraft to the ground station.

There are, of course, other pieces of radio equipment like the radio altimeter, the weather radio, and ground proximity warning system (GPWS). The GPWS provides visual and audio warnings in the case of dangerous flight path conditions are maintained that may result in inadvertent ground contact; the dangerous flight path conditions can be caused by excessive sink rate, excessive terrain closure rate, descent after takeoff, inadvertent proximity to terrain, or descent below ILS glide slope.

1.9.2 Visual Approach Slope Indicator

The *visual approach slope indicator* (VASI) is a system of lights arranged on the runway to provide visual descent guidance information to the aircraft during the approach to a runway. Certain installations have light units on one side of the runway while some other installations may have light units on both the sides of the runway. These lights are visible from 3 to 5 miles (4.8–8 km) during the day and up to 20 miles (32.2 km) or more at night.

1.9.3 Inertial Navigation System

The *inertial navigation system* (INS) works on a gyroscopic principle. The initialization is carried out at the bay where the coordinates—longitude, latitude, and altitude—are known. The system senses the component of acceleration along each coordinate and integrates the signal twice to estimate the new position along each axis. The system now refers to these coordinates and navigates in a straight line to the next coordinate requested by the operator. The system is like a two-dimensional coordinate system.

1.9.4 Magnetic Compass

The *magnetic compass* works on the principle of magnetism. It gives the heading of the airplane in degrees with respect to the Earth's magnetic north. It is generally a standby aid in modern aircraft which is used when other navigational aids are not available. The magnetic compass is a direction-seeking instrument and is simple in construction. However, it cannot be used when the aircraft is maneuvering a great deal in flight because the needle oscillates violently.

1.9.5 Heading Indicator

The *heading indicator* is fundamentally a mechanical instrument based on gyroscopic principles. It is also called the *direction indicator* or the *directional gyro*. It indicates the heading of the aircraft with respect to magnetic north, and enables the pilot to steer. In this instrument, the direction indicator is coupled to a gyroscopic wheel whose axis is horizontal and is kept aligned to a north-south direction by suitable devices. Heading information is displayed on the dial. The heading indicator is designed to facilitate the use of the magnetic compass. The heading indicator is not affected by the vibrations of the aircraft and, therefore, it works accurately even while the aircraft is flying in rough air currents.

Many modern aircraft use a *horizontal situation indicator* (HSI), which displays INS navigation information in addition to the information provided by the heading

indicator. A switch is provided to select either the INS navigation or magnetic heading display.

1.9.6 *Navigational Display*

The *navigational display* (ND) is a very versatile piece of equipment. With the help of a cathode ray tube (CRT), it has the capability of displaying on a single screen most of the information that is mentioned in the above paragraphs. The ND also displays wind speed, wind direction, and weather radar messages. When a failure affects an item of information that is displayed on the ND, this item is deleted until it is rectified or switched over to another source. If the ND is working satisfactorily, most other navigational equipment can be put on a standby basis because all of the information is shown on the ND.

1.10 Aircraft Weight

The weight of an aircraft is affected by the gravitational force exerted on it. The total weight of an aircraft that goes up in the air is an important design parameter that directly enters into almost all aircraft performance problems. The weight of an aircraft can be divided into various components. The aircraft weight combines with aerodynamic loads to generate stresses on the body of the aircraft.

1.10.1 *Weight and Stresses*

Weight and stresses are important design considerations in attempting to keep the weight of the aircraft as low as possible. An increase in weight would require an increase in runway length, more wing loading, and a higher stalling speed. The lowest-weight design means the lowest cost (both initial and operating) and better performance. An extra kilogram of weight means an increase in thrust required, wing area, fuel, etc., all leading to a further increase in the aircraft weight, and adversely affecting the cost and performance of the aircraft.

An aircraft structure is subjected to different types of stresses due to varying aerodynamic and inertial loads that may be imposed during flight. These different stresses are as follows: compression, tension, torsion (twisting), shearing (cutting), and bending. Skillful designers must be able to anticipate the magnitude, location, and type of load and stresses that the aircraft structure will have to endure, and make the aircraft sufficiently strong to withstand them. To do this, designers must have prior knowledge of the load distribution on the aircraft, and must subsequently calculate the stresses acting at different sections of the aircraft by theoretical and experimental stress analysis. The aircraft structure should also be able to withstand fatigue arising due to repeated loading and unloading. The problems encountered in structural design are further complicated by the fact that the aircraft structure must be light, strong, and rigid.

1.10.2 *All-Up Weight (Total Weight)*

The total weight of an aircraft that must be overcome to make it airborne is called the *all-up weight* (AUW) of the aircraft. The AUW is the weight of the aircraft that goes up in the air and acts vertically down at the center of gravity of the aircraft. It is also called the gross weight of the aircraft and denoted by W . The takeoff weight is the total weight of an aircraft at the moment of the start of the takeoff run. The takeoff weight plus the weight of the fuel required for the engine

run-up and taxiing, prior to the start of the takeoff run, is called *ramp* weight or taxiing weight.

The total weight of the aircraft continuously decreases during flight because of fuel consumption. In certain aircraft, the loss of weight can also be caused by the drops of paratroopers, missiles, bombs, and packages of food, clothes, medicine, or some other articles in flight; these drops bring discontinuous reductions in the weight of the aircraft. The total weight of the aircraft during flight can increase if refueling is undertaken during the flight.

The landing weight of the aircraft is generally considerably less than its takeoff weight; the reduction of weight by about 20–30% is not uncommon. This reduction in weight is taken into account by an aircraft designer while designing landing gear, flaps, or other such items used during landing. The smaller the aircraft weight, the less would be its impact load on the landing gears. The total weight at any instant, usually referred to in this book as simply weight, directly influences the point performance of the aircraft.

1.10.3 Weight Fractions

Expressing the total or gross weight of an aircraft as the sum of weights of the individual components and subsystems is very useful in design and performance. Broadly speaking, the total weight W can be considered to be made up of structural weight W_s , engine weight W_e , fuel weight W_f , and payload W_P , i.e.,

$$W = W_s + W_e + W_f + W_P \quad (1.1)$$

The structural weight includes the weights of airframe structure, equipment, comfort items for passengers (food, clothes, etc.), and flight and cabin crew. The engine weight consists of the weights of the engine(s), items associated with engine installation and operation, the fuel system, and the thrust reversal provisions. The payload consists of the weights of passengers, their baggage, cargo, and mail. The sum of W_s and W_e is called *operational empty weight* (OEW), or *basic operational weight* (BOW), or simply *empty weight* of the aircraft. The sum of OEW and W_P is called *zero fuel weight* (ZFW), and the sum of W_P and W_f is called the *useful load* of the aircraft. The weight of the aircraft without payload is called *operating weight* (OW), or *zero payload* of the aircraft; the OW of the aircraft is, therefore, the sum of OEW and the fuel weight W_f . The components of the total weight are briefly summarized in Fig. 1.3 for clarity. It is, of course, also possible to classify the total weight of an aircraft in some other different ways.

The contribution to total weight made by individual components becomes immediately clear if we work in terms of weight fractions. The weight fraction is the component weight divided by the total weight of the aircraft. Dividing Eq. (1.1) by W yields the relation,

$$W_s/W + W_e/W + W_f/W + W_P/W = 1 \quad (1.2)$$

where the ratio W_s/W is the structural weight fraction, W_e/W is the engine weight fraction, W_f/W is the fuel weight fraction, and W_P/W is the payload weight fraction. The sum of these individual weight fractions of the aircraft must always be unity.

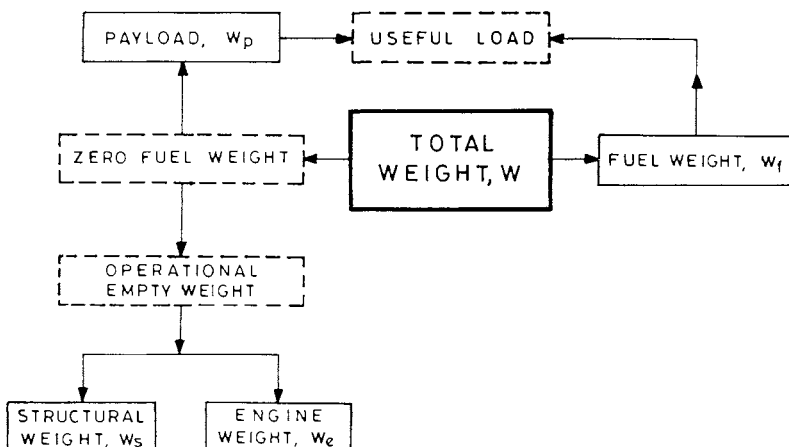


Fig. 1.3 Components of total weight of aircraft.

1.11 Forces Acting on Aircraft

An aircraft is acted on by aerodynamic, propulsive, and gravity forces in flight. An additional force between the wheels of the aircraft and the ground, called braking friction, also comes into play during the ground run (ground roll), either before liftoff or after the touchdown. These forces must be properly accounted for when forming the equations of motion of the aircraft dynamics.

1.11.1 True Presentation of Forces

The aerodynamic force is due to the interaction between the motion of the aircraft and the surrounding atmosphere. This force is exerted at each point of the aircraft that is exposed to the atmosphere. The resultant aerodynamic force acts at the center of pressure (CP) of the aircraft as shown in Fig. 1.4. The gravitational force is the total weight W of the aircraft, and it passes through the center of gravity of the aircraft. The CP coincides with the CG of the aircraft because of the aircraft's steady pitch and yaw attitudes. The propulsive thrust force acts along the thrust line shown in the figure. The thrust force may be due to a single engine or it may be the resultant thrust due to multiple engines. The propulsive unit may be either a piston-prop or a gas turbine engine. The thrust line passes very close

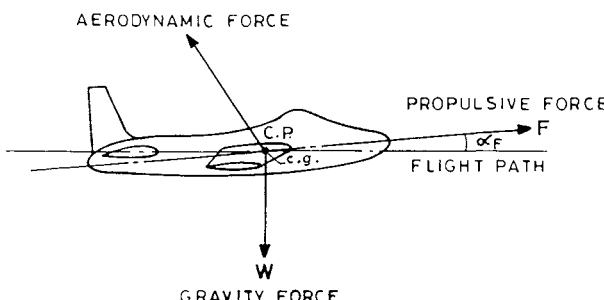


Fig. 1.4 True presentation of forces.

to the center of gravity of the aircraft. As a result of aerodynamic, propulsive, and gravity forces, the flight path is generally not along the thrust line. The angle α_F between the flight path and thrust line is generally very small.

1.11.2 Approximate Representation of Forces

In performance analysis, it is convenient to make certain valid approximations in representing the basic forces. The aircraft is regarded as a symmetric body. The resultant aerodynamic force is resolved into lift and drag forces, represented by the symbols L and D , respectively, whose lines of actions are orthogonal to each other. The lift force, by definition, acts normal to the flight path, and the drag force acts opposite to the direction of flight as shown in Fig. 1.5. The lift and drag are commonly expressed in nondimensional forms, as lift and drag coefficients, denoted by C_L and C_D , respectively, and defined as $C_L = 2L/(\rho V^2 S)$ and $C_D = 2D/(\rho V^2 S)$, where ρ is the density of air, S is the wing planform area, and V is the airspeed of the aircraft. The component of wind speed along the direction of flight is usually considered; the component of wind speed normal to the flight path has no appreciable influence if the wind speed is small. The thrust line is assumed to pass through the CG of the aircraft. The thrust line is also regarded coincident to the flight path because the angle α_F between them is very small. The aircraft is treated as rigid body so that no elastic forces are required for consideration.

1.11.3 Equations of Motion

The motion of a rigid body in space may consist of both translational and rotational motions. The motion of translation of the body can be considered independently of the motion of its rotation.¹¹ The independence of the two motions helps to solve body dynamics problems in general, and aircraft dynamics in particular. The performance problems of an aircraft require only translation motion, whereas the stability and control problems of the aircraft must also include its rotational dynamics.

The equations of motion of a body moving in space are obtained by applying Newton's laws of motion. According to the second law of motion, the sum of forces acting on a body in any direction is equal to the rate of change of momentum of the body in that direction. For example, if $\sum F_x$, $\sum F_y$, and $\sum F_z$ are the sum of forces acting on a body along the axes x , y , and z , respectively, the application

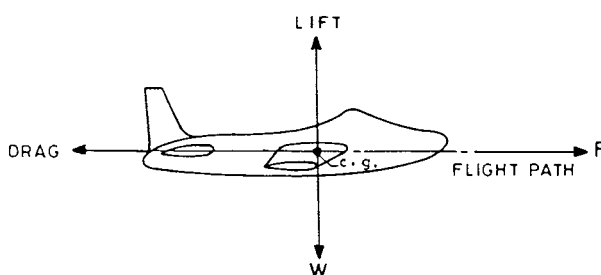


Fig. 1.5 Approximate representation of forces.

of the second law of motion yields the following three equations in the ground-axes system:

$$\sum F_x = \frac{d}{dt} \left(\frac{W}{g} V_x \right), \quad \sum F_y = \frac{d}{dt} \left(\frac{W}{g} V_y \right), \quad \text{and} \quad \sum F_z = \frac{d}{dt} \left(\frac{W}{g} V_z \right) \quad (1.3)$$

where V_x , V_y , V_z are the velocities along the axes of x , y , and z , respectively, g is the acceleration due to gravity, and W/g represents the mass of the aircraft.

In the cases where W is almost constant, or dW/dt is negligible, the above equations become, respectively,

$$\sum F_x = \frac{W}{g} \cdot \frac{dV_x}{dt}, \quad \sum F_y = \frac{W}{g} \cdot \frac{dV_y}{dt}, \quad \text{and} \quad \sum F_z = \frac{W}{g} \cdot \frac{dV_z}{dt} \quad (1.4)$$

and if the body does not have any acceleration, the above equations reduce to

$$\sum F_x = 0, \quad \sum F_y = 0, \quad \text{and} \quad \sum F_z = 0 \quad (1.5)$$

The above Eqs. (1.3), (1.4), and (1.5) are called the equations of equilibrium of the motion of the body. These equations are commonly used in formulating and preparing a theoretical base for aircraft performance.

1.12 What Is Aircraft Performance?

The meaning and scope of the term *aircraft performance* are explained here. It is shown that the subject of aircraft performance answers some of the most practical questions about flying that are not answered by other related disciplines.

1.12.1 Nature of the Basic Disciplines of Aircraft Performance

Consider first the disciplines that dictate the performance of an aircraft but individually cannot answer the questions demanded by the subject of aircraft performance. These disciplines are aerodynamics, aircraft structure, and aircraft propulsion. The function of each of these disciplines and their involvement are briefly explained below.

1.12.1.1 Aerodynamics. *Aerodynamics* is the study of the flowfield and the forces generated by the relative motion between the aircraft (or any other body) and the surrounding air. The *flowfield* deals with the nature of flow, involving steady and unsteady flows, laminar and turbulent flows, separated and attached flows, and rotational and irrotational flows. The concept of flowfield involves analyzing the difference between compressible and incompressible flows. In compressible flows, one studies compressibility effects, transonic flows, supersonic flows, mixed flow regions, and the formation of shocks and expansion waves. The study of aerodynamics involves calculating the velocity, temperature, and pressure fields arising due to relative motion between the body and the air. The velocity and pressure fields predict the flowfield and the forces due to friction. The pressure and friction forces acting at each point of the surface of the body give rise to lift, drag, and side forces. The study of aerodynamics helps one to calculate these

forces and to design surfaces with high lift and low drag. The ratio L/D is called the *aerodynamic efficiency*, which is denoted by E .

Aerodynamic forces affect the stability and control, and handling qualities of the aircraft. A stable aircraft returns to its original equilibrium position after it experiences a small disturbance. It is essential that the aircraft be stable during flight. The stability of aircraft is considered along all three of the mutually perpendicular axes passing through its center of gravity. *Longitudinal stability* deals with the aircraft's stability in pitch; *directional stability* studies its stability in yaw or sideslip; and lateral stability is concerned with the aircraft's stability in roll or bank. Their instabilities can be corrected by the corresponding control surfaces during flight or by a suitable design modification of the aircraft at the design stage. Aircraft stability can be both static and dynamic. Static stability is an essential requirement for the aircraft to be dynamically stable. Dynamic instability gives rise to different kinds of motions or oscillations. The longitudinal dynamic modes are phugoid motion (long-amplitude oscillations) and short-period oscillations, which can be dynamically stable or unstable. The lateral dynamic motions are Dutch roll oscillations, spiral divergence, and roll subsidence.²

1.12.1.2 Aircraft structure. An aircraft's structure is subjected to aerodynamic and structural loads. The primary function of the structural engineering group is to efficiently and optimally design the structure so that it is strong enough to safely withstand these loads under different operational conditions. These loads can even be due to gusts, impacts, or vibrations. An aircraft structure has several components consisting of different types of beams, columns, plates, and shells; these are usually thin-walled structures. Some of these structural components may be composed of stiffeners, a honeycomb-type construction, or composite materials. These components are subjected to compression, tension, bending, torsion, or combinations thereof. The subject of aircraft structure deals with the analysis of stress and strains. It predicts the conditions under which structural deformations, elastic instability, structural fatigue, fracture, and failure occur. An important objective of the structural design process is to maximize strength-to-weight ratio of the structure. It is very important that the weight of the structure should be at a minimum because this minimizes W/S , which is an important design parameter known as *wing loading*.

A perfectly rigid structure is only an ideal. All practical structures are elastic in nature. Since an aircraft structure must be as light as possible, this requirement results in a fairly flexible structure. The flexibility in the aircraft's structure gives rise to elastic forces that combine with aerodynamic forces to produce aeroelastic effects. These effects are important to all aircraft, particularly high-speed or high-performance aircraft. Flexibility (low rigidity) of the structure poses challenging problems from the point of view of the stability and control characteristics of the aircraft. The lower the rigidity, the larger the deflection under a given load. Excess deflection or bending under a load may lead to loss of control.

Aeroelastic problems may be grouped as 1) static or quasi-static problems, and 2) dynamic or unsteady problems. The static problems are concerned with steady (i.e., nonoscillatory) aerodynamic loads and the associated steady-state distortions. In the static problems, the aerodynamic loads distort the structure that gives rise to the corresponding elastic forces. This distortion produces an additional aerodynamic loading, which further distorts the structure. This process is continued until either an equilibrium condition is reached or structural failure occurs.

Certain important phenomena like wing torsional divergence and aileron reversal are caused by steady-state aeroelastic effects. Dynamic aeroelastic problems involve high-frequency oscillations in which inertia effects become important. The phenomena of flutter and buzz are caused by dynamic aeroelastic effects. *Flutter* is a particular type of resonance phenomena, in which energy is extracted from the airflow to build up the amplitude of oscillatory motion. Flutter may occur in different parts of aircraft. *Buzz* is a one-degree-of-freedom flutter involving only rotation of control surface. It consists of high-frequency oscillations of the control surface as a result of the movement of shock waves around the control surface at high airspeeds.

1.12.1.3 Aircraft propulsion. The primary job of the aircraft propulsion discipline is designing an engine powerful enough to push the aircraft forward, thus accelerating it to desirable airspeeds. Since the engine goes up in the air along with the aircraft, it must be reliable, lightweight, and must have the least possible drag during the flight. A propulsion unit generally consists of the processes of air diffusion, compression, fuel mixing, ignition, combustion, expansion of gases, and exhaust. The various components of the engine must be designed so that these processes can be efficiently carried out and matched to form a powerful power plant unit. The study of propulsion encompasses the design of diffusers, nozzles, compressors, fuel mixing system, fuel and ignition system, combustion chambers, turbines, and propellers. It also deals with the lubrication of power plants, the engine starting system and its acceleration and control, the engine cooling system, supercharging, the thrust augmentation system, and engine noise suppression. The power plant must be able to withstand varying atmospheric weather conditions, and other operational requirements of the aircraft.

Engines may be of different types, such as the reciprocating engine with propeller, the gas turbine engine, the ramjet engine, and the rocket engine. These engines have differing characteristics, and certain considerations must be taken into account during installations, including altitude and the Mach number range of the aircraft. The maximum thrust-to-weight ratio of the engine is its important design parameter; the ratio must be as high as possible. The rate of fuel consumption per unit of thrust (or power) is called thrust-specific fuel consumption (TSFC) or power-specific fuel consumption (PSFC). The TSFC (or PSFC), denoted by c (or \dot{c}), is an important engine parameter, which must be kept as low as possible.

Thus far, the activities of aerodynamics, aircraft structure, and propulsion groups have been explained. None of these activities indicates the performance of the aircraft. The basic forces generated by these disciplines, however, dictate the aircraft's performance. The word *performance* is a general term that connotes execution, fulfillment, or carrying out. If you ask an ordinary aircraft passenger what he understands by the term *aircraft performance*, you should not be surprised by his answer; he will probably say that good aircraft performance means that the flight is physically comfortable, the aircraft is not vibrating or bumping, noise level is low, the food and drinks are good, the airline attendants are cooperative, etc. These aspects do not belong to aircraft performance in the sense of the term as understood by the experts in the field of aeronautics. What then is the meaning of aircraft performance? We will explain the meaning of this term below.

1.12.2 Aircraft Performance and Its Parameters

The subject of aircraft performance is a part of the mechanics of flight; only the translational motion of the aircraft is considered by applying Newton's laws of motion. The study of aircraft performance deals with as its subject some of the most important questions about flight that cannot be answered by the other disciplines. Some of these questions are: how much is the takeoff distance, what is the angle of climb, what is the fastest possible rate of climb, what is the cruising speed of the aircraft, what is the geographic range covered and the time of the flight, how much fuel is consumed, what is the radius of turn, what is the fastest possible turn rate, etc. The content of these questions directly constitutes what we mean by performance parameters.

The various aircraft performance parameters will now be considered systematically by decomposing the flight into its various phases. These parameters depend on the phase of flight to which they belong. Starting from the beginning, these phases are takeoff, climb, cruise, turn, descent, and landing. A brief discussion to familiarize the reader with the various performance parameters is presented below for each phase of the flight.

1.12.2.1 Takeoff performance parameters. The takeoff flight, by definition, begins from the start of the aircraft's ground roll on the runway and ends when the lowest portion of the aircraft during its climb has reached the height of 35 ft (10.67 m) above the ground. This 35-ft height is called the *screen height* or *obstacle height*, which is taken to be the height of an imaginary obstacle; it is sometimes taken as 50 ft (15.24 m) depending on the flight regulations and aircraft. During takeoff, the aircraft first rolls on the ground until it has reached a specified airspeed; it is then rotated about the rear wheels for a short time (about 3 s) and then finally the aircraft becomes airborne when both the front and rear wheels are above the ground. Thereafter, the aircraft climbs and soon reaches a height of 35 ft (or 50 ft) above the ground to complete the takeoff phase. Thus, the performance parameters of takeoff flight are 1) ground roll distance and time, 2) rotation distance and time, and 3) airborne distance and time.

1.12.2.2 Climb performance parameters. The *climb phase*, by definition, starts from the height of 35 ft (or 50 ft, as the case may be) above the ground, and ends when the aircraft has completed climbing. The performance parameters of the climb phase are 1) angle of climb, 2) rate of climb, 3) airspeed or Mach number of climb, 4) time taken during climb, 5) horizontal distance covered in climb, 6) fuel consumption in climb, and 7) absolute and service ceilings (explained in Chapter 10).

1.12.2.3 Cruise performance parameters. The *cruising phase* starts soon after the completion of the climbing phase and ends when the aircraft has started descending or maneuvering. During the cruise, the aircraft moves steadily along a straight line in the horizontal plane. In other words, it is a steady (no acceleration), straight, and level (horizontal) flight. The performance parameters of the cruising flight are 1) airspeed and Mach number of the cruise, 2) range, i.e., horizontal distance covered in the cruise, 3) time taken to cover the range, and 4) fuel consumption in the cruise.

1.12.2.4 Turning performance parameters. In the cases of turning flight, the important performance parameters of the flight are 1) airspeed or Mach number of turn, 2) bank angle ϕ , and load factor $n (= L/W)$, 3) rate of turn, and 4) radius of turn.

1.12.2.5 Descent performance parameters. The descent phase starts when the aircraft has started losing height with the purpose of descending toward the ground and ends when the aircraft is 35 ft (or 50 ft) above the ground. Its performance parameters are 1) rate of descent, 2) angle of descent, 3) airspeed of descent, 4) time taken in descent, and 5) fuel consumption in descent.

1.12.2.6 Landing performance parameters The landing phase can be regarded as the reverse of the takeoff phase. By definition, the landing phase starts when the aircraft is at 35 ft (or 50 ft), above the ground. As soon as the airborne distance of the landing phase is completed, the rear wheels of the aircraft first touch the ground; soon after the nose wheels are also on the ground. Thereafter, a rapid deceleration of the aircraft takes place, first due to aerodynamic drag and then by braking friction, until it comes to a standstill. The performance parameters of the landing phase are 1) airborne distance and time, 2) rotation distance and time, and 3) ground roll distance and time.

Performance analysis goes further to optimize many of the above parameters of the different phases of flight. Thus we can obtain best range, maximum endurance, maximum rate of climb, fastest turn rate, etc. These are some of the very important performance parameters, called figures of merit (FOM), of the aircraft.

1.12.3 Solutions of Performance Problems

Performance solutions are expressed by means of aircraft design variables or parameters, which are listed here. It is generally convenient to make separate theoretical formulations for each phase of flight. Therefore, each different flight phase is generally considered in a separate chapter. The arrangement of different chapters in this book dealing with the formulation, analysis, and solution of each flight phase is presented here. We present basic information required for an understanding of the theoretical formulation and its analysis in the first few chapters. Other relevant information, affecting the aircraft performance but not generally treated mathematically, is also presented in separate chapters.

1.12.3.1 Performance solutions and design parameters. The solutions of aircraft performance problems require expressing the performance parameters in terms of known design parameters of the aircraft. These design parameters include those dealing with the aircraft's aerodynamic design, structural design, and power plant design. A brief understanding of these design parameters is necessary before one can proceed to obtain the solution of the performance problems. A detailed discussion of the aerodynamic design parameters is presented in Chapter 3; the power-plant design parameters are treated Chapters 4 and 5. The important design parameters that directly affect the aircraft performance are 1) zero-lift drag coefficient C_{D_0} ; 2) lift-dependent drag coefficient factor K ; 3) maximum aerodynamic efficiency of the aircraft; 4) maximum lift coefficient; 5) wing planform area S ; 6) total weight of aircraft W ; 7) maximum weight of fuel; 8) maximum load factor; 9) maximum net thrust F_m (or maximum power $P_{e,m}$) of the engine;

10) thrust (or power) specific fuel consumption; and 11) propeller efficiency, if a propeller exists.

Items 1–5 above are the aerodynamic design parameters; the quantities C_{D_0} and K are explained in Chapter 3. Items 6–8 are the structural design parameters, and items 9–11 are the power plant design parameters. Certain ratios associated with design parameters commonly occur in performance analysis, such as the wing loading W/S , the thrust/weight (power/weight) F/W (or P_e/W), and the thrust (or power) loading F/S (or P_e/S).

1.12.3.2 Discussions in different chapters. It is seen from the preceding discussions that the forces of aerodynamics, gravitation, and propulsion, and the design parameters associated with them, are relevant to the solutions of aircraft performance. Historically, powered flight could be achieved only after the relationship among these forces had reached a certain level. It is therefore appropriate to first present a more detailed discussion of these forces, as in Chapters 3–5. Chapter 3 discusses aerodynamic forces, flowfields, lifting surfaces, and the associated aerodynamic design parameters. We do not consider it necessary here to devote a full chapter to gravitational force (weight), because the information presented here in Sec. 1.10 is generally sufficient for performance analysis of the aircraft. Propulsive thrust of gas turbine engines, their components, and relevant design parameters are discussed in Chapter 4. Similarly, Chapter 5 discusses the reciprocating engine, its components, the propeller, and associated design parameters.

A discussion of the performance analysis of an aircraft begins in Chapter 7, which considers the performance solutions of unpowered or glider flights. Performance solutions of different phases of flight of turbojet aircraft are discussed in Chapters 8–11, and that of piston-prop aircraft in Chapters 12–15. Chapter 16 is devoted to both takeoff and landing phases; the analysis, as carried out in the chapter, is valid both for turbojet and piston-prop aircraft.

Discussions of performance solutions of different types of maneuvers are generally lacking in the aeronautical literature, probably because the theoretical analysis is not simple. This subject matter is, therefore, presented qualitatively in Chapter 17 in conjunction with a brief explanation of the different types of aircraft maneuvers and how they are performed.

A good performance solution of the aircraft should also incorporate the influence of atmosphere and weather. A brief review of the nature of the atmosphere and the effect of weather on flight is presented in Chapter 2. It is generally difficult to obtain theoretical performance solutions pertaining to different weather conditions that may prevail during flight. Therefore, only qualitative discussions are contained in Chapter 19, which deals with the nature of different weather hazards and their influence on flight. Chapter 20 explains how the enormous amount of meteorological information about the atmosphere and weather is collected, synthesized, and communicated to pilots to help them guide the aircraft better.

The performance solutions of an existing aircraft can be obtained directly from flight tests. A team consisting of a test pilot and two flight test engineers, along with the test aircraft, is generally sufficient to carry out the different flight tests. The various methods of obtaining the performance evaluation through flight tests is the subject matter of Chapter 18. The test pilot and flight test engineers frequently use different kinds of altitudes, airspeeds, and wind speeds which are explained in Chapter 6; this chapter, and certain discussions in other chapters, will help readers appreciate the practice of performance evaluation through flight tests.

1.12.4 Scope of Aircraft Performance

The subject of aircraft performance establishes the importance and utility of design parameters. It formulates the relationship between aircraft design and performance variables, which gives the designer a clear understanding of the qualitative and quantitative influence of the design parameters on aircraft performance. Improved aircraft design for better performance is an important goal of the designer.

The subject of aircraft performance is customer friendly. An aircraft customer is not interested in learning about aerodynamics, structures, or propulsion, as applied in the design of the aircraft. He would like to know how much runway length is required, how fast or high the aircraft can fly, how fast it can climb or turn, the aircraft's range or endurance, etc. All these questions belong to the subject of aircraft performance. The performance parameters are also utilized to distinguish one aircraft from another. They answer some of the most important questions that cannot be answered by other disciplines.

The subject of aircraft performance is also reader friendly. The mathematics used is simple and practical. The various concepts developed are realistic and can be grasped easily. The study of aircraft performance leads to greater interest and awareness among readers because the subject matter has always been of great interest to people.

It is necessary to achieve a theoretical understanding of the various parameters of aircraft performance. This is accomplished by applying the well-known laws of motion of a solid body and establishing the conditions of equilibrium of forces acting on the aircraft. It is rather surprising that some of the simplest equations of motion are capable of answering the most important questions about the performance of a complicated body like an aircraft.

The theoretical analysis developed for performance calculations of the conceptual and preliminary design phase of the aircraft has applications even in performance testing and evaluation. The various claims made by the designer and the manufacturer of the aircraft must be tested. There are some independent organizations devoted to the task of aircraft testing and evaluation. It is obvious that the cost of aircraft testing should be kept to a minimum. Thus, special methods of performance testing must be devised that would minimize fuel, effort, and would require the least amount of time and space.

Performance testing is carried out at various stages, like the production stage, prototype, and the final product. Any change made in the design of aircraft is again tested for its performance. Aircraft performance parameters form the base of comparing different aircraft. Performance analysis under standard atmospheric conditions is required to compare different flight tests of even the same aircraft.

Performance analysis and performance testing unite persons representing different disciplines of aircraft technology in a common effort devoted to suggesting, discussing, clarifying, and making improvements.

References

¹Torenbeek, E., *Synthesis of Subsonic Airplane Design*, Delft Univ. Press, Delft, The Netherlands, 1976.

²Nelson, R. C., *Flight Stability and Automatic Control*, McGraw-Hill, New York, 1990.

³Lambert, M. (ed.), *Jane's All the World's Aircraft*, 1991–1992.

⁴Bernard, R. H., and Philpott, D. R., *Aircraft Flight*, Longman, Harlow, England, UK, 1991.

⁵Perkins, C. D., and Hage, R. E., *Airplane Performance, Stability, and Control*, Wiley, New York, 1949.

⁶Davies, D. P., *Handling of Big Jets*, Civil Aviation Authority, London, 1985.

⁷MacDonalds, S. A. F., *From the Ground Up*, Himalayan Books, New Delhi, India, 1989.

⁸Stewart, S., *Flying the Big Jets*, 2nd ed., Airlife, Shrewsbury, England, UK, 1986.

⁹Middleton, D. H. (ed.), *Avionics Systems*, Longman, Harlow, England, UK, 1989.

¹⁰Pallet, E. H. J., *Microelectronics in Aircraft Systems*, Krieger, Malabar, FL, 1989.

¹¹Loney, S. L., *Dynamics of a Particle and of Rigid Bodies*, Cambridge Univ. Press, Cambridge, England, UK, 1952.

Problems

In the multiple choice problems below, mark the correct answer.

1.1 The tail portion of an aircraft, called the empennage, consists of a) vertical tail and elevator, b) horizontal tail and elevator, c) horizontal tail and vertical tail.

1.2 The speeds of 140, 320, and 450 m/s, respectively, correspond to a) low speed, low compressible speed, and transonic speed; b) low speed, transonic speed, and supersonic speed; c) low compressible speed, transonic speed, and supersonic speed.

1.3 The speeds of 150 kn, 200 m/s, and 1000 ft/s, respectively, correspond to a) low speed, transonic speed, and supersonic speed; b) low speed, low compressible speed, and transonic speed; c) low compressible speed, transonic speed, and supersonic speed.

1.4 A cockpit a) is normally situated near the middle of the fuselage, b) contains flight and navigational instruments, c) is a retiring room for all of the crew members.

1.5 The wings of aircraft provide both a) lift and roll, b) lift and pitch, c) roll and pitch.

1.6 Control surfaces are a) always in pairs on aircraft, b) always on the wings of the aircraft only, c) in pairs as well as occurring singly on aircraft.

1.7 The purpose of elevators is a) to provide additional lift to the aircraft, b) to control pitch, c) to stabilize the aircraft.

1.8 The purpose of the rudder is a) to stabilize in yaw, b) to control yaw, c) to stabilize in roll.

1.9 Starboard means a) right-hand-side wing, b) left-hand-side direction, c) right-hand-side direction.

1.10 Spoilers produce a) roll and pitch, b) speed brakes and yaw, c) roll and speed brakes.

1.11 Roll is the rotation of aircraft about the a) vertical axis, b) longitudinal axis, c) lateral axis.

1.12 Dutch roll of an aircraft consists of mostly a) yaw, b) yaw and roll, c) yaw, roll, and pitch.

1.13 Which of the following statements is correct? a) All aircraft have only one aileron on each side; b) Some aircraft have two ailerons on each side; c) Some aircraft have three ailerons on each side.

1.14 The starboard aileron is deflected down to cause a) rolling toward right, b) rolling toward left, c) to obtain more lift.

1.15 To enhance the roll, deflect the port aileron a) up and use the port spoiler, b) down and use the starboard spoiler, c) up and use the starboard spoiler.

1.16 Total pressure p_0 is used in a) airspeed indicator (ASI) only, b) Machmeter only, c) both in ASI and Machmeter.

1.17 Static pressure p is used in a) ASI only, b) ASI and altimeter only, c) ASI, altimeter, Machmeter, and VSI.

1.18 Aircraft structure should have a) maximum possible stiffness/weight ratio, b) maximum possible strength/weight ratio, c) maximum possible strength and stiffness.

1.19 Aeroelastic problems are primarily caused by a) the elastic nature of aerodynamic forces, b) a combination of elastic and gravitational forces, c) a combination of elastic and aerodynamic forces.

1.20 The phenomenon of aileron reversal is a) a static aeroelastic problem, b) a problem caused by poor maintenance of ailerons, c) a problem caused by excessive vibrations of wing.

1.21 A particular type of resonance phenomenon in which energy is extracted from the airflow to build up the amplitude of the oscillatory motion is called a) aerodynamic resonance, b) damped natural frequency, c) flutter.

1.22 Which of the following statements is correct? a) In a balanced turn the ball of the turn and slip indicator remains at the center; b) the altitude indicator does not display miniature aircraft; c) the DME does not give the slant range.

1.23 Which of these sets has all three gyroscopic instruments? a) VASI, attitude indicator, and INS; b) INS, accelerometer, and artificial horizon; c) heading indicator, attitude indicator, and INS.

1.24 Which of the following sets contains flight instruments? a) visual approach slope indicator, sidestick, and altimeter; b) ASI, magnetic compass, and PFD; c) turn coordinator, altimeter, and ASI.

1.25 Which of the following statements is not correct? a) An FBW system replaces mechanical linkages; b) Concorde was the first supersonic transport aircraft to have an FBW system; c) an FBW system is a particular type of powered flight control system; d) power-operated flying control surfaces are generally irreversible in nature.

1.26 Payload consists of a) fuel and passengers, b) passengers and baggage, c) fuel and baggage.

1.27 Operational empty weight consists of a) structural weight, engine, and fuel; b) engine, baggage, and fuel; c) structural weight and engine.

1.28 Useful load consists of a) fuel, passengers, and baggage; b) payload and structural weight; c) structural weight, engine, and passengers.

1.29 Which of the following statements is correct for a given aircraft: a) the sum of all weight fractions is unity throughout the flight; b) baggage is not a part of payload; c) ramp weight is less than takeoff weight.

1.30 Which of the following statements is correct: a) zero fuel load is the same as operational at empty weight, b) operational weight is the sum of passengers and fuel loads, c) useful load is the sum of payload and fuel load.

1.31 If an aircraft has a payload of 22% and fuel load of 17%, of the total weight of the aircraft, the weight fraction of operational empty weight is a) 0.52, b) 0.61, c) 0.75.

1.32 If in Problem 1.31 the engine weight fraction is 0.17, the structural weight fraction would be a) 0.22, b) 0.31, c) 0.40.

1.33 Which of the following statements is correct: a) fuel is generally placed inside the wings, b) landing gears are always retractable, c) an aircraft cannot have movable wings.

1.34 Which of the following statements is correct: a) maximum lift coefficient is a performance parameter, b) maximum aerodynamic efficiency is a design parameter, c) wing planform area is a structural design parameter.

1.35 Which of the following statements is correct: a) load factor is a design parameter, b) maximum fuel weight is a power plant design parameter, c) wing loading is a structural design parameter.

1.36 The three basic forces of aircraft performance of rigid structure are a) aircraft weight, wind force, and elastic force; b) gravitational force, aerodynamic force, and propulsive force; c) wind force, propulsive force, and aircraft weight.

1.37 The subject of aircraft performance determines a) how much distance a given aircraft can cover; b) at what air speed the aircraft becomes airborne; c) how much thrust is required during cruise.

2

The Atmosphere and Flying Weather

2.1 Introduction

Humans live at the base of an invisible ocean of air, which is referred to as the atmosphere. The atmosphere is always in a state of commotion and physical change, giving rise to changing weather conditions on extremely vast scales. The pilot has to recognize the “mood” of the atmosphere before he decides to go up in the air. He can take the help of weathermen and forecasters to understand meteorological conditions, but the final go or no-go decision rests with the pilot. The fundamentals of meteorology are undertaken in this chapter whereas hazardous weather is described in Chapter 19.

2.1.1 Elements of the Atmosphere

The *atmosphere* is the gaseous medium enveloping our Earth and revolving with it as an integral body. The weight of the atmosphere is about one millionth that of the Earth. The air is the basic gas composing the atmosphere, but to a very small extent it also contains water vapor and suspended tiny microscopic solid particles called aerosols. The atmosphere gets lighter with increasing altitude. More than 50% of the mass of the atmosphere is in the first 5 km altitude and about 99% of the mass of the atmosphere exists in the first 30 km altitude. The mass of the atmosphere is about 5×10^{15} tons,¹ which amazingly turns out to be just above 1/300 of the total mass of water (1.5×10^{18} tons) contained in all the rivers, lakes, and oceans on the Earth. The atmosphere regulates heat, air, and moisture. It also protects us from the sun’s harmful rays and from meteoroids, and maintains the ecological balance on the Earth. Flying takes place only in the relatively denser portion of the atmosphere.

Air is a mixture of many gases, and it contains an abundance of nitrogen and oxygen (99%). The percentage by volume of the first four largest gases is nitrogen 78%, oxygen 21%, argon 0.93%, carbon dioxide 0.031%; these constitute about 99.9% of the total clean air of the atmosphere. Within the remaining approximately 0.1% are found hydrogen, helium, ozone, neon, and some other trace gases. Without oxygen no life is possible on the Earth and, of course, without oxygen airbreathing engines would also have no “life.” Through nitrates, nitrogen constitutes food for all vegetation, and all plants breathe carbon dioxide. Ozone absorbs the sun’s ultraviolet rays and, therefore, shields us from its harmful effects on the cells of living beings. Water vapor in the atmosphere is the basic source of all fog, cloud, and precipitation. The aerosols in the atmosphere originate mostly from dust blown by wind, salt particles found in spray blown off the water, volcanic, debris, and smoke particles from forest fires and from human-made processes involving the burning of fossil fuels. These suspended particles are not completely parasites in the atmosphere because some of them significantly aid in the condensation of water vapor and help to freeze rain droplets.

A pilot of an aircraft, however, is not interested in the details of the composition of the air. A pilot views or senses atmosphere from its impact on flight performance.

2.1.2 *The Pilot's View of the Atmosphere*

A pilot generally finds the atmosphere quite friendly. It makes flying enjoyable to such an extent that he or she chooses flying as a career. The atmosphere exhibits its friendliness by giving sufficient "lift" to his aircraft. The atmospheric winds have inexhaustible energy that is utilized for windmills, generating electricity, cooling, and providing thrust and power to air-breathing engines.

The same atmosphere can sometimes be quite unfriendly too, and may even behave like an enemy. A pilot's concern is that the atmosphere also has its own independent motion which sometimes dangerously interacts with the motion of the aircraft. A pilot knows by experience that air is made up of changing wind speeds and directions, turbulence, vertical air currents, updrafts and downdrafts, gusts, circulations and vortices, microbursts, tornadoes, wind jets, and windshear. These may cause an aircraft to stall, roll, spin, yaw, sideslip, or engage in violent tossing that cannot be controlled. Atmospheric winds can uproot trees and houses, overthrow automobiles and railway carriages, and destroy bridges and tall buildings. For a pilot, water vapor causes fog, cloud, rain, snow, hail, thunder, lightning, rainbow, and halos. Many of these atmospheric phenomena put a pilot and his aircraft in difficult situations varying from discomfort to disaster. In certain catastrophes it becomes difficult to identify which is to blame—the pilot, the aircraft, or the atmosphere. This leads us to attempt to gain more knowledge of the atmosphere so that the pilot-aircraft-atmosphere system becomes more reliable.

2.2 Principles of Atmospheric Changes

The heat transfer processes distribute and diffuse the solar heating of the Earth which causes most meteorological changes.

2.2.1 *Heat Transfer Processes in the Atmosphere*

Heat flows from a higher temperature to a lower temperature. The three well-known heat transfer processes—radiation, convection, and conduction—also exist in the atmosphere. In *radiation*, the heat energy is transferred in the form of electromagnetic waves through empty space or through material medium. In *convection*, the heat is transferred by bodily movement of fluid particles. This movement may occur both vertically and horizontally. In meteorology, the vertical motion is called *convection* and the horizontal motion is referred to as *advection*. Rising of warm air or descending of cold air are the examples of convection currents, and similarly, the horizontal movements of hot or cold air masses are the examples of advection currents. The time and length scales of advection currents in the atmosphere are generally much longer than those of convection currents. The term *conduction* refers to the transfer of heat through contacts from molecule to molecule. In the atmospheric sciences, conduction is often neglected as compared to the other two modes of heat transfer, because air is an extremely poor conductor of heat. Conduction has importance only within a couple of meters above the ground. Heating or cooling of air in the immediate neighborhood of the Earth's surface is due to

conduction. As an example, during the day the air is warm and during the night the air is cool near the Earth's surface.

2.2.2 Solar Radiation, Absorptions, and Emissions

The sun is the basic source of energy for our Earth and the atmosphere. The surface temperature of the sun is about 6000°C and the average temperature of the Earth's surface is about 20°C. Therefore, there is continuous flow of solar heat energy from the sun to the Earth through short-wave radiation, which is also called *solar radiation*. Not all the solar radiation directed to the outer parts of the atmosphere reaches the Earth's surface. A part of the solar radiation is scattered by the individual molecules in the upper atmosphere which makes the sky look blue, and some is absorbed by the ozone layer. Some solar radiation is absorbed in the lower parts of the atmosphere by clouds (including its ice) and water vapor. Dry air is transparent to solar radiation because it does not absorb the solar radiation. The Earth does not absorb all the solar radiation that finally reaches it because part of it is simultaneously emitted back into the atmosphere as long-wave radiation. These long-wave radiations emitted by the Earth are commonly known as "terrestrial radiations," which are mostly absorbed by the water vapor and carbon dioxide of the atmosphere. The atmosphere is also simultaneously emitting long-wave radiation, part of which is directed toward the Earth and part of which goes to outer space. The net effect of absorption and emission is that out of the total solar energy received on our globe, about 20% is absorbed by the atmosphere, about 50% is absorbed by the land and ocean, and the rest—about 30%—is reflected back¹ into space by the clouds, atmosphere, and the Earth; out of this 30% reflection, called net global *albedo*, about 20% is reflected by clouds, 5% by scatter in the atmosphere, and 3% is reflected by the Earth's surface. This essentially means that the lower layers of the atmosphere are heated from below and not from above. Thus the terrestrial heating assumes significance. It is shown below that the terrestrial heating or cooling is not uniform, and this nonuniformity causes weather changes.

2.2.3 Differential Heating of Terrains

The amount of rise or fall in temperature of different substances by solar heating depends upon their specific heats and latent heats. The specific heat of a substance is the heat required to raise its unit mass by one degree. The latent heat is the amount of heat absorbed (or released) to change the state of unit mass of the substance from solid to liquid (or liquid to solid), or from liquid to gas (or gas to liquid), without change of temperature. Water has a high specific heat, ice has one-half, and moist soil has one-fifth of that value, dry soft surface has still less, while hard concrete surface or hard stones have still much less values of specific heats. Hard surfaces heat at a faster rate because the sun's rays are not able to penetrate deep inside the surface and, therefore, only a comparatively small amount of the Earth's layer absorbs all of them. On the other hand, the sun's rays penetrate several meters deep into water and, therefore, a large mass of the water absorbs the same rays. Moreover, all the heat received by water is not utilized to raise the water temperature, but instead it is used as latent heat to evaporate some water. Thus, substances having lower specific heats warm up or cool quickly. Since different types of terrain have different specific heats, the rise or fall in temperature is

also different. This differential heating of terrains causes vertical currents, winds, thermals, and clouds.

2.3 Temperature, Pressure, and Density of the Atmosphere

Temperature, pressure, and density are the three characteristic quantities of the atmosphere and it is important to know their behavior. They are not independent because they are related by the equation of state.

2.3.1 Atmospheric Temperature

Temperature is the most significant quantity which influences pressure and density of the air. The differential heating on Earth causes weather changes.

2.3.1.1 Temperature and its significance to flying. Air temperature is directly a measure of the average kinetic energy of air molecules. It is a physical quantity indicating the degree of heat or coldness of air. In a meteorological station, the temperature near the surface is measured in a shade at 1.25 m (4 ft) above the ground. It is measured either in degrees Celsius [degrees Centigrade ($^{\circ}\text{C}$)] or in degrees Fahrenheit ($^{\circ}\text{F}$). These two are linearly related as, $^{\circ}\text{F} = (9/5)(^{\circ}\text{C}) + 32$. This provides an excellent thumb rule which states: Double the Celsius reading, subtract one-tenth of this product, and add finally 32 to get Fahrenheit reading. The standard atmospheric temperature at sea level is taken as 15°C (59°F), normal human body temperature is 37°C (98.6°F), freezing temperature of water is 0°C (32°F) and its boiling point is 100°C (212°F). For flying, it is important to know air temperature at the time of takeoff and landing, and during flight. The temperature and pressure fix the air density, which in turn fixes the airspeed of the aircraft. The temperature maps of the atmosphere include lines of freezing temperature so that the pilot realizes the chances of icing acting as a hazard to an aircraft. The difference between temperature and dew-point temperature of the atmosphere indicates the probability of fog formation. The changes in temperature alter the Reynolds number and Mach number of flight. The temperature appears directly at several places during the data reduction from flight tests.

2.3.1.2 Minimum and maximum temperatures on Earth. The temperature is minimum at the antarctic, which is regarded as the Earth's ice house. Here low temperatures up to -75°C can be found. The hottest place on our Earth is the desert of Somali in Africa where the temperature may rise up to 65°C , and so this place is known as the Earth's furnace. Thus, the temperature variation on the Earth is -75°C to 65°C . At any fixed point also, on the Earth, the temperature may vary considerably. The average temperature on Earth is higher near the equator and decreases with the increase in latitude so that it is least at the poles.

2.3.1.3 Temperature aloft. Typical mean temperature variation with altitude is shown in Fig. 2.1. The zigzag behavior of the curve appears puzzling at first sight. At any particular point in space, there are variations of temperature with time during a year. This variation is more near the Earth and in the troposphere, and it reduces as the altitude increases. The mean temperature decreases with altitude in the troposphere and again in the mesosphere; terms like troposphere, mesosphere, mesopause, etc., are explained later in Sec. 2.16 of this chapter. The minimum

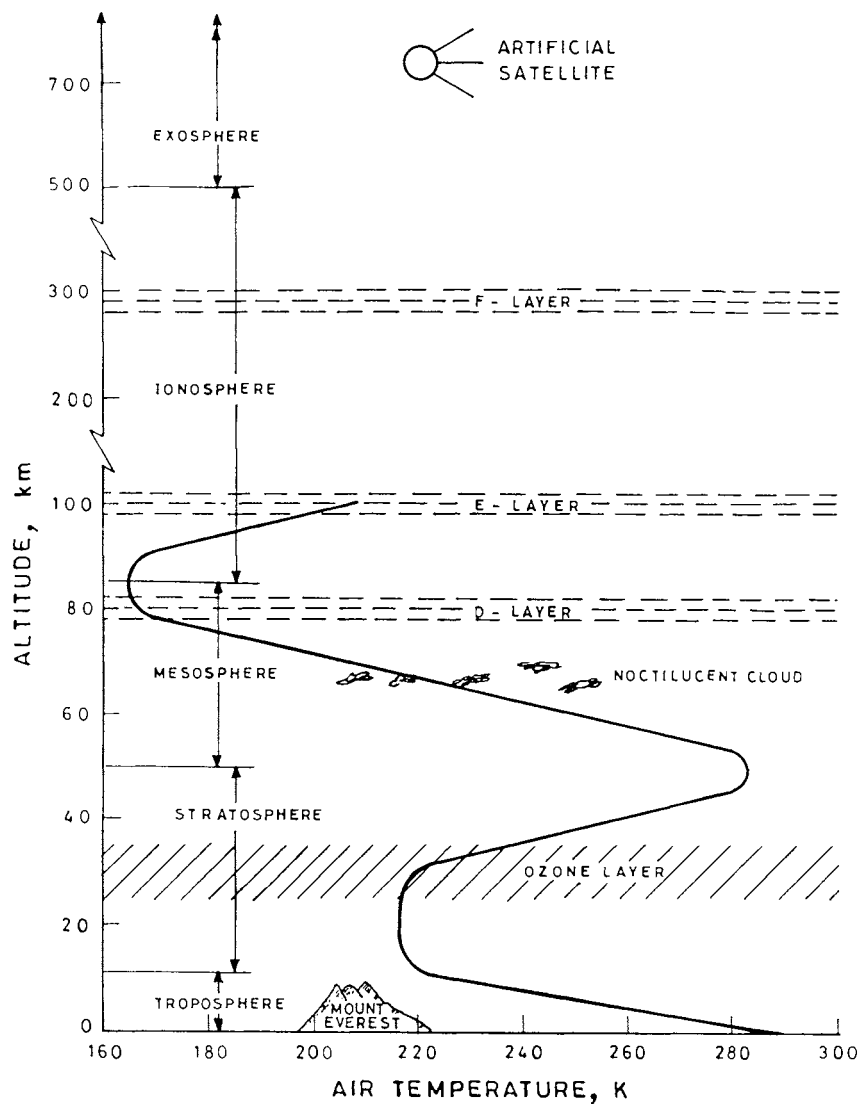


Fig. 2.1 Temperature variation with altitude in the atmosphere.

temperature in the upper atmosphere is observed as low as about -100°C in the mesopause over the Arctic continent.

2.3.1.4 Temperature lapse rate. The rate of change of temperature with height in the atmospheric layers at a place and time is called its *temperature lapse rate* or simply *lapse rate*, which is denoted by λ . The lapse rate, λ , is considered positive if the temperature decreases with height, and vice versa; $\lambda = -dT/dh$. The lapse rate is zero in isothermal layers. The lapse rate depends on whether the thermal process is adiabatic or nonadiabatic and on the moisture content in the

atmosphere. In the adiabatic process an air mass or air parcel (or any other gas) is compressed or expanded in volume without gaining or losing any heat to or from outside sources. The vertical motion of air parcels in the atmosphere is considered adiabatic because there is no heat exchange of heat energy from the external boundaries of the air parcel. In the rising currents, air expands and cools adiabatically. Similarly, in the descending layers, air is compressed and warms adiabatically.

The dry air adiabatic lapse rate (DALR) is 3°C per 1000 ft (304.8 m) or 1°C per 100 m. The saturated-air adiabatic lapse rate (SALR) is 1.5°C per 1000 ft or 0.5°C per 100 m; the concept of saturation of air is explained later in Sec. 6. Therefore, $\text{SALR} = 1/2 \text{ DALR}$. The moist air adiabatic lapse rate (MALR) would depend upon the moisture content, and its value would, therefore, fall between the values of DALR and SALR. Note that MALR is less than DALR. This is because the moist air in condensation releases the *latent heat of vaporization*; this released heat in turn reheats the air parcel to some extent, which slows the rate of cooling. The larger the moisture content, the lesser is the value of MALR.

2.3.1.5 Temperature inversions and isothermal layers. If the lapse rate changes sign from its usual sign of the lapse rate at any layer, it is called *temperature inversion* or simply *inversion* at that layer. For example, if the lapse rate in troposphere is negative (instead of usually being positive) at any layer, it will be called temperature inversion at that layer. In other words, if the temperature increases (instead of usually decreasing) at any layer in the troposphere, the layer is said to have undergone temperature inversion. If the temperature inversion takes place near the surface, it is called surface inversion. Similarly, if the temperature inversion takes place away from the Earth's surface, it is called upper layer inversion. Figure 2.2a shows the surface inversion, and Fig. 2.2b shows both the surface and upper layer inversions. If the temperature remains constant with altitude, as shown in Fig. 2.2c, it is called the isothermal layer.

Temperature inversions occur frequently in the atmosphere, but are generally confined to comparatively thin layers (about less than 2 km thick) in the

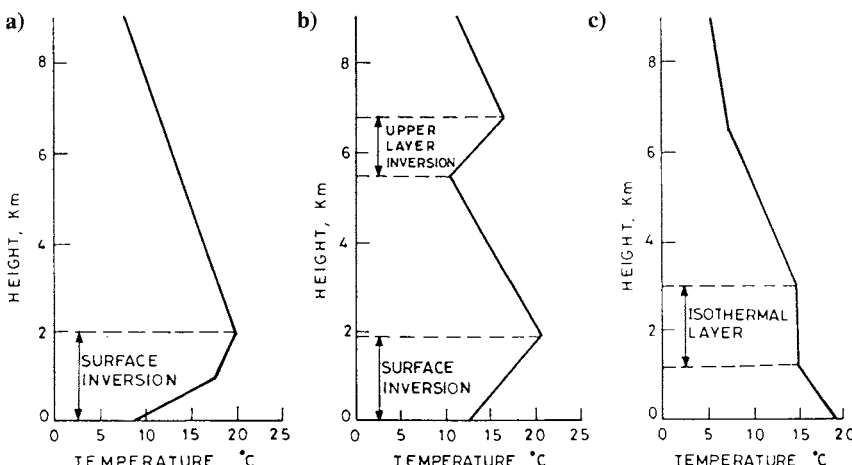


Fig. 2.2 Temperature inversions and isothermal layers: a) surface inversion, b) surface and upper-layer inversions, and c) isothermal layer.

troposphere. Temperature inversions are formed by the advection of warm air over cold air, over the cold Earth's surface, vertical descending currents, or by clouds. Temperature inversions are important in deciding the stability of the atmosphere.

2.3.2 Atmospheric Pressure

Knowledge of atmospheric pressure is important to pilots in determining altitude, understanding the functioning of altimeters, and forecasting the weather.

2.3.2.1 Pressure and its significance to flying. The pressure at any point in the atmosphere is the weight of the air column, of unit cross-sectional area directly above it, up to the top of the atmosphere. It is also called *barometric pressure* because it is usually measured by a mercury barometer. In aviation meteorology, the pressure is commonly measured in inches or millimeters of mercury but expressed in millibars where, $1 \text{ mb} = 1000 \text{ dyne/cm}^2 = 100 \text{ N/m}^2 = 0.07501 \text{ cm Hg}$. In FPS and SI systems, it is expressed as lb/ft^2 and N/m^2 , respectively. The sea level pressure in the atmosphere generally varies from 950 mb (about 28 in. Hg) to 1050 mb (31 in. Hg). The standard atmosphere sea level pressure is 1013.25 mb, 29.92 in. (760 mm) of Hg, 14.7 lb/in.^2 , or $1.013 \times 10^5 \text{ N/m}^2$ at 15°C of air temperature.

The winds move from the higher- to the lower-pressure side. The pressure distribution in the atmosphere controls the winds, which are of great importance to a pilot in planning cross-country flights. The aircraft altimeters are operated by atmospheric pressure and they must be properly set to obtain correct readings of altitude. Pressure maps are drawn at meteorological stations indicating isobars, high and low pressures, and pressure systems. These maps help to forecast weather to assist pilots.

2.3.2.2 Isobar and pressure gradient. An *isobar* is a locus of points in the horizontal plane at which barometric pressure of the atmosphere has the same constant value. An isobar is therefore a plane curve that is marked by the numerical value of its constant pressure in millibars. A pressure map contains many such lines. These lines are drawn on the map at 4-mb intervals, above and below the value of 1000 mb. They never cross each other, and form themselves into distinct areas of high and low pressures. Two different sets of isobars of a pressure map are shown in Fig. 2.3; one set encloses the high-pressure region, marked H, and the other set contains the low-pressure region, marked L.

The speed of winds depend on pressure gradient. The *pressure gradient* is defined as the rate of change of pressure with distance which is measured at right angles to the isobars. More concentrated lines of isobars, i.e., closely spaced isobars, indicate strong or steep pressure gradient across the isobars and therefore correspond to strong winds. The shallowly spaced isobars indicate a weak or flat pressure gradient and, therefore, the wind movement in such a region would be slow or light. If there exists only pressure gradient force, the wind direction would be normal to the isobars as shown by an arrow in Fig. 2.3. But due to the presence of other forces, the wind direction is inclined to an isobar.

2.3.2.3 Pressure systems. A pressure map containing isobars also shows regions of high pressure, ridge, trough, and col. These define pressure systems that are also known as pressure patterns. Since the winds are the result of these

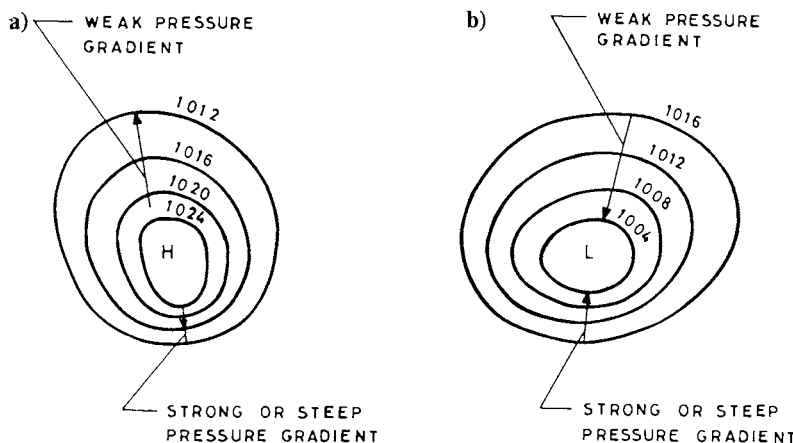


Fig. 2.3 Isobars and pressure gradients: a) high-pressure center and b) low-pressure center.

pressure systems, the wind and weather patterns can be better understood if we know more about the pressure systems.

2.3.2.3.1 Low-pressure and high-pressure regions. These regions are shown in Figs. 2.3, 2.4, and 2.5. The low- and high-pressure regions are marked by the letters L and H, respectively, as is the general practice in constructing a pressure map. The regions of low pressure are called cyclones, depressions, “valleys” of air, or simply lows. The low-pressure region has the lowest pressure at its center. A deep low has more concentrated isobar lines and large pressure gradients as in the case of a tornado. The depressions seldom stay long in one place but generally move in an easterly direction, i.e., their drift is generally toward the northeast or southeast. Their average rate of movement can be about 700 km (500 miles) per day in summer and 1125 km (700 miles) per day in winter. The drop in pressure makes weather windy, cloudy, and rainy. A low may cover a very small region which may be just recognized or it may extend across half a continent.

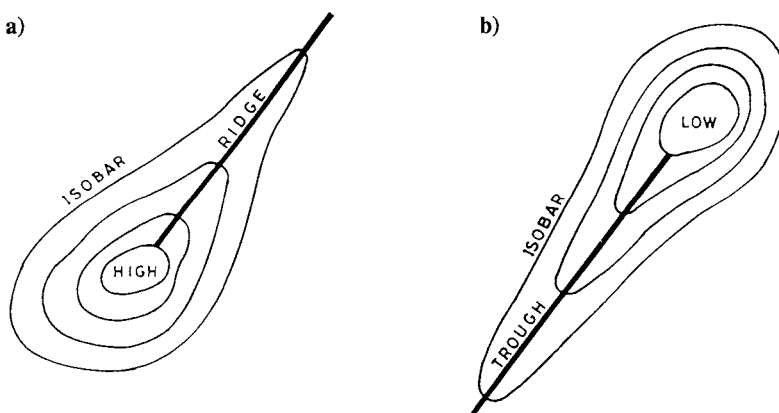


Fig. 2.4 Ridge and trough: a) high-pressure ridge and b) low-pressure trough.

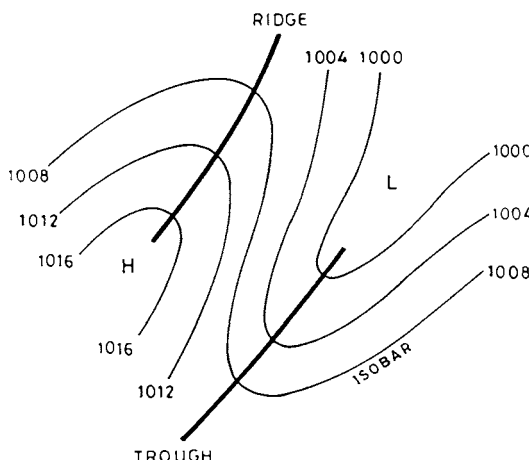


Fig. 2.5 Pressure system.

The high-pressure regions are called anticyclones, "hills" of air, or simply "highs." The highest pressure is at the center of the "high" and it decreases toward the outside. The "highs" move much more slowly across the country than depressions, and occasionally remain almost stationary for days at a time. The "high" brings usually fine, clear, and bright weather with moderately cool breezes.

2.3.2.3.2 Ridge, trough, and col. The high-pressure ridge or simply ridge is the thin elongated area of relatively high pressure in the atmosphere as shown by thick solid lines in Figs. 2.4a and 2.5. It is called a ridge because the pressure at any station on it is higher than that on its three sides, but lower than the fourth side (toward the high-pressure region). The word *ridge* means a long narrow top region, crest, or a narrow elevation. The ridge is also called a "wedge."

The low-pressure trough, or simply trough, is an elongated area of relatively low pressure, as shown by thick solid lines in Figs. 2.4b and 2.5. The word *trough* means a long narrow depression, a channel, or elongated U- or V-shaped area of low pressure. It is called a trough because at any station on the trough the pressure is lower than that on its three sides, but higher than the fourth side (toward the low-pressure region). A *col* is the saddleback-shaped area between two high- and two low-pressure regions. Cols may be regarded as regions of undependable weather.

2.3.2.4 Pressure tendency (barometric tendency). Meteorological stations observe not only the barometric pressure but also its tendency or behavior during the past given time (usually 3 h) immediately preceding the observation. This is called the pressure tendency or barometric tendency. It consists of 1) observing the total amount of change in barometric pressure, and 2) observing the nature or type of change in the barometric pressure. The second point shows how the change has occurred. For example, if the total change in the barometric pressure rises by 0.6 mb, it can be linear rise, or initial rise followed by fall, or initial fall then rise, etc., in such a way that finally a total rise of 0.6 mb is observed in the barometric pressure. The pressure tendency has a major role in weather forecasting. It helps us to understand the cause of weather change at a particular place. Generally, if the pressure drops, the weather may be windy, cloudy, and rainy. On the other hand, if the pressure rises, the weather may be clear and sunny.

2.3.2.5 Pressure aloft. The pressure is maximum at sea level and decreases with the increase in altitude. A rule of thumb valid for the lower parts of the troposphere is that, for every increase of altitude of 27 ft (8.2 m) there will be drop in pressure of 1 mb. At altitudes of 5, 10, and 20 km the pressures are, respectively, about 1/2, 1/4, and 1/20 of the sea-level pressure. The pressure decreases less and less slowly with the increase in altitude. The pressure of cold and heavy air decreases more rapidly with altitude than that of warm and light air. The pressure maps are provided for different pressure altitudes because pressure systems change with altitude. That is, the isobar contours and the regions of high pressure, low pressure, ridge, trough, and col can be quite different at different altitudes.

2.3.2.6 Station pressure, sea-level pressure, and altimeter setting. The *station pressure* is the reading of barometric pressure at the observing station. The higher the elevation (altitude) of the observing station, the lesser is the station pressure. To be consistent, each observing station translates its reading in terms of standard atmosphere sea level pressure which is usually reported in millibars.

The altimeter reading corresponds to standard atmospheric pressure. At sea level, the altimeter reading differs slightly from the ambient sea level pressure because the standard sea level pressure corresponds to 15°C. When correctly set, the altimeter then reads the true elevation of the airport at which the aircraft is parked. If the pilot does not know the altimeter setting but knows the elevation of the airport at which it is parked, he or she can enter the correct elevation on the dial and also get the correct altimeter setting. The altimeter setting is reported in inches of mercury (in. Hg).

2.3.2.7 Pressure pattern flying. Winds circulate anticlockwise around low-pressure regions, and clockwise around high-pressure regions. An experienced pilot can often take advantage of such pressure patterns so that the tail winds are available to him for longer duration. This kind of flight is known as the *minimal flight path* or the *least-time track*. Although this will not be the shortest distance, it may result in the shortest time between the two given stations. The pressure pattern flying technique is commonly practiced by birds.

2.3.3 Atmospheric Density

Air density is an invisible physical quantity that cannot be directly sensed by a human body. It is, however, a most important quantity in aircraft performance.

2.3.3.1 Density and its significance to flying. The density of atmospheric air at any given point is known as its mass per unit volume. Atmospheric air density is directly proportional to pressure and inversely proportional to absolute temperature. In the lower parts of the troposphere a 3°C rise in temperature corresponds to a 1% decrease in density, and vice versa. The density of standard atmosphere at sea level is 1.225 kg/m^3 or $0.002377 \text{ slug/ft}^3$. Atmospheric density decreases with increase in altitude, and its decrease is faster near the Earth than at higher altitudes. This is because, the air being compressible, more air mass is confined near the Earth's surface. At the altitudes of 5, 10, and 20 km the air density is about 60%, 35%, and 7%, respectively, of its value at sea level. The lines of constant density shown in a meteorological map are called *isosteric*.

The density also varies slightly with the change of place horizontally and with time. Density increases as one moves from the equator toward the poles, at any

altitude up to 8 km. At the altitude of 8 km, the density does not change with latitude. Above 8 km the density decreases from the equator toward the poles.

Aircraft performance, engine thrust or power output, and airspeed indicator readings are affected by the density of air. Aerodynamic forces are directly proportional to the density of the air. A given aircraft needs to fly faster to maintain a given altitude if the air density decreases. In fact, every aspect of aircraft operation—takeoff, climb, cruise, turn, descent, and landing—depends on the density of the air through which the aircraft is moving. Aircraft maneuvering limitations and ceiling also depend on air density. Propeller blades will produce less thrust in air of reduced density. Lower air density means a reduction in engine thrust, coincident with the need for higher takeoff and landing airspeeds, requiring a longer takeoff run. Alternatively, if a limited length of takeoff run is available, a lower density may necessitate a reduction in payload to meet the takeoff performance requirement.

There is no instrument on the flight deck panel that directly indicates the density of the atmosphere through which the aircraft is flying. The density can, however, be calculated after obtaining the measurements of the temperature and pressure of the atmosphere. The hazard of low air density must be guarded against, especially at unfamiliar airfields, at high altitudes, on hot days. The problem is further accentuated if the day is also humid, because humidity reduces the density of dry air.

2.3.3.2 Density of moist air. In the troposphere, air is generally moist (humid); this humidity is due to the presence of water vapor. The amount of water vapor present in the air varies with place and time. For air, water vapor, or any other gas, the density is given by the equation of state

$$p = \rho RT \quad \text{or} \quad \rho = p/(RT) \quad (2.1)$$

where R is the gas constant whose value depends upon the gas and the system of unit used. In SI units, the value of R in dry air, R_{da} , and in the presence of water vapor, R_{wv} , are given by

$$R_{da} = 287 \text{ m}^2/(\text{s}^2\text{K}) \quad \text{and} \quad R_{wv} = 459.2 \text{ m}^2/(\text{s}^2\text{K})$$

Note that $R_{wv} = (8/5)R_{da}$. For moist air the value of R is between 287 and 459.2 $\text{m}^2/(\text{s}^2\text{K})$ depending on the amount of water vapor present in the air. It is, however, not necessary to know the value of R every time when correspondingly different amounts of water vapor exist in the air. This is because the density of moist air can be obtained by adding the densities of dry air and water vapor as shown below.

If e is the vapor pressure at the point where the ambient atmospheric pressure is p , the pressure of dry air at that point would be $p - e$. Applying Eq. (2.1) to the dry air and the water vapor, respectively, the following two relations are obtained:

$$\rho_{da} = (p - e)/(R_{da}T) \quad \text{and} \quad \rho_{wv} = e/(R_{wv}T) = (5/8)e/(R_{da}T)$$

When one adds the above two equations, the density of air that contains water vapor is obtained as

$$\rho = \rho_{da} + \rho_{wv} = \frac{(p - e)}{R_{da}T} + \frac{(5/8)e}{R_{da}T} = \frac{p - (3/8)e}{R_{da}T}$$

The effect of e assumes importance in very moist tropical zones. In most practical cases, the effect of e is negligible, the above equation need not be

invoked, and one can continue to use Eq. (2.1) where $R = R_{da}$, the gas constant of dry air.

2.4 Winds

Different types of winds under different conditions move over the Earth. A brief account of these winds is presented here.

2.4.1 The Nature of Wind

Air in horizontal motion is called *wind*. Air moving vertically is referred to as *air current*. The time and length scales of winds are much greater than the vertical air currents. Wind has inexhaustible energy that creates no pollution. The utility of wind and also its destructive power are too well known. Winds are caused by the differences in pressures existing in the atmosphere, because the wind blows from higher- to lower-pressure regions. The pressure difference itself is created by differential solar heating, Earth's rotation, and the differences in heat absorption power of different terrains and sea. The higher the differential heating, the larger is the pressure difference and hence the faster will be the speed at which the wind blows. The speed and direction of wind varies with place and time. Also the wind velocities aloft may be quite different from those on the ground or at sea level. The wind speed may vary from nearly zero, as in calm conditions, to about 700 km/h, as in a tornado. Wind movements may be smooth, turbulent, unsteady, gusty, rotary, or a combination of these.

2.4.2 Forces Acting on Small Wind Element

The four basic forces that govern the horizontal motion of wind particles are due to pressure gradient, Coriolis, centripetal, and friction forces. The pressure gradient and friction are surface forces whereas Coriolis and centripetal are body forces acting on the small element. The pressure gradient force is by far the most important. In the absence of any other force, except the pressure gradient force, the air moves normal to isobars. Due to the presence of the other forces, the air motion is generally inclined to isobars; this inclination may even be up to 40 deg to isobars.

The Coriolis force was first mathematically described by the French professor, Gustave Gaspard de Coriolis,² who first described it in 1835. It is also commonly known as *geostrophic force* in meteorology. The Coriolis force arises due to the Earth's rotation which deflects the motion of air particles. This is called *geostrophic deflection*, and is at a maximum at the poles and vanishes at the equator. The law of geostrophic deflection states that "Any body moving over the Earth tends to be deflected to the right in the northern hemisphere and to the left in the southern hemisphere." The law of Buys-Ballot, called the law of storms,³ similarly states that "In the northern hemisphere, the lower pressure is always to the left and the higher pressure to the right, when looking downward; in the southern hemisphere the reverse holds good."

The centripetal force, also called the *cyclostrophic force*, arises only when the streamlines of wind are curved. It is more pronounced in whirling motion of the wind. It is absent in the stratosphere because there the wind moves straight and horizontally. The friction force is due to viscosity of the air. Viscosity retards the motion of air and produces windshear, turbulence, and vortices. The air velocity

distribution across the Earth changes because of friction; such change will be felt up to about 1000 m height for an average terrain.

2.4.3 Global Wind Circulation

Wind circulation refers to the large-scale winds moving over the Earth due to unequal distribution of the sun's energy on the Earth. This movement is continuous throughout the entire atmosphere. The wind circulation in the northern hemisphere is similar to that in the southern hemisphere. The nature of this circulation, and the different kinds of large-scale winds it produces, are explained here.

2.4.3.1 Three-cell theory of wind circulation. A three-cell theory of air circulation has been propounded according to which both the northern and southern hemispheres are divided into three different cells of equal spacing in latitudes between 0° (equator) and 90° (poles) as shown in Fig. 2.6a. Thus, on each hemisphere, the first cell is between the equator and 30° latitude, the second cell between 30° and 60° latitudes, and the third cell between 60° latitude and the pole; the regions near the north and south poles are called the arctic and antarctic regions, respectively. Each cell is bounded by high-pressure and low-pressure belts as shown in the figure. In the first cell lies the *tropic of Cancer* ($23^{\circ} 28'$ N) and the *tropic of Capricorn* ($23^{\circ} 28'$ S) lines. Being a tropical (very hot) region, hottest along the equator, it is also called a tropical zone in the lower parts of the troposphere. There exists a low-pressure belt along the equator and high-pressure belt along 30° latitude, both in the northern and southern hemispheres. The second cell near the Earth has the temperature zone of moderate climate which extends up to 60° latitude where again a low-pressure belt exists in both the hemispheres. As one approaches close to the poles in the third cell, it is very cold and the pressure increases.

The hot atmospheric air along the equator rises up and moves, toward north in the northern hemisphere and south in the southern hemisphere, until it has reached an altitude of about 60,000 ft (18,288 m). Thereafter, some part of it returns back to the Earth and strikes it at about 30° latitude where the pressure rises as shown in Fig. 2.6a. The other part of the air drifts toward the poles along the path A_N , B_N , C_N in the northern latitude and along A_S , B_S , C_S in the southern latitude. While moving toward the poles, they lose altitude to about 25,000 ft (7620 m) and finally move toward the Earth at the poles where again the pressure rises.

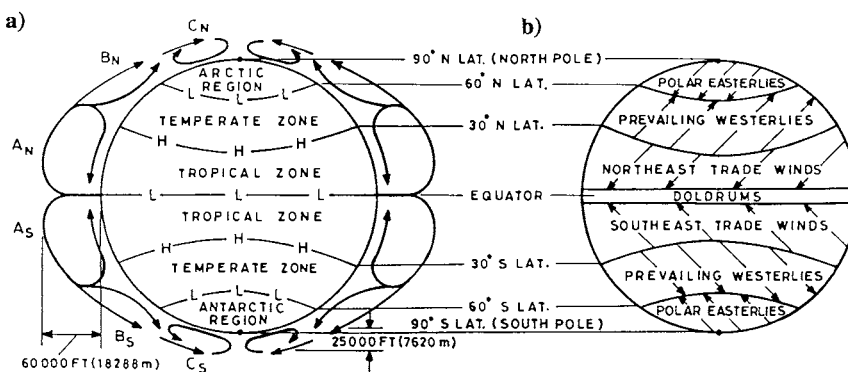


Fig. 2.6 Global wind circulation: a) three-cell pattern and b) general circulation.

This global movement of atmospheric air gives rise to winds which are named doldrums, trade winds, prevailing westerlies, and polar easterlies, as shown in Fig. 2.6b and explained below.

2.4.3.2 Doldrums. The doldrums are calm and baffling winds prevailing near the equator where low pressure exists. The word doldrum is probably the distortion of the word *dull*. The wind is either stagnant or wanders very slowly here as the gradients of pressure are undecided or very weak.

2.4.3.3 Trade winds. The trade winds blow in the tropical zone from the high-pressure subtropical belt to the equator. These are called northeast trade winds in the northern hemisphere because they come from the northeast direction. Similarly, the southern hemisphere has southeast trade winds. These trade winds blow approximately at constant speeds for days or even weeks without much variation in direction and they are rarely disturbed by cyclonic storms.

2.4.3.4 Prevailing westerlies. The westerlies are observed in the temperate zone. They blow southwesterly in the northern hemisphere and northwesterly in the southern hemisphere. These winds are also called the prevailing westerlies of the temperate zones because of their persistence in one direction more than the other. These winds are not as steady as the trade winds of the tropical zone.

2.4.3.5 Polar easterlies. The polar easterlies are extremely cold winds blowing almost throughout the year in the form of storms. In general, they are easterly winds over both the arctic region (north pole) and antarctic region (south pole). The cold air masses of the polar regions and the hot air masses of the tropics push against each other, in alternating waves. The intermixing region of cold and hot air masses is thus continuously changing. These changes influence the weather even in the middle latitudes.

2.4.4 Local Winds

Comparatively small-scale local winds also exist over the Earth. These winds are not continuously present with respect to time or place. Some of these winds may be quite pleasant while others can cause much destruction. The different types of local winds are described below.

2.4.4.1 Seasonal winds. A well-known local seasonal wind is the *monsoon*. The name is derived from the Arabic word *manusim*, meaning season. Monsoons occur not only in India and Arabia but also in Australia, Chile, Spain, and other parts of the world in different seasons. Monsoons are due to unequal heating of land and sea which causes differences in pressures needed for the movement of winds. In India, monsoon winds arise during the month of June and are warm, moist, and rainy. The occurrence of the monsoon is often interrupted by tropical cyclonic storms, locally known as typhoons. There are yet many other types of seasonal winds which have different names⁴ in different regions, like *sirocco*, *simum*, *haboob*, *levante*, *maestro*, *gregale*, *khamsin*, *harmattan*, *shamal*, *seistan*, etc.

2.4.4.2 Sea and land breezes. Sea and land breezes are local winds that occur almost daily in coastal areas. On sunny days, the land gets heated more than the sea. This causes air to rise above the land and, thereby, the pressure decreases over the land. The air over the sea then moves toward the land as shown in Fig. 2.7a. This gives rise to the sea breeze, so called because it comes from the sea. During the night the reverse situation exists; the land is cooler than the sea and this causes the land breeze as shown in Fig. 2.7b. Land and sea breezes are more pronounced in summer than in winter, and they can be more clearly recognized in the tropical zones than at higher latitudes. The land breeze is usually gentle as compared to the sea breeze, which may penetrate as much as 30 km into the land mass. In coastal airports, all landing and takeoff operations of aircraft are made against sea breezes.

2.4.4.3 Mountain and valley breezes. The formation of mountain and valley breezes is similar to that of land and sea breezes. During sunny days the air along the mountain slopes is heated more than in the valley. This causes convection of air currents from the mountain and, therefore, the air from the surrounding valley moves toward the mountain. This leads to the formation of daytime valley breezes. During the night, the air along the slopes of the mountain is cooled more than in the valley, which gives rise to mountain breezes.

2.4.4.4 Fall winds. A wind blowing down the slope on the leeward side, or any wind having a strong downward component is called a fall wind or katabatic (which means “moving down”) wind. The *foehn* (or *föhn*), *chinook*, *bora*, *mistral*, etc., are some names of winds belonging to the class of fall winds. If the wind is hot and dry and moves down the slope on the leeward side, it is called a foehn. Its formation is due to humid and stable air; when forced to move up a mountain slope, this type of air cools and condenses to form clouds and rains. After crossing the mountain peaks when it descends the mountain slope, the atmospheric pressure increases, and the air becomes hot due to adiabatic compression. Thus, it becomes hot, dry air. When foehn winds blow, the temperature can be 10°C higher than usual. Foehn winds make snow melt earlier, reduce the yield of cereal and fruit crops by making them ripen earlier, and increase the likelihood of forest fires. In some parts of the world, the foehn is called the chinook.

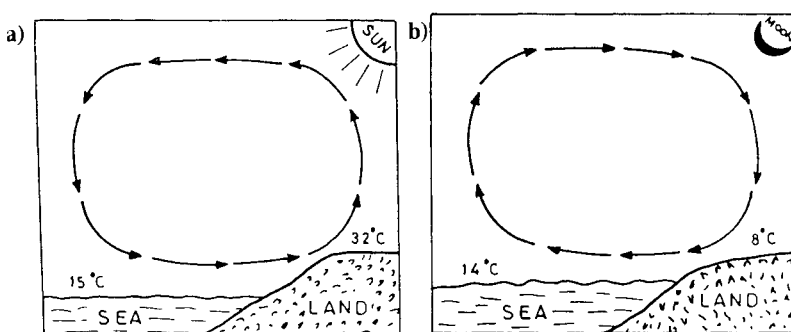


Fig. 2.7 Sea and land breezes: a) sea breeze during day and b) land breeze at night.

The bora is a quite different type of fall wind than foehn. A bora is a cold and fierce mountain wind moving down the leeward side of a mountain slope. When cold air is forced to move up a hill, it piles up on the peak of the hill and then rushes vigorously down the slope on the leeward side. This effect is further increased during long cold nights and in snow-covered mountains. The wind speed of the bora is very high, sometimes 100–150 km/h, and thus the bora can be regarded as a “cold air waterfall.” If the cold air is also dry, the bora is called the mistral.

2.4.4.5 Ravine, valley, and headland winds. The speed of winds is considerably increased when the oncoming winds have to pass through a narrow passage and the streamlines become closer. This is because the area of the oncoming wind passage decreases, causing the wind speed to increase. This is also referred to as the “funnel effect.” These situations arise due to topography of terrains usually found in ravines, valleys, and headlands. On certain occasions the wind speed may reach well over that of a gale.

2.4.4.6 Typhoon. A typhoon has strong cyclonic winds created by low-pressure regions due to convection currents in the atmosphere. It is known locally by various names, such as *cyclone*, *hurricane*, *baguio*, and *willy-willy*. In the case of a strong typhoon, the low-pressure region can reach below 900 mb which is about 10% lower than a standard atmosphere. A typhoon generally originates from the sea and occurs mostly in summer and autumn. The wind speeds are generally greater than 120 km/h, and produce heavy rainfall. The life of a typhoon is about 8 or 9 days on average and it may cover an area ranging from 150 to 800 km in diameter. The strong winds and heavy rains accompanying it for long periods of its life can cause serious damage to life, structures, trees, and communication. The most severe typhoon of the century occurred on November 12, 1970 in the Ganges delta north of the Bay of Bengal; it raised water surges up to 6 m high and about 3 lakhs (3×10^5) of people lost their lives. A typhoon has a central region with an average diameter of 20–30 km, which is called the “eye” of the typhoon. This “eye” is quite wonderful because despite all the activity of winds rushing furiously in spiral clouds around it, there is only gentle breeze and bright sunshine in the eye. The birds that are caught up in the typhoon always rush toward the eye for shelter.

2.4.4.7 Tornado. A tornado is also a cyclonic whirlwind but distinctly differs from a typhoon in size, duration, strength, and structure. Most tornadoes occur in the afternoon and are invariably associated with the occurrence of thunderstorm. A tornado is the most furious of all storms, with wind speed reaching even higher than 700 km/h. A tornado is much smaller in size than other storms, only about 100 to 1000 m in diameter, as compared to a typhoon. Its lifetime is also very small, mostly a quarter to one and a half hours, although occasionally it may exist for several hours. It travels with a medium speed of 50 to 100 km/h, similar to that of an automobile. It generally disappears after traveling about 1–5 km, but sometimes it may sweep over several hundred kilometers.

A tornado has amazing strength, which can cause enormous destruction. The United States is very vulnerable to tornadoes. In 1925 in the United States, a fierce tornado called Trister swept over 360 km at a speed of 100 km/h, killing 695 persons, wounding 2027 people, and causing a loss of property of about 40

million dollars. In Minnesota in 1931, a tornado lifted an 83-ton railway car with 117 passengers and placed it gently down in a gully at a distance of 20 m without hurting the passengers or the railway car. Sometimes a tornado may sweep up fish and shrimp from the sea, frogs from rivers, grain from barns, and then send them back down to the ground when the rain gushes, producing the interesting sight of fish rain, shrimp rain, frog rain, grain rain, etc.

A tornado has a very characteristic shape resembling a funnel hanging down in the mother body of thunderstorm clouds, or like an elephant trunk swinging in the sky. The lower part of this funnel or trunk swings up and down, sometimes touching or not touching the ground.

2.4.5 *Windshear*

Viscosity of air causes friction forces and wind-speed gradients in the atmosphere. These wind gradients across different layers are referred to as windshear, because the wind is sheared or torn. At ground level the wind speed is always zero but it increases as the distance from the ground increases. This can also be expressed by saying that the winds aloft are stronger than those near the ground. Above a certain height from the ground, called atmospheric boundary layer thickness, there is no more change in wind speed. The velocity gradient in the vertical plane is called vertical windshear, and similarly the velocity gradient in the horizontal plane is called horizontal windshear. Winds blowing in different, and even opposite, directions at the same place also form windshear. Windshear may cause turbulence, gust, and even loss of lift. Since the wind speed reduces near the ground, the aircraft experiences loss of lift during descent and landing. Windshear is commonly encountered by pilots near the ground during takeoff and landing. Windshear is further discussed in Sec. 19.7, of Chapter 19, Weather Hazards and Flying.

2.4.6 *Jet Streams*

Jet streams are the narrow bands of exceedingly high-speed winds that exist in higher altitudes near the tropopause. They encircle the entire hemisphere in a snakelike pattern. They shift location rapidly from day to day and with the seasons. The knowledge of jet stream is important to pilots who are planning long-range flights at high altitudes. Clear air turbulence is also associated with the jet stream. The nature of jet streams and flying through them is discussed in detail in Chapter 19.

2.5 Vertical Air Currents

The vertical movement of air is known as vertical air current or simply air current. These air currents are most important in carrying water vapor up in the sky. The air cools while ascending with the water vapor, so that the vapor condenses and becomes cloud. The ascending air is cooled adiabatically through expansion because some energy of the air parcel is utilized in the expansion process. The descending air is heated adiabatically through compression, because the density of the atmosphere increases with the decrease in altitude. There are various reasons such as thermal convection, mechanical convection, and convergence which produce vertical air currents.

This page intentionally left blank

This page intentionally left blank

The relative humidity of saturated air is 100%. Air is more humid or damp and its relative humidity is also higher in the rainy season than in winter. Relative humidity decreases with increasing temperature.

The relative humidity indicates how much water vapor the air can still hold. Relative humidity of 50% means that air can still hold as much water vapor as it already has. The relative humidity and dew point are obtained from the readings of wet and dry bulb thermometers. The relative humidity is a direct indication to a pilot of the potentiality of the atmosphere to form weather as cloud, rain, and icing if condensation occurs. A saturated atmosphere is like a loaded gun which can easily be triggered at any time.

2.7 Processes of Evaporation, Condensation, Sublimation, and Freezing

The interchange in the different states of water vapor is carried out by the fundamental processes of evaporation, condensation, sublimation, and freezing prevailing in the atmosphere.

2.7.1 *Evaporation*

In evaporation, water (or any other liquid) changes from liquid state to vapor state due to escape of water (or liquid) molecules as vapor in air from the free surface of water (or liquid). If the air is saturated with water vapor, there will be no net transfer of molecules between air and the free water surface. During the process of evaporation the heat is absorbed by the water as latent heat of vaporization, which is taken from the neighboring regions. Thus, surfaces in immediate contact with the free water surface get cooled. Therefore, evaporation is a cooling process. This explains why we feel cool and comfortable when our perspiring bodies in heat are exposed to the fan. In saturated air, water ceases to evaporate and wet clothes would not dry.

2.7.2 *Condensation*

The process of condensation is opposite to that of evaporation, because during condensation water vapor is transformed back to the water droplets. The condensation of pure water vapor, completely devoid of foreign particles, takes place in highly supersaturated air, requiring seven times as much water vapor pressure as is required for saturation at a given temperature. But the presence of extremely minute foreign particles in the atmosphere causes condensation even when air is close to saturation. Air usually contains a wide variety of airborne foreign particles (aerosols) of varying size with their radii ranging from 10^{-3} to 10μ . These minute particles are always present in the atmosphere in the form of smoke, dust, ash, salt, chemical particles, and water particles which act as condensation nuclei. The water vapor condenses to liquid around these particles even when water vapor is close to saturation. Some of the foreign particles that have a close affinity for water vapor are called hygroscopic particles, because condensation on them begins even before the air has become saturated. The nonhygroscopic particles require some degree of supersaturated air before acting as the centers of condensation nuclei.

During condensation heat is released from the water vapor into the air, and is called the latent heat of condensation. Therefore, condensation heats the surrounding air or it may lessen the cooling due to other processes in the air; this explains

why the inside of the clouds may be often warmer as compared to the surrounding regions. The release of this heat energy causes turbulence, thunderstorms, and the destructive forces found in hurricanes.

2.7.3 Sublimation

The process of sublimation is the direct change of water vapor (or gas) into ice crystals (or solid ice), or vice versa, without becoming the intermediate liquid state. The sublimation of water vapor takes place only below 0°C , and water vapor must be saturated before solidification into ice crystals. Heat is liberated to neighboring regions when solidification takes place whereas heat is absorbed when vaporization occurs.

2.7.4 Freezing

Freezing a large quantity of water, say water in a cup, is quite different from freezing water droplets of a cloud. The water of the cup can be frozen by cooling it a little below 0°C , whereas the droplet may often require a considerably lower temperature for freezing. Individual droplets of water will freeze at the temperature of -40°C without the aid of any freezing nuclei. Similar to condensation of water vapor around a condensation nuclei, the freezing process is also considerably facilitated by freezing nuclei around which water droplets may freeze. Freezing nuclei may be of different kinds and they number far less in the atmosphere than condensation nuclei. Some of the names⁶ of freezing nuclei are volcanic ash, biotite, silver iodide, ice crystal, etc. Different nuclei require different amounts of supercooling for water drops to freeze.

If the efficiency of a freezing nuclei is judged by the amount of supercooling of water necessary before it freezes, silver iodide is very efficient because water freezes on it at -4°C . The ideal freezing nuclei are the ice crystals themselves because water just below 0°C freezes on them and, therefore, requires no appreciable supercooling. The number of freezing nuclei increases considerably as the temperature decreases. For example, the number of effective freezing nuclei at -30°C may be 100 times as great as that required at -20°C . Below 0°C the vapor pressure over water is greater than that over ice, the difference being greatest between about -5° and -20°C . If both water droplets and ice crystals exist in a cloud whose temperatures are below the freezing point, the two cannot exist in equilibrium. Therefore, water droplets will evaporate making air supersaturated for ice so that water vapor condenses on ice crystals. When a supercooled water drop collides with an ice crystal, it at once freezes on the latter, imprisoning a little air. Thus, the droplets evaporate and the crystals of ice grow in size and begin to fall. The rising vertical air currents in the cloud may return the ice particles back to the top of the cloud. This process, repeated several times, produces large hailstones.

2.8 Moisture and Precipitation

Moisture and precipitation are important ingredients for different weather formations. They contaminate the runway and aircraft surfaces, and may produce weather hazards to flying.

2.8.1 **Moisture**

Moisture is a common name given to the various forms of water vapor. In the atmosphere it exists in three different states as solid, liquid, and gas. As a solid it is found in the form of frost, ice crystals, sleet, rime, snow, or hail. As a liquid it exists as water particles in dew, fog, cloud, drizzle, and rain. In a gaseous state it exists as invisible water vapor making the atmosphere humid or moist. Thick fog, icing, and thunderous clouds are some of the well-known hazards to flying produced by moisture.

2.8.2 **Precipitation**

Precipitation is a general name used for all types of falling moisture. That is, rain, snow, hail, sleet, etc. all are called precipitation. The accretion on objects in freezing temperatures is also called precipitation. For precipitation to occur it is necessary that the air must be saturated with water vapor and that condensation take place. Saturation is affected either by cooling or increasing the water vapor. Condensation is affected and accentuated by airborne particles in the atmosphere. Rain and drizzle are called liquid precipitation, whereas snow, hail, and other ice crystals are called freezing precipitation.

Any type of precipitation falling from clouds, but evaporating before reaching the Earth's surface, is called *virga*.

2.9 Dew, Frost, Fog, and Mist

Dew, fog, and mist are water particles, whereas frost contains ice particles. Dew is formed on plants, leaves, and cold surfaces, whereas fog and mist are formed in the atmosphere near the ground or ocean. They contaminate the runway and the surface of the aircraft, and deteriorate visibility through the atmosphere.

2.9.1 **Dew**

The condensation of saturated air in the immediate contact with a cold surface below the dew point appears as tiny water droplets known as dew on the Earth's surface. Dew does not fall from the atmosphere above the Earth. On cold nights dew is found deposited on grass or leaves of trees as tiny glistening droplets. During the daytime, the plants give out moisture making the surrounding air more humid, whereas during nights they lose heat quickly and get cooler than the dew point, so that dew is formed on leaves and plants. On the other hand, dry land and buildings absorb more heat and give it up slowly during the night so that they do not cool below the dew point and, therefore, no dew is formed on them.

A clear sky, still air, and moist soil favor the formation of dew. During daytime the heat of the sun is absorbed by the Earth which radiates it out during night. If the sky is not clear, the clouds will reflect the heat rays back to the Earth and evaporate the dew as soon as it is formed. Wind blowing past the leaves increases the rate of evaporation, which does not encourage the formation of dew.

2.9.2 **Frost**

On cool nights ice crystals formed directly from sublimation of water vapor and deposited on leaves is called *frost*. Frost is formed when the dew point is below the

freezing point of water. It is harmful to vegetation. Sometimes dew also freezes, but frozen dew is transparent whereas frost is opaque.

Frost occurs frequently on the metallic surfaces of automobiles or aircraft exposed to the cold atmosphere. The frost on the aircraft must be removed before takeoff because it causes considerable surface roughness which increases drag and can increase the stalling speed by about 10%. Frost is generally not formed during flight.

2.9.3 Fog and Mist

Fog is stratus cloud in contact with the ground. Fog is formed due to radiation cooling of the Earth. That is, the Earth radiates heat without heating the atmosphere near the ground. Therefore, the Earth cools below the dew point of the surrounding air. This cooling gets distributed to greater heights above the ground by the irregular and stirring motion of the air. Thus, when the air is damp and very cold, the moisture condenses into minute water droplets to form fog on the ground which may be several meters thick. Fog is also similarly formed on mountains, valleys, lakes, and the sea. Fog creates haziness to vision which can be a dangerous hazard to pilots because of the loss of visibility. If the terminal airport has thick fog, the pilot may need to go to an alternative airport for landing.

A mixture of smoke and fog is called *smog*. If the haziness is solely due to dust or smoke in the air, it is known as *dry fog* which may be found in a desert, dusty area, or in an industrial area emitting smoke.

There is no essential difference between mist and fog except for the degree of denseness. A very mild or thin fog is called *mist*. According to international agreement, if the visibility is less than 1 km it is known as fog, whereas mist produces visibility of more than 1 km.

2.10 Clouds

The knowledge of clouds, and their formation, classification, and significance, is particularly important to pilots in the forecasting of weather and the planning, and conducting of safe flights. Clouds give birth to rains, icing, lightning, and thunderstorms. Certain types of clouds help soaring while some others cause much inconvenience that may even damage the flight.

2.10.1 Cloud and Its Formation

A *cloud* is a visible aggregate accumulation of countless millions of minute particles of water or ice, or both, in the free atmosphere. This is due to condensation and sublimation of excess water vapor at certain regions in the atmosphere. In the initial development of a cloud the water droplets are very small, around 0.01 mm in diameter. Within the cloud these droplets grow in size so that they eventually become big enough to fall from the cloud as precipitation. Clouds are easily visible in the sky. If the base of fog is lifted 50 ft (15.24 m) or more above the ground or water surface, it is designated a cloud. The type of clouds and their movements indicate wind speed, direction, and weather condition that is likely to exist for some time ahead. The color of clouds depends on the size and concentration of component particles of clouds, the luminosity and color of sunlight or moonlight falling on the clouds, and the relative position of the light source (sun or moon), the cloud, and the observer. The brightness of a cloud depends on the reflection,

scattering, and transmission of light by the cloud particles. The shape of the cloud is guided by the thermal processes inside the cloud and the winds prevailing near the cloud.

Water vapor is the basic material source of cloud formation and it exists in abundance above ocean, river, marshy land, and vegetation. The three necessary conditions that need to be satisfied for cloud formation are 1) the existence of sufficient water vapor so that the air is close to saturation, 2) the existence of cooling process for air to be cooled below its dew point, and 3) the existence of condensation or sublimation for water vapor to become water or ice particles. The first and the third conditions have already been discussed in Secs. 2.6 and 2.7, respectively. The second condition, cooling of air, is obtained by the vertical air currents explained in Sec. 2.5. These vertical air currents expand adiabatically while ascending and as temperature decreases. The air gets further cooled below its dew point by mixing with the low-temperature atmosphere at high altitudes. The cloud is also formed if the base of the fog rises to heights above 50 ft due to heating of the Earth when the sun rises in the morning.

2.10.2 Nomenclature of Clouds

Clouds are generally named according to their outer appearance, behavior, or the height of their bases. Clouds were named by a London pharmacist, Luke Howard, in 1803, using Latin words. These names have been internationally agreed upon by meteorologists and are generally based on the outer appearances of clouds. A brief account of clouds with their photographs is given in Refs. 6 and 7. A very exhaustive account of clouds is presented in the *International Cloud Atlas* which was published in 1957 by the World Meteorological Organization in two volumes⁸ with colored pictures. For pilots the knowledge of certain clouds of frequent occurrence is essential and most of them are mentioned in the following paragraphs. The three main classes of clouds are cirrus, stratus, and cumulus clouds as shown in Fig. 2.8. Most of the other names of clouds are derived from these basic names.

2.10.2.1 Cirrus clouds. The Latin word *cirrus* means tufts of horse hair or bird feathers. These clouds have a white fibrous structure appearing as tufts, streaks, and tails as shown in Fig. 2.8a. These clouds are also known as mares' tails or cat's whiskers. The cirrus cloud is often abbreviated as Ci cloud. These are high clouds whose base is generally formed above 6 km where the temperature is below -25°C . Hence these clouds consist of tiny ice crystals which are responsible for the halos sometimes seen around the sun or moon. The cirrus clouds are indicative of fair and settled weather.

2.10.2.2 Stratus clouds. The Latin word *stratus*, abbreviated as St, stands for something spread out, extended, or flattened out. It refers to a wide extended

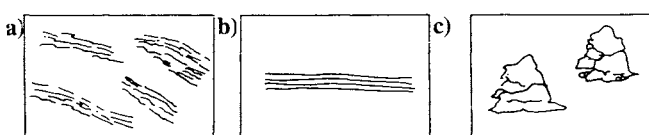


Fig. 2.8 Main classes of clouds: a) cirrus, b) stratus, c) cumulus.

horizontal sheet of clouds as shown in Fig. 2.8b. They are, therefore, also called sheet or layer clouds, although they may be several tens of meters thick. They resemble fog but do not rest on the ground and, unlike fog, they may persist for several days. These are low-level clouds having their bases usually within 300 to 600 m above the ground in a temperature warmer than -5°C . They are produced by slow, widespread lifting of damp air formed near the ground. Precipitation from them is normally in the form of light drizzle or closely spaced small water droplets.

The term *stratiform cloud* is applied to all types of clouds that are arranged in unbroken horizontal layers or sheets.

2.10.2.3 Cumulus clouds. The Latin word *cumulus* means an accumulation, pile, or heap. These clouds have upper surfaces bulging in dome-shaped rounded heaps while the base is nearly horizontal, as shown in Fig. 2.8c. These are sometimes also called heap, wool-pack, or cauliflower clouds because of their appearance when viewed from the side. The cumulus cloud is abbreviated as Cu cloud. These clouds are very thick, extending to several kilometers with vertical development. The base of these clouds is generally situated at altitudes ranging from 600 to 6000 m. These clouds are produced by local vertical air currents of about 1–5 m/s. The air inside the cloud and around it is turbulent. Cumulus clouds are also the source of the heaviest deposits of icing in the atmosphere.

The term *cumuliform cloud* is given to all types of dome-shaped clouds having protruding upper surfaces with generally horizontal bases. These clouds are separated from one another by clear spaces.

2.10.2.4 Cirrostratus, cirrocumulus, and stratocumulus clouds. Most frequently these clouds have mixed appearances and it becomes difficult to classify them as one of the above three basic clouds. Therefore, combined names have been assigned. For example, a cloud that appears both like cirrus and stratus clouds is referred to as a *cirrostratus cloud* and abbreviated as Cs. The cirrostratus is a very thin, high, sheet cloud, through which the sun or moon is invisible, producing a “halo” effect. The Cs cloud is indicative of an approaching warm front or occlusion and, therefore, of deteriorating weather. Similarly, there exist *cirrocumulus* and *stratocumulus clouds*, which are abbreviated as Cc and Sc clouds, respectively. Cirrocumulus clouds are often called “mackerel sky” and give little indication of the future weather conditions. In stratocumulus clouds icing is most frequently formed in winter.

2.10.2.5 Altostratus and altocumulus clouds. If stratus and cumulus clouds are formed at comparatively high altitudes, the prefix “alto” derived from the Latin word *altum*, is prefixed to the name. Thus, there are *altostratus clouds* and *altocumulus clouds*, which are abbreviated as As and Ac, respectively, and these are formed in the middle of the troposphere. The altostratus cloud is a thick veil of grey clouds that generally covers the whole sky. Some light rain or snow may fall from thick altostratus cloud. Altocumulus clouds form a layer or a series of patches of rounded masses of clouds and they are of little value as an indication of future weather development.

2.10.2.6 Fractostratus, fractocumulus, and fractonimbus clouds. Many times clouds are observed in fragments and they are specified by adding the word “fracto” before their names. The fragments of stratus cloud would be called *fractostratus cloud* and abbreviated as Fs cloud. Similarly, there are *fractocumulus clouds* and *fractonimbus clouds*, which are abbreviated as Fc and Fn clouds, respectively.

2.10.2.7 Nimbostratus and cumulonimbus clouds. Certain clouds precipitate into rains and they are classified by adding the Latin word *nimbus* (or *nimbo*), meaning rainy clouds. Thus there are *nimbostratus* and *cumulonimbus clouds*, which are abbreviated as Ns and Cb clouds, respectively. The cumulonimbus are dark grey rainy clouds close to the ground with no characteristic shapes.

Cumulonimbus clouds are another type of rainy clouds which are most hazardous to pilots. This type of cloud produces thunderstorms, lightning, heavy rain, hail, turbulence, and gusty winds. The cloud may be several kilometers thick with strong vertical currents ranging from 3 to 30 m/s inside the cloud. The top of the cloud spreads horizontally like an anvil containing ice with temperatures as cold as -50°C . This cloud requires special attention and, therefore, it is discussed in detail in Chapter 19.

2.10.2.8 Orographic clouds. These are the clouds⁹ formed in the mountain regions. The rising moist air over the mountain top and its wavy motion on the side gives rise to lenticular, wave, and rotor clouds.

2.10.2.9 Special clouds. There are yet some special types of clouds⁹ which are named differently, like arctic sea smoke, funnel cloud, waterspout, contrails, noctilucent cloud, etc.

2.10.3 Etages (Levels) of Clouds

The French word *étage* means floor, story, or level. All clouds can be grouped into three different categories, based on the altitudes (levels), which are called etages of clouds. There can be high-, medium-, and low-level clouds. The altitudes of these clouds depend on whether they belong to tropical, temperate, or polar regions. The clouds and their levels in various regions are presented in Table 2.1.

2.10.4 Stability of Atmosphere and Clouds

Air generally tends to flow horizontally but certain disturbances may cause vertical updrafts or downdrafts. Air is said to be stable if it resists upward or downward displacement and tends to return to its original horizontal level. Air is said to be unstable when on disturbance it tends to move further away from the original horizontal position. Stability is, therefore, atmospheric resistance to vertical motion of an air parcel.

When a parcel of air is warmer than its surrounding air, it is unstable because it would tend to rise further when disturbed. Similarly, when the parcel of air is cooler than its surrounding air, it is stable because it would tend to return back on disturbance.

Table 2.1 Etages (levels) of clouds

Etages	Names of clouds	Altitudes		
		Tropical region	Temperate region	Polar region
High	Cirrus	6–18 km	5–13 km	3–8 km
	Cirrocumulus			
	Cirrostratus			
Middle	Altostratus	2–8 km	2–7 km	2–4 km
Low	Altocumulus			
	Stratus	0–2 km	0–2 km	0–2 km
	Stratocumulus			
	Nimbostratus			
	Cumulus			
	Cumulonimbus			
	Fractionimbus			

The lapse rate of air with no vertical currents is important in determining the stability of the air. If the lapse rate becomes steeper, the colder air aloft tends to sink and the warmer air of lower levels will rise. Therefore, a steeper lapse rate makes the atmosphere unstable. The explanation for this is that if the air becomes cooler in the upper levels or warmer in the lower levels, it will have a steeper lapse rate and, therefore, an unstable atmosphere will result. A layer of air having a small temperature lapse rate will be stable because there will be little tendency for vertical currents to develop.

The stability of the atmospheric layer or air parcel at a certain place and time depends on the values of DALR and SALR in the layers of air as shown in Fig. 2.9. If the environmental lapse rate (ELR) curve lies on the right-hand side of the SALR curve, i.e., $ELR < SALR$, as shown by the dotted line in the figure, this represents the condition of absolute stability. Isothermal layers and temperature inversion layers are examples of absolute stability. If the ELR curve lies on the left-hand side of the DALR line, i.e., $ELR > DALR$, as shown by the dashed line in Fig. 2.9, this is called a condition of absolute instability. If the ELR curve falls in between the curves of DALR and SALR, i.e., $DALR > ELR > SALR$, as shown by the dash-dot line in the figure, it is called conditional stability. In the case of conditional stability, if the air layer is saturated, it will be unstable; if saturated, it will be stable. Therefore, in conditional stability, the amount of moisture content decides whether the air is stable or unstable. Conditional stability is also called conditional instability. Finally, if the ELR curve coincides with DALR or SALR, this is a situation of neutral stability (or neutral instability). In neutral stability, the air parcel when displaced upward or downward will remain at its new level without showing any tendency to continue to rise or descend when the displacing force is removed.

There may still be situations⁹ when a stable parcel of air at a low level is lifted mechanically to a higher level, and it may become unstable; this is called potential (or convective) instability. Similarly, there can be a condition of potential (or convective) stability in which the initial unstable layer at a low level becomes stable at a higher level.

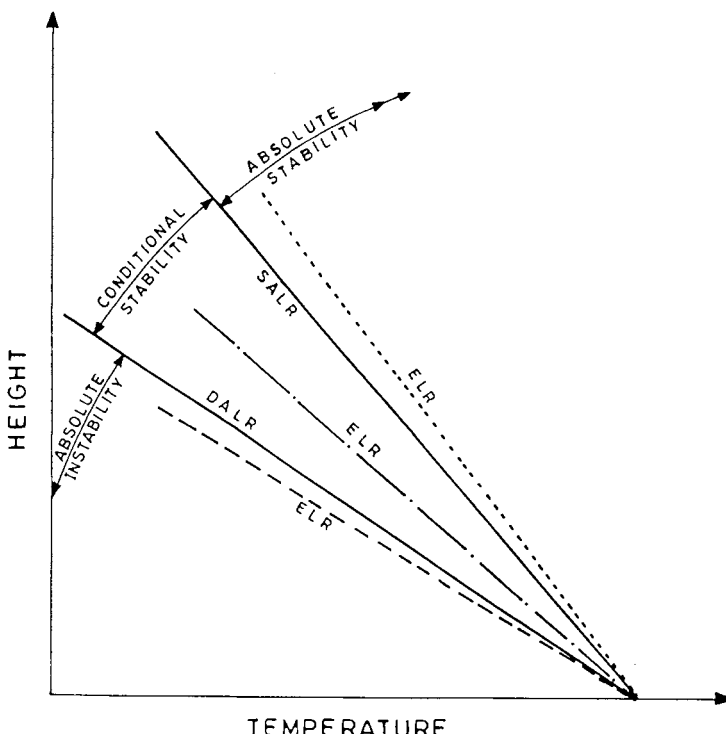


Fig. 2.9 Stability criteria.

In unstable regions, clouds develop vertically in the form of cumulus or cumulonimbus clouds and turbulence is created. The vertical development of clouds may also generate thunderstorms. In stable regions, clouds, if present, would have a layer type such as stratus and the flying conditions would be smooth.

2.10.5 *Ceiling of Clouds*

The ceiling of clouds is simply called the *ceiling*. By definition, the concept of ceiling¹⁰ arises only when six-tenths (more than half) or more of the sky is covered with clouds. Clouds can be of different types and at different levels. The ceiling is then defined as the vertical height above the ground or water of the base of that lowest cloud layer, which in conjunction with all other lower layers of clouds covers six-tenths or more of the sky. The ceiling may range between zero and unlimited. If one-half or less of the sky is covered with clouds, the ceiling is said to be unlimited. When the cloud base cannot be seen at all due to heavy rain or fog, the ceiling is said to be zero.

2.11 Rain and Drizzle

The terms *rain* and *drizzle* designate small water droplets falling from clouds but are categorized differently.

2.11.1 Rain

The precipitation that reaches the Earth's surface as water drops is called rain. Raindrops vary in size from 0.5 mm up to even 6 mm diam. Considering their average diameter to be about 1 mm, the diameter of raindrops is 100 times more than the average diameter of a droplet in the cloud. This means that the volume of a rain drop is about one million times greater than the volume of a cloud droplet. It follows that about one million droplets in the cloud must combine to form only one rain drop. The freely moving cloud droplets mix with each other, i.e., coalesce, to become water droplets and this process is known as *coalescence*. If the temperature of the cloud is much below freezing, say below -15°C , some of the water droplets of the cloud may become ice crystals which grow in size before they fall. During this fall, when these ice crystals pass through the temperatures above 0°C , they melt and become raindrops. Not all raindrops reach the Earth because some smaller raindrops may evaporate before reaching the Earth. Rains are classified as light, moderate, or heavy. Rains can be intermittent or continuous.

2.11.2 Drizzle

Drizzle is basically rain whose drops are smaller (less than 0.5 mm diam) than that of rain. Drizzle is due to precipitation from stratus clouds. The fact that these tiny water drops which appear to float in the atmosphere are able to reach the Earth indicates the absence of turbulence in the atmosphere. Drizzle is also classified as light, moderate, or heavy, and can be either intermittent or continuous.

2.12 Hail and Snow

Hail and *snow* are two important solid forms of water vapor which fall on the ground under certain atmospheric conditions.

2.12.1 Hail

Hail consists of grains of ice falling from clouds. These grains are also referred to as hailstones. They are mostly spherical, and their diameters range from less than 0.5 cm to about 8 cm, although a hailstone of about 14 cm diameter weighing 0.7 kg has also been reported; the process of formation of hailstones is mentioned in Sec. 2.7 above. Hailstones of diameter 0.5–2 cm are most common. Hailstorms occur most frequently in the middle latitudes and diminish toward the poles, equator, or over the sea. The duration of hail fall may vary from 10 s to 40 min, but a duration of about 5 min is most common. Hail does not stick to the surface of an aircraft but has the potential of causing much physical damage to it.

2.12.2 Snow

Water vapor that freezes directly in crystalline form and unites to form flakes (the term *flake* means small flat layer) is called snow. Ice crystals may also exist in different forms like pellet, sleet, needle, etc. Snowfall can occur at surface temperatures up to 4°C . One foot of freshly fallen snow is approximately equal to an inch of rainfall. Dry snow does not stick to an aircraft surface but wet snow does stick.

2.13 Air Masses and Air Fronts

Global atmosphere in the lower layers consist of certain large air masses whose boundaries form air fronts.

2.13.1 Air Masses

An *air mass* is a large body of air held together, extending to hundreds of kilometers with common physical properties. Its temperature, lapse rate, and moisture content are nearly uniform horizontally. An air mass may contain fog, clouds, rain, and ice particles. Global atmospheric air may contain several of such air masses. Knowledge of weather characteristics of the air mass helps a pilot to make probable predictions of flying conditions within the given air mass.

The properties of an air mass are decided by the place of its origin, the path over which it travels, and the age of the mass. If due to certain meteorological conditions an air mass has largely remained confined to a particular area for days or even weeks, this may be called the place of its origin. The air mass picks up its properties from the physical and geographical nature of the surface over which it existed. Therefore, an air would be warm or cold depending on whether it is born in tropical or arctic regions. Similarly, the air mass would be dry or moist depending on whether its origin is continental or maritime, respectively.

The initial properties of an air mass that are acquired at the place of its origin may undergo changes depending on the path over which it travels. The slower the speed of the air mass, the greater the influence of the path of travel. An air mass is called hot or cold depending on whether the underneath surface temperature of the Earth is less or more, respectively, compared to that of the air mass. An air mass of 40°C traveling over a surface of 30°C temperature would be called a hot air mass, and when it travels over a surface of 50°C it would be termed a cold air mass. The extent to which the surface conditions are able to spread vertically depends on the age of the air mass.

There are four basic types of air masses: 1) dry cold air which is referred to as *continental polar air* by weather forecasters, 2) moist cold air which is referred to as *maritime polar air*, 3) dry warm air which is commonly called *continental tropical air*, and 4) moist warm air which is known as *maritime tropical air*. Each of these air masses has certain characteristic features² with regard to temperature, humidity, lapse rate, precipitation, clouds, and visibility. If the air masses are broadly classified as cold and hot air masses, their typical characteristics can be presented in broader terms. Cold air mass is characterized by instability, turbulence, good visibility, cumuliform clouds, and precipitation in the form of showers, hail, or thunderstorms. Similarly, a warm air mass would have stability, smooth winds, poor visibility, stratiform clouds, fog, and precipitation in the form of drizzle.

2.13.2 Air Fronts

The term *air front* is defined here and different types of air fronts are explained. The knowledge of air fronts help a pilot to predict the weather change in the atmosphere.

2.13.2.1 Frontal zones and their origin. The *front* or *frontal zone* is a relatively narrow belt of interface or transition zone, defining the boundary

between two different air masses. The weather term “front” was coined during the First World War; the word front was taken from the fronts of the battle fields. Since the two air masses may be very different and foreign to one another, they clash and fight, and their line of battle resembles a battle field or front. In a frontal zone, the air cannot be identified with either air mass since it is a mixture of both. The fronts have a sloping boundary whose slopes may range from 1 in 50 to 1 in 300. The width across the frontal zone can vary from about 5 to 80 km (3 to 50 miles).

Fronts are of great importance in aviation because they cause considerable weather changes which create hazards to flying. The growth of new fronts and the regeneration of old, weak, and decaying fronts is called *frontogenesis*, or *frontal development*. Similarly, the opposite process, the decaying and dissipation of existing fronts is called *frontolysis*, or *frontal breakdown*. Fronts are generated by the meeting of the air masses of different temperatures so that steep gradients of temperature and density, amounting to temperature and density discontinuity, occur. Fronts are destroyed by the release of their energy in frontal activity by mixing of air in the two masses along the frontal zone. This reduces the steep temperature gradient to a broad zone of gradual transition, leading to the weakening or destruction of the front.

A pilot can feel the crossing of a front when he finds steep temperature change, shift in wind direction, change in barometric pressure, and change in cloud conditions.

2.13.2.2 Different types of fronts. There are several types of fronts, namely, the *polar front*, the *cold front*, the *warm front*, the *stationary front*, and the *occluded front*.

2.13.2.2.1 Polar fronts. A polar front is the interface between the cold air mass of the polar region and the warm air mass of the tropical region. This is the biggest “battle front” in the atmosphere, exhibiting severe weather changes. The polar front is semipermanent and semicontinuous with dynamic moving boundary. Weather activity along the polar front also considerably influences the weather in the mid-latitudes as the polar front itself may reach as far as 60° north in the summer.

2.13.2.2.2 Cold fronts and squall lines. A cold front is the zone of interface where cold air displaces the mass of warm air. Violent weather changes may also be associated with the cold front. Since cold air is denser than warm air, the cold air stays on the surface with steep velocity gradient across the surface of the Earth. Cold fronts tend to move much faster than warm fronts. The steep slope of the cold front makes warm air rise almost abruptly which leads to the formation of cumulus-type clouds. The cold front may lead to the formation of rain, snow, or hail in the turbulent atmosphere which is the greatest hazard in flying. Cold fronts can be slow moving or fast moving.

The air in a rapidly moving cold front is often proceeded by squall lines of heavy showers and thunderstorms. These squall lines may be as much as 80 km (50 miles) to 160 km (100 miles) ahead of the cold front. The exact cause of these squall lines is still a matter of research. It is suspected that the strong downdrafts within the thunderstorms carry cold air from aloft to the surface and diverge, forming a cold air ahead of the front. A squall line is more violent than the associated cold front and lasts only a few minutes.

2.13.2.2.3 Warm fronts. A warm front is the zone of interface where warm air overtakes a mass of retarding cold air. The warm air, being lighter, ascends

over the cold air in a long gentle slope. Warm fronts move at relatively low speeds. The precipitation associated with the warm front may be in the form of rain, snow, sleet, or freezing rain, depending on the temperature around the warm front. Flight hazards associated with a warm front are due to fog and poor visibility.

2.13.2.2.4 Stationary fronts. A front that is moving at a speed less than or equal to 5 kn (2.6 m/s, 8.4 ft/s) is called a stationary or quasistationary front. Both cold and warm fronts on certain occasions gradually lose speed and show little movement, and develop into quasistationary fronts. The weather conditions attending a cold front are similar to those associated with the warm front but are generally less intense. A stationary front usually weakens and finally dissipates. Sometimes after several days it may, however, revive its activity and begin to move, either as a warm front or a cold front.

2.13.2.2.5 Occluded fronts. Sometimes when hot and cold fronts meet, their common boundary is lifted upward from the Earth's surface. This merging or absorption of the two fronts is called *occlusion*. The instability of the frontal waves is often considered² to be a cause of occlusion.

2.14 Atmospheric Pollution

The increasing and apparently never-ending demand for more comfort to human beings is adding to atmospheric pollution. This comes about mainly through industrialization of cities. Millions of tons of pollutants are being poured¹ into the atmosphere every year. Pollution has started increasing at alarming rates. Human beings in many industrial towns inhale polluted air which is even visible to the unaided eye.

There may be different views as to what constitutes pollution of the atmosphere. Atmospheric pollution may be defined¹¹ as "the presence in the atmosphere of substances or energy in such quantities and of such duration liable to cause harm to human, plant, or animal life, or damage to human-made materials and structures, or changes in the weather and climate, or interference with the comfortable enjoyment of life or property or other human activities."

Different types of pollutants and their effects are briefly described here. It has become imminent to control pollution as it decreases the quality and span of our lives.

2.14.1 Pollutants and Their Origin

The suspended particles and gases introduced by human activity into the atmosphere, that may lead to harmful effects on living beings, soil, vegetation, civil and metallic structures, are atmospheric pollutants. The suspended particles are that of solids and liquids. The pollutants in particle form are chiefly ash, soot, smoke, carbon and sulfur particles, and metallic particles. The gas pollutants¹² are mainly sulfur dioxide, oxides of nitrogen, and carbon monoxide. These pollutants originate from domestic heating and from a wide range of industrial, and power plants. Natural calamities like volcanic eruptions and forest fires also produce pollutants. The tremendous increase in the use of diesel and gasoline-powered vehicles has considerably increased the gas pollutants. Oxides of nitrogen are produced by nitrogen-based agricultural fertilizers, bacterial action in the soil, lightning and volcanic eruptions, nuclear weapon tests, and by human activity during combustion processes at temperatures higher than about 1000°C.

Five toxic metals found in air—beryllium, cadmium, lead, mercury, and nickel—act as pollutants. Lead is very commonly used and is widely dispersed throughout the environment as compared to the other toxic metals. They are usually found in certain metal-refining industries, production industries, and waste dumps.

Several thousands of synthetic chemicals are currently available and many are toxic chemicals which act as pollutants. Toxic chemicals originate from chemical industries, industrial incinerators, waste disposal facilities, and sewage treatment plants.

Certain radioactive materials present in the environment as the result of natural processes and human technological developments are also pollutants. These materials produce x-rays, gamma rays, alpha-particles, beta-particles, electrons, protons, neutrons, and cosmic rays. They ionize the atoms of substances through which they penetrate. Photochemical oxidants are regarded as secondary pollutants¹² which are produced by the action of sunlight on an atmosphere containing reactive hydrocarbons and oxides of nitrogen.

Noise is another frequently cited irritant found in residential as well as in industrial areas. Noise disturbance in the home arises from trucks, cars, locomotives, aircraft, nearby industrial premises, construction sites, barking dogs, radio and television sets, people shouting in the street or at home, and for various other reasons.

Certain odors that affect the well being of people by eliciting unpleasant sensations are also considered as pollutants. Odors may arise most commonly from sewage and refuse disposal, paint spraying operations, manufacture of paints and plastics, fish and animal products processing, food processing, chemical and petroleum industries.

Waste energy discharged from the burning of fuels from residential and industrial areas may also be considered as a pollutant because it unbalances the natural solar energy input of the Earth's atmosphere system and may affect weather and climate.

2.14.2 Effects of Pollution

The adverse effects of pollution appear in several ways. It damages the health of human beings, animals, birds, and insects. It is detrimental to the growth of vegetation including crops. It may harm or cause soiling of certain human-made materials. Pollution can even affect the weather and climatic changes.

2.14.2.1 Effects on health. Particle and gas pollutants may aggravate and/or cause chronic bronchitis, asthma, respiratory and heart diseases. They may cause shortness of breath, coughing, excess sputum, throat tickle, nausea, headache, and burning of the eyes. Increased exposure to certain toxic metals and chemicals may decrease the hemoglobin level in the blood, cause anemia, skin lesions, and cancer, produce dysfunction of the brain, and may cause subtle neurological damage. In extreme cases death may also occur.

Prolonged exposure to radiation may cause abnormalities in cell development, chromosomal damage, leukemia, cancer of thyroid, lung, and breast. It may also impair growth and development, and cause an increase in fetal, infant, and general mortality. Radiation effects may even be genetic and hereditary, affecting succeeding generations.

Noise pollution can disturb people's work, communications, rest, and sleep. Prolonged exposure to noise can induce stress causing high blood pressure, fatigue, and irritability. High-intensity noise can damage the eardrums, and can evoke psychological, physiological, and possibly pathological reactions.¹³

Certain odors are generally considered unhealthy annoyances to be removed from the air. They may elicit unpleasant sensations and may cause nausea, vomiting, and headaches. Odors may induce shallow breathing and coughing, and upset sleep, stomach, and appetite. They may also cause irritation of eyes, nose, and throat. They may also decrease heart rate, and produce constriction of blood vessels of the skin and muscles.

Similar to its effects on human beings, pollution also affects animals, birds, and insects. Prolonged exposure and high concentrations of pollutants may even kill these living beings.

2.14.2.2 Effects on vegetation. Pollution affects leaves, plants, vegetation, and crops. Suspended particles of pollutants are deposited on the leaves and plug the stomata, thereby reducing the absorption of carbon dioxide from the atmosphere and the intensity of sunlight reaching the interior of the leaves. This suppresses the growth of plants. Specific particles such as fluorides cause additional damage. Atmospheric pollution effects vegetation in several other ways; whatever the form of damage, the result is a reduction in growth and yield.

2.14.2.3 Effects on materials. Suspended particles of pollutants in the atmosphere may be deposited on the materials and soil or blacken their surfaces. Sulfur dioxide is an important pollutant in damaging materials. It combines chemically with limestone, sandstone, and mortar of buildings and monuments to form calcium sulfate (gypsum) which causes blistering and disintegration of the surface, with the loose material being washed away by rain. Certain historical monuments and monuments of older civilizations have been damaged due to an increase in atmospheric pollution in the past few decades. Fabrics, paper, leather, electrical contacts, paint, and medieval stained glass are all adversely affected by sulfur dioxide. Metals like iron, steel, zinc, copper, and nickel are corroded by the presence of sulfur dioxide, which forms sulfuric acid on metal surface under moist conditions. Ozone reduces the strength of certain textiles and all oxidants cause some fading of fabrics and dyes.

2.14.2.4 Atmospheric effects. Climatic conditions are affected by pollution. The total amount of heat released by human activities on our Earth is about 0.01% of the solar energy absorbed by the Earth. In certain industrial regions, however, the waste heat discharged by human activity may be comparable with that obtained from the sun. The burning of fossil fuels (coal and oil) increases carbon dioxide and decreases oxygen in the atmosphere. Carbon dioxide absorbs infrared radiation from the Earth's surface, which causes a rise in temperature of the atmosphere at the rate of 0.3°C for each 10% increase in its concentration. Actually the temperature on the Earth's surface is decreasing on the average in the last few decades, which shows that the impact of carbon dioxide is nullified by some more important factors in the atmosphere. The increase in heat, due to absorption of Earth's radiation as well as by the waste heat generated by burning of fossils in industry, produces more water vapor, which leads to thicker clouds,

and, therefore, less radiational heating from the sun. The waste heat discharged by an industrial city may amount to more than seven times the quantity of heat the city receives from the sun. The oxides of nitrogen react with the ozone to decrease the ozone content of the atmosphere; this means more ultraviolet rays reach the Earth and this leads to a higher incidence of skin cancer. The increase in suspended particles in the atmosphere increases scatter and reflection of radiation, which means less solar radiation and less radiation from the Earth's surface, and consequently lowers the global mean atmospheric temperature. The increase of suspended particles in the atmosphere accelerates the formation of fog, which reduces visibility.

2.14.3 Acid Rain

An important consequence of air pollution is the production of acid rain, because certain pollutants are easily dissolved in water to produce sulfuric, nitric, and carbonic acids during rain. Acid rain damages the health of human beings, retards the growth of vegetation and forests, corrodes metals, deteriorates the quality of soil, and spoils lake water which may even kill fish, even to the point of the extinction of some species. Suspended acidic liquid particles in atmosphere produce acid hazes causing loss of visibility.

2.14.4 Atmospheric Pollution and Aircraft

The atmospheric pollution affects aircraft too, just as it affects other materials. It may soil and corrode the surface of aircraft, causing increase in skin friction and reduction in structural strength. This may appreciably increase the aerodynamic drag force on the aircraft and more energy may be required to propel the aircraft, as well as necessitating an increase in the lengths of takeoff and landing runs. Atmospheric pollution may also contaminate runway fields, causing difficulties in takeoff and landing runs. Air pollution also adversely affects the efficiency of the aircraft's airbreathing engine that may even lead to engine shutdown.

Aircraft also create atmospheric pollution through exhaust gases and noise. Exhaust gases contain pollutants in the form of particles and gases. Engine exhausts of high-speed and high-altitude modern aircraft directly pollute the stratosphere and interact with the ozone layer. Aircraft noise is the sum total of all the noises caused by different sources of the aircraft-atmosphere system, such as jet noise, airframe noise, propeller noise, fan and compressor noise, turbine noise, combustion noise, shock-associated noise, jet mixing noise, and the noise of thrust reversal. A detailed account of these noises has been presented by Smith.¹³ Aircraft noise is a serious atmospheric pollution problem, especially since the introduction of large high-speed aircraft, and with the increase in population around airports during the last few decades.

2.14.5 Efforts to Minimize Pollution

People have become aware of the ill effects of pollution since they have occurred more frequently with serious consequences during the past few decades. In certain modern industrial towns in developing countries, atmospheric pollution exists on a 24-h basis. Print, electronic media, and national and international conferences have sufficiently underlined the seriousness of this problem. Research activity has been undertaken to precisely understand the origin and effects of each pollutant.

Environmental deterioration and atmospheric pollution has become a political issue in some developed countries. Individuals, pressure groups, organizations, and governments are trying to reduce pollution. Pollution is no longer a local problem—it has national and international repercussions. International organizations such as the United Nations have devoted much attention to environmental protection. Pollution control strategies has been laid down for designating the level of pollution demand acceptable and for controlling pollutant emissions. A variety of economic strategies has been used to control air pollution. Legislation affecting pollution control has been framed and in some countries industrial and automotive pollution control is mandatory, which is achieved by devices that yield pollution-free discharge of gases, limiting pollution to acceptable levels.

Certain physical and chemical processes in the atmosphere also do not allow pollutants to occupy a permanent place in the atmosphere. Some pollutants, due to the force of gravity, may ultimately fall to the Earth's surface after a few days or months in the atmosphere. Some are washed away by rain and others are transformed into other substances by oxidation or bacteria. However, some pollutants may also be transformed to new pollutants through photochemical reactions.

2.15 Visibility

Visibility is the horizontal distance at which prominent objects may be seen by a naked eye and identified during the day, and also applies similarly to prominent lighted objects at night. The object should be of a size commensurate with its distance from the observer and should ideally be of a dark color when seen in daylight. Visibility is considerably reduced by the presence of rain, fog, snow, smoke, sand, or dust in the atmosphere. If visibility varies in different directions, the visibility in the poorest direction is reported by meteorologists.

Visibility is of major importance to a pilot, and based on the degree of visibility he decides whether to fly by visual flight rules (VFR). For a pilot, visibility means the horizontal distance at which mountains, television and radio towers, high-rise buildings, and such other obstructions to flight can be seen. Visibility can range from zero to unlimited. If one can see an object clearly at 16.09 km (10 miles) or more, the visibility is said to be unlimited. There may be different categories of visibility such as prevailing visibility, runway visibility, runway visual range, flight visibility, and approach light contact flight. These are explained below.

2.15.1 *Prevailing Visibility*

It has been mentioned above that the visibility need not necessarily be the same in all directions. This has led to the definition of *prevailing visibility*. It is the greatest visibility in miles and its fractions, which is equaled or surpassed throughout at least half of the horizon. The segments constituting this half of the horizon need not be adjacent to one another as explained in Fig. 2.10. The observer is at the center of the circle, the number inside each segment indicates visibility in miles in that segment. The number at the bottom of the circle indicates prevailing visibility in each case.

2.15.2 *Runway Visibility*

Runway visibility refers to the visibility observed along a specific runway, expressed in miles and its fractions.

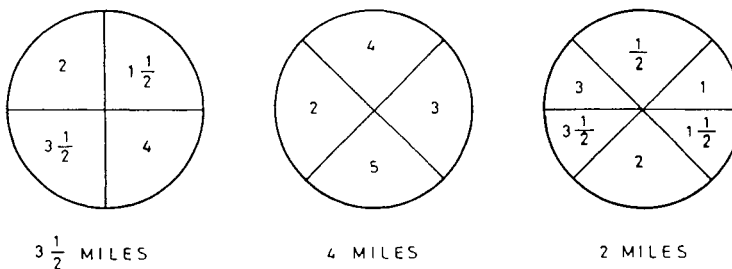


Fig. 2.10 Determination of prevailing visibility.

2.15.3 Runway Visual Range

The runway visual range (RVR) is the distance a pilot approaching at the threshold of the runway during landing operation can be expected to see when looking down the runway. The RVR can be based on either visual contrast of well-known objects (not lights) or high-intensity runway lights, whichever of the two yields the greater visual range. It is reported in hundreds of feet. The RVR is a measurement service provided by Air Traffic Control (ATC); it is not a forecast. If the RVR is measured by instruments (transmissometers), it is called instrumented runway visual range (IRVR).

2.15.4 Flight Visibility

The flight visibility is the visibility toward the flight direction as observed by a pilot from the cockpit of his aircraft during flight.

2.15.5 Approach Light Contact Height

The approach light contact height is based on visibility. It is the height at which a pilot can see the approach lights. This is based on the pilot's slant visual range.

2.16 Classification of Atmosphere into Zones

The atmosphere at higher altitudes differs significantly from the corresponding lower layers. The knowledge of the higher layers of the atmosphere has become important with the development of high-speed and high-altitude aircraft, rockets, and space vehicles. With the advancement of atmospheric sciences it is now possible to make more reliable descriptions instead of ambiguous assumptions.

2.16.1 Basis of Classification

The atmosphere changes from homogeneous (up to about 90 km) to heterogeneous, or from nonionospheric (up to about 60 km) to ionospheric. Many interesting physical phenomena also take place in the atmosphere. Therefore, it is possible to classify the atmosphere in different ways. In meteorology, it is common to classify the atmosphere in accordance with thermal conditions such as troposphere, stratosphere, mesosphere, ionosphere, and exosphere. The temperature variation in these layers is shown in Fig. 2.1 which also depicts some more information of the layers.

2.16.2 *Troposphere*

The troposphere is closest to us because one of its boundaries is the Earth's surface. It varies in height with latitude, from about 16 km at the equator to about 9 km at the poles. Its height also varies with the seasons because it is higher in the summer than in winter. The standard atmosphere regards the altitude of the troposphere as up to 11 km. The pressure and density decreases rapidly with altitude. The temperature also generally decreases with altitude at about the constant rate of about $6.5^{\circ}\text{C}/\text{km}$. The air in this region moves both horizontally and vertically, hence the name troposphere from the Greek word *tropos* which means turning. Most of the water vapor exists in the lower parts of the troposphere. It may be preferable to call this region the "weather-sphere" because practically all weather phenomena occur in this region due to the presence of water vapor and vertical air currents.

The top layer of the troposphere is called the *tropopause*, and its temperature is about -56°C . The tropopause is the boundary region between the troposphere and the stratosphere; it is not a clear-cut boundary region and its height varies from place to place as stated earlier. Fast-moving jet streams are found to exist near the tropopause. Modern jet airlines fly either in the tropopause or in the lower parts of the stratosphere.

2.16.3 *Stratosphere*

The region above the tropopause, extending up to about 50 km altitude, is known as the stratosphere. The pressure and density continue to decrease with altitude. The lower part of the stratosphere has a constant temperature in the vicinity of -56°C up to about 20 km altitude and, thereafter, the temperature rises to nearly 0°C at about 50 km. Here the air moves almost horizontally, with practically no vertical air currents, hence the name *stratosphere*. Near the base of stratosphere, especially over the polar regions in winter, one may frequently find jet streams of winds as mentioned in Sec. 2.4.6 above. There is practically no water vapor, cloud, or rainfall in the stratosphere. The top layer of the troposphere is known as the *stratopause*, which forms the boundary region between the stratosphere and mesosphere.

2.16.4 *Mesosphere*

The zone of the mesosphere starts from an altitude of about 50 km and ends at an altitude of about 85 km. It is the middle zone of the atmospheric classification into five zones, hence the name mesosphere. The temperature decreases with the increase in altitude in this region. This decrease in temperature is similar to that which exists in the troposphere; therefore, the mesosphere is also referred to as the upper troposphere. A very small amount of water vapor deposits on nickel-containing cosmic dust (acting as condensation nuclei) form noctilucent clouds of silver-white and light blue color which are cirruslike in shape. A series of intense photochemical reactions take place in this region, i.e., dissociations and recombinations of various elements of the atmosphere under the action of the sun's ultraviolet radiation. Since the mesosphere is colder in the upper part and warmer in the lower, this gives rise to convective motion of air in the mesosphere. The presence of both horizontal and vertical motions of air maintains the homogeneity of the atmosphere. The top layer of the mesosphere is called the *mesopause* where

the temperature may fall down to about -100°C , which is the coldest temperature in the entire atmosphere. The mesopause is the boundary region between the mesosphere and ionosphere.

2.16.5 Ionosphere

This region extends from about 85 to 500 km altitude. The temperature increases uniformly with altitude from about -85°C at 85 km to about 1600°C at 500 km. The air particles are electrically charged (ionized by the sun's ultraviolet radiation) and congregate in three main layers, designated *D*, *E*, and *F*. Layer *D* is closest to the Earth and *F* is the farthest away. These layers reflect certain radio waves back to the ground and, therefore, they have importance to pilots for transmission and propagation. Fortunately, the ionosphere does not reflect very high and superhigh frequencies so that microwaves can be used to relay telephones, telegrams, radio, teletypes and television programs via satellites. In the lower parts of the ionosphere meteors from outer space burn up as they meet the increased resistance of the air.

It becomes difficult to define an upper limit of altitude of the atmosphere because the air gradually becomes thinner with increasing altitude. One usually enters into the realm of satellites at about 145 km (90 miles) where the aerodynamic lift is no longer a requirement for maintaining height above the ground. This region is accepted by some authorities as the boundary of outer space and 145 km is also regarded as the limit of national sovereignty.

2.16.6 Exosphere

This is the outermost part of the Earth's atmosphere and hence the name exosphere, because the Greek word *exo* means outside. This is the boundary region between the Earth's atmosphere and interplanetary space. This region may be considered to begin from about 500 km and extend up to 1500 km or even greater. Here atoms and molecules move almost freely under the action of gravity with hardly any collision among themselves. Most molecules that go up, return back due to gravity, like the return of a spray from a jet of water. This region is, therefore, sometimes known as the *spray region*.¹⁴ The heavier atoms or molecules exist on the lower levels of exosphere while the lighter ones, those of helium or hydrogen, exist at higher levels. Because of very high velocity at high temperature, some of these lighter molecules may also leave the Earth's atmosphere forever.

2.17 Standard Atmosphere

The knowledge of standard atmosphere is required for producing pressure instruments, performing data reductions of flight tests, and pronouncing certain safety regulations for the aircraft.

2.17.1 Necessity for Standard Atmosphere

The physical characteristics of the atmosphere are not steady and constant but change with altitude, location (longitude and latitude) on the globe, season, and time of the day, and with the solar sunspot activity. The performance of an aircraft depends on the physical characteristics of the atmospheric air through which it flies. The performance data of an aircraft or comparison of the performance of different aircraft have meaning only if they are considered with respect to

some commonly agreed upon reference atmosphere. This reference atmosphere is usually the *standard atmosphere*, where the temperature, pressure, and density vary with altitude only. The fixation of standard atmosphere allows for the design of instruments for measuring altitude and airspeed. The pressure altitude, temperature altitude, and density altitude have meaning only after the standard atmosphere has been specified; these different altitudes have been defined in Sec. 6.2.4.

It is presently possible to specify the prevailing atmospheric conditions up to an altitude of 2000 km at any latitude and longitude of our globe. If desired, each country can have its own standard atmosphere. For general aviation purposes it is pertinent to develop internationally known reference atmosphere. Several reference atmospheric models have been established, which are summarized by Whitten and Vaughan.¹⁵ Some of the commonly known standard atmospheric models are as follows: 1) The Air Research and Development Command (ARDC) model¹⁶ proposed in 1959 by the U.S. Air Force (this name has now been changed to Air Force Systems Command). 2) The International Civil Aviation Organization (ICAO) standard atmosphere¹⁷ proposed in 1964; this standard has been used by European countries. 3) The U.S. standard atmosphere proposed in 1962; this was revised¹⁸ in 1976 and presents the standard atmosphere up to 1000 km of altitude. All these standard atmospheres are basically the same up to about 30 km but at higher altitudes they differ appreciably. These standard atmospheres approximate average atmospheric conditions around the latitude of 45°N in North America, but are also valid in the southern hemisphere around the latitude of 45°S for all longitudes.

Since the prevailing meteorological conditions in the tropics are different from those in the mid-latitudes, an International Tropical Reference Atmosphere (ITRA) has been suggested by Ananthasayanam and Narasimha,¹⁹ which is valid in the latitudes of around 30°N to about 30°S.

2.17.2 Method of Calculation and Presentation

Air temperature distribution is the most important element of the atmosphere as it also controls the other elements of the atmosphere. In a standard atmosphere, the temperature distribution is obtained by making several measurements at different altitudes. The temperature distribution of the U.S. standard atmosphere¹⁸ 1976, is presented in Fig. 2.11 up to an altitude of 110 km only. The temperature distribution in the standard atmosphere (Fig. 2.11) consists of mostly straight lines. Thus, the atmosphere has either isothermal regions of zero lapse rate, or constant gradient regions of positive or negative lapse rates. The lapse rate is positive in troposphere and mesosphere. The isothermal regions in Fig. 2.11 are 1) from 11 km (more precisely 11.1 km) to 20 km, 2) from 47 km (more precisely 47.4 km) to 51 km, and 3) from 86 km to 91 km. The lapse rates $\lambda (= -dT/dh)$ in different regions can be calculated.

Having obtained the temperature variation empirically, the pressure and density variations are calculated from the hydrostatic relation and the equation of state by assuming that the medium of air is continuum, perfect gas, and at rest. It will be shown here that the variations of pressure and density with altitude can be expressed analytically.

Consider a small cylindrical element of air at rest, of height dh and cross-section area dA , as shown in Fig. 2.12. The continuum approach implies that p , ρ , T , and

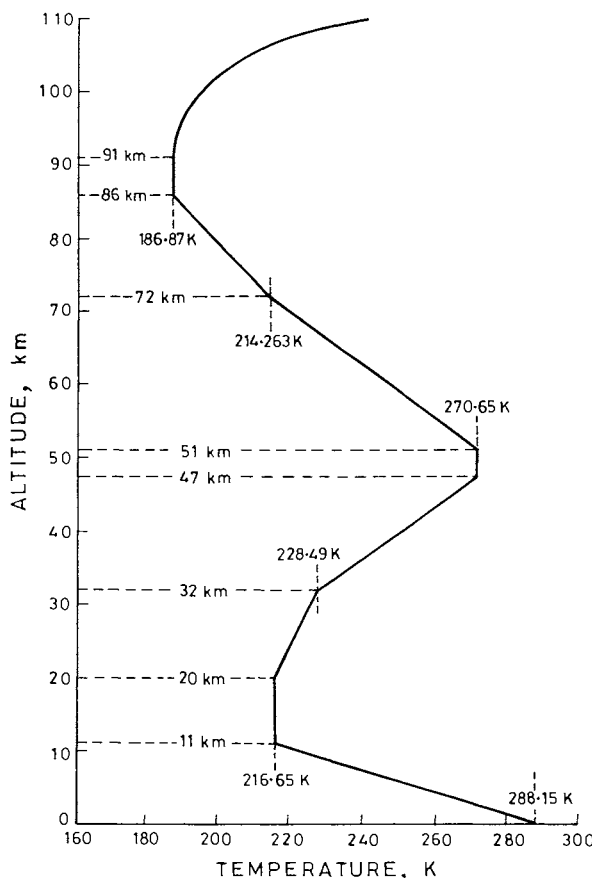


Fig. 2.11 Temperature variation in the standard atmosphere.

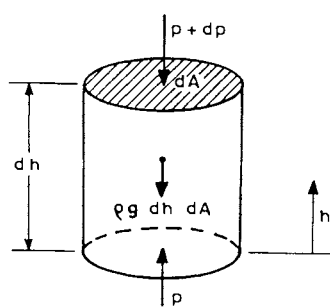


Fig. 2.12 Vertical forces on cylindrical air-element.

other fluid properties are continuous functions of space and time in the fluid medium. The forces acting on the element in a vertical direction are due to surface pressures p and $p + dp$ acting on the two opposite faces, and the gravitational force acting at the center of gravity of the element. The balance of forces in vertical direction gives the following hydrostatic relation,

$$dp/dA - (p + dp)/dA - \rho g dh/dA = 0, \quad \text{i.e.,} \quad dp = -\rho g dh \quad (2.2)$$

Using the equation of state for perfect gas, $p = \rho RT$, Eq. (2.2) can be written as

$$dp/p = -(g/R) dh/T$$

Let p_1 and p be the pressures at the true altitudes h_1 and h ($h > h_1$), respectively, the integration of the above relation yields

$$p/p_1 = \exp \left\{ -(1/R) \int_{h_1}^h (g/T) dh \right\} \quad (2.3)$$

In general, the right-hand-side integral of the above equation has to be solved numerically. Considerable simplification arises by noting that the temperature distribution (Fig. 2.11) in the standard atmosphere consists of straight lines; the vertical lines denote the isothermal regions and the sloping lines denote the constant temperature gradient regions. In both these regions it is possible to integrate the integral in Eq. (2.3) and obtain the results analytically as shown below.

Let another altitude h_G be defined by satisfying the relationship

$$g dh = g_{SL} dh \quad (2.4)$$

where g_{SL} is the value of g at sea level. The length scale h_G is commonly called the geopotential altitude. A further discussion of h_G is reserved for Sec. 6.2 where the relationship between h and h_G is obtained as

$$h_G = rh/(r + h) \quad (2.5)$$

where r is the radius of the Earth. If $h \ll r$, as is usually the case even for modern aircraft, h_G can be regarded equal to h .

Equation (2.3) after using Eq. (2.4) can be written as

$$p/p_1 = \exp \left\{ -(g_{SL}/R) \int_{h_{G,1}}^{h_G} dh_G/T \right\} \quad (2.6)$$

where h_G and $h_{G,1}$ are the values of geopotential altitudes at h and h_1 , respectively. The integral on the right-hand side of the above relation can be easily integrated both for isothermal and constant temperature-gradient regions.

1) *Isothermal region.* In isothermal regions the temperature remains constant; $T = T_1$, a constant. From the equation of state it follows that, $p/p_1 = \rho/\rho_1$. From Eq. (2.6), the following relation for the pressure and density ratios is obtained,

$$p/p_1 = \rho/\rho_1 = \exp \{ -g_{SL}(h_G - h_{G,1})/(RT_1) \} \quad (2.7)$$

where the subscript 1 refers to the known initial values. The above relation expresses the ratios p/p_1 and ρ/ρ_1 as functions of h_G . Since, from Eq. (2.5), h can be obtained for the known value of h_G , the ratios p/p_1 and ρ/ρ_1 can also be obtained as functions of h .

2) *Constant temperature gradient region.* In the case of constant temperature gradient the temperature distribution is linear and can be represented as $T = T_1 - \lambda(h_G - h_{G,1})$, where T_1 is the absolute temperature at $h_{G,1}$ which is the geopotential altitude at the base of the sloping line. Equation (2.6), after using the above expression for T and integrating the integral term, becomes

$$p/p_1 = \{1 - \lambda(h_G - h_{G,1})/T_1\}^{g_{SL}/(\lambda R)} = (T/T_1)^{g_{SL}/(\lambda R)} \quad (2.8)$$

and using the equation of state, the density ratio is obtained as

$$\rho/\rho_1 = \{1 - \lambda(h_G - h_{G,1})/T_1\}^{\{g_{SL}/(\lambda R)\}-1} = [T/T_1]^{\{g_{SL}/(\lambda R)\}-1} \quad (2.9)$$

In the above Eqs. (2.8) and (2.9), the g_{SL} , R , and λ are the known quantities. The quantities with superscript 1 are the known initial values. These relations, therefore, express p/p_1 and ρ/ρ_1 as function of h_G . Using Eq. (2.5), the ratios p/p_1 and ρ/ρ_1 can be expressed as functions of h .

In case it is desired to use the above Eqs. (2.8) and (2.9) of the standard atmosphere from the sea level, $h_{G,1} = 0$, $T_1 = T_{SSL}$, and $\rho_1 = \rho_{SSL}$, where the subscript SSL represents the standard atmosphere sea level condition. The ratios, p/p_{SSL} and ρ/ρ_{SSL} , denoted as δ and σ , respectively, become

$$\delta = p/p_{SSL} = (1 - \lambda h_G / T_{SSL})^{g_{SL}/(\lambda R)} = (T/T_{SSL})^{g_{SL}/(\lambda R)} \quad (2.10)$$

and

$$\sigma = \rho/\rho_{SSL} = \{1 - \lambda h_G / T_{SSL}\}^{\{g_{SL}/(\lambda R)\}-1} = [T/T_{SSL}]^{\{g_{SL}/(\lambda R)\}-1} \quad (2.11)$$

where $T_{SSL} = 288.15$ K, $\rho_{SSL} = 1.225$ kg/m³, $\lambda = 6.5$ K/km, $R = 287$ m²/(s²K), and $g_{SL} = 9.8066$ m/s². For day to day work, it is common to regard $T_{SSL} = 288$ K, and $g_{SL} = 9.81$ m/s².

The variations of pressure and density ratios with the increase in altitude h can now be calculated by first using Eqs.(2.10) and (2.11) up to an altitude of $h = 11$ km ($h_G = 10.981$ km). Thereafter, for higher altitudes use Eq. (2.7) for isothermal regions, and Eqs. (2.8) and (2.9) for constant temperature gradient regions; the values of λ , $h_{G,1}$, and T_1 , belonging to the region concerned should be used.

The temperature, pressure, and density variations in standard atmosphere is usually presented both for geopotential and geometric altitudes. We have presented in Tables 2.2 the U.S. standard atmosphere, 1976, at certain selected geometric altitudes up to 25 km (82,000 ft) in the form of atmospheric property ratios. The ratios of T/T_{SSL} and a/a_{SSL} are denoted by θ and a^* , respectively, where $a (= \sqrt{\gamma RT})$ is the speed of sound in air, and γ is the ratio of specific heats of air. The a^* is obtained from the relation $a^* = \sqrt{T/T_{SSL}}$. The last columns of Tables 2.2a and 2.2b show a^* , which are useful ratios in calculating the Mach number

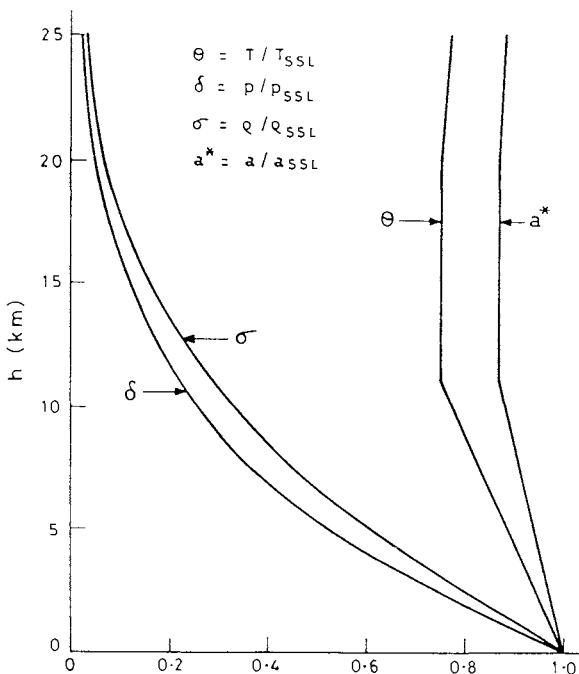


Fig. 2.13 Variations of θ , δ , σ , and a^* with altitude.

of the flight at standard altitude if the airspeed is specified. The curves of the variations of θ , σ , δ , and a^* with altitude in the standard atmosphere are shown in Fig. 2.13.

The performance analysis of aircraft powered by airbreathing engines is mainly concerned with the atmospheric region below 30 km. For this region, it is reasonable to approximate $g = g_{SL}$, and this implies that $h_G = h$. The error involved by using this approximation increases as the altitude increases, becoming about 0.5% in h at the altitude of 30 km.

2.17.3 Approximate Representation of Density Ratio Variation

Equation (2.11) giving the density ratio is generally not found convenient for obtaining analytical results of performance calculations. For a preliminary design of the aircraft, it is useful to approximate the density ratio variation by an exponential law.

Angelo Miele²⁰ uses the exponential relation, $\sigma = e^{-h/\beta}$ where $\beta = 23,800$ ft (7254.24 m), for the altitude interval between sea level and 2.5×10^5 ft (76.2 km), Hale²¹ has used the exponential expression,

$$\sigma = e^{-h/\beta} \quad (2.12)$$

where β depends on the altitude interval as follows: for $h < 11$ km, $\beta = 30,500$ ft (9296 m), and for $11 < h \leq 76$ km, $\beta = 23,800$ ft (7254 m). The exponential representation used by Hale, however, has the discontinuity at $h = 11$ km as

Table 2.2a Standard atmosphere property ratios, SI units

Altitude <i>h</i> , m	Temperature ratio θ	Density ratio σ	Pressure ratio δ	Sound speed ratio a^*
0	1.0000	1.0000	1.0000	1.0000
1,000	0.9774	0.9075	0.8870	0.9886
2,000	0.9549	0.8217	0.7846	0.9772
3,000	0.9324	0.7422	0.6920	0.9656
4,000	0.9098	0.6689	0.6085	0.9538
5,000	0.8873	0.6012	0.5334	0.9419
6,000	0.8648	0.5389	0.4660	0.9299
7,000	0.8423	0.4816	0.4057	0.9177
8,000	0.8198	0.4292	0.3518	0.9054
9,000	0.7973	0.3813	0.3040	0.8929
10,000	0.7748	0.3376	0.2615	0.8802
11,000	0.7523	0.2978	0.2240	0.8673
12,000	0.7519	0.2546	0.1914	0.8671
13,000	0.7519	0.2176	0.1636	0.8671
14,000	0.7519	0.1860	0.1398	0.8671
15,000	0.7519	0.1590	0.1195	0.8671
16,000	0.7519	0.1359	0.1022	0.8671
17,000	0.7519	0.1162	0.0873	0.8671
18,000	0.7519	0.0993	0.0747	0.8671
19,000	0.7519	0.0849	0.0638	0.8671
20,000	0.7519	0.0726	0.0546	0.8671
21,000	0.7551	0.0618	0.0467	0.8690
22,000	0.7585	0.0527	0.0399	0.8709
23,000	0.7620	0.0449	0.0342	0.8729
24,000	0.7654	0.0383	0.0293	0.8749
25,000	0.7689	0.0327	0.0252	0.8769

$$\theta = T/T_{SSL}, \quad \sigma = \rho/\rho_{SSL}, \quad \delta = p/p_{SSL}, \quad \text{and} \quad a^* = a/a_{SSL}$$

Standard atmosphere sea level (SSL) values:

$$T_{SSL} = 288.15 \text{ K} = 15^\circ \text{ C} \quad R = 287 \text{ m}^2/(\text{s}^2\text{K})$$

$$\rho_{SSL} = 1.225 \text{ kg/m}^3 \quad \gamma = 1.4$$

$$p_{SSL} = 1.01325 \times 10^5 \text{ N/m}^2 \quad g_{SL} = 9.8067 \text{ m/s}^2$$

$$a_{SSL} = 340.3 \text{ m/s}$$

shown in Fig. 2.14. In this book we use the following exponential approximation for the density ratio:

$$\rho/\rho_{SSL} = \epsilon e^{-(h-h^*)/\beta} \quad (2.13)$$

where the values of ϵ , h^* , and β are chosen as for $h \leq 11 \text{ km}$, $\epsilon = 1$, $h^* = 0$, $\beta = 9296 \text{ m}$, and for $h > 11 \text{ km}$, $\epsilon = 0.3063$, $h^* = 11000 \text{ m}$, $\beta = 6216 \text{ m}$.

The curve represented by Eq. (2.13) is shown by a dotted line in Fig. 2.14. In the troposphere ($h < 11 \text{ km}$), the curves given by Eqs. (2.12) and (2.13) are just the same but differ considerably at higher altitudes as shown in Fig. 2.14. The curve presented by Eq. (2.13) is continuous at $h = 11 \text{ km}$ and represents more closely the values of the standard atmosphere.

Table 2.2b Standard atmosphere property ratios, engineering units

Altitude <i>h</i> , ft	Temperature ratio θ	Density ratio σ	Pressure ratio δ	Sound speed ratio a^*
0	1.0000	1.0000	1.0000	1.0000
2,000	0.9862	0.9428	0.9298	0.9931
4,000	0.9725	0.8881	0.8637	0.9862
6,000	0.9588	0.8359	0.8014	0.9792
8,000	0.9450	0.7861	0.7429	0.9721
10,000	0.9313	0.7386	0.6878	0.9650
12,000	0.9175	0.6933	0.6361	0.9579
14,000	0.9038	0.6502	0.5877	0.9507
16,000	0.8901	0.6092	0.5422	0.9434
18,000	0.8763	0.5702	0.4997	0.9361
20,000	0.8626	0.5332	0.4599	0.9288
22,000	0.8489	0.4980	0.4227	0.9214
24,000	0.8352	0.4646	0.3880	0.9139
26,000	0.8214	0.4330	0.3557	0.9063
28,000	0.8077	0.4030	0.3256	0.8987
30,000	0.7940	0.3747	0.2975	0.8911
32,000	0.7803	0.3479	0.2715	0.8833
34,000	0.7666	0.3227	0.2474	0.8756
36,000	0.7529	0.2988	0.2250	0.8677
38,000	0.7519	0.2719	0.2044	0.8671
40,000	0.7519	0.2471	0.1858	0.8671
45,000	0.7519	0.1945	0.1462	0.8671
50,000	0.7519	0.1531	0.1151	0.8671
55,000	0.7519	0.1205	0.0906	0.8671
60,000	0.7519	0.0949	0.0714	0.8671
65,000	0.7519	0.0747	0.0562	0.8671
70,000	0.7562	0.0586	0.0443	0.8696
75,000	0.7615	0.0459	0.0350	0.8726
80,000	0.7668	0.0361	0.0276	0.8757
82,000	0.7689	0.0327	0.0252	0.8769

$$\theta = T/T_{SSL}, \quad \sigma = \rho/\rho_{SSL}, \quad \delta = p/p_{SSL}, \quad \text{and} \quad a^* = a/a_{SSL}$$

Standard atmosphere sea level (SSL) values:

$$T_{SSL} = 518.69^\circ\text{R} \quad R = 1.7165 \times 10^3 \text{ ft}^2/\text{s}^2 \text{ }^\circ\text{R}$$

$$\rho_{SSL} = 0.0023769 \text{ slug}/\text{ft}^3 \quad \gamma = 1.4$$

$$p_{SSL} = 2116.2 \text{ lb}/\text{ft}^2 \quad g_{SL} = 32.174 \text{ ft}/\text{s}^2$$

$$a_{SSL} = 1116.4 \text{ ft/s}$$

2.17.4 Limitations of Standard Atmosphere

The standard atmosphere standardizes only temperature, pressure, and density variations with altitude. It does not give the amount of fluctuations that these quantities would have with time at different altitudes and at different places. Moreover, it would be a most pleasant surprise if any one could ever find exactly the same distribution as provided by the standard atmosphere at any instant of time in a year. The standard atmosphere does not standardize many weather conditions such as air currents, clouds, rain, hail, or thunderstorms. In fact, the standard atmosphere is presumed to be free from these weather conditions. The standard atmosphere lapse rate lies between DALR and SALR, making it only conditionally stable.

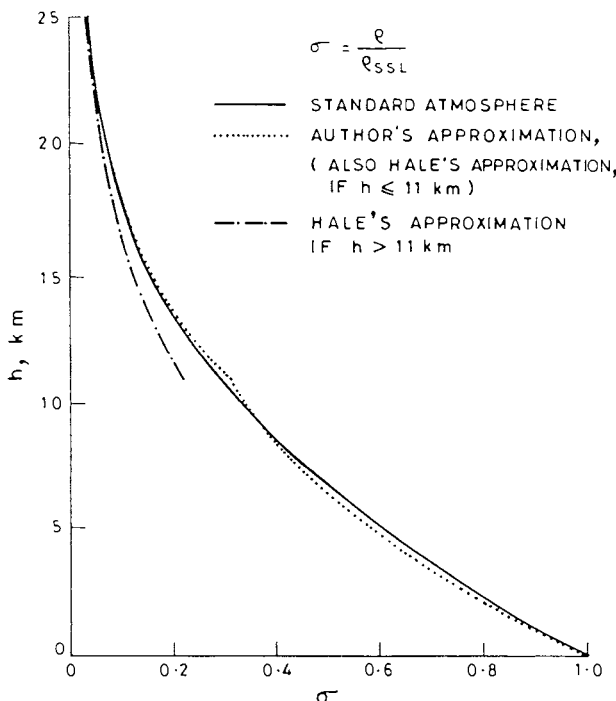


Fig. 2.14 Variation of σ in standard atmosphere and its approximations.

References

- ¹Zhongjia, Y., *Meteorology*, China Science and Technology Press, Beijing, PRC, 1985.
- ²Cagle, M. W., and Halpine, C. G., *A Pilot's Meteorology*, Van Nostrand Reinhold, New York, 1970.
- ³Richel, H., *Introduction to the Atmosphere*, McGraw-Hill, New York, 1972.
- ⁴Bennett, D. C. T., *The Complete Air Navigator*, Pitman, London, 1967.
- ⁵Barry, R. G., and Horley, R. J., *Atmosphere, Weather and Climate*, The English Language Book Society and Methuen, England, UK, 1976.
- ⁶Mason, B. J., *Clouds, Rain and Rainmaking*, Cambridge Univ. Press, Cambridge, England, UK, 1962.
- ⁷Ludlam, F. H., and Scorer, R. S., *Cloud Study*, John Murray, London, 1957.
- ⁸*International Cloud Atlas*, Vol. 2, World Meteorological Organization, 1987.
- ⁹Underdown, R. B., *Ground Studies for Pilots*, Vol. 4, *Meteorology*, BSP Professional Books, London, 1990.
- ¹⁰*WBAN Manual of Surface Observations*, 'Circular N,' U.S. Weather Bureau, Washington, DC.
- ¹¹Elsom, D., *Atmospheric Pollution*, Blackwell, England, 1987.
- ¹²Grennfelt, P., and Schjoldager, J., "Photochemical Oxidants in the Troposphere: A Mounting Menace," *Ambio*, Vol. 13, Nos. 61-67, 1984.
- ¹³Smith, J. T. M., *Aircraft Noise*, Cambridge Univ. Press, Cambridge, England, UK, 1989.
- ¹⁴Dobson, G. M. B., *Exploring the Atmosphere*, Clarendon, Oxford, England, UK, 1968.

¹⁵Whitten, R. C., and Vaughan, W. W., *Guide to Reference and Standard Atmospheric Models*, AIAA, Washington, DC, 1988.

¹⁶Minzner, R. A., Champion, K. S. W., and Pond, H. L., *The ARDC Model Atmosphere*, 1959, Air Force Cambridge Research Center Rept. No. TR-59-267, U.S. Air Force, Bedford, MA, 1959.

¹⁷*Manual of the ICAO Standard Atmosphere*, Doc. 7488/2, 2nd ed., 1964.

¹⁸*U.S. Standard Atmosphere*, 1976, National Oceanic and Atmospheric Administration (NOAA), National Aeronautics and Space Administration (NASA), U.S. Air Force, Washington, DC, October 1976.

¹⁹Ananthasayamam, M. R., and Narasimha, R., "A Proposed International Tropical Reference Atmosphere up to 1000 km," *Advances in Space Research*, Vol. 7, No. 10, pp. (10)117-(10)131, 1987.

²⁰Miele, A., *Flight Mechanics, Vol. 1, Theory of Flight Paths*, Addison-Wesley, Reading, MA, 1962.

²¹Hale, F. J., *Aircraft Performance, Selection, and Design*, Wiley, New York, 1984.

Problems

In the multiple choice problems below, mark the correct answer.

2.1 Earth receives heat and loses heat by a) long waves and short waves, respectively; b) short waves and long waves, respectively; c) short waves only.

2.2 Albedo of the Earth means a) the absorbing power of the Earth which raises its surface temperature, b) the net solar radiation reflected back into space by the Earth and its atmosphere, c) the total energy received by the Earth.

2.3 Which of the following statements are correct? a) The approximate ratio of oxygen to nitrogen in the atmosphere by volume is 1 : 4 and by weight 1 : 3; b) The carbon dioxide content of the atmosphere is 0.3%; c) Moist air has lower density than dry air; d) If $y^{\circ}\text{F}$ correspond to $x^{\circ}\text{C}$, $y = (2x - x/5) + 32$. e) 0°C , 15°C , 37°C , and 100°C are equal to 32°F , 59°F , 98.6°F , and 212°F , respectively.

2.4 The rise in the surface temperature during day would be a) the same over both wet and dry lands, b) greater over wet land than over dry land, c) less over wet land than over dry land.

2.5 Temperature inversion in the atmosphere causes a) increase in temperature with altitude in stratosphere, b) increase in temperature with altitude in troposphere, c) temperature to remain constant with the change of altitude.

2.6 At a given pressure, the density of air varies a) directly with the temperature in K , b) inversely with the temperature in $^{\circ}\text{C}$, c) inversely with the temperature in K .

2.7 The value of the gas constant for moist air is a) more than that of the dry air, b) less than that of the dry air, c) the same as that of the dry air.

2.8 The intertropical convergence zone is a) the zone of convergence between northeast and southeast trade winds, b) an area of low-pressure trough over the Indian Ocean, c) a trough of low pressure over the Pacific Ocean.

2.9 Winds move a) normal to the Earth, b) inclined to the Earth's surface, c) approximately parallel to the Earth's surface.

2.10 A katabatic wind is a) a warm wind that blows up the mountain slopes, b) a cold wind that blows up the mountain slopes, c) a cold wind that blows down the mountain slopes.

2.11 In the northern hemisphere the winds are deflected to the right due to rotation of Earth. The force causing this deflection is called a) Buys-Ballot's force, b) force due to pressure gradient, c) Coriolis force.

2.12 Which of the following storms is not a tropical revolving storm a) cyclone, b) tornado, c) typhoon.

2.13 Thermal currents are due to a) convergence of air on the ground, b) lifting of air by upslopes of mountains, c) local heating at certain places on the Earth.

2.14 Changes in temperature cause variation in a) the Reynolds number of flight, b) the Mach number of flight, c) both the Reynolds and Mach numbers of flight.

2.15 The mass of water vapor per unit mass of dry air, expressed generally in grams per kilogram, is referred to as a) relative humidity, b) mixing ratio, c) absolute humidity.

2.16 At a given temperature and pressure, the water vapor has a) a greater density than dry air, b) a lesser density than dry air, c) the same density as dry air.

2.17 Clouds with "stratus" in their names are a) rain bearing, b) fibrous, c) layer type.

2.18 In India, the heights of clouds a) are generally lower in summer than in winter, b) are generally higher in summer than in winter, c) do not vary with the seasons.

2.19 A sheet of cloud that produces a halo around the sun is a) cirrostratus, b) altostratus, c) nimbostratus.

2.20 When cumulonimbus clouds are reported a) stratus clouds may also be present, b) stratus clouds will not be present, c) both stratus and nimbostratus clouds will also be present.

2.21 Isosterics are the lines of a) constant humidity, b) constant density, c) constant pollution.

2.22 The dry adiabatic lapse rate is a) $9.8^{\circ}\text{C}/\text{km}$, b) $6.5^{\circ}\text{C}/\text{km}$, c) $5.5^{\circ}\text{C}/\text{km}$.

2.23 In conditional instability the environmental lapse rate a) lies between DALR and SALR, b) is more than dry-air adiabatic lapse rate, c) is less than saturated air adiabatic lapse rate.

2.24 Which of the following statements are not correct? a) Among the clouds, altostratus, stratocumulus, and stratus, the last cloud has the lowest base height. b) Temperature inversion indicates that the atmosphere is absolutely stable. c) Isothermal layer indicates that the atmosphere is absolutely stable. d) Water absorbs more heat than sand. e) On a hot humid day at an airfield, the air density will be more than the average of the year at that place.

2.25 Which of the following statements are correct? a) Differential heating is caused due to different specific heats of terrains. b) Water has more specific heat than ice. c) Materials with low specific heats get cool and are warmed quickly. d) Water vapor has more specific heat than dry air. e) Increase in vapor pressure causes reduction in air density.

2.26 Which of the following statements are correct? a) Easterly winds blow toward the east. b) Arctic sea smoke is a cloud. c) When the whole sky is covered with clouds, the cloud ceiling is said to be unlimited. d) Standard atmosphere does not consider winds. e) Pressure altitude is the standard altitude.

2.27 Which of the following statements are correct? a) Tailwinds are favorable to reducing the time of travel. b) Pressure pattern flying is practiced by birds. c) Temperature inversions are formed by radiation heating. d) In the troposphere, lapse rate is negative. e) The atmospheric boundary layer is generally about 10 m thick.

2.28 Which of the following statements are not correct? a) Formation of frost over the aircraft surface increases drag. b) Clouds are always harmful to flight. c) Flight is not seriously affected by cumulonimbus clouds. d) Fog may sometimes become cloud. e) Pressure patterns help a pilot in weather forecasting.

2.29 A front is a) a boundary of thunderstorms, b) a narrow transition zone between two different types of air masses, c) a boundary of thick layer of clouds.

2.30 A warm front brings a) good flying weather, b) clear but not unstable air, c) fog and poor visibility.

2.31 The altitude of tropopause a) is highest near the equator and lowest near the poles, b) is lowest near the equator and highest near the poles, c) does not vary with latitude.

2.32 Noise pollution is maximum near a) nose of the aircraft, b) jet exhaust, c) seats of passengers.

2.33 Atmospheric pollution may a) increase the length of takeoff run, b) decrease the landing roll, c) decrease the aerodynamic drag.

2.34 Using Eq. (2.5), Eqs. (2.8–2.11), and Fig. 2.11, find the values of θ , δ , and σ for standard atmosphere at a) $h_G = 22$ km, and b) $h_G = 25$ km.

2.35 Using Eq. (2.5), Eqs. (2.8–2.11), and Fig. 2.11, find the values of θ , δ , and σ for standard atmosphere at a) $h = 22$ km, and b) $h = 25$ km.

2.36 Find the percentage error in the values of θ , δ , and σ for standard atmosphere at the altitudes of $h = 22$ km and $h = 25$ km when h is considered equal to h_G (the results of Problems 2.34 and 2.35 can be used).

2.37 Find the values of θ , δ , and σ at the altitude of $h = 11$ km when a) $\lambda = -5$ K/km, b) $\lambda = 0$ K/km, and c) $\lambda = 5$ K/km. Find the percentage error in each case when compared with the standard atmospheric values given in Table 2.2a.

This page intentionally left blank

3

Aerodynamic Forces on Aircraft

3.1 Introduction

The subject of *aerodynamics* deals with the behavior of air flow and the forces the air exerts on a body during their relative motion. Air is invisible and is a very light, fluid medium, but it has the capability of lifting modern jumbo jets weighing around 400 tons. A discipline dealing with such “unbelievable” capacities has to be of interest to most of us. The subject of aerodynamics is covered in so many standard books that it is difficult to justify presenting its most important ideas in just one chapter. Therefore, some basic ideas of aerodynamics are described here that make this book self-contained for the purpose of calculating the performance of aircraft during the preliminary design stage, and estimating their performance through flight tests.

It is important to understand air flow behavior because it is intimately connected with the pressure field around the body. Certain elements of the vocabulary of aerodynamic flows are explained here first before discussing the airfoil, which is the fundamental lifting element. A good knowledge of the flow and pressure fields around an airfoil is necessary for understanding the nature of aerodynamic forces on wings, fuselage, aircraft, or any other lifting or nonlifting surface. A more practical aerodynamic surface is a wing which is used for producing lift in an aircraft. Research has been carried out to discover wing designs with maximum lift and minimum drag, and this has led to the development of many high-lift devices which are commonly used on a modern aircraft. In addition, small lifting surfaces are used to stabilize and control the motion of an aircraft.

Performance calculations require lift and drag forces acting on the complete aircraft. Aerodynamic characteristics of an aircraft are discussed here because its lift and drag coefficients, drag polar, and maximum lift coefficient enter directly into performance calculations.

Both experiments and theory have led to the development of certain useful concepts in aerodynamics. Experiments are usually carried out in wind tunnels. The measurements of velocity and pressure fields, determination of aerodynamic forces, and flow visualization studies, are important characteristic features of aerodynamic experiments. Aerodynamics is one of those fortunate subjects that has a sound theoretical base, but the difficulties lie in solving its theoretical formulation. Several simplifications are made but only some of their results are presented here, and these are used in the subsequent chapters of this book.

3.2 Air Flow Characteristics

Atmospheric air is the fluid medium through which an aircraft moves and generates aerodynamic forces. Flowfield around an aircraft or any other body is directly connected with its pressure field, which dictates aerodynamic forces. Air

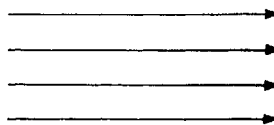


Fig. 3.1 Particle path in laminar flow.

flow characteristics mentioned here are common to all gas flows and most of them remain the same to all Newtonian fluids.

3.2.1 Viscous and Inviscid Flows

Viscosity is the property of fluid that distinguishes it from one fluid (liquid or gas) to another. The shear stress at a point varies linearly with the rate of strain in a Newtonian fluid. The constant of proportionality of this linear variation is called the *coefficient of viscosity* which is usually denoted by μ ; air is a Newtonian fluid whose $\mu = 1.79 \times 10^{-5}$ kg/(ms) in the standard atmosphere at sea level. If the stress-strain variation is not linear it is called non-Newtonian fluid. The viscosity causes the layers of fluid particles in contact with the solid surface to stick to the surface over which the fluid flows. All the real fluids are viscous. An inviscid fluid has no viscosity and it is also referred to as an ideal fluid. An inviscid fluid is just an idealization of a real fluid for mathematical simplification which has served useful purposes in understanding certain fluid flow phenomena.

3.2.2 Steady and Unsteady Flows

A fluid flow is *steady* when its velocity field is invariant with time, both in magnitude and direction. Similarly, there is no change in pressure, density, and temperature with time in a steady flow. If the flow is not steady it is called *unsteady flow*. A fluid flow in nature is generally unsteady. The atmospheric changes, turbulence, flow separation over surfaces, and aircraft vibrations cause unsteady flow of air past an aircraft.

3.2.3 Laminar and Turbulent Flows

The flow with fluid particles moving smoothly over one another in parallel layers or *laminas*, is called laminar flow, as shown in Fig. 3.1. There is no intermixing between the adjacent layers or particles on molar scale. At a fixed point in laminar flow the speed and direction of the flow does not change erratically with time. While moving over a surface, the laminar flow may become unstable and turbulent after a short distance.

In a turbulent flow the mixing of fluid layers is on molar scale, because the fluid particles of different sizes coming from neighboring layers are continuously in the process of agglomeration, disintegration and moving erratically from one place to another, as shown in Fig. 3.2. The velocity fluctuations at a point shown

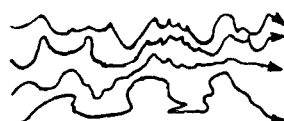


Fig. 3.2 Particle path in turbulent flow.

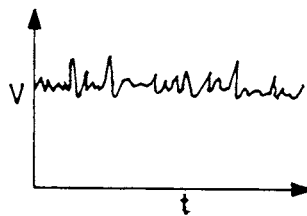


Fig. 3.3 Velocity fluctuations in turbulent flow.

in Fig. 3.3 are irregular and of high frequency. In nature, the flow of air or water over solid surfaces is mostly turbulent. A turbulent flow is less prone to separation from the surface over which it flows, as compared to a laminar flow.

3.2.4 One-, Two-, and Three-Dimensional Flows

A flow is generally three-dimensional in nature because it is free to move in any direction in space. One- or two-dimensional flows are approximations of real flows for mathematical simplification depending on the situations involved. One-dimensional flow neglects the variations of flow properties normal to the direction of flow. In two-dimensional flow, the motion of fluid particles is identical in the parallel planes containing the direction of flow.

3.2.5 Boundary-Layer Flow, Its Separation, and Its Reattachment

The external flowfield over the surface of a body in most real cases can be divided into boundary-layer flow near the surface, and potential flow away from the surface. The boundary layer (b.l.) region is a thin layer in the immediate neighborhood of the surface of a body. The viscous effects are predominant and velocity changes rapidly across the boundary layer. The dashed line in Fig. 3.4 is the common boundary between the boundary layer and the potential flow regions. The flow in the potential region is irrotational and can be regarded as inviscid. The boundary layer is laminar from the leading edge at O (Fig. 3.4) to station A, and it becomes fully turbulent from station B. The short length AB is the transition region of the boundary layer containing partly laminar and partly turbulent flows. The concept of the boundary layer has been found very useful in aerodynamics and it has been further extended to higher-order boundary layers.¹

In adverse pressure gradients along the surface, the boundary layer may separate from the surface as shown in Fig. 3.5. The flow separation alters the pressure

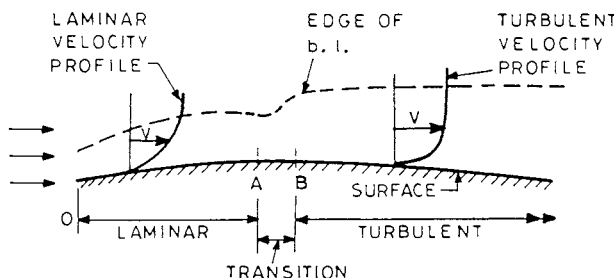


Fig. 3.4 Boundary-layer flow.

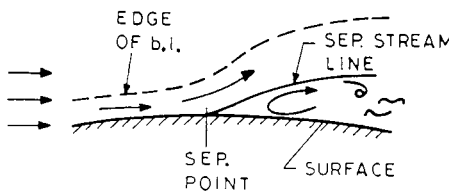


Fig. 3.5 Boundary-layer separation.

and velocity fields, reduces the lift of a lifting surface, and increases its drag. If a laminar boundary layer separates, it may in certain cases reattach again as a turbulent boundary layer at the downstream of the two-dimensional flow as shown in Fig. 3.6. The region between the laminar separation and the turbulent reattachment is called the *laminar separation bubble*. The three-dimensional boundary layer flow separations and reattachments are distinguished by Maskell² on the basis of limiting streamlines on the surface.

3.2.6 Wake and Vortices

The boundary layer, or its separation, after leaving the trailing edge becomes a free shear layer which is commonly referred to as the *wake*. The wake region starts from the trailing edge and extends far downstream as shown in Fig. 3.7 for the flow past an airfoil. The wake thickness increases slowly in the downstream direction and the velocity across the wake is nonuniform and unsteady. The larger the separated flow region, the thicker the wake, the smaller the pressure recovery near the trailing edge, and hence the higher the pressure drag on the body.

The localized regions of a fluid medium, moving in circular or helical path in the boundary layer or wake regions, are called *vortices*. A laminar separation bubble has a steady vortex or vortices. Flow separations behind two-dimensional objects have alternate shedding of vortices, called the *Karman vortex street*.³ Fluid particles separating from the tip of a wing and moving in a helical path are called *tip vortices*, which become a part of the trailing edge vortices.⁴ Similar vortices also emerge from the leading edge of a highly swept-back wing and continue to show their presence in the wake region.

3.2.7 Irrotational and Rotational Flows

A flowfield is irrotational if the curl of the velocity vector \bar{V} at each point in the flowfield vanishes. This is more of an idealization for mathematical simplification found for inviscid flows. In an irrotational flow the velocity potential ϕ exists,

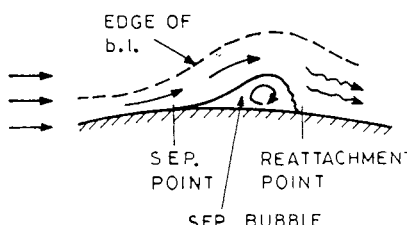


Fig. 3.6 Laminar separation bubble.

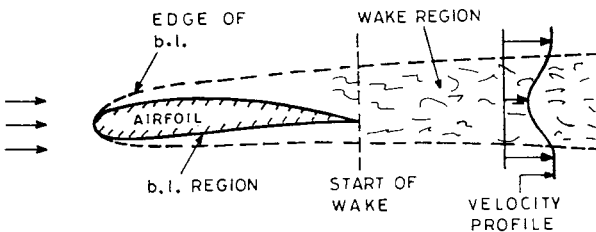


Fig. 3.7 Wake behind airfoil.

such that the differentiation of ϕ in any particular direction gives the velocity in that direction. Potential flow theory has given rise to the concepts of source, sink, vortex, doublet, etc., which are called singularities of the flowfield. The flows in nature in the neighborhood of objects are generally rotational where $\text{curl } \vec{V} \neq 0$. In other words, the flows in the boundary layers, wakes, shear layers, and trailing vortices are all rotational flows.

3.2.8 Incompressible and Compressible Flows

Air is certainly a compressible gas, but the flow of air can be regarded as that of incompressible air if the airspeed is much below the speed of sound. It may apparently appear strange at first sight to find the occurrence of the speed of sound in the flowfield. Its importance can, however, be explained. The relative motion between the object and the air continuously sends the infinitesimally small pressure waves in all directions with the speed of sound. The ability of the fluid particles to adjust themselves and acknowledge the presence of the object depends on how much earlier they have realized the presence of the object through the pressure signals. If the relative velocity is sufficiently less than the speed of sound in the fluid medium, the fluid particles are able to adjust themselves without feeling compression and the flow is said to be incompressible. The density changes in incompressible flow are negligible compared to the pressure changes in the fluid medium. It is shown below in Sec. 3.3 that Mach number is an important parameter in a compressible flow. Along with compressibility, the corresponding changes in the density, temperature, and viscosity of air also enter into the flow problem.

3.2.9 Shock and Expansion Waves

The formation of shock and expansion waves is a characteristic feature of a supersonic flow. A supersonic flow generally decelerates through single or multiple shocks, and accelerates through expansion waves. A *shock wave* is a thin boundary surface in the flowfield across which the pressure, velocity, density, and static temperature change almost discontinuously. A shock wave is formed whenever the supersonic flow turns into the oncoming flow, as shown in Figs. 3.8 and 3.9. The shock waves shown in these figures are *oblique shocks*, but if the shock surface is perpendicular to the oncoming flow, it is called *normal shock*. The higher the static pressure rise across the shock, the greater the shock strength. Across a shock, the stagnation (total) temperature remains constant, whereas the stagnation pressure decreases and consequently there is a loss of flow energy across the shock.

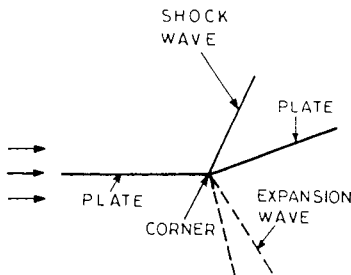


Fig. 3.8 Shock and expansion waves at the corner.

An expansion wave is formed whenever there is turning, away from the oncoming flow, as shown in Figs. 3.8 and 3.9. Unlike a shock wave, an expansion wave occupies a finite width which is shown by the dashed-line boundaries in the figures. Across an expansion wave the static pressure, density, and temperature decrease rapidly and smoothly. The airspeed and Mach number increase across the expansion wave and there is no loss of flow energy across it.

3.3 Flow Parameters

Flow parameters are the groups of fluid flow variables that help to reduce the total number of variables in a flow problem. This simplifies experimental and analytical works and improves on their presentation to a more compact form. For example, the pressure p at a fixed point around a given body depends on the density ρ , velocity V , temperature T , coefficient of viscosity μ , and the speed of sound a , in the fluid medium. Instead of working with these variables, it is possible to find nondimensional flow parameters that would control the nondimensional pressure field around the body. The two important flow parameters are Reynolds number and Mach number. These parameters can be obtained either by applying Buckingham's π -theorem or by nondimensionalizing the Navier–Stokes equations, which are the fundamental governing equations for all Newtonian fluid flow problems. There are also some other flow parameters⁵ but they are not of interest in the context of this book.

3.3.1 Reynolds Number

The existence of the Reynolds number is due to British scientist Osborne Reynolds (1842–1912). The nondimensional quantity $\rho V c / \mu$ is called Reynolds

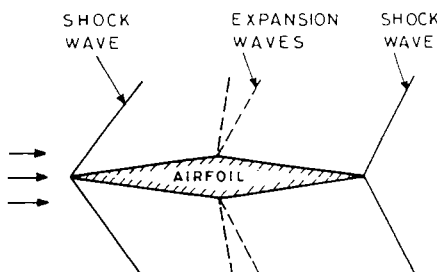


Fig. 3.9 Shock and expansion waves on supersonic airfoil.

number, where the ratio μ/ρ is known as kinematic viscosity and c is the characteristic length of the body, say chord length in the case of an airfoil. In a flowfield past an aircraft, Reynolds number mostly varies from about 10^4 to 10^9 . The influence of Reynolds number is negligible on streamlined bodies exhibiting no appreciable regions of flow separation. The influence of Reynolds number is noticeable when the separated flow regions extend appreciably on the surface of the body.

3.3.2 Mach Number

The existence of the Mach number is due to a German scientist, Ernst Mach (1838–1916), who recognized the importance of the ratio of airspeed V to the speed of sound a . The ratio V/a is called the Mach number which is denoted by M . If M is less than about 0.3, the flow is considered incompressible. The compressibility effects increase with the increase of M . The design of aerodynamic surfaces depends upon the Mach number range in which they mostly operate. Airspeeds are often classified in terms of Mach numbers. Thus there may be low airspeed ($M \ll 1$), subsonic airspeed ($M < 1$), transonic airspeed ($M \approx 1$), supersonic airspeed ($M > 1$), and hypersonic airspeed ($5 < M < 40$). Each Mach number range has certain characteristic flow features and their mathematical formulations and solutions are also different.

3.4 Airfoils

An airfoil is a streamlined body, or a lifting surface, of simple shape that provides sufficient lift and considerably less drag at small angles of attack. An airfoil is considered to be a two-dimensional body because its geometric sections normal to span do not change. Modern airfoils have evolved after years of theoretical and experimental research. The design philosophy of an airfoil, is useful in many other disciplines that use Newtonian fluids. The geometric and aerodynamic characteristics of airfoils used in the design of wings of an aircraft are explained here.

3.4.1 Geometric Features of Airfoils

The characteristic geometric features of an airfoil distinguishing it from one airfoil to another are shown in Fig. 3.10. The distance between its leading edge (LE) and trailing edge (TE) is called the chord length or simply *chord* of the airfoil, which is denoted by c . The maximum distance between the upper and lower

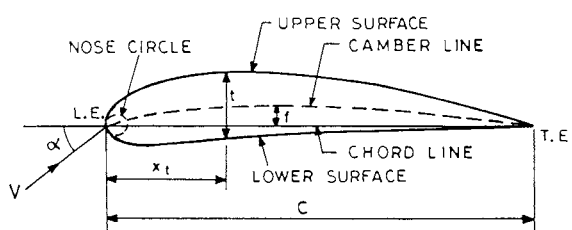


Fig. 3.10 Airfoil geometry.



Fig. 3.11 Subsonic airfoils: a) low-speed airfoil, b) high-subsonic airfoil, and c) supercritical airfoil.

surfaces of an airfoil, measured normal to its chord line, is called the maximum thickness or simply the thickness t . The position x_t of the maximum thickness, aft of the LE, measured along the chord line, is also an important geometric variable of the airfoil. A *camber line* or *mean line* is the locus of points, halfway between the upper and lower surfaces of the airfoil when measured normal to the chord line. The maximum distance of the camber line from the chord line is called the maximum camber or simply camber, which is denoted by f . The position x_f of the maximum camber, aft of the LE, is also specified. An airfoil that is symmetrical about its chord line has zero camber. An airfoil surface is highly curved at the LE and it is common to specify the LE radius. The angle between the chord line and the oncoming flow direction is called the *angle of attack* or *incidence* of the airfoil and is denoted by α . It is customary to express t , x_t , f , x_f as a percentage of chord. Typical low-speed airfoils have maximum thickness of 12–18% of chord ($t/c = 0.12$ –0.18), the position of maximum thickness is at 30–40% of chord ($x_t/c = 0.3$ –0.4), and the camber is 2–3% of the chord ($f/c = 0.02$ –0.03). Various nomenclatures exist^{7,8} to designate the airfoils. To obtain the precise shape of a subsonic airfoil surface, the LE radius and the coordinates of the upper and lower surfaces from the chord line are specified at close intervals.⁸

High subsonic and transonic airfoils have the same characteristic features as above except that these are thinner with thin, round, leading edges. These airfoils are designed to delay the critical and drag-rise Mach numbers. Recently, *supercritical airfoils* have been designed⁵ for transonic flows which considerably delay the drag-rise Mach number. Figure 3.11 shows a low-speed airfoil and two high-subsonic airfoils.

Supersonic airfoils are quite different from low-speed or high-subsonic airfoils. These are of sharp leading edge, thinner, have no camber, and are doubly symmetrical. Three different supersonic airfoils, namely, biconvex, double wedge (diamond shape), and quadruple wedge (hexagonal shape) are shown in Fig. 3.12. They are designed to obtain sufficient lift with minimum wave drag. Airfoil thickness and asymmetry with respect to mid-chord do not contribute to lift but only add to drag in a supersonic flow. Some minimum thickness is, however, required for structural strength and storage.

3.4.2 Aerodynamic Characteristics of Airfoils

Aerodynamic characteristics deal with the important features of velocity and pressure fields and the behavior of aerodynamic forces on the body. The streamlines

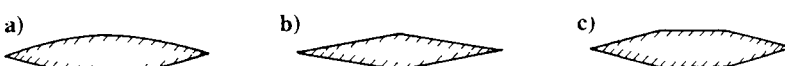


Fig. 3.12 Supersonic airfoils: a) biconvex airfoil, b) double-wedge airfoil, and c) hexagonal airfoil.

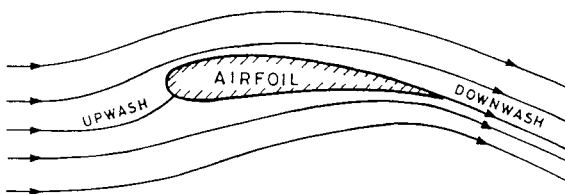


Fig. 3.13 Streamlines of flow without separation on airfoil.

of flow past an airfoil in the absence of their separation from the surface are shown in Fig. 3.13. The turning of streamlines upward, below the LE of the airfoil, is called *upwash*, and the downward turning, downstream of its trailing edge, is called *downwash*. The larger the upwash and downwash, the higher the lift due to increase in flow circulation⁹ around the airfoil.

The flowfield past an airfoil at small incidence consists of boundary-layer flow near the surface and the outer inviscid flow. Initially the boundary layer is laminar near the LE, and after a short distance downstream, it usually becomes turbulent on both the upper and lower surfaces. The turbulent boundary layer separates on the upper surface near the TE because of adverse pressure gradients. The separation point moves upstream with increase in the incidence of the airfoil and causes large regions of flow separation on the surface. Certain thin subsonic airfoils exhibit the formation of a laminar separation bubble on the upper surface near the LE. These bubbles are of two types—short and long—which have different characteristics.^{10,11} With the increase in airfoil incidence, the short bubble contracts in length but increases in height (Fig. 3.14) until at some incidence it fails to reattach, and this failure of reattachment is called *bursting* of the short bubble. The length and height of a long bubble, on the other hand, progressively increases with the increase in incidence, as shown in Fig. 3.15. The flow separations and bubble formations cause the three different types of stalls,¹⁰ which are called TE, LE, and thin airfoil stalls.

The static pressure distribution p on the upper and lower surfaces of the airfoil is usually expressed in the form of nondimensional pressure coefficient, C_p , which is defined as $C_p = 2(p - p_\infty)/\rho V^2$, where p_∞ , ρ , and V are, respectively, the pressure, density, and velocity of the oncoming freestream. A typical variation of C_p against x/c is shown in Fig. 3.16, where x is the distance along the chord line, measured from the LE of the airfoil. On the upper surface of the airfoil, the pressure first decreases, which is called a negative or favorable pressure gradient, and then slowly increases. The increasing pressures in the direction of flow are called positive or adverse pressure gradients, and are responsible for the flow separation on the surface. According to inviscid flow theory, the pressure coefficient at a point in subsonic flow is related to the incompressible flow pressure coefficient at the same point. If the subscripts c and i represent compressible subsonic and

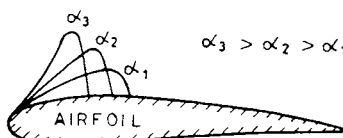


Fig. 3.14 Development of a short bubble.

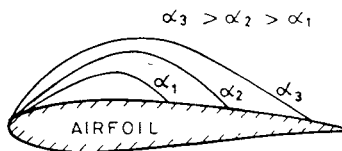


Fig. 3.15 Development of a long bubble.

incompressible flows, respectively, the pressure coefficients in the two regions are obtained from the Prandtl-Glauert similarity rule,¹² $C_{p_c} = C_{p_i}/\sqrt{1 - M^2}$, where M is the freestream Mach number. This shows that the pressure coefficient at a point in subsonic flow is increased due to compressibility.

The forces due to static pressure and skin friction, acting at each point on the surface of the airfoil, constitute the basic aerodynamic forces whose resultant acts at the center of pressure. The component of this resultant force along the normal to the oncoming flow direction is called lift force or *lift*. Similarly, the component of resultant force along the downstream direction of the oncoming flow is called drag force or *drag*. The directions of lift and drag are orthogonal to each other. These forces are usually expressed in the forms of lift and drag coefficients which are, respectively, denoted by C_l and C_d , and are defined as $C_l = 2l/(\rho V^2 c)$ and $C_d = 2d/(\rho V^2 c)$, where l and d are, respectively, the lift and drag per unit span of the airfoil.

For a given cambered airfoil at specified Reynolds and Mach numbers, the variations of C_l and C_d with angle of attack are shown in Figs. 3.17 and 3.18, respectively. The C_l versus α curve has the maximum value of lift coefficient, $C_{l,m}$, at $\alpha = \alpha_s$, which is called the *stalling angle* of the airfoil. The airfoil stalls due to large regions of flow separation on its upper surface. The C_l versus α curve of a given airfoil depend on the Reynolds number and Mach number of the flow. The dependence on the Reynolds number becomes important near the stalling angle.¹³ Mach numbers assume importance in compressible flow regions, and more significantly so when a shock appears on the surface.

The movement of shock on an airfoil surface in transonic flow is shown in Fig. 3.19. First a shock appears on the upper surface (Fig 3.19a). As the Mach number increases, the upper surface shock moves downstream and another shock appears on the lower surface (Fig. 3.19b) which moves faster and reaches the

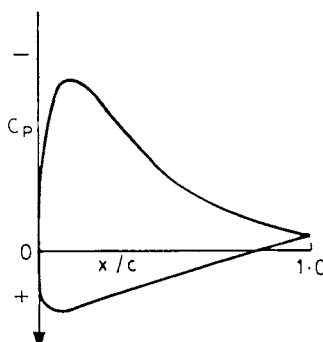
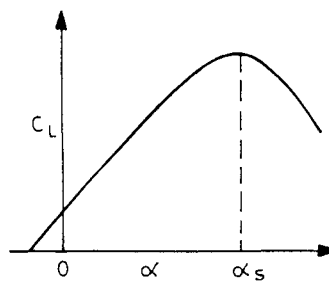
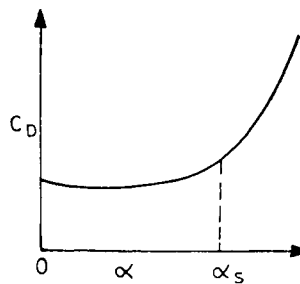
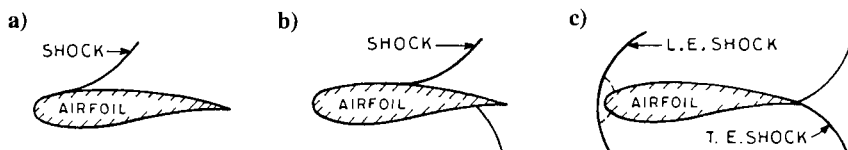


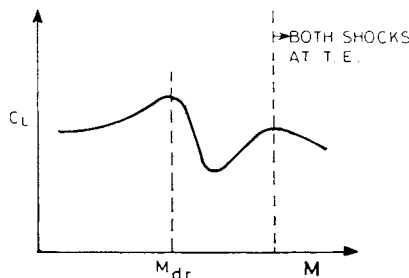
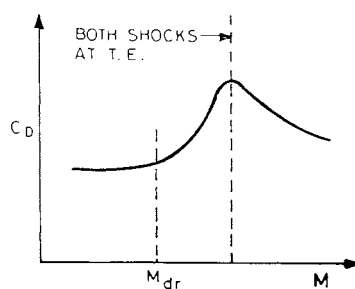
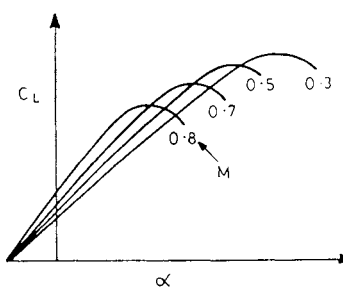
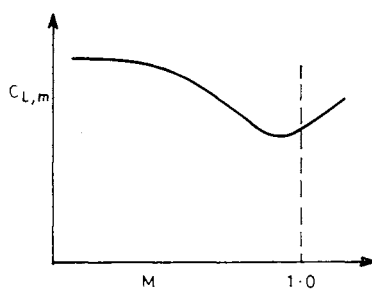
Fig. 3.16 Surface C_p distribution.

Fig. 3.17 C_L versus α .Fig. 3.18 C_D versus α .

trailing edge earlier. The strengths of these shocks also increase during their downstream movement, and the upper surface shock may cause a large-scale flow separation resulting in shock stall. In a supersonic flow, the shocks on the upper and lower surfaces settle at the trailing edge and another shock appears in front of the LE as shown in Fig. 3.19c. The movements of these shocks change C_l and C_d with the increase in freestream Mach number as shown in Figs. 3.20 and 3.21. The relationship between C_l and C_d at a fixed Mach number is mathematically approximated by a parabola, called *drag polar*. The effect of Mach number on C_l versus α curve is shown in Fig. 3.22. Although the lift coefficient at a given angle of attack increases with Mach number, yet the stalling angle and the maximum lift coefficient decrease. The variation of $C_{l,m}$ versus M , as obtained from Fig. 3.22, is plotted in Fig. 3.23.

The value of the freestream Mach number, at which the local Mach number somewhere on the surface of the airfoil reaches unity, is called the *critical Mach number* of the airfoil. In subsonic flow, above the critical Mach number, the flow over the airfoil is partly subsonic and partly supersonic. Increasing the freestream

Fig. 3.19 Movement of shock in transonic flow: a) $0.6 < M_1 < 1$, b) $M_1 < M < 1$, c) $M_1 > 1$.

Fig. 3.20 Changes in C_L with Mach number.Fig. 3.21 Changes in C_D with Mach number.Fig. 3.22 C_L versus α curves for different M .Fig. 3.23 $C_{L,m}$ versus M .

Mach number above the critical Mach number produces shock that becomes stronger to cause shock stall. The value of the freestream Mach number in a subsonic flow, at which the drag of the airfoil starts rising rapidly due to shock, is called the *drag rise Mach number* and is denoted by M_{dr} .

3.5 Wings

A *wing* is a thin lifting surface of finite span. The thickness of a wing is much less than its span or chord. Generally a wing is symmetrical about the normal plane passing through the root chord of its central section. The geometric features and aerodynamic characteristics of wings are explained here.

3.5.1 Geometric Features of Wings

There are several geometric features that distinguish one wing from the other, such as wing planform, taper ratio, span, aspect ratio, sweep angle, and twist. The most important is the shape of wing and the area of its *wing planform*. The wing planform is the projection of the wing surface onto a plane parallel to the wing chords; in the case of a twisted wing the projection is made onto a specified plane. The wing planform area S is commonly used for nondimensionalizing aerodynamic forces and moments. The shape of a wing planform can be rectangular, elliptical, crescent, delta, etc.¹⁴ The chord of a wing generally varies along the span, which is called a tapered wing planform. The chords at the root and the tip are called the root-chord and the tip-chord, respectively, as shown in Fig. 3.24 for a swept-back tapered wing. The ratio of the tip-chord to the root-chord is called the *taper ratio*, and is generally less than unity. Similarly, the thickness distribution of a wing may be tapered along the span. The linear distance between the two tips of a wing is called the *span* of the wing.

The *aspect ratio* (AR) of a wing is the ratio $(\text{span})^2/S$. It is an important nondimensional geometric parameter of the wing, indicating how many times the wing span can be compared to its mean chord. The angle (in degrees) that the quarter-chord line makes with the lateral axis is called the *sweep angle*, denoted by Λ ; sometimes the LE line or maximum thickness line of the wing is considered instead of the quarter-chord line for defining the sweep angle. If the incidence of its airfoil sections varies along the span, the wing is said to be a *twisted wing*; the chord lines of a twisted wing are not parallel. In case the plane of the wing is inclined to the horizontal on both of its symmetrical sides, the wing is said to be *dihedral*, a design that is able to stabilize rolling moment during sideslip of the aircraft.

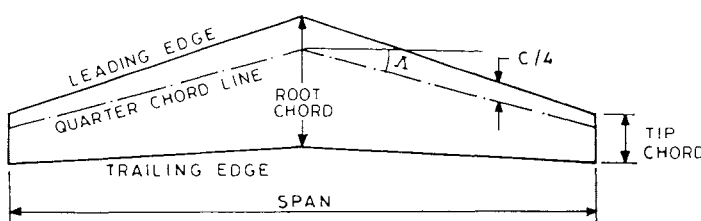


Fig. 3.24 Basic wing geometry.

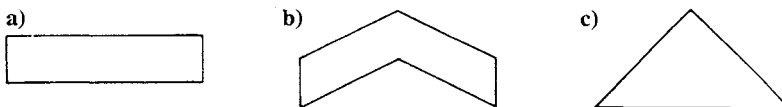


Fig. 3.25 Three different wing planforms: a) rectangular wing, b) swept-back wing, and c) delta wing.

The numerical values of different wing design parameters mentioned above can be found in Torenbeek's book¹⁵ for different aircraft. Low-speed wings have a large AR, are tapered, have no sweep, and use low-speed airfoil sections. High-subsonic wings have medium AR, are tapered, are swept-back (generally) or swept forward, and use high-subsonic airfoil sections. Supersonic wings are thin, have a low AR, are highly swept-back or of delta wing design, and employ supersonic airfoil sections. Three different wing planforms corresponding to the three different Mach number regions are shown in Fig. 3.25.

3.5.2 Aerodynamic Characteristics of Wings

Since a wing is the envelope of its airfoil sections, the aerodynamic properties of the wing resemble those of the airfoil but are appreciably influenced by the three-dimensional behavior of the flow past the wing; the smaller the span, the larger is the three-dimensional behavior of the flowfield. The boundary layer flow past a wing is initially laminar near the leading edge but becomes turbulent as it moves toward the trailing edge. The boundary layer flow may separate near the trailing edge and the separation line shifts upstream and extends along the span, producing larger separation regions as the angle of attack of the wing increases. Over swept-back wings the boundary layer drifts toward the tips, which causes it to separate earlier near the trailing edge close to the tips. The region of the first boundary layer separation and its spread with increasing angle of attack depends on the type of the wing, as shown in Fig. 3.26. The wavy lines in the figure show the boundary layer separation regions and the arrows show the direction of their spread as the angle of attack increases. The boundary layer on rectangular or moderately tapered wings separates first near the root, whereas on highly tapered or swept-back wings it separates first near the tip. A wing is swept back to alleviate compressibility effects.¹⁶ A special feature of wings is the formation of tip vortices which pass downstream in a helical path as shown in

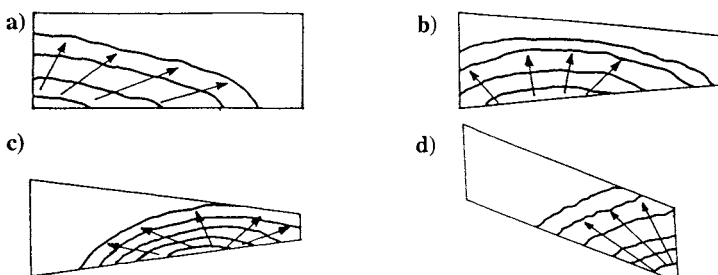


Fig. 3.26 Spread of separation regions on different wings: a) rectangular wing, taper ratio, $\lambda = 1.0$; b) moderate-taper wing, taper ratio, $\lambda = 0.5$; c) high-taper wing, taper ratio, $\lambda = 0.25$; and d) swept-back wing.

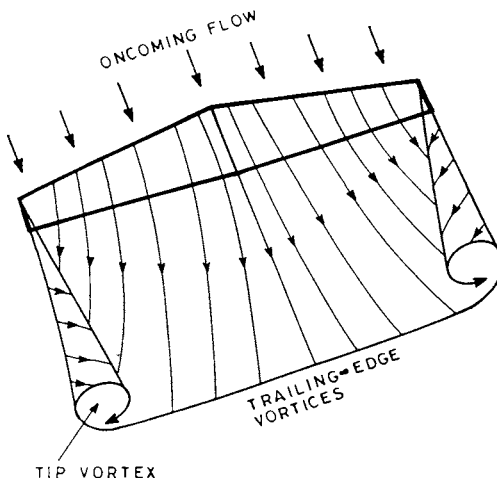


Fig. 3.27 Trailing-edge and tip vortices of a wing.

Fig. 3.27. Similar vortices emerge from the LEs of highly swept-back or delta wings.

The surface pressure distribution over a wing section normal to the span resembles that shown in Fig. 3.16. The magnitude of C_p varies along the span, causing variations in the sectional lift and drag coefficients, denoted by C_l and C_d , respectively. A typical variation of the sectional lift coefficient along the span is shown in Fig. 3.28 for straight and swept-back wings. The swept-back wing has more aerodynamic load at the tip than that of the straight wing, and the sectional lifts of both the wings drop to zero at the tips.

The lift and drag forces are the orthogonal components of aerodynamic forces acting on the wing. The lift force, by definition, is normal to the oncoming flow, and the drag force is in the downstream direction of the oncoming flow. The lift and drag forces are denoted by L and D , respectively, and are often used in non-dimensional forms as lift and drag coefficients. The lift and drag coefficients are denoted by C_L and C_D , respectively, and are defined as $C_L = 2L/(\rho V^2 S)$ and $C_D = 2D/(\rho V^2 S)$, respectively.

The lift and drag coefficients of a specified wing depend on its angle of attack, Mach number, and AR. The variations of C_L and C_D of a wing, along with changes in α and freestream Mach number, are similar to that shown for an airfoil. The

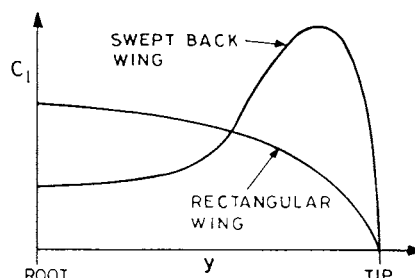


Fig. 3.28 Variation of sectional lift coefficient along wing span.

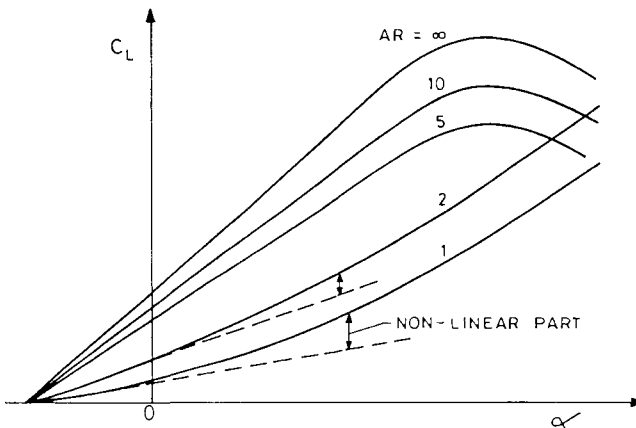


Fig. 3.29 Effects of aspect ratio AR on C_L versus α curve.

critical and drag rise Mach numbers of a wing are defined in the same way as for an airfoil. The variation of $C_{L,m}$ with M is shown in Fig. 3.23. Since a wing is a streamlined body, the effect of the Reynolds number is negligible at low incidences. The effect of the AR on C_L versus α curve is shown in Fig. 3.29. The lift coefficient curve is linear at small incidences, except when the AR is very small, less than about 3. The slope of the lift coefficient curve $dC_L/d\alpha$ increases with the increase in AR. The value of $dC_L/d\alpha$ of a wing, taking into account the effects of AR, sweep, and compressibility, is given by Nicolai¹⁷ as

$$\frac{dC_L}{d\alpha} = \frac{2\pi(AR)}{2 + [4 + (AR)^2\{(1 - M^2) + \tan^2 \Lambda\}]^{1/2}} \text{ per rad}$$

where AR is the aspect ratio, Λ is the sweep angle of the maximum thickness line of the wing, and M is the freestream Mach number.

3.5.3 Relationship Between Lift and Drag Coefficients

The lift and drag coefficients of a specified wing at low incidences depend on the angle of attack and freestream Mach number. This implies that for a given Mach number, there is relationship between C_L and C_D , and a typical form of this relationship is shown in Fig. 3.30. The turning back of the curve at large angles of attack is due to stalling. The curve can be fairly accurately represented, except near the stalling angle, by the quadratic expression

$$C_D = C_{D,\min} + K_1(C_L - C_{L_0})^2 \quad (3.1)$$

where K_1 is a constant and $C_{D,\min}$ is the minimum drag coefficient where the lift coefficient is C_{L_0} .

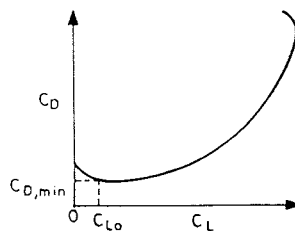


Fig. 3.30 Relationship between lift and drag coefficients.

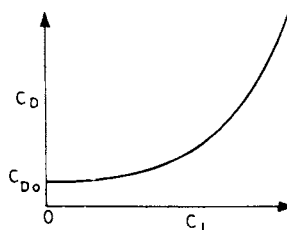


Fig. 3.31 Drag polar.

It has been found convenient to approximate the above expression by the following relation, called the *drag polar*,

$$C_D = C_{D_0} + KC_L^2 \quad (3.2)$$

which is shown in Fig. 3.31. The first term on the right-hand side C_{D_0} is the zero-lift drag coefficient, which is also called the parasite drag coefficient. The second term, $K C_L^2$, is the lift-dependent drag coefficient, where K can be referred to as the lift-dependent drag coefficient factor. The quantities C_{D_0} and K are constants for a given wing and Mach number.

At comparatively low speeds, up to about Mach 0.6, there is no appreciable influence of compressibility on the drag polar, but it increases with a further increase in Mach number. The drag polar curves at different Mach numbers are shown in Fig. 3.32. Each curve of this figure is a parabolic curve which can be represented by Eq. (3.2) provided the values of C_{D_0} and K are modified according to Mach number. Typical variations of C_{D_0} and K with Mach number are shown in Figs. 3.33 and 3.34, respectively.

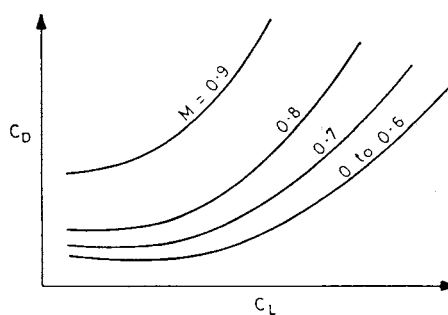


Fig. 3.32 Compressibility effect on drag polar.

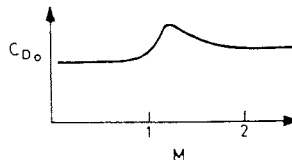


Fig. 3.33 Effect of Mach number on C_{D_0} .

3.6 High-Lift Devices for Wings

Wings of modern aircraft are provided with high-lift devices for achieving higher C_L at a given angle of attack and increasing the value of the maximum lift coefficient $C_{L,m}$, which is a design parameter. The higher the $C_{L,m}$, the lower are the stalling, takeoff, and landing speeds. Consequently, this makes the flight safer, reduces the runway length, and improves flight maneuvers. The high-lift devices are generally used for short duration only when they are required.

3.6.1 Principles of High-Lift Devices

It was seen earlier that the adverse pressure gradients near the leading and trailing edges cause flow separation and drift the boundary layer toward the wingtips. Consequently, the lift is reduced and the control surfaces tend to become less effective. Therefore, the basic principles involved in the high-lift devices are to alleviate the adverse pressure gradients, energize the boundary layer, and minimize the boundary layer drift. This is generally achieved by adding auxiliary movable surfaces near the leading and trailing edges of the wing. Some immovable thin plates protruding above the upper surface of the wing are also used. Many of these devices also act as additional lifting surfaces and increase the effective camber for augmenting flow circulation and total lift of the wing. The lift is also increased in some cases by the normal component of its thrust vector.

The high-lift devices discussed in Secs. 3.6.2–3.6.5 are called mechanical high-lift devices. The earliest wings of the Wright brothers' aircraft had $C_{L,m}$ of about 1.2, whereas modern aircraft, by using mechanical high-lift devices, have increased the $C_{L,m}$ by three times; the present-day Boeing 737 aircraft has achieved the $C_{L,m}$ close to 3.8 by using full-span flaps. There is still need to further improve the maximum lift coefficient, especially in the cases of vertical or short takeoff and landing (V-STOL) aircraft. This has led to the development of the concept of powered high-lift devices discussed in Sec. 3.6.6, and has increased the maximum lift coefficient to about 8.

3.6.2 Auxiliary Devices near the Leading Edge

The most commonly used high-lift devices near the leading edge of a wing are due to the slat, drooped leading edge, and flap. These devices alleviate the adverse

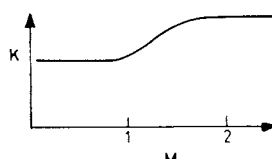


Fig. 3.34 Effect of Mach number on K .



Fig. 3.35 Leading-edge slat.

pressure gradient effects near the LE of a wing and energize the boundary layer to avoid flow separation.

The LE slat is a miniature auxiliary lifting surface mounted ahead of the leading edge of the basic wing as shown in Fig. 3.35. It can be fixed or retractable with a carefully designed gap (slot) between them. If any flow separation exists on the upper surface of the slat, its wake is discharged into the main stream without appreciably affecting the lift of the main wing. The slat is more effective at high incidences. The drag at high incidences is reduced but appreciably increases at low incidences if the slat is not retractable.

A drooped leading edge is a device shown in Fig. 3.36 where a portion near the leading edge of a wing can be drooped whenever required at higher incidences, and again retracted back to its original position at small incidences of the wing; in a lighter mood one could say that this device is like a host (wing) who politely bends his head downward (drooped leading edge) to welcome his guest (oncoming flow) so that later (downstream of leading edge) no problem (flow separation) is created. This diminishes the undesirable large turning of the flow near the LE at high incidences. It produces a small camber effect on the wing. The stalling angle here is generally not as high as in the case of a LE slat on a conventional wing.

A thin plate extending forward from the LE portion of the wing is known as the LE flap, as shown in Fig. 3.37. It is generally retractable either to the upper surface as in Fig. 3.37a or to the lower surface as in Fig. 3.37b; the latter type is called the Kruger flap. This device was extensively used during the Second World War. Leading-edge flaps are found more effective than slotted wings on highly swept-back wings. These are usually employed over the outer-half span for reducing the tip stall.

3.6.3 Trailing-Edge Flaps

A trailing-edge flap is a movable flat plate or a small auxiliary wing located at the rear portion of the main wing. The angle between the chords of the main wing and the flap is the deflection angle of the flap. A downward deflection of the flap about its hinge line increases the lift and aerodynamic efficiency of the wing without appreciably influencing its aerodynamic center. Different types of flaps have been used¹⁸ such as split flap, plain flap, slotted flap, Fowler flap, and multiple flaps.

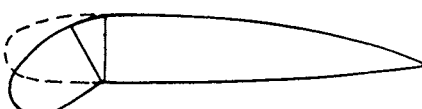


Fig. 3.36 Drooped leading edge.

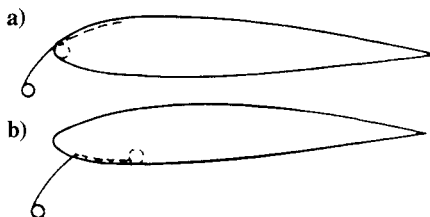


Fig. 3.37 Leading-edge flaps: a) flap at upper surface and b) flap at lower surface (Kruger flap).



Fig. 3.38 Split flap.



Fig. 3.39 Plain flap.



Fig. 3.40 Slotted flap.

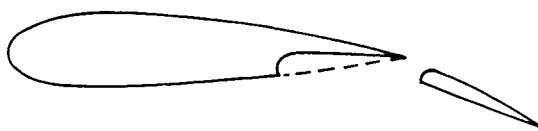


Fig. 3.41 Fowler flap.

A *split flap* is just a retractable simple thin plate attached to the lower surface as shown in Fig. 3.38. It can be deflected down when required for higher lift, otherwise it remains flush with the lower surface. A *plain flap* is a small auxiliary wing used as a flap with no gap between the trailing edge of the main wing and the leading edge of the flap as shown in Fig. 3.39. If the gap exists, it is called a *slotted flap* as shown in Fig. 3.40. Through the slot, the air from the lower surface of the wing rushes over to the upper surface of the flap and energizes its boundary layer. The slotted flap is generally retractable so that the gap is closed when in its original position. If the flap is not only deflected but can also be slides considerably to the back of the main wing, it is referred to as a *Fowler flap*, as shown in Fig. 3.41; the flap is so much behind the main wing that it behaves more like another independent wing and provides increased surface area in addition to a camber effect.

A brief and useful comparative study of the aerodynamic characteristics of these different types of flaps can be obtained by plotting their typical lift coefficient and drag polar curves as shown in Figs. 3.42 and 3.43, respectively. These figures clearly bring out the advantages of using TE flaps. Although the flaps may increase drag, the lift and aerodynamic efficiency of the wing are increased which provides a powerful reason for deploying flaps. In practice, the flaps have been deflected to as much as 80° to augment lift. Because of the utility of flaps, there are two or even three flaps on the wings of certain aircraft; these are called multiple flaps.

Furthermore, it has been found advantageous to use both the leading edge auxiliary devices and the TE flaps, such as Kruger–Fowler flap configuration to the basic wing. Some modern Boeing aircraft use three TE flaps in addition to the leading edge slat as shown in Fig. 3.44; the actions of the slat and flaps are coordinated during the flight. The flaps for high lift are situated in the inboard regions of the wing, because the outboard regions are occupied by the ailerons. This reduces flap effectiveness for high lift and moves the center of lift force inward on each wing.

3.6.4 Boundary-Layer Suction and Injection

The adverse effects of a sluggish boundary layer are controlled by removing it by suction or energizing it by blowing high-energy air into the boundary

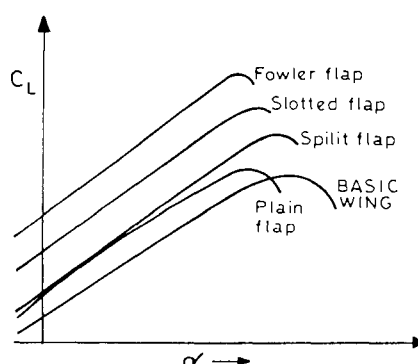


Fig. 3.42 Influence of trailing-edge flaps on C_L versus α curve.

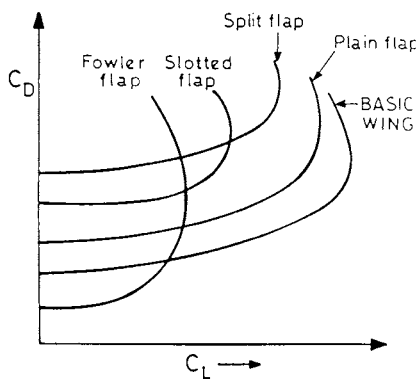


Fig. 3.43 Influence of trailing-edge flaps on drag polar.

layer. These methods are used because the loss on extra power required here is negligible.

In boundary-layer suction, the boundary layer is mainly sucked from the upper surface of the wing by creating lower pressure inside the wing as shown in Fig. 3.45. The wing surface at the places of suction has to be porous, perforated, or slotted. For high lift, it is sufficient to use suction near the LE, TE, or both, as required for preventing separations. This increases the lift and the stalling angle, and decreases the drag, without affecting the lift curve slope and the zero-lift angle of attack. If the emphasis is on obtaining laminar flow over the complete surface of the wing for minimizing its drag or drag power, the suction is performed almost over the entire upper and lower surfaces of the wing.

In boundary-layer suction, an additional mass of air is blown tangentially, as a high-velocity jet, into the sluggish boundary layer, to postpone or eliminate the flow separation. This type of blowing is highly favored by aeronautical engineers as compared to suction, because the high-pressure air is readily available in plentiful supply from the aircraft engine which can be bled into the boundary layer of the wing. Blowing of an additional air mass can be performed near the minimum pressure point on the upper surface as shown in Fig. 3.46, or at any other station. In many cases, this type of blowing is performed at the nose of its flap and a small amount of air mass blowing may altogether eliminate boundary-layer separation even at large flap deflections. Lift is considerably increased and drag is reduced as compared to controlling the adverse effect of the boundary layer, by means of slotted flap, which does not involve blowing air.

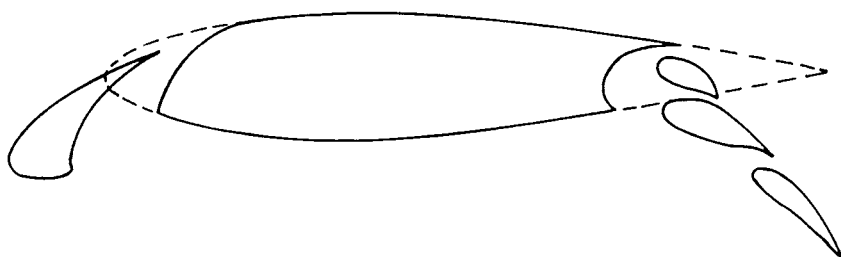


Fig. 3.44 Wing section with leading-edge slat and trailing-edge flaps.

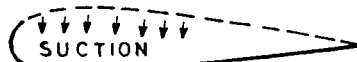


Fig. 3.45 Boundary-layer suction.

3.6.5 Boundary-Layer Fences and Vortex Generators

Boundary-layer fences and vortex generators are simple, immovable devices used to stop or minimize the drift of the boundary layer toward the outboard portion of the wing.

Boundary-layer fences are thin strips on the upper surface normal to the wing, extending in the chordwise direction. A strip usually starts near the leading edge of the wing and extends up to about half the chord length. The height of a strip is about five times the boundary-layer thickness, and three or four such strips are fitted at different spanwise locations.

A *vortex generator* is a thin plate of very small aspect ratio and span, which is mounted at a short distance above the wing. A few such vortex generators are mounted at various spanwise locations. They generate vortices close to the wing surface whose axes are along the chordwise direction of the wing. The vortices energize the boundary layer by bringing the high-energy outer stream into the boundary layer and simultaneously pushing the sluggish boundary layer into the outer stream. This extends the linear portion of the C_L versus α curve such that the maximum lift coefficient and the stalling angle are increased by about one and a half times. At low incidences, C_D is increased but at higher incidences it is reduced by avoiding TE separation. Certain wings have notches in the LE whose effect is similar to that of vortex generators.

3.6.6 Powered High-Lift Concepts

The increase in lift by the mechanical high-lift devices discussed so far can still be considerably increased, but at the cost of engine power. High-lift devices using appreciable engine power are called powered high-lift devices. These are used for V-STOL aircraft and some of them are described by Goodmanson and Gratzer.¹⁹ Devices of this type in common use are upper surface blowing (USB), externally blown flap (EBF), internally blown flap (IBF), augmentor wing (AW), and vectored thrust (VT). Most of these devices utilize the principle of the Coanda effect, according to which a jet of fluid on meeting a curved surface adheres to it and the jet can be sufficiently turned.

In USB, the engine jet exhaust is blown over the upper surfaces of the wing and TE flaps. In the EBF, the jet exhaust hits the trailing-edge flaps directly, and consequently the jet is deflected down. In the IBF, a part of the engine jet exhaust is diverted to blow tangentially near the leading edges of the wing and its trailing-edge flaps. In the VT devices, almost the whole of the jet exhaust is deflected

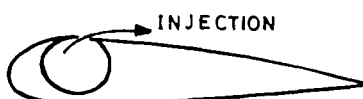


Fig. 3.46 Boundary-layer injection.

down by tilting the exhaust nozzle, whereas the wings continue to make use of the mechanical high-lift devices.

3.7 Fuselage

The *fuselage* is the cylindrical central body of an aircraft for carrying the crew members, passengers, cargo, baggage, instruments, and sometimes the fuel as well. The exact shape and size of the fuselage is a design problem, but it is generally symmetrical about the normal plane passing through the longitudinal axis of the aircraft. Its length-to-diameter ratio is called the *fineness ratio* of the fuselage. It is generally a nonlifting body that substantially contributes to drag. The drag on the fuselage is the sum of its pressure and skin friction drags. At high subsonic or supersonic speeds, shock waves may appear on the fuselage. For minimum drag, a fineness ratio of 3 is suggested for subsonic speeds and one of 14 for supersonic speeds.²⁰ If the aircraft flies about half the time at subsonic speeds, and half the time at supersonic speeds, the selection of the fineness ratio should be a compromise between the two conflicting criteria.

3.8 Aircraft Configuration

An aircraft configuration consists mainly of the wing, fuselage, tail unit, and the air inlet of its power plant. All these components produce drag, while lift is mainly produced by the wing. The aerodynamic forces that produce lift also produce drag, and in addition, there are also other aerodynamic factors that contribute to drag. The ratio L/D (lift/drag) is called the *aerodynamic efficiency* of the aircraft and is an important performance variable.

3.8.1 Flowfield and Forces on Aircraft

A *flowfield* in the immediate neighborhood of an aircraft consists of the boundary layer over its surfaces, separated flows near the trailing edges of aircraft components, shear layers, trailing-edge vortices including the tip-vortices emerging from the tail plane and the tips of the wings, and the wake downstream of the aircraft. These are schematically shown in Fig. 3.47. In the case of an aircraft using propellers, there would also be slipstreams ensuing from its blades. The flowfield away from the surface, which lies above the boundary layer and shear layers, behaves like an inviscid potential flow. In a transonic flow, there would be shocks at certain places on the surface of the aircraft, and in supersonic flow the shocks would be confined to the leading and trailing edges of the aircraft components. The stalling behavior of an aircraft depends on the nature of flow separation over the wings and how it progresses with the increase in angle of attack.

Each and every point on the surface of an aircraft is acted on by pressure and skin friction forces. The pressure at a point is normal to the surface and the skin friction force is tangential to the surface. Resolving these forces in a particular direction and integrating them throughout the surface of the aircraft gives the component of aerodynamic force in that direction. Generally the lift, drag, and lateral forces are obtained. The lateral force is generated by asymmetry in the flowfield about the normal plane of the aircraft. These forces can also be obtained regarding the individual components of the aircraft configuration, as this is usually required for understanding the contribution made by each of these components to the aircraft's stability. The analysis of aircraft performance, however, requires

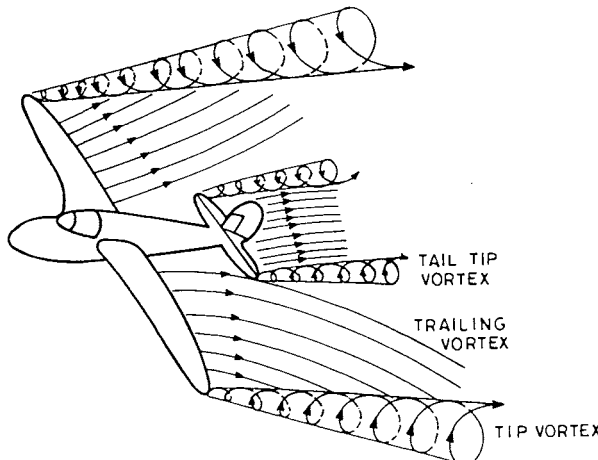


Fig. 3.47 Simplified schematic diagram of flow past an aircraft.

only the calculation of the total aerodynamic force acting on the surface of the aircraft, and this force is the vector sum of the aerodynamic forces acting on the components of the aircraft configuration.

Lift and drag forces are the two most important aerodynamic forces, because an aircraft, and its flowfield, is generally symmetrical about its normal plane. These forces are defined in the same way as that for a wing. The lift force L of an aircraft is the component of its aerodynamic force normal to its flight path in the plane of symmetry and the drag force D is the component in the downstream direction along the flight path. These forces are commonly expressed in nondimensional forms as lift and drag coefficients. The lift coefficient C_L and the drag coefficient C_D are defined as

$$C_L = 2L/(\rho V^2 S) \quad \text{and} \quad C_D = 2D/(\rho V^2 S) \quad (3.3)$$

where V is the airspeed of the aircraft relative to air along the flight path, and S is the reference wing planform area obtained by extending the wing, without interruption through its fuselage, up to the center line of the aircraft, as shown in Fig. 3.48. The lift and drag coefficients depend on the attitude and configuration of the aircraft, and in the operating range of an aircraft they are weak functions

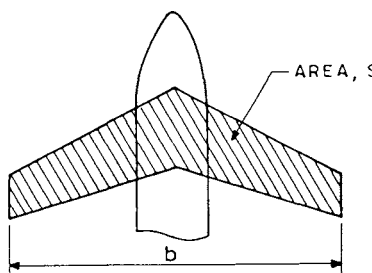


Fig. 3.48 Reference wing planform area S .

of the Reynolds number. At higher speeds, C_L and C_D also depend on the Mach number.

In the case of a straight and steady flight of an aircraft in the horizontal plane (level flight), $L = W$ and the airspeed is obtained from Eq. (3.3) as

$$V = \sqrt{2(W/S)/(\rho C_L)} = \sqrt{2(W/S)/(\rho_{SSL} \sigma C_L)} \quad (3.4)$$

which expresses the airspeed in terms of the wing loading, air density (and thus altitude), and lift coefficient. This explains why heavy, high-altitude aircraft fly at higher speeds. Equation (3.4) is a very versatile relationship which is used at several places in the analysis of aircraft performance.

In view of Eq. (3.3), the lift and drag can be expressed as

$$L = (1/2)\rho V^2 S C_L = (\gamma/2) p_{SSL} M^2 \delta S C_L$$

and

$$D = (1/2)\rho V^2 S C_D = (\gamma/2) p_{SSL} M^2 \delta S C_D$$

where $\delta = p/p_{SSL}$, p_{SSL} is the standard atmosphere sea level pressure, and $\gamma (= 1.4)$ is the ratio of specific heats of air. If $L = W$, and $D = F$, as in the case of straight level flight, the above two equations can be expressed, respectively, as

$$W/\delta = (\gamma/2) p_{SSL} M^2 S C_L \quad \text{and} \quad F/\delta = (\gamma/2) p_{SSL} M^2 S C_D \quad (3.5)$$

which for a given aircraft can be written in the functional form as

$$W/\delta = f(M, C_L) \quad \text{and} \quad F/\delta = f(M, C_D) \quad (3.6)$$

where it is understood that the functional form f appearing in the above two relations of Eq. (3.6) are different. It can also be remarked here that the two relations of Eq. (3.6) are not dimensionally correct, but they have usually become understandable and acceptable as long as they are used only for a specified aircraft. Such functional forms are commonly used in the performance evaluation of a given aircraft through flight tests.

3.8.2 Components of Drag and Drag Polar

Pressure and skin friction are the two fundamental causes producing aerodynamic drag force on an aircraft. Pressure drag is sometimes called *form drag*. Any other agency producing drag, like *induced drag*, *wave drag*, *cooling drag*, *trim drag*, *base drag*, *interference drag*, and *leakage drag*, can cause drag only by affecting pressure and skin friction drags. This is schematically shown in Fig. 3.49. The induced drag is primarily a pressure drag due to the trailing edge and tip vortices of the lifting surface. The wave drag arises in a compressible flow due to shocks over the surface of the aircraft; shocks inside the inlet duct give rise to ram drag, and shocks ahead of the body produce additive or spillage drag. Cooling drag is due to the power plant installation that cools the engine, oil, and accessories. Trim drag results from the deflection of control surfaces for the purpose of trimming the aircraft about its center of gravity. Base drag is due to blunt base, boat

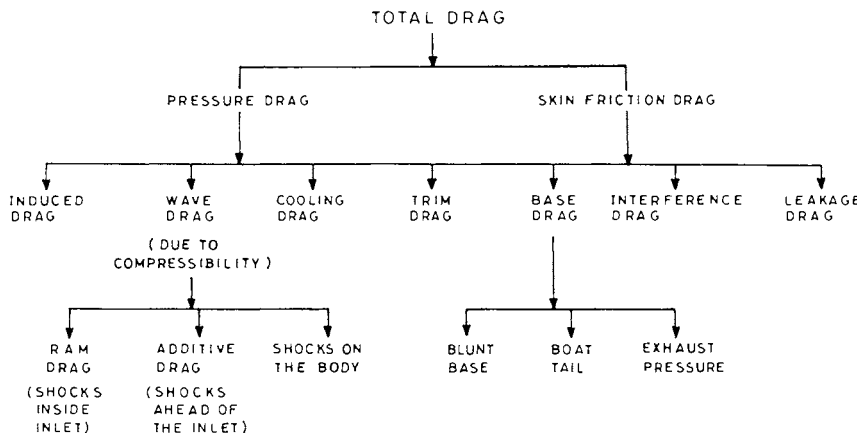


Fig. 3.49 Components of total drag.

tail, or exhaust pressure. Interference drag arises due to aerodynamic interference among the different components of an aircraft configuration. Leakage drag is due to leaks caused by the differential pressure between the inside and outside of the aircraft, or between the upper and lower surfaces of the aircraft components through joints.

The names of profile and parasite drags are also quite common in the aerodynamic drag literature. The sum of pressure and skin friction drags is called *profile drag*. *Parasite drag* is the sum of the drag forces caused by nonlifting components of the aircraft.

In the operational range of an aircraft of specified configuration and Mach number, its drag coefficient C_D depends on C_L . The relationship between the C_L and C_D is regarded as parabolic, similar to that shown in Fig. 3.31, and it can be expressed as

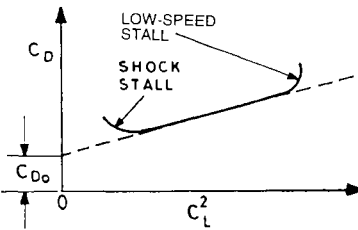
$$C_D = C_{D_0} + KC_L^2 \quad (3.7)$$

where C_{D_0} is the zero-lift drag coefficient, and K is the lift-dependent drag coefficient factor whose value can be given by

$$K = 1/\{\pi(AR)e\} \quad (3.8)$$

where e is Oswald's span efficiency factor. Both C_{D_0} and K are positive quantities, much less than unity, and depend on Mach number in compressible flow. The quantities C_{D_0} and KC_L^2 are formed due to the various components of the drag, but the effect of the induced drag is more predominant in the KC_L^2 term.

The drag polar in Eq. (3.7) will represent a straight line if C_D is plotted against C_L^2 as shown by the dashed line in Fig. 3.50. The behavior of the curve in practice is shown by a solid line in the Fig. 3.50, where it rapidly moves up at the lower values of C_L due to compressibility (shock stall), and then moves up at the higher values of C_L due to low-speed stall.

Fig. 3.50 Variation of C_D against C_L^2 .

3.8.3 Aerodynamic Efficiency of an Aircraft

The lift to drag ratio L/D of an aircraft is called its aerodynamic efficiency and is denoted by E . Therefore,

$$E = L/D = C_L/C_D = C_L/(C_{D_0} + K C_L^2) \quad (3.9)$$

Using Eq. (3.3) and writing $L = W$, the above equation can be written as

$$E = 2(W/S)\rho V^2 / \{C_{D_0}\rho^2 V^4 + 4K(W/S)^2\} \quad (3.10)$$

It is now also possible to obtain the velocity V_{E_m} for maximum aerodynamic efficiency E_m by differentiating the above equation with respect to V , putting $dE/dV = 0$, and solving the resulting equation. This gives

$$V_{E_m} = \{2(W/S)/\rho\}^{1/2} (K/C_{D_0})^{1/4} \quad (3.11)$$

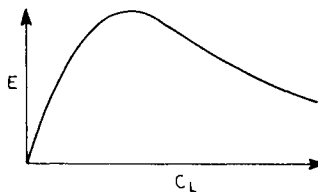
The values of lift and drag coefficients C_{L,E_m} and C_{D,E_m} , respectively, at the maximum aerodynamic efficiency are obtained from Eq. (3.3) by putting $V = V_{E_m}$, and similarly, E_m is obtained from Eq. (3.10). This gives

$$C_{L,E_m} = (C_{D_0}/K)^{1/2}, \quad C_{D,E_m} = 2C_{D_0}, \quad \text{and} \quad E_m = 1/(2\sqrt{C_{D_0}K}) \quad (3.12)$$

The maximum aerodynamic efficiency is an important aerodynamic design variable. An increase in E_m improves the performance of the aircraft. The orders of magnitudes of E_m for different types of aircraft are shown in Table 3.1. A typical variation of E with C_L as obtained from Eq. (3.9) is shown in Fig. 3.51, and a variation of E with Mach number, obtained from Eq. (3.10), is shown in Fig. 3.52.

Table 3.1 Values of E_m for different types of aircraft

Types of aircraft	E_m
High performance sailplanes	40
Transport aircraft ($M = 0.8$)	18
Subsonic fighters	10
Supersonic aircraft	7
Helicopters	3

Fig. 3.51 Changes in E with C_L .

3.9 Flight Control by Aerodynamic Surfaces

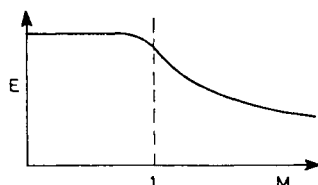
Attitudes and airspeeds of aircraft during flight are often controlled by movable aerodynamic surfaces called *control surfaces*. These control surfaces and their effectiveness are discussed here.

3.9.1 Nature of Control Surfaces

Flight control means turning or changing the attitude of an aircraft that is otherwise stable along the three orthogonal axes passing through its center of gravity. Flight control is affected by applying additional forces in suitable directions during the flight. These additional forces are provided by deflecting or extending the control surfaces, which are generally thin streamline bodies specially designed for the purpose. Each control surface is much smaller in area as compared to the wing surface. The primary control surfaces are usually located at extreme positions from the center of gravity of the aircraft for providing large moment arms. A control surface is usually deflected about its hinge line and the moment of deflecting force about the hinge is called the *hinge moment*.

3.9.2 Primary Flight Controls

The ailerons, elevators, and rudders are called the *primary flight controls*. The locations of these control surfaces and their functions have already been explained in Sec. 1.5. (Chapter 1). The aerodynamics of a control surface for generating additional force is similar to that of the trailing-edge flap for additional lift force, as explained in Sec. 3.6. The ailerons provide lateral control (control in the lateral plane) by causing roll displacements about the longitudinal axis. The elevators provide longitudinal or pitch control about the lateral axis of the aircraft by causing nose-up or nose-down attitude of the aircraft. The rudder provides yawing moments, or directional control, about the normal axis of the aircraft by turning the aircraft toward the left or the right, depending on the direction of the rudder deflection.

Fig. 3.52 Changes in E with M .

3.9.3 Effectiveness of Flight Controls

The change in the moment produced, for a given control deflection, measures the effectiveness of primary flight controls. The larger the change in moment, the greater the effectiveness of the controls. The moment of force produced depends on the magnitude of the aerodynamic force and the length of its moment arm. The aerodynamic force generally increases with an increase in airspeed and in surface area of the control surface. At higher airspeeds the controls are more effective and only a small movement of the control surface is required, and similarly at lower airspeeds larger movements of the control surface are needed.

A control surface remains effective only for a limited amount of its deflection. If the deflection exceeds this limit, large regions of flow separation may prevail, rendering the control surface ineffective.

In many large aircraft the control surfaces are arranged in pairs, i.e., an inboard and outboard aileron on each wing, an inboard and outboard elevator, and an upper and lower rudder. The existence of both inboard and outboard ailerons ensures control effectiveness at low airspeeds as well as at high airspeeds. At low airspeeds, only the outboard ailerons are used for providing lateral control. At high airspeeds the outboard ailerons are locked and the lateral control is taken over by the inboard ailerons so that the deflecting forces act closer to the longitudinal axis of the aircraft for reducing wing-twisting. The duplication of elevators and rudders is a safety precaution. In addition, each elevator and rudder is operated independently to ensure that one control surface of a pair remains effective in case the other fails.

3.9.4 Combined Controls

The primary flight controls in certain classes of aircraft are arranged such that one type of control surface may combine its function with that of another. For example, a control surface on the delta wing of a Concorde aircraft can perform the function of both an aileron and elevator, and such a control surface is called an *elevon*. When a control system is used as both a flap (for high lift) and, aileron, it is called a *flaperon*. In some aircraft with a V-shaped or “butterfly” tail, the control surfaces operate either as a rudder or elevator, and for this reason, they are known as *ruddervators*.

Elevators are dispensed with in some aircraft, and they are replaced by a movable horizontal stabilizer, called a *stabilator*.

3.9.5 Trim Tabs

During a flight, the deflection of a control surface may need to be maintained for a long time, which may be quite tiring for the pilot. Therefore, it is usual to have a secondary control system whose aerodynamic forces can be separately adjusted to provide the necessary force on the primary control, thus relieving the pilot of undue physical strain. The operation of such a system is referred to as *trimming*.

The use of the tab is an important basic device for trimming. A *tab* is an auxiliary surface (small flap) hinged at the trailing edge of the primary control surface, as shown in Fig. 3.53. The forces F_1 and F_2 acting on the control surface and the tab, respectively, are shown in the figure. The tab is operated by a trim wheel in the cockpit; the wheel is arranged so that it can be rotated in the same sense as the

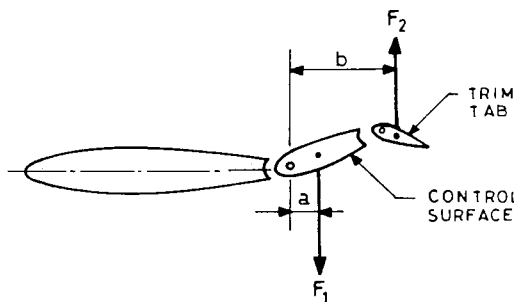


Fig. 3.53 Principle of a trim tab.

required trim change. Figure 3.53 illustrates the case where the tab is hinged to the elevator when the aircraft is required to adopt the nose-up attitude for a straight and level flight. If the trim tab did not exist, this would require that the elevators be displaced to an upward position by a constant pull on the control column by the pilot. However, by employing the trim tab, the pilot can set up the required elevator deflection simply by rotating the trim wheel in the appropriate direction, in this case rearward. As shown in Fig. 3.53, the tab will move downward and the aerodynamic load acting on the tab will deflect the elevator upward, also moving the control column to a rearward position. In terms of moments, that produced by the elevators, F_1a , must be equal and opposite to the moment F_2b , which is produced by the tab; the lines of action of aerodynamic forces F_1 and F_2 acting on the elevator and tab, respectively, are at the distances of a and b from the hinge line of the elevator, as shown in Fig. 3.53.

Tabs are also designed for purposes other than the trimming, and may act as such as a balancing device, or in some cases as part of the primary control surface.²¹ Similarly, trimming is also carried out by certain other means,²² such as an all-moving tail, a flying tail, and Mach trim.

3.10 Aerodynamic Interference Effects

Flowfield past a body is affected by the presence of another body in its neighborhood, and consequently its pressure field is also disturbed; this is called the aerodynamic interference effect. In a subsonic flow, this disturbance is in both the upstream and downstream directions, whereas it spreads only downstream in a supersonic flow. Different types of interactions are explained here.

3.10.1 Interference Among the Components of an Aircraft

The components of an aircraft's configuration, such as fuselage, wing, tail plane, and air inlet, may be quite efficient individually in their aerodynamic design. When these components are assembled to form an aircraft, the flow over each component may change appreciably because of aerodynamic interference. The flow over one component interferes with the smooth flow over the other components and the magnitude of this interference may increase with a change in attitude and airspeed of the aircraft. Interference of flows between the wing and tail plane, the wing and fuselage, and the inlet duct and fuselage (or wing), is quite common. In a piston-prop aircraft, the flow past its propeller blades interferes with the flow

over the other components of the aircraft. The interference changes the stalling characteristics and handling qualities of the aircraft.

The wake of the wing may hit the tail plane. The wake region, being unsteady, turbulent, and of low-energy air, reduces the effectiveness of the tail and may cause buffeting. The downwash of the wing reduces the effective incidence of the tail plane. Wing interference with the tail in many modern aircraft is minimized by placing the tail plane sufficiently above the plane of the wing.

The flow over the fuselage interferes with the flow over the wing and tail plane, and is normally confined to the narrow regions of the boundary layer of the fuselage. This interference, however, spreads rapidly during yaw or sideslip of the aircraft when the wake of the fuselage passes over the appreciable portions of the wing and tail plane, and this produces the side force. This blanking effect of the fuselage is shown in Fig. 3.54 by the shaded portion, which is more pronounced on swept-back wings as shown in Fig. 3.55. When the fuselage wake passes over the wing and tail plane, their lift and aerodynamic efficiency drops. The decrease in the lift of the affected wing becomes more pronounced due to reduction in its effective aspect ratio caused by the yaw. The decrease in lift over one wing causes rolling toward the side of the inner wing (affected wing). During yaw, the outer wing moves faster than the inner wing and consequently the lift on the inner wing is less than the outer wing, which further adds to the rolling toward the side of inner wing (affected wing). Thus the yawing motion leads to rolling motion of the aircraft, called *yaw-roll coupling*. Change in the direction of the yaw reverses the direction of its roll. If yaw and roll are not checked, this may lead to *Dutch roll*, which is an oscillatory mode caused by the combinations of yawing and rolling motions. The rolling motion in Dutch roll is more noticeable and the aircraft proceeds with continuously reversing roll action.

Interference between the fuselage and the wing at transonic speeds contributes significantly to the transonic drag rise of the aircraft. This interference can be minimized if the distribution of the total cross-sectional area along the longitudinal axis of the aircraft follows a smooth pattern.²³ This is commonly called *the transonic area rule* and is usually applied to all high-speed aircraft.

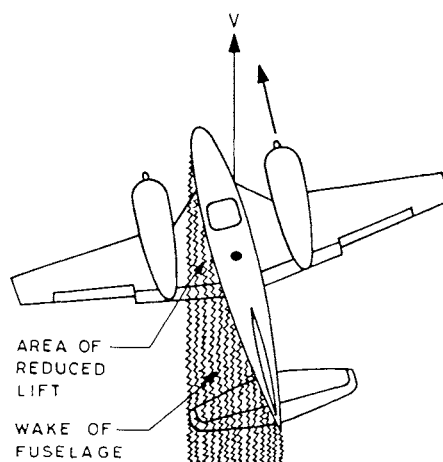


Fig. 3.54 Blanking effect on wing by fuselage.

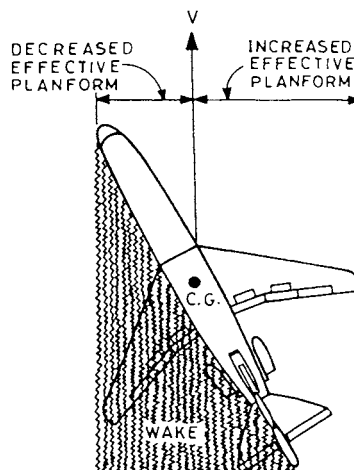


Fig. 3.55 Blanking effect more pronounced on swept-back wing.

Flow separation over the inlet of the air duct may spoil the smooth flow over the fuselage or the wing, depending on its location. Flow separation at the lip of the inlet may enter the duct and spoil the flow at the compressor face which lowers the efficiency of the compressor blades and the engine. In the case of piston-prop aircraft, the rotation of the propeller produces asymmetrical flow over the wings and the tail plane.

3.10.2 Wind Tunnel Wall Interference

An aircraft, its components, and other bodies are frequently tested in a wind tunnel. These tests do not simulate free-flight tests exactly. The straight solid walls of a closed jet tunnel require that the streamlines must be straight near the walls, whereas in a free flight they would be curved. The limited boundaries of a tunnel alter the flowfield around the test model. In other words, the finite area of the test section constrains the flowfield, which in turn affects the surface pressure distribution on the test model.

In mathematical terms also, the outer boundary condition in a wind tunnel test is different from that of a free flight. Therefore, the solution of a flow problem around a specified object in a wind tunnel (closed or open jet) would differ from that in a free flight. If the maximum cross-section area of the model is less than about 5% of the cross-sectional area of the test section, the effect of the wind tunnel walls is generally negligible, otherwise a suitable correction must be applied. Various analytical approaches have been devised to apply wind tunnel wall corrections,²⁴ but presently this problem is solved on computers.²⁵

Boundary-layer growth along the solid wall of a test section reduces its effective cross-sectional area, accelerates the flow, and reduces the static pressure along the length of the test section. This reduction in static pressure gives rise to *horizontal buoyancy* on the model, producing drag force. The horizontal buoyancy effect becomes appreciable on long models and it is experimentally avoided by providing a suitable divergence to the test section that produces a constant static pressure along the length of the empty test section during its operation.

3.10.3 *Ground Interference*

The air flow around an aircraft flying or moving close to the ground or sea is not the same as in free flight far away from the Earth. The proximity of the ground or the sea, acting as a solid boundary, influences the flowfield around the aircraft, similar to a wind tunnel wall. Effects produced by the ground are noticeable when the aircraft is about one wing span or low above the ground.²⁶ The closer the ground, the greater is its effect, which can be approximately estimated.²⁷

The proximity of the Earth primarily causes reduction in upwash and downwash of the wing and decreases the strength of its tip vortices. This reduces the induced drag and the total drag force, but increases the lift; the lift is increased due to the overpowering influence of the increased velocity and incidence caused by the ground effect, as can be established by the method of images. These effects are clearly seen in the tendency of a light aircraft to "float" during its landings. Since the decrease in thrust or power required reduces the requirement of fuel, the ground effect is used in emergency flying over an ocean when the fuel available is low or critical. Birds make use of the ground effect by soaring close to the ocean waves.

The proximity of the ground modifies the pressure field around the aircraft which in turn changes its pitching moment and increases the static pressure below the wings. If the static pressure holes of an airspeed indicator are located below the wing, the ground effect would cause them to indicate a lesser airspeed than the actual airspeed when the aircraft is very close to the Earth.

The ground effect can be estimated mathematically by the method of images using potential flow theory. It can be shown that the effect of the ground close to an aircraft is the same as that of an inverted aircraft "flying in formation below the ground" at the same distance.⁴

3.10.4 *Interference Between Two Aircraft*

The tip vortices created at high angles of attack, such as during the liftoff or landing-flare, produce very powerful rolling moments which may easily exceed the roll control capability of a light aircraft. The tangential velocity of air within these vortices may exceed 80.9 m/s (150 kn), and a small aircraft coming within them may be uncontrollable.²⁸ The various situations that may occur are shown in Fig. 3.56 where a small aircraft is shown crossing the vortex or flying closely along the vortex line.

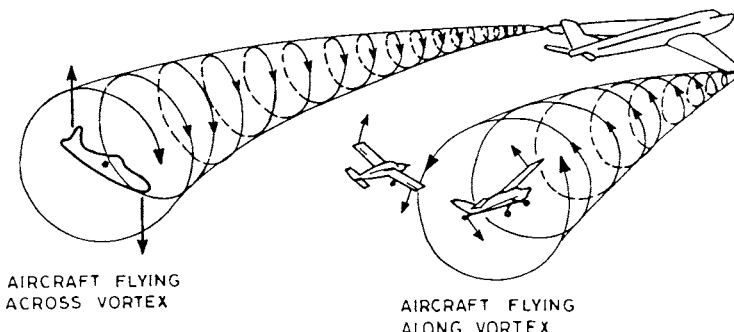


Fig. 3.56 Interference between two aircraft.

The two vortices emerging continuously from the wingtips move outward and downward behind the generating aircraft and remain active for several minutes before they finally break up and disintegrate. A certain minimum spacing or a minimum time interval is recommended when an aircraft is directly behind another aircraft, or when it crosses behind the leading aircraft at the same height or less than 305 m (1000 ft) below the leading aircraft. The spacing varies from 3 to 8 n miles and the time interval varies from 2 to 4 min depending on the types of the leading and the following aircraft. Naturally the spacing and the time interval would be on the higher side when a light aircraft follows the heavy aircraft. It is considered safer for the following aircraft to fly a little higher than the leading aircraft because the vortices of a leading aircraft move downward in case there are no air currents.

On the ground, while the leading aircraft is taxiing or running its engines, the following aircraft must stay at a sufficient distance downstream of the leading aircraft so that it is not under the influence of jet blast, or slipstream of the propeller, of the leading aircraft.

3.11 Experimental Methods in Aerodynamics

A wind tunnel is the most important facility for conducting experiments in aerodynamics. Measurements of pressure, velocity, forces, and flow visualization studies are routine activities of experimental aerodynamics.

3.11.1 Wind Tunnels

A wind tunnel utilizes the fact that aerodynamic force remains unaltered as long as the relative motion between the air and the test model is the same. In other words, irrespective of the fact whether the body is moving in still air, or the air is moving past a fixed body, the aerodynamic forces remain the same if the same relative velocity between the free air and the body is maintained. In a wind tunnel, the test model is generally kept fixed and the air is made to move past it. The oncoming flow of air in a wind tunnel is generally uniform but it can be simulated to a specified nonuniform flow whenever required for a particular experiment.

Wind tunnels of different sizes, designs, and Mach number ranges exist.^{29,30} The size of a wind tunnel is identified by the size of the cross section of its test section, which may be rectangular, square, octagonal, elliptical, or circular. The jet of air in the test section may be open or closed, and the passage of air in it may be an open circuit or closed circuit.

Wind tunnels are very widely used for both aeronautical and nonaeronautical purposes. Aeronautical uses consist of testing streamlined bodies, aircraft components, model aircraft, and even full-scale aircraft. The aerodynamic behavior of bullets, rockets, and missiles is also studied in wind tunnels. The nonaeronautical uses of wind tunnels include testing small-scale models of long bridges, high buildings, towers, chimneys, automobiles, railway cars, etc. The movements of wind over a city, field, hill, etc. may also be simulated in wind tunnels.

3.11.2 Pressure, Velocity, and Force Measurements

Surface pressure measurements are made by drilling very tiny holes on the surface of the body and connecting them to a manometer through a system of tubes inside the body. The static pressure measurements away from the body are

carried by the static tubes. In a low-speed flow, alcohol, water, or any other low-density and nonsticking liquid is usually used as a gauging fluid in the manometer. For high subsonic, transonic, and supersonic speeds, a mercury manometer is used. Bordan gauges and piezoelectric transducers are also used for high-speed flows. The velocity at a point is obtained from the measurements of static and total pressures at that point. Direct measurement of velocity can be made by different classes of wind velocity meters.³¹ Unsteady and rapidly fluctuating velocities are measured by a hot-wire anemometer³² or by a laser doppler velocimeter.³³

Because of practical considerations, the knowledge of lift, drag, and lateral forces acting on a body are more important than the details of velocity and pressure field in the flow. Although the pressure forces can be obtained by suitably integrating the surface pressure distribution, they do not give skin friction force. Therefore, mechanical or strain gauge balances³⁴ are frequently used to directly obtain lift, drag, and lateral forces on the body in a wind tunnel.

3.11.3 Flow Visualization

Flow visualization activities are important in most experimental aerodynamic studies. Air or water is a transparent fluid medium in which no streamlines are visible. Seeing is believing, which forces us to adopt methods of visualizing streamlines. Moreover, before one undertakes velocity and pressure measurements, it is pertinent to know the overall picture of the flowfield, especially in the close vicinity of the body. The knowledge of the direction of streamlines help to align pressure and velocity probes for obtaining accurate and quick measurements. It also helps to decide which part of the flowfield one should concentrate on more for measurements.

Various methods of flow visualization are used.³⁵ Surface flow patterns at low speeds are usually obtained by using thin tufts, introducing smoke filaments, and spreading thin liquid film on the surface of the body. Other methods of incompressible flow visualization around the body are adopted by employing a water tunnel and introducing hydrogen bubbles, using suspended and floating particles, and using colored liquid filaments. In transonic and supersonic flows, shocks and expansion fans are observed by means of a schlieren system.¹²

3.12 Pressure, Velocity, and Density Relationships

Aerodynamics is the mechanics of Newtonian fluid. Most of the low-density fluids in nature, such as water, gasoline, alcohol, air, and other gases, are classified as Newtonian fluids. The number of molecules of air at sea level is of the order of 10^{19} per cubic centimeter. This number is so large that the air can be regarded as a continuous (continuum) and homogeneous fluid medium. This considerably simplifies the mathematical formulation of aerodynamics which remains valid far beyond the altitudes at which the most modern supersonic or hypersonic aircraft fly.

The mathematical formulation of a flow problem and some of its simplifications are briefly described here. The emphasis is on obtaining the pressure, velocity, and density relationships that serve useful purposes in later chapters.

3.12.1 Fundamental Equations

The natural laws of motion of Newton, when applied to a Newtonian fluid, give rise to the well-known Navier–Stokes equations of motion.³ These governing

partial differential equations are mathematically difficult and remain intractable for solving many practical problems even with modern high-speed computers. Many simplifications of these equations have been extensively used, and try to cope with reality in a limited sense.

Flow problems in aerodynamics have commonly been solved by neglecting viscous terms because the coefficient of viscosity of air is extremely small, of the order of 10^{-5} . This reduces the Navier–Stokes equations to Euler's equations of inviscid flow theory, which in vector notation can be written as

$$\rho D\bar{V}/DT = -\text{grad } p \quad \text{and} \quad \text{div}(\rho \bar{V}) = 0 \quad (3.13)$$

where \bar{V} is the velocity vector at a point in the flowfield, D/Dt is the total derivative, and the force of gravity is neglected because air is a very light fluid medium. The first equation above is the momentum equation obtained by the principle of conservation of momentum, and the second equation is the continuity equation obtained by the principle of conservation of mass. If the flow is irrotational, $\text{curl } \bar{V} = 0$, and Eq. (3.13) reduces to another well-known Laplace equation, $\nabla^2 \phi = 0$, where ϕ is the velocity potential. With advances in computers, the Laplace equation in aerodynamics is now commonly solved by a panel method³⁶ by using surface singularities.

The above Eq. (3.13) can be integrated³⁷ along a streamline, and the resulting equation is the integral form of Bernoulli's equation,

$$V^2/2 + \int dp/\rho = \text{const} \quad (3.14)$$

which is valid both for incompressible and compressible flows. Equation (3.14) can also be independently obtained¹⁴ by balancing the momentum flux and the forces across a small element of the inviscid fluid along a streamline. It will be seen in the following subsections that the above equation, in conjunction with the equation of state,

$$p = \rho RT \quad (3.15)$$

provides many useful simple algebraic relations, where T is the absolute temperature and R is the gas constant whose value is $287 \text{ m}^2/(\text{s}^2\text{K})$ for air.

3.12.2 Incompressible Flow Relations

An incompressible flow has constant density. Equation (3.14) in such a case reduces to

$$p + \rho V^2/2 = \text{const} = p_0 \quad (3.16)$$

where p is the static pressure, p_0 is the total pressure, and the difference $p_0 - p$ is called the dynamic pressure whose value is $\rho V^2/2$ in incompressible flow. The p_0 is constant throughout the irrotational flowfield, otherwise in rotational flow it varies with the change in streamline. The pressure p_0 is also called the stagnation pressure, which is defined as the pressure attained at the point when the flow is brought to rest isentropically at that point. Another common name of p_0 is the

pitot pressure because it is measured by a pitot tube, where the name Pitot is due to its inventor Henry Pitot, born in 1695 in France.³⁸

The above Eq. (3.16) is a well-known Bernoulli equation for an incompressible inviscid flow. It is obtained by neglecting the term ρgh due to the force of gravity, which is generally much smaller in aerodynamics as compared to the other terms; the quantity h can be the height above a suitably chosen reference line. The term ρgh is to be included on the left-hand side of Eq. (3.16) when the fluid is liquid or where the gaseous flow velocity is too low, as in the case of a creeping motion.

The air flow velocity V at a point is obtained from Eq. (3.16) as

$$V = \sqrt{(p_0 - p)/\rho} \quad (3.17)$$

where p_0 and p at a point in the flowfield can be measured, and ρ is the known density of air. The above relation helps in defining equivalent airspeed and designing an airspeed indicator, as explained in Chapter 6.

3.12.3 Compressible Flow Relations

An adiabatic inviscid compressible flow free from shock waves is isentropic. In the presence of shocks, departure from the isentropic flow exists only in the narrow regions along the shock waves. Flow with very weak shocks is usually approximated as an isentropic flow. In a compressible isentropic flow, the equation of state assumes the form,

$$p/\rho^\gamma = \text{const} = p_0/\rho_0^\gamma \quad (3.18)$$

where the subscript 0 represent the stagnation condition. Using the above relation, Eq. (3.14) can be written as

$$V^{1/2} + \{\gamma/(\gamma - 1)\}p/\rho = \text{const} = \{\gamma/(\gamma - 1)\}p_0/\rho_0 \quad (3.19)$$

Eliminating ρ_0 from Eqs. (3.18) and (3.19), the velocity at a point in the flowfield can be expressed as

$$V = \left[\frac{2\gamma}{\gamma - 1} \cdot \frac{p}{\rho} \left\{ \left(\frac{p_0 - p}{p} + 1 \right)^{(\gamma-1)/\gamma} - 1 \right\} \right]^{1/2} \quad (3.20)$$

which is used in Chapter 6 for defining the calibrated and equivalent airspeeds in a compressible flow

Equations (3.18) and (3.19), respectively, can be written as

$$\rho/\rho_0 = (p/p_0)^{1/\gamma} \quad (3.21)$$

and

$$1 + (\gamma - 1)V^2/(2\gamma p/\rho) = (\rho/\rho_0)/(p/p_0) \quad (3.22)$$

Eliminating ρ/ρ_0 from the above two relations and noting that $\gamma p/\rho = \gamma RT = a^2$,

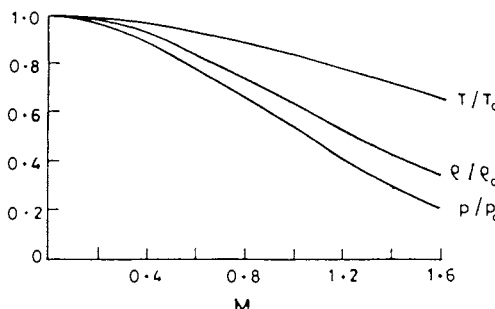


Fig. 3.57 Variations of p/p_0 , ρ/ρ_0 , and T/T_0 with Mach number.

Eq. (3.22) can be written as

$$p/p_0 = \{1 + (\gamma - 1)M^2/2\}^{-\gamma/(\gamma-1)} \quad (3.23)$$

and is commonly used for obtaining the Mach number by measuring p_0 and p in the flowfield.

In the case $(\gamma - 1)M^2/2 < 1$, the right-hand side of the above equation can be expanded by a binomial theorem, yielding

$$p_0 - p = (1/2)\gamma p M^2(1 + M^2/4 + \dots) = (1/2)\rho V^2(1 + M^2/4 + \dots)$$

which shows that the dynamic pressure $p_0 - p$ in a compressible isentropic flow exceeds $\rho V^2/2$ by a factor $(1 + M^2/4 + \dots)$.

Combining Eqs. (3.21) and (3.23) gives the density ratio ρ/ρ_0 as

$$\rho/\rho_0 = [1 + (\gamma - 1)M^2/2]^{1/(\gamma-1)} \quad (3.24)$$

and using Eqs. (3.15), (3.23), and (3.24), the temperature ratio T/T_0 can be expressed as

$$T/T_0 = \{1 + (\gamma - 1)M^2/2\}^{-1} \quad (3.25)$$

The above equation is used in Chapter 18 for defining the temperature recovery factor and obtaining the absolute temperature T in the flowfield. Figure 3.57 shows the variations of p/p_0 , ρ/ρ_0 , and T/T_0 with the increase in Mach number of the flowfield.

References

¹Narasimha, R., and Ojha, S. K., "Effect of Longitudinal Surface Curvature on Boundary Layers," *Journal of Fluid Mechanics*, Vol. 29, Pt. 1, July 1967, pp 187–199.

²Maskell, E. C., *Flow Separation in Three Dimensions*, Royal Aircraft Establishment, Rept. Aero. 2565, 1955.

³Schlichting, H., *Boundary Layer Theory*, 7th ed. (translated by Dr. J. Kestin), McGraw-Hill, New York, 1979.

⁴Houghton, E. L., and Carruthers, N. B., *Aerodynamics for Engineering Students*, 3rd ed., Edward Arnold, 1987.

- ⁵Kuethe, A. M., and Chow, C.-Y., *Foundations of Aerodynamics*, 3rd ed., Wiley, New York, 1976.
- ⁶Eppler, R., *Airfoil Design and Data*, Springer-Verlag, New York, 1990.
- ⁷Riegels, F. W., *Aerofoil Sections*, Butterworth, London, 1961.
- ⁸Abbott, I. H., and Von Doenhoff, A. E., *Theory of Wing Sections*, Dover, New York, 1959.
- ⁹Karamcheti, K., *Principles of Ideal Fluid Aerodynamics*, Wiley, New York, 1966.
- ¹⁰McCullough, G. B., and Gault, D. E., *Examples of Three Representative Types of Airfoil Section Stall at Low Speed*, NACA Technical Note 2502, 1951.
- ¹¹Ojha, S. K., "An Experimental Study of Laminar Separation Bubbles," *Journal of the Aeronautical Society of India*, Vol. 21, No. 3, Aug. 1969, pp. 275–303.
- ¹²Liepmann, H. W., and Roshko, A., *Elements of Gas Dynamics*, Wiley, New York, 1957.
- ¹³Thwaites, B., *Incompressible Aerodynamics*, Clarendon, Oxford, England, UK, 1960.
- ¹⁴Clancy, L. J., *Aerodynamics*, Pitman, England, UK, 1975.
- ¹⁵Torenbeek, E., *Synthesis of Subsonic Airplane Design*, Delft Univ. Press, Delft, The Netherlands, 1976.
- ¹⁶Kuchemann, D., *The Aerodynamic Design of Aircraft*, Pergamon, Oxford, England, UK, 1978.
- ¹⁷Nicolai, L. M., *Fundamentals of Aircraft Design*, METS, CA, 1975.
- ¹⁸Stinton, D., *The Design of the Aeroplane*, Granada, England, UK, 1983.
- ¹⁹Goodmanson, L. T., and Gratzer, L. B., *Recent Advances in Aerodynamics for Transport Aircraft*, Pt. I—Aero. Astro. 11, 1973; Pt. II—Aero. Astro. 12, 1974.
- ²⁰Miele, A., *Flight Mechanics, Vol. I, (Theory of Flight Paths)*, Addison-Wesley, Reading, MA, 1962.
- ²¹Perkins, C. D., and Hage, R. E., *Airplane Performance Stability and Control*, Wiley, New York, 1958.
- ²²Pallatt, E. H. J., *Automatic Flight Control*, 2nd ed., Granada, England, UK, 1983.
- ²³Lomax, H., and Heaslet, M. A., "Recent Developments in the Theory of Wing-Body Wave Drag," *Journal of Aeronautical Sciences*, Vol. 23, 1956, pp. 1061–1074.
- ²⁴Pankhurst, R. C., and Holder, D. W., *Wind-Tunnel Technique*, Pitman, England, UK, 1952.
- ²⁵Ojha, S. K., and Shevare, G. R., "Exact Solution for Wind Tunnel Interference Using the Panel Method," *Computers and Fluids*, Vol. 13, No. 1, 1985, pp. 1–14.
- ²⁶Dole, C. E., *Flight Theory and Aerodynamics*, Wiley, New York, 1981.
- ²⁷McCormick, B. W., *Aerodynamics, Aeronautics and Flight Mechanics*, Wiley, New York, 1979.
- ²⁸Campbell, R. D., *Flight Safety in General Aviation*, William Collins Sons, Collins Professional Books, England, UK, 1987.
- ²⁹Pope, A., and Harper, J. J., *Low Speed Wind Tunnel Testing*, Wiley, New York, 1966.
- ³⁰Pope, A., and Goin, K. L., *High Speed Wind Tunnel Testing*, Wiley, New York, 1965.
- ³¹Sachs, P., *Wind Forces Engineering*, 2nd ed., Pergamon, Oxford, England, UK, 1978.
- ³²Sandborn, V. A., *Resistance Temperature Transducers*, Metrology Press, CO, 1972.
- ³³Doebelin, E. O., *Measurement Systems*, 4th ed., McGraw-Hill, New York, 1990.
- ³⁴Dally, J. W., Riley, W. F., and McConnell, K. G., *Instrumentation for Engineering Measurements*, Wiley, New York, 1984.
- ³⁵Merzkirch, W., *Flow Visualization*, Academic, New York, 1974.

³⁶Moran, J., *An Introduction to Theoretical and Computational Aerodynamics*, Wiley, New York, 1984.

³⁷Yuan, S. V., *Foundations of Fluid Mechanics*, Prentice-Hall, Englewood Cliffs, NJ, 1967.

³⁸Anderson, J. D., Jr., *Introduction to Flight*, 3rd ed., McGraw-Hill, New York, 1989.

Problems

In the multiple choice problems below, mark the correct answer.

3.1 A Newtonian fluid is defined as the fluid that a) was discovered by Newton, b) is viscous and produces vortices, c) has the shearing stress proportional to the rate of strain.

3.2 Boundary-layer flow is always a) either laminar or turbulent and irrotational, b) turbulent and rotational, c) viscous with rapid changes in velocity across it.

3.3 In a two-dimensional rotational flow a) streamlines are always curved, b) fluid particles rotate about their own axes, c) streamlines can be straight and parallel.

3.4 Find the Reynolds number and Mach number of the motion of a circular cylinder of diameter 5 cm if it has the velocity of 100 m/s in a standard atmosphere at sea level.

3.5 Find the Mach number in Problem 3.4 if the cylinder is at an altitude of 12 km.

3.6 An incompressible flow of air is passing convergent-divergent duct. The velocity at station 1 of the duct is 60 m/s where the area is 0.5 m^2 . Find the velocity at station 2 where the area is three times more than at station 1.

3.7 The ambient temperature and pressure are 25°C and 75 cm Hg, respectively, where the duct of Problem 3.6 is situated. Find the pressure difference between stations 1 and 2.

3.8 An aircraft is flying at the standard altitude of 4 km with an airspeed of 70 m/s. Assuming incompressible flow, find the pressure at the point on the surface of the aircraft where the airspeed is 85 m/s.

3.9 In a convergent-divergent supersonic duct, the stagnation temperature and stagnation pressure are, respectively, 25°C and 8 atm. Assuming the airflow to be isentropic, find the pressure and density at the station where the pressure is 1 atm.

3.10 Consider an aircraft flying with an airspeed of 250 m/s at a standard altitude of 5 km. At a point on its wing, the airspeed is 320 m/s. Find the pressure at this point.

- 3.11** A supersonic aircraft is flying at a temperature altitude of 15 km with an airspeed of 2400 km/h. The temperature at a point on the wing is 440 K, find the airspeed at this point.
- 3.12** Find the Mach number of an aircraft cruising at an airspeed of 300 m/s at a temperature altitude of 12 km.
- 3.13** The camber of an airfoil is a) its mean line, b) its maximum thickness, c) the maximum height of its mean line above its chord line.
- 3.14** In an incompressible flow the value of C_p at stagnation point is a) 0, b) 1, c) ∞ .
- 3.15** An airfoil has a) stagnation point always at the leading edge, b) the slope of $2\pi/\text{rad}$ of its lift coefficient curve, c) zero lift, always at the zero angle of attack.
- 3.16** With the increase in aspect ratio a) the value of $dC_L/d\alpha$ decreases, b) wing area increases, c) span to chord ratio of a rectangular wing increases.
- 3.17** Supersonic wings are generally a) highly swept back, b) moderately swept back, c) not swept back.
- 3.18** The critical Mach number is a) the same as the drag rise Mach number, b) larger than the drag rise Mach number, c) the flight Mach number at which sonic velocity is first formed on the surface.
- 3.19** An airflow in the test section of a wind tunnel has the velocity, static pressure, and temperature of 250 km/h, 0.98 atm, and 21°C, respectively. Find the pressure measured by the pitot tube.
- 3.20** An aircraft is flying with a velocity of 60 m/s at the pressure altitude of 2 km where the temperature is 10°C. If at a point on its wing the pressure is $0.75 \times 10^5 \text{ N/m}^2$, find the pressure coefficient at that point.
- 3.21** An aircraft is flying at an airspeed of 60 m/s. If the velocity at a point on its surface is 70 m/s, find the pressure coefficient at that point.
- 3.22** A minimum pressure coefficient on the surface of a wing is -0.92 . What is the critical Mach number of the wing at sea level in the standard atmosphere?
- 3.23** An aircraft is flying with a velocity of 70 m/s at the pressure altitude of 3 km where the temperature is -1°C . It has the lift coefficient of 1.1 and wing planform area of 10 m^2 . Find the all-up weight of the aircraft.
- 3.24** High-lift devices should be used a) throughout the flight, b) only during takeoff, c) during takeoff and landing.
- 3.25** Vortex generators on the wing surface are used to a) stabilize the aircraft, b) obtain high lift, c) minimize drag.

3.26 Pressure coefficient variation along the surface of an airfoil can predict a) positions of flow separation and reattachment, b) regions of laminar and turbulent flows, c) regions of favorable and adverse pressure gradients.

3.27 Flow separation on the surface of a wing causes increase in the drag due to primarily a) increase in skin friction, b) change in surface pressure distribution, c) separated flow becoming unsteady.

3.28 Maximum aerodynamic efficiency means a) lift is maximum, b) drag is minimum, c) lift to drag ratio is maximum.

3.29 Maximum aerodynamic efficiency of an aircraft depends on its a) wing loading and altitude, b) configuration, c) airspeed and thrust.

3.30 The wings of an aircraft have an aspect ratio of 7 and Oswald's span efficiency factor of 0.88. The drag coefficient of the aircraft at zero lift is 0.05. Find the lift and drag coefficients, and calculate the aerodynamic efficiency of the aircraft during its steady level flight.

3.31 Find the maximum aerodynamic efficiency of the aircraft in Problem 3.30.

3.32 A wing is tested in a subsonic wind tunnel at a speed of 60 m/s. If the velocity at a point on the wing is 70 m/s, find the pressure coefficient at that point.

3.33 In Problem 3.32, if the tunnel speed is increased to 270 m/s and the test section air temperature is 20°C, find the pressure coefficient at the same point.

3.34 An aircraft wing of aspect ratio 7.5, and wing area 17 m^2 has an Oswald's span efficiency factor, of 0.75. If the aircraft weighs 10,000 N and is flying at an standard altitude of 2 km with a velocity of 320 km/h, find the lift-dependent drag of the aircraft.

3.35 Find the lift-dependent drag of the aircraft in Problem 3.34 at its stalling airspeed of 90 km/h in a standard atmosphere at sea level.

3.36 Aircraft control surfaces are generally a) cambered, b) not cambered, c) immovable.

3.37 Flow visualization is generally carried out to predict a) velocity field, b) pressure field, c) streamline pattern.

This page intentionally left blank

Propulsive Thrust by Jet Engines

4.1 Introduction

The concept of jet propulsion became a reality when the Germans used it in their military aircraft during the Second World War. Later on the technology developed to a more sophisticated level¹ in the United States, with the result that most modern airlines successfully use jet propulsion in their gas turbine engine aircraft. The advent of supersonic flights greater than Mach 2 or 3, requiring high thrust, led to the development of ramjet engines that are far simpler. Another important chapter in jet propulsion was opened by the development of rockets, which are nonairbreathing engines and do not depend on atmospheric air for propulsion; this paved the way for outerspace travel.

Aircraft engines can be broadly classified into airbreathing and nonairbreathing engines. An airbreathing engine can be either a reciprocating engine (piston engine) or a jet engine, as shown in Fig. 4.1. The jet engine can be either a ramjet or a gas turbine engine. The ramjet fully utilizes the air-jet for thrust but operates efficiently at supersonic Mach numbers exceeding 2 or 3. The gas turbine engine only partly utilizes the jet for thrust purposes because some energy of the jet is extracted to rotate its turbine for developing shaft power. Gas turbine engines can be classified as turbojet, turboprop, and turbofan.

The thrust or power characteristics of an aircraft engine, especially with respect to airspeed and altitude, dictate the performance of an aircraft. These characteristics depend on the type of engine being used. In a book of this size it is not possible to pronounce performance calculation methods for all the different types of engines. Therefore, only reciprocating and turbojet engines are chosen for carrying out different aspects of aircraft performance. A reciprocating engine is representative of a low-speed aircraft, which is described in the next chapter. The present chapter describes gas turbine engines with emphasis on a turbojet engine that can be regarded as representative of a high-speed and high-performance aircraft. For the sake of completeness of propulsive devices of an aircraft, the important aspects of ramjets and rockets are also summarized.

4.2 Jet Propulsion and Gas Turbine Engines

A jet propulsion engine is based on Newton's third law of motion, namely, that to every action there is always an equal and opposite reaction. A jet propulsion device uses gas turbine engines where Newton's third law of motion can be applied in different ways, resulting in different types of gas turbine engines.

4.2.1 Principle of Jet Propulsion

A jet engine forces the incoming finite air-jet stream to accelerate. It works on the principle that any device forcing a jet stream to accelerate will in turn experience an equal and opposite force of reaction as thrust. The thrust produced

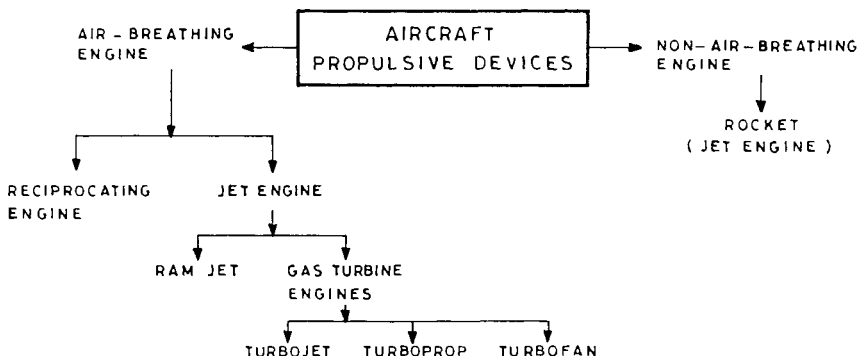


Fig. 4.1 Classification of aircraft propulsive devices.

by the engine can be calculated by the rate of change of momentum it imparts to the air-jet stream. The physical mechanism by which an air stream, or any other fluid medium, communicates force to the solid surface is through surface pressure and skin friction forces acting at each point over the surface. If the axial components of these two forces are added and integrated over the complete surface of the engine, the thrust force acting along the axis of the engine is obtained. The skin friction force, being negligibly small, is usually not considered in calculating thrust. The principle of producing thrust by a propeller or fan is also the same.

4.2.2 Gas Turbine Engines

A gas turbine engine is an airbreathing engine. The term *gas turbine* is used to differentiate it from a steam or water turbine. A *turbine* is a mechanical device used to extract power from high-speed moving fluids. The gas turbine extracts power from high-speed hot expanding gases. These gases are mostly air (more than 98%) but also contain a negligibly small amount (less than 2%) of gas resulting from fuel combustion. The engine first produces high-speed hot gas that passes over its turbine, which extracts mechanical energy from the gas. The extracted energy appears in the form of shaft power (SP) of the turbine, or thrust power from the exhaust gas, or both. Different types of gas turbine engines are available that can be broadly classified as turbojet, turboprop, and turbofan. The turbojet engine produces mostly jet thrust, the turboprop engine produces mostly power and only a small amount of jet thrust, and the turbofan engine produces both thrust and power of comparable magnitudes.

The processes and their sequence, which are common to all gas turbine engines, and the characteristic differences among the turbojet, turboprop, and turbofan engines, are shown in Fig. 4.2. The atmospheric air entering the airbreathing inlet is compressed, burned with the fuel in the combustion chamber, and the resulting hot, high-speed gases expand and pass through the turbine and exhaust nozzle for extraction of energy. The turbine extracts some energy from the gases and converts it into SP, and the rest of the gas passes through the nozzle as a jet stream, producing thrust. A turbojet engine produces only jet thrust, because the power extracted by the turbine is consumed by the engine itself for running the compressor and accessories. In a turboprop engine, the turbine produces mostly SP to run both the compressor and the propeller. The propeller of a turboprop

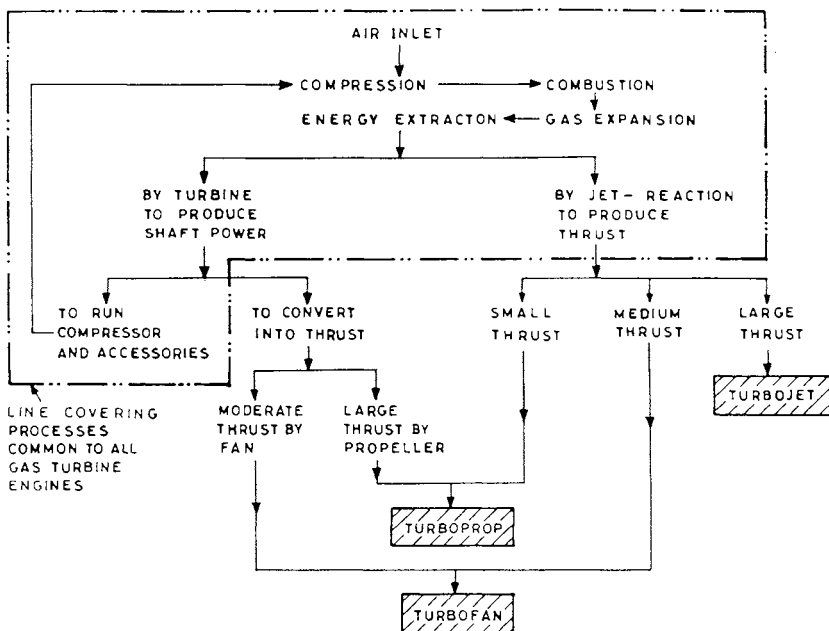


Fig. 4.2 Processes common to all gas turbine engines, and differences among turbojet, turbodrop, and turbofan engines.

converts SP into thrust, and only a small portion of thrust is also obtained from the jet of its exhaust gases. A turbofan engine produces comparable amounts of both thrust and SP. The thrust of a turbofan engine is produced by the exhaust jet, and the SP is produced by its turbine to run the fan, which produces additional thrust. A detailed description of the three gas turbine engines and their relative advantages are presented in subsequent sections.

4.2.3 Engine Ratings

The turbine inlet temperature depends on the amount of fuel being introduced into the combustion chamber. There is a maximum allowable temperature that the turbine can withstand under the high stresses of its rotation. This allowable temperature forms the genesis of engine ratings.

A turbojet engine generally produces more thrust than is required for takeoff and flight. The maximum thrust is generally not allowed to be used in most of the operations of the aircraft. Only a certain fraction of the maximum thrust is usually used. The thrust that an engine is allowed to develop for a particular mode of operation of the aircraft is called the engine rating of the aircraft for that mode. Thus, there are engine ratings for takeoff, climb, cruise, etc. These engine ratings are required for certification of the aircraft. The thrust at the time of takeoff is termed the *maximum allowable thrust*. The ratings can also be time limited and may depend on the altitude and atmospheric conditions. The ratings for takeoff usually have time limitations of about 5 min. The rating can also specify the maximum thrust that can be continuously used for emergency operations at the discretion of the pilot.

4.3 Turbojet Engine

The components of a turbojet engine and the nature of the fundamental thrust equation are described here. Knowledge of variation of thrust and its specific fuel consumption with airspeed and altitude is important for performance calculation. Thrust augmentation devices and the relative merits of a turbojet engine are also explained below.

4.3.1 Components of a Turbojet Engine

The most important components of a turbojet engine are its air inlet duct, compressor, combustion chamber, gas turbine, and the exhaust nozzle, as shown in Fig. 4.3. The purpose and the characteristic features of these components are explained here.

4.3.1.1 Air inlet duct. An air inlet duct is usually a diffuser that decreases velocity and increases static pressure of the air while it is passing through the inlet duct. It converts the kinetic energy of the freestream into pressure energy in an efficient manner. Normally, the air inlet duct is considered a part of an airframe, and not a part of its engine. However, the duct is quite important to engine performance and this must be taken into account when discussing the engine as a whole. The inlet duct has three important functions for the engine and one for the airframe. First, it must supply a required quantity of air mass flow rate in the duct, which fixes the size of the duct. Second, it must reduce the airspeed with minimum total pressure loss. The total pressure recovery across the length of the duct is called the *ram recovery*. To minimize total pressure loss, i.e., to maximize total pressure recovery, the pressure and skin friction losses should be kept at a minimum. Third, the duct must be able to provide uniform flow across its cross section at the compressor face. Last, in regard to its function in the aircraft, the duct should have minimum drag and should not interfere with the smooth flow of air over the aircraft.

The inlet duct would be either a subsonic or a supersonic diffuser, depending on whether the aircraft is subsonic or supersonic. A *subsonic diffuser* is a divergent duct while a *supersonic diffuser* is a convergent duct. The design of a supersonic diffuser is quite different from that of a subsonic diffuser; this is to be expected from the differences in subsonic and supersonic flows. The formation of shock waves is generally inevitable in supersonic air diffusion. These shocks produce additional pressure loss, called *wave drag*, which also must be reduced. Some supersonic inlets use a movable central body to tailor the strength and location of the shock waves and to help in forming a suitable convergent-divergent nozzle

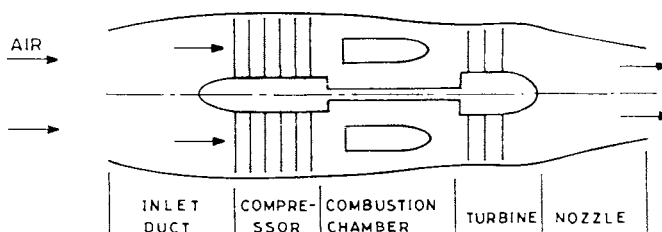


Fig. 4.3 Elements of a turbojet engine.

for diffusion. Supersonic diffuser design is an important subject that has been discussed in detail by Seddon and Goldsmith.²

4.3.1.2 Compressor. The combustion of fuel and air at atmospheric pressure does not produce sufficient power that can be extracted from the expanding gases at a reasonable level of efficiency. A compressor produces the increased pressure that is required to increase the efficiency of combustion. The compressor first imparts kinetic energy to the airflow by increasing its airspeed, and then diffuses it by decreasing the airspeed to increase the static pressure of the airflow. A compressor can be either a centrifugal or axial flow type.

4.3.1.2.1 Centrifugal compressor. A centrifugal compressor has three main parts: an impeller, a diffuser, and a compressor manifold. The outside air enters the compressor near the central hub and the high-speed rotation of the impeller about its own axis imparts high-velocity rotational kinetic energy to the air. The air from the impeller is pushed into the diffuser by centrifugal force. The diffuser converts the high-velocity energy into low-velocity, high-pressure energy, and diverts the flow to the manifold. The manifold delivers the air to the combustion face at a velocity and pressure that will be satisfactory for use in the burning section of the engine. The maximum compression ratio of about 4 or 5 can be achieved by a single centrifugal compressor, which has an efficiency of about 70–85%. Multiple centrifugal compressors can be mounted in tandem on the same shaft, but this arrangement has the disadvantage of diverting the flow through 180 deg from the exit of one compressor to the inlet of the other compressor. Many earlier turbojet engines and even some current ones use centrifugal compressors. This type of compressor is also used as a supercharger, and for pumping water and other liquids.

4.3.1.2.2 Axial flow compressor. An axial flow compressor achieves a much higher pressure ratio with better efficiency than a centrifugal compressor. The axial flow may develop thrust per unit area of about $71,820 \text{ N/m}^2$, $7326 \text{ kg}_f/\text{m}^2$ (1500 lb/ft^2) that is about four times the amount of thrust per unit area developed by the average centrifugal flow engine, which developed about $19,152 \text{ N/m}^2$, $1954 \text{ kg}_f/\text{m}^2$ (400 lb/ft^2). Axial flow compressors are most commonly used in gas turbine engines, especially those requiring high thrust. The compressor consists of a series of alternating stationary and rotating wheels that have blades in radial directions. The blade sections are made up of thin airfoils. The stationary blades are called *stators* and the rotating blades are called *rotors*. The stator blades are also called guide vanes, straighteners, or diffusers because the blades serve these purposes.

The air enters axially into the inlet of the axial flow compressor and it first meets the first set of stator blades, called *guide vanes*. These guide vanes guide the flow according to the requirements of the following first set of rotor blades. The most modern engines do not have guide vanes because the rotor blades themselves are designed accordingly. The rotor blades by their rotation impart kinetic energy to the airflow by creating pressure difference across the surface of the blades. The static pressure also rises slightly as the air passes over the rotor blades. This rise in static pressure is further increased by diffusion as it passes through the next set of stator blades. The stator blades reduce the velocity and guide the flow to meet the following rotor blades at a proper angle of attack. The process is repeated through the remaining stages of the compressor. After the last set of stator

blades, many compressors have one or two sets of more stator blades to straighten the flow and reduce the airspeed prior to its entry into the combustion chamber; if these later stator blades are also meant to provide additional air turbulence, which is sometimes necessary to alleviate combustion problem, they are called *mixer blades*.

The pressure ratio accomplished per stage of compression, which is called the *stage pressure ratio* (SPR), is about 1.2–1.6. This relatively low-pressure ratio in a single stage is the reason for providing a number of stages in a single axial flow compressor unit. The total pressure ratio (TPR) of an n -stage compressor is given by $\text{TPR} = (\text{SPR})^n$. For example, a 10-stage compressor with an average SPR of 1.36 would give, $\text{TPR} = (1.36)^{10} = 21.6$.

It may appear that a single axial flow compressor can be built by carrying as many stages as necessary for achieving the required total compression pressure ratio. But this would cause the rearmost stages, which have small blades, to become inefficient, and the front stages with large blades therefore become overloaded. This produces flow separation on blades leading to *compressor stall*, also referred to as *surge*. Therefore, when very high total compression ratio is required, it is better to have two axial flow compressor units that are fitted one after another independently, each connected to its own turbine. In the dual axial flow compressor, also sometimes called the split or twin-spool compressor, the two units are connected to the two turbines through two coaxial circular shafts. The front compressor is called the low-pressure (LP) compressor and the rear one, operating at high pressure, is called the high-pressure (HP) compressor.

4.3.1.3 Combustion chamber. After leaving the compressor exit, the air enters the combustion chamber. Fuel is injected at the beginning of the combustion chamber and mixes with a part of the oncoming air. The combustible mixture is ignited, which releases heat energy at constant pressure and the gas expands in the combustion chamber. The combustion chamber provides the delivery of gas, at proper temperature level and proper temperature profile, to the turbine face. Combustion chambers of different types³ serve the same purpose.

The fuel air ratio for combustion is between 0.04 and 0.15, since beyond these limits burning ceases to exist. The lower number (0.04) is called a *lean limit* of flammability and the higher number (0.15) is called a *rich limit* of flammability. A combustion chamber maintains the fuel air mixture ratio within these allowable limits, and generally within more stringent limits, if efficient burning is to occur. All the air that leaves the compressor is not mixed with the fuel, because this would require more fuel to maintain the proper fuel air ratio and the heating of the gas would be in excess of the maximum allowable turbine blade inlet temperature. Only 25–40% of the air is allowed to take part in combustion while the rest of the air is mixed with the combusted gas later in the combustion chamber to bring the delivery temperature (turbine entry temperature) within allowable limits.

The combustion cannot be maintained unless the three *T* of combustion—temperature, turbulence, and time—are also satisfied. The temperature of the mixture must be kept above its ignition temperature. This requires the mixture to first be ignited by electric spark, and therefore the heat released by combustion is much greater than the ignition temperature necessary to keep the burning continuous. Turbulence is required to maintain the fuel air mixture ratio constant and homogeneous within allowable limits. A sufficient time interval must be

maintained for complete burning of the fuel, requiring low airspeed in the combustion chamber. If the airspeed is greater than the flame speed (about 18–30 m/s), the flame will be blown down the combustion chamber and out of the engine, causing *flameout*.

4.3.1.4 Gas turbine. The hot gases coming out of the combustion chamber at high speeds pass through the gas turbine blades. The purpose of a gas turbine is to extract mechanical energy from the high-velocity hot gases and develop SP to drive the compressor. The turbine also supplies power to the auxiliary equipment, such as fuel pumps, oil pumps, and electrical generators. In the case of turboprop and turbofan engines, the turbines are designed to extract much more mechanical energy from the gases, because in addition to driving the compressor here, the turbines also drive the propeller and fan. This extraction of mechanical energy is more in the turboprop than in the turbofan engine.

A turbine has a disc, coaxially fitted to the central shaft, and around the circumference of the disc the blades are radially mounted. For efficient functioning of the turbine, the oncoming flow must be directed to the leading edge of the turbine blades at a particular angle. This angle is generally achieved by means of fixed blades, called guide vanes or nozzles, placed ahead of the rotating turbine blades. When the high-velocity gases produced by the nozzles pass through the turbine blades, lift force is generated on each blade of the turbine. Thus, the turbine wheel turns at a great speed producing torque to the central shaft which is used for running the rotary compressor itself. If more SP is required from the gases, it is common to mount two or more turbine wheels one behind the other on the same shaft. Between the two turbine wheels, fixed blades known as *stator blades* are mounted that do not rotate. These stator blades correct the entry of the gas flow into the following set of rotary turbine wheel blades and also neutralize the rotary motion of the gases that is induced by the first set of rotary turbine wheel blades. The flow of gases through a turbine is an expansion process causing a drop in static pressure when the gases pass through the turbine. This is the only component in the whole gas turbine engine that extracts power from the hot, high-velocity gases. Hence, this is the most important component; in fact, the term the *gas turbine engine* is derived from this component.

4.3.1.5 Exhaust nozzle. At the exit section of the turbine, the static pressure of gases is generally higher than the ambient atmospheric pressure outside the region. Therefore, the gas flow can be further expanded and the jet velocity can be increased to enhance the thrust by simply incorporating an exhaust nozzle at the rear of the engine. The exhaust nozzle is designed so that the static pressure of the gases at the discharge section is the same as the ambient atmospheric pressure, because the exhaust nozzle reduces the pressure drag. The exhaust duct is generally axisymmetric but can be also two-dimensional. The exhaust duct can be either a convergent nozzle, or a convergent-divergent nozzle, depending on its type and the use it is designed for. If the engine is meant for subsonic flight, the exhaust duct is a convergent nozzle so that the exit velocity is subsonic or at the most sonic. If the engine is meant for a supersonic aircraft, the exhaust duct may be a convergent or convergent-divergent nozzle. In order to achieve optimum performance over the entire airspeed range of the flight, the exhaust nozzle is a variable-area nozzle so that the ratio of its exit area to throat area can be changed to make the exit pressure of the gas equal to the ambient pressure.

4.3.1.6 Variation of flow properties among the components. The variation of gas flow properties such as airspeed, pressure, temperature, and force along the length of each component of the turbojet engine during flight is shown in Fig. 4.4. The static temperature continuously increases until the end of combustion chamber, then it decreases. The total temperature increases during the compression and combustion but decreases during the passage through the turbine. The total temperature is constant in the inlet duct and again in the exhaust nozzle. The static pressure continuously increases up to the end of compression, remains almost constant in the combustion chamber and thereafter decreases until the end of the exhaust nozzle is reached. The total pressure falls slightly in the inlet duct, then rises sharply during compression, remains almost constant in the combustion chamber, falls in the turbine region, and falls again very slightly in the exhaust nozzle. The velocity falls in the inlet duct (diffuser) and then rises. In the turbine region the net increase in velocity is almost negligible.

The forward force distribution contributing to the thrust is also shown in the bottom portion of Fig. 4.4. Both forward force distribution and thrust are shown for both static and flight conditions. The positive slopes contribute to forward force while the negative slopes contribute to backward force (drag). The unbal-

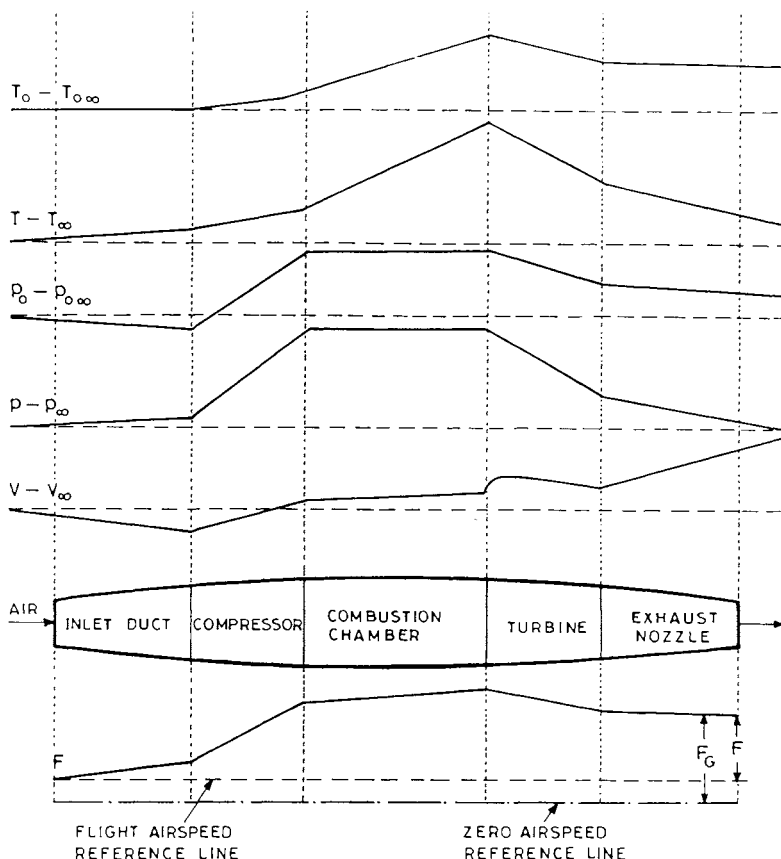


Fig. 4.4 Variation of gas flow properties in a turbojet engine.

anced force, designated as F , is the net force that is available to the aircraft for propulsion during flight, and F_G is the gross thrust available on the ground during the start of takeoff.

4.3.2 Thrust and Its Determination

Thrust is an important variable for carrying out various flight operations. The pilot controls thrust by throttling the fuel pipeline. By reducing the throttle, the fuel supply to the combustion chamber is constrained so that the thrust is reduced. By increasing the throttle, thrust increases, so that at full throttle (valve fully open) thrust is at its maximum—this is also referred to as *thrust available*. The fundamental equation of the thrust is discussed here without entering into its derivation, and the determination of thrust is briefly explained.

4.3.2.1 The fundamental thrust equation. The fundamental equation of the thrust force of a turbojet engine is obtained by considering the change in momentum flux of the air entering into the inlet duct and the unbalanced force acting at the nozzle exit due to the difference between the exit and ambient pressures. V and p , respectively, represent the airspeed and pressure, the subscript ∞ denotes the ambient or upstream condition near the entrance of the inlet duct, and the subscript e denotes the condition at the exit of the exhaust nozzle.

The momentum flux at the entry of the inlet duct is $\dot{m}_{\text{air}} V_\infty$, where \dot{m}_{air} is the mass flow rate of air at the inlet. The momentum flux of the exhaust gases is $(\dot{m}_{\text{air}} + \dot{m}_f) V_e$ where \dot{m}_f is the mass flow rate of the fuel. The pressure p_e at the exit of the nozzle can be greater or less than the ambient atmospheric pressure p_∞ , and if this is true, the pressure imbalance will provide an additional term $(p_e - p_\infty) A_e$ to the thrust, where A_e is the area of the exit portion of the nozzle. The equation for the net thrust force F is given by¹

$$F = (\dot{m}_{\text{air}} + \dot{m}_f) V_e - \dot{m}_{\text{air}} V_\infty + (p_e - p_\infty) A_e \quad (4.1)$$

This is the fundamental equation of thrust. Since $\dot{m}_f \ll \dot{m}_{\text{air}}$, the above relation can be written as

$$F = \dot{m}_{\text{air}} (V_e - V_\infty) + (p_e - p_\infty) A_e \quad (4.2)$$

When the aircraft and engine are static, $V_\infty = 0$, the net thrust F is called the gross thrust or static thrust, and is represented by F_G . Therefore, from Eq. (4.2),

$$F_G = \dot{m}_{\text{air}} V_e + (p_e - p_\infty) A_e \quad (4.3)$$

During the motion of an aircraft, $V_\infty \neq 0$, the net thrust F becomes less than the gross thrust F_G . They become equal, $F = F_G$, when the aircraft is static, $V_\infty = 0$.

An important design consideration is to keep $p_e = p_\infty$ and in such cases the net thrust given by Eq. (4.2) becomes

$$F = \dot{m}_{\text{air}} (V_e - V_\infty) \quad (4.4)$$

and the gross thrust becomes

$$F_G = \dot{m}_{\text{air}} V_e \quad (4.5)$$

When the term "thrust" is used by itself in discussing a gas turbine engine or an aircraft, the reference is usually to net thrust, unless otherwise stated.

4.3.2.2 Thrust determination. The thrust equations presented in Sec. 4.3.2.1 serve a useful purpose in helping us to understand the effects of several variables encountered during flight and on the ground.

The static thrust of an engine is measured directly by use of an engine test stand. The stand is generally constructed in such a way that it usually floats, pushing against a calibrated scale that accurately measures the thrust. Thrust stands, which measure the static thrust of an aircraft, are also available and are often used.

Direct measurement of net thrust when the aircraft is in motion becomes usually impracticable. The net propulsive thrust during flight is indicated by the measurements of compressor revolutions per minute (rpm) and turbine discharge pressure (or engine pressure ratio), which vary with the thrust being developed.

4.3.3 Influence of Airspeed, Altitude, and Atmosphere

For a given engine, the thrust varies with the airspeed, altitude, and the atmospheric conditions of pressure, temperature, and humidity. For performance calculations it is necessary to know these variations for any given throttle setting. These variations can be explained from the basic equations of thrust mentioned above.

4.3.3.1 Thrust variation with airspeed. The variation of thrust with airspeed is nearly constant except at the initial part of the ground roll during the start of takeoff when the airspeeds are too low, as shown in Fig. 4.5. During the flight of an aircraft the airspeeds are not small and it is reasonable to assume that the thrust remains constant with airspeed. This can be explained by Eq. (4.4), which shows that the thrust is the product of the mass flow rate of air \dot{m}_{air} and the velocity difference $V_e - V_\infty$. As the airspeed V_∞ increases, the mass flow rate of air also increases. But the exit velocity V_e is not much affected by the increase in V_∞ because the exhaust nozzle generally operates under choked throat conditions, so that $V_e - V_\infty$ decreases with the increase in airspeed V_∞ . Thus, the thrust—determined by the product $\dot{m}_{\text{air}}(V_e - V_\infty)$ —remains approximately constant. The assumption of that thrust remains constant with airspeed implies

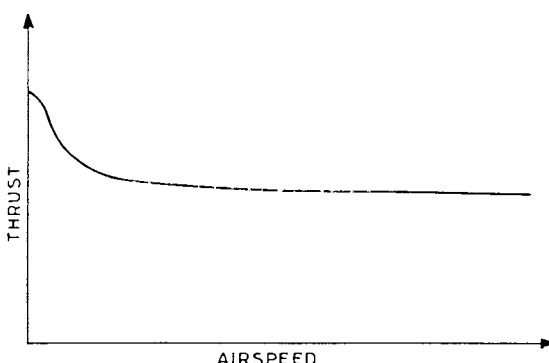


Fig. 4.5 Thrust variation of turbojet engine with airspeed.

that $dF/dV = 0$, which considerably simplifies many performance calculations related to turbojet aircraft, and the results can be presented analytically.

4.3.3.2 Thrust variation with altitude. A knowledge of thrust variation with altitude (and thus with air density) is important because the density enters directly into almost all the performance calculations, and the aircraft flies at different altitudes. Since mass flow rate of air is represented by $\dot{m}_{\text{air}} = \rho A V_{\infty}$, Eq. (4.4) can be written as

$$F = \rho A V_{\infty} (V_e - V_{\infty}) \quad (4.6)$$

which shows that the thrust is directly proportional to the ambient air density. In view of the above relation for a given aircraft, it would be reasonable to write that for a given throttle setting,

$$F/F_{\text{SSL}} = \rho/\rho_{\text{SSL}} = \sigma \quad (4.7)$$

where the subscript SSL represents standard atmosphere sea level condition. In practice, the above relation is more satisfactory in the stratosphere. In the troposphere it takes the form

$$F/F_{\text{SSL}} = \sigma^{0.7} \quad (4.8)$$

For the sake of simplicity and for the purpose of obtaining certain performance results analytically, Eq. (4.7) is used both in the troposphere and stratosphere, for a constant throttle setting. At any given altitude, however, a pilot can vary the thrust considerably by changing the throttle setting.

4.3.3.3 Effects of pressure, temperature, and humidity. The effects of ambient atmospheric pressure and temperature on thrust are obtained from Eq. (4.6) by writing it as

$$F = p A V_{\infty} (V_e - V_{\infty}) / (RT) \quad (4.9)$$

where R is the gas constant of air. This shows that the thrust decreases with the decrease in ambient pressure and consequently it is at a maximum at sea level.

Similarly, Eq. (4.9) shows that the thrust decreases with increase in atmospheric temperature, indicating that on hotter days engine thrust would decrease whereas on colder days it would increase.

Humid air is lighter than dry air and the gas properties of humid air are slightly different from those of dry air. The effect of humidity on thrust is not appreciable because even with 100% relative humidity of the air, the effect on thrust and engine performance is only about 1%. The effect of humidity is taken into account only when extreme accuracy is desired.

4.3.4 Thrust Augmentation Devices

The desire to achieve better takeoff performance, higher rate of climb, and improved combat maneuvers demands methods for increasing the thrust output of an aircraft. The two most common methods used for thrust augmentation are

This page intentionally left blank

This page intentionally left blank

Equation (4.11) has six variables with three fundamental units. According to Buckingham's π theorem, Eq. (4.11) can be written in terms of three dimensionless variables as

$$F/(pD^2) = f(ND/\sqrt{T}, M)$$

Similarly, the functional relationship for the fuel flow rate \dot{W}_f can be written as

$$\dot{W}_f/(pD^2\sqrt{T}) = f(ND/\sqrt{T}, M)$$

Introducing the notations $\delta = p/p_{SSL}$ and $\theta = T/T_{SSL}$, the above two relations can, respectively, be written as

$$F/(\delta p_{SSL} D^2) = f(ND/\sqrt{T_{SSL}\theta}, M)$$

and

$$\dot{W}_f/(\delta D^2\sqrt{\theta T_{SSL}}) = f(ND/\sqrt{T_{SSL}\theta}, M)$$

where p_{SSL} and T_{SSL} are constants, and for a given engine, D is also a constant. Therefore, for a specified engine, it is common to express the above two equations, respectively, as

$$F/\delta = f(N/\sqrt{\theta}, M) \quad \text{and} \quad \dot{W}_f/(\delta\sqrt{\theta}) = f(N/\sqrt{\theta}, M) \quad (4.12)$$

For example, consider a set of typical turbojet engine curves given by the first relation of Eq. (4.12), as shown in Fig. 4.6. This single plot represents the thrust performance of the engine at all altitudes, Mach numbers, and engine rpm, over the range shown in the figure. If the parameters are not used, it would require many curves and graphs to present the same information. The parametric representation, therefore, saves considerable time and money when the performance characteristics are calculated or determined by flight or wind-tunnel tests.

4.3.7 Advantages and Disadvantages of a Turbojet Engine

Turbojet engines of various sizes are available ranging from 22.7 kg_f (50 lb) to 27,216 kg_f (60,000 lb) of thrust. The uninstalled engine thrust/weight ratio is about 4 to 8. Turbojet engines are much lighter and have smaller frontal areas as compared

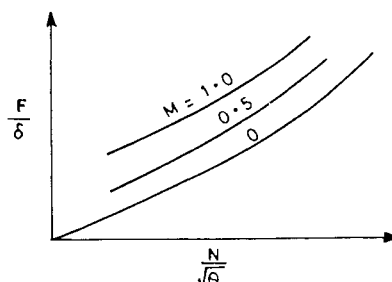


Fig. 4.6 Functional relationship of turbojet engine.

to piston-prop engines. At higher airspeeds, the inlet of a jet engine captures higher mass flow rate which increases the efficiency of the engine. This efficiency is further increased at high altitudes because the pressure and temperature drop through the turbine is greater in the less dense and cooler atmosphere. Thus, turbojet engines are most suited to high-speed and high-altitude flying.

The TSFC of a turbojet engine is higher than that of a turboprop or turbofan engine, but this disadvantage decreases as the altitude and airspeed increases. Turbojet engines are not suitable for very high thrust at low airspeed. Therefore, an aircraft powered by a turbojet engine takes longer time for ground roll, takeoff, and climb.

Piston-prop engines are efficient around Mach 0.3 and turbojets are efficient at around Mach 0.8 and above. Thus, there appeared a need to design engines that are efficient in the region of Mach 0.3–0.8. This also suggests that if one could develop an engine that employed both propeller and jet simultaneously for thrust, the efficiency of the engine could be expected to lie between that of the piston-prop and turbojet engines. This concept has led to the development of turboprop and turbofan engines which are classified as different versions of the gas turbine engines.

4.4 Turboprop Engine

The components of a turboprop engine are discussed here. It has a propeller that is mounted in front of the engine. The thrust produced by its propeller is much more than that produced by the jet of its exhaust gases. It is a dual-flow engine whose power is expressed in terms of equivalent shaft power.

4.4.1 Engine Components

A turboprop engine has all the components of a turbojet engine and, in addition, it has a propeller in front of the engine. The propeller is connected to the compressor or a separate power turbine through a central shaft and a gear, as shown schematically in Fig. 4.7. Its components such as inlet duct (diffuser), compressor, combustion chamber, and exhaust nozzle work in the same fashion as those of a turbojet engine. The only difference is that the turbine here extracts much more power than it does in the turbojet engine, because the turbine provides power for both the compressor and the propeller. A turboprop engine, like a turbojet engine,

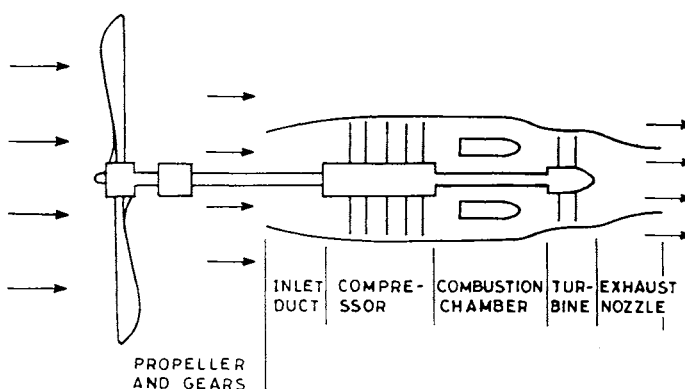


Fig. 4.7 Elements of a turboprop engine.

may have either a single-stage or multistage centrifugal compressor, or otherwise a single compressor or a dual axial compressor. The reduction gear that controls the propeller rpm is generally connected directly to the central shaft. In the case of a dual-axial compressor, the reduction gear is connected to a low-speed compressor drive shaft. In certain turboprop engines the propeller is driven by a turbine of its own, independently of the compressor.

In addition to the compressor, if the shaft of a gas turbine drives an external rotor, the engine is called a *shaft turbine* or *turboshaft engine*. Turboshaft engines are commonly used in helicopters, where the engine axis is vertical and the rotor rotates in a horizontal plane. These engines are normally smaller in size but run at high rpm, and power the helicopter rotor through a gear box. The rpm of a turboshaft engine are generally much higher (20,000–40,000 rpm) than that of a turboprop engine (10,000–15,000 rpm).

4.4.2 Importance of the Propeller

The turbines extract most of the energy of the high-velocity hot gases for driving both propeller and compressor, with the result that only a small portion of the energy is left for producing jet thrust. The sum of the thrusts developed by the propeller and the jet exhaust is the total thrust produced by the engine. The propeller produces about 85% of the thrust and the remaining 15% comes from the jet exhaust. The rotational speed of the central shaft of a gas turbine engine is too high and, therefore, the reduction gears are installed at the back of the propeller for reducing the rpm of the propeller. The tip velocity of the propeller blades is thus not allowed to exceed sonic velocity, which ensures the efficiency of the propeller blades. The propeller of a turboprop engine is similar to that of a large piston-prop engine. As the airspeed increases beyond a certain limit, the efficiency of the propeller drops, but this is compensated to a certain extent by the increased efficiency of the jet thrust at the tail. Thus, a turboprop engine is more efficient at high airspeeds, as compared with a piston-prop engine.

4.4.3 Turboprop as a Dual-Flow Engine

The jet exhaust of hot gases (air + fuel) emerging from the nozzle at the tail is called *primary flow*. The air flow through the propeller is called *secondary flow*. The mass flow rate of the secondary flow is considerably higher than that of the primary flow. Therefore, a turboprop has two kinds of flows, and so it is classified as a *dual-flow* or *multiple-flow* engine. The propulsive thrust is provided by the dual momentum change of the air, first by the propeller to the secondary flow, and second by the jet exhaust to the primary flow. The sum of these two thrusts is the total thrust of the engine.

4.4.4 Equivalent Shaft Power

A turboprop essentially produces SP because about 85% of the total power comes from the central shaft, which provides power to the propeller. The remaining 15% of the total power comes from the jet exhaust. This makes it common to designate the engine in terms of SP or horsepower rather than in terms of thrust. Since the jet exhaust is converted into power based on the design airspeed of the engine, it is necessary to designate the engine in terms of equivalent shaft power

(ESP), or equivalent shaft horsepower (ESH), instead of simply brake power (or horsepower). The equivalent SP is defined as

$$\text{ESP} = \text{shaft power} + F_j V / (k\eta_p)$$

where V is the design airspeed of the turboprop aircraft, F_j is the jet thrust, and η_p is the propeller efficiency. The quantity k is the conversion factor whose value depends on the units used in the shaft power. For example, $k = 550 \text{ ft-lb/s hp}$, 1000 W/kW , or 1, respectively, depending on whether the SP is specified in horsepower, kilowatts, or watts.

The variation in power of the engine with altitude can be made to behave like that of a supercharged piston-prop engine by a technique known as *derating*.⁴

Having defined ESP above, it is now also possible to define equivalent power-specific fuel consumption (EPSFC). It will be denoted by \hat{c}^* , which is defined as $\hat{c}^* = \dot{W}_f / \text{ESP}$. Therefore, EPSFC is the ratio of the rate of fuel consumed \dot{W}_f to the ESP.

4.4.5 Advantages and Disadvantages of a Turboprop Engine

Turboprop engines are available in the range of ESHP of 373–4474 kW (500–6000 hp) and sometimes even up to 7457 kW (10,000 hp). The power-weight ratio of a turboprop engine is about 3.288 kW/kg_f (2 hp/lb), and a turboprop engine is one-fourth the weight of a piston engine of the same horsepower. The performance of a turboprop engine is much superior to that of a turbojet or turbofan engine during takeoff and climb; this is due to the ability of its propeller to accelerate a large mass of air at relatively low flight speed. A turboprop usually flies in the Mach number range of 0.4–0.7. The propulsive efficiency of a turboprop engine remains nearly constant in the normal cruising speed range. The specific fuel consumption of a turboprop is somewhat more than that of a piston-prop, but much less than that of a turbojet engine. Its frontal area is less than that of a piston-prop engine but somewhat more than a turbojet engine. Although the initial cost of a turboprop engine is higher than that of a piston-prop engine, the maintenance cost is much less and it is more reliable. A turboprop engine is heavier than a turbojet or a turbofan engine.

4.5 Turbofan Engine

The components of a turbofan engine are mentioned here, with emphasis on its fan, which is installed in the front portion of the engine. It is also a dual-flow engine whose thrust is expressed in terms of equivalent thrust. The thrust produced by the fan is comparable with that produced by the jet exhaust of its engine.

4.5.1 Engine Features

A turbofan engine combines the characteristic features of both turboprop and turbojet engines. The turbofan version of a gas turbine engine is schematically shown in Fig. 4.8. It has all the components of a turbojet engine, i.e., inlet duct, compressor, combustion chamber, gas turbine, and exhaust nozzle. The geared propeller of a turboprop is replaced here by a ducted fan which is also driven by the turbine. The blades of the fan are much smaller than that of a propeller so that the fan rpm can be increased to higher values without the tip airspeed reaching

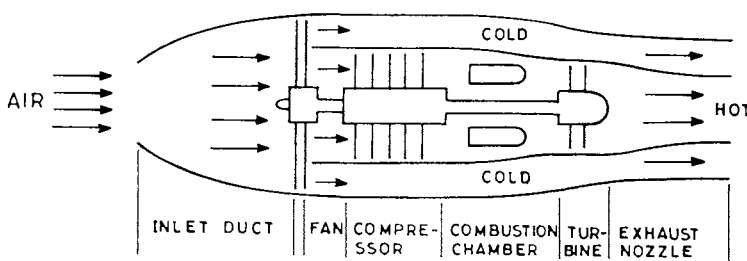


Fig. 4.8 Elements of a turbofan engine.

sonic velocity. The cross section of a fan blade is similar to that of a thin airfoil. Although the primary purpose of the fan is to convert SP into thrust, since it is located in front of the compressor it also provides a small amount of compression with a pressure ratio of about 1.5 to 2. In a two-spool turbofan engine, the fan and the compressor are driven by separate turbines through coaxial shafts. In some different versions of turbofan, the outer parts of the compressor blades or turbine blades serve the purpose of the fan, and there is no separate fan as such.

The turbine of a turbofan engine, like that of a turboprop engine, provides power to both the fan and the compressor. Unlike the turboprop engine, there is considerable energy available in the gases downstream of the turbine. These gases are further expanded in the exhaust nozzle to increase the jet velocity for producing thrust. In a turbofan engine about 30–60% of the propulsive force is produced by the fan, and the rest comes from the jet thrust of the exhaust gases. Thus, the thrust produced by the fan is either approximately equal or comparable to that produced by the exhaust jet of the gases.

4.5.2 Turbofan as a Dual-Flow Engine

The air, after passing through the inlet duct and the fan, is allowed to split into two parts, called primary and secondary flows. The primary flow moves to the compressor, combustion chamber, and gas turbine, finally emerging from the exhaust nozzle as hot gases (air + fuel). The secondary flow enters the bypass duct around the periphery of the engine; it is cold and of lower velocity because it does not pass through the various components of the engine. The bypass air (secondary flow) joins the exhaust gases (primary flow) at the back of the engine. Like a turboprop, the turbofan is also a dual-flow or multiple-flow engine.

4.5.3 Bypass Ratio

The *bypass ratio* (BPR) is an important parameter of the performance of a turbofan engine. It is defined as the ratio of the mass flow rate of cold air (secondary flow) that is allowed to bypass to the mass flow rate of hot gases (primary flow) passing through the combustion chamber and turbine of the engine. That is,

$$\text{Bypass ratio} = \frac{\text{Mass flow rate of cold air (secondary flow)}}{\text{Mass flow rate of hot gases (primary flow)}}$$

If the ratio is zero, the turbofan is more like a turbojet engine. On the other hand, the turbofan resembles a turboprop engine if the BPR is sufficiently increased. In some modern turbofan engines the BPR may go as high as 6, and in engines

using a prop-fan the BPR may reach 10. The engine thrust and the rate of fuel consumption depend on the BPR.

4.5.4 Equivalent Thrust

Although a turbofan engine may produce more power through the fan than through the exhaust jet at a high BPR, it is common to designate power in terms of thrust, similar to a turbojet engine. This requires that the SP, or HP, also be converted into thrust. It is then necessary to designate the engine in terms of equivalent thrust (ET), denoted here by F^* . The ET is defined as

$$F^* = F_j + k\eta(\text{SP})/V$$

where F_j is the jet thrust, V is the design airspeed of the turbofan engine aircraft, η is the fan efficiency, and k is the conversion factor whose numerical value depends on the units to be used, as mentioned above. The last term on the right-hand side is due to conversion of the SP to thrust by the fan. It is now also possible to define c^* , the equivalent thrust specific fuel consumption (ETSCF), as $c^* = \dot{W}_f/F^*$, where $\dot{W}_f = dW_f/dt$ is the weight of the fuel flow rate. The value of c^* may be around 0.6–0.8/h for high-bypass turbofans, which is much less than that of a turbojet engine but somewhat more than that of a turboprop. The value of c^* also varies with airspeed and this variation is greater in turbofan engines than in turboprop engines.

4.5.5 Advantages and Disadvantages of a Turbofan Engine

Turbofans are available in the maximum thrust range of 20,000 lb (9072 kg_f) to 60,000 lb (27,216 kg_f). Turbofan aircraft usually fly in the Mach number range of 0.65–0.85, but more recently this Mach number range has been extended to 1.5. The thrust-weight ratio of its engine is around 5 or 6. The turbofan engine is even simpler and lighter than a turboprop engine because it does not require the propeller, the intricate mechanism to alter its pitch, on the heavy gears. The air flow through the ducted fan is not much affected by the airspeed so that the decrease in propulsive efficiency is not very significant, as in case of the propeller of a turboprop engine. Since the bypass air is not heated, the turbofan has lower TSFC than that of the turbojet engine. The turboprop loses its efficiency rapidly at airspeeds above 741 km/h (400 kn) at cruising altitude, while turbofan engines produce thrust efficiently even at higher airspeeds. The mixing of the high-velocity hot gases with the cold and slower bypass air reduces the average velocity and temperature of the exhaust gases. This decrease in exhaust velocity lowers engine noise, and the decrease in temperature increases the propulsive efficiency of the turbofan engine. Therefore, it is quieter than either a turbojet engine or a turboprop engine producing the same thrust. Thrust augmentation devices, like the afterburner and water injection, as in case of a turbojet, can also be installed. Many transport aircraft today use turbofan engines. The frontal area of a turboprop engine is, however, larger than that of a turbojet engine, but this does not mean that the drag would also be proportionately higher. The turbofan engine has a lower speed limit than the turbojet.

4.6 Comparative Study of Different Gas Turbine Engines

A comparative study of the performance of different versions of gas turbine engines is important for understanding them better and for selecting among them.

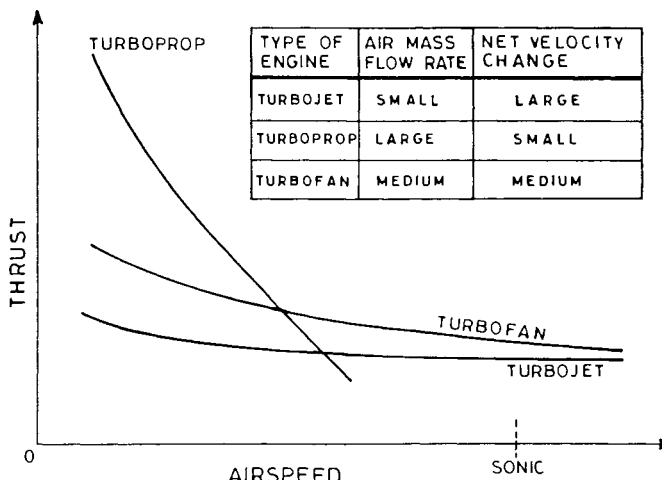


Fig. 4.9 Thrust variation with airspeed for different engines.

The relative advantages of different types of gas turbine engines have already been mentioned earlier in the concluding parts of Secs. 4.3.7, 4.4.5, and 4.5.5. The emphasis here is on the behavior of their thrust (or power) and TSFC (or PSFC) because these enter directly into several performance calculations of the aircraft.

The variation in thrust with airspeed is shown in Fig. 4.9 for different versions of the gas turbine engine, each having the same core engine. The turboprop engine gives more thrust up to moderately high subsonic airspeeds. The thrust of the turbofan, as expected, lies between that of the turboprop and turbojet. The curves of the turbojet and turbofan engines are flatter than those of the turboprop.

Every aircraft engine designer endeavors to achieve higher thrust coupled with lesser engine weight. There has been considerable improvement in the values of F/W_e of gas turbine engines during the last few decades, where W_e is the weight of the engine. This results in higher thrust-weight ratio, F/W , of an aircraft, which is an important parameter in the calculation of aircraft performance.

It is also an important task of an engine designer to achieve minimum specific fuel consumption. The variation of the TSFC with airspeed is shown in Fig. 4.10

Table 4.1 TSFC (or PSFC) and typical Mach number ranges

Engine	TSFC or PSFC	Mach no.
Piston-prop	0.4–0.5	<0.35
Turboprop	0.3–0.6	0.40–0.80
Turbofan (high bypass ratio)	0.3–0.7	0.65–0.85
Turbofan (low bypass ratio)	0.4–0.8	0.65–1.5
Turbojet	0.8–1.0	0.8–3.0
Turbojet (with afterburner)	1.6–2.0	0.8–3.0
Ramjet	3.0	3.0–5.0
Rocket	10.0	>5.0

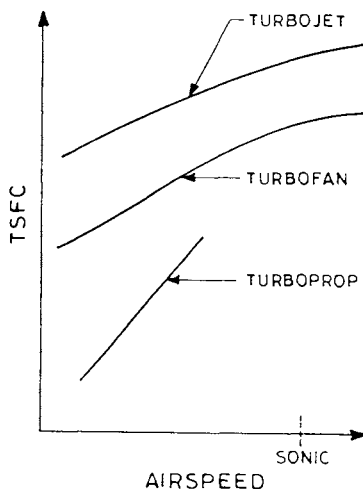


Fig. 4.10 Change in thrust-specific fuel consumption (TSFC) with airspeed for different engines.

for different engines. Up to moderately high subsonic airspeeds the turboprop engine is the most economical in terms of fuel consumption. The turbojet at all airspeeds is the most thirsty as compared to other versions of gas turbine engines. The TSFC (or PSFC) of different engines and the Mach number ranges at which they generally operate are presented in Table 4.1.

The propulsive efficiency of different engines is shown in Fig. 4.11. The turboprop has the highest efficiency at low airspeeds whereas at very high airspeeds the efficiency of the ramjet is better. No engine can compare with the ramjet among the airbreathing engines at very high Mach numbers.

4.7 Ramjet and Rocket Engines

A ramjet and a rocket are very different types of jet engines. The ramjet requires atmospheric air for propulsion whereas the rocket does not need it. The desire to fly at high supersonic speeds and even at hypersonic speeds led to the development of ramjets. The need to fly higher, in outer space where no trace of atmospheric air exists, led to the discovery of rocket engines. These two types of engines are very briefly described here.

4.7.1 Ramjet

A *ramjet* is an airbreathing engine useful only at supersonic speeds of Mach 2 and above. It does not require a compressor and consequently has no turbine to drive it. As the engine's name suggests, air compression is achieved through the ram effect in the inlet portion of the ramjet which is moving at supersonic speed. The appearance of shocks at the mouth of the inlet produce compression. For example, at Mach 2 the compression ratio across the shock may be about 4, which may be acceptable to replace the mechanical compressor. At higher Mach numbers, higher compression is achieved without any compressor. After compression the air is mixed with the fuel and ignited as shown in Fig. 4.12. Since no turbine exists, temperature limits can be raised much higher than in the

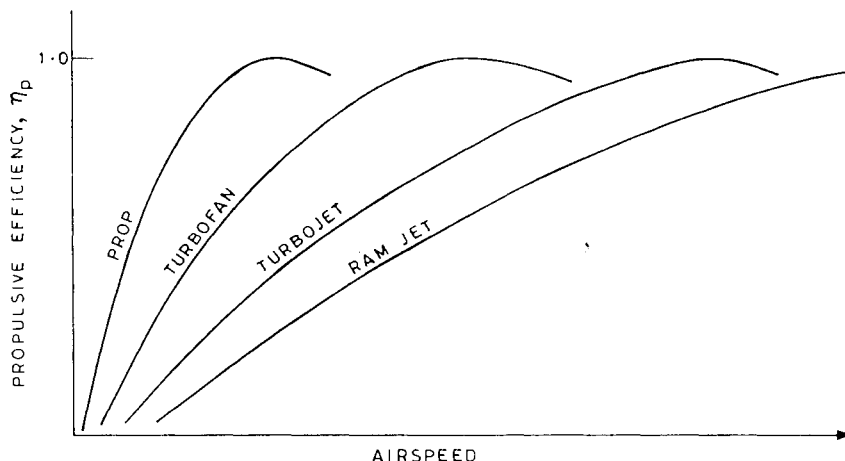


Fig. 4.11 Propulsive efficiency of different airbreathing engines.

case of turbine engines; this is because the walls of the combustion zone can withstand much higher temperatures than the material of the turbine. The higher temperature at the combustion zone results in the gases being pushed at higher exhaust velocities through the nozzle, thus producing thrust. The TSFC of a ramjet may be around 2.5/h at Mach 2.

The ramjet is a most simple engine with no moving parts and therefore no lubrication requirement. Due to its simplicity and functional behavior, the ramjet is sometimes called a *flying stove* or *aerothermodynamic duct*. In a conventional ramjet the air flow in the combustion zone is at low subsonic speeds. This makes the temperature of the compressed air prohibitively high (air may disintegrate even before it burns) for large supersonic or hypersonic flight. The air temperature after compression can be reduced if the compressed airflow can be kept supersonic. This has led to proposals that supersonic combustion ramjets be used for hypersonic flight.

A ramjet is prohibitively expensive to operate below Mach 1 because of its poor efficiency. It cannot be started on its own because it produces thrust only when sufficient airspeed is present. Thus it is necessary to have an auxiliary device of propulsion, such as a rocket, for starting and gaining airspeed until the ramjet can be deployed.

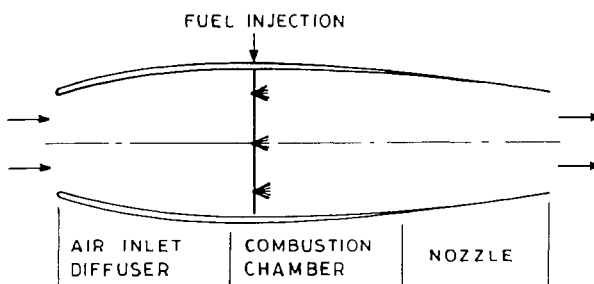


Fig. 4.12 Elements of a ramjet.

4.7.2 Rocket

A rocket is not an air-breathing engine, as is the case with the other types of engines discussed in this chapter. It does not depend on atmospheric air for producing thrust. *Rockets* are a different class of jet engine with a unique capability of propulsion even in outer space where atmospheric air is nonexistent. The history of rocketry and space travel has been presented by Von Braun.⁵ A rocket carries its own propellant, which is a fuel–oxidizer combination, either in liquid or solid form. This suggests that only light-weight propellants can be used, such as kerosene–oxygen or hydrogen–oxygen. The propellant on being ignited produces gases of extremely high temperature, which rush through the exit nozzle. The change in the momentum flux of the gases produces thrust to the rocket.

As all the propellant, i.e., the mass creating thrust, must be carried inside the rocket itself, this offers greatest disadvantage to rocket use, and becomes uneconomical. The thrust-specific fuel consumption of a rocket is about 10/h. Therefore, rockets are generally used as auxiliary devices to other means of propulsion, for launching missiles and satellites, and for steering and stopping outer space vehicles. Humans have reached the moon using craft powered solely by rocket engines, and the rocket is the ultimate high-thrust propulsive device for outer space vehicles.

References

- ¹Anderson, J. D., Jr., *Introduction to Flight*, 3rd ed., McGraw-Hill, New York, 1989.
- ²Seddon, J., and Goldsmith, E. L., *Intake Aerodynamics*, William Collins, London, 1985.
- ³Cohen, E., and Rogers, G. F. C., *Gas Turbine Theory*, 3rd ed., Longman, Harlow, England, UK, 1987.
- ⁴Hale, F. J., *Introduction to Aircraft Performance, Selection and Design*, Wiley, New York, 1984.
- ⁵Von Braun, W., and Ordway, F. I., *History of Rocketry and Space Travel*, 3rd ed. rev., Crowell, New York, 1975.

Problems

In the multiple choice problems below, mark the correct answer.

- 4.1** The principle of jet propulsion is primarily based on a) Newton's third law of motion, b) first law of thermodynamics, c) second law of thermodynamics.
- 4.2** A turbine rotor extracts power from a) hot, high-speed gases, b) compressed air, c) hot gas from combustion chamber of the engine.
- 4.3** A turbojet engine a) produces thrust by the change in momentum across the engine, b) produces thrust by the energy change across the engine, c) produces power by the turbine that is comparable with the thrust power produced by the jet exhaust.
- 4.4** Which of the following statements are true? a) The fan of a turbofan engine is powered by the compressor of the engine. b) The fan of a turbofan is powered by the turbine of the engine. c) A turbine is powered by the compressor in all gas turbine engines.

4.5 Engine ratings are a) different for different modes of flight i.e., takeoff, cruise, and landing; b) the same for all modes of flight; c) defined in terms of test-bed results only.

4.6 The central body of a supersonic air inlet is used to a) tailor the strength and location of shock waves, b) prevent entry of birds, c) improve the slenderness of the engine.

4.7 All the air leaving the compressor is not used for combustion with the fuel because a) this would require more fuel to increase fuel air ratio, b) the turbine entry temperature would become in excess of the maximum allowable turbine temperature, c) excess fuel gives a better combustible mixture.

4.8 Consider a stationary turbojet aircraft at the start of its ground roll. The mass flow rate of air entering the inlet is 50 kg/s, and the jet velocity at its exhaust is 80 m/s. Find the thrust developed by the engine and the rate at which the energy is being wasted by the exhaust gas.

4.9 Consider a stationary turboprop aircraft at the start of its ground roll. A mass flow rate of 250 kg/s is passing through its propeller, which increases the velocity by 16 m/s. Find the thrust produced by the propeller and the rate at which the energy is being wasted by the slipstream of the propeller.

4.10 Compare the thrust of the aircraft in Problems 4.8 and 4.9. Which is the more efficient propulsive device?

4.11 Calculate the gross thrust, net thrust, and TSFC of a turbojet where the weight of air flow entering the engine is $80 \text{ kg}_f/\text{s}$, inlet and exit velocities of air are 200 m/s and 450 m/s, respectively, the exit and ambient pressures are equal, and the fuel flow rate is $0.46 \text{ kg}_f/\text{s}$.

4.12 The mass flow rate of air entering the inlet of a turbojet engine is 120 kg/s, and the airspeeds at the inlet and exhaust are 240 and 430 m/s, respectively. The ambient and exhaust pressures are $2.61 \times 10^4 \text{ N/m}^2$ and $2.65 \times 10^4 \text{ N/m}^2$, respectively, and the area of the exhaust nozzle at the exit is 0.9 m^2 . The mass flow rate of the fuel supplied is 1.5% that of the air entering the inlet. Calculate the gross thrust, net thrust, and TSFC of the turbojet.

4.13 A turbojet aircraft is flying at an airspeed of 800 km/h at a standard altitude of 9 km. The airspeed and pressure of the exhaust gas at the exit are 490 m/s and $30,640 \text{ N/m}^2$, respectively. The area at the entrance of the air inlet duct of the engine is 0.65 m^2 and that at the exit of its exhaust nozzle is 0.42 m^2 . Find the thrust produced by the turbojet engine.

4.14 The inlet and exit areas of a turbojet are the same, both equal to 0.50 m^2 . The exhaust gas has velocity, pressure, and temperature, respectively, of 420 m/s, 1.0 atm, and 770 K, during the testing of the turbojet on a stationary test bed at sea level. Find the static thrust of the engine.

4.15 Explain the concept of the afterburner in a turbojet engine.

- 4.16** Explain how the total pressure is increased in a compressor.
- 4.17** Discuss the three *T*s of combustion.
- 4.18** What is the purpose of the air inlet duct of a gas turbine engine?
- 4.19** What is the purpose and function of a gas turbine engine?
- 4.20** Explain the concepts of equivalent thrust (ET) and equivalent shaft power (ESP).
- 4.21** What is the purpose of exhaust nozzle in a gas turbine engine?
- 4.22** The turbojet engine of an aircraft has inlet and exit areas of 1.3 and 1.0 m^2 , respectively. The velocity and pressure of the exhaust gas at the exit are 470 m/s, and $21,500\text{ N/m}^2$, respectively. If the aircraft is flying at a standard altitude of 12 km with an airspeed of 850 km/h, calculate the thrust developed by the engine.
- 4.23** The exit velocity and pressure of the exhaust gas are 300 m/s and 1 atm, respectively, of a ramjet that is moving with a velocity of 630 m/s at sea level and producing a thrust of 4500 N. Find the area at the entry of the inlet duct.
- 4.24** The mass flow rate of the mixture of fuel and oxidizer through a rocket engine is 30 kg/s. If the exit area, velocity, and pressure are 2.2 m^2 , 4100 m/s, and $19,000\text{ N/m}^2$, respectively, find the thrust at a standard altitude of 55 km where the ambient pressure is 48.37 N/m^2 .
- 4.25** Static pressure at the exit of the turbine is generally kept a) higher than the ambient pressure, b) lower than the ambient pressure, c) equal to the ambient pressure.
- 4.26** The inlet duct for a supersonic aircraft is a) convergent type, b) divergent type, c) convergent-divergent type.
- 4.27** A ramjet engine is a) an airbreathing engine, b) a nonairbreathing engine, c) an engine with rotating parts.
- 4.28** A ramjet is useful a) for flight exceeding Mach 2, b) for transonic airspeed, c) for the takeoff phase of flight.
- 4.29** Which of the following statements are correct? a) A turbofan mainly produces shaft power only. b) A turboprop produces thrust only by its propeller. c) A turbojet produces mainly thrust power.
- 4.30** The fan of turbofan produces a pressure ratio of about a) 115, b) 15, c) 1.5.
- 4.31** An ideal exhaust nozzle is designed to make the static pressure of the exhaust at the discharge section to be the same as the ambient atmospheric pressure because a) it reduces the pressure drag, b) it reduces the skin friction drag, c) it maximizes the momentum thrust.

This page intentionally left blank

5

Propulsive Power by Piston-Prop Engines

5.1 Introduction

In the early days of aviation, reciprocating engines were used and they are still the most efficient propulsive device at low speeds. A reciprocating engine is also called a *piston engine*. It is similar to an automobile engine with reliability and reduction in weight and drag becoming high-priority considerations in an aircraft engine. A piston engine develops the necessary torque and power and transmits it to its central shaft as shaft power. The rotating shaft of a piston engine cannot by itself push an aircraft unless it is converted into thrust power by means of the rotation of a propeller, which is usually fitted at the front of the piston engine. The propeller must be highly efficient, otherwise it will be just rotating at high speed without producing any significant thrust, like the rotation of wheels of an automobile on a slippery road. The combination of the piston engine and the propeller is called piston-propeller, or simply *piston-prop*, and is the subject matter of this chapter.

The piston-prop had the honor of powering the first successful flight by the Wright brothers on December 17, 1903; they used a 9-kW (12-hp) engine, weighing 445 N (100 lb) without fuel and oil, and the propeller efficiency was 0.7. Although piston engines and propellers existed much before 1903, the first successful flight could not be accomplished until engines were made sufficiently lighter without compromising power, and the propellers made more efficient. Since then, there has been rapid growth in all aspects of aviation and certain minimum standards have been laid down for the safety of flight operations. An account of the historical development of piston engines and propellers is provided by Anderson.¹ Until the beginning of the 1950s, piston-props were the only type of power plants for aircraft propulsion. Today piston engines may have as much as 2610 kW (3500 hp) and the propellers of 90% efficiency. Piston-props are still the best choice for a low-speed general aviation aircraft whose cruising speed does not exceed about 483 km/h (300 miles/h).

5.2 Piston Engine

The principle of operation and the characteristic features of a piston engine are explained here.

5.2.1 Engine Configuration and Principle of Operation

The piston-prop is an airbreathing, internal combustion, reciprocating piston engine. Atmospheric air is brought at the inlet of the carburetor where the fuel is also injected. The carburetor vaporizes the fuel and mixes it with the incoming air in proper proportion. The mixture passes through the throttle into the intake manifold and then to combustion cylinders where it is burned. A piston engine employs gasoline fuel with a density of 718.8 kg/m^3 , which is about 10% lighter

than the fuel of a gas turbine engine. The chemical energy of fuel released during combustion is changed into heat energy that develops high gas pressure in the cylinders of the engine. The gas pressure in the cylinders, acting through the piston-connecting rod-crankshaft linkages, applies torque to the engine shaft. The primary objective of the piston engine is to develop a certain amount of power and torque in the shaft located at the center. A more powerful engine would give higher torque to the central shaft.

The power of a piston engine is determined by the engine rpm and manifold pressure, where the manifold pressure is the pressure of the fuel-air mixture in the intake manifold. The pressure is given in inches of mercury above absolute pressure, so the readings of the manifold pressure may be above or below 29.92 in. Hg, which is the pressure of the standard atmosphere at sea level. As manifold pressure increases, the power output of the engine increases provided the rpm remains constant. Likewise, the power increases as rpm increases provided that the manifold pressure remains constant.

A piston engine can be characterized by the number of cylinders, the pattern of their arrangement, and their cooling devices, as decided by the engine designer.

5.2.2 Types of Piston Engines

Piston-prop engines are often classified by the type of arrangement of their cylinders around the central crankshaft. The arrangement of these cylinders can be radial, horizontally opposed, or in-line, and can be of different shapes, of which some are shown in Fig. 5.1. Figures 5.1a and 5.1b show radial arrangements of single-row and double-row cylinders, respectively. A radial arrangement of four rows is common for obtaining more power for the same frontal area. This type of engine always has an odd number (five, seven, nine, etc.) of cylinders. It has the disadvantage of increasing parasite drag by increasing frontal area of the engine.

The horizontally opposed arrangement of the cylinders is shown in Fig. 5.1c, and is most commonly used in general aviation aircraft. It has two rows of cylinders directly opposite to each other in the horizontal plane and working on the same crankshaft. This type of engine has the advantage of smaller frontal area, producing less drag.

Different in-line arrangements of the cylinders are shown in Figs. 5.1d–5.1f. Figure 5.1d shows four cylinders along a single line, Fig. 5.1e shows eight cylinders forming a V-shape, and Fig. 5.1f shows six cylinders in an H-shape. There is a

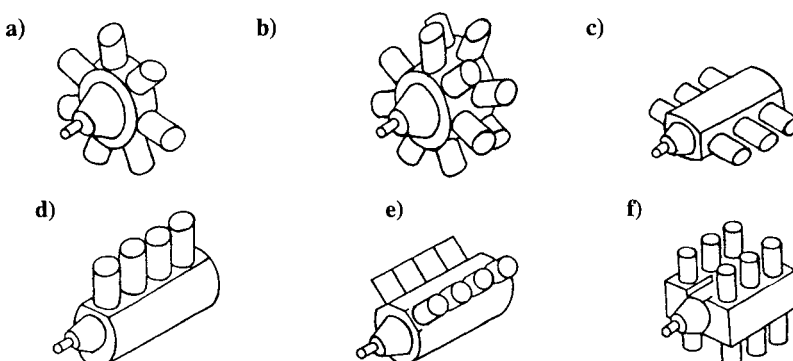


Fig. 5.1 Types of arrangements of cylinders in piston engines.

practical limit of six cylinders in one row because a long crankshaft may cause vibrations. Some of these arrangements may have two crankshafts side by side. These types of engines are mostly found in vintage aircraft.

5.2.3 *Cooling of Cylinders*

The cooling of these cylinders is essential because the material of the cylinder cannot withstand high temperatures of about 2500–3000°C, caused by the ignition of the fuel–air mixture inside. Engines are either air-cooled or liquid-cooled. The cylinders of air-cooled engines have fins over their outer surface offering the maximum area of contact with the cooling air flowing over them. The cylinders of air-cooled engines are always arranged along radial directions as shown in Fig. 5.1a and 5.1b, whereas the rest of the other arrangements of Fig. 5.1 may be either air-cooled or water-cooled. The cylinders of a liquid-cooled engine are surrounded by a “water jacket” carrying either water, ethylene glycol, or a mixture of the two. The cooling fluid is in constant circulation, by the action of a pump, and passes through a radiator where the excess heat is dissipated to the atmosphere. Thus, the water-cooled engine is also eventually air-cooled. Both types of cooling must be controlled so that there is enough cooling when the aircraft is at rest, and also not excessive cooling when it is flying at speed. Air-cooled engines are more common than liquid-cooled engines. The engine installation provided for cooling the engine, oil, and accessories, produce aerodynamic drag that is called *cooling drag*.

5.3 Carburetor

The carburetor of a piston engine has certain important functions. It may also cause ice formation, which is a hazard during flight.

5.3.1 *Function of a Carburetor, Fuel–Air Mixture, and Throttle Control*

The function of a carburetor is to admit the correct quantity of fuel (gasoline), vaporize this fuel, mix it with air in the proper proportion, and deliver the mixture to the cylinders.

The proper proportion of fuel/air ratio of the mixture varies from the leanest (about 1:20) to the richest mixture (about 1:8). The fuel/air ratio of the mixture in practice lies in between these two ratios. For example, the fuel/air ratio of the mixture for the best power is about 1:14, and for the lowest fuel consumption it is about 1:18. If the mixture is too lean, or too rich, it may cause overheating, appreciable loss of power, or even engine failure.

The mixture of vaporized fuel and air is first regulated in volume by the throttle valve as it enters the intake manifold and is then distributed to the individual cylinders. The throttle is positioned immediately after or at the exit of the carburetor; it throttles the flow of the mixture into the cylinders. The throttle valve is connected to the throttle control on the instrument panel in the cockpit of the aircraft. Forward movement of the throttle control opens the throttle valve, increases the volume of the mixture, and consequently the speed (rpm) of the engine. Similarly, backward movement of the throttle control reduces the speed of the engine. When the engine is idling the throttle valve is nearly closed, but not fully closed. A complete carburetor is a complicated unit that incorporates devices to control the fuel/air ratio of the mixture under widely varying conditions imposed on a modern aircraft.

5.3.2 Carburetor Icing

The formation of ice inside the carburetor is an important topic as this may cause a hazard to flying, leading to engine failure. Ice formation can take place even when the outside atmosphere temperature is well above freezing; earlier pilots failed to appreciate that it caused fatal accidents.

There are three types of carburetor icing—fuel ice, throttle ice, and impact ice. *Fuel ice* is due to cooling of the air in the vaporized fuel-air mixture. The vaporization of fuel requires a latent heat of vaporization that is taken from the air in the fuel-air mixture. Thus, incoming air is cooled by as much as 30°C . Therefore, it is possible for icing to occur by freezing of the water vapor of air, when the outside air temperature is 30°C . The ice so formed is deposited over the inside surfaces and on the throttle valve of the carburetor, choking the flow of the mixture. When the atmospheric temperature is around 15°C , fuel ice is the most likely to form, especially when the atmosphere is humid. The minimum humidity for icing is generally 50%, and further increase in the humidity increases the chances of icing. If the atmospheric temperature is below -5°C , there may not be sufficient water vapor in the atmosphere at so a low temperature for carburetor ice to form; the small amount of moisture that might be present in the air will be frozen and will pass harmlessly through the carburetor.

Throttle ice is formed by the cooling of the fuel-air mixture as it passes through the throttle valve. The sudden increase in the area just downstream of the partially closed valve lowers both pressure and temperature. This drop in the temperature is rarely more than 3°C and, therefore, throttle ice is not a problem when the outside ambient temperature is above 4°C . Any ice formation inside the carburetor is the cumulative effect of both the fuel ice and throttle ice phenomena.

Impact ice is formed when supercooled water droplets, snow, or sleet impinge on the surfaces of the carburetor and its other elements.

5.3.3 Prevention of Carburetor Icing

A modern aircraft is fitted with devices to combat icing. Generally, hot air, obtained from the exhaust of the piston engine, is directed into the carburetor air intake. Hot air can be used both as an anti-icing device (for preventing ice formation) or as a deicing device (for removing ice). It is always better to prevent ice formation than to remove it after it has formed. It requires much more heat to melt ice that has already formed than to prevent its formation.

In order to prevent carburetor ice formation, the hot air is so regulated that the inlet air temperature is maintained at $29\text{--}32^{\circ}\text{C}$ ($85\text{--}90^{\circ}\text{F}$). This is the temperature of air just before entering the carburetor and it can be measured by the *carburetor air inlet temperature gauge* of the instrument panel in the cockpit. Many aircraft are fitted with a *carburetor mixture temperature gauge* to measure the temperature of the fuel-air mixture. The temperature of this mixture should be maintained at $4\text{--}7^{\circ}\text{C}$ ($40\text{--}45^{\circ}\text{F}$) in flight by regulating the hot air of the mixture.

Introducing hot air to the carburetor reduces engine power because the hot air is lighter than cold air. This suggests that during takeoff, or other such operations of the aircraft requiring full power, the carburetor heat control should be kept at the cold air position. If no carburetor ice is present, the application of carburetor heat causes loss of power as indicated by a drop in the manifold pressure; this method can be used to check whether carburetor ice is forming or not, especially when there is no carburetor heat measuring device.

It should also be kept in mind that sometimes full heat or no heat is better, instead of partial heat. Under certain conditions the partial heat application may be worse than none at all. Partial heating of the carburetor may raise the temperature of the mixture from temperatures that are less prone to icing (around -8°C) to temperatures where icing is more likely to occur (about -1°C). Moreover, certain dry ice crystals, which otherwise would have harmlessly passed downstream, may melt due to partial heating and become harmful by being deposited again as ice on the surface of the carburetor. Partial heating should not be used when a gauge measuring the temperature of carburetor air (or fuel-air mixture) is not installed in the aircraft.

5.4 Fuel Injection System

An aircraft fitted with fuel injection dispenses with the carburetor and hence with the hazard of carburetor icing. The fuel injection pump delivers the fuel from the fuel reservoir to the nozzles where it is atomized into a fine spray. This fine spray is discharged in proper proportion into the air stream entering the intake manifold. The fuel injection system has the advantage of saving fuel by providing more uniform distribution of fuel to all the cylinders. It also produces more power since the need to heat the carburetor air is eliminated. A detailed account of the functioning of different fuel injection systems is provided by McKinley and Bent.²

5.5 Aspirated Engine, Supercharging, and Critical Altitude

The first generation of reciprocating engines were all aspirated engines. These engines lose their power as the density of air decreases. The present generation of reciprocating engines are supercharged, which enables their power to remain constant up to a certain altitude.

5.5.1 Aspirated Engine

A reciprocating engine (piston engine) is an airbreathing engine requiring a constant supply of air for proper functioning. If the mass flow rate of air is not maintained constant, the engine aspirates. The word *aspirate* means rough breathing or longing for more air.

An engine designed for operating at sea level atmospheric pressure is normally called an *aspirated engine*. The diminishing of atmospheric pressure and density at higher altitudes reduces the mass flow rate of air intake into the engine, causing it to aspirate. It also reduces the mass of fuel to be burned because for efficient combustion only a narrow range of fuel-to-air proportions are required in the combustion cylinders. Consequently, the power of the aspirated engine is reduced.

5.5.2 Supercharging

It was mentioned above that a normal aspirated engine loses power with an increase in altitude. This situation is rectified by supercharging the engine. A *supercharger* is generally a centrifugal compressor for increasing the pressure and density of the air moving into the cylinder. The compressor of a supercharged engine may be either gear-driven or turbine-driven.

In earlier supercharged engines, the compressor was gear-driven by a gear-train from the engine crankshaft, and consequently they were known as gear-driven supercharged piston engines. It may take as much as about 16% of the engine's

power to drive the supercharger. The compressor is installed downstream of the carburetor so that it compresses the fuel-air mixture after it leaves the carburetor.

Later, the supercharged piston engines employed turbine-driven compressors in which the turbine is powered by the engine's exhaust. These engines are termed *turbosupercharged* or simply *turbocharged* piston engines. An additional compressor (supercharger), located between the air intake and the carburetor, compresses the air before it is mixed with fuel in the carburetor. The additional turbocharger of the engine has the advantage that its compressor does not utilize the power of the engine, but instead uses the energy of the exhaust gases that normally would have been wasted. The turbocharged piston engine is also able to maintain sea level-rated power up to much higher altitudes than a gear-driven supercharged engine.

5.5.3 Critical Altitude

The supercharged piston engine has given rise to the concept of critical altitude of the engine. The altitude up to which sea level power can be maintained constant is called the *critical altitude*. The critical altitude depends on the ambient temperature—on cooler days the critical altitude is greater and on hotter days it is less. The critical altitude is generally around 6 km (20,000 ft).

5.6 Engine Power and Engine Ratings

Different types of engine power exist and their differences must be clearly understood. An important engine parameter is the brake power, which directly enters into calculations of aircraft performance. The maximum power of an engine is not commonly used; this gives rise to engine ratings for different aircraft operations during flight.

5.6.1 Engine Power

The power developed in the engine cylinders is known as indicated horsepower (IHP), which is measured from the pressure-volume diagram of the parametric changes occurring in the gases inside the cylinders. The power communicated to the central shaft through linkages is the shaft horsepower, commonly known as the brake horsepower (BHP). The word *brake* stems from the fact that the brake mechanism is used in laboratory tests for measuring the horsepower of the shaft. The BHP is always less than the IHP because of inevitable loss occurring in mechanical friction that is being dissipated as heat. The mechanical efficiency η_{mech} of the engine may be defined as the ratio of BHP to IHP. In a well-designed piston engine, $\eta_{\text{mech}} \approx 0.85$, meaning that only about 85% of the indicated power of the engine is transferred to the shaft as shaft power (brake power). For the performance analysis of a propeller or an aircraft, the BHP is an important quantity because it is the power input for the rotation of propeller. The brake power, henceforth, is referred to as the engine power, which is denoted by P_e .

5.6.2 Power-Specific Fuel Consumption

The rate of fuel consumption of a piston engine can be regarded as directly proportional to the brake power developed by the engine. This means

$$\frac{dW_f}{dt} = \hat{c}P_e, \quad \text{i.e.,} \quad \hat{c} = \dot{W}_f / P_e \quad (5.1)$$

where $\dot{W}_f = dW_f/dt$ is the weight of fuel flow rate, and \hat{c} is the *power-specific fuel consumption* (PSFC). This defines the PSFC as the fuel flow per unit of time for unit brake power of the engine. It is one of the most important parameters used in comparing different engines. PSFC is a measure of the fuel consumed to power developed, hence it is also a measure of the fuel economy.

5.6.3 Engine Ratings

Engine ratings are essentially its power ratings and their purpose is the same as in the case of gas turbine engines. Engine ratings safeguard against structural, mechanical, and thermal failures of the engine by limiting the use of engine power, both in magnitude and duration. In practice, an engine rarely operates at its maximum power because generally this is neither necessary nor desirable. Most of the commonly used aircraft operations during flight require only a fraction of the maximum engine power output. Engine ratings are also defined as the fractions of the maximum power output of the engine, but are expressed as percentages. The maximum power output of a piston engine is determined by its maximum rpm and manifold pressure.

The takeoff power rating is generally quite close to maximum power, but such power may only be needed for a period of 1–5 min. The maximum continuous power is also called the *maximum except takeoff* (METO) power. The METO power is guaranteed by the manufacturer of the engine under specified conditions and it is called the *rated power* or the *standard engine rating*.

5.7 Power Variations with Altitude, Airspeed, Temperature, and Humidity

An aircraft operates at different altitudes and airspeeds, and under varying atmospheric conditions. It becomes pertinent to know the corresponding behavior of its engine under these situations.

5.7.1 Power Variations With Altitude and Airspeed

Engine power is significantly affected by changes in altitude. The variation of power with altitude depends on whether the engine is aspirated (unsupercharged) or supercharged.

In the case of an aspirated engine, power decreases with the increase in altitude, and it is convenient to represent the variation as

$$P_e/P_{e,SSL} = \rho_e/\rho_{SSL} = \sigma \quad (5.2)$$

where SSL denotes the standard atmosphere at sea level.

In the case of a supercharged engine, power variation depends whether the altitude is below or above the critical altitude. For altitudes below and up to the critical altitude h_{cr} , the power of the supercharged engine is considered constant, and may be represented as

$$P_e/P_{e,SSL} = 1.0 \quad \text{for } h \leq h_{cr} \quad (5.3)$$

and for the altitudes above the critical altitude, the power variation is presented by

$$P_e/P_{e,SSL} = \rho/\rho_{cr} = (\rho/\rho_{SSL})/(\rho_{cr}/\rho_{SSL}) = \sigma/\sigma_{cr} \quad \text{for } h > h_{cr} \quad (5.4)$$

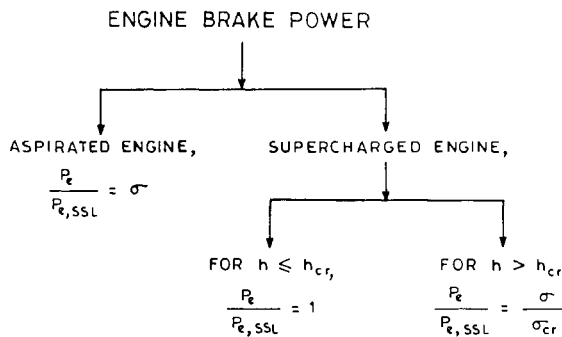


Fig. 5.2 Schematic presentation of engine power approximations.

Equations (5.2–5.4) are convenient in calculating the performance of a piston-prop aircraft. These approximations of engine power with respect to altitude are schematically presented in Fig. 5.2.

The variation of engine power with the airspeed is twofold. As the airspeed increases, the ram pressure increases and so the manifold absolute pressure (MAP) also increases, which has the effect of increasing the power output of the engine. On the other hand, the increase in ram pressure also increases the air temperature at the inlet of the carburetor, and this reduces the power output of the engine. The net effect is the engine power remains approximately constant in the operating range of airspeeds in which the piston engine aircraft mostly fly.

5.7.2 Effects of Temperature and Humidity

The BHP of a piston engine is usually found from the engine performance curves supplied by its manufacturer. These curves are based on the standard atmosphere. The correction for nonstandard atmosphere is made by a rule of thumb that increases the power by 1% for each 6°C (10°F) decrease in temperature from the standard ambient condition. Similarly, the power decreases by 1% for each 6°C rise of temperature from the standard atmospheric condition.

The effect of humidity on engine power is generally negligible. The water vapor in the air reduces the engine power to a negligible amount. The water vapor, being lighter and incombustible, causes a somewhat richer mixture and incomplete combustion. It has been found that 100% relative humidity at 32°C of ambient temperature causes a loss of power of less than 2%. On very hot and humid days when the aircraft is heavily loaded, the effect of humidity might be worth remembering while calculating the takeoff run and climb performance of the aircraft.

5.8 Engine Instruments

A successful engine operation requires different measuring instruments; the most important are those that measure rpm, pressure, and temperature.

5.8.1 Tachometer

The tachometer measures the rpm of the engine shaft, hence it is also called rpm indicator. Tachometers can be either mechanical or electrical. Since the rpm

are directly proportional to the engine power, the reading of the tachometer is a measure of the engine power. The tachometer is color coded to help the pilot operate in the proper range of engine rpm. The green arc indicates the normal range of operation, the yellow arc is the caution range, and the red line is the maximum limit. Exceeding the recommended operating range may cause excessive mechanical stresses leading to engine failure.

5.8.2 Manifold Pressure Gauge

The manifold pressure gauge indicates the pressure of the vaporized fuel-air mixture in the intake of the manifold between the carburetor and the cylinders. The pressure at the intake of the manifold is equal to the ambient atmospheric pressure if the engine is not running. This pressure is reduced as the engine operates.

The manifold pressure gauge indicates the reading that is taken inside the intake of the manifold. When the rpm are decreased, the engine runs more slowly, the flow speed of the mixture decreases, and hence the intake manifold pressure increases due to Bernoulli's theorem. Similarly, when the rpm are increased, the engine speeds up, the flow speed of the mixture increases, and hence the intake manifold pressure decreases. Thus the decrease in the rpm results in an increase in manifold pressure and vice versa.

If the manifold pressure and the engine rpm are known, the brake power of the engine can be obtained from the engine performance charts after applying the temperature correction. Excessive manifold pressure raises the temperature and the compression pressure, resulting in high stresses in the cylinders and burned-out valves. The manifold pressure gauge, like the tachometer, has colored markings to indicate normal operating range and operational limits.

5.8.3 Oil Pressure Gauge

The oil pressure gauge indicates the oil pressure supplied by the oil pump to lubricate the engine. Oil pressure that is too high will force oil into the combustion chamber, causing a smoking exhaust and carbon deposits on engine parts. Low oil pressure causes more serious trouble since the friction between the moving surfaces increases. The recommended minimum oil pressure is about 40% of the maximum pressure at cruising power.

5.8.4 Oil Temperature Gauge

The oil temperature gauge measures the temperature of the oil. The temperature changes the viscosity and pressure of the oil. Excessively high or low oil temperatures are undesirable.

5.8.5 Cylinder Head Temperature Gauge

The cylinder head temperature gauge measures the temperature of one (or more) of the engine cylinder heads. Measurement of this temperature provides a good indication of the effectiveness of the engine cooling system. High head temperatures decrease the strength of metals, cause detonation, preignition, and eventual engine failure.

5.8.6 Carburetor Air Temperature Gauge

The carburetor air temperature gauge records the temperature of the intake air entering into the carburetor; it may also record the temperature of the vaporized fuel-air mixture entering the manifold, depending on where the temperature-sensing element is installed. This instrument enables the pilot to maintain the temperature that will ensure maximum operating efficiency of the carburetor, which is especially important for avoiding ice formation inside the carburetor. If the temperature-sensing element measures intake air temperature, this should be maintained at about 29–32°C when the icing conditions exist. Similarly, if the temperature-sensing element measures the temperature of the mixture, the temperature should be maintained at about 4–7°C to avoid the chance of ice formation.

5.8.7 Outside Air Temperature Gauge

The outside air temperature gauge records the ambient air temperature of the atmosphere that exists around the aircraft. The sensing element of the temperature gauge is shielded from the sun's radiation and located at a place that reproduces the conditions of the free atmosphere. Knowledge of the ambient temperature helps the pilot to select the proper manifold pressure. This temperature also enables the pilot to calculate the true airspeed and the altitude, and warns of conditions causing ice formation.

5.9 Propeller

The propeller can be placed either in the front or at the rear of the aircraft. The propellers pulling from the front of the aircraft are quite common and they are sometimes referred to as *tractors*, whereas those attached at the back of the aircraft, for pushing forward, are referred to as *pushers*. In both cases the principle of operation of a propeller and its basic features remain the same.

5.9.1 Principle of Operation

The purpose of the propeller is to change the rotary motion of the shaft of a piston engine into the forward motion of the aircraft. The rotation of the propeller converts the torque (brake power) of the shaft into the thrust power of the aircraft. This conversion is done by drawing a large mass of air and giving it a small increment of velocity (about 10 m/s) so that the change in momentum flux of air imparts thrust force on the propeller blades. The imparting of thrust is through the modification of pressure and skin friction at each point on the surface of the blade; the sum of these components along the axis of rotation of the propeller yields the thrust force. This thrust force when multiplied by the forward airspeed of the aircraft gives thrust power. Thus, the propeller is a device for absorbing the shaft power (brake power) of the engine and generating the thrust power for propelling the aircraft. In early literature, the propeller was often referred to as an *airscrew* because it screws itself through the air without slipping.

5.9.2 Propeller Geometry and Pitch

A propeller has blades in the radial directions whose number may vary from two to five depending on the designer; three or four blades are generally quite common. A three-blade propeller is shown in Fig. 5.3. All propeller blades are exactly the same shape and are mounted on a conical hub or spinner. The aerodynamic design

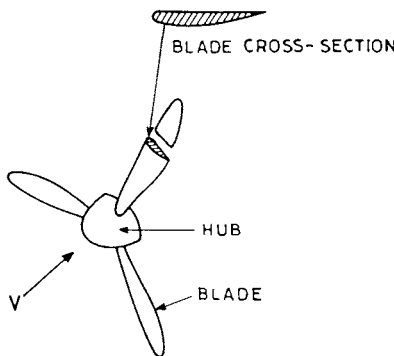


Fig. 5.3 Three-blade propeller, showing blade cross section.

of a blade requires that it should be able to produce maximum thrust power with minimum consumption of drag power. This design requirement is similar to that for a wing of maximum lift with minimum drag. A cross section of the propeller blade is very much like that of a low-drag or high-subsonic airfoil. The angle between the plane of rotation (the plane of propeller) and the chord line of the airfoil at any section of the blade is called the *pitch angle* or simply *pitch* and is denoted by β . The pitch angle is not constant along the length of the propeller blade. That is, $\beta = \beta(r)$, which means that the pitch angle β is a function of the radial distance r , which may be measured from the root of the propeller. Figure 5.4 shows the pitch angles at two different cross sections along the radial direction. The pitch angle is the least (close to zero) at the tip but increases to nearly $\pi/2$ when one approaches closer to the root of the propeller.

It is worth mentioning that in early literature the propeller pitch is defined as the distance traveled by the plane of the propeller in one complete revolution.

5.9.3 Relative Velocity and Its Direction

During the motion of an aircraft, each section of the blade experiences simultaneously the two different velocities, which are generally orthogonal to each other. One is the circumferential velocity $r\omega$ in the plane of rotation, where $\omega = 2\pi N$ is the angular velocity of rotation of the propeller that is making N number of

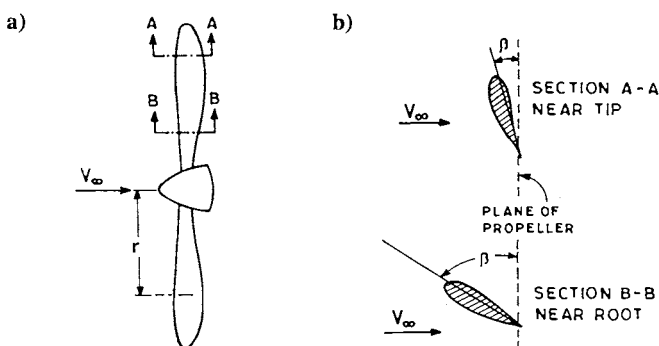


Fig. 5.4 Propeller blades showing pitch angles near the tip and root: a) side view of propeller blades and b) top view of airfoil sections.

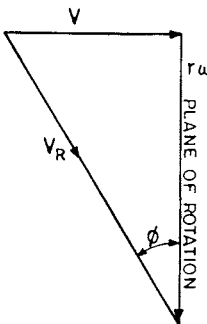


Fig. 5.5 Relative airspeed and its direction at a blade section.

revolutions per unit of time. The other is the forward velocity V normal to the plane of rotation of the propeller, due to the motion of the aircraft. Each blade section (airfoil), faces the relative (resultant) airspeed V_R , which is the vector sum of the velocities V and $r\omega$ as shown in Fig. 5.5. The magnitude of V_R and its direction ϕ from the plane of rotation are given by

$$V_R = \sqrt{V^2 + r^2\omega^2} \quad \text{and} \quad \phi = \tan^{-1}\{V/(r\omega)\} \quad (5.5)$$

Thus, both V_R and ϕ depend on V , r , and ω . The circumferential velocity $r\omega$ can be increased either by increasing r by moving toward the tip of a blade, or increasing ω by increasing the rpm of the propeller. The effect of increasing the circumferential velocity is to reduce ϕ which brings the relative airspeed closer to the plane of rotation. Similarly, increasing the airspeed V brings the magnitude and direction of V_R closer to that of V .

For a given forward velocity V , and a given rpm of the propeller, the maximum V_R and the minimum ϕ are obtained at the tip of the blade. These can be written as, respectively,

$$V_{R.m} = V_{R.tip} = \sqrt{V^2 + R^2\omega^2} \quad \text{and} \quad \phi_{\min} = \phi_{\text{tip}} = \tan^{-1}\{V/(R\omega)\}$$

where R is the radial distance of the tip of the blade, and the subscripts m and \min refer to maximum and minimum, respectively. The above two relations can also be, respectively, written as

$$M_{R.m} = M_{R.tip} = M\sqrt{1 + (\pi/J)^2} \quad \text{and} \quad \phi_{\min} = \phi_{\text{tip}} = \tan^{-1}(J/\pi)$$

where $M_{R.m}$ ($= V_{R.m}/a$) and M ($= V/a$) are the Mach numbers corresponding to the resultant and forward velocities, respectively, and a is the local speed of sound. The quantity J is called the *advance ratio of the propeller*, which is defined as $J = V/ND$, where D ($= 2R$) is the diameter of the propeller whose radius is R . The advance ratio is an important parameter of propeller motion.

5.9.4 Angle of Attack

The angle between V_R and the chord line is defined as the *angle of attack* α of the airfoil or blade section. As seen from Fig. 5.6a the angle of attack is given by

$$\alpha = \beta - \phi \quad (5.6)$$

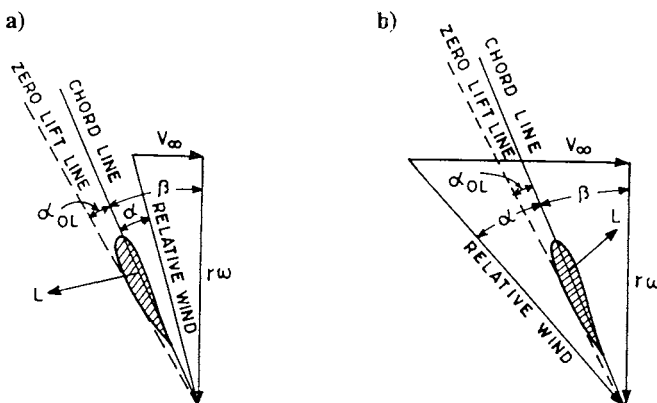


Fig. 5.6 Angles of attack of blade section: a) +ve in advance and b) -ve in advance.

Since the angle of attack must be positive to produce a reasonable thrust, it follows that β must be greater than ϕ . The pitch β at a blade section is an important geometric parameter of the propeller because it fixes the angle of attack at the section for a given ϕ or advance ratio J .

In cases where V is greater than or comparable to $r\omega$, the angle ϕ may exceed β and, therefore, the angle of attack α would become negative as shown in Fig. 5.6b. At such blade sections the thrust would be negative, which is unwanted. It can be easily seen that such situations may arise either near the roots of the blades or when the propeller is rotating slowly during forward motion.

5.9.5 Fine-Pitch and Coarse-Pitch Propellers

The pitch angle of a propeller blade decides whether it is a fine-pitch or a coarse-pitch propeller. If the pitch angle β is small, this is called fine pitch, and the large pitch angle is referred to as coarse pitch. Fine pitch is also sometimes called low pitch, and coarse pitch is sometimes called high pitch. In modern piston-prop aircraft, the pitch angle can be changed during flight. As the pitch changes from fine to coarse at a given rpm, the thrust increases and consequently the airspeed of the aircraft also increases. In this sense, the pitch is like a gear of an automobile, with the fine pitch corresponding to a lower gear, and the coarse pitch corresponding to a higher gear.

A propeller set for fine pitch has less drag (in the plane of rotation), or torque, and consequently rotates at higher speed, enabling the engine to develop greater power. Therefore, a propeller set for fine pitch gives the aircraft better takeoff and climb performance. A coarse-pitch propeller gives better performance for high-speed cruising and high-altitude flight.

5.10 Thrust and Torque Calculations of a Propeller

The rotation of the propeller in air produces aerodynamic forces due to changes in pressure and skin friction at each point on the surface of the propeller blades. These forces, when resolved along the normal to the plane of rotation, give the thrust force, commonly known as thrust of the propeller, which is responsible for the forward motion of the aircraft. If the moment of these aerodynamic forces is taken at each point of the propeller about the axis of rotation of the propeller,

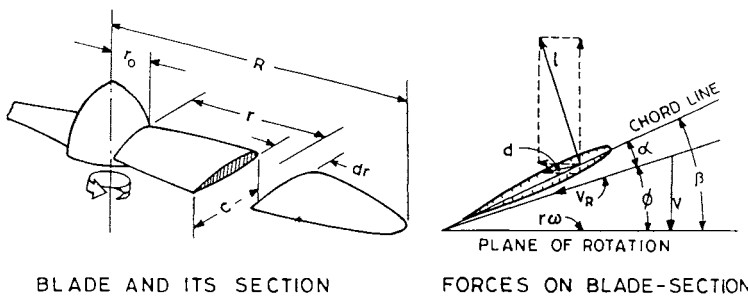


Fig. 5.7 Blade of a propeller and forces acting on its section.

this gives the torque experienced by the propeller shaft. It is possible to calculate the thrust and torque theoretically with reasonable accuracy by properly resolving the aerodynamic forces at each section of the blades. First, the forces on a small section dr of the blade are obtained, then they are integrated along the length of the blades, and finally they are multiplied by the number of propeller blades, as explained below.

Figure 5.7 shows one blade of the propeller and the forces acting on its section. Let l and d denote the lift and drag forces, respectively, per unit length of the blade at a radial distance r . If F_r and Q_r are the sectional thrust and torque, respectively, per unit length of the blade, at a radial distance r , they can be expressed as

$$F_r = l \cos \phi - d \sin \phi \quad (5.7)$$

and

$$Q_r = (l \sin \phi + d \cos \phi)r \quad (5.8)$$

where the quantity inside the bracket in Eq. (5.8) is the force per unit span of the blade in the plane of rotation, but normal to the radial direction. Representing the sectional lift and drag coefficients per unit length of the blade by C_l and C_d , respectively, the l and d can be expressed as

$$l = C_l \rho V_R^2 c / 2 \quad \text{and} \quad d = C_d \rho V_R^2 c / 2$$

where $V_R = V / \sin \phi$. Equations (5.7) and (5.8) can now be written as

$$F_r = \rho V^2 c (C_l \cos \phi - C_d \sin \phi) r / (2 \sin^2 \phi)$$

and

$$Q_r = \rho V^2 c (C_l \sin \phi + C_d \cos \phi) r / (2 \sin^2 \phi)$$

The variation in F_r along the length of the blade is shown in Fig. 5.8. The inner portion of the blade close to the hub produces hardly any thrust, which justifies putting a fairly big hub at the center of the propeller. The space inside the hub can be utilized for installing a pitch change actuator system.

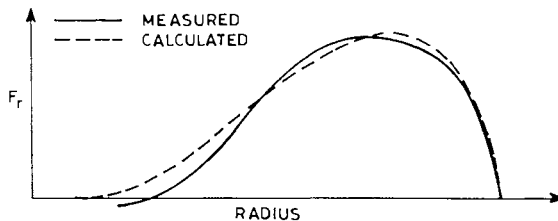


Fig. 5.8 Calculated and measured F_r along the blade length.

The total thrust F and the total torque Q produced by the propeller would be, respectively, given by

$$F = B \int_{r_0}^R F_r dr \quad \text{and} \quad Q = B \int_{r_0}^R Q_r dr$$

where B is the number of blades of the propeller, R is the radial distance of the tip of the blade, and r_0 is the external radius of the hub where the root of the blade is fixed. The thrust and torque, respectively, can now be obtained as

$$F = B(\rho V^2/2) \int_{r_0}^R (C/\sin^2 \phi)(C_l \cos \phi - C_d \sin \phi) dr \quad (5.9)$$

and

$$Q = B(\rho V^2/2) \int_r^R (c/\sin^2 \phi)(C_l \sin \phi + C_d \cos \phi)r dr \quad (5.10)$$

where the quantities inside the integral sign vary nonlinearly along the radial direction. It is generally not possible to evaluate these integrals analytically. The determination of F and Q depends on the accuracies at which C_l and C_d can be calculated. The sectional lift and drag coefficients are calculated by either the blade element theory or vortex theory, which have been developed for a propeller after the earliest and simplest Rankine–Froude momentum theory of the propeller. A detailed discussion of these theories can be obtained in Dommasch et al.² The following two paragraphs provide the characteristic features of this theory.

The Rankine–Froude momentum theory replaces the propeller by an infinite number of blades forming an actuator disc. The flow of air is regarded as incompressible, inviscid, and one-dimensional. Although it is assumed that there is a sudden increase in static pressure across the disc, the velocity is assumed to vary smoothly across it. The theory does not consider the shape of the blade and does not predict lift and drag at any blade section. The theory predicts the ideal total thrust F and the ideal efficiency η_p of the propeller as

$$F = (\pi D^2/2)\rho(V + v)v \quad \text{and} \quad \eta_p = V/(V + v)$$

where V is the velocity of the undisturbed oncoming flow of air; when it reaches at the plane of the propeller the velocity has increased to $(V + v)$. The actual efficiency in practice is about 85% of this ideal efficiency.

The blade element and vortex theories of the propeller are more realistic as they both take into account the geometry of each blade section and predict the sectional lift and drag coefficients, C_l and C_d , at each radial station. The development of the blade element theory is similar to the incompressible, inviscid, and potential flow theory of a wing, which considers only pressure force and neglects the skin friction force because it is generally very small.

Experimentally the propeller thrust, torque, and power can be directly measured by strain gauge instruments. A propeller can be tested in a wind tunnel designed for this specific purpose and equipped with variable-speed and variable-power electric motors for driving the propeller.

5.11 Propeller Parameters

The important characteristic parameters of a propeller are its advance ratio J , thrust coefficient C_F , torque coefficient C_Q , power coefficient C_P , and the propeller efficiency η_P . Similar to many other aerodynamic problems, the aerodynamics of the propeller also make it convenient to express the thrust F , the torque Q , and the power P in suitable nondimensional forms. If D represents the diameter of the propeller making N revolutions per unit of time, take the reference length as D , reference area as D^2 , reference velocity as ND , and the reference pressure as $\rho(ND)^2$. The nondimensional coefficients of thrust, torque, and power can be, respectively, defined as

$$C_F = F/\{\rho(ND)^2 D^2\} = F/(\rho N^2 D^4)$$

$$C_Q = Q/\{\rho(ND)^2 D^2 D\} = Q/(\rho N^2 D^5)$$

and

$$C_P = P/\{\rho(ND)^2 D^2 ND\} = P/(\rho N^3 D^5)$$

If the quantities C_F , C_Q , and C_P are known for a specific propeller, the thrust, torque, and power of the propeller, or another similar propeller, can be obtained from the following relations, respectively:

$$F = \rho N^2 D^4 C_F, \quad Q = \rho N^2 D^5 C_Q, \quad \text{and} \quad P = \rho N^3 D^5 C_P \quad (5.11)$$

The thrust, torque, and power of a propeller strongly depend on its diameter and rpm, and are directly proportional to the density of air.

The coefficients of a propeller's thrust, torque, and power would generally depend on the shape of its blade, pitch angle, Reynolds number (Re), Mach number, and advance ratio, i.e.,

$$C_F = C_F(\text{shape}, \beta, Re, M, J), \quad C_Q = C_Q(\text{shape}, \beta, Re, M, J)$$

and

$$C_P = C_P(\text{shape}, \beta, Re, M, J)$$

Since a propeller is a streamlined body during rotation, the influence of Reynolds number is very weak. The propellers are generally used well below transonic speeds so that the maximum relative velocity at the tip of the blade is less than the

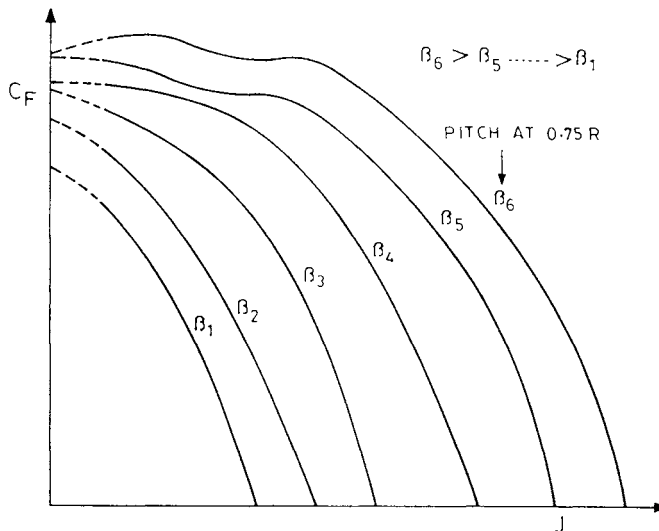


Fig. 5.9 Thrust coefficient versus advance ratio for different pitch angles.

sonic velocity incorporating no compressibility effects. It follows that for a given propeller, the above relations would simplify to

$$C_F = C_F(\beta, J), \quad C_Q = C_Q(\beta, J), \quad \text{and} \quad C_P = C_P(\beta, J) \quad (5.12)$$

This shows that the coefficients C_F , C_Q , and C_P depend only on the pitch angle β and the advance ratio J . A typical variation of C_F against the propeller advance ratio J for different values of the pitch angles is shown in Fig. 5.9. Since the pitch angle varies along the radial direction, the pitch at $0.75 R$ is specified to distinguish different pitch angles of the same propeller.

If the torque Q is known, the power P is obtained from the relation, $P = 2\pi N Q$, which after using the last two relations of Eq. (5.11) can be written as $C_P = 2\pi C_Q$.

There is, however, another propeller parameter, known as the speed-power coefficient, which is denoted by C_S and defined as

$$\begin{aligned} C_S &= J/(C_P)^{1/5} = \{V/(ND)\}/\{P/(\rho N^3 D^5)\}^{1/5} \\ &= \{\rho V^5/(PN^2)\}^{1/5} = C_S(\beta, J) \end{aligned}$$

C_S also depends on β and J . If C_S is specified, this simplifies the selection of the propeller since it does not involve the diameter of its blade.

5.12 Propeller Efficiency

Propeller efficiency is the most important parameter of a propeller for the purpose of propulsion. Propeller efficiency is defined here and the effects of pitch angle and advance ratio are presented.

5.12.1 Definition of Propeller Efficiency

The propeller efficiency is an important characteristic parameter of the propeller arising due to its rotation in the air. It answers the question, how efficiently is the engine power (power input or brake power) utilized for obtaining the thrust power (power output). It is defined as

$$\begin{aligned}\text{Propeller efficiency} &= \frac{\text{Power output (thrust power)}}{\text{Power input (brake power)}} \\ &= \frac{\text{Thrust} \times \text{forward velocity}}{\text{Torque of the engine shaft} \times \text{angular velocity}}\end{aligned}$$

If the propeller efficiency is denoted by η_p and the torque of the engine shaft by Q_e , the above relation can be written as

$$\eta_p = P/P_e = FV/(Q_e 2\pi N) \quad (5.13)$$

where the thrust F can be given by Eq. (5.9) and V is the forward airspeed of the aircraft. Since the shaft of an engine generally rotates at a constant rpm, the engine torque Q_e is spent in overcoming the aerodynamic torque Q , so that $Q_e = Q$, where Q is given by Eq. (5.10). The above relation becomes, $\eta_p = FV/(2\pi N Q)$, and after using the relations for F and Q in Eq. (5.11) the propeller efficiency can be expressed in terms of the dimensionless quantities as

$$\eta_p = (C_F/C_Q)J/(2\pi)$$

This shows that η_p is also a function of β and J , whose effects will be examined below.

5.12.2 Effects of Pitch and Advance Ratio

A typical variation of η_p with J for different values of β is presented in Fig. 5.10 for a given propeller. The characteristic features of these curves are explained below.

For any given β , the propeller efficiency first rises to some maximum value and then drops rapidly. This is because a propeller is designed for a particular rpm and V so that the angle of attack α of each airfoil section of the blade is at its maximum aerodynamic efficiency (C_l/C_d maximum). Any change in either

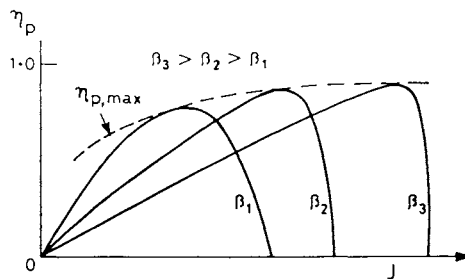


Fig. 5.10 Variation in propeller efficiency with advance ratio for different pitch angles.

the rpm or V changes this incidence at each radial distance and consequently the propeller efficiency η_p falls from its optimum value.

The optimum efficiency is less than unity. This is because some part of the input power is lost by the propeller in 1) skin friction and pressure drag of the blade elements and the hub, 2) inducing rotation to oncoming flow, 3) forming tip vortices of the blades, 4) causing turbulence to the oncoming flow, and 5) compressibility loss caused at high subsonic Mach numbers makes it prohibitive to use the propeller in this range of Mach numbers.

At any fixed pitch β , the propeller efficiency is maximum for only one value of J . This means that a given propeller moving at a given rpm will have maximum efficiency at only one value of its forward airspeed. All the first-generation aircraft had fixed-pitch propellers rigidly mounted on the engine shaft and a pilot had no option of changing the blade angle. Later two-pitch propellers were designed, one pitch angle for climbing speed and the other for cruising speed. Modern propeller-driven aircraft use variable-pitch propellers, which are explained below along with certain other types of propellers.

5.13 Types of Propellers

An efficient use of the propeller requires fixing suitable pitch angles. The effect of pitch on propeller efficiency has been extensively studied. This has historically led to the development of different types of propellers based on the method of using the pitch angles. The modern generation of aircraft use variable-pitch propellers. The different types of propellers and their relative merits are explained below.

5.13.1 Constant-Pitch Propeller

In a constant-pitch propeller, the pitch angle β has the same constant value at each blade section (airfoil). That is, the value of β is independent of the radial distance of the propeller, and it also does not change with the forward speed of the aircraft.

It is seen in the previous section (Eq. 5.5) that the direction ϕ of the relative velocity varies with the changes in V , r , and rpm. It follows from Eq. (5.6) that the angle of attack α of the blade section would also change with V , r , and rpm. Even after keeping both rpm and V as constants, the angle of attack α at each blade section would change along its radial direction. This may increase or decrease α at certain sections beyond certain limits such that 1) exceeding the stalling angle would cause large regions of flow separations at those sections, or 2) decreasing beyond the zero-lift angle would produce negative thrust. Both these situations are most undesirable and should be avoided by suitably twisting the blades at each radial station, at least for the design values of V and rpm of the propeller. This has given rise to the concept of a fixed-pitch propeller, as explained below.

5.13.2 Fixed-Pitch Propeller

The difference between constant pitch and fixed-pitch propellers should be clearly distinguished. In a fixed-pitch propeller, unlike a constant pitch propeller, the pitch β varies along the radial direction of the blade, i.e., $\beta = \beta(r)$. The values of β at all radial sections are geometrically fixed by the designer and the blades of the propeller are rigidly mounted on the hub. In a fixed-pitch propeller, the pitch angle $\beta(r)$ at each blade section is fixed with respect to the design airspeed of the

aircraft. The pilot therefore, cannot change the pitch angle $\beta(r)$ during flight. The fixed-pitch propeller would be most efficient for the design values of V and rpm, and for their other values the efficiency would drop. The pitch of a fixed-pitch propeller is maximum (close to $\pi/2$) near the root and minimum (close to zero) near the tip of the blade. This is because ϕ is maximum at the root and minimum at the tip, and it follows from Eq. (5.6) that the pitch β has to be suitably adjusted to make the angle of attack α remain positive and below the stalling angle. If a propeller's pitch can be adjusted on the ground, it is called an *adjustable-pitch propeller*, which has the advantage of changing pitch to suit a particular situation.

5.13.3 Variable-Pitch Propeller

It was seen below in Fig. 5.10 that for each J there is a different value of β for achieving maximum efficiency of a given propeller. The dashed lines in the figure are the locus of points of maximum efficiency for different values of β . It follows that the maximum propeller efficiency at different airspeeds and rpm can be obtained only if the variable-pitch propeller is used. If a propeller's pitch can be adjusted by a pilot to various angles during flight, it is called a *controllable- or variable-pitch propeller*. Most present-day aircraft propellers are fitted with a mechanically variable pitch device inside the hub. This mechanism rotates each blade about its own axis along the length of the blade, known as the *feathering axis* of the blade. Thus, the pitch can be continuously varied to maintain maximum efficiency of the propeller at all the flight airspeeds and rpm.

5.13.4 Constant-Speed (rpm) Propeller

In practice, the rpm of propellers are kept constant during flight because a normal piston-engine requires a particular rotational speed (rpm) to obtain maximum brake power. These are also commonly referred to as constant-speed propellers because their rotational speed is kept constant during flight. If the blade of a propeller has a pitch angle that is too high for that required for a particular airspeed, the blade will need more torque from the engine than the engine can deliver and, therefore, the engine shaft rpm will be reduced. Similarly, if the pitch angle is too small or the throttle setting is too high, the propeller will not be able to absorb the engine torque and consequently the engine rpm will start increasing, which may cause structural damage to the engine and the propeller. In order to have an efficient blade setting under all conditions and at the same time avoid the possibility of excessive or insufficient torque, constant-speed propellers are fitted with a variable-pitch device. The pitch of the blade in this device is automatically corrected so that a constant rotational speed is maintained, regardless of the throttle setting. A pilot simply selects the desired rotational speed; fixing the pitch of the propeller blade subsequently is fully automatic. Thus, the efficiency of the propeller always automatically remains at its maximum on the curve shown by the dashed lines in Fig. 5.10, as the airspeed or the advance ratio changes. The maximum efficiency of a modern propeller lies between 0.80 and 0.90. Therefore, it is a common practice to regard $\eta_p = 0.85$ if the propeller efficiency is not specified.

5.14 Different Propeller States

There are four important different propeller states: the propeller state, the brake state, the windmill state, and the feathering state. In the *propeller state*, the propeller absorbs the power of the shaft and delivers it as thrust power to the aircraft. In

the *brake state* (propeller reversing), the propeller absorbs power from the shaft and converts it into drag power (negative thrust) to the aircraft. In the *windmill state*, the propeller absorbs power from the wind and delivers it to the shaft as shaft power.

In case the aircraft engine becomes inoperative, it is desirable to turn the blades to the extreme coarse pitch position to minimize the drag of the propeller along the flight path. This is called the *feathering state* of the propeller. It also stops the propeller from windmilling, which may possibly cause damage to the inoperative engine.

5.15 Trends in Propeller Design

More powerful engines have become essential with advances in aircraft weight and speed. This means that the propellers must be able to absorb high shaft power as in the case of turboprops of gas turbine engines. High power absorption can be achieved by increasing the number of blades, diameter, and rpm of the propellers. Increasing the number of blades increases hub diameter and creates large aerodynamic interference problems between the blades. Five blades in a propeller is considered to be the maximum number that is operationally feasible. Therefore, counter-rotating propellers in two different parallel planes of the hub are used. This increases the number of blades absorbing more shaft power. The additional advantage of counter-rotating propellers is to nullify slipstream effect and out-of-balance torque due to the front propeller of the aircraft. Counter-rotating propellers, however, increase weight, complexity, and cost.

The increase in propeller diameter is sometimes not feasible because of ground and airframe clearance problems. The increase in the length of the blades or rpm increases tip velocity, causing the compressibility effect. This is currently minimized by providing swept-back propeller blades. This reduces wave drag in a fashion similar to a swept-back wing. The concept of the shrouded or ducted propeller is also used for increasing the efficiency of the propeller system.

References

- ¹Anderson, J. D., Jr., *Introduction to Flight*, McGraw-Hill, New York, 1989.
²McKinley, J. L., and Bent, R. D., *Powerplants of Aerospace Vehicles*, 3rd ed., McGraw-Hill, New York, 1965.
³Dommash, D. O., Sherby, S. S., and Connolly, T. F., *Airplane Aerodynamics*, 4th ed., Pitman, New York, 1967.

Problems

In the multiple choice problems below, mark the correct answer.

5.1 Piston engine produces torque to overcome a) drag force of aircraft, b) moment of drag forces on propeller in the plane of rotation, c) rotation of aircraft.

5.2 The horizontally opposed system of cylinders of a piston engine is preferred because it a) offers less drag, b) produces more power, c) is easy to cool.

5.3 Cooling drag of an aircraft is the a) drag of aircraft when flying in extreme cold atmosphere, b) drag of aircraft in cooling exhaust gases, c) drag of installation for the purpose of cooling engine, oil, and its accessories.

5.4 In a supercharged engine a) power remains constant as the altitude increases, b) power decreases as the altitude increases, c) power remains constant up to a certain altitude and then decreases.

5.5 A turbocharger is a) a turbine placed in the exhaust gases, b) a compressor placed downstream of the carburetor, c) a compressor placed upstream of the carburetor.

5.6 List the important requirements of an aircraft engine.

5.7 What is meant by indicated horsepower?

5.8 What is critical altitude of an engine?

5.9 Explain rated power of an engine.

5.10 What is a rich mixture and when it is used?

5.11 What fuel/air ratio produces the best power?

5.12 Explain the advantages of a fuel injection system.

5.13 Carburetor icing is dangerous because a) it tends to block the passage of the fuel-air mixture, b) it cools the surfaces of the carburetor, c) ice particles are introduced in the mixture.

5.14 Dangers of carburetor icing can be suspected when the ambient temperature is about a) -10°C , b) 20°C , c) 40°C .

5.15 The carburetor heat is most effective at a) full throttle, b) partial throttle, c) throttle for idling engine.

5.16 When using the carburetor heat for prolonged periods, the mixture should be kept a) rich, b) moderate, c) lean.

5.17 As soon as the heat is applied to remove carburetor icing, there is initially a) no change in engine power, b) loss in engine power, c) gain in engine power.

5.18 During takeoff the carburetor heat control position should be a) at cold air position, b) at hot air position, c) at moderate air position.

5.19 Which of the following statements are not correct? a) Hot air reduces engine power. b) Avoid clouds as much as possible to prevent carburetor icing. c) The word "carburetor" means mixer.

5.20 A propeller is a device that takes a) a large mass of air and imparts small acceleration to it, b) a large mass of air and imparts large acceleration to it, c) a small mass of air and imparts large acceleration to it.

- 5.21** When the propeller pitch control is moved during flight, from fine pitch to coarse pitch, the manifold pressure gauge would indicate a) increase in pressure, b) decrease in pressure, c) no change in pressure.
- 5.22** In a fixed-pitch propeller a) pitch is constant along the blade length, b) pitch varies along the blade length, but the blade is fixed at root, c) rotational speed of propeller is constant.
- 5.23** In a constant-speed propeller a) pitch remains constant, b) forward speed remains constant, c) rpm remains constant.
- 5.24** A propeller blade generally has a) more pitch at the tip than at the root, b) more pitch at the root than at the tip, c) no change in pitch along the blade length.
- 5.25** With the change in pitch a) angle of attack also changes, b) angle of attack does not change, c) only the direction of relative velocity changes.
- 5.26** If a piston engine is running at a constant power, the increase in pitch angle would a) increase the rpm, b) decrease the rpm, c) not change the rpm.
- 5.27** The efficiency of a modern propeller is about a) 0.65, b) 0.75, c) 0.85.
- 5.28** Thrust is delivered a) more by the outer radius of blade, b) more by the inner radius of blade, c) constant along the radial direction.
- 5.29** Advance ratio of propeller indicates a) ratio of root chord to tip chord, b) ratio of airspeed to wind speed, c) ratio of forward airspeed to tip speed.
- 5.30** Which of the following statements are correct? a) Critical altitude does not vary with ambient temperature. b) Propeller blades are not twisted. c) The feathering state of a propeller produces more vibrations.
- 5.31** How does a propeller produce thrust?
- 5.32** Why does a propeller blade angle change from the hub to the tip?
- 5.33** Explain propeller efficiency.
- 5.34** Explain the purpose of a constant-speed propeller.
- 5.35** What is a feathering propeller state?

This page intentionally left blank

6

Altitudes, Airspeeds, and Wind Speeds

6.1 Introduction

An aircraft flies at different altitudes and airspeeds, and may encounter different wind speeds. These three different variables are frequently used by pilots, designers, and aircraft performance evaluators. It is pertinent to understand them clearly since different types exist in each one of the three variables.

A pilot knows the altitude and airspeed of his aircraft from consulting the flight instruments in the cockpit. The altitude is obtained from an altimeter whereas the airspeed is given by an airspeed indicator. These instruments, however, do not predict the true altitude and true airspeed (TAS). Therefore, it is most pertinent to learn what altitudes and airspeeds these instruments predict and, if possible and whenever required, to obtain the true altitude and true airspeed of the aircraft.

6.2 Altitude

The height above the ground is an important quantity during climb or when landing, or when flying near high ground, hills, or mountains. The term *altitude* does not generally designate the height above ground. *Altitude* is defined as the vertical distance or height above sea level. The seven different types of altitude that are referred to in the aeronautical literature are the geometric, absolute, geopotential, pressure, temperature, density, and standard altitudes. Some of these altitudes are commonly used in flight manuals and flight tests.

6.2.1 Geometric Altitude (True Altitude)

The *geometric altitude* of an object is its height above sea level. Consider Fig. 6.1 where points *A*, *B*, and *S* are along the same vertical line. Point *S* is at sea level, point *B* is on the ground, and point *A* is above the ground. Let the distances $SB = h_B$, $BA = h_1$, and $SA = h_A = h_B + h_1$. The geometric altitudes of points *A* and *B* are h_A and h_B , respectively, because they are measured from sea level. Generally, the land height of a city is specified in terms of its geometric altitude. The geometric altitude is also called the *tape-line altitude* or *true altitude*. In practice, the geometric altitude is important during climb, landing, or when approaching high ground. The true altitude is generally of primary concern in performance calculations of an aircraft.

6.2.2 Absolute Altitude

The *absolute altitude* is measured from the center of the Earth. If r is the radius of the Earth as shown in Fig. 6.1, the absolute altitude h_a of the point *A* would be

$$h_a = r + h_A$$

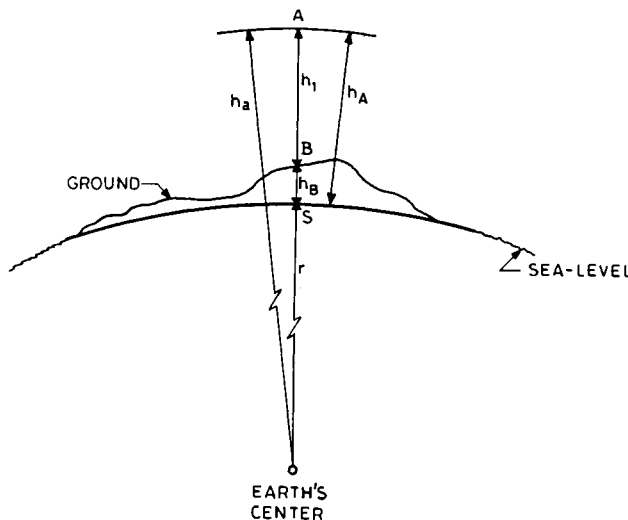


Fig. 6.1 Geometric and absolute altitudes.

That is, if the radius of the Earth is added to its geometric altitude, this becomes the absolute altitude of the point.

6.2.3 Geopotential Altitude

Geopotential altitude is usually defined by the transformation of the geometric altitude h into the geopotential altitude h_G by the following differential relation:

$$gdh = g_{SL}dh_G \quad (6.1)$$

where g_{SL} is the acceleration due to gravity at sea level. Geopotential altitude expresses the “apparent loss” of potential energy (due to reduction in g) of a given mass when it is raised to a higher altitude.¹ With the help of the above equation and using Newton’s law of gravitation, it is possible to express h_G in terms of the true altitude h as shown below.

Consider both h_G and h to be zero at sea level, and h_G is the geopotential altitude where the corresponding geometric altitude is h . The integration of Eq. 6.1 gives

$$\int_0^{h_G} dh_G = \int_0^h (g/g_{SL})dh \quad (6.2)$$

From Newton’s law of gravitation, it is known that g varies inversely as the square of the distance from the center of the Earth. Therefore,

$$g/g_{SL} = (r/h_a)^2 = \{r/(r+h)\}^2$$

and Eq. (6.2) becomes

$$\int_0^{h_G} dh_G = r^2 \int_0^h dh/(r+h)^2$$

which on solving the integrals gives

$$h_G = rh/(r + h) \quad (6.3)$$

This defines the geopotential altitude in terms of the geometric altitude. Thus, $h_G < h$ for distances above sea level ($h > 0$) and the reverse is the case below sea level where $h < 0$.

Modern aircraft generally fly in the lower parts of atmosphere at altitudes of less than 20 km. Therefore, the Earth's radius $r \gg h$, and so for many practical purposes, $h_G = h$. As an example, if $r = 6357$ km, it can be easily verified that at the altitudes of 20 and 65 km, the values of h_G would be less than h by about 0.3 and 1%, respectively.

6.2.4 Pressure, Temperature, and Density Altitudes

These altitudes have meaning only if a standard atmosphere table (or graph) exists, because these altitudes are defined with respect to the standard atmosphere. The pressure altitude is defined here first, because the temperature and density altitudes can be similarly defined. Consider an aircraft flying at an altitude where the atmosphere pressure is p . Now look at the standard atmosphere table (or graph) and find the altitude h_p corresponding to the pressure p ; the h_p is the pressure altitude. Similarly, the temperature and the density altitudes are defined. These altitudes generally differ among themselves for a given geometric altitude.

As an example, consider a pilot flying an aircraft at an altitude where the ambient atmospheric pressure $p = 0.472 \times 10^5$ N/m² and temperature $T = 254.4$ K. From the equation of state, calculate the density, $\rho = p/(RT) = 0.472 \times 10^5 / (287 \times 254.4) = 0.646$ kg/m³, where R is the gas constant of air. Now look at the standard atmosphere table or graph and find that these pressure, temperature, and density values exist at the altitudes of 6, 5.2, and 6.2 km, respectively. This means that the aircraft is flying at the pressure altitude of 6 km and, simultaneously, at the temperature altitude of 5.2 km and density altitude of 6.2 km. Its geometric altitude would be yet another different quantity.

6.2.5 Standard Altitude

The *standard altitude* is also defined with respect to the standard atmosphere table or graph. At standard altitude, the values of pressure, temperature, and density are simultaneously the same as those of the standard atmosphere at that altitude. By definition, any altitude in the standard atmosphere is the standard altitude.

6.2.6 Altitude Measurements

The standard atmosphere table is of importance in designing altimeters. The most common altimeter is the pressure altitude indicator. The pressure altitude of standard atmosphere is a function of altitude only. It is, therefore, possible to design an instrument that senses the pressure of the atmosphere and converts it into the pressure altitude. The altimeter has evacuated metal bellows that sense ambient atmospheric pressure from the static hole of pitot-static tube. The bellows expands or contracts with the changes in the outside ambient pressure. The bellows is connected to a series of gears and levers that make the pointer move along the scale of its dial, which directly reads pressure altitude in feet or meters.

An altimeter to read temperature altitude could be similarly designed but it is not common because of large temperature fluctuations over the Earth. An altimeter to read density altitude directly could also be designed if an instrument were available to measure the density of the atmosphere directly.

6.3 Airspeed

Airspeed is the velocity of an aircraft along its flight path. It is the most important variable of aircraft performance, and emphasis is laid on determining it accurately because the aerodynamic forces are proportional to the square of airspeed. Aircraft maneuvers during takeoff, turns, and landing are initiated only at specified airspeeds. Different names, which generally do not correspond to the same airspeed, are in use in the flight test literature, such as indicated airspeed (IAS), equivalent airspeed (EAS), calibrated airspeed (CAS), true airspeed (TAS), ground speed, stalling airspeed, etc. For someone calculating aircraft performance, the airspeed is simply the TAS, which is written as V . But for a pilot or for someone evaluating an aircraft through flight tests, the airspeed is the value that the airspeed indicator (ASI) in the cockpit shows during flight. The ASI, however, does not indicate TAS; this is due to its sensing element and to the design philosophy behind the airspeed measuring instrument. Terms such as IAS, EAS, and CAS originated due to the airspeed measuring equipment. Therefore, airspeed measurement is described first before explaining the different types of airspeeds.

6.3.1 Airspeed Measurement

The two basic elements of the system that measure airspeed are the pitot-static tube and the mechanical instrument called the ASI. The pitot-static tube senses the ambient pressure which is converted into IAS by the linkages according to a specified algebraic relation. The IAS is not the TAS, because the instrument is designed to indicate or read the EAS in incompressible flow and the CAS in compressible flow. The sensing element, design principle (algebraic equation), and the mechanical instrument are explained below.

6.3.1.1 Sensing element. The sensing element is the pitot-static tube for simultaneously sensing total pressure p_0 (called the pitot pressure) and the static pressure p of the airflow field. The pitot-static tube has two coaxial metallic tubes smoothly joined at the leading edge (mouth) such that the inner tube is kept open at the mouth for sensing total pressure p_0 as shown in Fig. 6.2a.

At a short distance downstream of the mouth there are about four or more tiny holes with the same cross section in the outer tube. These tiny holes sense static pressure and, therefore, the outer tube senses static pressure. These two

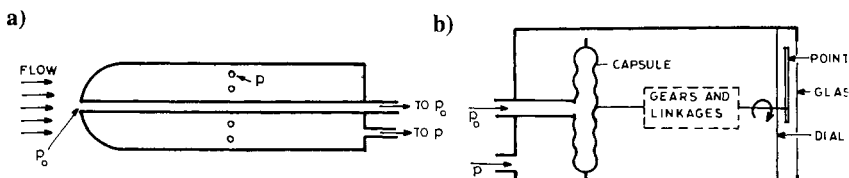


Fig. 6.2 Schematic views of a) pitot-static tube and b) airspeed indicator (ASI).

tubes sense p_0 and p of the ambient conditions correctly when the axis of the pitot-static tube is parallel to the flight path and is located at a place that is not affected by the pressure field of the aircraft. There is a provision for electrical heating of the mouth of the tube to avoid its blocking due to ice formation in the icing zones of the atmosphere. The electrical heating, however, does not affect the readings of total and static pressures. The exit portions of the two coaxial tubes of the pitot-static tube are independently connected to two flexible tubings, which are in turn connected to the ASI placed in the cockpit. The pitot-static tubes may be of different design, and those used in large modern aircraft are thick and sturdy and may even stand the impact of hailstones.

6.3.1.2 Design principle. In incompressible flow regions the airspeed V (TAS) is related to p_0 and p by Eq. (3.17) as

$$V = \{2(p_0 - p)/\rho\}^{1/2} \quad (6.4)$$

The differential pressure $p_0 - p$ can be regarded as a single variable, instead of the individual pressures p_0 and p being taken as separate variables. Hence, the TAS is a function of the two variables $(p_0 - p)$ and ρ . This causes complications in the design of the ASI, because it is much simpler to design a mechanical instrument if V depends only on the single variable $p_0 - p$. In the case of incompressible flow, the instrument is designed by keeping $\rho = \rho_{SSL}$ a constant, where the subscript SSL represents standard atmosphere sea level condition. It will then not read the TAS at any other altitude except at the sea level in standard atmosphere.

In compressible flow regions, the TAS V is related to the pressures p_0 and p by Eq. (3.20) as

$$V = \left[\frac{2\gamma p}{(\gamma - 1)\rho} \left\{ \left(\frac{p_0 - p}{p} + 1 \right)^{(\gamma-1)/\gamma} - 1 \right\} \right]^{1/2} \quad (6.5)$$

Here the TAS is a function of the three different variables, $(p_0 - p)$, p , and ρ . This will cause more complications in the design of airspeed measuring instruments for compressible flow regions. It therefore becomes necessary to keep p and ρ as constants in the above equation, by assigning $p = p_{SSL}$ and $\rho = \rho_{SSL}$ and without disturbing the variable $p_0 - p$. An instrument designed with $p_0 - p$ as the only independent variable will not indicate the TAS at any other altitude except at sea level in the standard atmosphere.

6.3.1.3 Airspeed indicator. The ASI is a mechanical instrument that has a phosphor bronze pressure capsule whose case is sealed. It is schematically shown in Fig. 6.2b. The total pressure p_0 is applied to the inside of the capsule and the static pressure, p , to its outside, so that the differential pressure $p_0 - p$, sensed by the instrument, puts the capsule into motion. This movement of the capsule is transmitted to the pointer of the dial, by magnifying the linkage and gear movements, to obtain a uniform scale of airspeed. The instrument includes a suitable damping device and a proper compensation for temperature variation.

6.3.2 Ground Speed (Flight Speed)

The *ground speed* of an aircraft is its speed along its flight path with respect to a fixed location on the ground, like the speed of an automobile. It is denoted by V_g and it is also referred to as the *flight speed* of the aircraft. The ground speed is used in referring to mileage or in connection with the endurance of the aircraft. Because of certain practical considerations, the ground speed of an aircraft is more important than other kinds of airspeed. The presence of wind causes differences between the ground speed and the TAS of the aircraft. The ground speed is also the TAS of the aircraft in the case of no wind.

6.3.3 True Airspeed

The presence of wind is generally inevitable. The TAS is defined as the velocity of the center of gravity of the aircraft with respect to the wind velocity. If V_w is the wind velocity parallel to the flight path and V_g is the ground speed of the aircraft, the TAS V would be given by

$$V = V_g \pm V_w \quad (6.6)$$

where the positive sign is for the headwind and the negative sign is for the tailwind. A *headwind* is an oncoming wind that moves in the direction from head to tail as shown in Fig. 6.3a and its reverse direction is called a tailwind as shown in Fig. 6.3b. In the case of wind velocity being inclined to the flight path, its component along the flight path is considered.

The airspeed (TAS) of an aircraft is defined with respect to the wind due to the following reasons: 1) The speed-sensing element (pitot-static tube) senses p_0 and p of the speed of the aircraft with respect to wind, and 2) it is the speed that the aircraft configuration feels; the aerodynamic forces and moments over the aircraft are proportional to the square of the relative speed, and these forces and moments are nondimensionalized with respect to the relative speed of the aircraft.

In this book, the word “airspeed” is generally used to refer to the TAS of the aircraft. If the wind velocity is much less than the ground speed of the aircraft, the TAS can be regarded to be the same as the ground speed of the aircraft. In most chapters of this book that calculate aircraft performance, the wind speed is considered to be negligible because most modern aircraft fly at a sufficiently high speed as compared to the wind speed. In all such cases, the TAS is the same as the ground speed of the aircraft. In the concluding sections of some chapters dealing with low-speed aircraft, the effect of wind speed is also considered.

6.3.4 Indicated Airspeed

The airspeed pointed out by the indicator of the dial of airspeed indicator of the aircraft is known as indicated airspeed, which a pilot reads in his cockpit. It



Fig. 6.3 Headwinds and tailwinds: a) headwind and b) tailwind.

is commonly abbreviated IAS and its value is denoted by V_i . The readings of the ASI would not generally be free from error if certain corrections were not applied to it. The three important errors that may arise are instrument error, lag error, and position error (or pressure error). A detailed discussion on these errors and their corrections can be obtained in the *Flight Test Manual*.²

The instrument error arises due to certain imperfections in the instrument, the friction of linkages, and the changes due to wear and tear of the instrument. The instrument correction ΔV_{ins} is generally small and since it varies with time, frequent calibration of the instrument is desirable for precise results. The instrument error is obtained empirically and it is applied first before any other correction. Lag errors are present only when transient atmospheric or flow conditions exist such as during changing altitude, attitude, and airspeed. The lag correction ΔV_{lag} is generally established in ground tests because it is difficult to measure lag error in flight. The lag error is absent in steady, level flight. The position error ΔV_{posi} arises because the pitot-static tube may be positioned at a place that is under the influence of the pressure or velocity field of the aircraft. It is difficult to find a fixed position in the vicinity of the aircraft that has an undisturbed pressure or velocity field in relation to all the attitudes and airspeeds of the aircraft. In subsonic flow, the position error in regard to total pressure is negligible in practice as compared to that regarding static pressure. As far as possible, the pitot-static tube should not be installed in the boundary-layer or shear-layer region, the localized region of supersonic flow, behind the leading edge shock of a wing or nose, or behind the propeller. Generally, it is possible to avoid these difficulties by locating the pitot-static tube ahead of the wing leading edge or the nose of the aircraft. The error due to shock forming near the leading edge of the pitot-static tube can be corrected by using normal shock-wave relation of a supersonic flow.

The IAS, even after applying all the corrections mentioned above, does not generally read the TAS because it is not designed accordingly. It is designed to read the EAS in incompressible flow, whereas in the compressible flow regions it is designed to read the CAS. The definitions of these two airspeeds and the method of obtaining the TAS are explained in the following two subsections.

6.3.5 Equivalent Airspeed

The EAS is defined both for incompressible and compressible flows. First it is defined here for incompressible flow, since it can be similarly defined for compressible flow.

6.3.5.1 EAS in incompressible flow. The TAS V in incompressible flow is given by Eq. (6.4), which is a function of the two independent variables $p_0 - p$ and ρ . In order to facilitate the design of the airspeed measuring instrument, ρ is kept constant by assigning $\rho = \rho_{SSL}$. This leads to defining V_e , the EAS, in incompressible flow as

$$\boxed{V_e = \sqrt{2(p_0 - p)/\rho_{SSL}}} \quad (6.7)$$

The equivalent airspeed V_e is a function of the single variable $p_0 - p$, and the

airspeed measuring instrument can now be easily designed but it will read EAS, which is not the TAS. The EAS = TAS only at sea level in the standard atmosphere. At any other altitude, the EAS would be different from the TAS. The IAS, after one corrects all errors in arriving at its values, is nothing but the EAS.

At any altitude, the dynamic pressure $p_0 - p$ sensed by the airspeed measuring instrument is $\rho_{SSL} V_e^2 / 2$ and that given by the TAS is $\rho V^2 / 2$. It follows that

$$\rho V^2 / 2 = \rho_{SSL} V_e^2 / 2$$

which gives

$$V = V_e / \sqrt{\sigma}, \quad \text{where } \sigma = \rho / \rho_{SSL} \quad (6.8)$$

The above equation is important because it connects the EAS with the TAS. Having obtained V_e from the corrected V_i , the above equation gives the true airspeed V . It will be shown below (Eq. 6.10) that the above relationship also holds good for compressible flows.

In incompressible flow, the method of obtaining the TAS V from the IAS V_i can thus be summarized below:

$$V_i + \Delta V_{ins} + \Delta V_{lag} + \Delta V_{posi} = \text{corrected } V_i = V_e$$

and

$$V_e / \sqrt{\sigma} = V$$

The EAS differs from the TAS due to σ being different from unity, i.e., due to change in atmosphere from the standard atmosphere at sea level. The value of σ generally decreases with increasing altitude. It is possible for a pilot to keep either a constant EAS or a constant TAS during a climbing flight.

6.3.5.2 Advantages of EAS in incompressible flow. The ASI records EAS rather than TAS. This would appear to be a drawback at first sight, but it has certain advantages as follows:

1) The instrument measuring EAS is simple and has a high degree of accuracy, and the TAS can always be easily determined from the EAS. The measurement of V or M would require a more complex system with less precision.

2) Since the dynamic pressure, $p_0 - p = \rho V^2 / 2 = \rho_{SSL} V_e^2 / 2$, it follows that the dynamic pressure at any altitude depends solely on V_e . Many performance variables of a given aircraft depend on the dynamic pressure, and hence only on V_e .

3) It is often convenient to work in terms of EAS rather than TAS. As an example, consider an aircraft operating at maximum lift coefficient, $C_{L,m}$, at the time of landing. The weight W of the aircraft during landing can be expressed as

$$W = \rho V^2 C_L S / 2 = \rho_{SSL} V_{e,land}^2 C_{L,m} S / 2$$

where S is the wing planform area and $V_{e,land}$ is the EAS at the time of landing. It follows that

$$V_{e,land} = \sqrt{2(W/S) / (\rho_{SSL} C_{L,m})}$$

which shows that V_e for landing of a given aircraft depends only on W ; the V_e does not depend on the altitude, pressure, and temperature of the atmosphere. Once the W is fixed, the V_e for landing at higher altitudes is just the same as at sea level. The case is similar during takeoff or stall, because the pilot needs to consider only one factor—weight.

4) Certain performance data can be presented more concisely if presented against V_e . For example, the drag force of a given aircraft when plotted against V gives different curves at different altitudes. All these curves collapse into a single curve (Fig. 8.4) when the drag is plotted against the EAS.

6.3.5.3 EAS in compressible flow. Like EAS in incompressible flow, the EAS in compressible flow can be similarly defined and is denoted by $V_{e,comp}$. Here also ρ is replaced by ρ_{SSL} in Eq. (6.5), and the EAS is obtained as

$$V_{e,comp} = \left[\frac{2\gamma}{\gamma - 1} \cdot \frac{p}{\rho_{SSL}} \left\{ \left(\frac{p_0 - p}{p} - 1 \right)^{(\gamma-1)/\gamma} - 1 \right\} \right]^{1/2} \quad (6.9)$$

The $V_{e,comp}$ is a function of the two variables $(p_0 - p)$ and p . Therefore, the above equation is generally not used in designing the airspeed measuring instrument. Equation 6.9, however, follows the relationship

$$V = V_{e,comp} / \sqrt{\rho} \quad (6.10)$$

which is the same as that for an incompressible flow (Eq. 6.8). As such, $V_{e,comp}$ has no real meaning, but it will be seen in Sec. 6.3.6, below, that it is used as an intermediate step in obtaining the true airspeed V from the CAS.

6.3.6 Calibrated Airspeed

The concept of calibrated airspeed exists for compressible flow. It is commonly abbreviated as CAS and its value is denoted here by V_c . If p and ρ in Eq. (6.5) are replaced by p_{SSL} and ρ_{SSL} , respectively, without affecting the term $p_0 - p$, the CAS can be defined as

$$V_c = \left[\frac{2\gamma}{(\gamma - 1)} \cdot \frac{p_{SSL}}{\rho_{SSL}} \left\{ \left(\frac{p_0 - p}{p} + 1 \right)^{(\gamma-1)/\gamma} - 1 \right\} \right]^{1/2} \quad (6.11)$$

The CAS is a function of the single variable $p_0 - p$ and, therefore, it becomes easier to design an ASI that reads V_c after sensing the differential pressure $(p_0 - p)$. This means that the IAS, if corrected for instrument, lag, and position errors, would yield CAS in the compressible flow.

It can be seen that in a standard atmosphere at sea level, the TAS V , the EAS $V_{e,comp}$ for compressible flow, and the V_c would all be equal. At any other altitude on any day, or at sea level in nonstandard atmosphere, these three airspeeds would be different. The CAS does not depend on ρ (and thus altitude).

The difference between V_c and $V_{e,comp}$ defines a useful correction ΔV_{SA} as

$$\Delta V_{SA} = V_c - V_{e,comp} \quad (6.12)$$

which is used for obtaining $V_{e,comp}$ if V_c and ΔV_{SA} are known. The quantity ΔV_{SA} is commonly known as *scale-altitude correction*. The quantity ΔV_{SA} is also called

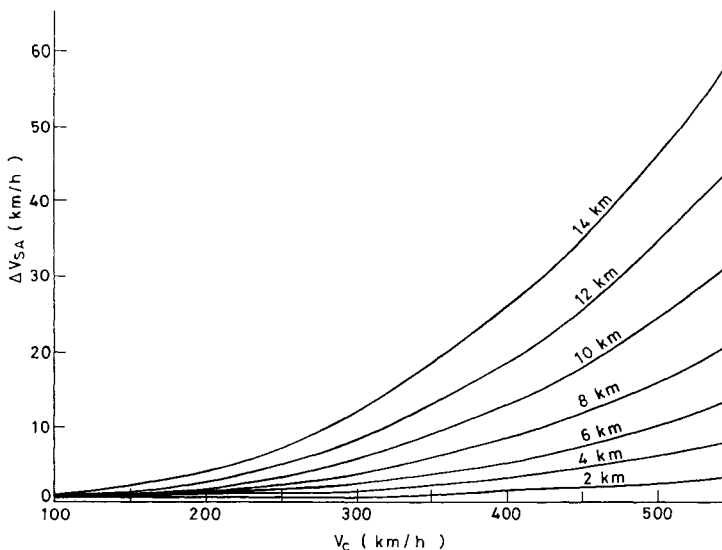


Fig. 6.4 Scale-altitude correction.

the *compressibility correction*, although it is not related to the compressibility effect because both terms V_c and $V_{e,comp}$, which define ΔV_{SA} , are obtained from the compressible flow.

It can be seen from Eq. (6.11) that the differential pressure $p_0 - p$ is a function of V_c . It follows from Eq. (6.9) that $V_{e,comp}$ is a function of V_c and p (and thus h_p). Therefore, the known functional form of ΔV_{SA} can be written from Eq. (6.12) as

$$\Delta V_{SA} = f(V_c, p) = f(V_c, h_p)$$

which is plotted in Fig. 6.4 against V_c for different values of the pressure altitude h_p . Having obtained V_c and h_p from the measuring instruments, the scale-altitude correction ΔV_{SA} can be found from this figure.

The process of obtaining the TAS from the IAS airspeed in the compressible flow region can now be summarized as follows:

$$V_i + \Delta V_{ins} + \Delta V_{lag} + \Delta V_{posi} = \text{corrected } V_i = V_c$$

$$V_c - \Delta V_{SA} = V_{e,comp}$$

$$V_{e,comp}/\sqrt{\sigma} = V$$

The process of obtaining the TAS from the IAS is again summarized schematically in Fig. 6.5, both for compressible and incompressible flows.

6.3.7 Airspeeds Based on Functional Uses

The names of airspeeds are also frequently based on the associated flow phenomenon or the limitations imposed by the designer of the aircraft. These airspeeds vary from one aircraft to another. Some of these names are stalling airspeed, cruising airspeed, maximum airspeed, minimum airspeed, maximum flap extended

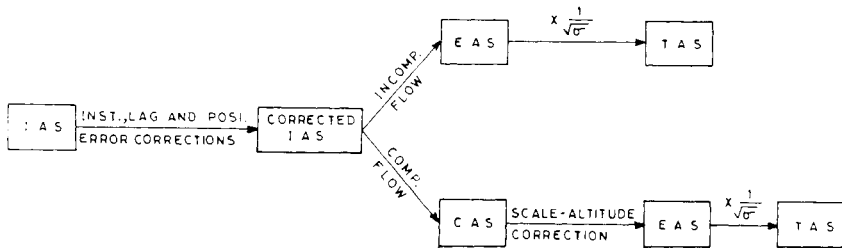


Fig. 6.5 Schematic presentation of obtaining TAS from IAS.

airspeed, minimum control airspeed, takeoff safety airspeed, rotation airspeed, maneuvering airspeed, diving airspeed, landing airspeed, etc.^{3,4} All these airspeeds are generally specified in terms of TAS or IAS.

6.3.8 Relationships Among TAS, EAS, M, and Atmospheric Ratios

Certain useful relationships exist among V , V_e , and Mach number M , involving the pressure ratio $\delta (= p / p_{SSL})$, temperature ratio $\theta (= T / T_{SSL})$, and density ratio σ .

From the speed of sound, $a = \sqrt{\gamma RT}$, the following relationship is obtained:

$$a/a_{SSL} = \sqrt{\theta} \quad (6.13)$$

and similarly from the equation of state, $p = \rho RT$, where R is the gas constant, the following relationship is obtained:

$$\delta = \sigma\theta \quad (6.14)$$

The above Eq. (6.14) is the nondimensional form of the equation of state. Using Eq. (6.14), Eq. (6.8) can also be written as

$$V_e/\sqrt{\sigma} = V/\sqrt{\theta} \quad (6.15)$$

The Mach number is $M = V/a = V/(a_{SSL}\sqrt{\theta})$, which can also be written as

$$M = V_e/(a_{SSL}\sqrt{\delta}) \quad (6.16)$$

The above equation is important because M can be obtained from the easily measured quantities of V_e and δ during flight.

The above relations predict the variations of TAS and Mach number when the EAS is kept constant during the climb of an aircraft. This is shown in Fig. 6.6 for three different constant values of the EAS ($V_e = 300, 400$, and 500 km/h). Both V and M are found to increase rapidly with altitude. Similarly, it is possible to keep constant TAS during the climb, and Fig. 6.7 shows the variations of V_e and M for three different constant values of the true airspeed ($V = 300, 400$, and 500 km/h). The EAS is found to decrease with increase in altitude. Here the Mach number increases slowly with the increase in altitude in the troposphere, and becomes constant in the stratosphere.

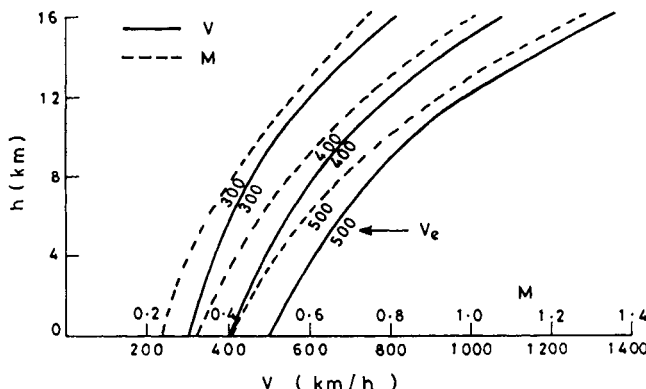


Fig. 6.6 Variations of TAS and M with altitude at constant EAS.

6.4 Wind Speeds

Air moving horizontally is termed *wind*; if it is moving vertically it is called an *air current*. Every weather reporting station measures wind speed and its direction either continuously or intermittently. Terminology describing different kinds of wind speed, wind direction, and the methods of measuring wind speed, are explained below.

6.4.1 Mean Wind Speed

The average wind speed of 1 h duration is known as the *hourly mean wind speed*. A typical variation of the mean wind speed during 24 h of a day in various seasons is shown in Fig. 6.8, which occurs at Madras, India; the abbreviations MN and MD in the figure are used for morning and midday, respectively. This shows that the wind speeds are generally low at early hours in the morning, but around 6 or 7 a.m. the wind speed starts increasing and reaches to a maximum value at about 16 h in the afternoon (4 p.m.) and, thereafter, it starts decreasing.

6.4.2 Gust and Lull

The wind speed generally fluctuates irregularly around its mean value as shown in Fig. 6.9. A sudden strong rush of winds shown by higher peaks above the

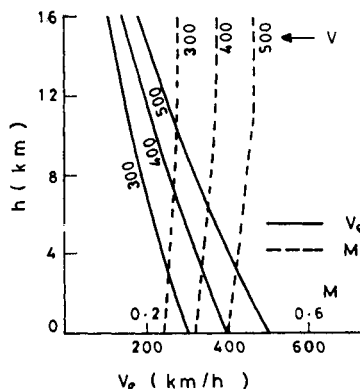


Fig. 6.7 Variations of EAS and M with altitude at constant TAS.

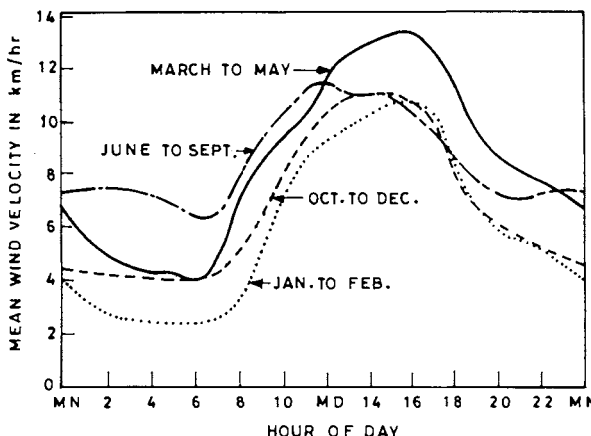


Fig. 6.8 Diurnal variation of wind speed at Madras, India.

mean is called a *gust*. Some of these gusts are marked as A, B, C in the figure. A temporary increase in wind speed above its mean value lasting for a few seconds is called the *gust speed*.

A *lull* is just opposite of a gust. The lower peaks below the mean value are called lulls, and some of these are marked A', B', C' in the figure. A gust or lull persists for only a few seconds, less than a minute. Only the magnitude of wind speed, and not its direction, is of concern for defining a gust or lull.

6.4.3 Gustiness, Gust, and Gust Load Factors

The *gustiness factor* is a meteorological term that quantifies the amount of gustiness prevailing in relation to the mean wind speed. It is usually defined in percentage as

$$\text{Gustiness factor} = \frac{\text{Range of wind speed from lull to gust}}{\text{Mean wind speed}} \times 100$$

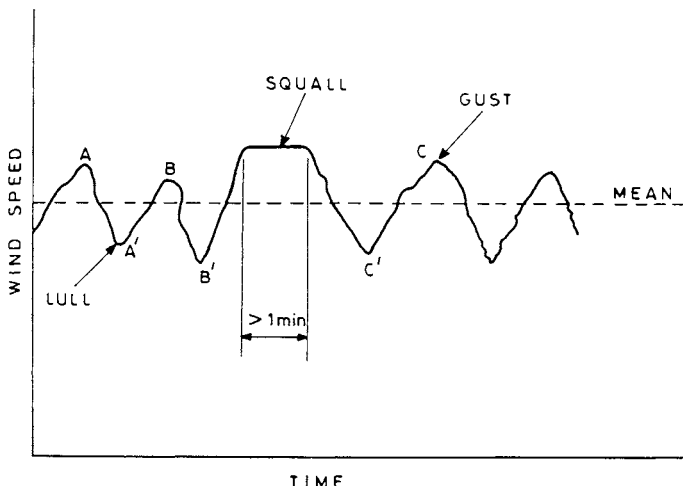


Fig. 6.9 Wind gusts, lulls, and squall.

For example, if a mean wind speed of 20 m/s dropping to 15 m/s in lull but going to 30 m/s in gust, the gustiness factor of the wind is given by

$$\text{Gustiness factor} = \frac{(20 - 15) + (30 - 20)}{20} \times 100 = 75\%$$

The term *gust factor* is commonly used by civil engineers when designing civil structures that are exposed to winds.⁵ The ratio of the gust speed to the mean hourly wind speed is called the gust factor, which generally varies between 1.3 and 2.5 depending on the surface roughness of the terrain. The lower factor is typical of wind near smooth terrains and near the surface where the level of gustiness is low. The rougher the terrain, the higher is the gust factor.

There is yet another term, commonly used by aeronautical engineers⁶: the *gust-load factor*. It is the increase in load factor of the aircraft caused by a sudden increase in its angle of attack when it strikes an ascending air current. For example, if an aircraft in level flight with airspeed V meets an ascending air current of speed v , the increase in angle of attack $\alpha = v/V$ would correspondingly increase the load factor of the aircraft, which is called the gust-load factor.

6.4.4 Squall

If a gust persists for more than a minute, it is called a *squall*. The squall is shown in Fig. 6.9. It is usually associated with a meteorological feature such as thunderstorm.

6.4.5 Beaufort Scale

Wind speeds were classified as early as 1805 by a British admiral, Sir Francis Beaufort. The classification is based on the influence of the wind speed on natural surroundings of the terrain. This classification is described in Table 6.1. The descriptive terms of the winds have also been assigned numbers ranging from 0 to 12, which are called *Beaufort numbers*. In order to qualify for the Beaufort scale, the wind speed is measured at a height of 10 m above an open flat ground.

6.4.6 Wind Direction, Veering, and Backing

The wind is commonly named on the basis of the direction from which it blows. For example, if the wind blows from the east toward west, it is called easterly or east wind. Similarly, a northwest wind is one that blows from a northwest direction toward a southeast direction.

The magnitude of wind direction is measured from north in the clockwise direction. The terms *veering* and *Backing* are commonly used for expressing the shifts in the wind's direction. The wind is said to be *veering* if its direction shifts in a clockwise direction, i.e., shifts to the right of the direction from which it had been blowing. *Backing* is the opposite of the veering.

6.4.7 Wind Speed Measurement

An accurate measurement of wind speed is important because the wind force is generally proportional to the square of the wind speed. For example, a true wind speed of 35 m/s being read as 40 m/s would cause an error 31% in the wind force.

Table 6.1 Beaufort scale for winds

Beaufort number	Wind	Wind speed, km/h (miles/h)		Land effect
0	Calm	<1	(<1)	Smoke rises straight up
1	Light air	1–5	(1–3)	Direction shown by smoke drift
2	Light breeze	6–11	(4–7)	Wind felt on face; leaves rustle
3	Gentle breeze	12–19	(8–12)	Leaves in constant motion; wind extends light flags
4	Moderate breeze	20–28	(13–18)	Raise dust and loose paper, small branches move
5	Fresh breeze	29–38	(19–24)	Small trees and leaves begin to sway
6	Strong breeze	39–49	(25–31)	Large branches in motion; whistling of telegraph wires
7	Moderate gale	50–61	(32–38)	Whole tree in motion; difficulty in walking
8	Gale	62–74	(39–46)	Breaks twigs off trees
9	Strong gale	75–88	(47–54)	Some damage to vegetation and structure
10	Storm	89–102	(55–63)	Trees uprooted; considerable damage
11	Violent storm	103–117	(64–72)	Widespread damage
12	Hurricane	>118	(>73)	

Near the Earth's surface the wind is measured by anemometers⁴ such as the pressure anemometer, cup anemometer, and windmill anemometer. The pressure anemometer is essentially a pitot-static tube that is provided with a vertical vane at its back to obtain wind direction. A cup anemometer has three or four cups in the horizontal plane rotating about vertical axis due to wind force on the cups. The rate of rotation of the cups is proportional to the wind speed. In a windmill anemometer, the windmill or propeller rotates in the vertical plane. The whole instrument is rotatable about the vertical axis so that the wind vane at its back always maintains the wind direction. All these anemometers are calibrated frequently due to wear in mechanical friction. An instrument that makes a running record of the wind velocity is called *anemograph*. The record traced by the anemometer is called *anemogram*.

The *gust anemometer* is used for measuring wind gust. It has a perforated ball placed at the end of a cantilevered arm. The wind force on the ball bends the cantilever whose strains are measured by strain gauges that can be calibrated. There is also a hot wire anemometer to measure wind speed and wind gust. The heated wire of the instrument is cooled by the winds. This causes changes in the resistance and voltage across the wire, which can be calibrated.

Winds aloft are measured by pilot balloons or rawinsondes, which are explained in Chapter 20 of this book.

References

- ¹Layton, D., *Aircraft Performance*, Matrix Publishers, 1988.
- ²Durbin, E. J., et. al. (eds.), *Flight Test Manual*, Vol. 1, (Performance), published on behalf of AGARD, Pergamon, New York, 1962.
- ³Stinton, D., *The Design of the Aeroplane*, Granada, England, UK, 1983; distributed by ASIAA, Washington, DC.
- ⁴MacDonalds, S. A. F., *From the Ground Up*, Himalayan Books, New Delhi, 1989.
- ⁵Sachs, P., *Wind Forces Engineering*, 1st ed., Pergamon, New York, 1972.
- ⁶Peery, D. J., *Aircraft Structures*, McGraw-Hill, New York, 1950.

Problems

In the multiple choice problems below, mark the correct answer.

- 6.1** The ground level of a town is usually measured in terms of a) geometric altitude, b) standard altitude, c) geopotential altitude.
- 6.2** Flight tests for the evaluation of an aircraft performance usually measure a) pressure altitude, b) standard altitude, c) temperature altitude.
- 6.3** Geopotential altitude is due to change in a) weather temperature, b) winds, c) acceleration due to gravity.
- 6.4** Find the various altitudes where the ambient atmospheric conditions are a) $p = 54,000 \text{ N/m}^2$, $T = 256 \text{ K}$, b) $\rho = 0.6 \text{ kg/m}^3$, c) $\delta = 0.350$, $\theta = 0.80$, d) $\sigma = 0.320$.
- 6.5** At any positive altitude a) $\sigma\delta = \theta$, b) $\delta/\theta < \sigma$, c) $\theta < \sigma < \delta$.
- 6.6** Pressure altimeter measures a) standard altitude, b) pressure altitude, c) true altitude.
- 6.7** Find the true altitude where the difference $h - h_G$ is 1.5% of h .
- 6.8** Which of the following statements are correct? a) Geopotential altitude is positive below sea level. b) Percentage difference between geometric and geopotential altitude decreases with the increase in altitude. c) If g does not vary with altitude, $h = h_G$.
- 6.9** During the altitude measurement from pitot-static system, the sensing element is a) static hole, b) pitot hole, c) both static and pitot holes.
- 6.10** Which of the following statements are correct? a) It is easy to realize a standard altitude in practice by a pilot. b) If pressure and temperature altitudes are the same, it must be standard altitude. c) Pressure altitude can be obtained from the temperature altitude.
- 6.11** Static hole of a pitot-static system is used for a) ASI only, b) altimeter only, c) both ASI and altimeter.

6.12 In an altimeter calibration, it is found that the altimeter yields altitude readings that are too high. This means that a) ambient pressures are too high, b) ASI would also read too high, c) ASI would also read too low.

6.13 TAS depends on $p_0 - p$ and ρ only in a) compressible flow, b) incompressible flow, c) both incompressible and compressible flows.

6.14 In general, TAS depends on a) p , ρ , and T only, b) p , p_0 , and T only, c) $p_0 - p$ and ρ only.

6.15 EAS = TAS in the a) standard atmosphere at any altitude, b) standard atmosphere at sea level, c) nonstandard atmosphere at sea level.

6.16 Acceleration of an aircraft is the rate of change of its a) EAS, b) CAS, c) TAS.

6.17 TAS is equal to ground speed of the aircraft in the case of winds moving a) parallel to flight path, b) inclined to flight path, c) normal to flight path.

6.18 If an aircraft maintains constant TAS of 350 kn during climb, what is its Mach number at the altitudes of 5, 10, and 15 km.

6.19 If an aircraft is climbing at constant TAS of 300 kn, find the EAS at 4, 8, and 12 km.

6.20 If an aircraft is climbing at constant EAS of 400 kn, find the TAS at the altitudes of 3, 6, and 9 km.

6.21 If an aircraft has constant EAS of 350 kn during climb, find its Mach number at 4, 8, and 12 km.

6.22 A high-speed subsonic aircraft is flying at a pressure altitude of 10 km where the ambient temperature is 225 K. A pitot-tube at its wingtip measures a pressure of 4.51×10^4 N/m². Calculate TAS, Mach number, and CAS.

6.23 A high-speed subsonic aircraft is flying at Mach 0.62. Its pitot-tube on the wingtip measures a pressure of 112,000 N/m². What altitude would be predicted by its altimeter?

6.24 The altimeter of a low-speed aircraft reads 2 km where the outside air temperature is 274 K. If the ASI reads 53 m/s, find the TAS of the aircraft.

6.25 Wind speeds are generally low at a) early hours in the morning, b) noon, c) late in the evening.

6.26 Wind direction is measured from a) east in anticlockwise direction, b) north in clockwise direction, c) south in anticlockwise direction.

6.27 Wind is said to be veering if its a) direction shifts anticlockwise, b) direction shifts clockwise, c) magnitude increases.

6.28 If a gust persists more than 1 min, it is called a) gustiness, b) strong wind, c) squall.

6.29 The ratio of gust wind speed to the mean hourly wind speed is called a) gust, b) gustiness factor, c) gust factor.

6.30 It is said to be calm if only a) wind speed is zero, b) winds make no noise, c) wind speed is less than 2 km/h.

6.31 If the wind speed is 40–50 km/h, it is called a) fresh breeze, b) moderate gale, c) strong breeze.

6.32 If the wind speed is 125 km/h, it is called a) gale, b) hurricane, c) violent storm.

6.33 Calculate gust factor of the wind that has a gust speed of 25 m/s in wind having a mean hourly speed of 18 m/s.

Gliding and Unpowered Flights

7.1 Introduction

An unpowered flight may be caused by various reasons. The aircraft itself may not have any propulsive device such as in gliders or sailplanes. It may also arise when an aircraft runs out of fuel, or when one or more engines have become inoperative due to certain reasons. Engine failure is a serious matter and most of present-day aircraft are designed to take into account this eventuality by incorporating special design features for safe landing.

The word *glide* means to fly without power. In the case of gliders starting from the ground, the initial pull to a desired airspeed may be provided by a winch, which is a cylindrical drum enveloped by a long flexible rope over its circumference. One end of the rope is attached to the hook at the nose of the glider, which is standing at a far distance from the winch. When the winch rotates, the rope continuously pulls the glider to a desired airspeed until it has acquired sufficient altitude. Thereafter, the process of gliding starts as soon as the pilot releases the rope and the glider is left on its own to fly without power.

Equations of motion of gliding flight are formulated here and analytical solutions are obtained for different flight parameters. The theoretical analysis is extended to optimize the gliding flight for the best range as well as for the best endurance. The cases of constant-lift coefficient glide (constant glide angle) and constant-airspeed glide are of interest here.

Gliding as a hobby or sport is fairly common. Most of the professional glider pilots aim for soaring. The phenomenon of soaring is discussed at the end of this chapter.

7.2 Equations of Motion

The gliding flight starts soon after the pilot has released the rope after the glider has attained suitable height. The unpowered aircraft does not have now any external agency to push it forward. The forward force is provided by the component of the aircraft weight acting in the direction of flight. The aircraft generally descends during a gliding flight, which is assumed here to be in the vertical plane. The flight path at any instant of time is inclined below the horizontal line as shown in Fig. 7.1. The climb is possible only in ascending air currents, or in zoom where the kinetic energy of the aircraft motion is temporarily utilized for climbing.

The angle between flight path and horizontal line will be referred to as the gliding angle γ . This definition is just the same as for the climb angle, except for the fact that the gliding angle is negative when the climb angle is considered positive. In practice the gliding angle is sufficiently small so that $\sin \gamma = \gamma$ (radians) and $\cos \gamma = 1$. Referring to Fig. 7.1, let W be the weight of aircraft, L and D be the lift and drag forces, V be the forward airspeed along the flight path, and x be the horizontal distance traveled by the aircraft in time t during the gliding flight.

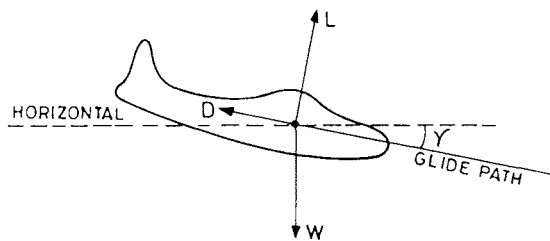


Fig. 7.1 Forces on unpowered aircraft.

Resolving the forces acting on the aircraft along the flight path and normal to it, respectively, the following two equations of motion for a steady glide are obtained,

$$D + W\gamma = 0 \quad (7.1)$$

and

$$L - W = 0 \quad (7.2)$$

In addition, the following two kinematic relations are

$$\frac{dx}{dt} = V \quad (7.3)$$

and

$$\frac{dh}{dt} = V\gamma \quad (7.4)$$

which express that the rate of change of distances x and h are the components of the ground speed of the aircraft. The weight of the aircraft is considered to remain constant during the glide, giving,

$$\frac{dW}{dt} = 0 \quad (7.5)$$

The above Eqs. (7.1–7.5) are the basic equations of a gliding or unpowered flight.

7.3 Gliding Flight Parameters

The gliding flight parameters of interest are the gliding angle, rate of descent, time taken, and the horizontal distance covered during the gliding flight. These parameters are obtained here in terms of the aircraft design parameters.

7.3.1 Gliding Angle and Rate of Descent

The gliding angle is obtained from Eqs. (7.1) and (7.2) as

$$\gamma = -D/W = -D/L = -1/E \quad (7.6)$$

where $E (= L/D)$ is the aerodynamics efficiency of the aircraft. The magnitude of the gliding angle is the inverse of the aerodynamic efficiency. Since E is a positive quantity, the gliding angle becomes negative, which is in accordance with our sign

convention. Introducing the nondimensional lift and drag coefficients, C_L and C_D , defined, respectively, as

$$C_L = \frac{2L}{\rho V^2 S} = \frac{2(W/S)}{\rho_{SSL}\sigma V^2} \quad \text{and} \quad C_D = \frac{2D}{\rho_{SSL}\sigma V^2 S} \quad (7.7)$$

where S is the wing planform area, ρ is the density of air, $\sigma = \rho/\rho_{SSL}$, and the subscript SSL refers to standard atmosphere sea level condition. The lift and drag coefficients are related by the parabolic drag polar,

$$C_D = C_{D_0} + K C_L^2 \quad (7.8)$$

where C_{D_0} is the zero-lift drag coefficient. The quantity K is the lift-dependent drag coefficient factor, which can be obtained from the relation

$$K = 1/(\pi A Re) \quad (7.9)$$

provided the aspect ratio $A R$ of the wing, and the Oswald's span efficiency factor e , are specified. The larger the $A R$ or e , the smaller would be the value of K .

The $1/E$ can be written as $1/E = D/L = C_D/C_L$, which after using Eqs. (7.7) and (7.8) becomes

$$1/E = \rho_{SSL}\sigma V^2 C_{D_0}/\{2(W/S)\} + 2K(W/S)/(\rho_{SSL}\sigma V^2) \quad (7.10)$$

The gliding angle γ in Eq. (7.6) can now be expressed in terms of the aircraft design variables as

$$\gamma = -[\rho_{SSL}\sigma V^2 C_{D_0}/\{2(W/S)\} + 2K(W/S)/(\rho_{SSL}\sigma V^2)] \quad (7.11)$$

The rate of decrease in altitude during descent is called the *rate of descent*, which is denoted by R/D or $-\dot{h}$. A positive value of the rate of descent implies that the rate of climb is negative. That is,

$$R/D = -R/C = -dh/dt = -\dot{h} \quad (7.12)$$

and using Eqs. (7.4) and (7.6), the rate of descent is obtained as

$$-\dot{h} = -V\gamma = V/E \quad (7.13)$$

Substituting the value of γ or $1/E$ in the above relation gives

$$-\dot{h} = \rho_{SSL}\sigma C_{D_0} V^3 / \{2(W/S)\} + 2K(W/S)/(\rho_{SSL}\sigma V) \quad (7.14)$$

which expresses the rate of descent in terms of the aircraft design variables.

7.3.2 Range

The horizontal distance x traveled during the glide is called the range of the gliding flight. It is obtained from the instantaneous range to altitude exchange ratio dx/dh which after using Eqs. (7.3), (7.4), and (7.6) can be written as

$$dx/dh = (dx/dt)/(dh/dt) = V/(V\gamma) = 1/\gamma = -E$$

If x is the range covered when the aircraft loses altitude from h_2 to h_1 , the integration of the above relation gives

$$x = - \int_{h_2}^{h_1} E \, dh \quad (7.15)$$

The right-hand-side integral can be generally evaluated numerically because E of a given aircraft can be obtained from Eq. (7.10) if σ and V are known at different altitudes. However, if either C_L or V is constant during the glide, it is possible to integrate the right-hand side of Eq. (7.15) analytically; these two cases will be discussed here.

7.3.2.1 Range of constant lift coefficient glide. The lift coefficient of the aircraft is kept constant here. It follows from the drag polar Eq. (7.8) that both C_D and E would also be constant, and consequently the gliding angle γ [Eq. (7.6)] would also remain constant. Hence the constant lift coefficient glide is synonymous to the constant angle glide. The range x_{C_L} for constant C_L glide is obtained from Eq. (7.15) as

$$x_{C_L} = -E \int_{h_2}^{h_1} dh = E(h_2 - h_1) \quad (7.16)$$

where the subscript C_L refers to the fact that the lift coefficient is kept constant. The range is thus the product of the aerodynamic efficiency and the loss of height during the glide. The range can be increased by increasing the lift/drag ratio E of the aircraft and the height interval $h_2 - h_1$ of the gliding flight.

7.3.2.2 Range of constant airspeed glide. The airspeed is kept constant during the glide here. Introducing the notations A and B as

$$A = \rho_{SSL} C_{D_0} V^2 / \{2(W/S)\} \quad \text{and} \quad B = 2K(W/S) / (\rho_{SSL} V^2) \quad (7.17)$$

the expression for E obtained from Eq. (7.10) can be written as $E = \sigma / (A\sigma^2 + B)$, where A and B are constant quantities for a given aircraft because V is considered constant during the glide. The range x_V of the constant-airspeed glide is obtained from Eq. (7.15) as

$$x_V = -(1/A) \int_{h_2}^{h_1} \sigma dh / \{\sigma^2 + (B/A)\} \quad (7.18)$$

Since a gliding or unpowered flight usually takes place in the troposphere, the variation of σ with h for standard atmosphere can be written as [Eq. (2.13)],

$$\sigma = e^{-h/\beta}, \quad \beta = 9296 \text{ m} \quad (7.19)$$

Using this value of σ , the right-hand side of Eq. (7.18) can be integrated and the range can be expressed as

$$x_V = \frac{\beta}{B} \left\{ \tan^{-1} \left(\frac{A}{B} e^{-h_1/\beta} \right) - \tan^{-1} \left(\frac{A}{B} e^{-h_2/\beta} \right) \right\}$$

Replacing the notations A and B from Eq. (7.17), the above expression for range becomes

$$x_V = \frac{\beta \rho_{SSL} V^2}{2K(W/S)} \left[\tan^{-1} \left\{ \frac{C_{D_0} \rho_{SSL}^2 V^4 e^{-h_1/\beta}}{4K(W/S)^2} \right\} - \tan^{-1} \left\{ \frac{C_{D_0} \rho_{SSL}^2 V^4 e^{-h_2/\beta}}{4K(W/S)^2} \right\} \right] \quad (7.20)$$

This is the expression for range in terms of the aircraft design parameters for a constant airspeed glide.

7.3.3 Endurance

The time taken during the gliding flight is called the *endurance* of the glide and is denoted by t . The endurance is obtained from the time to altitude exchange ratio dt/dh which can be written as

$$dt/dh = 1/(dh/dt) = 1/(V\gamma) = -E/V \quad (7.21)$$

The endurance of the descent from an altitude h_2 to a lower altitude h_1 is obtained by integrating the above relation as

$$t = - \int_{h_2}^{h_1} (E/V) dh \quad (7.22)$$

In the cases of constant C_L and constant V flights, it is possible to integrate the right-hand side of the above relation analytically as shown below.

7.3.3.1 Endurance of constant lift coefficient glide. The constant C_L implies that E is also constant during the glide. The endurance t_{C_L} of the constant C_L glide can be expressed as

$$t_{C_L} = -E \int_{h_2}^{h_1} dh/V \quad (7.23)$$

The airspeed V is given by $V = \sqrt{2(W/S)/(\rho_{SSL}\sigma C_L)}$, where W/S and C_L are constant quantities during the glide. The endurance given by Eq. (7.23) becomes

$$t_{C_L} = -E [\rho_{SSL} C_L / \{2(W/S)\}]^{1/2} \int_{h_2}^{h_1} \sqrt{\sigma} dh$$

Using Eq. (7.19) the above integral can be integrated and the endurance can be written as

$$t_{C_L} = 2\beta E[\rho_{SSL} C_L / \{2(W/S)\}]^{1/2} (e^{-h_1/2\beta} - e^{-h_2/2\beta}) \quad (7.24)$$

This is the endurance of the glide whose range is given by Eq. (7.16). The endurance increases with the increase in lift/drag ratio E , but it decreases with the increase in wing loading.

7.3.3.2 Endurance of constant airspeed glide. The right-hand side of Eq. (7.22) can be integrated analytically here after putting V outside the integral sign. Since the airspeed is kept constant, the endurance can be directly obtained from Eq. (7.20) by dividing the range by the airspeed, i.e., $t_V = x_V/V$. This gives

$$t_V = \frac{\beta \rho_{SSL} V}{2K(W/S)} \left[\tan^{-1} \left\{ \frac{C_{D_0} \rho_{SSL}^2 V^4 e^{-h_1/\beta}}{4K(W/S)^2} \right\} - \tan^{-1} \left\{ \frac{C_{D_0} \rho_{SSL}^2 V^4 e^{-h_2/\beta}}{4K(W/S)^2} \right\} \right] \quad (7.25)$$

This is the endurance of the glide whose range is given by Eq. (7.20).

7.4 Best- (Maximum-) Range Glides

The best-range glide of a given aircraft gives the maximum range for the specified altitudes h_2 and h_1 of the gliding flight. This mode of flying assumes special importance in the case of an engine failure or fuel starvation. The best range depends on the gliding flight program. The two cases of the glides, constant C_L and constant V , are considered here as in Sec. 7.3.2. The best-range glide parameters will be denoted by the subscript br.

7.4.1 Best Range at Constant Lift Coefficient (Flattest Glide)

The simplification of optimization process for determining the best range of constant C_L glide is provided by Eq. (7.16). This immediately suggests the value of E for optimum range, and consequently the other flight parameters can be deduced.

7.4.1.1 Aerodynamic efficiency and airspeed. Equation (7.16) suggests that the aerodynamic efficiency E_{br,C_L} for the best-range of constant C_L glide will be given by

$$E_{br,C_L} = E_m = 1/(2\sqrt{C_{D_0} K}) \quad (7.26)$$

where E_m is the maximum aerodynamic efficiency. It follows that the lift coefficient, C_{L,br,C_L} , and the drag coefficient, C_{D,br,C_L} , for the best-range glide will be given by

$$C_{L,br,C_L} = C_{L,E_m} = \sqrt{C_{D_0}/K} \quad (7.27)$$

and

$$C_{D,\text{br};C_L} = C_{D,E_m} = 2C_{D_0} \quad (7.28)$$

where the subscript E_m refers to the condition of maximum aerodynamic efficiency. The lift and drag coefficients, and the aerodynamic efficiency, remain constant during the best-range glide.

The airspeed $V_{\text{br};C_L}$ of the best-range glide is similarly obtained as

$$V_{\text{br},C_L} = V_{E_m} = \left\{ \frac{2(W/S)}{\rho_{\text{SSL}}\sigma} \right\}^{1/2} \left(\frac{K}{C_{D_0}} \right)^{1/4} = \frac{V_{E_m,\text{SSL}}}{\sqrt{\sigma}} \quad (7.29)$$

The airspeed decreases as the aircraft approaches the ground because σ is increasing during the descent. The pilot must control the airspeed according to Eq. (7.29) for the best-range glide at constant lift coefficient.

7.4.1.2 Range and endurance. The best range $x_{\text{br};C_L}$ of constant C_L glide for a specified interval $h_2 - h_1$ of the altitude is given by Eq. (7.16) as

$$x_{\text{br};C_L} = E_m(h_2 - h_1) \quad (7.30)$$

The best range increases with the increase in E_m , or with the decrease in C_{D_0} and K , which are design parameters. The decrease in zero-lift drag coefficient C_{D_0} demands that the aircraft must have a more streamlined body, smooth surface, and laminar flow as far as possible with a minimum of flow separation regions over the surface. As seen from Eq. (7.9), the reduction in K requires, that the aspect ratio of the wing and Oswald's span efficiency factor should be large. This explains why gliders have large-span wings with smooth surfaces.

The endurance of the flight $t_{\text{br};C_L}$ is obtained from Eq. (7.24) as

$$t_{\text{br};C_L} = 2\beta E_{\text{br};C_L} [\rho_{\text{SSL}} C_{L,\text{br};C_L} / \{2(W/S)\}]^{1/2} (e^{-h_1/2\beta} - e^{-h_2/2\beta})$$

which after using Eqs. (7.26) and (7.27) can be written as

$$t_{\text{br};C_L} = 2\beta E_m [\rho_{\text{SSL}} / \{2(W/S)\}]^{1/2} (C_{D_0}/K)^{1/4} (e^{-h_1/2\beta} - e^{-h_2/2\beta}) \quad (7.31)$$

This gives the endurance in terms of the aircraft design parameters.

7.4.1.3 Gliding angle and rate of descent. The gliding angle $\gamma_{\text{br};C_L}$ of the best range of the constant C_L glide is obtained from Eqs. (7.6) and (7.26) as

$$\gamma_{\text{br};C_L} = -1/E_{\text{br};C_L} = -1/E_m = -2\sqrt{C_{D_0}K} \quad (7.32)$$

The gliding angle being minimum here, the flight program is also called the *flattest glide*. The rate of descent of the flattest glide is obtained from Eq. (7.13) as $(R/D)_{\text{br};C_L} = (-\dot{h})_{\text{br};C_L} = V_{\text{br};C_L}/E_{\text{br};C_L}$, which after using Eqs. (7.26) and (7.29) becomes

$$(R/D)_{\text{br};C_L} = (-\dot{h})_{\text{br};C_L} = \frac{1}{E_m} \left\{ \frac{2(W/S)}{\rho_{\text{SSL}}\sigma} \right\}^{1/2} \left(\frac{K}{C_{D_0}} \right)^{1/4} = \frac{V_{E_m,\text{SSL}}}{E_m \sqrt{\sigma}} \quad (7.33)$$

The rate of descent of the glider decreases with the decrease in C_{D_0} and K , and also with the decrease in altitude. The rate of descent also decreases with the decrease in wing loading, which explains why gliders are generally lightweight.

7.4.2 Best Range at Constant Airspeed

The airspeed is kept constant here and its value is chosen to yield the best range. The range of constant-airspeed glide is given by Eq. (7.20). The presence of arc tangent function in the equation prohibits obtaining the best-range airspeed in analytic form; it is, of course, possible to use a graphical or numerical method for optimization. The arc tan function can, however, be simplified to facilitate the optimization process for obtaining analytic solutions.

7.4.2.1 Approximation to range, and best-range airspeed. For the sake of brevity, introducing the notations a and b as

$$a = \frac{C_{D_0} \rho_{SSL}^2 e^{-h_1/\beta}}{4K(W/S)^2} \quad \text{and} \quad b = \frac{C_{D_0} \rho_{SSL}^2 e^{-h_2/\beta}}{4K(W/S)^2} \quad (7.34)$$

where a and b are constants for specified altitudes h_1 and h_2 of a given aircraft. The range given by Eq. (7.20) is

$$x_V = [\beta \rho_{SSL} V^2 / \{2K(W/S)\}] \{\tan^{-1}(aV^4) - \tan^{-1}(bV^4)\}$$

which can be written as

$$x_V = [\beta \rho_{SSL} V^2 / \{2K(W/S)\}] \tan^{-1}\{(a - b)V^4 / (1 + abV^8)\} \quad (7.35)$$

It may be noted that in many cases of practical interest, the function $(a - b)V^4 / (1 + abV^8)$ being generally much less than unity, it is possible to write

$$\tan^{-1}\{(a - b)V^4 / (1 + abV^8)\} = (a - b)V^4 / \{(1 + ab)V^8\} \quad (7.36)$$

and Eq. (7.35) becomes

$$x_V = \beta \rho_{SSL} (a - b)V^6 / \{2K(W/S)(1 + abV^8)\}$$

where, except for V , all the other quantities on the right-hand side are constant. It is now much simpler to optimize x_V with respect to V from the above relation. Differentiating the above relation with respect to V , putting $dx_V/dV = 0$, and solving the resulting algebraic equation for $V = V_{br;V}$ yields

$$V_{br;V} = \{3/(ab)\}^{1/8} \quad (7.37)$$

Replacing the notations a and b from Eq. (7.34), the above relation becomes

$$V_{br;V} = (\sqrt{3}K/C_{D_0})^{1/4} \{2(W/S)/\rho_{SSL}\}^{1/2} e^{(h_1+h_2)/8\beta} \quad (7.38)$$

This shows that the best-range airspeed of a given aircraft depends on the average altitude $(h_1 + h_2)/2$ of the descent.

7.4.2.2 Aerodynamic efficiency, range, and endurance. The lift and drag coefficients are obtained from Eqs. (7.7) and (7.8), respectively, as

$$C_{L,\text{br};V} = 2(W/S)/(\rho_{SSL}\sigma V_{\text{br};V}^2) \quad \text{and} \quad C_{D,\text{br};V} = C_{D_0} + KC_{L,\text{br};V}^2$$

which after using Eq. (7.38) can be written as

$$C_{L,\text{br};V} = \left\{ C_{D_0}/(\sqrt{3}K) \right\}^{1/2} e^{h/\beta} \cdot e^{-(h_1+h_2)/4\beta} \quad (7.39)$$

and

$$C_{D,\text{br};V} = C_{D_0} \left\{ 1 + \left(e^{2h/\beta}/\sqrt{3} \right) \cdot e^{-(h_1+h_2)/2\beta} \right\}$$

The aerodynamic efficiency of the best range is obtained as

$$E_{\text{br};V} = C_{L,\text{br};V}/C_{D,\text{br};V}$$

which gives

$$E_{\text{br};V} = 2(3)^{1/4} E_m \left\{ \frac{e^{-(h_1+h_2)/4\beta}}{e^{-h/\beta}\sqrt{3} + e^{h/\beta}e^{-(h_1+h_2)/2\beta}} \right\} \quad (7.40)$$

The best-range $x_{\text{br};V}$ is obtained from Eq. (7.35), which after using Eqs. (7.34) and (7.38) becomes

$$\begin{aligned} x_{\text{br};V} &= 2(3)^{1/4} \beta E_m e^{(h_1+h_2)/4\beta} \\ &\times \tan^{-1} \left[\frac{\sqrt{3}}{4} \left\{ e^{(h_2-h_1)/2\beta} - e^{-(h_2-h_1)/2\beta} \right\} \right] \end{aligned} \quad (7.41)$$

Making use of the fact that the airspeed is kept constant, the endurance is obtained from the relation, $t_{\text{br};V} = X_{\text{br};V}/V_{\text{br};V}$, which gives

$$\begin{aligned} t_{\text{br};V} &= 2(3)^{1/4} \beta E_m \left[\frac{C_{D_0}}{\sqrt{3}K} \right]^{1/4} \left\{ \frac{\rho_{SSL}}{2(W/S)} \right\}^{1/2} e^{(h_1+h_2)/8\beta} \\ &\times \tan^{-1} \left[\frac{\sqrt{3}}{4} \left\{ e^{(h_2-h_1)/2\beta} - e^{-(h_2-h_1)/2\beta} \right\} \right] \end{aligned} \quad (7.42)$$

Equations (7.41) and (7.42), respectively, give the range and endurance of the best-range glide at constant airspeed in terms of the aircraft design parameters.

7.4.2.3 Gliding angle and rate of descent. The gliding angle, $\gamma_{\text{br};V}$, and the rate of descent, $\dot{h}_{\text{br};V}$, for the best range at constant airspeed are obtained from Eqs. (7.6) and (7.13), respectively, as $\gamma_{\text{br};V} = -1/E_{\text{br};V}$, and $-\dot{h}_{\text{br};V} = V_{\text{br};V}/E_{\text{br};V}$, which after using Eqs. (7.38) and (7.40) can, respectively, be expressed as

$$\gamma_{\text{br};V} = - \left\{ \frac{e^{-h/\beta}\sqrt{3} + e^{h/\beta} \cdot e^{-(h_1+h_2)/2\beta}}{2(3)^{1/4} E_m e^{-(h_1+h_2)/4\beta}} \right\} \quad (7.43)$$

and

$$\begin{aligned} -\dot{h}_{br;V} &= \left\{ \frac{e^{-h/\beta} \sqrt{3} + e^{h/\beta} \cdot e^{-(h_1+h_2)/2\beta}}{2(3)^{1/4} E_m} \right\} \\ &\times \left(\frac{\sqrt{3} K}{C_{D_0}} \right)^{1/4} \left(\frac{2(W/S)}{\rho_{SSL}} \right)^{1/2} e^{3(h_1+h_2)/8\beta} \end{aligned} \quad (7.44)$$

Equations (7.43) and (7.44) express the gliding angle and rate of descent of the best-range glide at constant airspeed in terms of the aircraft design parameters.

7.4.3 Comparison of Best-Range Glides

The performance characteristics of the best-range constant lift coefficient glide will now be compared here with the best-range constant airspeed glide of a given aircraft. Comparison of the best ranges obtained from Eqs. (7.41) and (7.30) gives

$$\frac{X_{br;V}}{X_{br;C_L}} = \frac{2(3)^{1/4} \beta}{h_2 - h_1} e^{(h_1+h_2)/4\beta} \tan^{-1} \left[\frac{\sqrt{3}}{4} \{ e^{(h_2-h_1)/2\beta} - e^{-(h_2-h_1)/2\beta} \} \right] \quad (7.45)$$

and the ratio of their endurance is obtained from Eqs. (7.42) and (7.31) as

$$\frac{t_{br;V}}{t_{br;C_L}} = \frac{(3)^{1/8} e^{(h_1+h_2)/8\beta}}{e^{-h_1/2\beta} - e^{-h_2/2\beta}} \tan^{-1} \left[\frac{\sqrt{3}}{4} \{ e^{(h_2-h_1)/2\beta} - e^{-(h_2-h_1)/2\beta} \} \right] \quad (7.46)$$

The ratio of angles of descents is given by Eqs. (7.43) and (7.32) as

$$\frac{\gamma_{br;V}}{\gamma_{br;C_L}} = \frac{\sqrt{3} e^{-h/\beta} + e^{h/\beta} e^{-(h_1+h_2)/2\beta}}{2(3)^{1/4} e^{-(h_1+h_2)/4\beta}} \quad (7.47)$$

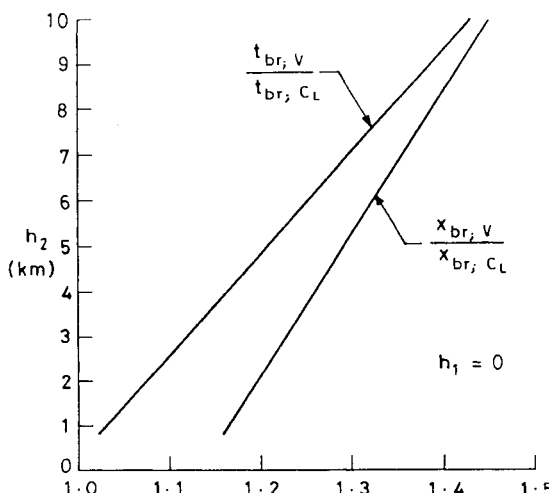


Fig. 7.2 Ratios of best ranges, and of their endurance, in aircraft gliding from different altitudes to sea level.

and the ratio of the rates of descents is obtained from Eq. (7.44) and (7.33) as

$$\frac{(-\dot{h})_{br;V}}{(-\dot{h})_{br;C_L}} = \frac{e^{-h/2\beta} \cdot e^{3(h_1+h_2)/8\beta}}{2(3)^{1/8}} \left\{ \sqrt{3}e^{-h/\beta} + e^{h/\beta} \cdot e^{-(h_1+h_2)/2\beta} \right\} \quad (7.48)$$

It can be seen from the above Eqs. (7.45–7.48) that the ratios of the performance quantities for the best range of a given aircraft depend only on the altitude during the descent.

The above ratios will now be graphically presented by considering the cases of the best-range flights starting from the altitude h_2 to sea level ($h_1 = 0$). Figure 7.2 shows the ratios of the best ranges and of their endurance for flights starting from different altitudes h_2 to sea level. Since the ratio $x_{br;V}/x_{br;C_L}$ is always greater than unity, this implies that the best range of the constant-airspeed glide is greater than the best range of the constant lift coefficient glide. Similarly, for the best range, it can also be seen that the endurance of the constant-airspeed glide is greater than the endurance of the constant lift coefficient glide.

The ratios of gliding angles and of their rates of descents are plotted in Fig. 7.3 for only two cases (10 and 5 km) of h_2 for gliding flights up to sea level ($h_1 = 0$). The figure shows the variations of ratios of gliding angles and the rates of descent during the glide. The gliding angle of the constant-airspeed glide is greater than that of the constant lift coefficient glide. The ratio of rates of descent changes slowly initially but becomes faster when the aircraft approaches the ground.

7.5 Best- (Maximum-) Endurance Glides

The best-endurance glide of a given aircraft is the maximum time taken during a specified loss of height $h_2 - h_1$. The best endurance depends on the program of gliding flight. The two programs of glides, namely, the constant C_L and the

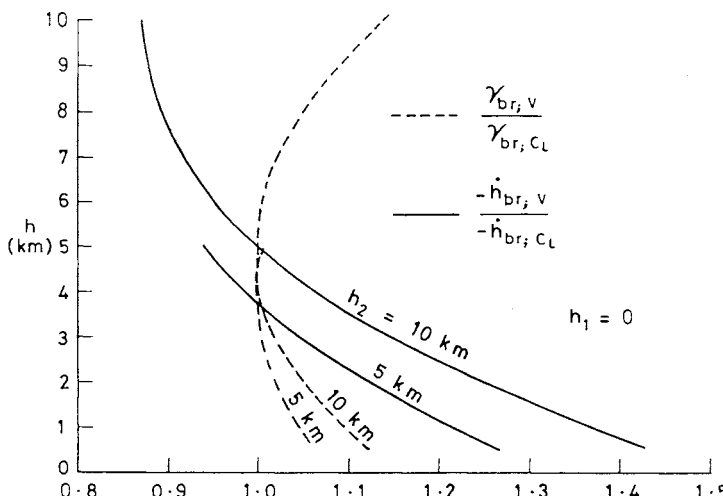


Fig. 7.3 Ratios of gliding angles, and of rates of descent, in the best-range glides from 10- and 5-km altitudes to sea level.

constant V , are considered here. The subscript be is used to denote the condition of best endurance in each case.

7.5.1 Best Endurance at Constant Lift Coefficient

The best endurance, its range, and the associated flight parameters are obtained here for the constant lift coefficient glide. First the lift coefficient is obtained and, thereafter, the other quantities are deduced. The subscript be; C_L denotes the best-endurance condition for constant lift coefficient glide.

7.5.1.1 Lift coefficient, aerodynamic efficiency, and airspeed. Equation (7.24) suggests that the optimum value of t_{C_L} for specified h_1 and h_2 would be obtained by maximizing $E\sqrt{C_L}$ with respect to lift coefficient. This requires that

$$\frac{d}{dC_L}(E\sqrt{C_L}) = \frac{d}{dC_L} \left\{ \frac{C_L^{3/2}}{C_{D_0} + KC_L^2} \right\} = 0 \quad \text{for } C_L = C_{L,\text{be};C_L}$$

which gives

$$C_{L,\text{be};C_L} = \sqrt{3C_{D_0}/K} \quad (7.49)$$

The drag coefficient and aerodynamic efficiency are given by

$$C_{D,\text{be};C_L} = C_{D_0} + KC_{L,\text{be};C_L}^2 = 4C_{D_0}$$

and

$$E_{\text{be},C_L} = C_{L,\text{be};C_L}/C_{D,\text{be};C_L} = \sqrt{3}E_m/2 \quad (7.50)$$

The airspeed $V_{\text{be};C_L}$ of the flight for best endurance can be found from the relation

$$V_{\text{be};C_L} = \{2(W/S)/(\rho C_{L,\text{be};C_L})\}^{1/2} = \{2(W/S)/(\rho_{SSL}\sigma)\}^{1/2} \{K/(3C_{D_0})\}^{1/4}$$

where $\sigma = e^{-h/\beta}$. This shows that the best-endurance airspeed decreases with the decrease in altitude.

7.5.1.2 Gliding angle and rate of descent. The gliding angle $\gamma_{\text{be};C_L}$ and the rate of descent $-\dot{h}_{\text{be};C_L}$ are obtained from Eqs. (7.6) and (7.13), respectively, as

$$\gamma_{\text{be};C_L} = -1/E_{\text{be};C_L} = -2/(\sqrt{3}E_m) = -1.155/E_m \quad (7.51)$$

and

$$\dot{h}_{\text{be};C_L} = -V_{\text{be};C_L} \gamma_{\text{be};C_L} = \frac{2}{\sqrt{3}E_m} \left\{ \frac{2(W/S)}{\rho_{SSL}\sigma} \right\}^{1/2} \left(\frac{K}{C_{D_0}} \right)^{1/4} \quad (7.52)$$

The angle of descent remains constant during the glide because it is a constant C_L (i.e., constant E) glide. The rate of descent decreases as the aircraft approaches the ground.

7.5.1.3 Range and endurance. The range $x_{\text{be};C_L}$ of the best endurance at constant lift coefficient glide is obtained from Eq. (7.16) as

$$x_{\text{be};C_L} = E_{\text{be};C_L}(h_2 - h_1) = \sqrt{3}E_m(h_2 - h_1)/2 \quad (7.53)$$

The best endurance of the glide is obtained from Eq. (7.24) as

$$t_{\text{be};C_L} = 2\beta E_{\text{be};C_L} [\rho_{\text{SSL}} C_{L,\text{be};C_L}/(2(W/S))]^{1/2} (e^{-h_1/2\beta} - e^{-h_2/2\beta})$$

which after using Eqs. (7.49) and (7.50) can be written as

$$t_{\text{be};C_L} = \sqrt{3}\beta E_m \{\rho_{\text{SSL}}/(2W/S)\}^{1/2} (3C_{D_0}/K)^{1/4} (e^{-h_1/2\beta} - e^{-h_2/2\beta}) \quad (7.54)$$

It can be seen that the gliding flight parameters, range and endurance, as given by Eqs. (7.49–7.54) can also be obtained by optimizing (minimizing) the rate of descent, $-\dot{h}$ of Eq. (7.14) with respect to airspeed.

7.5.2 Best Endurance at Constant Airspeed

It is required here to find the particular constant airspeed of an aircraft that will yield the best (maximum) endurance while the aircraft is gliding from specified altitude h_2 to h_1 . Endurance of a constant-airspeed glide is given by Eq. (7.25) as

$$t_V = [\beta\rho_{\text{SSL}}V/(2K(W/S))] \tan^{-1} \{(a - b)V^4/(1 + abV^8)\} \quad (7.55)$$

where the constants a and b are given by the relations of Eq. (7.34). The t_V will be optimized here with respect to airspeed and the corresponding flight parameters, range and endurance, will be obtained. The subscript $\text{be}; V$ is used to denote the condition of best-endurance glide at constant airspeed.

7.5.2.1 Approximation to endurance and best-endurance airspeed. Making use of the simplification provided by Eq. (7.36), the expression for endurance [Eq. (7.55)] can be written as

$$t_V = \beta\rho_{\text{SSL}}(a - b)V^5/(2K(W/S)(1 + abV^8))$$

where, except V , all the other quantities on the right-hand side are constant. Differentiating the above relation with respect to V , putting $dt_V/dV = 0$, and solving the resulting equation gives

$$V_{\text{be};V} = \{5/(3ab)\}^{1/8}$$

which after using Eq. (7.34) can be written as

$$V_{\text{be};V} = (5/3)^{1/8} \{2(W/S)/\rho_{\text{SSL}}\}^{1/2} (K/C_{D_0})^{1/4} e^{(h_1+h_2)/8\beta} \quad (7.56)$$

This shows that the best-endurance airspeed, like the best-range airspeed at constant V , also depends on the average altitude $(h_1 + h_2)/2$ of the descent.

7.5.2.2 Aerodynamic efficiency, gliding angle, and rate of descent. The lift and drag coefficients are obtained from Eqs. (7.7) and (7.8), respectively, as

$$C_{L,\text{be};V} = 2(W/S)/(\rho_{SSL}\sigma V_{\text{be};V}^2) \quad \text{and} \quad C_{D,\text{be};V} = C_{D_0} + KC_{L,\text{be};V}^2$$

which after using Eq. (7.56) can be written as

$$C_{L,\text{be};V} = (3/5)^{1/4}(C_{D_0}/K)^{1/2}e^{h/\beta}e^{-(h_1+h_2)/4\beta} \quad (7.57)$$

and

$$C_{D,\text{be};V} = C_{D_0}\left\{1 + (3/5)^{1/2}e^{2h/\beta}e^{-(h_1+h_2)/2\beta}\right\}$$

The aerodynamic efficiency of the best endurance is obtained from the relation, $E_{\text{be};V} = C_{L,\text{be};V}/C_{D,\text{be};V}$, which gives

$$E_{\text{be};V} = \frac{2(3/5)^{1/4}E_m e^{-(h_1+h_2)/4\beta}}{e^{-h/\beta} + (3/5)^{1/2}e^{h/\beta}e^{-(h_1+h_2)/2\beta}} \quad (7.58)$$

The gliding angle $\gamma_{\text{be};V}$ and the rate of descent $-\dot{h}_{\text{be};V}$ are obtained from Eqs. (7.6) and (7.13), respectively, as

$$\gamma_{\text{be};V} = -1/E_{\text{be};V} \quad \text{and} \quad -\dot{h}_{\text{be};V} = V_{\text{be};V}/E_{\text{be};V}$$

which, after using Eqs. (7.58) and (7.56), give, respectively,

$$\gamma_{\text{be};V} = -\frac{e^{-h/\beta} + (3/5)^{1/2}e^{h/\beta}e^{-(h_1+h_2)/2\beta}}{2(3/5)^{1/4}E_m e^{-(h_1+h_2)/4\beta}} \quad (7.59)$$

and

$$\begin{aligned} -\dot{h}_{\text{be};V} &= \frac{(5/3)^{3/8}}{2E_m} \left\{ \frac{2(W/S)}{\rho_{SSL}} \right\}^{1/2} \left(\frac{K}{C_{D_0}} \right)^{1/4} e^{3(h_1+h_2)/8\beta} \\ &\times \left\{ e^{-h/\beta} + (3/5)^{1/2}e^{h/\beta}e^{-(h_1+h_2)/2\beta} \right\} \end{aligned} \quad (7.60)$$

The above relations (7.57–7.60) show that the lift coefficient, aerodynamic efficiency, gliding angle, and the rate of descent vary during the gliding flight.

7.5.2.3 Range and endurance. The range of the best-endurance flight is obtained from Eq. (7.35) by putting $V = V_{\text{be};V}$. This gives

$$\begin{aligned} x_{\text{be};V} &= 2(5/3)^{1/4}\beta E_m e^{(h_1+h_2)/4\beta} \\ &\times \tan^{-1} \left[(\sqrt{15}/8) \left\{ e^{(h_2-h_1)/2\beta} - e^{-(h_2-h_1)/2\beta} \right\} \right] \end{aligned} \quad (7.61)$$

The best endurance of the constant-airspeed glide is obtained from $t_{be;V} = x_{be;V} / V_{be;V}$, which gives

$$\begin{aligned} t_{be;V} &= 2(5/3)^{1/8} \beta E_m \{\rho_{SSL}/(2W/S)\}^{1/2} (C_{D_0}/K)^{1/4} e^{(h_1+h_2)/8\beta} \\ &\times \tan^{-1} [(\sqrt{15}/8) \{e^{(h_2-h_1)/2\beta} - e^{-(h_2-h_1)/2\beta}\}] \end{aligned} \quad (7.62)$$

Equations (7.61) and (7.62) predict the range and endurance, respectively, of the best-endurance glide at constant airspeed in terms of the aircraft design parameters.

7.5.3 Comparison of Best-Endurance Glides

The constant lift coefficient and the constant-airspeed glides of a given aircraft will now be compared here for their best endurance. The ratio of best endurance obtained from Eqs. (7.54) and (7.62) gives

$$\begin{aligned} \frac{t_{be;V}}{t_{be;C_L}} &= \frac{2(5)^{1/8}}{(3)^{7/8}} \cdot \frac{e^{(h_1+h_2)/8\beta}}{(e^{-h_1/2\beta} - e^{-h_2/2\beta})} \\ &\times \tan^{-1} \left[\left(\frac{\sqrt{15}}{8} \right) \{e^{(h_2-h_1)/2\beta} - e^{-(h_2-h_1)/2\beta}\} \right] \end{aligned} \quad (7.63)$$

and the ratio of their corresponding ranges can be found from Eqs. (7.53) and (7.61) as

$$\frac{x_{be;V}}{x_{be;C_L}} = \frac{4(5)^{1/4}\beta}{(3)^{3/4}} \cdot \frac{e^{(h_1+h_2)/4\beta}}{h_2 - h_1} \tan^{-1} \left[\left(\frac{\sqrt{15}}{8} \right) \{e^{(h_2-h_1)/2\beta} - e^{-(h_2-h_1)/2\beta}\} \right] \quad (7.64)$$

The ratio of angles of descent of the two best endurance glides is given by Eqs. (7.51) and (7.59) as

$$\frac{\gamma_{be;V}}{\gamma_{be;C_L}} = \frac{(15)^{1/4}}{4} [e^{-h/\beta} + (3/5)^{1/2} e^{h/\beta} e^{-(h_1+h_2)/2\beta}] e^{(h_1+h_2)/4\beta} \quad (7.65)$$

and the ratio of their rates of descent is obtained from Eqs. (7.52) and (7.60) as

$$\frac{-\dot{h}_{be;V}}{-\dot{h}_{be;C_L}} = \frac{(5)^{3/8}(3)^{1/8}}{4} e^{-h/2\beta} e^{3(h_1+h_2)/8\beta} [e^{-h/\beta} + (3/5)^{1/2} e^{h/\beta} e^{-(h_1+h_2)/2\beta}] \quad (7.66)$$

The different ratios of performance quantities of a given aircraft, as given by Eqs. (7.63–7.66), depend only on the altitudes during the descent.

Consider the cases of a given aircraft for glides starting from an altitude h_2 to sea level ($h_1 = 0$). The ratios of best endurance and of their corresponding ranges, for flights starting from different altitudes h_2 to sea level, are shown in Fig. 7.4. The ratio $t_{be;V} / t_{be;C_L}$ is greater than unity at higher altitudes, whereas at the lower altitudes it is less than unity. This suggests that for taking greater advantage of the constant-airspeed glide over that of the constant lift coefficient glide, it is better to

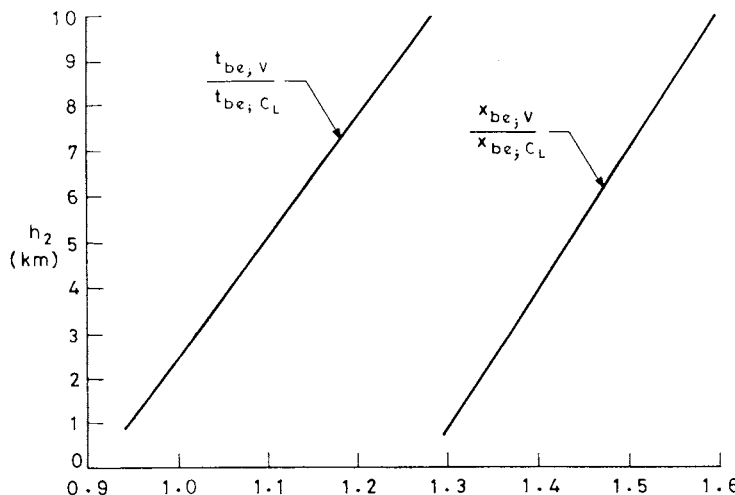


Fig. 7.4 Ratios of best endurance, and of their ranges, in aircraft gliding from different altitudes to sea level.

start gliding from higher altitudes. The range $x_{be;v}$ of the constant airspeed glide is always greater than the range $x_{be;C_L}$ of the constant lift coefficient glide.

The gliding angle of a constant-airspeed glide varies during the flight whereas that of the constant lift coefficient glide remains constant. Their ratio $\gamma_{be;v}/\gamma_{be;C_L}$ is plotted in Fig. 7.5 for the two cases (10 and 5 km) of h_2 for gliding to sea level ($h_1 = 0$). The gliding angle $\gamma_{be;v}$ is generally less than $\gamma_{be;C_L}$, except for altitudes above about 9 km. The rates of descent of both constant-airspeed glides and constant lift coefficient glides vary during the glide. Their ratio $-\dot{h}_{be;v}/-\dot{h}_{be;C_L}$ is also plotted in Fig. 7.5 for the same two cases (10 and 5 km) of h_2 for the flights to

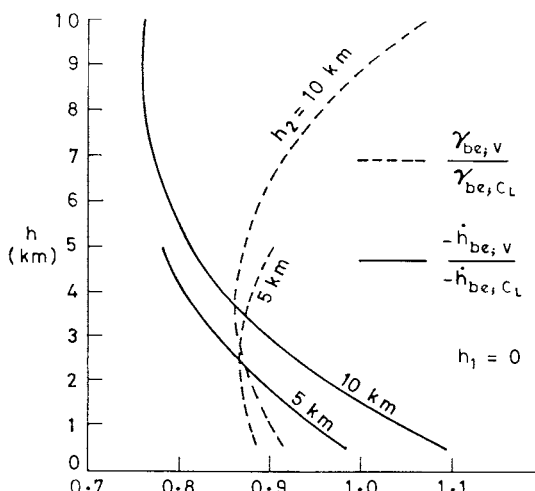


Fig. 7.5 Ratios of gliding angles, and of rates of descent, in the best-endurance glides from 10- and 5-km altitudes to sea level.

sea level. The ratio of rates of descent changes slowly initially but becomes faster as the aircraft approaches the ground.

7.6 Soaring

To *soar* means to fly aloft, to rise to a great height, or to glide in a rising current. Soaring is quite common among gliders and sailplanes. Some light powered aircraft also attempt at soaring. Soaring is also a sport where one attempts to achieve the maximum climb, maximum range, or maximum endurance. Birds have known how to soar for millennia, whereas man has learned soaring only comparatively recently. Dhawan¹ has studied and summarized the application of the basic principles of incompressible aerodynamics to the flapping and gliding flight of birds. The principles of soaring, and the locations where it is customarily practiced, are explained below.

7.6.1 Principle of Soaring

Soaring is possible basically because of rising air currents in the atmosphere. These currents superimpose the vertical velocity v , as shown in Fig. 7.6. The resultant velocity V_R and the corresponding angle of attack α_R become, respectively,

$$V_R = \sqrt{V^2 + v^2} \quad \text{and} \quad \alpha_R = \alpha + \tan^{-1} \frac{v}{V}$$

Since $V_R > V$, and $\alpha_R > \alpha$, the rising air currents increase both the airspeed and the angle of attack. The increase in angle of attack increases both the lift and the lift coefficient, and so the aircraft can be made to climb higher. The gliding can also be made flatter, which increases the range and endurance. This explains why experienced soaring pilots are always in search of rising air currents that are usually found in thermals, clouds, and uphill winds.

7.6.2 Soaring in Thermals

The most widely used rising air currents for soaring are those due to thermal effects. These air currents are called *thermals*. The differential solar heating of terrains creates thermals, as explained in Chapter 2. For thermals to exist, it is necessary that the local air mass over the Earth be unstable and relatively warmer than the surrounding air. It is not essential that the atmospheric air be hot because it is possible to have good thermals even in severe winter weather.

Dry ground or dry fields are better sources of thermals than moist areas and forests. Hard, concrete, black surfaces, buildings, metallic tops of buildings, rocks, and hills are still better for generating thermals. Water surfaces may also act as thermals because during cold days the water may be warmer than the surrounding

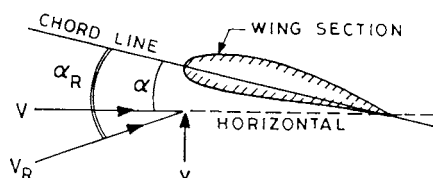


Fig. 7.6 Principle of soaring.

land; the thermal activity is further helped by the water vapor, which makes the air lighter. Strong surface winds hamper thermal activity because of mixing of cold air with the warmer air of the thermal, and the tendency for an air mass to remain only for a short duration over the hot spot on the Earth. However, certain protected areas during strong winds, like the leeward side of a hill, may have thermals, called *wind shadow thermals*. It has been explained² that the air masses at the tops of hills or mountains are frequently better sources of thermals due to instability, whereas simultaneously the air may be stable at the lower levels.

The strongest lift to an aircraft can be found in the central regions of thermals. Therefore, it is advisable to make tighter turns around the central region inside thermals for obtaining the maximum lift. The details of flow structure inside thermals have been studied² by meteorologists, aerodynamics specialists, and soaring pilots.

Nature sometimes helps directly to indicate the areas where the soaring pilot should approach to find thermals. A swirling wind in a field of growing crops, at the top of trees, or in dust devils is indicative of the existence of a thermal. Some of these thermals may be too small and of too short duration for a soaring pilot to circle inside. Rising columns of smoke, dust, or haze also indicate the position of thermals. The soaring of birds can also be a good guide in locating thermals.

Soaring should not be attempted when the pilot is just a few hundred feet above the Earth, because some thermals have severe turbulence and the pilot may not have sufficient height and time to control his aircraft in an adverse situation.

7.6.3 Soaring in Clouds

Vertical air currents exist inside clouds that can be used for soaring. Clouds are formed by the lifting up of warm moist air. A cloud continues to move and develop upward as long as the vertical air currents supply moisture and energy to it. The vertical air currents inside the cloud are further increased by the condensation process, which releases heat inside the cloud. It should be remembered that all clouds do not have air currents sufficient for soaring. The most sought-after cloud for soaring is the growing cumulus cloud. Once the cumulus cloud has grown to a cumulonimbus cloud, it becomes dangerous to continue flying inside it. The cumulonimbus cloud may become a weather hazard as explained in Chapter 19. Some pilots have developed instincts that tell them at a glance whether a cloud is growing or dissipating.

7.6.4 Soaring in Upslope Winds

When air strikes a hill, mountain, or ridge, the upslope motion of air may have a sufficient vertical component of velocity to qualify for calling it vertical air current. An experienced glider pilot can use such an air current by soaring inside it and yet keep a safe distance away from the hill. If the uphill side is facing the sun, the rise of air due to heating may further augment the vertical currents. Piggott³ prescribes advice on how soaring conditions may be used by powered light aircraft as well as by gliders.

References

¹Dhawan, S., *Bird Flight, Sadhana (Indian Academy of Sciences)*, Vol. 16, Pt. 4, Dec. 1991, pp. 275–352.

²Cagle, M. W., and Halpine, C. G., *A Pilot's Meteorology*, 3rd ed., Van Nostrand Reinhold, 1970.

³Piggott, D., *Understanding Flying Weather*, A&C Black, London, 1988.

Problems

Major specifications of two different unpowered aircraft that are used in the problems of this chapter are presented in the table below.

Major specifications of aircraft 1 and 2

Specifications	Aircraft 1 (glider)	Aircraft 2 (unpowered aircraft)
Total weight, N	3920	12,470
Wing area, m ²	15	16.20
C_{D_0}	0.015	0.020
K	0.03	0.059
$C_{L,m}$	1.20	1.45

7.1 Aircraft 1 is gliding at an altitude of 2 km in standard atmosphere with an airspeed of 30 m/s. Find the gliding angle and the rate of descent.

7.2 Solve Problem 7.1 if the aircraft glides at an altitude of 4 km with an airspeed of 30 m/s. Find the change in gliding angle and the rate of descent as compared to that in Problem 7.1.

7.3 Aircraft 1 is gliding at an altitude where the ambient pressure and temperature are 0.76×10^5 N/m² and 2°C, respectively. If the airspeed of the glider is 25 m/s, find the gliding angle and the rate of descent.

7.4 Aircraft 1 is gliding at an angle of 2 deg in standard atmosphere at an altitude of 1.5 km. Find the airspeed, drag, and rate of descent.

7.5 Aircraft 1 is descending at the rate of 1.8 m/s during the glide in standard atmosphere at an altitude of 2 km. Find the airspeed and glide angle.

7.6 Aircraft 2 is gliding at an angle of 3 deg in the atmosphere where the ambient pressure and temperature are 0.7×10^5 N/m² and -2°C, respectively. Find the airspeed, lift/drag ratio, and rate of descent of the aircraft.

7.7 Aircraft 2 is gliding at an altitude of 5 km in standard atmosphere with an airspeed of 180 km/h. Find its gliding angle and rate of descent.

7.8 The weight of aircraft in Problem 7.7 is reduced by 200 kg_f. Find the changes in its gliding angle and rate of descent.

7.9 Find the range and endurance of Aircraft 1 in Problem 7.1 during its gliding flight from an altitude of 2 km to sea level at constant lift coefficient.

7.10 How much will the range and endurance of Aircraft 1 in Problem 7.1 change, while gliding from 2 km to sea level at constant lift coefficient, if the airspeed of the aircraft is increased from 30 to 35 km/h.

7.11 Find the range and endurance of the aircraft in Problem 7.7 if it descends from an altitude of 5 km to sea level at constant gliding angle.

7.12 Find the range and endurance of the aircraft in Problem 7.7 while gliding from 5 km to sea level at constant airspeed.

7.13 Aircraft 1 is gliding at a constant gliding angle of 3 deg while descending from an altitude of 3 km to sea level. Find the range covered and time taken during the glide.

7.14 Find the range and endurance of the aircraft in Problem 7.1 if it is gliding at constant airspeed from an altitude of 2 km to sea level.

7.15 Find the range and endurance of Aircraft 2 in Problem 7.7 if it glides at constant lift coefficient from an altitude of 5 km to sea level.

7.16 The aircraft in Problem 7.7 glides from an altitude of 5 km to sea level with constant-airspeed. Find the range and endurance. Compare these results with those of Problem 7.15.

7.17 Solve Problem 7.13 for Aircraft 2 and compare the results with those of Aircraft 1.

7.18 The design variables of Aircraft 2 are changed to the following: 1) W/S is increased by 10%, 2) C_{D_0} is decreased by 5%, 3) K is decreased by 5%. The aircraft starts gliding from an altitude of 4 km to sea level at an airspeed of 200 km/h. If the gliding angle is kept constant, calculate a) the range and the endurance, and b) the variation of the rate of descent.

7.19 In Problem 7.18 if the airspeed is kept constant during the glide, calculate a) the range and the endurance, and b) the variation of the rate of descent and the gliding angle.

7.20 Aircraft 1 is descending from an altitude of 3 km to sea level at constant lift coefficient. Find the ranges at constant lift coefficients of 0.4, 0.5, 0.6, 0.7, 0.8, and 0.9. Plot this variation of range with lift coefficient and mark the lift coefficient for best range.

7.21 Solve Problem 7.20 for Aircraft 2.

7.22 Aircraft 2 is gliding from an altitude of 6 km to sea level in the standard atmosphere at constant airspeed. Find the ranges if the gliding starts at a constant airspeed of 45, 50, 55, 60, and 65 m/s. Plot the variations of range with airspeed and mark the airspeed for best range.

7.23 Consider that Aircraft 1 starts gliding in standard atmosphere from an altitude of 5 km to sea level at constant lift coefficient. Find the endurance in each of the cases of the constant lift coefficients of 0.4, 0.5, 0.6, 0.7, 0.8, and 0.9. Plot the variation of endurance with lift coefficient and mark the lift coefficient that gives the best endurance.

7.24 Solve Problem 7.23 for Aircraft 2.

7.25 Calculate the endurance of Aircraft 2 in Problem 7.22 at the specified airspeeds. Plot the variations of endurance with airspeed and mark the airspeed for best endurance.

7.26 Calculate the best range and its endurance for Aircraft 1, gliding from an altitude of 4 km to sea level at constant lift coefficient. Also calculate its rate of descent at the start of the glide and at sea level.

7.27 Aircraft 2 glides at constant airspeed. Calculate the best range airspeeds and the best ranges when it glides, a) from 8 km to sea level, b) from 7 to 1 km, and c) from 6 to 2 km.

7.28 In Problem 7.27 also find the endurance and the gliding angles at the top and bottom of the altitudes mentioned in each case.

7.29 Aircraft 1 glides from an altitude of 6 km to sea level at the best-range airspeed. Find the best ranges covered and their endurance in the cases of a) constant C_L glide, and b) constant-airspeed glide. Compare the two glides and find the percentage changes in the best range and its endurance.

7.30 Solve Problem 7.29 for Aircraft 2.

7.31 Aircraft 2 glides from an altitude of 8 km to sea level at the best-endurance airspeed. Find the best endurance and the range at best endurance in the cases of a) constant C_L glide and b) constant-airspeed glide. Compare the two glides and find the percentage changes in the best endurance and its range.

7.32 Solve Problem 7.31 if the aircraft glides from an altitude of 4 km to sea level.

7.33 Solve Problem 7.31 for Aircraft 1, gliding from an altitude of 5 km to sea level.

This page intentionally left blank

Cruising Flights of Turbojet Aircraft

8.1 Introduction

A natural sequence of flight starts from takeoff then climb before the aircraft starts cruising. The sequence in which chapters are presented in this book is not the same as the natural sequence of flight. For the purpose of theoretical analysis, cruising flight is considered here first because it is simpler mathematically, and practically it is the most comfortable and the safest flight.

The meaning of the word *cruise* is explained here and the equations of motion of a cruising flight are obtained. A necessary condition for cruising is deduced and the thrusts required at different airspeeds, altitudes, and weights are established.

Range, fuel consumption, and endurance are the important performance parameters of a cruising flight. There can be different types of cruising flight profiles or programs, each flight yielding different values of the flight parameters. Three different types of cruising flights are discussed here that are practically feasible by a pilot and mathematically amenable to providing analytical solutions.

8.2 Cruise, Cruising Range, and Endurance

The dictionary meaning of the word *cruise* is to fly at a speed economical in terms of fuel, or to wander about seeking something. In practice, the aircraft performs no acceleration, climbing, turning, or any other maneuver during cruising. A cruising flight is a steady-state (unaccelerated), straight, and level (horizontal) flight. Cruising airspeed lies between the maximum and minimum airspeeds of the aircraft at the specified altitude. The cruising flight can be started soon after the completion of the climb phase when the thrust and airspeed corresponding to the climb are changed to the cruising thrust and cruising airspeed. The cruising flight ends when descent, turning, or any other maneuver commences. During the cruise, the lift force is equal to the weight of the aircraft at any instant of time, and similarly the engine thrust balances the drag force. The equations of motion of a cruising flight are thus considerably simple.

The *cruising range* is the horizontal distance x traveled with respect to the surface of the Earth during the cruising flight. The term *range* refers here to the cruising range.

The *endurance* is generally the length of time of the flight during which an aircraft remains airborne. Certain aircraft are often required to undertake special missions where endurance is more important than range. These missions can be patrolling, observation, antisubmarine warfare, loitering. All aircraft are expected to loiter while awaiting clearance for further flight to the destination, or for letdown and landing. This chapter is confined to *cruising endurance*, which is the time taken by the aircraft during the cruising flight. The term *endurance* used here refers to cruising endurance.

8.3 Equations of Motion of Cruising Flight

The forces of lift, drag, weight, and thrust acting on an aircraft in steady, straight, and level flight are shown in Fig. 8.1. *Lift* and *drag* are the aerodynamic forces, denoted by L and D , respectively. The *thrust* is the net propulsive force of the engine, denoted by F , and the weight of aircraft W is the gravitational force. The lift and drag forces act at the center of pressure, and the weight acts at the center of gravity of the aircraft. The lift-weight couple is equal and opposite to the thrust-drag couple. The lines of action of the thrust and drag forces lie very close to each other, so that the moment of this couple is negligible. This means that the lift-weight couple is also negligible, and the center of pressure can be regarded coincident with the center of gravity of the aircraft.

The lift and weight are the equal and opposite forces acting along the vertical line. The condition of equilibrium in the vertical direction gives

$$L - W = 0 \quad (8.1)$$

The thrust line is considered to be the same as the flight path because the angle between them is very small. The thrust and drag forces, therefore, act along the same line but in opposite directions. The condition of equilibrium along the straight flight path in the horizontal plane gives

$$F - D = 0 \quad (8.2)$$

Equations (8.1) and (8.2) assert that the aircraft is in cruising flight.

The aircraft is flying parallel to the ground, which is regarded as horizontal and at rest with respect to the motion of the aircraft. This gives a simple kinematic relation

$$\frac{dx}{dt} = V \quad (8.3)$$

where x is the horizontal distance traveled during the cruise in the time t , and V is the airspeed of the aircraft. The above relation expresses that the rate of change of x -distance is equal to the airspeed of the aircraft. It should be kept in mind that the above Eq. (8.3) is true only for the no-wind component along the flight path.

There is yet another important relation that connects the rate of fuel consumption with thrust. Considering that the reduction in weight of an aircraft is solely due to its fuel consumption, it gives

$$-\frac{dW}{dt} = cF \quad (8.4)$$

where c is the *thrust-specific fuel consumption* (TSFC). Equations (8.1–8.4) are the basic relations of a cruising flight.

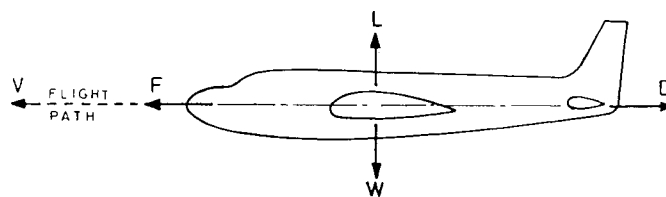


Fig. 8.1 Forces on cruising aircraft.

An important deduction can be made from Eqs. (8.1) and (8.2) that

$$F/W = 1/E \quad (8.5)$$

where $E = L/D$ is the aerodynamic efficiency of the aircraft. This expresses that the thrust per unit weight is the inverse of the aerodynamic efficiency during the cruise.

From the definition of lift coefficient C_L , the airspeed can be expressed as

$$V = \{2(W/S)/(\rho C_L)\}^{1/2} = \{2(W/S)/(\rho_{SSL}\sigma C_L)\}^{1/2} \quad (8.6)$$

where S is the wing planform area, ρ is the density of air, $\sigma = \rho/\rho_{SSL}$, and the subscript SSL denotes standard atmosphere at sea level. It shows that V increases with the increase in wing loading and altitude and with the decrease in lift coefficient. It is one of the most useful relations and is being used occasionally throughout this book.

8.4 Airspeed

In the case of jet engine aircraft, it is possible to express airspeed analytically in terms of its design parameters. Starting from the definition of drag coefficient, the expression for drag force of the aircraft can be written as

$$D = q S C_D$$

where $q = \rho V^2/2$ is the dynamic pressure and C_D is the drag coefficient. Using the parabolic drag polar for C_D , the above relation can be written as

$$D = q S (C_{D_0} + K C_L^2)$$

where C_{D_0} is the zero-lift drag coefficient, $K = 1/(\pi A Re)$ is the lift-dependant drag coefficient factor, AR is the aspect ratio of the wing, and e is Oswald's span efficiency factor. Since $D = F$ and $L = W$, the above relation becomes

$$F = q S C_{D_0} + K W^2 / (q S) \quad (8.7)$$

which after rearrangement can be written as

$$q^2 - \{(F/S)/C_{D_0}\}q + K(W/S)^2/C_{D_0} = 0$$

The above algebraic equation is quadratic in q , whose solution is

$$q = \{(F/S)/(2C_{D_0})\} \{1 \pm \sqrt{1 - 4K C_{D_0} (W/F)^2}\}$$

and noting that $E_m = 1/2\sqrt{K C_{D_0}}$, the above relation can also be written as

$$V = [\{(F/S) \cdot (W/S)/(\rho_{SSL}\sigma C_{D_0})\} \{1 \pm \sqrt{1 - 1/(E_m F/W)^2}\}]^{1/2} \quad (8.8)$$

The above relation expresses airspeed in terms of the design variables of aircraft. It can be seen that the increase in airspeed requires increasing thrust and altitude, reducing the wing area and C_{D_0} . This explains why high-speed aircraft have more powerful engines, fly at higher altitudes, have wings with a lesser aspect ratio, and have smoother surfaces with improved streamline bodies. The existence of the \pm sign in the above relation suggests the possibility of two different airspeeds for cruise at a specified altitude, for a given aircraft and throttle setting.

8.5 Necessary Condition of Flight

A necessary condition for cruising flight can be deduced from Eq. (8.8). Since the right-hand side of Eq. (8.8) must provide real values in practice, it follows that

$$F/W \geq 1/E_m \quad (8.9)$$

which expresses that for cruising flight the thrust/weight ratio must be greater than or equal to the inverse of the maximum aerodynamic efficiency of the aircraft.

In the case $F/W > 1/E_m$, the two real values of V are obtained from Eq. (8.8). The larger of the two values of V is obtained by using the positive sign and it is called the *high-speed solution*. The use of the negative sign gives the smaller value of V , which is referred to as the *low-speed solution*.

In the case $F/W = 1/E_m$, only one value of V is possible, which is the cruising airspeed at its absolute ceiling. Equation (8.9) is the relation among the basic forces of an aircraft establishing the necessary condition of cruising flight.

8.6 Thrust Required and Thrust Available

The thrust required is less than the thrust available from the power plant of an aircraft during cruise. The characteristics of the thrust-required curve are different from the thrust-available curve of a given aircraft. These characteristics are discussed here because they decide the positions of steady equilibrium in cruising flight.

8.6.1 Thrust Required Variation with Airspeed

The thrust required is equal to drag force acting on the aircraft during the cruising flight. The expression for thrust required is obtained in terms of aircraft design parameters from Eq. (8.7) as

$$F(\text{or } D) = \rho V^2 S C_{D_0}/2 + 2KS(W/S)^2/(\rho V^2) \quad (8.10)$$

This relationship shows that the variation of thrust required with airspeed is nonlinear for a given aircraft, as presented in Fig. 8.2. The figure also shows the positions of minimum-thrust (or minimum-drag) airspeed $V_{F_{\min}}$ (or $V_{D_{\min}}$) and the stalling airspeed V_S of the aircraft. Below the stalling airspeed, the continuous-line curve obtained from Eq. (8.10) differs from the dashed line curve, which occurs

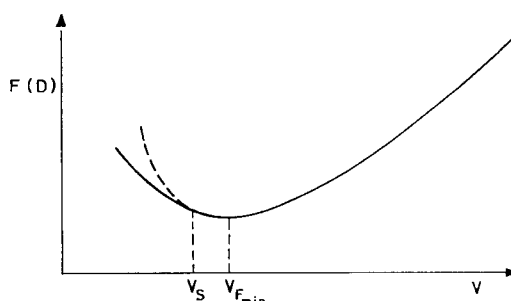


Fig. 8.2 Variation of thrust required (or drag) with airspeed.

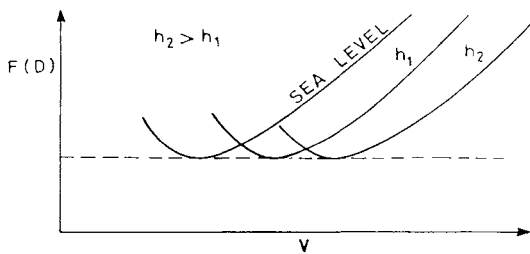


Fig. 8.3 Effect of altitude on thrust required.

in practice. The large increase of thrust required in practice, below the stalling airspeed, is due to large regions of flow separation over the wings. Therefore, high drag penalty is to be paid for flying above the stalling angle. It is generally not advisable to fly above the stalling angle because it may make the aircraft unsteady and uncontrollable.

Equation (8.10) also establishes the effects of altitude, weight, and other design parameters on the thrust-required curve as explained below.

8.6.2 Influence of Altitude and Weight

The thrust-required (or drag) versus airspeed curves of a given aircraft for three different altitudes is shown in Fig. 8.3. The curves shift toward the right with the increase in altitude such that the magnitude of F_{\min} or D_{\min} is not altered in each case. If the curves are plotted against the equivalent airspeed V_e ($= V\sqrt{\sigma}$), they merge into a single curve as shown in Fig. 8.4; this is also indicated by Eq. (8.10). It can be noted from Eq. (8.6) that for cruising flight at constant C_L of a given aircraft, the ratio of airspeeds is $V_1/V_2 = \sqrt{\rho_2/\rho_1}$, where the subscripts 1 and 2 correspond to the two different altitudes.

The effect of variation of the weight of a given aircraft on the thrust-required curve is shown in Fig. 8.5; the same lift coefficient is maintained when the weight of the aircraft is increased from W_1 to W_2 . The curve shifts upward with the increase in weight. It follows from Eq. (8.6) that the airspeed would be proportional to the square root of the weight of aircraft, i.e., $V \propto \sqrt{W}$.

The constant lift coefficient during the flight implies that both C_D and E are also constant. From Eq. (8.5), $F = W/E$, showing that the thrust-required for constant C_L flight is directly proportional to the weight of the aircraft.

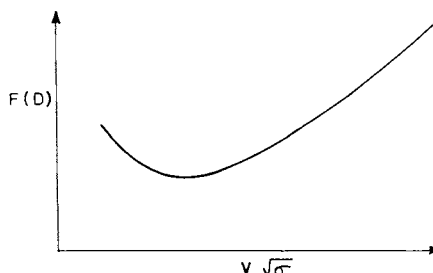


Fig. 8.4 Variation of thrust required with equivalent airspeed.

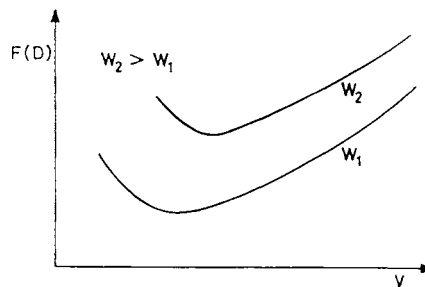


Fig. 8.5 Effect of weight on thrust required.

Equation (8.10) also shows that the thrust required is directly proportional to the zero-lift drag coefficient C_{D_0} , and lift-dependent drag coefficient factor K , which are the aerodynamic design parameters. The reductions in the values of these parameters reduce the thrust required.

8.6.3 Thrust Available and Steady Equilibrium Positions

The net thrust available F_{av} to an aircraft from its engines is generally much more than the thrust-required F during cruise. The characteristics of F_{av} curves with airspeed and altitude are significantly different from the thrust-required curves. Both the F_{av} and F curves can be drawn against airspeed as shown in Fig. 8.6, and the points where they cross or meet each other are the positions of equilibrium for a steady flight.

The thrust available is a function of both altitude and power setting, i.e., $F_{av} = F_{av}(h, \pi)$, where π represents power (or throttle) setting. The two curves, $F_{av}(h, \pi_1)$ and $F_{av}(h, \pi_2)$, of the thrust available for the power settings π_1 and π_2 ($\pi_2 < \pi_1$), respectively, at the same altitude h are shown in Fig. 8.6 against the airspeed. The curve $F_{av}(h, \pi_1)$ is shown by a continuous line and the curve $F_{av}(h, \pi_2)$ is shown by a dashed line. The thrust-available curves are nearly independent of airspeed in the range of airspeeds usually encountered during flight.

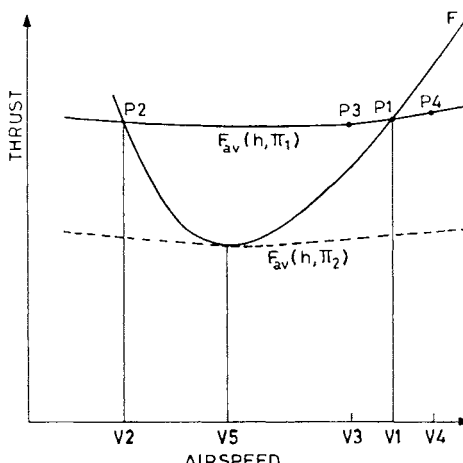


Fig. 8.6 Thrust-available curves and steady equilibrium positions $V1$ and $V2$, or $V5$.

Thus, the F_{av} curve can be raised or lowered at a given altitude by changing the throttle setting. Similarly, the F_{av} curve can also be raised or lowered at a given throttle setting by changing the altitude; raising the altitude would lower the curve and vice versa.

Consider now the $F_{av}(h, \pi_1)$ curve of Fig. (8.6) where the power setting is π_1 at an altitude of h . The figure also shows the thrust-required curve at the same altitude by a continuous line and it crosses the $F_{av}(h, \pi_1)$ curve at the points $P1$ and $P2$ where the airspeeds are $V1$ and $V2$, respectively. These two points are called equilibrium positions because the thrust required here is equal to thrust available and the aircraft can fly in the equilibrium condition at these two points. Therefore, for a given throttle setting and altitude, generally two possible airspeeds, $V1$ and $V2$, exist at which cruising flight is possible. The values of these two airspeeds are obtained from Eq. (8.8); the airspeed $V1$ is the high-speed solution and $V2$ is the low-speed solution.

The nature of static equilibrium at points $P1$ and $P2$ can now be examined. Consider first the position $P1$ where the airspeed is $V1$. If $V1$ is decreased to $V3$ at position $P3$, the thrust required is less than the thrust available, which will cause the aircraft to accelerate until the airspeed $V1$ is reached; a similar situation arises when the airspeed is reduced to any value between $V1$ and $V2$. If the aircraft is moved to point $P4$ by increasing the airspeed from $V1$ to $V4$, the thrust required more than the thrust available, which will cause the aircraft to decelerate until the airspeed $V1$ is reached. Therefore, the aircraft at $P1$ is in statically stable equilibrium condition. Similarly, the equilibrium condition at station $P2$ can be examined and it can be seen that, if the airspeed $V2$ is increased or decreased, in both cases the aircraft will move away from the position $P2$. Therefore, position $P2$ is in a statically unstable equilibrium condition.

It should be kept in mind that the airspeeds $V1$ and $V2$ may not always be achieved in practice. This is because $V1$ may be higher than the drag rise airspeed due to compressibility and $V2$ may be lower than the stalling airspeed of the aircraft. The two airspeeds can be brought closer either by reducing the throttle or increasing the altitude. If the thrust-available curve, as shown by the dashed line in Fig. 8.6, just touches the thrust-required curve, there is only one possible equilibrium position $P5$ where the airspeed is $V5$. The altitude at which this occurs is called the *ceiling altitude* for that power setting. The concept of ceiling altitudes is discussed further in Chapter 10.

8.7 Range and Its Flight Parameters

The basic expression for range of a cruising flight is in integral form. The integral can be solved analytically under certain conditions that give rise to different flight profiles or programs. The ranges attained by three such flight programs, and the associated flight parameters in each case, are presented here.

8.7.1 Basic Integral Relation for Range

The horizontal distance covered by an aircraft during cruise depends on the amount of fuel consumed by the power plant during the cruising flight. If a relationship of the range increment dx due to the fuel consumption $-dW$ or dW_f can be established, the expression for range x can be obtained. This relationship is provided by dividing Eq. (8.3) by the equal terms of Eq. (8.4), which gives

$$dx/(-dW) = V/(cD) \quad (8.11)$$

The left-hand-side quantity ($-dx/dW$) is the exchange ratio between the range and fuel at any specified point or time in the flight path. This is also referred to as *instantaneous range* or *specific range* because it gives the range covered for unit consumption of fuel. It may be kilometers per kilogram of fuel; this is analogous to the concept of mileage of an automobile or aircraft. Cruising performance determines the range covered for a given amount of fuel consumed, or vice versa. It also obtains the values of flight parameters during the cruise. The range is established by integrating the point performance equation (8.11) over the interval between the specified initial and the final points of the cruise. This gives

$$x = - \int_1^2 \{V/(cD)\} dW$$

where the numbers 1 and 2 in the integral sign represent the initial and the final points, respectively, of the cruise. The thrust-specific fuel consumption (TSFC) c will be considered constant during the cruise. Therefore,

$$x = -\frac{1}{c} \int_1^2 (V/D) dW \quad (8.12)$$

Noting that $1/D = (L/D)/W = (C_L/C_D)/W$, the above equation for range becomes

$$x = -\frac{1}{c} \int_1^2 V(C_L/C_D) dW/W \quad (8.13)$$

and if Eq. (8.6) is used for V , the above equation is

$$x = -\frac{1}{c} \int_1^2 \{2W/(\rho S C_L)\}^{1/2} (C_L/C_D) dW/W \quad (8.14)$$

The above three equations [(8.12–8.14)] are just different forms for expressing the range with c being a constant.

8.7.2 Different Flight Programs

The integrals in Eqs. (8.12–8.14) depend on the altitude, airspeed, lift coefficient, and weight of the aircraft. If any two of these parameters are kept fixed and express the third parameter as a function of weight of the aircraft, it would be possible to integrate these integrals and obtain analytical expression for range. This leads to different flight programs depending on the parameters that are being kept constant during the flight. Like that of Hale,¹ the three flight programs considered here are 1) constant altitude–constant lift coefficient flight; this is referred to as constant $h-C_L$ flight; 2) constant airspeed–constant lift coefficient flight; this is referred to as constant $V-C_L$ flight; and 3) constant altitude–constant airspeed flight; this is referred to as constant $h-V$ flight, or sometimes called hard altitude–hard airspeed flight.

In the first two flight programs the lift coefficient C_L is kept constant, but a pilot usually does not fly in practice with such a flight program. Although these two flight programs appear to be of academic interest, they provide excellent

examples for showing the influence of flight program on the range and other flight parameters. The third flight program has much practical application for general aviation pilots. These different flight programs are now discussed in detail in the following three subsections when the aircraft loses weight due to fuel consumption only during the cruise.

8.7.3 Range and Flight Parameters of Constant Altitude–Constant Lift Coefficient Flight

The altitude and lift coefficient are kept constant here during the cruising flight. That is, $h = h_1$, and $C_L = C_{L,1}$, throughout the cruise, where the subscript 1 represents initial condition at the start of the cruise. The subscript 2 represents the condition at the end of the cruise. The other flight parameters like the thrust and airspeed may vary during the cruise as guided by the flight program. Since C_L is constant throughout the cruise, it follows that the drag coefficient C_D , and the aerodynamic efficiency E , would also remain constant, because the drag polar (C_D vs C_L curve) of an aircraft is a single-valued function of the lift coefficient. If x_{h-C_L} denotes the range of the constant h - C_L flight program, Eq. (8.14) can be written as

$$x_{h-C_L} = -\frac{1}{c}\sqrt{2C_{L,1}/(\rho_1 S)}(1/C_{D,1}) \int_1^2 dW/\sqrt{W}$$

The integral on the right-hand side of the above equation can be evaluated to give the range

$$x_{h-C_L} = \frac{2}{c}\sqrt{2W_1/(\rho_1 S C_{L,1})}(C_{L,1}/C_{D,1})(1 - \sqrt{W_2/W_1}) \quad (8.15)$$

and since $V_1 = \sqrt{2W_1/(\rho_1 S C_{L,1})}$ and $E_1 = C_{L,1}/C_{D,1}$, the above equation becomes

$$x_{h-C_L} = (2E_1 V_1/c)(1 - \sqrt{W_2/W_1}) \quad (8.16)$$

If ΔW_f is the weight of fuel consumed during the cruise, $\Delta W_f = W_1 - W_2$. Defining the cruise/fuel weight fraction ζ as

$$\zeta = \Delta W_f / W_1 \quad (8.17)$$

the ratio of weights W_2/W_1 can be expressed as

$$W_2/W_1 = \{W_1 - (\Delta W_f)\}/W_1 = 1 - \Delta W_f/W_1 = 1 - \zeta \quad (8.18)$$

where $\zeta = 0$ at the start of the cruise, representing the initial condition. Equation (8.16) can be written as

$$x_{h-C_L} = 2E_1 V_1(1 - \sqrt{1 - \zeta})/c \quad (8.19)$$

This equation can also predict the cruise-fuel weight fraction ζ or the weight of the fuel consumed ΔW_f , for a specified range x_{h-C_L} of the given aircraft. The

factor $E_1 V_1/c$ is called the *range factor* of the turbojet aircraft where the ratio V_1/c is the *propulsive efficiency* of the aircraft. Therefore, the range factor is the product of aerodynamic and propulsive efficiencies of the aircraft. It can be seen from the above equation that the range increases with the increase in E_1 , V_1 , and ΔW_f . The range also increases with the decrease in c .

The variations in flight parameters like V , F , and W during the flight can also now be obtained. From Eqs. (8.6) and (8.18),

$$V/V_1 = \sqrt{W/W_1} = \sqrt{1-\zeta} \quad (8.20)$$

where V and W are the airspeed and weight of the aircraft, respectively, at the end of the cruise; the end point of the cruise is regarded as a variable point by dropping the subscript 2. Since $F = D = \rho V^2 S C_D / 2$, the constant h - C_L flight gives

$$F/F_1 = D/D_1 = V^2/V_1^2 = 1 - \zeta \quad (8.21)$$

Equations (8.20) and (8.21) present the variations of flight parameters during the cruise as a function of the cruise-fuel weight fraction ζ . These variations are shown in Fig. 8.7. The topmost curve is a horizontal line arising due to the flight specifications. The variations of F/F_1 and W/W_1 against ζ are linear, whereas the variation of V/V_1 is nonlinear.

This flight program has the drawback that it requires continuous reduction of the airspeed by adjusting throttle setting during the flight. The air traffic regulations also do not permit change in the airspeed since they require constant airspeed with an accuracy of within ± 18.52 km/h (10 kn).

8.7.4 Range and Flight Parameters of Constant Airspeed–Constant Lift Coefficient Flight

The airspeed and lift coefficient are kept constant here during the cruising flight. These constant values are $V = V_1$ and $C_L = C_{L,1}$, where the subscript 1 represents

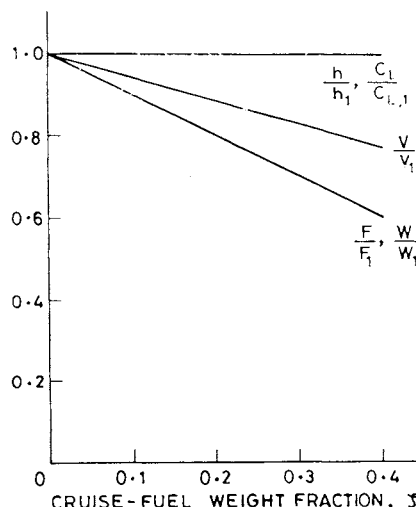


Fig. 8.7 Variations of flight parameters in constant h - C_L flight.

the condition at the start of the cruise. The altitude and thrust may vary during the flight. The constant C_L implies, as in the previous case, that both C_D and E are also constant during the flight. Therefore, the quantities V , C_L , and C_D can be taken out of the integral sign of Eq. (8.13), which gives

$$x_{V-C_L} = -(V_1/c)(C_{L,1}/C_{D,1}) \int_1^2 dW/W$$

where x_{V-C_L} denotes the cruising range of the constant V - C_L flight, and the limits of integration 1 and 2 correspond to the start and the end of the cruise, respectively. Integrating the right-hand-side integral, the above equation becomes

$$x_{V-C_L} = (V_1/c)(C_{L,1}/C_{D,1}) \ln(W_1/W_2) \quad (8.22)$$

Introducing the cruise-fuel weight fraction ζ , the above equation becomes

$$x_{V-C_L} = (E_1 V_1/c) \ln\{1/(1 - \zeta)\} \quad (8.23)$$

This is commonly called Breguet's range formula. The variables that influence the range of constant V - C_L flight are the same as for the constant h - C_L flight. Equation (8.23) can also predict the cruise-fuel weight fraction ζ , or the amount of fuel consumed ΔW_f , during the cruise if the range x_{V-C_L} is specified.

The factor EV/c is the range factor, which can also be expressed as WV/\dot{W}_f , where \dot{W}_f is the fuel flow rate; the latter expression for the range factor is commonly used during flight tests (Chapter 18) of a cruising flight, because it can be obtained from the measurements during the test.

The flight parameters of the program can now be obtained as a function of ζ . Writing as before,

$$W/W_1 = 1 - \zeta, \quad D = \rho V^2 S C_D / 2, \quad \text{and} \quad V = \sqrt{2(W/S)/(\rho C_L)} \quad (8.24)$$

the following relations are obtained:

$$F/F_1 = D/D_1 = \rho/\rho_1 = W/W_1 = 1 - \zeta \quad (8.25)$$

which represent the flight parameters as a function of ζ .

The constant V - C_L flight implies, from the last relationship of Eq. (8.24), that the ratio W/ρ is also constant. Since W decreases due to fuel consumption, ρ must also decrease and h must increase during the flight. Therefore, the constant V - C_L flight is also referred to as *cruise-climb flight*. The increase in altitude is small, however, which is usually neglected in the performance analysis. The increase in altitude can be calculated from Eq. (2.13),

$$\rho/\rho_{SSL} = \epsilon e^{-(h-h^*)/\beta}$$

where the values of ϵ , h^* and β depend whether the flight is performed in the troposphere ($h \leq 11$ km) or in the stratosphere. Using the above equation, the ratio ρ/ρ_1 can be found from

$$\rho/\rho_1 = (\rho/\rho_{SSL})/(\rho_1/\rho_{SSL}) = e^{-(h-h_1)/\beta} \quad (8.26)$$

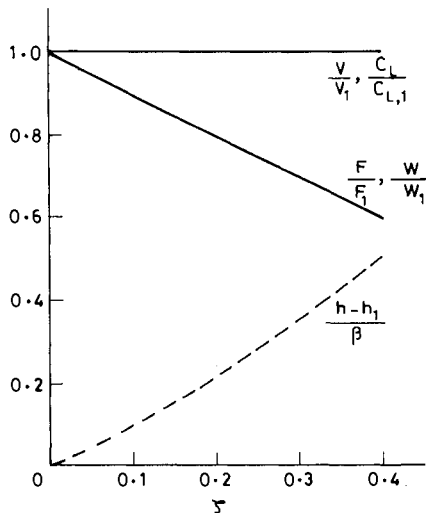


Fig. 8.8 Variations of flight parameters in constant $V \cdot C_L$ flight.

for the cases where both h ($h > h_1$) and h_1 lie either in the troposphere or in the stratosphere. Equating the expressions for ρ/ρ_1 from Eqs. (8.25) and (8.26) gives

$$(h - h_1)/\beta = -l_n(1 - \zeta) \quad (8.27)$$

If h_1 lies in the troposphere and h is in the stratosphere, the increase in altitude is obtained by using the above equation twice—first in the troposphere with $h = 11,000$ m, then in the stratosphere with $h_1 = 11,000$ m.

The flight parameters given by Eq. (8.25) and the increase in altitude obtained from Eq. (8.27) are plotted against ζ in Fig. 8.8. The thrust and weight decrease linearly with ζ , whereas the increase in altitude is nonlinear.

8.7.5 Range and Flight Parameters of Constant Altitude—Constant Airspeed Flight

The constant h - V flight program is commonly operated by the pilots of long-range transport aircraft. Here the altitude and airspeed are kept constant during the cruise. Since the altitude h is constant, the density ρ would also be regarded as constant. The constant values are V_1 and ρ_1 that exist at the start of the cruise. The lift and drag coefficients, aerodynamic efficiency, and thrust required would vary during the cruise. The range x_{h-V} covered between the stations 1 and 2 of the constant h - V flight can be obtained from Eq. (8.13) as

$$x_{h-V} = -(V_1/c) \int_1^2 (C_L/C_D) dW/W \quad (8.28)$$

For the sake of brevity, the notation a_1 is introduced as

$$a_1 = K/(q_1^2 S^2 C_{D_0}) \quad \text{where} \quad q_1 = \rho_1 V_1^2/2 \quad (8.29)$$

and the ratio C_L/C_D is written as

$$C_L/C_D = C_L/(C_{D_0} + KC_L^2) = W/\{q_1 SC_{D_0}(1 + a_1 W^2)\}$$

where both q_1 and a_1 are constants during the flight. Equation (8.28) can now be written as

$$x_{h-v} = -\{V_1/(cq_1 SC_{D_0})\} \int_1^2 dW/(1 + a_1 W^2) \quad (8.30)$$

which after integrating the right-hand side can be expressed as

$$x_{h-v} = \{V_1/(cq_1 SC_{D_0}\sqrt{a_1})\} \{\tan^{-1}(\sqrt{a_1}W_1) - \tan^{-1}(\sqrt{a_1}W_2)\} \quad (8.31)$$

If ν_1 and ν_2 are defined as

$$\tan \nu_1 = \sqrt{a_1}W_1 \quad \text{and} \quad \tan \nu_2 = \sqrt{a_1}W_2 \quad (8.32)$$

Eq. (8.31) becomes

$$x_{h-v} = V_1(\nu_1 - \nu_2)/(cq_1 SC_{D_0}\sqrt{a_1})$$

Noting that $\nu_1 - \nu_2 = \tan^{-1} \tan(\nu_1 - \nu_2)$, the above relation can be written as

$$x_{h-v} = \{V_1/(cq_1 SC_{D_0}\sqrt{a_1})\} \tan^{-1} \{(\tan \nu_1 - \tan \nu_2)/(1 + \tan \nu_1 \tan \nu_2)\}$$

which after using the relations of Eq. (8.32) becomes

$$x_{h-v} = \{V_1/(cq_1 SC_{D_0}\sqrt{a_1})\} \tan^{-1} \{\sqrt{a_1}(W_1 - W_2)/(1 + a_1 W_1 W_2)\}$$

Replacing the notation a_1 from Eq. (8.29), the above equation becomes

$$x_{h-v} = \frac{V_1}{c\sqrt{KC_{D_0}}} \tan^{-1} \left\{ \frac{q_1 S \sqrt{KC_{D_0}}(W_1 - W_2)}{q_1^2 S^2 C_{D_0} + K W_1 W_2} \right\} \quad (8.33)$$

Since $C_{L,1} = W_1/(q_1 S)$, and $\sqrt{KC_{D_0}} = 1/(2E_m)$, Eq. (8.33) can also be written as

$$x_{h-v} = \frac{2V_1 E_m}{c} \tan^{-1} \left[\frac{C_{L,1}(1 - W_2/W_1)}{2E_m \{C_{D_0} + KC_{L,1}^2(W_2/W_1)\}} \right] \quad (8.34)$$

Station 2 can be regarded as a variable point by dropping the subscript 2. Using the relations

$$E_1 = C_{L,1}/C_{D,1}, \quad C_{D,1} = C_{D_0} + KC_{L,1}^2 \quad \text{and} \quad W_2/W_1 = W/W_1 = 1 - \zeta$$

Eq. (8.34) becomes

$$x_{h-v} = (2V_1 E_m/c) \tan^{-1} [E_1 \zeta / \{2E_m(1 - KE_1 C_{L,1} \zeta)\}] \quad (8.35)$$

This expresses the range of the constant h - V flight in terms of the aircraft design parameters. If the range x_{h-V} is specified, the above equation can also predict the cruise-fuel weight fraction ζ , or the amount of fuel consumed, ΔW_f , during the cruise.

The flight parameters C_L , E , and F (or D), vary during the cruise and they can also now be obtained. Since $V = V_1$, it follows that $\sqrt{2W/(\rho SC_L)} = \sqrt{2W_1/(\rho_1 SC_{L,1})}$, which gives

$$C_L/C_{L,1} = W/W_1 = 1 - \zeta \quad (8.36)$$

The ratio of aerodynamic efficiencies can be expressed as

$$E/E_1 = (C_L/C_D)/(C_{L,1}/C_{D,1}) = (C_L/C_{L,1})C_{D,1}/C_D$$

which after using Eq. (8.36) can be written as

$$E/E_1 = (1 - \zeta)C_{D,1}/C_D \quad (8.37)$$

From the drag polar of the aircraft, the ratio $C_{D,1}/C_D$ can be written as

$$C_{D,1}/C_D = C_{D,1}/(C_{D_0} + KC_L^2)$$

which after using Eq. (8.36) becomes

$$C_{D,1}/C_D = C_{D,1}/\{C_{D_0} + K(1 - \zeta)^2 C_{L,1}^2\} = 1/\{1 + \zeta(\zeta - 2)KE_1C_{L,1}\} \quad (8.38)$$

Therefore, Eq. (8.37) can be written as

$$E/E_1 = (1 - \zeta)/\{1 + \zeta(\zeta - 2)KE_1C_{L,1}\} \quad (8.39)$$

The thrust is given by $F = D = C_D q S$, where $q = q_1$ is a constant. It follows that

$$F/F_1 = D/D_1 = C_D/C_{D,1}$$

which after using Eq. (8.38) becomes

$$F/F_1 = D/D_1 = 1 + \zeta(\zeta - 2)KE_1C_{L,1} \quad (8.40)$$

where $\zeta = \zeta_1 = 0$, at the start of the cruise.

The present flight program, unlike the previous two flight programs, does not depend on ζ only. It depends both on ζ and the product $KE_1C_{L,1}$. Considering an aircraft having $KE_1C_{L,1} = 0.3$, the nonlinear variations of E/E_1 and F/F_1 against ζ are plotted in Fig. 8.9. The thrust required diminishes during the flight and can be monitored either manually or by a combination of altitude and airspeed (or Mach number) hold modes applied by the pilot. The horizontal line in the figure is due to flight specification that h and V remain constant. The variations of $C_L/C_{L,1}$ and W/W_1 against ζ are linear and follow the same straight line.

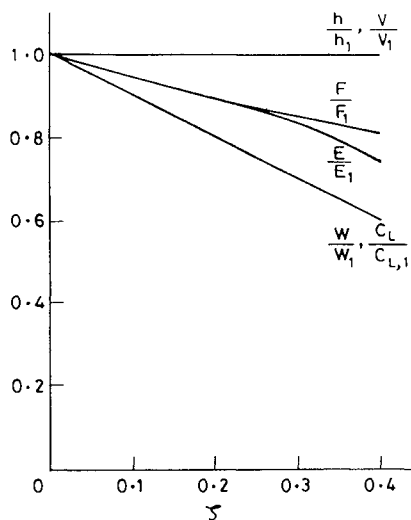


Fig. 8.9 Variations of flight parameters in constant h - V flight.

8.8 Endurance of Cruising Flight

Endurance here is the time taken during the cruising flight. A basic integral equation for the endurance would be deduced and the endurance of the three different flight programs, mentioned above, would be obtained.

8.8.1 Basic Integral Equation and Specified Flight Programs

The basic governing equation for yielding the endurance is obtained by inverting the fuel consumption Eq. (8.4) as

$$-dt/dW = 1/(cD) = E/(cW) \quad (8.41)$$

The left-hand-side term $-dt/dW$ is the instantaneous endurance giving the exchange ratio between the time and fuel consumption; it is the time during which the aircraft will remain airborne in cruise for a unit consumption of fuel. Integration of the above equation gives

$$t = -\frac{1}{c} \int_1^2 E \, dW/W \quad (8.42)$$

where t is the endurance of the cruising flight between stations 1 and 2. The integral on the right-hand side of Eq. (8.42) can be evaluated analytically in the cases of constant h - C_L , constant V - C_L , and constant h - V flights. It can be noted that constant h - C_L and constant V - C_L flights will yield the same endurance because the constant C_L implies that E is also constant which can be taken out of the integral sign, leaving the same integral in both the cases. Therefore, only constant C_L and constant h - V flights are considered here.

8.8.2 Endurance of Constant Lift Coefficient Flight

A constant lift coefficient during the flight implies that both C_D and E are constant during the flight. This flight program includes both constant $h\text{-}C_L$ and constant $V\text{-}C_L$ flights, because their endurance would be the same. Equation (8.42) in this case can be written as

$$t_{C_L} = -(E_1/c) \int_1^2 dW/W \quad (8.43)$$

where t_{C_L} denotes the endurance of the constant C_L flight between stations 1 and 2. The aerodynamic efficiency $E = E_1$ is constant during the flight. Integration of the right-hand side of the above equation gives $t_{C_L} = (E_1/c) \ln(W_1/W_2)$. Since $W_2/W_1 = 1 - \zeta$, the endurance can also be written as

$$t_{C_L} = (E_1/c) \ln\{1/(1 - \zeta)\} \quad (8.44)$$

This equation could also have been directly obtained from Eq. (8.23) by dividing $x_{V\text{-}C_L}$ by V_1 because the airspeed is kept constant in the constant $V\text{-}C_L$ flight. It can be seen that for a given cruise-fuel weight fraction ζ , the endurance can be increased by increasing the aerodynamic efficiency and by decreasing the thrust-specific fuel consumption.

8.8.3 Endurance of Constant Altitude–Constant Airspeed Flight

The aerodynamic efficiency E does not remain constant in this case. This gives rise to the same integral that exists in Eq. (8.28) and therefore the procedure of its evaluation would be just the same. However, making use of the fact that the airspeed V_1 is constant during the flight, the endurance $t_{h\text{-}V}$ can be easily obtained by dividing the range $X_{h\text{-}V}$ [Eq. (8.35)] by V_1 . This gives

$$t_{h\text{-}V} = (2E_m/c) \tan^{-1}[E_1\zeta/\{2E_m(1 - KE_1C_{L,1}\zeta)\}] \quad (8.45)$$

which expresses the endurance of the constant $h\text{-}V$ flight in terms of the aircraft design parameters.

8.9 Engine-Inoperative Cruise

In the event of one or more engines becoming inoperative, the maximum range at the optimum altitude is less than that for all engine operation. The drag of the aircraft increases due to 1) additional drag of the inoperative engine and 2) the engine failure may require flying the aircraft with an unclean configuration. This means that the aerodynamic efficiency L/D of the aircraft will be lower than it would be with all engines operating.

The engine-inoperative aircraft has a different drag polar, which should be used for finding range and other flight parameters by the same formulas that have been developed for all engine operation.

The thrust required per engine becomes higher in the event of engine failure or other radical loss of thrust in cruise. A descent to a lower altitude and an adjustment in speed is usually necessary. A drift-down procedure to minimize loss of range is usually provided in the pilot's flight manual. The thrust levers on the operating

engines are advanced to obtain maximum continuous thrust and the aircraft is allowed to descend to a specified speed that is compatible with the speed at which the engine-inoperative cruise is flown.

8.10 Application to an Aircraft

Consider a turbojet aircraft whose wing loading is 4000 N/m^2 , TSFC is $0.8/\text{h}$, and whose cruise-fuel weight fraction is 0.3 during its cruising flight. The aspect ratio of its wing is 7.2 and the Oswald's span efficiency factor is 0.85. The zero-lift drag coefficient of the aircraft is 0.016. The aircraft started cruising flight at an altitude of 9 km with an airspeed of 800 km/h. Calculate the lift and drag coefficients, aerodynamic efficiency, thrust/weight ratio, range, and endurance of the flight in standard atmosphere for the cases of constant $h-C_L$, constant $V-C_L$, and constant $h-V$ flights.

The values given here are $W/S = 4000 \text{ N/m}^2$, $c = 0.8/\text{h} = 0.8/3600/\text{s}$, $\zeta = 0.3$, $AR = 7.2$, $e = 0.85$, $C_{D_0} = 0.016$, $V = V_1 = 800 \text{ km/h} = 222.22 \text{ m/s}$, and $h = 9 \text{ km} = 9000 \text{ m}$.

At the altitude of 9 km the value of $\sigma = 0.3813$ as obtained from the standard atmospheric table. The value of the lift-dependent drag coefficient factor K is obtained as

$$K = 1/(\pi AR e) = 1/(3.1416 \times 7.2 \times 0.85) = 0.052$$

The maximum aerodynamic efficiency of the aircraft is $E_m = 1/2\sqrt{KC_{D_0}} = 1/2\sqrt{0.052 \times 0.016} = 17.33$.

1) *Constant h-C_L flight.* The lift and drag coefficients are obtained as

$$C_L = C_{L,1} = \frac{2(W/S)}{\rho_{SSL}\sigma V_1^2} = \frac{2(4000)}{1.225 \times 0.3813 \times (222.22)^2} = 0.3468$$

and

$$C_D = C_{D,1} = C_{D_0} + KC_L^2 = 0.016 + 0.052(0.3468)^2 = 0.0222$$

The aerodynamic efficiency is given by $E = E_1 = C_L/C_D = 0.3468/0.0222 = 15.62$ and the thrust/weight ratio is obtained from the relation $F/W = 1/E = 1/E_1 = 1/15.62 = 0.0640$.

The range is obtained from Eq. (8.19) as

$$x_{h-C_L} = \frac{2 \times 15.62 \times 222.22}{0.8/3600} (1 - \sqrt{1 - 0.3}) = 5,102,690 \text{ m} = 5103 \text{ km}$$

and the corresponding endurance is given by Eq. (8.44) as

$$t_{h-C_L} = \frac{15.62}{0.8/3600} \ln\left(\frac{1}{1 - 0.3}\right) = 25070.7 \text{ s} = 6.964 \text{ h}$$

2) *Constant V-C_L flight.* The values of C_L , C_D , and E , are the same as in the case of constant $h-C_L$ flight considered above. Since $F/W = 1/E$, the value of

F/W is also the same as that obtained for constant $h\text{-}C_L$ flight. The range is given by Eq. (8.23) as

$$x_{V-C_L} = \frac{15.62 \times 222.22}{0.8/3600} \ln\left(\frac{1}{1 - 0.3}\right) = 5,571,206.9 \text{ m} = 5571.2 \text{ km}$$

and the endurance t_{V-C_L} , would be just the same as that obtained for the constant $h\text{-}C_L$ flight.

3) *Constant h-V flight.* In this case, C_L , C_D , and E vary during the flight. Their initial values would be the same as given in the case of constant $h\text{-}C_L$ flight, i.e., $C_{L,1} = 0.3468$, $C_{D,1} = 0.0222$ and $E_1 = 15.62$. In this case, $KE_1C_{L,1} = 0.052 \times 15.62 \times 0.3468 = 0.2817$. The variations of C_L , C_D , and E during the flight are given by Eqs. (8.36), (8.38) and (8.39), respectively, as

$$C_L = (1 - \zeta)0.3468, \quad C_D = \{1 + \zeta(\zeta - 2)0.2817\}0.0222$$

and

$$E = (1 - \zeta)15.62/\{1 + \zeta(\zeta - 2)0.2817\}$$

The thrust/weight ratio is obtained as

$$F/W = 1/E = \{1 + \zeta(\zeta - 2)0.2817\}/\{(1 - \zeta)15.62\}$$

The range is obtained from Eq. (8.35) as

$$\begin{aligned} x_{h-V} &= \frac{2 \times 222.22 \times 17.33}{0.8/3600} \\ &\times \tan^{-1} \left\{ \frac{15.62 \times 0.3}{2 \times 17.33(1 - 0.052 \times 0.3468 \times 15.62 \times 0.3)} \right\} \\ &= 5,081,760 \text{ m} = 5081.76 \text{ km} \end{aligned}$$

and the endurance is given by

$$t_{h-V} = x_{h-V}/V = 5081.76/800 \text{ h} = 6.352 \text{ h}$$

The results of the above calculations can be summarized by the following table.

Flight	C_L	C_D	E	F/W	x, km	t, h
Constant $h\text{-}C_L$	0.347	0.022	15.6	0.064	5103	6.96
Constant $V\text{-}C_L$	0.347	0.022	15.6	0.064	5571	6.96
Constant $h\text{-}V$	0.347*	0.022*	15.6*	0.064*	5082	6.35

The values marked (*) are only at the start of the cruise. It can be clearly seen that the constant $V\text{-}C_L$ flight gives the longest range among the three different flight programs calculated above.

Reference

¹Hale, F. J., *Aircraft Performance, Selection, and Design*, Wiley, New York, 1984.

Problems

Major specifications of three different turbojet aircraft are presented below; they are used in many problems in this chapter and Chapters 9–11.

Major specifications of turbojet aircraft A, B, and C

Specifications	Aircraft A (jet trainer)	Aircraft B (executive)	Aircraft C (long-range)
Total weight, N	12,500	66,750	2,700,000
Maximum fuel, N	3,200	24,500	1,000,000
Wing area, m ²	6.12	21.5	475
Maximum thrust, N	2,600	26,250	800,000
C_{D_0}	0.032	0.026	0.017
K	0.10	0.084	0.042
M_{dr}	0.72	0.82	0.85
$C_{L,m}$	1.22	1.32	2.2
c , N/h/N	1.18	0.95	0.8

In the multiple choice problems below, mark the correct answer.

- 8.1** Cruising flight consists of a) unaccelerated, straight, and horizontal flight with no bank or yaw, b) steady, straight, horizontal, and accelerated flight, c) accelerated and horizontal flight.
- 8.2** The thrust required during cruise is a) more than the thrust available, b) equal to the thrust available, c) less than the thrust available.
- 8.3** In a constant lift coefficient flight program a) both C_D and E remain constant, b) only C_D remains constant, c) none of these two is true.
- 8.4** In a constant lift coefficient flight program a) $F \propto W$, b) $F \propto \sqrt{W}$, c) $F \propto 1/W$.
- 8.5** Which of the following flight programs is commonly used by pilots for long-range transport flights: a) constant $h-C_L$, b) constant $V-C_L$, c) constant $h-V$.
- 8.6** The range factor is a) a factor to obtain range from aerodynamic efficiency, b) a factor to obtain range from propulsive efficiency, c) the product of aerodynamic and propulsive efficiencies.

8.7 An aircraft of wing area 140 m^2 is cruising at a lift coefficient of 0.6 and aerodynamic efficiency of 16. Find its lift and drag forces at sea level, 6 km, and 12 km for each of the airspeeds of 200, 400, and 800 km/h.

8.8 If the aircraft of the above problem weighs 686,000 N, find the airspeeds required to cruise at sea level, 6 km, and 12 km.

8.9 For Aircraft A, cruising in standard atmosphere at sea level, obtain the following: a) Estimate the minimum and maximum airspeeds and the associated lift coefficients and aerodynamic efficiencies. Can these airspeeds be physically attained? b) Plot the variation of aerodynamic efficiency with airspeed, and from the plot find the maximum aerodynamic efficiency and the corresponding value of the airspeed. Also obtain E_m theoretically. c) Plot the required thrust/weight ratio, F/W , and the available thrust/weight ratio, F_{av}/W , as functions of the true airspeed of the aircraft in km/h in the same figure. From the plot, obtain the minimum and maximum airspeeds.

8.10 Repeat Problem 8.9 when Aircraft A is flying at an altitude of a) 2 km and b) 4 km.

8.11 Repeat Problem 8.9 for Aircraft B.

8.12 Repeat Problem 8.9 for Aircraft B flying at an altitude of a) 5 km and b) 10 km.

8.13 Repeat Problem 8.9 for Aircraft C.

8.14 Repeat Problem 8.9 for Aircraft C flying at an altitude of a) 6 km and b) 12 km.

8.15 For Aircraft A, plot the following as a function of altitude in the same figure: a) the minimum and maximum airspeeds, b) the stalling airspeed, and c) the drag-rise airspeed.

8.16 Repeat Problem 8.15 for Aircraft B.

8.17 Repeat Problem 8.15 for Aircraft C.

8.18 Aircraft A is flown at a 75% thrust rating with a weight of 1200 kg at a) sea level, and b) an altitude of 4 km. Find the cruising airspeeds in both cases. Give both the high-speed and low-speed solutions. Are these airspeeds realizable in practice?

8.19 Repeat Problem 8.18 for Aircraft C, which is cruising at 80% of its maximum thrust at an altitude of a) 7 km and b) 12 km.

8.20 An aircraft weighing 3000 kg is cruising in standard atmosphere at sea level with an airspeed of 300 km/h. At this airspeed its lift/drag ratio is maximum. Its drag polar is given by $C_D = 0.02 + 0.06C_L^2$. Calculate the total drag on the aircraft.

8.21 Suppose an aircraft encounters a wind disturbance causing the airspeed to increase momentarily. How would the aircraft behave following the disturbance if it is flying at a) the high-speed equilibrium position, and b) the low-speed equilibrium position.

8.22 Aircraft A is cruising at sea level with constant lift coefficient. Its airspeed is 200 km/h at the start of the cruise and it has a cruise-fuel weight of 260 kg_f. Obtain the following: a) The range covered in the cruising flight, b) The specific range at the start and at the end of the cruise, c) The fuel flow rate at the start and at the end of the cruise, d) The amount of fuel consumed when 50% of the cruising range has been covered.

8.23 Repeat Problem 8.22 when Aircraft A is cruising at an altitude of 2 km and at an airspeed of 300 km/h at the start of the cruise. Also find the airspeed at the end of the cruise and the time taken during the cruise.

8.24 Repeat Problem 8.22 when Aircraft A is cruising at an altitude of 4 km and at an airspeed of 400 km/h at the start of the cruise. Also find the airspeed at the end of the cruise and the time taken during the cruise.

8.25 Solve Problem 8.22 when Aircraft A has a constant-lift coefficient and maintains the initial airspeed constant throughout the cruise.

8.26 Solve Problem 8.22 when Aircraft A has started cruising at an initial altitude of 2 km, and maintains a constant airspeed of 300 km/h with constant-lift coefficient. Also find the altitude at the end of the cruise and the time taken during the cruise.

8.27 Solve Problem 8.22 when Aircraft A has started cruising at an initial altitude of 4 km, and maintains a constant airspeed of 400 km/h with constant lift coefficient. Also find the altitude at the end of the cruise and the time taken for the cruise.

8.28 Aircraft B cruises at a constant airspeed of 500 km/h and maintains a constant lift coefficient. It starts cruising at an altitude of 5 km and it has a cruise-fuel weight of 19,000 N. Obtain the following: a) Range covered in the cruising flight, b) Specific range (km/kg_f) at the start and at the end of the cruise, c) Fuel flow rate (kg_f/min) at the start and at the end of the cruise, d) Amounts of fuel consumed (kg_f) when 40%, 60%, and 80% of the cruising ranges have been covered.

8.29 Solve Problem 8.28 if Aircraft B cruises at a constant airspeed of 700 km/h and the cruising has started at an altitude of 10 km. Also find the average climb angle.

8.30 Solve Problem 8.28 when Aircraft B maintains the initial airspeed and altitude as constants.

8.31 Solve Problem 8.28 when Aircraft B cruises at a constant airspeed of 700 km/h at a constant altitude of 10 km.

8.32 Aircraft B cruises at Mach 0.6 at an altitude of 10 km, with a weight of 4600 kg_f and a fuel weight of 1500 kg_f . Answer the following: a) Find the range that can be covered using this fuel for a cruise climb flight. b) If a drop tank of weight 60 kg_f is added to the aircraft, with a capacity of 600 kg_f of fuel, find the additional range that the aircraft can cover. c) If the drop tank is ejected following the consumption of its fuel, find the extra range that can be covered.

8.33 Aircraft C cruises with an airspeed of 700 km/h at an altitude of 12 km for a period of 1 h. Assume maximum aircraft weight and fuel weight. Calculate the range covered, the fuel consumed, and the lift coefficient at the end of the cruise for a constant $h-C_L$ flight.

8.34 Aircraft B starts cruising at an altitude of 5 km and uses a cruise-fuel weight fraction of 0.3. Calculate and plot the variation in range covered with airspeed and from the plot find the airspeed for the maximum range when it is in a) constant $h-V$ flight, b) constant $h-C_L$ flight, and c) cruise climb flight.

8.35 Repeat Problem 8.34, this time plotting the variation of the time spent in cruise with the airspeed, and thereby find the airspeed for the maximum endurance.

8.36 Aircraft B starts cruising at an altitude of 5 km and has to cover a range of 1000 km. Calculate and plot the variation of the fuel spent in cruise with the airspeed and find the airspeed for minimum fuel consumption when the aircraft is in a) constant $h-V$ flight, b) constant $h-C_L$ flight, and c) cruise climb flight.

Optimization of Cruising Flights of Turbojet Aircraft

9.1 Introduction

A cruising flight is usually undertaken at optimum airspeed. This optimum airspeed can be chosen for the purposes of achieving minimum thrust, maximum range, or maximum endurance, and these different cases are considered here. Flight parameters of minimum thrust are obtained here first. Cruising flights are optimized with respect to airspeed for achieving maximum range. Maximum range and the associated flight parameters are discussed here for the same three different flight programs that were undertaken in Chapter 8. Maximum endurance and the flight parameters of the three flights are also discussed.

An aircraft is often subjected to certain restrictions on its airspeed. These restrictions may be due to aerodynamic or structural considerations. Air traffic regulations further restrict airspeed and altitude. The optimization of these constrained flights is also discussed here.

9.2 Minimum-Thrust (or Minimum-Drag) Flight

Flying at the airspeed required by minimum thrust gives a minimum rate of fuel consumption and provides the most economical flight. Since thrust is equal to drag, the minimum thrust F_{\min} is synonymous with the minimum drag D_{\min} , and the performance parameters of minimum thrust required would be just the same as those of minimum drag. The airspeed for minimum thrust is obtained first, which helps one to deduce the values of the other corresponding flight parameters.

9.2.1 Airspeed for Minimum Thrust

The expression for thrust given by Eq. (8.10) of the previous chapter is

$$F = \rho V^2 S C_{D_0} / 2 + 2 K S (W/S)^2 / (\rho V^2) \quad (9.1)$$

The airspeed for minimum thrust is obtained by differentiating the above equation with respect to V and putting $dF/dV = 0$. The resulting algebraic equation is solved for obtaining the minimum-thrust airspeed $V_{F_{\min}}$ as

$$V_{F_{\min}} = \{2(W/S)/(\rho_{SSL} \sigma)\}^{1/2} (K/C_{D_0})^{1/4} = V_{E_m} \quad (9.2)$$

This equation shows that the airspeed for minimum thrust is the same as that required for maximum aerodynamic efficiency. The airspeed increases with the increase in wing loading and altitude. The performance of a given aircraft for minimum thrust depends on whether the altitude or the airspeed is kept constant.

In the case of the altitude being kept constant, $\sigma = \sigma_1$ during minimum-thrust flight and the airspeed $V_{F_{\min},h}$ is obtained from Eq. (9.2) as

$$V_{F_{\min},h} = \{2(W/S)/(\rho_{SSL}\sigma_1)\}^{1/2} (K/C_{D_0})^{1/4} \quad (9.3)$$

This shows that the airspeed decreases with the decrease in weight and altitude of the aircraft during the flight.

In the case of the airspeed being kept constant, $V = V_{F_{\min},V}$, it follows from Eq. (9.2) that $W/\sigma = \text{constant} = W_1/\sigma_1$, and the airspeed is given by

$$V_{F_{\min},V} = \{2(W_1/S)/(\rho_{SSL}\sigma_1)\}^{1/2} (K/C_{D_0})^{1/4} \quad (9.4)$$

This shows that for flights where W/σ is constant, the altitude increases (σ decreases) as the weight of the aircraft decreases during the cruise. Such a flight is, therefore, often referred to as a *cruise-climb flight*. When climb is slow, the flight is regarded as horizontal for theoretical analysis of the cruising flight.

9.2.2 Lift Coefficient and Aerodynamic Efficiency

The lift and drag coefficients, aerodynamic efficiency, and thrust can now also be obtained for the minimum-thrust flight. The lift coefficient for minimum thrust $C_{L,F_{\min}}$ is obtained as

$$C_{L,F_{\min}} = 2(W/S)/(\rho V_{F_{\min}}^2) = 2(W/S)/(\rho_{SSL}\sigma V_{F_{\min}}^2)$$

which, after using Eq. (9.2), becomes

$$C_{L,F_{\min}} = \sqrt{(C_{D_0}/K)} = C_{L,E_m} \quad (9.5)$$

The lift coefficient for minimum thrust is the same as that required for maximum aerodynamic efficiency of the aircraft. The drag coefficient for minimum thrust $C_{D,F_{\min}}$ (or $C_{D,\min}$) is obtained by using the drag polar relation,

$$C_{D,F_{\min}} = C_{D_0} + K C_{L,F_{\min}}^2 = 2C_{D_0} \quad (9.6)$$

The aerodynamic efficiency $E_{F_{\min}}$ for the minimum thrust is given by

$$E_{F_{\min}} = C_{L,F_{\min}}/C_{D,F_{\min}} = 1/(2\sqrt{KC_{D_0}}) = E_m \quad (9.7)$$

Substituting the value of minimum-thrust airspeed [Eq. (9.2)] in Eq. (9.1), the minimum thrust is $F_{\min} = 2W\sqrt{KC_{D_0}} = W/E_m$, which gives the thrust/weight ratio

$$F_{\min}/W = 1/E_m \quad (9.8)$$

Equation (9.8) can also be directly obtained from Eq. (8.5). Thus, the minimum thrust required per unit weight of the aircraft is equal to the inverse of the maximum aerodynamic efficiency of the aircraft.

The minimum-thrust (or minimum-drag) flight parameters of a given aircraft are thus found to be just the same as that required for maximum aerodynamic efficiency.

9.3 Maximum-Range Flights

The maximum-range flight parameters are important to a pilot or a designer for covering a longer distance during cruise for a given amount of fuel consumption. Optimization for maximum range is carried out here for three different flight programs. First, the airspeed for maximum range is established in each case and the corresponding lift coefficient, aerodynamic efficiency, range, and thrust/weight ratio are then obtained. The results are presented analytically, and the contributions of different design and flight variables for achieving the maximum range are calculated. It is not always possible to fly at the maximum-range airspeed as predicted by theory because of aerodynamic or structural constraints, or due to air traffic regulations. Such constrained flights and their optimizations are discussed in the last two subsections of this section.

9.3.1 Maximum Range of Constant Altitude–Constant Lift Coefficient Flight

The range of constant h - C_L flight is given by Eq. (8.19) as

$$x_{h-C_L} = (2E_1 V_1/c)(1 - \sqrt{1 - \zeta}) \quad (9.9)$$

where the thrust-specific fuel consumption c is constant. For a given cruise-fuel weight fraction ζ , the range would be maximum if the product $E_1 V_1$ is maximum. The value of V_1 for which $E_1 V_1$ is maximum is given by

$$d(E_1 V_1)/dV_1 = 0 \quad (9.10)$$

and then solving the resulting equation for V_1 . Noting that

$$E_1 = C_{L,1}/C_{D,1}, \quad C_{D,1} = C_{D_0} + K C_{L,1}^2, \quad \text{and} \quad C_{L,1} = 2(W_1/S)/(\rho_1 V_1^2)$$

the product $E_1 V_1$ can be expressed as

$$E_1 V_1 = \left\{ 2W_1/(\rho_1 S) \right\} \left\{ C_{D_0} V_1 + 4K W_1^2 / (\rho_1^2 S^2 V_1^3) \right\}^{-1}$$

Substituting the above expression of $E_1 V_1$ in Eq. (9.10) and performing the required differentiation yields

$$C_{D_0} - 12K W_1^2 / (\rho_1^2 S^2 V_1^4) = 0 \quad \text{for} \quad V_1 = V_{1mr;h-C_L}$$

where $V_{1mr;h-C_L}$ is the value of V_1 for the maximum range of the constant h - C_L flight. From the above relation, the maximum-range airspeed is obtained as

$$V_{1mr;h-C_L} = \{2(W_1/S)/(\rho_{SSL} \sigma_1)\}^{1/2} (3K/C_{D_0})^{1/4} = 3^{1/4} V_{1E_m} = 1.32 V_{1E_m} \quad (9.11)$$

where V_{1E_m} is the airspeed for maximum aerodynamic efficiency at the start of the cruise. The above relation shows the influence of the various design parameters on the maximum-range airspeed. It can be seen that an aircraft flying at an altitude of about 10 km will have $V_{1mr;h-C_L}$, which is about 72% more than at sea level.

The lift coefficient $C_{L,1\text{mr};h-C_L}$, which is constant during maximum-range flight, is

$$C_{L,\text{mr};h-C_L} = C_{L,1\text{mr};h-C_L} = 2(W_1/S)/(\rho_1 V_{1\text{mr};h-C_L}^2)$$

which after using the value of $V_{1\text{mr};h-C_L}$ becomes

$$C_{L,1\text{mr};h-C_L} = \sqrt{C_{D_0}/(3K)} = C_{L,E_m}/\sqrt{3} \quad (9.12)$$

The drag coefficient for the maximum range is given by

$$C_{D,\text{mr};h-C_L} = C_{D,1\text{mr};h-C_L} = C_{D_0} + K C_{L,1\text{mr};h-C_L}^2$$

which after using Eq. (9.12) becomes

$$C_{D,1\text{mr};h-C_L} = 4C_{D_0}/3 = 2C_{D,E_m}/3 \quad (9.13)$$

The aerodynamic efficiency for the maximum range is given by

$$E_{\text{mr};h-C_L} = E_{1\text{mr};h-C_L} = C_{L,1\text{mr};h-C_L}/C_{D,1\text{mr};h-C_L}$$

which after using Eqs. (9.12) and (9.13) can be written as

$$E_{1\text{mr};h-C_L} = \sqrt{3}/(4\sqrt{KC_{D_0}}) = \sqrt{3}E_m/2 = 0.866E_m \quad (9.14)$$

The maximum range $x_{\text{mr};h-C_L}$ of the constant $h\text{-}C_L$ flight is obtained from Eq. (9.9) as

$$x_{\text{mr};h-C_L} = (2E_{1\text{mr};h-C_L} V_{1\text{mr};h-C_L})(1 - \sqrt{1 - \zeta})/c$$

which after using Eqs. (9.11) and (9.14) can be written as

$$x_{\text{mr};h-C_L} = (3^{3/4} E_m V_{1E_m}/c)(1 - \sqrt{1 - \zeta}) \quad (9.15)$$

where

$$E_m = 1/(2\sqrt{KC_{D_0}})$$

and

$$V_{1E_m} = \{2(W_1/S)/(\rho_{\text{SSL}}\sigma_1)\}^{1/2} (K/C_{D_0})^{1/4}$$

Therefore, Eq. (9.15) becomes

$$x_{\text{mr};h-C_L} = \left(\frac{3\sqrt{3}}{2}\right)^{1/2} \left\{\frac{2(W_1/S)}{\rho_{\text{SSL}}\sigma_1}\right\}^{1/2} \frac{1}{c} \left(\frac{E_m}{C_{D_0}}\right)^{1/2} (1 - \sqrt{1 - \zeta}) \quad (9.16)$$

Equation (9.16) expresses the maximum range of constant $h\text{-}C_L$ flight in terms of aircraft design parameters. Increasing the wing loading W_1/S increases the maximum range, but it should be attempted by reducing the wing planform area S and not by increasing W_1 . This is, first, because the increase in W_1 would decrease

ζ , which reduces the factor $(1 - \sqrt{1 - \zeta})$, thereby reducing the range. Second, the increase in W_1 increases the thrust required for maximum range, as can be seen from Eq. (9.19). The increase in altitude (and thus decrease in σ_1) also increases the maximum range.

The increase in maximum aerodynamic efficiency, or the decrease in K and C_{D_0} , increases the maximum range. Writing $E_m = 1/2\sqrt{KC_{D_0}}$ in Eq. (9.16), it can be seen in the equation that K is raised to the power 1/4, and C_{D_0} is raised to the power 3/4, which is close to unity. Since both C_{D_0} and K are much less than unity, the dependence of maximum range on K is much more effective than the dependence of maximum range on C_{D_0} . This implies that the reduction in K should be emphasized first before attempting to reduce C_{D_0} for increasing the maximum range. The reduction in K is obtained by increasing the aspect ratio of the wing. The reduction in C_{D_0} is achieved by streamlining the aircraft configuration and providing smooth external surfaces.

The airspeed $V_{mr;h-C_L}$ and thrust $F_{mr;h-C_L}$ vary during the cruise according to Eq. (8.21). This gives

$$F_{mr;h-C_L}/F_{1mr;h-C_L} = V_{mr;h-C_L}^2/V_{1mr;h-C_L}^2 = 1 - \zeta \quad (9.17)$$

where $V_{1mr;h-C_L}$ is given by Eq. (9.11), and $F_{1mr;h-C_L}$ is obtained from Eq. (8.5) as

$$F_{1mr;h-C_L}/W_1 = 1/E_{1mr;h-C_L} = 1/(0.866E_m) \quad (9.18)$$

From Eq. (8.5), the thrust per unit weight during the cruise is given by

$$F_{mr;h-C_L}/W = 1/E_{mr;h-C_L} = 1/(0.866E_m) = 1.155/E_m \quad (9.19)$$

Therefore, the thrust $F_{mr;h-C_L}$ varies during the cruise but the thrust per unit weight of the aircraft remains constant.

It is shown in the following subsection that the endurance $t_{mr;h-C_L}$ of constant $h-C_L$ flight is the same as the endurance $t_{mr;V-C_L}$ of constant $V-C_L$ flight.

9.3.2 Maximum Range of Constant Airspeed–Constant Lift Coefficient Flight

The range of the constant $V-C_L$ flight program is given by Eq. (8.23) as

$$x_{V-C_L} = (E_1 V_1/c) \ln\{1/(1 - \zeta)\} \quad (9.20)$$

where the thrust-specific fuel consumption is considered constant. For a given ζ , here also the range is maximum if the product $E_1 V_1$ is maximum. This situation is exactly the same as in Sec. 9.3.1 for constant $h-C_L$ flight. It follows that

$$V_{mr;V-C_L} = V_{1mr;V-C_L} = V_{1mr;h-C_L} = 3^{1/4} V_{1E_m} \quad (9.21)$$

$$C_{L,mr;V-C_L} = C_{L,1mr;V-C_L} = C_{L,1mr;h-C_L} = C_{L,E_m}/\sqrt{3} \quad (9.22)$$

$$C_{D,mr;V-C_L} = C_{D,1mr;V-C_L} = C_{D,1mr;h-C_L} = 2C_{D,E_m}/3$$

and

$$E_{mr;V-C_L} = E_{1mr;V-C_L} = E_{1mr;h-C_L} = \sqrt{3}E_m/2 \quad (9.23)$$

The expression for the maximum range is obtained from Eq. (9.20) as

$$x_{mr; V-C_L} = (E_{1mr; V-C_L} V_{1mr; V-C_L} / c) \ln \{1/(1 - \xi)\} \quad (9.24)$$

which after using Eqs. (9.21) and (9.23) becomes

$$x_{mr; V-C_L} = \{3^{3/4} E_m V_{E_m} / (2c)\} \ln \{1/(1 - \xi)\} \quad (9.25)$$

and using the value of V_{E_m} , it can be written as

$$x_{mr; V-C_L} = \frac{1}{2c} \left(\frac{3\sqrt{3}}{2} \right)^{1/2} \left\{ \frac{2W_1/S}{\rho_{SSL}\sigma_1} \right\}^{1/2} \left(\frac{E_m}{C_{D_0}} \right)^{1/2} \ln \left(\frac{1}{1 - \xi} \right) \quad (9.26)$$

The above relation expresses the maximum range of constant $V-C_L$ flight in terms of its aircraft design parameters. The influence of these parameters is the same as in the case of the maximum range of constant $h-C_L$ flight.

The altitude and thrust vary during constant $V-C_L$ flight. The variation of altitude is given by Eq. (8.27) as

$$(h - h_1)/\beta = - \ln(1 - \xi) \quad (9.27)$$

where both h and h_1 lie in the same atmospheric region, which is either the troposphere or the stratosphere. The thrust varies according to Eq. (8.25) as

$$F_{mr; V-C_L} / F_{1mr; V-C_L} = 1 - \xi \quad (9.28)$$

The thrust variation per unit weight is given by

$$F_{mr; V-C_L} / W = 1/E_{mr; V-C_L} = 2/(\sqrt{3}E_m) \quad (9.29)$$

and since the right-hand side is a constant quantity, the thrust per unit weight of the aircraft remains constant during the flight.

Since the airspeed is constant here, the endurance $t_{mr; V-C_L}$ of maximum-range flight is obtained as

$$t_{mr; V-C_L} = x_{mr; V-C_L} / V_{mr; V-C_L} = (E_{mr; V-C_L} / c) \ln \{1/(1 - \xi)\}$$

which after using Eq. (9.23) becomes

$$t_{mr; V-C_L} = (\sqrt{3}E_m / 2c) \ln \{1/(1 - \xi)\} \quad (9.30)$$

We observed in Chapter 8 that the endurance of constant $h-C_L$ and constant $V-C_L$ flights are the same. Therefore, the endurance $t_{mr; h-C_L}$ for the maximum range of the constant $h-C_L$ flight would be the same as that given by the above relation.

In this section and in Sec. 9.3.1, the maximum-range flight parameters are obtained by differentiating the range with respect to airspeed. However, the same maximum-range conditions can also be obtained¹ by optimizing the instantaneous range by setting $d(-dx/dW)/dV = 0$, and solving the resulting equation for V .

9.3.3 Maximum Range of Constant Altitude–Constant Airspeed Flight

The range is obtained from Eq. (8.35) as

$$x_{h-V} = (2V_1 E_m / c) \tan^{-1} [E_1 \zeta / (2E_m (1 - K E_1 C_{L,1} \zeta))] \quad (9.31)$$

where the thrust-specific fuel consumption is constant; here the subscript 1 represents the condition at the start of the cruise,

$$C_{L,1} = 2(W_1/S) / (\rho V_1^2), \quad E_m = 1 / (2\sqrt{K C_{D_0}}), \quad \zeta = \Delta W_f / W_1 \quad (9.32)$$

and

$$E_1 = \frac{C_{L,1}}{C_{D_0} + K C_{L,1}^2} = \frac{2(W_1/S) / \rho_1 V_1^2}{C_{D_0} + 4K(W_1/S)^2 / \rho_1^2 V_1^4} \quad (9.33)$$

To optimize for the maximum range with respect to airspeed, substitute the values of $C_{L,1}$ and E_1 from Eqs. (9.32) and (9.33) in Eq. (9.31). Thereafter, make $dx_{h-V}/dV_1 = 0$, and solve for V_1 the resulting equation for getting the maximum-range airspeed $V_{1mr,h-V}$. However, this resulting equation cannot be solved in analytic form as it involves the arc tan function.

It is possible to obtain analytic expression for the maximum-range airspeed if it is noted that the function $E_1 \zeta / (2E_m (1 - K E_1 C_{L,1} \zeta))$ is much smaller than unity in many practical cases of cruising flights.² The arc tan function can now be approximated as

$$\tan^{-1} \left\{ \frac{E_1 \zeta}{2E_m (1 - K E_1 C_{L,1} \zeta)} \right\} \cong \frac{E_1 \zeta}{2E_m (1 - K E_1 C_{L,1} \zeta)} \quad (9.34)$$

and Eq. (9.31) reduces to

$$x_{h-V} = E_1 V_1 \zeta / \{c(1 - K E_1 C_{L,1} \zeta)\} \quad (9.35)$$

which after using Eqs. (9.32) and (9.33) can be written as

$$x_{h-V} = 2(W_1/S) \rho_1 \zeta V_1^3 / [c \{C_{D_0} \rho_1^2 V_1^4 + (1 - \zeta) 4K(W_1/S)^2\}] \quad (9.36)$$

It is now simpler to optimize the range x_{h-V} with respect to airspeed. Before differentiating the above relation with respect to V_1 , it is necessary that all the other quantities on its right-hand side must be regarded as constant. This requires that ζ must also be fixed beforehand. Therefore, let $\zeta = \zeta^*$ be the known cruise-fuel weight fraction that has been used in covering the range, the above relation becomes

$$x_{h-V} = 2(W_1/S) \rho_1 \zeta^* V_1^3 / [c \{C_{D_0} \rho_1^2 V_1^4 + (1 - \zeta^*) 4K(W_1/S)^2\}] \quad (9.37)$$

Differentiate the above equation with respect to V_1 and put $dx_{h-V}/dV_1 = 0$. The solution of the resulting equation gives the maximum-range airspeed $V_{1mr,h-V}$ as

$$V_{1mr,h-V} = \left\{ \frac{2(W_1/S)}{\rho_{SSL} \sigma_1} \right\}^{1/2} \left\{ \frac{3K(1 - \zeta^*)}{C_{D_0}} \right\}^{1/4} = 3^{1/4} V_{1E_m} (1 - \zeta^*)^{1/4} \quad (9.38)$$

Note that in the case of a constant $h-V$ flight, the maximum-range airspeed depends on ζ^* . This means that the maximum-range airspeed can be obtained if the amount of fuel consumed during the cruise is known beforehand. The maximum-range airspeed decreases with the increase in ζ^* .

The values of the other flight parameters of the maximum range can now also be obtained. Since the altitude (and thus ρ) and the airspeed are constant, the lift coefficient for the maximum range $C_{L,\text{mr};h-V}$ is given by

$$C_{L,\text{mr};h-V} = 2(W/S) / (\rho_1 V_{1\text{mr};h-V}^2) = (W/W_1) [C_{D_0}/\{3K(1 - \zeta^*)\}]^{1/2}$$

where $W/W_1 = 1 - \zeta$. Therefore,

$$C_{L,\text{mr};h-V} = (1 - \zeta) [C_{D_0}/\{3K(1 - \zeta^*)\}]^{1/2} \quad (9.39)$$

The drag coefficient for the maximum range is given by

$$C_{D,\text{mr};h-V} = C_{D_0} + K C_{L,\text{mr};h-V}^2$$

which after using Eq. (9.39) can be written as

$$C_{D,\text{mr};h-V} = \{3(1 - \zeta^*) + (1 - \zeta)^2\} C_{D_0} / \{3(1 - \zeta^*)\} \quad (9.40)$$

The aerodynamic efficiency for the maximum range, $E_{\text{mr};h-V}$, is obtained from the relation

$$E_{\text{mr};h-V} = \frac{C_{L,\text{mr},h-V}}{C_{D,\text{mr};h-V}} = \frac{2E_m(1 - \zeta)\sqrt{3(1 - \zeta^*)}}{3(1 - \zeta^*) + (1 - \zeta)^2} \quad (9.41)$$

The thrust/weight ratio for the best range is obtained from Eq. (8.5) as

$$\frac{F_{\text{mr},h-V}}{W} = \frac{1}{E_{\text{mr};h-V}} = \frac{3(1 - \zeta^*) + (1 - \zeta)^2}{2E_m(1 - \zeta)\sqrt{3(1 - \zeta^*)}} \quad (9.42)$$

The above flight parameters help to determine the maximum range that will be obtained from Eq. (9.31); it can be remarked here that within the framework of the approximation presented by Eq. (9.34), Eq. (9.35) can also be used for obtaining the maximum range. Equation (9.31) for the maximum range can be written as

$$x_{\text{mr},h-V} = \frac{2E_m V_{1\text{mr};h-V}}{c} \tan^{-1} \left\{ \frac{E_{1\text{mr},h-V}\zeta}{2E_m(1 - KE_{1\text{mr},h-V}C_{L,1\text{mr},h-V}\zeta)} \right\} \quad (9.43)$$

where $V_{1\text{mr},h-V}$ is given by Eq. (9.38), $C_{L,1\text{mr},h-V}$ and $E_{L,1\text{mr},h-V}$ are obtained from Eqs. (9.39) and (9.41), respectively, as

$$C_{L,1\text{mr},h-V} = (C_{L,\text{mr},h-V})_{\zeta=0} = [C_{D_0}/\{3K(1 - \zeta^*)\}]^{1/2} \quad (9.44)$$

and

$$E_{1\text{mr},h-V} = (E_{\text{mr},h-V})_{\zeta=0} = \frac{2E_m\sqrt{3(1 - \zeta^*)}}{1 + 3(1 - \zeta^*)} \quad (9.45)$$

Using Eqs. (9.38), (9.44), and (9.45), the maximum range given by Eq. (9.43) can be written as

$$x_{mr;h-V} = \frac{2E_m V_{1E_m}}{c} \{3(1 - \zeta^*)\}^{1/4} \tan^{-1} \left\{ \frac{\zeta \sqrt{3(1 - \zeta^*)}}{(1 - \zeta) + 3(1 - \zeta^*)} \right\} \quad (9.46)$$

which after substituting the expression for V_{1E_m} becomes

$$\begin{aligned} x_{mr;h-V} &= \frac{1}{c} \left(\frac{2E_m}{C_{D_0}} \right)^{1/2} \left\{ \frac{2(W_1/S)}{\rho_{SSL}\sigma_1} \right\}^{1/2} \{3(1 - \zeta^*)\}^{1/4} \\ &\times \tan^{-1} \left\{ \frac{\zeta \sqrt{3(1 - \zeta^*)}}{(1 - \zeta) + 3(1 - \zeta^*)} \right\} \end{aligned} \quad (9.47)$$

The above relation expresses maximum range of the constant h - V flight in terms of the aircraft design parameters.

The endurance $t_{mr;h-V}$ corresponding to the maximum range of constant h - V flight can be obtained from the relation $t_{mr;h-V} = x_{mr;h-V} / V_{mr;h-V}$, which after using Eqs. (9.38) and (9.46) can be written as

$$t_{mr;h-V} = \frac{2E_m}{c} \tan^{-1} [\zeta \sqrt{3(1 - \zeta^*)} / ((1 - \zeta) + 3(1 - \zeta^*))] \quad (9.48)$$

Like airspeed, all the other flight parameters also depend on ζ^* . Having fixed ζ^* , Eqs. (9.47) and (9.48), respectively, show the variations of range and endurance with ζ of maximum-range flight for $\zeta = \zeta^*$.

The effectiveness of ζ^* will now be investigated by defining the two functions F_x and F_t as

$$F_x = (1 - \zeta^*)^{1/4} F_t \quad \text{and} \quad F_t = \tan^{-1} \left\{ \frac{\zeta \sqrt{3(1 - \zeta^*)}}{(1 - \zeta) + 3(1 - \zeta^*)} \right\}$$

These two functions appear in expressions for the range and endurance, respectively. Both are functions of ζ and ζ^* only, and do not depend on the aircraft design parameters. These functions are plotted in Fig. 9.1 against ζ for the three different values (0.1, 0.3, and 0.5) of ζ^* . The solid lines represent F_x and the dashed lines F_t . The three solid lines for F_x are so extremely close that it becomes difficult to distinguish them. This shows that F_x is an extremely weak function of ζ^* . The three dashed lines of F_t are, however, quite distinct, showing that the change in ζ^* appreciably influences F_t . Therefore, unlike the range, the endurance is appreciably affected by changes in ζ^* .

If it is desired to obtain the maximum-range flight parameters for each given value of ζ , put $\zeta^* = \zeta$ in Eqs. (9.38–9.42). The airspeed, lift and drag coefficients, aerodynamic efficiency, and the thrust per unit weight, of the maximum range for each ζ are, therefore, given by the following relations:

$$V_{mr;h-V} = \left\{ \frac{2(W_1/S)}{\rho_1} \right\}^{1/2} \left\{ \frac{3K(1 - \zeta)}{C_{D_0}} \right\}^{1/4} = 3^{1/4} V_{1E_m} (1 - \zeta)^{1/4} \quad (9.49)$$

$$C_{L,mr;h-V} = \{C_{D_0}(1 - \zeta)/(3K)\}^{1/2}, \quad C_{D,mr;h-V} = (4 - \zeta)C_{D_0}/3 \quad (9.50)$$

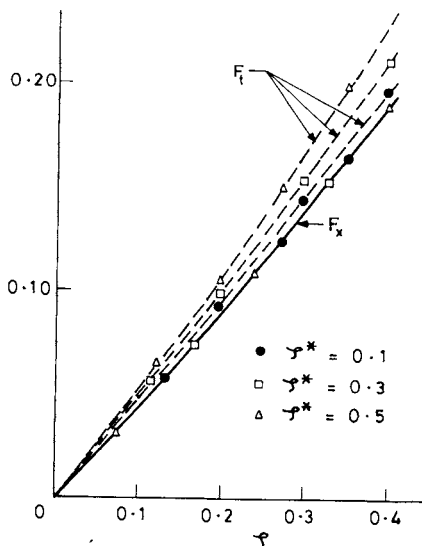


Fig. 9.1 Changes in F_x and F_t with ξ showing the influence of ζ^* .

$$E_{mr;h-V} = \frac{2E_m\sqrt{3}(1-\zeta)}{4-\zeta} \quad \text{and} \quad \frac{F_{mr;h-V}}{W} = \frac{4-\zeta}{2E_m\sqrt{3}(1-\zeta)} \quad (9.51)$$

Similarly, the maximum range and its endurance for each ζ are obtained by putting $\zeta^* = \zeta$ in Eqs. (9.47) and (9.48). This gives

$$x_{mr;h-V} = \frac{1}{c} \left(\frac{2E_m}{C_{D_0}} \right)^{1/2} \left\{ \frac{2(W_1/S)}{\rho_{SSL}\rho_1} \right\}^{1/2} \{3(1-\zeta)\}^{1/4} \tan^{-1} \left(\frac{0.433\zeta}{\sqrt{1-\zeta}} \right) \quad (9.52)$$

and

$$t_{mr;h-V} = (2E_m/c) \tan^{-1} (0.433\zeta/\sqrt{1-\zeta}) \quad (9.53)$$

In Eqs. (9.49–9.53), each change in ζ represents a different constant h - V flight for maximum range. The above relations will not give the variations of the flight parameters against ζ for a given ($\zeta = \zeta^*$) maximum-range flight.

9.3.4 Comparison of Different Maximum-Range Flights

It is of interest to compare the ranges of the three different maximum-range flights discussed in Secs. 9.3.1–9.3.3. Thus, we enquire here about the flight program of a given aircraft that would cover the largest range among the three different maximum-range flights for a specified amount of fuel consumption. It will be seen below that the ratios of the different maximum ranges are purely a function of ζ , which makes the comparison easier.

From Eqs. (9.15) and (9.25),

$$\frac{x_{mr;V-C_L}}{x_{mr;h-C_L}} = \frac{\ln\{1/(1-\zeta)\}}{2(1-\sqrt{1-\zeta})} \quad (9.54)$$

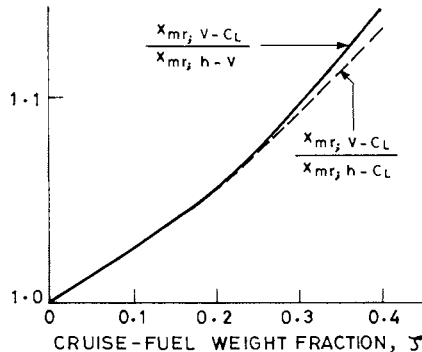


Fig. 9.2 Ratios of maximum ranges of different flights against ζ .

and, similarly, from Eqs. (9.25) and (9.52),

$$\frac{x_{mr;V-C_L}}{x_{mr;h-V}} = \frac{\sqrt{3} \ln\{1/(1-\zeta)\}}{4(1-\zeta)^{1/4} \tan^{-1}\{0.433\zeta/(\sqrt{1-\zeta})\}} \quad (9.55)$$

Equations (9.54) and (9.55) are plotted against ζ in Fig. 9.2. Both curves lie above unity for all ζ , showing that the maximum range of the constant $V-C_L$ flight, i.e., the cruise-climb flight, is better than that of the other two maximum-range flights. The difference between the two curves is negligible initially but increases as the cruise-fuel weight fraction ζ increases. This means that differences in the maximum ranges among the various flights become significant for long-range flights.

9.3.5 Maximum Range for a Specified Constant Airspeed

It may happen that the maximum-range airspeed of a specified flight program may exceed the allowable limit provided by the aerodynamic, structural, or the other operational constraints. In such cases one is required to obtain the maximum range. There are two flight programs, constant $V-C_L$ and constant $h-V$, that keep the airspeed constant. Both these programs are considered here for obtaining the maximum range with specified (allowable) constant airspeed, which is different from the maximum-range airspeed.

In the case of constant $V-C_L$ flight, it is seen that the maximum range is obtained if the product $E_1 V_1$ is maximum. Since V_1 is specified, the product $E_1 V_1$ is maximized by maximizing E_1 . This gives the aerodynamic efficiency $E_{mr;V_1-C_L}$ of the constant $V-C_L$ flight as

$$E_{mr;V_1-C_L} = E_m \quad (9.56)$$

and the value of the lift coefficient $C_{L,mr;V_1-C_L}$ during the flight would be given by

$$C_{L,mr;V_1-C_L} = C_{L,E_m} = \sqrt{C_{D_0}/K} \quad (9.57)$$

The specified airspeed V_1 during the cruise follows the relationship

$$V_1 = \left\{ 2(W_1/S)/(\rho_{SSL}\sigma_1 C_{L,mr;V_1-C_L}) \right\}^{1/2} \quad (9.58)$$

Since the lift coefficient is fixed by Eq. (9.57), the specified V_1 can be achieved either by altering the wing loading at the design stage or by flying the aircraft at the initial altitude corresponding to σ_1 given by the above relation. In Eq. (9.58), both the airspeed and lift coefficient are constant, it follows that $W_1/\sigma_1 = W/\sigma = \text{constant}$, which corresponds to a cruise-climb flight. The maximum range $x_{\text{mr}; V_1 - C_L}$ of the constant $V - C_L$ flight for a specified airspeed is obtained from Eq. (9.20) as

$$x_{\text{mr}; V_1 - C_L} = (E_m V_1 / c) \ell_n \{1/(1 - \zeta)\} \quad (9.59)$$

This shows that the maximum range of the specified airspeed for a given ζ is obtained by maximizing the aerodynamic efficiency and minimizing the thrust-specific fuel consumption.

Consider now the case of constant $h - V$ flight of an specified airspeed V_1 which is different from V_{mr} . In this case, the maximum range would be obtained by optimizing the range given by Eq. (9.35) with respect to $C_{L,1}$. Equation (9.35), after using the first relation of Eq. (9.33), becomes

$$x_{h-V_1} = (C_{L,1} V_1 \zeta) / [c \{C_{D_0} + K C_{L,1}^2 (1 - \zeta)\}] \quad (9.60)$$

To optimize the range x_{h-V_1} with respect to $C_{L,1}$, the value of ζ also has to be fixed. Therefore, let $\zeta = \zeta^*$ be the cruise fuel weight fraction that is being consumed during the cruise. The above relation can be written as

$$x_{h-V_1} = C_{L,1} V_1 \zeta^* / [c \{C_{D_0} + K C_{L,1}^2 (1 - \zeta^*)\}] \quad (9.61)$$

Differentiating the above relation with respect to $C_{L,1}$ and putting $dx_{h,V}/dC_{L,1} = 0$, an algebraic equation is obtained whose solution gives¹

$$C_{L,\text{mr}; h-V_1} = \sqrt{C_{D_0} / \{K(1 - \zeta^*)\}} \quad (9.62)$$

The aerodynamic efficiency of the flight is obtained as

$$E_{\text{mr}; h-V_1} = \frac{C_{L,\text{mr}; h-V_1}}{C_{D_0} + K C_{L,\text{mr}; h-V_1}^2} = 2E_m \frac{\sqrt{1 - \zeta^*}}{1 + (1 - \zeta^*)} \quad (9.63)$$

The maximum range for the specified airspeed ($\neq V_{\text{mr}}$) is obtained from Eq. (9.31), which after using Eqs. (9.62) and (9.63) can be written as

$$x_{\text{mr}; h-V_1} = \frac{2E_m V_1}{c} \tan^{-1} \left\{ \frac{\zeta \sqrt{1 - \zeta^*}}{(1 - \zeta^*) + (1 - \zeta)} \right\} \quad (9.64)$$

The above relation gives the maximum range $x_{\text{mr}; h-V}$ for $\zeta = \zeta^*$ only. For the other values of ζ , it gives the variation of the range with ζ . To obtain the maximum range $x_{\text{mr}; h-V_1}$ for each value of ζ , put $\zeta^* = \zeta$ in the above relation, which gives

$$x_{\text{mr}; h-V_1} = (2E_m V_1 / c) \tan^{-1} \{ \zeta / (2\sqrt{1 - \zeta}) \} \quad (9.65)$$

Here also it is found that the maximum range for the specified airspeed V_1 ($\neq V_{\text{mr}}$) would be achieved by flying at the maximum aerodynamic efficiency of the aircraft and keeping the thrust-specific fuel consumption of the engine as low as possible.

9.3.6 Maximum Range in Practice (Stepped-Altitude Flight)

It has been seen in Sec. 9.3.4 that the cruise-climb flight gives the largest range for a given ζ , but it is not compatible with the air traffic control regulations which require constant $h\text{-}V$ flight. However, the traffic control may allow the change in altitude at certain intervals. Even-numbered altitudes (in thousands of feet) are assigned to air traffic in one direction and odd-numbered altitudes are assigned to air traffic in the opposite direction. This implies that steps in altitude must be in multiples of 609.6 m (2000 ft). The present air traffic control regulations limit such steps to 1219.2 m (4000 ft), although airlines would prefer 609.6 m (2000 ft).

In practice, a long-range flight, such as an intercontinental or transoceanic flight, is broken into a number of segments. During each segment the altitude and airspeed are kept constant. The increase in altitude in a step of 1219.2 m (4000 ft) takes place when the next segment is reached. Such a flight program is called a *stepped-altitude flight*. If the number of segments is allowed to increase while keeping the airspeed the same as that of a cruise-climb flight, the stepped-altitude flight resembles more closely the cruise-climb flight. In the stepped-altitude flight, the airspeed is kept the same as the maximum-range airspeed of the cruise-climb flight.

A stepped-altitude flight path is shown in Fig. 9.3. The top inclined thin straight line is the flight path of the cruise-climb flight. This flight path has been approximated by breaking it into stepped altitudes consisting of horizontal segments at different altitudes. The stepped-altitude path is shown by a thicker line in Fig. 9.3 which is an idealized (approximate) representation of the actual flight path for the purpose of theoretical analysis, since such sharp vertical turns in practice are not possible by an aircraft. In each of these horizontal segments, numbered $1, 2, 3, \dots, n - 1, n$, the airspeed and altitude are kept constant and Eq. (9.31) can be used in each segment. Therefore, putting

$$V_1 = V_{1mr; V-C_L}, \quad C_{L,1} = C_{L,1mr; V-C_L}, \quad \text{and} \quad E_1 = E_{1mr; V-C_L}$$

in Eq. (9.31), and using Eqs. (9.21–9.23), Eq. (9.31) becomes

$$x_{h-V} = \left\{ 2(3)^{1/4} E_m V_{E_m} / c \right\} \tan^{-1} \left\{ 0.433 \zeta / (1 - 0.25 \zeta) \right\} \quad (9.66)$$

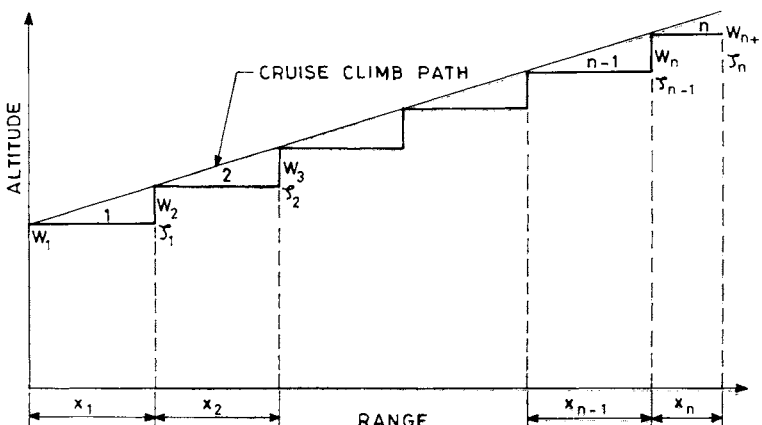


Fig. 9.3 Stepped-altitude flight.

where

$$V_{E_m} = \{2(W_1/S)/(\rho_{SSL}\sigma_1)\}^{1/2} (K/C_{D_0})^{1/4} \quad (9.67)$$

If ξ_i denotes the cruise-fuel weight fraction that has been used in the segment i of length x_i , where $i = 1, 2, 3, \dots, n$, Eq. (9.66) for each segment is

$$x_i = \{2(3)^{1/4} E_m V_{E_m}/c\} \tan^{-1} \{0.433 \xi_i / (1 - 0.25 \xi_i)\} \quad (9.68)$$

where

$$\xi_i = (W_i - W_{i+1})/W_i \quad (9.69)$$

If $\Delta h_i (= h_{i+1} - h_i)$ is the cruise climb covered at the end of each segment during which ξ_i is consumed, Eq. (9.27) yields

$$\xi_i = 1 - \exp(-\Delta h_i/\beta) \quad (9.70)$$

The air traffic regulations require $\Delta h_i = 1219.2$ m (4000 ft) for each segment. Taking $\beta = 6216$ m (20,395 ft), because modern long-range aircraft fly in the tropopause or above, the above relation becomes

$$\xi_i = 1 - \exp(-1219.2/6216) = 0.1781$$

for $i = 1, 2, 3, \dots, n - 1$, which does not include the last segment ξ_n . It follows that

$$\xi_1 = \xi_2 = \xi_3 = \dots = \xi_{n-1} = 0.1781 \quad (9.71)$$

Substituting the above value of ξ_i in Eq. (9.68), the length x_i of each segment, $i = 1, 2, 3, \dots, n - 1$, which does not include the last segment x_n , is obtained as

$$x_i = 0.21244 E_m V_{E_m}/c \quad (9.72)$$

The airspeed V_{E_m} is constant along the inclined line (cruise-climb flight path) because W/ρ is constant at each of its point. Therefore, V_{E_m} will have the same value at each of the points where the step touches the cruise-climb path (Fig. 9.3). Thus, for a given aircraft, E_m , V_{E_m} , and c are the known constants, yielding equal horizontal segments

$$x_1 = x_2 = x_3 = \dots = x_{n-1} \quad (9.73)$$

and these are now known quantities as obtained from Eq. (9.72).

The last segment x_n is obtained from the relation

$$x_n = x_R - \sum_{i=1}^{n-1} x_i$$

where x_R is the total range of the cruising flight, which is known beforehand. Making use of the equalities of Eq. (9.73), the above relation becomes

$$x_n = x_R - (n - 1)x_1 \quad (9.74)$$

The weight W_i of the aircraft at the end of each segment is obtained from Eq. (9.69) which can be written as

$$W_{i+1} = (1 - \zeta_i) W_i$$

where $\zeta_i = 0.1781$, for $i = 1, 2, 3, \dots, n - 1$. This gives

$$W_{i+1} = (1 - 0.1781) W_i \quad (9.75)$$

for $i = 1, 2, 3, \dots, n - 1$. From the repeated application of the recurrence relation (Eq. 9.75), one obtains

$$W_i = (1 - 0.1781)^{i-1} W_1 \quad (9.76)$$

where $i = 2, 3, \dots, n$, and W_1 is the known weight of the aircraft at the start of the cruise. The above relation gives $W_2, W_3, W_4, \dots, W_n$ which are the weights of the aircraft at the end of each of the equal segments $x_1, x_2, x_3, \dots, x_{n-1}$, respectively. The weight W_{n+1} at the end of the cruise is still unknown, and can be obtained by using Eqs. (9.68) and (9.69) for $i = n$. This gives

$$x_n = \left\{ 2(3)^{1/4} E_m V_{E_m} / c \right\} \tan^{-1} \left\{ 0.433 \zeta_n / (1 - 0.25 \zeta_n) \right\} \quad (9.77)$$

where

$$\zeta_n = (W_n - W_{n+1}) / W_n \quad (9.78)$$

Since x_n and W_n are the known quantities from Eqs. (9.74) and (9.76), respectively, one first obtains ζ_n from Eq. (9.77) then W_{n+1} from Eq. (9.78). Now $W_i, i = 1, 2, 3, \dots, n + 1$, are the known weights. The total amount of the fuel consumed ΔW_f during the cruise, and the corresponding cruise-fuel weight fraction ζ are given by

$$\Delta W_f = \sum_{i=1}^n (W_i - W_{i+1}) = W_1 - W_{n+1} \quad \text{and} \quad \zeta = \Delta W_f / W_1$$

The above method of calculating the fuel consumption in the stepped-altitude flight is only approximate because the fuel consumed during the climb by an altitude of 1219.2 m (4000 ft) at the end of each segment is not taken into account.

9.4 Maximum-Endurance Flights

Endurance of different flights is obtained in Sec. 8.8, their optimizations will be discussed here. It was found that the endurance of the constant $h-C_L$ and constant $V-C_L$ flights are just the same; this was called the endurance of the constant C_L flight. Therefore, the maximum endurance and the associated flight parameters of the constant C_L and constant $h-V$ flights are obtained here. These maximum-endurance values are compared with the endurance values for different maximum-range flights. The subscript me is used to denote the condition of maximum endurance t_m .

9.4.1 Maximum Endurance of Constant Lift Coefficient Flight

The endurance of a constant C_L flight is given by Eq. (8.44) as

$$t_{C_L} = (E_1/c) \ln \{1/(1 - \zeta)\}$$

It is clear that for a given ζ , the maximum endurance $t_{m:C_L}$ of the constant lift coefficient flight would be achieved if $E_1 = E_m$. Therefore,

$$t_{m:C_L} = (E_m/c) \ln \{1/(1 - \zeta)\} \quad (9.79)$$

which shows that the maximum endurance is independent of altitude and wing loading. This essentially means that a turbojet aircraft with a given fuel load can stay in the air just as long at a higher altitude as at sea level. It is therefore the increased airspeed at the higher altitude that is responsible for the greater range.

It also follows that the aerodynamic efficiency, lift coefficient, and airspeed, respectively, of the flight are given by

$$E_{me:C_L} = E_m, \quad C_{L,me:C_L} = C_{L,E_m}, \quad \text{and} \quad V_{me:C_L} = V_{E_m} \quad (9.80)$$

The thrust per unit weight for maximum endurance of the constant C_L flight is obtained from Eq. (8.5) as

$$F_{me:C_L}/W = 1/E_{me:C_L} = 1/E_m$$

which expresses that the thrust per unit weight has to be at a minimum for maximum endurance.

The flight parameters for maximum endurance at constant C_L flight are, therefore, the same as those required for maximum aerodynamic efficiency, i.e., for maximum lift/drag ratio.

These flight parameters can now be compared with the corresponding flight parameters for maximum-range flight discussed above. Comparison of lift coefficients and aerodynamic efficiencies gives

$$\frac{C_{L,me:C_L}}{C_{L,mr;V-C_L}} = \sqrt{3} = 1.732 \quad \text{and} \quad \frac{E_{me:C_L}}{E_{mr;V-C_L}} = \frac{2}{\sqrt{3}} = 1.155$$

which shows that the lift coefficient and aerodynamic efficiency for maximum endurance flight are higher than those for maximum-range flight. Comparing the airspeeds gives

$$V_{me:C_L}/V_{mr;V-C_L} = 1/3^{1/4} = 0.76$$

which shows that for a given aircraft the maximum-endurance airspeed is 24% slower than the maximum-range airspeed of the constant C_L flight. Similarly, comparing Eqs. (9.30) and (9.79), it is found that

$$t_{m:C_L}/t_{mr;V-C_L} = 2/\sqrt{3} = 1.155$$

which indicates that the flight time of a maximum-endurance flight for a given aircraft is 15.5% higher than that for a maximum-range flight with constant C_L .

9.4.2 Maximum Endurance of a Constant Altitude–Constant Airspeed Flight

The endurance of a constant h - V flight is obtained from Eq. (8.45) as

$$t_{h-V} = (2E_m/c) \tan^{-1}[E_1\zeta/\{2E_m(1 - KE_1C_{L,1}\zeta)\}] \quad (9.81)$$

Following the approximation of the arc tan function presented by Eq. (9.34), the above relation can be written as

$$t_{h-V} = E_1\zeta/\{c(1 - KE_1C_{L,1}\zeta)\}$$

which after using Eqs. (9.32) and (9.33) for $C_{L,1}$ and E_1 , respectively, becomes

$$t_{h-V} = 2(W_1/S)\rho_1\zeta V_1^2/[c\{C_{D_0}\rho_1^2V_1^4 + (1 - \zeta)4K(W_1/S)^2\}]$$

If $\zeta = \zeta^*$, is the value of ζ for which t_{h-V} is to be optimized, the above relation can be written as

$$t_{h-V} = 2(W_1/S)\rho_1\zeta^* V_1^2/[c\{C_{D_0}\rho_1^2V_1^4 + (1 - \zeta^*)4K(W_1/S)^2\}]$$

Differentiate the above equation with respect to V_1 , and put $dt_{h-V}/dV_1 = 0$. The resulting algebraic relation can be solved, giving the maximum-endurance airspeed $V_{me;h-V}$ of constant h - V flight as

$$V_{me;h-V} = \left\{ \frac{2(W_1/S)}{\rho_{SSL}\sigma_1} \right\}^{1/2} \left\{ \frac{K(1 - \zeta^*)}{C_{D_0}} \right\}^{1/4} = V_{E_m}(1 - \zeta^*)^{1/4} \quad (9.82)$$

The lift coefficient $C_{L,me;h-V}$ for the maximum endurance of the constant h - V flight is given by

$$C_{L,me;h-V} = 2(W/S)/(\rho_1 V_{me;h-V}^2)$$

which after using Eq. (9.82) becomes

$$C_{L,me;h-V} = \frac{W}{W_1} \left\{ \frac{C_{D_0}}{K(1 - \zeta^*)} \right\}^{1/2} = (1 - \zeta) \left\{ \frac{C_{D_0}}{K(1 - \zeta^*)} \right\}^{1/2} \quad (9.83)$$

The aerodynamic efficiency is obtained by

$$E_{me;h-V} = C_{L,me;h-V}/C_{D,me;h-V} = C_{L,me;h-V}/(C_{D_0} + K C_{L,me;h-V}^2)$$

which after using Eq. (9.83) can be written as

$$E_{me;h-V} = 2E_m(1 - \zeta)\sqrt{(1 - \zeta^*)}/\{(1 - \zeta^*) + (1 - \zeta)^2\} \quad (9.84)$$

The maximum endurance $t_{m;h-V}$ is now obtained from Eq. (9.81) as

$$t_{m;h-V} = \frac{2E_m}{c} \tan^{-1} \left\{ \frac{E_{1me,h-V}\zeta}{2E_m(1 - KE_{1me,h-V}C_{L,1me;h-V}\zeta)} \right\}$$

where

$$C_{L,1\text{me};h-V} = [C_{L,\text{me};h-V}]_{\zeta=0} = \sqrt{C_{D_0}/\{K(1-\zeta^*)\}}$$

and

$$E_{1\text{me};h-V} = [E_{\text{me};h-V}]_{\zeta=0} = 2E_m\sqrt{(1-\zeta^*)/\{1+(1-\zeta^*)\}}$$

Therefore, the maximum endurance value can be expressed as

$$t_{m;h-V} = (2E_m/c) \tan^{-1}[\zeta\sqrt{(1-\zeta^*)}/\{(1-\zeta)+(1-\zeta^*)\}] \quad (9.85)$$

Thus, the maximum endurance for a given ζ^* is achieved by flying at the maximum aerodynamic efficiency and keeping the thrust-specific fuel consumption as low as possible.

Equations (9.82–9.85) give the variations in maximum-endurance flight parameters with ζ for the flight; these equations are meant for calculating maximum endurance with values $\zeta = \zeta^*$ only. To obtain maximum endurance parameters for all the values of ζ , put $\zeta^* = \zeta$ in Eqs. (9.82–9.85), which, respectively, give

$$V_{\text{me};h-V} = \{2(W_1/S)/\rho_1\}^{1/2} \{K(1-\zeta)/C_{D_0}\}^{1/4} \quad (9.86)$$

$$C_{L,\text{me};h-V} = \sqrt{C_{D_0}(1-\zeta)/K}, \quad E_{\text{me};h-V} = 2E_m\sqrt{1-\zeta}/\{1+(1-\zeta)\} \quad (9.87)$$

and

$$t_{m;h-V} = (2E_m/c) \tan^{-1}\{\zeta/(2\sqrt{1-\zeta})\} \quad (9.88)$$

In the above four relations, each change in ζ corresponds to a different flight.

It is now of interest to compare the endurance yielded by different flight programs. From Eqs. (9.30), (9.53), (9.79), and (9.88), respectively, it is seen that $(c/E_m)t_{\text{mr};V-C_L}$, $(c/E_m)t_{\text{mr};h-V}$, $(c/E_m)t_{m;C_L}$, and $(c/E_m)t_{m;h-V}$ depend only on the cruise-fuel weight fraction ζ . These values are plotted against ζ in Fig. 9.4 which shows that the maximum-endurance flight of a given aircraft cruises for longer periods of time, as compared to the maximum-range flight, for a specified amount of ζ . It is further seen that for a given ζ , there is no appreciable difference between the maximum endurance of the constant C_L and constant $h-V$ flights. Similarly, there is no difference between the endurance of the maximum ranges of constant $V-C_L$ and constant $h-V$ flights.

9.5 Application to an Aircraft

Consider the aircraft of Sec. 8.10, starting its cruising flight at an altitude of 9 km. Find the maximum-range airspeeds and the maximum ranges of constant $h-C_L$, constant $V-C_L$, and constant $h-V$ flights.

For a constant $h-C_L$ flight, the maximum-range airspeed at the start of the cruise is obtained from Eq. (9.11) as

$$V_{1\text{mr};h-C_L} = \left\{ \frac{2(4000)}{1.225 \times 0.3813} \right\}^{1/2} \left[\frac{3 \times 0.052}{0.016} \right]^{1/4} = 231.26 \text{ m/s} = 832.5 \text{ km/h}$$

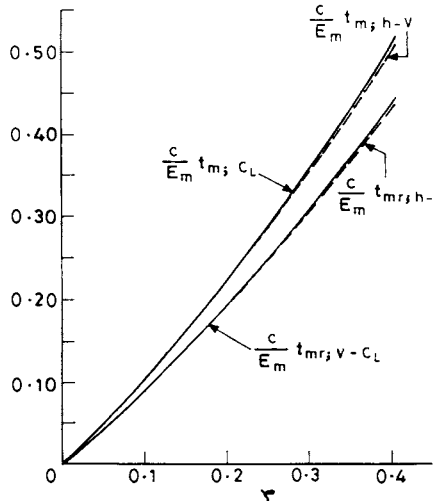


Fig. 9.4 Maximum endurance, and endurance of maximum ranges, of different flights.

and since, $E_{1mr;h-C_L} = 0.866 E_m = 0.866 \times 17.33 = 15$, the range is given by

$$\begin{aligned} x_{mr;h-C_L} &= (2E_{1mr;h-C_L} V_{1mr;h-C_L})(1 - \sqrt{1 - \zeta})/c \\ &= \frac{2 \times 15 \times 231.26}{(0.8/3600)} (1 - \sqrt{1 - 0.3}) = 5,099,490 \text{ m} = 5099 \text{ km} \end{aligned}$$

For a constant $V-C_L$ flight the maximum-range airspeed is obtained from Eq. (9.21) as

$$V_{mr;V-C_L} = V_{1mr;h-C_L} = 231.26 \text{ m/s} = 832.5 \text{ km/h}$$

and since $E_{mr;V-C_L} = E_{1mr;h-C_L} = 15$, the range is given by

$$\begin{aligned} x_{mr;V-C_L} &= (E_{1mr;V-C_L} V_{1mr;V-C_L}/c) \ln\{1/(1 - \zeta)\} \\ &= \frac{15 \times 231.26}{(0.8/3600)} \ln\left(\frac{1}{1 - 0.3}\right) = 5,567,714 \text{ m} = 5568 \text{ km} \end{aligned}$$

For a constant $h-V$ flight, the maximum-range airspeed is obtained from Eqs. (9.38) and (9.21) as

$$\begin{aligned} V_{1mr;h-V} &= 3^{1/4} V_{1E_m} (1 - \zeta^*)^{1/4} = V_{1mr;h-C_L} (1 - \zeta^*)^{1/4} = 231.26 (1 - 0.3)^{1/4} \\ &= 211.53 \text{ m/s} = 761.5 \text{ km/h} \end{aligned}$$

and since from Eqs. (9.44) and (9.45), respectively,

$$C_{L,1mr;h-V} = [0.016/\{3 \times 0.052(1 - 0.3)\}]^{1/2} = 0.3828$$

and

$$E_{1mr;h-V} = 2 \times 17.33 \sqrt{3(1 - 0.3)}/\{1 + 3(1 - 0.3)\} = 16.20$$

the maximum range is obtained from Eq. (9.43) as

$$\begin{aligned} x_{\text{mr}; h-V} &= \frac{2 \times 17.33 \times 211.53}{0.8/3600} \\ &\times \tan^{-1} \left\{ \frac{16.20 \times 0.3}{2 \times 17.33(1 - 0.052 \times 16.20 \times 0.3828 \times 0.3)} \right\} \\ &= 5,081,078 \text{ m} = 5081 \text{ km} \end{aligned}$$

Therefore, the maximum-range airspeeds of constant $h \cdot C_L$, constant $V \cdot C_L$, and constant $h \cdot V$ flights are respectively, 832.5 km/h of cruise, 832.5 km/h, and 761.5 km/h (at the start of cruising). Similarly, the maximum ranges achieved by these flights are 5099, 5568, and 5081 km, respectively.

References

- ¹Hale, F. J., *Aircraft Performance, Selection, and Design*, Wiley, New York, 1984.
²Ojha, S. K., "Optimization of Constant Altitude–Constant Airspeed Flight of Turbojet Aircraft," *Journal of Aircraft*, Vol. 29, No. 4, 1992, pp. 731–734.

Problems

The major specifications of Aircraft A, Aircraft B, and Aircraft C, which are needed to solve many of these problems, are presented at the beginning of the Problems Section in Chapter 8.

9.1 Aircraft A starts cruising at an altitude of 3 km using minimum thrust. Assuming the initial weight to be the gross weight of the aircraft, find the following:
 a) The airspeed, thrust, weight, and aerodynamic efficiency after a period of 1 h, if the aircraft flies at the constant altitude. b) If the aircraft cruises at constant airspeed, calculate the thrust, weight, aerodynamic efficiency, and altitude, after a period of 1 h.

9.2 Repeat Problem 9.1 for Aircraft B and find the corresponding quantities after a period of 2 h, if the aircraft starts cruising at sea level.

9.3 Repeat Problem 9.1 for Aircraft C and find the corresponding quantities after a period of 4 h if the aircraft starts cruising at an altitude of 12 km.

9.4 Aircraft A is cruising at sea level. Plot the variation of E against V , where V varies from the minimum to the maximum airspeed. Note the airspeed for maximum E .

9.5 Solve Problem 9.4 if Aircraft A is flying at an altitude of 4 km with 90% of its gross weight.

9.6 Solve Problem 9.4 if Aircraft B is cruising at an altitude of a) 5 km and b) 10 km.

9.7 Solve Problem 9.4 if Aircraft C is cruising at an altitude of a) 6 km, and b) 12 km.

9.8 Aircraft B cruises at an altitude of 4 km under constant $h\text{-}C_L$ flight program. It uses a cruise-fuel weight fraction of 0.22. For a) maximum range, and b) maximum endurance, calculate the following: i) airspeed at the beginning and at the end of the cruise; ii) lift and drag coefficients, aerodynamic efficiency, and thrust-weight ratio; iii) the cruising range and its endurance.

9.9 Repeat Problem 9.8 if Aircraft B cruises at an altitude of 8 km.

9.10 Repeat Problem 9.8 if Aircraft B cruises at an altitude of 12 km.

9.11 Solve Problem 9.8 if it is now Aircraft A that cruises at an altitude of a) 2 km and b) 4 km. Use the same cruise-fuel weight fraction of 0.22 as in Problem 9.8.

9.12 Solve Problem 9.8 if it is Aircraft C that cruises at an altitude of a) 6 km and b) 12 km. Use a cruise-fuel weight fraction of 0.22.

9.13 For a cruise-climb flight program of Aircraft B that uses 80% of the fuel for cruise, find the maximum ranges when its cruising starts at the altitudes of a) 4 km, b) 6 km, c) 8 km, d) 10 km, and e) 12 km.

9.14 Aircraft C is flying under cruise-climb flight program and uses 80% of its maximum fuel for cruise. Find the maximum range when the cruising has started at the altitude of a) 4 km, b) 8 km, and c) 12 km.

9.15 Aircraft C cruises at an altitude of 4 km under constant $h\text{-}V$ flight program and consumes 640,000 N fuel during the cruise. For a) maximum range, and b) maximum endurance, calculate the following: i) The airspeed and Mach number. Can these airspeeds be realized in practice? ii) Lift coefficient, aerodynamic efficiency, and thrust-weight ratio at the beginning and at the end of the cruise. iii) The range and its endurance.

9.16 Solve Problem 9.15 if Aircraft C is cruising at an altitude of 8 km.

9.17 Solve Problem 9.15 if Aircraft C is cruising at an altitude of 12 km.

9.18 Plot the variations of the lift coefficient, aerodynamic efficiency, and thrust-weight ratio in the cases of a) Problem 9.15, b) Problem 9.16, and c) Problem 9.17.

9.19 Solve Problem 9.15 if Aircraft B is cruising at an altitude of 4 km and uses a cruise-fuel weight fraction of 0.28 for the cruise.

9.20 Solve Problem 9.15 if Aircraft B is cruising at an altitude of 7 km and uses a cruise-fuel weight fraction of 0.28 for the cruise.

9.21 Solve Problem 9.15 if Aircraft B is cruising at an altitude of 10 km and uses a cruise-fuel weight fraction of 0.28 for the cruise.

9.22 Aircraft A starts cruising at an altitude of 2 km and consumes 75% of its fuel in the cruise. Compare the aircraft's constant $h\text{-}C_L$, constant $V\text{-}C_L$, and constant $h\text{-}V$ flights, for the cases of a) maximum-range airspeeds, b) maximum ranges, c) maximum-endurance airspeeds, and d) maximum endurance.

9.23 Repeat Problem 9.22 if Aircraft A starts cruising at an altitude of 4 km.

9.24 Solve Problem 9.22 if Aircraft B starts cruising at an altitude of 6 km and consumes 80% of its fuel for the cruise.

9.25 Solve Problem 9.22 if Aircraft C starts cruising at an altitude of 12 km and consumes 80% of its fuel for the cruise.

9.26 Aircraft C starts cruising at an altitude of 10 km at constant airspeed and consumes a cruise-fuel weight fraction of 0.24. Aerodynamic constraint fixes its cruising Mach number at 0.7. Find the maximum range and its altitude for constant $V\text{-}C_L$ flight.

9.27 Solve Problem 9.26 for Aircraft C cruising under constant $h\text{-}V$ flight program.

9.28 Aircraft C cruises at an altitude of 12 km initially, under maximum range conditions, using the stepped-altitude flight program with a) 609.6 m (2000 ft) steps, and b) 1219.2 m (4000 ft) steps. Find the range covered in kilometers in both the cases if 80% of the fuel is spent in the cruise. Also find the final altitude and the time spent during the cruise.

9.29 Aircraft A is scheduled to cover a range of 2000 km under maximum range conditions and starts cruising at an initial altitude of 2 km. Find the fuel required and the cruise-fuel weight fraction for a) constant $h\text{-}V$ flight, b) cruise-climb flight, and c) constant $h\text{-}C_L$ flight.

9.30 Repeat Problem 9.29 for Aircraft C, at an initial altitude of 11 km.

9.31 Solve Problem 9.29 for Aircraft C, using a stepped-altitude flight program when the increase in each step height is a) 609.6 m (2000 ft) and b) 1219.2 m (4000 ft).

9.32 Aircraft B cruises under maximum-range conditions at an altitude of 10 km, with a weight of 4600 kg_f and a fuel weight of 1500 kg_f . Answer the following: a) Find the range that can be covered using this fuel for a cruise-climb flight; b) If a drop tank of weight 60 kg_f is added to the aircraft, with a capacity of 600 kg_f of fuel, find the additional range that the aircraft can cover; c) If the drop tank is ejected following the consumption of its fuel, find the extra range covered.

Climbing Flights of Turbojet Aircraft

10.1 Introduction

A climbing flight is always required for reaching a necessary altitude after liftoff. Air traffic control regulations or the pattern of winds may also require changing the altitude of aircraft during its cruise. The climb performance of a military aircraft may become a primary design requirement for the need to reach a specified altitude and airspeed in minimum time. Sufficient attention is paid toward climb performance while designing an aircraft, because many fatal accidents have occurred during the climb phase of flights.

The basic equations of climb are obtained here both for steady and unsteady climbs. In a steady climb, the airspeed of aircraft remains constant, whereas in an unsteady climb, the aircraft accelerates and the airspeed continuously changes during the climb. The performance parameters of interest during the climbing phase are the angle of climb, rate of climb, horizontal distance covered, time taken, and the fuel consumed in climb. First, steady climb is considered here and subsequently the unsteady climb is discussed.

In a steady climb, the angle of climb and the rate of climb can generally be obtained in analytic forms, but the horizontal distance covered, time taken, and the fuel consumed have integral forms. Steady climb performance is optimized with respect to airspeed, both for the steepest and fastest climbs. These two cases are of much practical interest and are regarded as figures of merit of the aircraft. Under certain conditions it is possible to express all the climb performance parameters in analytic forms. The analytical results are obtained here for the case of standard atmosphere, but the analysis developed later in Chapter 18 for reducing aircraft performance data of nonstandard atmosphere to standard atmosphere conditions can also be applied here in reverse order, for obtaining the results of performance in nonstandard atmosphere from that of the standard atmosphere conditions.

The accelerated climb assumes importance in modern jet aircraft. The acceleration of aircraft gives rise to an inertia force in the equations of motion which makes performance analysis more difficult. Accelerated climbs are sometimes preferred for optimization by energy methods, involving calculus of variations. The method is only very briefly discussed here since it is also detailed in Chapter 18.

10.2 Basic Equations of Climb

The angle that the flight path makes with the horizontal during climb is called the *climb angle* and is denoted by γ . Consider an aircraft of weight W climbing at an angle γ as shown in Fig. 10.1. The flight path and the basic forces acting on the aircraft during climb are shown in this figure. Let F be the thrust force required during the climb, D the aerodynamic drag force, and x and h the horizontal and vertical distances traveled, respectively, in the climb. A steady climb of constant airspeed is considered here so that the aircraft has no acceleration along the flight

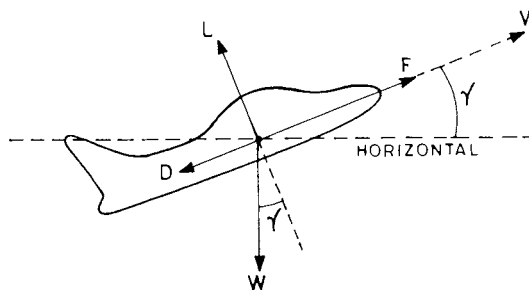


Fig. 10.1 Forces on aircraft during climb.

path. Application of Newton's second law of motion along the flight path and normal to it, respectively, gives

$$F - D - W \sin \gamma = 0 \quad (10.1)$$

and

$$L - W \cos \gamma = 0 \quad (10.2)$$

Equation (10.1) is valid only for steady flight. In the case of acceleration along the flight path, the inertia force $-(W/g)dV/dt$, where g is the acceleration due to gravity, should be added to the left-hand side of Eq. (10.1), and such cases are considered in Secs. 10.7 and 10.8. Equation (10.2) suggests that the lift force is less than the weight of the aircraft during climb. This may at first sight appear to be rather an anomaly, but it is not so because the lift force, by definition, is always taken normal to the flight path and not vertically up.

The velocity V is the airspeed along the flight path. The horizontal velocity dx/dt , and the vertical velocity dh/dt , are the components of airspeed along the horizontal and vertical directions, respectively. This gives rise to the two kinematic relations

$$dx/dt = V \cos \gamma \quad (10.3)$$

and

$$dh/dt = V \sin \gamma \quad (10.4)$$

which will be used later in the calculations of horizontal and vertical distances traveled during the climb. The term dh/dt is called the rate of climb, which is briefly written as R/C or \dot{h} . The above two relations are true when the wind effect is negligible.

The expression for the rate of fuel consumption is just the same as for the cruising flight (Eq. 8.4),

$$-dW/dt = cF \quad (10.5)$$

where c is the thrust-specific fuel consumption (TSFC). For a well-designed aircraft that is climbing efficiently, the fuel burned during the climb is a small

fraction of the total weight of the aircraft. It is often convenient for theoretical analysis to regard the weight of the aircraft as constant during the climb. The above five relations help to deduce important climb parameters.

10.3 Climbing Flight Parameters

The important climbing flight parameters of aircraft performance are the climb angle γ , the rate of climb h , the time taken in climb t , and the horizontal distance traveled x during the climb. The methods of calculating them for a given aircraft will be discussed here.

10.3.1 Climb Angle

The climb angle is obtained from Eq. (10.1) as

$$\sin \gamma = (F - D)/W \quad (10.6)$$

The difference $F - D$ is called the *excess thrust* that may be available at the altitude. The quantity $(F - D)/W$ is the excess thrust per unit weight, called the *specific thrust* of the aircraft. The excess thrust per unit weight directly fixes the climb angle. The increase in excess thrust of a given aircraft increases its climb angle, and vice versa. The excess thrust at any altitude can be varied by controlling F by throttling the aircraft power plant.

Equation (10.6), after using Eq. (10.2), can be written as

$$\sin \gamma = F/W - D/W = F/W - \cos \gamma/E \quad (10.7)$$

where the aerodynamic efficiency E is the lift/drag ratio L/D of the aircraft. In practice the climb angle γ (in radians) is generally small so that $\sin \gamma$ can be approximated as γ and $\cos \gamma$ becomes equal to unity. This approximation gives reasonable accuracy up to about $\gamma = 30$ deg. The climb angle does not exceed this limit in many practical cases; for most conventional subsonic aircraft the angle of climb is limited¹ to about 10–15 deg. The above relation simplifies to

$$\gamma = F/W - 1/E \quad (10.8)$$

where γ is in radians. The thrust per unit weight and the aerodynamic efficiency decide the climb angle.

The term $1/E$ of the above relation can be further expressed in terms of aircraft design parameters and γ can be written in a different form as shown below:

$$1/E = C_D/C_L = (C_{D_0} + K C_L^2)/C_L = C_{D_0}/C_L + K C_L$$

where C_L and C_D are the lift and drag coefficients, respectively, C_{D_0} is the zero-lift drag coefficient, and K is the lift-dependent drag coefficient factor. From the definition of lift coefficient,

$$C_L = \frac{2L}{\rho V^2 S} = \frac{2W \cos \gamma}{\rho V^2 S} \cong \frac{2(W/S)}{\rho V^2} = \frac{2(W/S)}{\rho_{SSL} \sigma V^2} \quad (10.9)$$

where the density ratio $\sigma = \rho/\rho_{SSL}$ and the subscript SSL represents standard atmosphere at sea level. The expression for $1/E$ can be written as

$$1/E = \rho_{SSL}\sigma V^2 C_{D_0}/\{2(W/S)\} + 2K(W/S)/(\rho_{SSL}\sigma V^2) \quad (10.10)$$

and the climb angle γ of Eq. (10.8) becomes

$$\gamma = F/W - [\rho_{SSL}\sigma V^2 C_{D_0}/\{2(W/S)\} + 2K(W/S)/(\rho_{SSL}\sigma V^2)] \quad (10.11)$$

The climb angle decreases with the increase in altitude (and thus decrease in σ) because the decline in thrust is faster. The decrease in C_{D_0} and K increases the climb angle.

10.3.2 Rate of Climb

The rate of climb of an aircraft is the change in its altitude per unit time. Having obtained the climb angle γ in the previous subsection, we may obtain the rate of climb from Eq. (10.4) as

$$\dot{h} = dh/dt = R/C = V \sin \gamma \quad (10.12)$$

In practice, γ (in radians) is small, and the above relation can be written as

$$\dot{h} = V\gamma = (F/W)V - V/E \quad (10.13)$$

which shows that the rate of climb increases by increasing F and E . The above relation can also be expressed as

$$\dot{h} = (FV - DV)/W \quad (10.14)$$

where the difference $FV - DV$ is called the *excess power*. The quantity $(FV - DV)/W$ is the excess power per unit weight, called *specific excess power* of the aircraft. The excess power per unit weight directly gives the rate of climb. The excess power is an important quantity in a maneuver of the aircraft; the higher the excess power, the greater is the maneuverability.

The rate of climb in terms of aircraft design parameters is obtained by using Eq. (10.10) in Eq. (10.13). This gives

$$\dot{h} = (F/W)V - [(\rho_{SSL}\sigma V^3 C_{D_0})/\{2(W/S)\} + 2K(W/S)/(\rho_{SSL}\sigma V)] \quad (10.15)$$

It can be seen that the rate of climb decreases with the increase in the altitude. A decrease in the design parameters K and C_{D_0} increases the rate of climb.

10.3.3 Time Taken in Climb

The time taken in climb can be written in differential form, $dt = dh/\dot{h}$, which on integration gives

$$t = \int_{h_1}^{h_2} dh/\dot{h} \quad (10.16)$$

where t is the time taken in climbing from an altitude h_1 to h_2 . The rate of climb in terms of aircraft design parameters is given by Eq. (10.15). This functional form of \dot{h} is generally such that it is not possible to integrate the right-hand side of the above relation in an analytical form; it would thus require numerical integration. It may, however, be possible to integrate it analytically in certain specific situations, or after making certain simplifying assumptions as discussed below in Secs. 10.4 and 10.5.

10.3.4 Distance Traveled in Climb

The horizontal distance x traveled during the climb would be calculated here. This is obtained from the exchange ratio dx/dh between the horizontal and vertical displacements, which can be expressed as

$$dx/dh = (dx/dt)/(dh/dt) = V \cos \gamma / (V \sin \gamma) = \cos \gamma / \sin \gamma$$

Since γ is small in practice, the above relation can be written as, $dx/dh = 1/\gamma$, i.e., $dx = dh/\gamma$, which on integration gives

$$x = \int_{h_1}^{h_2} dh/\gamma \quad (10.17)$$

where x is the horizontal distance traveled by the aircraft while climbing from an altitude h_1 to h_2 . The integration of the right-hand side of the above relation in a closed form depends on the functional form of the climb angle γ , otherwise it can be integrated numerically.

10.3.5 Fuel Consumption in Climb

The amount of fuel consumed in the climb can be calculated from the fuel-altitude exchange ratio dW/dh by writing

$$dW/dh = (dW/dt)/(dh/dt) = -c F / \dot{h}$$

which in differential form can also be written as

$$dW/W = -c(F/W)dh/\dot{h} \quad (10.18)$$

If W_1 and W_2 are the weights of the aircraft at altitudes h_1 and h_2 , respectively, the integration of the above relation gives

$$\int_{W_1}^{W_2} dW/W = -c \int_{h_1}^{h_2} (F/W)dh/\dot{h} \quad (10.19)$$

where c is taken as constant. The loss of weight of the aircraft will be considered due to its fuel consumption only. The left-hand side of the above relation can be integrated to yield

$$W_2/W_1 = \exp \left\{ -c \int_{h_1}^{h_2} (F/W)dh/\dot{h} \right\} \quad (10.20)$$

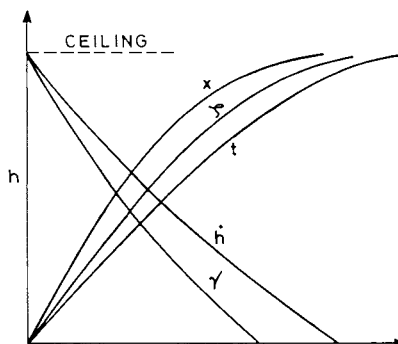


Fig. 10.2 Typical variations of γ , \dot{h} , x , t , and ζ with altitude in climb.

Introducing the climb-fuel weight fraction ζ as

$$\zeta = \Delta W_f / W_1, \quad \Delta W_f = W_1 - W_2 \quad (10.21)$$

where ΔW_f is the weight of fuel consumed during the climb, Eq. (10.20) becomes

$$\zeta = 1 - \exp \left\{ -c \int_{h_1}^{h_2} (F/W) dh / \dot{h} \right\} \quad (10.22)$$

The power of the exponential on the right-hand side is in the integral form whose integration in a closed form would depend on the functional form of the integrand, otherwise it can be integrated numerically.

The typical variations of γ , \dot{h} , x , t , and ζ with altitude during climb of an aircraft are shown in Fig. 10.2. The angle γ and \dot{h} decrease, whereas x , t , and ζ increase, with an increase in the altitude during the climb. The figure also shows the ceiling altitude by a dashed line, which is the subject matter of the following section.

10.3.6 Ceiling Altitudes

It has been seen that for a constant throttle setting the rate of climb of aircraft is continuously decreasing with the increasing altitude, until the rate of climb eventually vanishes. The *ceiling altitude* of an aircraft is defined as the altitude where it has a specified rate of climb for the given throttle setting. At the absolute ceiling the maximum rate of climb is zero, whereas it has certain specified rates of climb in the other types of ceiling altitudes.

10.3.6.1 Absolute ceiling. A ceiling altitude of a given aircraft depends on its throttle setting. The altitude at which the rate of climb becomes zero for a particular throttle setting is called the absolute ceiling for that throttle setting. The more the throttle, the higher is its absolute ceiling. The absolute ceiling achieved when the throttle is fully open is called the *absolute ceiling* or simply *ceiling* of the aircraft. It is possible to calculate the altitude and airspeed at the absolute ceiling for constant throttle climb.

At the absolute ceiling, the thrust required and the thrust-available curves meet each other tangentially, as shown in Fig. 8.6. At the ceiling altitude only one

airspeed in the horizontal direction is possible. This implies that the radicand in Eq. (8.8) must be zero at absolute ceiling, which gives

$$F_C/W_C = 1/E_m \quad (10.23)$$

where subscript C represents the condition at the absolute ceiling. For a constant throttle climb,

$$F_C/F_{SSL} = \sigma_C \quad (10.24)$$

which after using Eq. (10.23) becomes

$$\sigma_C = 1/\{(F_{SSL}/W)E_m\} \quad (10.25)$$

where F_{SSL} is not necessarily the maximum available thrust $F_{m,SSL}$ in standard atmosphere at sea level. The altitude corresponding to σ_C can be obtained from the table or graph of the standard atmosphere.

It is clear from Eq. (10.25) that σ_C can be decreased, and thus the ceiling for a given throttle setting can be increased, by increasing the throttle. If $\sigma_{C,\min}$ denotes the minimum value of σ_C , it is obtained from Eq. (10.25) as

$$\sigma_{C,\min} = 1/\{(F_{m,SSL}/W)E_m\} \quad (10.26)$$

The altitude corresponding to $\sigma_{C,\min}$ would be the *absolute ceiling* or simply the *ceiling* of the aircraft.

The airspeed V_C at the ceiling is obtained from Eq. (8.8) by putting its radicand equal to zero. This gives

$$V_C = \left\{ \frac{(F_C/W)(W/S)}{\rho_{SSL}\sigma_C C_{D_0}} \right\}^{1/2} = \left\{ \frac{(F_{SSL}/W)(W/S)}{\rho_{SSL} C_{D_0}} \right\}^{1/2} \quad (10.27)$$

which shows the influence of aircraft design parameters on the airspeed at ceiling altitude. The V_C would be horizontal velocity because an aircraft is unable to climb beyond its ceiling altitude.

The absolute ceiling of an aircraft is only its theoretical measure of the maximum altitude, because the absence of excess power at that altitude leaves the aircraft with very poor handling qualities, making it most undesirable to fly at the ceiling. Any disturbance to the aircraft may put it in a nonequilibrium condition with no excess thrust to control the aircraft at the ceiling altitude. An aircraft can, however, temporarily fly for a short time above its absolute ceiling by zooming. The act of zooming exchanges the kinetic energy of the aircraft with its potential energy, but soon it has to come down to its absolute ceiling altitude or below.

10.3.6.2 Service and performance ceilings. Since absolute ceiling is a theoretical measure, it is better to define another ceiling altitude that can be a practical measure of maximum operating height and yet close to absolute ceiling. This height is called the *service ceiling* of the aircraft, which is defined as the altitude where the maximum rate of climb is 0.51 m/s (100 ft/min) for a jet aircraft. The service ceiling is commonly used for performance or design specification of a military aircraft. For civil aircraft, a ceiling altitude called the *performance ceiling*

is used,² which is defined as the altitude where the maximum rate of climb is 0.762 m/s (150 ft/min). There is yet another ceiling altitude of an aircraft that is referred to as the *operational ceiling*,³ which is defined as the altitude where the maximum rate of climb is 2.54 m/s (500 ft/min).

10.4 Steepest Climb

The analytical expressions for γ and \dot{h} , and the integral forms for x , t , and ξ have been obtained earlier for a climbing flight. These quantities will now be obtained for the particular cases of special interest—steepest climb, fastest climb, and the most economical climb. The study of steepest climb is undertaken here first and the subsequent Secs. 10.5 and 10.6 deal with the other two cases.

The *steepest climb* is the one where the climb angle is always maintained at its maximum possible angle during the climb. The subscript SC will be used to represent the condition of steepest climb angle γ_m . The steepest climb flight establishes the upper limit of the climb angle that an aircraft can achieve. It has better capability of clearing the obstacles safely around an airport than any other type of climb.

10.4.1 Climb Angle and Airspeed of Steepest Climb

The maximum climb angle γ_m is directly obtained from Eq. (10.8) as

$$\gamma_{\text{SC}} = \gamma_m = F_m / W - 1/E_m \quad (10.28)$$

where γ_m is in radians, and both F_m and E_m are design parameters of the aircraft. Considering that, for a given throttle setting, the engine thrust varies linearly with the density of the atmosphere, the thrust ratio F/F_{SSL} can be written as

$$F/F_{\text{SSL}} = F_m/F_{m,\text{SSL}} = \rho/\rho_{\text{SSL}} = \sigma \quad (10.29)$$

Using the value of F_m from the above relation, Eq. (10.28) becomes

$$\gamma_m = (F_{m,\text{SSL}}/W)\sigma - 1/E_m \quad (10.30)$$

This shows that the steepest climb is achieved by maximizing the thrust/weight ratio and the aerodynamic efficiency. The E_m and $F_{m,\text{SSL}}$ being constant quantities of a given aircraft, the steepest climb angle γ_m varies linearly with σ if W is assumed constant during the climb.

A quick estimate of γ_m can be obtained by retaining only the first term on the right-hand side of Eq. (10.30), giving $\gamma_m \approx (F_{m,\text{SSL}}\sigma)/W$. As an example, for $F_{m,\text{SSL}}/W = 0.25$, which is a typical value for a subsonic jet transport aircraft, the maximum climb angle γ_m will not exceed 14 deg during the climb. As the altitude increases, the γ_m decreases and ultimately reduces to zero at the absolute ceiling. It is seen above that the steepest climb is achieved by flying at the maximum aerodynamic efficiency. Therefore, the airspeed V_{SC} of the steepest climb would be given by

$$V_{\text{SC}} = V_{E_m} = \left\{ \frac{2(W/S)}{\rho_{\text{SSL}}\sigma} \right\}^{1/2} \left(\frac{K}{C_{D_0}} \right)^{1/4} = \left(\frac{W}{W_o} \right)^{1/2} \frac{V_{E_m,\text{SSL}}}{\sqrt{\sigma}} \quad (10.31)$$

where W_o is the takeoff weight of the aircraft, and $V_{E_m,SSL}$ is the value of V_{E_m} in standard atmosphere at sea level. Since the airspeeds for minimum drag and maximum aerodynamic efficiency are the same, it follows that the steepest climb airspeed is the same as that required for the minimum-drag airspeed. This is also an obvious conclusion by looking at the thrust required and thrust available curves of Fig. 8.6, which shows that the maximum excess thrust occurs when the drag is minimum. It is pertinent to note that the steepest climb airspeed is independent of the engine thrust. It can also be seen from Eq. (10.31) that the steepest climb airspeed increases slowly with the increase in altitude because the decrease in σ with altitude is faster than the decrease in wing loading due to fuel consumption. The slow increase in V_{SC} with altitude may justify the omission of acceleration term (inertia force) from Eq. (10.1).

10.4.2 Rate of Climb of Steepest Climb

The rate of climb \dot{h}_{SC} of the steepest climb is obtained from Eq. (10.12) as $\dot{h}_{SC} = V_{SC} \sin \gamma_m$, and with the assumption that γ_m is generally small, the steepest rate of climb becomes

$$\dot{h}_{SC} = V_{SC} \gamma_m \quad (10.32)$$

Using the values of γ_m and V_{SC} from Eqs. (10.28) and (10.31), respectively, the expression for \dot{h}_{SC} can be written as

$$\dot{h}_{SC} = \{2(W/S)/(\rho_{SSL}\sigma)\}^{1/2} (K/C_{D_0})^{1/4} (F_m/W - 1/E_m) \quad (10.33)$$

which after using Eq. (10.29) for constant throttle climb becomes

$$\dot{h}_{SC} = \{2(W/S)/(\rho_{SSL}\sigma)\}^{1/2} (K/C_{D_0})^{1/4} \{(F_{m,SSL}/W)\sigma - 1/E_m\} \quad (10.34)$$

It can now be seen from Eq. (10.34) that \dot{h}_{SC} increases with the increase in wing loading W/S , maximum thrust/weight ratio $F_{m,SSL}/W$, and the maximum aerodynamic efficiency E_m , of the aircraft.

10.4.3 Time and Distance Covered in Steepest Climb

The time taken t_{SC} in the steepest climb from an altitude h_1 to h_2 is obtained from Eq. (10.16) as

$$t_{SC} = \int_{h_1}^{h_2} dh / \dot{h}_{SC} \quad (10.35)$$

where \dot{h}_{SC} is given by Eq. (10.34). Introducing the notations A and B for the sake of brevity as

$$A = \{2(W/S)/\rho_{SSL}\}^{1/2} (K/C_{D_0})^{1/4} (1/E_m) = (W/W_0)^{1/2} V_{E_m,SSL}/E_m \quad (10.36)$$

and

$$B = E_m (T_{m,SSL}/W) = \{E_m/(W/W_0)\} (T_{m,SSL}/W_0) \quad (10.37)$$

where both A and B are constants because the change in weight of the aircraft due to fuel consumption is considered insignificant in the climb, i.e., $W \cong W_o$ during the climb. Equation (10.34) can thus be written as

$$\dot{h}_{SC} = A(B\sigma - 1)/\sqrt{\sigma} \quad (10.38)$$

and Eq. (10.35) becomes

$$t_{SC} = \frac{1}{A} \int_{h_1}^{h_2} \sqrt{\sigma} dh / (B\sigma - 1) \quad (10.39)$$

For integrating the right-hand side of the above equation, express the density ratio σ according to Eq. (2.13) as

$$\sigma = \epsilon e^{-(h-h^*)/\beta} \quad (10.40)$$

where the values of ϵ , h^* , and β depend on whether the climb is taking place in the troposphere ($h \leq 11$ km) or in the stratosphere ($h > 11$ km) as follows: for $h \leq 11$ km, the values are

$$\epsilon = 1.0, \quad h^* = 0, \quad \text{and} \quad \beta = 9296 \text{ m} \quad (10.41)$$

and for $h > 11$ km, the values are

$$\epsilon = 0.3063, \quad h^* = 11000 \text{ m}, \quad \text{and} \quad \beta = 6216 \text{ m} \quad (10.42)$$

Using Eq. (10.40), the t_{SC} of Eq. (10.39) can be expressed as

$$t_{SC} = -(\beta/A) \int_{\sigma_1}^{\sigma_2} d\sigma / \{(B\sigma - 1)\sqrt{\sigma}\} \quad (10.43)$$

where σ_1 and σ_2 are the values of σ at h_1 and h_2 , respectively. Solving the right-hand-side integral of Eq. (10.43), t_{SC} can be expressed in analytic form as

$$t_{SC} = \frac{\beta}{A\sqrt{B}} \ln \frac{(\sqrt{\beta\sigma_1} - 1)(\sqrt{\beta\sigma_2} + 1)}{(\sqrt{\beta\sigma_1} + 1)(\sqrt{\beta\sigma_2} - 1)} \quad (10.44)$$

where σ_1 and σ_2 can be obtained from Eq. (10.40) as

$$\sigma_1 = \epsilon e^{-(h_1-h^*)/\beta} \quad \text{and} \quad \sigma_2 = \epsilon e^{-(h_2-h^*)/\beta} \quad (10.45)$$

Using these values of σ_1 and σ_2 in Eq. (10.44) the expression for t_{SC} becomes

$$t_{SC} = \frac{\beta}{A\sqrt{B}} \ln \frac{(\sqrt{B\epsilon} e^{-(h_1-h^*)/2\beta} - 1)(\sqrt{B\epsilon} e^{-(h_2-h^*)/2\beta} + 1)}{(\sqrt{B\epsilon} e^{-(h_1-h^*)/2\beta} + 1)(\sqrt{B\epsilon} e^{-(h_2-h^*)/2\beta} - 1)} \quad (10.46)$$

where ϵ , h^* , and β , are given by Eqs. (10.41) and (10.42), and A and B are obtained from Eqs. (10.36) and (10.37), respectively.

The horizontal distance covered x_{SC} in the steepest climb will be obtained from Eq. (10.17) as

$$x_{SC} = \int_{h_1}^{h_2} dh / \gamma_m$$

which after using the expression for γ_m from Eq. (10.30) becomes

$$x_{SC} = E_m \int_{h_1}^{h_2} dh / (B\sigma - 1) \quad (10.47)$$

The above equation after using Eq. (10.40) can be written as

$$x_{SC} = -\beta E_m \int_{\sigma_1}^{\sigma_2} d\sigma / \{\sigma(B\sigma - 1)\}$$

where the right-hand-side integral can be evaluated and x_{SC} can be expressed as

$$x_{SC} = \beta E_m \ln[\{B - (1/\sigma_1)\}/\{B - (1/\sigma_2)\}] \quad (10.48)$$

which after using the relations of Eq. (10.45) becomes

$$x_{SC} = \beta E_m \ln[\{B\epsilon - e^{(h_1-h^*)/\beta}\}/\{B\epsilon - e^{(h_2-h^*)/\beta}\}] \quad (10.49)$$

where the values of ϵ , h^* , and β are given by Eqs. (10.41) and (10.42), and A and B are obtained from Eqs. (10.36) and (10.37), respectively.

10.4.4 Fuel Consumption in Steepest Climb

The amount of fuel consumed (ΔW_f)_{SC} in the steepest climb from an altitude h_1 to h_2 is obtained here in a nondimensional form of the climb-fuel weight fraction ξ_{SC} . It is obtained from Eq. (10.22) as

$$\xi_{SC} = 1 - \exp\left\{-c \int_{h_1}^{h_2} (F_m/W) dh / \dot{h}_{SC}\right\} \quad (10.50)$$

Using Eqs. (10.29) and (10.38) for F_m and \dot{h}_{SC} , respectively, the above equation can be written as

$$\xi_{SC} = 1 - \exp\left[\{-c(F_{m,SSL}/W)/A\} \int_{h_1}^{h_2} \sigma \sqrt{\sigma} dh / (B\sigma - 1)\right] \quad (10.51)$$

which after using Eq. (10.40) becomes

$$\xi_{SC} = 1 - \exp\left[\{\beta c(F_{m,SSL}/W)/A\} \int_{\sigma_1}^{\sigma_2} \sqrt{\sigma} d\sigma / (B\sigma - 1)\right]$$

Solving the right-hand-side integral, the above equation becomes

$$\begin{aligned}\xi_{SC} = 1 - \exp & \left[\frac{2\beta c(F_{m,SSL}/W)}{AB} \left\{ (\sqrt{\sigma_2} - \sqrt{\sigma_1}) \right. \right. \\ & \left. \left. + \frac{1}{2\sqrt{B}} \ln \frac{(\sqrt{B\sigma_2} - 1)(\sqrt{B\sigma_1} + 1)}{(\sqrt{B\sigma_2} + 1)(\sqrt{B\sigma_1} - 1)} \right\} \right] \quad (10.52)\end{aligned}$$

and expressing σ_1 and σ_2 as given by the relations of Eq. (10.45), the above equation becomes

$$\begin{aligned}\xi_{SC} = 1 - \exp & \left[\frac{2\beta c(F_{m,SSL}/W)}{AB} \left\{ (\sqrt{\epsilon} e^{-(h_2-h^*)/2\beta} - \sqrt{\epsilon} e^{-(h_1-h^*)/2\beta}) \right. \right. \\ & \left. \left. + \frac{1}{2\sqrt{B}} \ln \frac{(\sqrt{B\epsilon} e^{-(h_2-h^*)/2\beta} - 1)(\sqrt{B\epsilon} e^{-(h_1-h^*)/2\beta} + 1)}{(\sqrt{B\epsilon} e^{-(h_2-h^*)/2\beta} + 1)(\sqrt{B\epsilon} e^{-(h_1-h^*)/2\beta} - 1)} \right\} \right] \quad (10.53)\end{aligned}$$

where ϵ , h^* , and β are obtained from Eqs. (10.41) and (10.42), and A and B are given by Eqs. (10.36) and (10.37), respectively.

The steepest climb parameters of the aircraft considered below in Sec. 10.9 are shown in Figs. 10.3 and 10.4. The variations of airspeed, climb angle, and rate

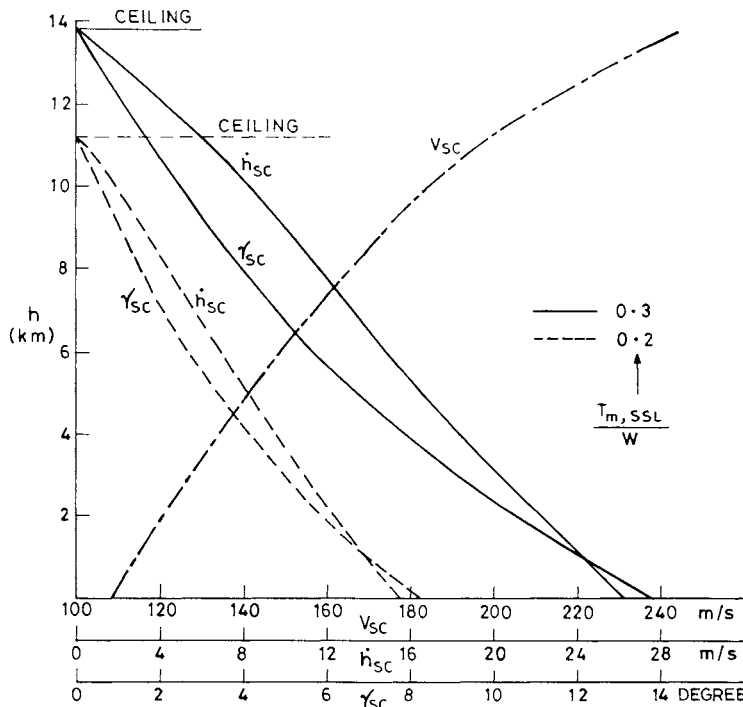


Fig. 10.3 Changes in V_{SC} , γ_{SC} , and \dot{h}_{SC} , with altitude.

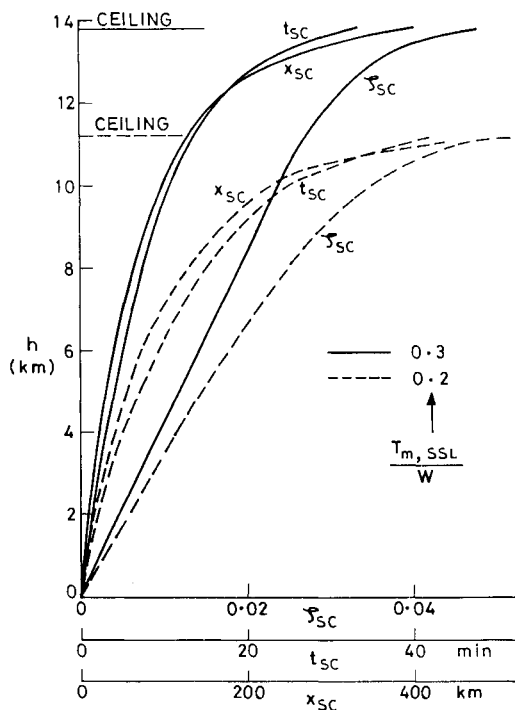


Fig. 10.4 Changes in t_{SC} , x_{SC} , and ζ_{SC} with altitude.

of climb against altitude are shown in Fig. 10.3 for two different values (0.2 and 3) of the maximum thrust/weight ratio at sea level. The ceiling altitudes are also marked in the two cases. Similarly, the horizontal distance covered, time taken, and fuel consumed during the climb are shown in Fig. 10.4 for the two cases of maximum thrust/weight ratio at sea level.

10.5 Fastest Climb

The maximum rate of climb is called the *fastest climb*. The subscript FC will be used to represent the condition of fastest climb \dot{h}_m . The fastest climb takes minimum time to climb to a specified altitude and it is quite close to the minimum fuel consumption climb. Its importance to air traffic control lies in keeping the intervening air space clear of traffic for a longer duration. Generally the fastest climb has greater importance than the steepest climb, and it is a figure of merit of the aircraft.

10.5.1 Airspeed and Climb Angle of Fastest Climb

The airspeed V_{FC} of the fastest climb is obtained by optimizing \dot{h} of Eq. (10.14) with respect to V . This requires

$$\frac{d\dot{h}}{dV} = \frac{d\{(FV - DV)/W\}}{dV} = 0 \quad (10.54)$$

Assuming W to be constant during the climb, the above relation on completing the differentiation gives the condition of fastest climb as

$$F - D - VdD/dV = 0 \quad (10.55)$$

for $V = V_{FC}$. The drag force in the above relation can be expressed as $D = C_D \rho V^2 S/2 + (C_{D_0} + K C_L^2) \rho V^2 S/2$, which after making the level-flight approximation, $L = W$ as in Eq. (10.9), becomes $D = C_{D_0} \rho V^2 S/2 + 2K W^2 / (\rho V^2 S)$. Substitution of this value of D and its derivative dD/dV in Eq. (10.55) gives

$$(3C_{D_0}\rho^2S^2)V^4 - (2\rho SF)V^2 - 4KW^2 = 0$$

for $V = V_{FC}$. The solution of the above algebraic equation is

$$V_{FC}^2 = \frac{F/S}{3\rho C_{D_0}} \left\{ 1 \pm \sqrt{1 + 12C_{D_0}K(W/F)^2} \right\}$$

and retaining only positive sign so that V_{FC} remains a real quantity, the above relation can be written as

$$V_{FC} = \left[\frac{(F/W)(W/S)}{3\rho_{SSL}\sigma C_{D_0}} \left\{ 1 + \sqrt{1 + \frac{3}{E_m^2(F/W)^2}} \right\} \right]^{1/2} \quad (10.56)$$

The fastest climb airspeed is found to increase with the increase in wing loading, thrust/weight ratio, and altitude.

For the sake of brevity, introduce the notation Γ as

$$\Gamma = \left[1 + \sqrt{1 + 3/E_m^2(F/W)^2} \right]^{1/2} \quad (10.57)$$

where Γ is a nondimensional quantity that is quite useful in obtaining the analytic expressions of the fastest climb parameters. Some observations can be made about the magnitude of Γ which suggest that Γ can be regarded as constant. At sea level F/W is maximum so that the value of Γ approaches 2. On the other hand, at ceiling altitude, $E_m(F/W) = 1$ [Eq. (8.9)], and so the Γ approaches 3 at the ceiling. Therefore, the value of Γ ranges between 2 and 3 for any given aircraft. Consequently, the changes in E_m and (F/W) of different aircraft do not have a powerful influence on Γ . This suggests that for mathematical simplification Γ can be regarded as constant. Hale⁴ considers $\Gamma = 2$ as a constant value in climb performance. We have regarded Γ as constant without assigning any particular value to it when it occurs inside an integral sign. After solving the integral, Γ can be treated as variable [Eq. (10.57)] or $\Gamma = 2.3$ for improving the results.

The fastest climb airspeed expressed by Eq. (10.56) can be written as

$$V_{FC} = \left\{ (F/W)(W/S)\Gamma / (3\rho_{SSL}\sigma C_{D_0}) \right\}^{1/2} \quad (10.58)$$

The fastest climb angle γ_{FC} for a given thrust/weight ratio is obtained from Eq. (10.8) as

$$\gamma_{FC} = F/W - 1/E_{FC} \quad (10.59)$$

where E_{FC} is the aerodynamic efficiency of the fastest climb. The term $1/E_{FC}$ can be obtained in terms of aircraft design parameters by writing $V = V_{FC}$ in Eq. (10.10) and using Eq. (10.58). This gives

$$1/E_{FC} = (F/W)\Gamma/6 + 3/\{2E_m^2(F/W)\Gamma\}$$

The γ_{FC} can now be obtained from Eq. (10.59) as

$$\gamma_{FC} = (F/W)(1 - \Gamma/6) - 3/\{2E_m^2\Gamma(F/W)\} \quad (10.60)$$

which shows that the fastest climb angle increases with the increase in thrust/weight ratio, F/W , and maximum lift/drag ratio E_m .

For a constant throttle climb $F = F_{SSL}\sigma$, the above Eq. (10.60) becomes,

$$\gamma_{FC} = (F_{SSL}/W)(1 - \Gamma/6)[\sigma - \{(2/3)\Gamma(1 - \Gamma/6)E_m^2(F_{SSL}/W)^2\sigma\}^{-1}] \quad (10.61)$$

where

$$\Gamma = 1 + \sqrt{1 + 3/\{E_m^2(F_{SSL}/W)^2\sigma^2\}} \quad (10.62)$$

Equation (10.61) predicts the fastest climb angle in terms of the aircraft design parameters.

10.5.2 Fastest (Maximum) Rate of Climb

The maximum rate of climb \dot{h}_m is obtained from Eq. (10.13) as

$$\dot{h}_m = \dot{h}_{FC} = V_{FC} \cdot \gamma_{FC} \quad (10.63)$$

where V_{FC} and γ_{FC} are obtained from Eqs. (10.58) and (10.60), respectively. Substitution of these values in the above relation gives

$$\dot{h}_m = \left\{ \frac{(W/S)\Gamma}{3\rho_{SSL}\sigma C_{D_0}} \right\}^{1/2} \left(\frac{F}{W} \right)^{3/2} \left(1 - \frac{\Gamma}{6} \right) \left\{ 1 - \frac{3}{2\Gamma(1 - \Gamma/6)E_m^2(F/W)^2} \right\} \quad (10.64)$$

where Γ is given by Eq. (10.57).

If the throttle is kept constant during the climb, $F = F_{SSL}\sigma$, and Eq. (10.64) becomes

$$\begin{aligned} \dot{h}_m &= \left\{ \frac{(W/S)\Gamma}{3\rho_{SSL}C_{D_0}} \right\}^{1/2} \left(\frac{F_{SSL}}{W} \right)^{3/2} \left(1 - \frac{\Gamma}{6} \right) \\ &\times \left\{ \sigma - \frac{1}{(2/3)\Gamma(1 - \Gamma/6)E_m^2(F_{SSL}/W)^2\sigma} \right\} \end{aligned} \quad (10.65)$$

where Γ is given by Eq. (10.62). The above relation gives maximum rate of climb in terms of the aircraft design parameters.

10.5.3 Time and Distance Covered in Fastest Climb

The time taken t_{FC} , and the horizontal distance covered x_{FC} , in the fastest climb from an altitude h_1 to h_2 will be calculated here. The fastest climb takes minimum time to climb t_{min} , which is obtained from Eq. (10.16) as

$$t_{min} = t_{FC} = \int_{h_1}^{h_2} dh / \dot{h}_m \quad (10.66)$$

Considering that the throttle is kept constant during climb, Eq. (10.65) can be used for \dot{h}_m , but the above integral cannot generally be evaluated analytically. In view of the observations made earlier about Γ it is possible to obtain analytical solutions as shown below.

For the sake of brevity, introducing the notation b as

$$b = \{(2\Gamma/3)(1 - \Gamma/6)\}^{1/2} (F_{SSL}/W) E_m \quad (10.67)$$

where b will be constant when both Γ and W are considered constant during the climb. Equation (10.65) can be written as

$$\dot{h}_m = \left\{ \frac{(W/S)\Gamma}{3\rho_{SSL} C_{D_0}} \right\}^{1/2} \left(\frac{F_{SSL}}{W} \right)^{3/2} \left(1 - \frac{\Gamma}{6} \right) \left(\sigma - \frac{1}{b^2\sigma} \right) \quad (10.68)$$

and Eq. (10.66) becomes

$$t_{FC} = \left\{ \frac{3\rho_{SSL} C_{D_0}}{(W/S)\Gamma} \right\}^{1/2} \frac{1}{(F_{SSL}/W)^{3/2}(1 - \Gamma/6)} \int_{h_1}^{h_2} \frac{b^2\sigma}{b^2\sigma^2 - 1} dh$$

The above integral can be solved by using Eq. (10.40) and the t_{FC} can be obtained as

$$t_{FC} = \left\{ \frac{3\rho_{SSL} C_{D_0}}{(W/S)\Gamma} \right\}^{1/2} \frac{\beta b}{2(F_{SSL}/W)^{3/2}(1 - \Gamma/6)} \ln \left\{ \frac{(b\sigma_1 - 1)(b\sigma_2 + 1)}{(b\sigma_1 + 1)(b\sigma_2 - 1)} \right\} \quad (10.69)$$

which after using the relations of Eq. (10.45) becomes

$$t_{FC} = \left\{ \frac{3\rho_{SSL} C_{D_0}}{(W/S)\Gamma} \right\}^{1/2} \frac{\beta b}{2(F_{SSL}/W)^{3/2}(1 - \Gamma/6)} \ln \left\{ \frac{\{b\epsilon e^{-(h_1-h^*)/\beta} - 1\}}{\{b\epsilon e^{-(h_1-h^*)/\beta} + 1\}} \right. \\ \times \left. \frac{\{b\epsilon e^{-(h_2-h^*)/\beta} + 1\}}{\{b\epsilon e^{-(h_2-h^*)/\beta} - 1\}} \right\} \quad (10.70)$$

where ϵ , h^* , and β are given by Eqs. (10.41) and (10.42), b is obtained from Eq. (10.67), and Γ can be obtained from either Eq. (10.62) or $\Gamma = 2.3$ for simplicity.

The horizontal distance covered during the fastest climb is obtained from Eq. (10.17) as

$$x_{FC} = \int_{h_1}^{h_2} dh / \gamma_{FC} \quad (10.71)$$

where γ_{FC} after using Eqs. (10.61) and (10.67) can be written as

$$\gamma_{FC} = (F_{SSL}/W)(1 - \Gamma/6)\{\sigma - 1/(b^2\sigma)\}$$

and Eq. (10.71) becomes

$$x_{FC} = [1/\{(F_{SSL}/W)(1 - \Gamma/6)\}] \int_{h_1}^{h_2} b^2\sigma dh / (b^2\sigma^2 - 1)$$

The above integral can be evaluated by using Eq. (10.40) and x_{FC} can be obtained as

$$x_{FC} = \frac{\beta b}{2(F_{SSL}/W)(1 - \Gamma/6)} \ln \left\{ \frac{(b\sigma_1 - 1)(b\sigma_2 + 1)}{(b\sigma_1 + 1)(b\sigma_2 - 1)} \right\} \quad (10.72)$$

which can also be written as

$$x_{FC} = \frac{\beta b}{2(F_{SSL}/W)(1 - \Gamma/6)} \ln \left\{ \frac{\{b\epsilon e^{-(h_1-h^*)/\beta} - 1\}\{b\epsilon e^{-(h_2-h^*)/\beta} + 1\}}{\{b\epsilon e^{-(h_1-h^*)/\beta} + 1\}\{b\epsilon e^{-(h_2-h^*)/\beta} - 1\}} \right\} \quad (10.73)$$

where the values of ϵ , h^* , β , b , and Γ are the same as stated in the lines below Eq. (10.70).

10.5.4 Fuel Consumption in Fastest Climb

The amount of fuel consumed in the fastest climb is obtained in the nondimensional form of ξ_{FC} , which is given by Eq. (10.22) as

$$\xi_{FC} = 1 - \exp \left\{ -c \int_{h_1}^{h_2} (F/W)dh / \dot{h}_m \right\} \quad (10.74)$$

Writing $F = F_{SSL}\sigma$ for constant throttle climb, and using Eq. (10.68) for \dot{h}_m , the above equation can be written as

$$\xi_{FC} = 1 - \exp \left[-c \left\{ \frac{3\rho_{SSL} C_{D_0}}{(F_{SSL}/W)(W/S)\Gamma} \right\}^{1/2} \frac{1}{(1 - \Gamma/6)} \int_{h_1}^{h_2} \frac{b^2\sigma^2}{b^2\sigma^2 - 1} dh \right]$$

The integral on the right-hand side of the above equation can be solved by using Eq. (10.40), and ξ_{FC} can be obtained as

$$\xi_{FC} = 1 - \exp \left[\left\{ \frac{3\rho_{SSL} C_{D_0}}{(F_{SSL}/W)(W/S)\Gamma} \right\}^{1/2} \frac{\beta c}{2(1 - \Gamma/6)} \ln \frac{(b^2\sigma_2^2 - 1)}{(b^2\sigma_1^2 - 1)} \right] \quad (10.75)$$

Using the expressions of σ_1 and σ_2 from the relations of Eq. (10.45), the above equation becomes

$$\zeta_{FC} = 1 - \exp \left[\left\{ \frac{3\rho_{SSL} C_{D_0}}{(F_{SSL}/W)(W/S)\Gamma} \right\}^{1/2} \times \frac{\beta c}{2(1 - \Gamma/6)} \ln \frac{\{b^2 \epsilon^2 e^{-2(h_2 - h^*)/\beta} - 1\}}{\{b^2 \epsilon^2 e^{-2(h_1 - h^*)/\beta} - 1\}} \right] \quad (10.76)$$

where the values of ϵ , h^* , β , b and Γ are the same as stated in the lines below Eq. (10.70).

The fastest climb parameters of the aircraft considered below in Sec. 10.9 are shown in Figs. 10.5 and 10.6. The variations of airspeed, climb angle, and rate of climb are shown in Fig. 10.5 for two different values (0.2 and 0.3) of the maximum thrust/weight ratio at sea level. Similarly, the horizontal distance covered, time taken, and the fuel consumed are shown in Fig. 10.6 for the two cases of maximum thrust/weight ratio at sea level.

10.5.5 Numerical Method

The analytic expressions for V_{FC} , γ_{FC} , and \dot{h}_m were obtained in Secs. 10.5.1 and 10.5.2. The quantities t_{FC} , x_{FC} , and ζ_{FC} , obtained in Secs. 10.5.3 and 10.5.4

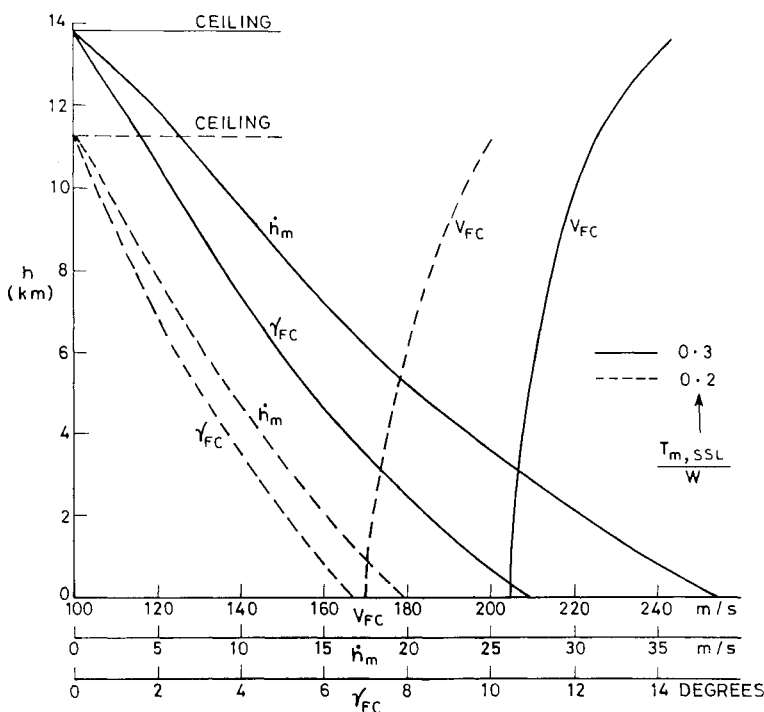


Fig. 10.5 Variations in V_{FC} , γ_{FC} , and \dot{h}_m with altitude.

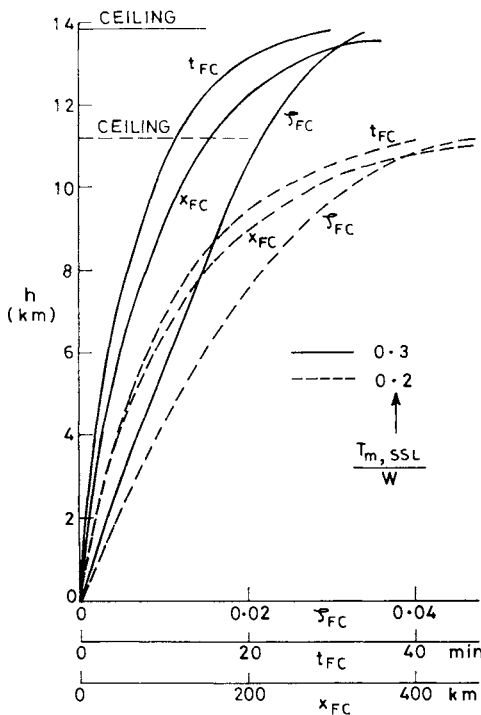


Fig. 10.6 Variations in t_{FC} , x_{FC} , and ζ_{FC} with altitude.

involved integrals that were evaluated by approximating Γ as constant. This approximation can be withdrawn by having recourse to numerical integration. The scheme of numerical integration explained here can be adopted for solving many other such integrals.

The numerical integration requires the altitude h of the climb to be divided into a number of intervals, each of length Δh_i ($i = 1, 2, 3, 4, n$), where $\Delta h_i = h_{i+1} - h_i$, and $\sum_{i=1}^n \Delta h_i = h$. The interval lengths can be chosen, say 50 m or smaller, and they need not to be of equal length. The subscript i represents the end-points, called the *pivotal points* of the intervals. The $i = 1$ and $n + 1$, respectively, correspond to the starting and end-points of the climb under consideration.

The method requires that the values of σ_i , $(\gamma_{FC})_i$, and $(\dot{h}_m)_i$ must be known beforehand at each pivotal point h_i ($i = 1, 2, 3, \dots, n, n + 1$). The value of σ_i at each altitude h_i is obtained from Eq. (10.40) or from the standard atmosphere table. A constant throttle setting is assumed during the climb; the relaxation of this condition would require the value of $(F/W)_i$ at each pivotal point during the climb. The values of $(\gamma_{FC})_i$ and $(\dot{h}_m)_i$ at the altitude h_i are obtained from Eqs. (10.61) and (10.65), respectively.

The average values $\sigma_{i,\text{ave}}$, $(\gamma_{FC})_{i,\text{ave}}$, and $(\dot{h}_m)_{i,\text{ave}}$ in each interval are now obtained from the forward difference relations,

$$\sigma_{i,\text{ave}} = (\sigma_i + \sigma_{i+1})/2$$

$$(\gamma_{FC})_{i,\text{ave}} = \{(\gamma_{FC})_i + (\gamma_{FC})_{i+1}\}/2$$

and

$$(\dot{h}_m)_{i,\text{ave}} = \{(\dot{h}_m)_i + (\dot{h}_m)_{i+1}\}/2$$

where $i = 1, 2, 3, 4 \dots, n$. The integrals in Eqs. (10.66), (10.71), and (10.74) can be replaced by summations that give t_{FC} , x_{FC} , and ζ_{FC} , respectively, as

$$t_{\text{FC}} = (t_{\text{FC}})_{i=n+1} = \sum_{i=1}^n dh_i / (\dot{h}_m)_{i,\text{ave}}$$

$$x_{\text{FC}} = (x_{\text{FC}})_{i=n+1} = \sum_{i=1}^n dh_i / (\gamma_{\text{FC}})_{i,\text{ave}}$$

and

$$\zeta_{\text{FC}} = (\zeta_{\text{FC}})_{i=n+1} = 1 - \exp \left\{ -c \left(\frac{F_{\text{SSL}}}{W} \right) \sum_{i=1}^n \frac{\sigma_{i,\text{ave}}}{(\dot{h}_m)_{i,\text{ave}}} dh_i \right\}$$

As an example of the above method, for the aircraft of Sec. 10.9 we calculated the values of t_{FC} , x_{FC} , and ζ_{FC} for $F_{m,\text{SSL}}/W = 0.3$ by taking the steps of $\Delta h_i = 50$ m. The values so obtained were within 2% of the values presented in Fig. 10.6.

10.6 Most Economical Climb

The *most economical climb* flight uses the least amount of fuel during the climb. For any commercial airline it is important to keep the cost of flying as low as possible. The aviation fuel consumed by an aircraft contributes very significantly toward the cost of flying. Reduction of fuel consumption during each segment of flying is a most welcome feature, especially when fuel cost is significant.

The minimization of fuel consumption requires the optimization of $-dh/dW$ which is obtained from Eqs. (10.5) and (10.14) as $-dh/dW = -(dh/dt)/(dW/dt) = (FV - DV)/(WcF)$. To optimize $-dh/dW$ with respect to V , it is necessary to have $d((FV - DV)/(WcF))/dV = 0$. Since the c is considered constant and the F of a turbojet is independent of airspeed, the above condition reduces to $d((FV - DV)/W)/dV = 0$, which is just the same as Eq. (10.54) for the fastest climb. This implies that the fastest climb is the most economical climb for a turbojet aircraft.

It has been pointed out⁴ that if the actual variation in F and c are considered during the climb, the airspeed at each altitude for the most economical climb lies between V_{SC} and V_{FC} , but it is sufficiently closer to V_{FC} . Therefore, for preliminary performance analysis of an aircraft, the fastest climb can be regarded as the most economical climb.

10.7 Climb with Allowance for Acceleration

The steady-state climb equation along the flight path is given by Eq. (10.1) where it is mentioned that in the presence of acceleration during the climb the equation should be modified as

$$F - D - W \sin \gamma - (W/g)dV/dt = 0 \quad (10.77)$$

The last term on the right-hand side of Eq. (10.77) is the inertia force due to acceleration. The acceleration dV/dt can be expressed as $dV/dt = (dV/dh)dh/dt = (dV/dh)V \sin \gamma$, which helps in writing Eq. (10.77) as $F - D - W\{1 + (V/g)dV/dh\} \sin \gamma = 0$. Considering that γ is small in practice, $\sin \gamma = \gamma$, the above relation yields the climb angle

$$\gamma = \{(F - D)/W\}\{1 + (V/g)dV/dh\}^{-1} \quad (10.78)$$

The rate of climb \dot{h} is obtained from $\dot{h} = V \sin \gamma \simeq V\gamma$, which after using Eq. (10.78) becomes

$$\dot{h} = \{(FV - DV)/W\}\{1 + (V/g)dV/dh\}^{-1} \quad (10.79)$$

It is seen from Eqs. (10.78) and (10.79) that γ and \dot{h} for accelerated climb are obtained by multiplying their steady-state values by the factor $\{1 + (V/g)dV/dh\}^{-1}$, which can be called the *acceleration correction factor*. Since dV/dh is positive for acceleration, the correction factor will be less than unity during acceleration. Equation (10.78) shows that for a given excess thrust per unit weight of the aircraft, the climb angle of accelerated flight would be less than that required for steady flight. Similarly, Eq. (10.79) shows that for given excess power per unit weight of the aircraft, the rate of climb of accelerated flight would be less than that required for steady flight. This is because a part of the given excess thrust or excess power is utilized in accelerating the aircraft.

In an accelerated climb, if $(V/g)dV/dh$ is constant, the acceleration correction factor becomes constant and such a climb can be called a *quasi-steady climb*.

Climbing flights in which either equivalent airspeed (EAS), or Mach number, is kept constant, are of special interest to pilots. In both these cases the true airspeed varies during the climb and the corresponding acceleration correction factors are theoretically obtained below for flights in the standard atmosphere.

10.7.1 Constant EAS Climb

The relation between true airspeed (TAS) and equivalent airspeed (EAS) is given by

$$V = V_e / \sqrt{\sigma} = (V_e / \sqrt{\epsilon}) e^{(h-h^*)/2\beta}$$

where V_e is the EAS. Differentiation of the above relation with respect to h gives

$$dV/dh = \{V_e/(2\beta\sqrt{\epsilon})\} e^{(h-h^*)/2\beta}$$

and, therefore,

$$(V/g)dV/dh = \{V_e^2/(2\beta\epsilon g)\} e^{(h-h^*)/2\beta} = V^2/(2\beta g)$$

The acceleration correction factor $\{1 + (V/g)dV/dh\}^{-1}$ can be expressed as

$$\{1 + (V/g)dV/dh\}^{-1} = [1 + \{V_e^2/(2\beta\epsilon g)\} e^{(h-h^*)/\beta}]^{-1} \quad (10.80)$$

In the troposphere, $\epsilon = 1$, $h^* = 0$, and $\beta = 9296$ m, therefore the above equation reduces to

$$\{1 + (V/g)dV/dh\}^{-1} = \left\{1 + (V_e^2/182, 202)e^{h/9296}\right\}^{-1}$$

which shows that the correction factor depends on the EAS and the altitude. For example, at sea level ($h = 0$), if the EASs are 50 m/s and 200 m/s, the corresponding acceleration correction factors are 0.986 and 0.820, respectively.

In the stratosphere, $\epsilon = 0.3063$, $h^* = 11,000$ m, and $\beta = 6216$ m, Eq. (10.80) becomes

$$\{1 + (V/g)dV/dh\}^{-1} = \left\{1 + (V_e^2/37318)e^{(h-11,000)/6216}\right\}^{-1}$$

where $h > 11,000$ m. Here also the correction factor depends on the EAS and the altitude.

The values of the correction factor can be improved⁶ if the exact relationship between σ and h is used as given by Eq. (2.11).

10.7.2 Constant Mach Number Climb

The relationship between TAS and the Mach number can be written as

$$V = Ma = Ma_{SSL}a/a_{SSL} = Ma_{SSL}\sqrt{T/T_{SSL}} \quad (10.81)$$

In the region of troposphere, $T = T_{SSL} - \lambda h$, where $\lambda = 0.0065$ K/m is the temperature lapse rate. Equation (10.81) becomes

$$V = Ma_{SSL}(1 - \lambda h/T_{SSL})^{1/2}$$

Therefore, $(V/g)dV/dh = -\lambda a_{SSL}^2 M^2 / (2gT_{SSL}) = -0.133M^2$ and the value of the acceleration correction factor becomes

$$\{1 + (V/g)dV/dh\}^{-1} = (1 - 0.133M^2)^{-1}$$

which shows that the correction factor is greater than unity in the constant Mach number climb. This is because the aircraft decelerates during the climb in this case.

In the case of flight in the stratosphere, $T = \text{constant}$, and a constant Mach number climb implies from Eq. (10.81) that TAS is also constant. Therefore, the value of the acceleration factor would be unity, implying that there would not be any change in the rate of climb or the climb angle.

10.8 Energy Method of Optimal Climb

The concept of energy method of optimal climb is useful to high-performance aircraft that may rapidly accelerate during climb. The emphasis here is on maximizing the rate of change of energy height rather than on maximizing the rate of change of height. An analytical solution of the optimal climb becomes more difficult and usually a graphical method of solution is adapted. The graphical method has also been used for evaluating the optimal climb performance through flight tests.

The basic Eq. (10.77) of climb with acceleration can be multiplied by V and written in a different form as

$$(FV - DV)/W = dh/dt + (V/g)dV/dt \quad (10.82)$$

where the left-hand-side quantity is the specific excess power. The two terms on the right-hand side are, respectively, the rate of climb and acceleration terms. The above equation shows that the specific excess power is utilized both in climbing and accelerating the aircraft. The above equation can also be written as

$$(FV - DV)/W = d(h + V^2/2g)/dt$$

where the quantity $(h + V^2/2g)$ is called energy height or specific energy. The specific excess power and energy height are important quantities in the analysis of optimal climb.

10.8.1 Total Energy

The *total energy* E_T of an aircraft at any instant is the sum of its potential and kinetic energies. The potential energy Wh is due to the altitude at which the aircraft is flying and the kinetic energy $(W/2g)V^2$ is due to its airspeed. This can be expressed as

$$E_T = Wh + (W/2g)V^2 \quad (10.83)$$

During climb the potential energy increases either at the expense of chemical energy of the power plant or by decreasing the kinetic energy of the aircraft. During descent the potential energy decreases, which may or may not be accompanied by a change in kinetic energy; e.g., a constant TAS descent involves a decrease in both the potential energy and the total energy due to work done by the aircraft in overcoming the drag force.

10.8.2 Specific Energy (Energy Height)

The specific total energy, or simply the *specific energy*, of an aircraft is its total energy per unit weight of the aircraft. Writing E_s for the specific energy and using Eq. (10.83), E_s can be expressed as

$$E_s = E_T/W = h + (V^2/2g) \quad (10.84)$$

The first term on the right-hand side may be called the specific potential energy and the second term $V^2/2g$ may be called the specific kinetic energy. The specific energy is a convenient parameter when analyzing the performance of aircraft of different weights. It is also an important parameter in evaluating climbs and maneuvers of high-speed aircraft.

The specific energy is also called the *energy height* because it has dimension of height (length), and is denoted by h_e . Therefore

$$h_e = E_s = h + V^2/(2g) \quad (10.85)$$

Physically the energy height represents the altitude that the aircraft would attain without loss of energy if all its kinetic energy were converted to potential energy.

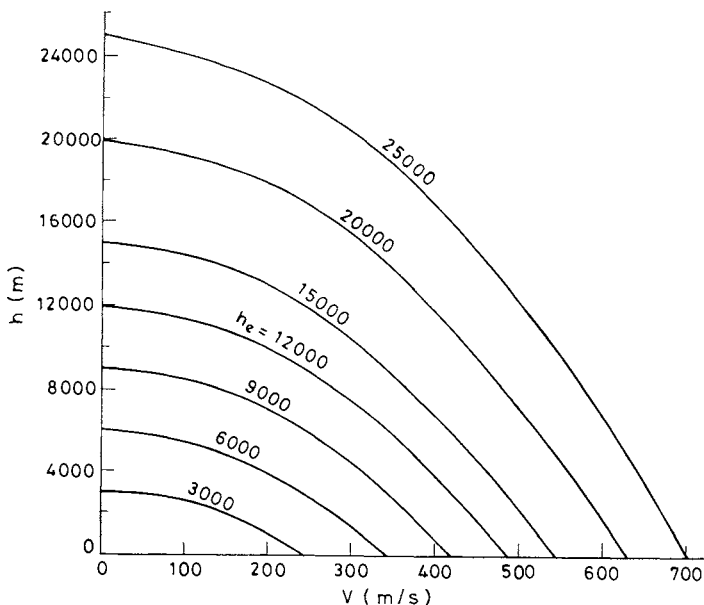


Fig. 10.7 Energy height curves on h - V axes.

Alternatively, if all the altitude (potential energy) were converted into kinetic energy, the corresponding true airspeed would be the maximum airspeed that can be attained for a given specific energy of the aircraft.

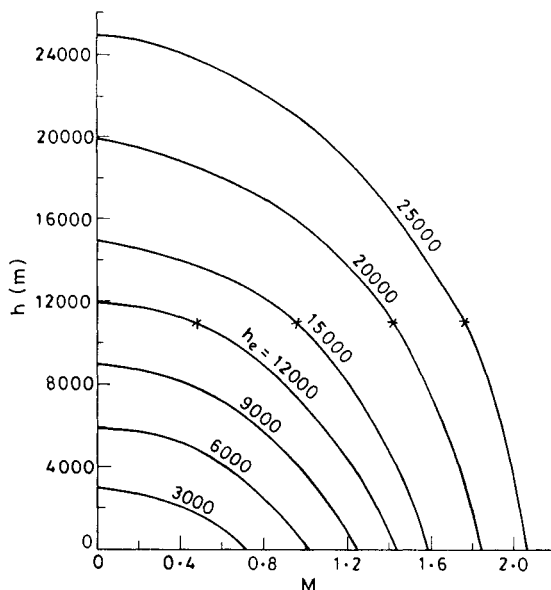
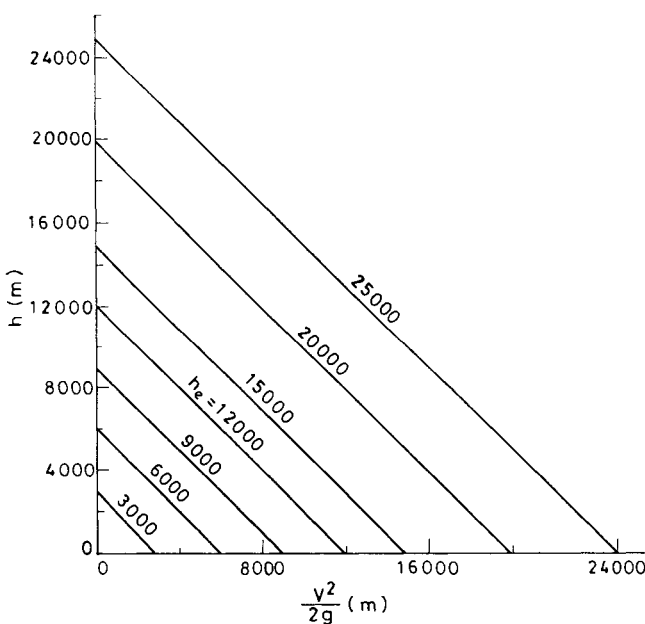
The energy height (specific energy) is a function of the altitude and airspeed. From Eq. (10.85), constant energy height curves can be drawn on the h - V plane as shown in Fig. 10.7. Along each curve in the figure, the energy height is a constant whose numerical value is indicated on the curve, and this constant value changes on shifting from one curve to another curve. The energy height curves do not depend on the aircraft and need to be drawn only once—they remain valid for all aircraft. It will be seen in Sec. 10.8.6 below that these curves are useful in obtaining graphical solutions for optimal climb performance.

Alternative ways of plotting these curves are also possible, as shown in Figs. 10.8 and 10.9. The altitude–Mach number axes of energy height (specific energy) contours in Fig. 10.8 are common to supersonic aircraft in operationally oriented aircraft literature; the slopes of certain curves are discontinuous at the points marked with an asterisk because the sonic speed is constant in the lower part of the stratosphere. Another method of presenting the energy height curves is on the h - $V^2/(2g)$ axes as shown in Fig. 10.9; such a plot is useful in locating the points of tangency with the other curves.

10.8.3 Specific Excess Power

The *specific excess power* is the excess power per unit weight of the aircraft as already stated in Sec. 10.3.2. It is denoted by P_s , which on using Eq. (10.82) can be written as

$$P_s = (F - D)V/W = dh/dt + (V/g)dV/dt \quad (10.86)$$

Fig. 10.8 Energy height curves on h - M axes.Fig. 10.9 Energy height curves on h - $\frac{V^2}{2g}$ axes.

The right-hand side of the above relation is the same as dE_s/dt or dh_e/dt obtained from Eq. (10.85). Therefore

$$P_s = \dot{E}_s = \dot{h}_e = dh/dt + (V/g)dV/dt \quad (10.87)$$

where the overdot denotes differentiation with respect to time. This shows that the specific excess power is the rate of change of specific energy or energy height. For a given aircraft and power setting, \dot{h}_e indicates the capacity of change in energy as a function of h and V . The larger the \dot{h}_e (or P_s), the higher is the maneuvering capability of the aircraft.

If the thrust and drag characteristics of the aircraft are known, Eq. (10.86) can be used to obtain P_s over a range of airspeeds at constant altitude. A set of curves of \dot{h}_e (or P_s) versus V for different altitudes can be drawn as shown in Fig. 10.10. These curves show that the excess power at a given airspeed of the aircraft falls as the altitude increases. From this figure, at a constant \dot{h}_e the values of h can be obtained for different V . This gives rise to constant \dot{h}_e contours that are plotted over the orthogonal h - V axes in Fig. 10.11; each \dot{h}_e contour is valid for only one power setting, one weight, one load factor, one configuration, and one set of atmospheric conditions.

The peak points of the curves in Fig. 10.11 are the points of tangency that the lines of $h = \text{constant}$ make with the lines of $\dot{h}_e = \text{constant}$; one such peak point B at the altitude h_B is shown in the figure. These peak points represent the maximum values of \dot{h}_e at the altitude at which the peaks exist; e.g., the peak point B in Fig. 10.11 for $\dot{h}_e = 200$ is the maximum value of \dot{h}_e at the altitude of $h = h_B$. The locus of these points is the curve ABC representing the climb schedule of the aircraft for maximum \dot{h}_e at each altitude. In the case of zero acceleration during

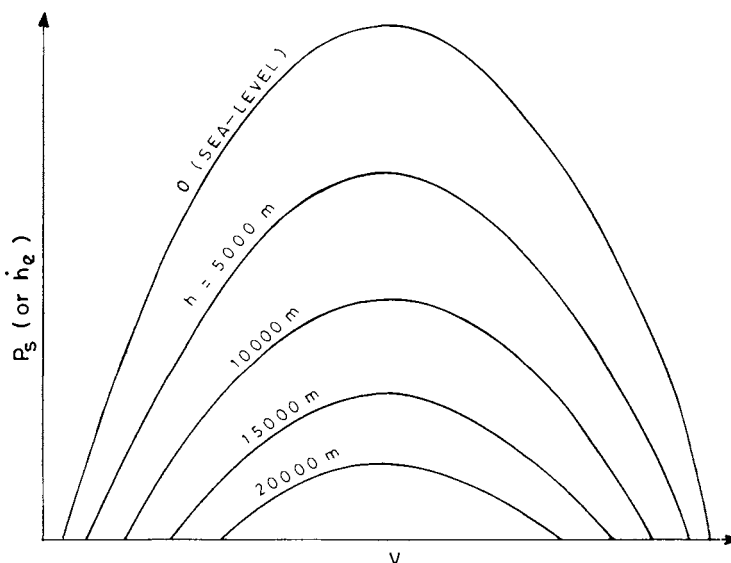


Fig. 10.10 Specific power variation with airspeed at different altitudes.

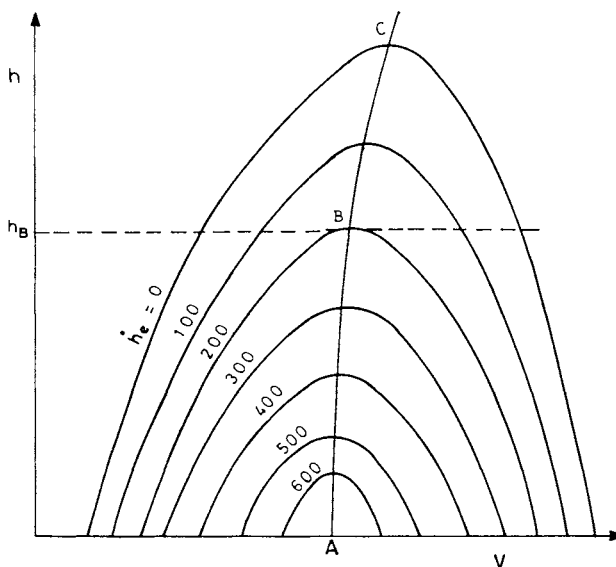


Fig. 10.11 Specific power curves on h - V axes.

climb, $\dot{h}_e = \dot{h}$, and the curve ABC also gives the climb schedule for maximum rate of climb \dot{h} , as may generally happen in the case of a low-performance aircraft.

The $\dot{h}_e = 0$ contour in Fig. 10.11 has a special significance because it is the locus of states corresponding to $F = D$. At any point on the $\dot{h}_e = 0$ contour, the aircraft has no capability of maneuvering, as long as the throttle setting, load factor, weight, or the aircraft configuration, do not change. Along the $\dot{h}_e = 0$ contour, the aircraft would be in the stabilized, steady state, and level flight. Increasing the drag or the load factor, or reducing the thrust, have the effect of shrinking the $\dot{h}_e = 0$ contour as shown in the Fig. 10.12 by a dashed line; this shrinkage is not a proportional shrinkage because the $\dot{h}_e = 0$ contour may also change (distort) the shape. The $\dot{h}_e = 0$ contour, or any other \dot{h}_e contour, does not recognize the aircraft limitations, such as those due to aerodynamic or structural factors, or

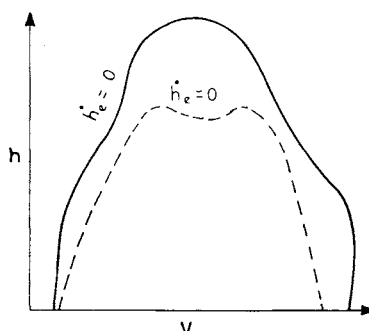


Fig. 10.12 Effect of increasing drag, decreasing load factor, or reducing thrust.

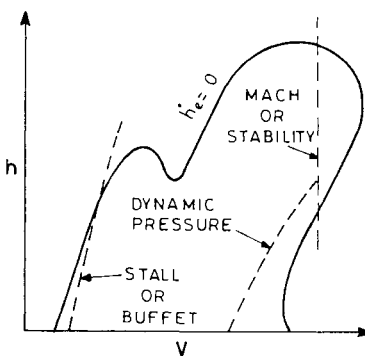


Fig. 10.13 Possible aircraft limits.

controllability. These limitations may modify the usable h_e envelope as shown in Fig. 10.13.

10.8.4 Need for Energy Optimization

The variation of airspeed with altitude that a pilot should maintain during the climb phase of an aircraft is called the *climb schedule*. It is important for a pilot to know the climb schedule before preparing for the climb. The best climb schedule is generally chosen because it gives the maximum rate of climb airspeeds at different altitudes. At any altitude the optimum climb airspeed V_{opt} is found by optimizing the rate of climb \dot{h} with respect to V . This is expressed mathematically by writing,

$$\{\partial(\dot{h}/dt)/\partial V\}_h = 0 \quad \text{for} \quad V = V_{\text{opt}} \quad (10.88)$$

The above relationship helps in finding the best climb schedule of a given aircraft, both theoretically and practically. The importance of the best climb schedule also lies in the fact that it yields the minimum time to climb.

For a high-performance aircraft, it may be more important to reach a particular specific energy level (energy height) h_e in a minimum time rather than to reach a particular altitude h in a minimum time. If the aircraft arrives at a specified altitude with a very low airspeed, an additional amount of time is required to accelerate it to the fighting airspeed at that altitude before the aircraft's mission can be performed. Thus, it is necessary that both h and V be achieved simultaneously rather than attaining only h . The energy height h_e , involving both h and V , can be regarded as a good measure to be achieved, during the climb. Therefore, the essential problem of a high-performance aircraft is that of flying from one energy height to another energy height, in the minimum time.

High-performance jet engine aircraft have large excess thrust available for providing very rapid rates of climb with significant acceleration. The acceleration term in Eq. (10.87) assumes importance in such cases. The maximum energy climb method provides a solution to climb performance by allowing for accelerated climbs.

In the case of a low-performance aircraft, such as a reciprocating engine aircraft, the acceleration term $(V/g)dV/dt$ in Eq. (10.87) is negligible as compared to the term $d\dot{h}/dt$; this is because the acceleration dV/dt is negligible during the climb. The optimum climb airspeed at any altitude is simply the airspeed at which the

rate of climb \dot{h} is maximum. Since in the case of low-performance aircraft $\dot{h}_e = \dot{h}$, it makes little difference whether the rate of climb \dot{h} or the rate of energy height climb \dot{h}_e is optimized.

10.8.5 Theoretical Formulation of Energy Optimization

The time taken t to climb from one energy height $h_{e,1}$ to another energy height $h_{e,2}$ is given by

$$t = \int_{h_{e,1}}^{h_{e,2}} (\frac{dt}{dh_e}) dh_e \quad (10.89)$$

Presenting the time in the above form has, however, one disadvantage; it predicts zero time to climb (or descent) from an altitude h_1 to h_2 if they lie on the same energy height, i.e., if $h_{e,1} = h_{e,2}$, because in such a case $dh_e = 0$. This means that, although the aircraft has changed both altitude and airspeed in arriving from h_1 to h_2 , it has taken zero time—this is impossible. Excluding such situations, Eq. (10.89) is useful in optimizing the energy height climb.

The problem in hand is that of minimizing the right-hand-side integral of Eq. (10.89). This is an intricate mathematical problem involving the calculus of variations and it is beyond the scope of this book to go deeper into its theory. The fact that this powerful mathematical tool can be applied to aircraft performance was pointed out by Rutowski.⁷ The resulting mathematical conditions that must be satisfied are written here to obtain the optimal airspeed at each energy height for the best energy height climb. The integral Eq. (10.89) would be minimum if the partial derivatives of the integrand dt/dh_e with respect to h and V , evaluated at $h_e = \text{constant}$, are both zero. This implies that the partial derivatives of dh_e/dt are also zero for achieving the optimum condition. That is,

$$\{\partial(dh_e/dt)/\partial V\}_{h_e=\text{const}} = \{\partial(dh_e/dt)/\partial h\}_{h_e=\text{const}} = 0 \quad (10.90)$$

The climb schedule of flight, satisfying the above conditions, can be determined graphically as explained below.

10.8.6 Graphical Method of Solution

The constant \dot{h}_e (or P_s) curves are first drawn on h - V axes, as in Fig. 10.11; one can also use h - M or h - $V^2/(2g)$ axes, if so desired. On the same plot of h - V axes, draw the constant h_e curves, as in Fig. 10.7. This amounts to combining Figs. 10.7 and 10.11 on the same graph for producing Fig. 10.14. The conditions presented in Eq. (10.90) are satisfied at the points where the constant h_e contours are tangent to the constant \dot{h}_e curves as shown in Fig. 10.14. The point of tangent represents the maximum value of the specific excess power \dot{h}_e for the energy height (specific energy) h_e that exists at the point of contact. For example, consider a tangent point D in Fig. 10.14 where $h_e = h_{e,D}$ and $\dot{h}_e = \dot{h}_{e,D}$. Along the constant \dot{h}_e ($= \dot{h}_{e,D}$) contour, which starts from the altitude h_D , the maximum value of \dot{h}_e would be $\dot{h}_{e,D}$ which exists at the tangent point D .

The locus of the tangent points mentioned above is the curve ADE in Fig. 10.14. This locus is the best climb schedule for the maximum \dot{h}_e climb of the aircraft. This climb schedule is often referred to as the *maximum-energy climb* and it is

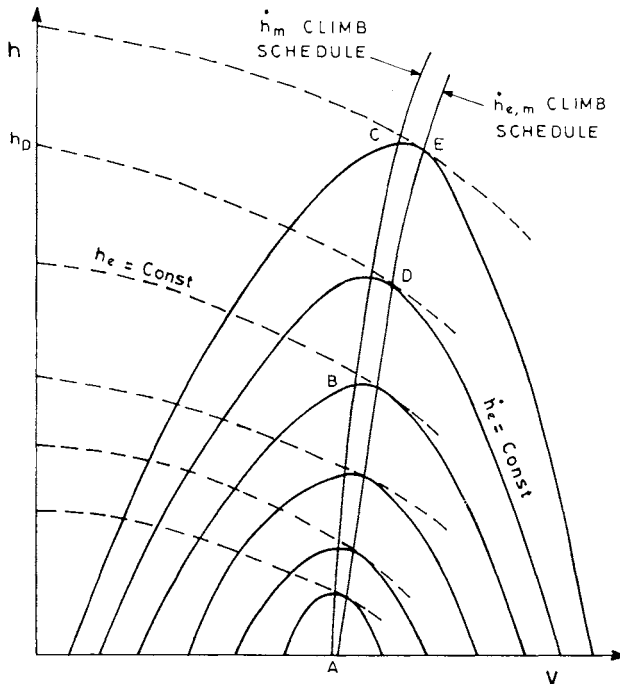


Fig. 10.14 Specific excess power and energy height contours for obtaining optimum climb schedules.

distinct from the best (maximum) rate of climb schedule. This distinction nearly disappears in the case of low-performance aircraft. At any altitude, the airspeed for the maximum-energy climb is always slightly greater, by about 5%, than that for the maximum rate of climb.⁸ The maximum energy climb schedule is also called the *nominal best climb schedule* of the true altitude.

10.8.7 Energy Height Climb from Subsonic to Supersonic

The shapes of the constant h_e (or E_s) lines and constant \dot{h}_e (or P_s) lines shown in Fig. 10.14 are typical of subsonic regions of flight. In Fig. 10.15 such curves are depicted both for subsonic and supersonic regions of flight. The \dot{h}_e lines assume quite different shapes in supersonic regions. The maximum-energy climb schedule is shown by the thick line starting from rest at point 0 until the aircraft reaches the ceiling altitude at E which is the uppermost point of the $\dot{h}_e = 0$ line. The flight starting from the point 0 until the aircraft reaches the point E can be divided into five segments: from 0 to A , A to B , B to C , C to D , and finally from D to E .

In the first segment 0 to A , the aircraft starts from point 0 and accelerates on the ground until it reaches point A where the climb starts. The second segment is the locus AB where the aircraft climbs according to the best (maximum) energy climb schedule in the subsonic region. The third segment BC is along the constant energy height where the aircraft dives to lose potential energy and thereby gains airspeed for moving from the subsonic region at point B to the supersonic region at point C . The constant energy height curve containing the segment BC is such that it is tangent at B to a constant \dot{h}_e curve in the subsonic region, and it is also

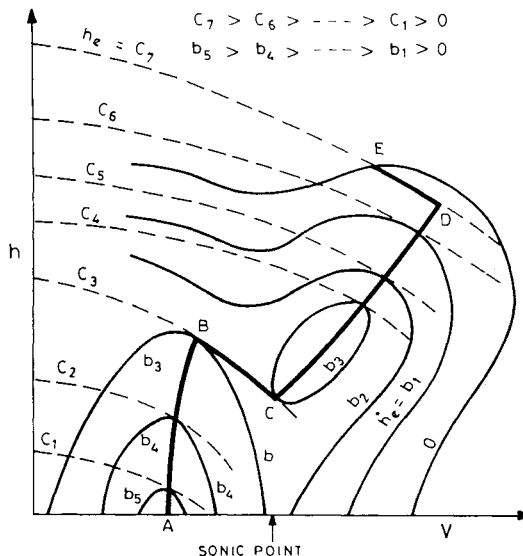


Fig. 10.15 Energy height climb from subsonic to supersonic.

tangent at C to the same numerical constant \dot{h}_e curve in the supersonic region; the value to this constant \dot{h}_e curve is b_3 in Fig. 10.15. The fourth segment is the locus CD where the aircraft climbs at supersonic airspeeds according to the best (maximum) energy climb schedule. The supersonic segment CD is generally very close to a constant calibrated airspeed (CAS) climb. Point D is at the intersection of the locus CD and the constant energy height curve passing through point E . At point D the aircraft zooms to the ceiling altitude at point E along the constant energy height curve. During zooming, the aircraft loses airspeed (kinetic energy) by gaining height (potential energy), ideally in zero time.

10.9 Application to an Aircraft

The aircraft considered in Sec. 8.10 is used as an example here for calculating the performance of the fastest and steepest climbing flights from sea level to the ceiling altitude for two cases (0.3 and 0.2) of $F_{m,SSL}/W$. The aircraft has $W/S = 4000 \text{ N/m}^2$, $C_{D_0} = 0.016$, $K = 0.052$, $E_m = 17.33$, and $c = 0.8/h = 0.8/3600/\text{s}$.

From the standard atmosphere table, $\rho_{SSL} = 1.225 \text{ kg/m}^3$. The values of σ at different altitudes are obtained from Eq. (10.40), and that of Γ are obtained by using Eq. (10.62).

The performance of fastest climb is considered first, and the steepest climb can be similarly obtained. The V_{FC} is obtained from Eq. (10.58) where $F/W = (F_{m,SSL}/W)\sigma$. The values of γ_{FC} and $\dot{h}_{FC} (= \dot{h}_m)$ are obtained from Eqs. (10.61) and (10.65), respectively. The weight of the aircraft is assumed constant during the climb. The results of these calculations are plotted in Fig. 10.5 by solid lines for the case of $F_{m,SSL}/W = 0.3$, and by dashed lines for the case of $F_{m,SSL}/W = 0.2$. The ceiling altitudes are also marked.

The values of t_{FC} , x_{FC} , and ζ_{FC} are obtained from Eqs. (10.70), (10.73), and (10.76), respectively, where Γ is obtained from Eq. (10.62). In the troposphere

($h \leq 11,000$ m), $h^* = 0$, $\epsilon = 1$, $\beta = 9296$ m, and since the climb is from sea level, $h_1 = 0$, and $h_2 = h$ is a known variable altitude. In the stratosphere ($h > 11,000$ m), $h^* = 11,000$ m, $\epsilon = 0.3063$, $\beta = 6216$ m, $h_1 = 11,000$ m, and $h_2 = h$ is a known variable altitude whose first value is 11,000 m and whose last value is the ceiling altitude; the values of t_{FC} , x_{FC} , and ζ_{FC} so obtained should be added to the corresponding values found at 11,000 m during the flight in the troposphere. The results of these calculations are plotted in Fig. 10.6 by solid lines for the case of $F_{m,SSL}/W = 0.3$, and by dashed lines for the case of $F_{m,SSL}/W = 0.2$. For a given change Δh , the changes in Δt_{FC} , Δx_{FC} , and $\Delta \zeta_{FC}$ increase with the increase in altitude.

The performance calculations of the steepest climb can be similarly carried out by using the appropriate relations in Sec. 10.4. The values of V_{SC} , γ_{SC} , and \dot{h}_{SC} , are plotted in Fig. 10.3 and that of t_{SC} , γ_{SC} , and ζ_{SC} are plotted in Fig. 10.4. It can be seen that both in the fastest and steepest climbs the fuel consumption is about 4% of the takeoff weight of the aircraft reaching near-ceiling altitudes; this justifies assuming the aircraft weight to be constant during the climbs.

References

- ¹Torenbeek, E., *Synthesis of Subsonic Airplane Design*, Delft Univ. Press, Delft, The Netherlands, 1976.
- ²Stinton, D., *The Design of the Aeroplane*, Blackwell Science, Osney Mead, England, UK, distributed by AIAA, Washington, DC, 1983.
- ³Mair, W. A., and Birdsall, D. L., *Aircraft Performance*, Cambridge Univ. Press, Cambridge, England, UK, 1992.
- ⁴Hale, F. J., *Introduction to Aircraft Performance, Selection and Design*, Wiley, New York, 1984.
- ⁵Ojha, S. K., "Fastest Climb of a Turbojet Aircraft," *Journal of Aircraft*, Vol. 30, No. 1, Jan.–Feb. 1993, pp. 127–129.
- ⁶Houghton, E. L., and Carruthers N. B., *Aerodynamics for Engineering Students*, 3rd ed., Edward Arnold, 1984.
- ⁷Rutowski, E. S., "Energy Approach to the General Aircraft Performance Problem," *Journal of the Aeronautical Sciences*, Vol. 21, No. 3, 1954, pp. 187–195.
- ⁸Lush K. J., *The Loss in Climb Performance, Relation to the Optimum, Arising from the Use of a Practical Climb Technique*, AAEE, Research Paper 243, England, UK.

Problems

Major specifications of Aircraft A, Aircraft B, and Aircraft C, which are required to solve many of these problems, are presented at the beginning of the Problems section in Chapter 8.

10.1 Aircraft A is climbing from sea level at a constant airspeed of 100 m/s. Plot the variation with altitude of a) climb angle and b) rate of climb.

10.2 Solve Problem 10.1 if Aircraft A has airspeeds of a) 70 km/h, b) 90 km/h, c) 110 km/h, and d) 130 km/h.

10.3 Aircraft A has to climb to an altitude of 4 km. Assuming that the climb has started from sea level at a constant airspeed of 100 m/s, find a) the time to climb, b) distance traveled, and c) fuel consumed.

10.4 Solve Problem 10.1 for Aircraft B climbing at a constant airspeed of a) 400 km/h, b) 500 km/h, and c) 600 km/h.

10.5 Aircraft B climbs at a constant airspeed of 500 km/h at constant throttle setting. For a climb from sea level to 6 km, find the a) time to climb, b) distance traveled, and c) fuel consumed.

10.6 Solve Problem 10.5 for Aircraft B if it has to climb from an altitude of 6 to 12 km.

10.7 Solve Problem 10.1 for Aircraft C climbing at a constant airspeed of a) 500 km/h, b) 600 km/h, and c) 700 km/h.

10.8 Solve Problem 10.5 for Aircraft C, climbing at a constant airspeed of 600 km/h.

10.9 Solve Problem 10.5 for Aircraft C, climbing at a constant airspeed of 600 km/h from an altitude of 6 to 12 km.

10.10 Calculate and plot the variation of climb angle with airspeed for Aircraft A, at a) sea level and b) 4 km, for 100% throttle setting and for 75% throttle setting. From these plots obtain the airspeeds for the steepest climbs. Compare these values with the theoretically obtained values.

10.11 Repeat Problem 10.10 for Aircraft B at a) sea level and b) an altitude of 8 km.

10.12 Repeat Problem 10.10 for Aircraft C at altitudes of a) 6 km and b) 12 km.

10.13 Aircraft A climbs at the steepest climb angle. Find the horizontal distance traveled, time taken, and fuel consumed in climbing from a) sea level to 2 km, b) sea level to 3 km, c) sea level to 4 km, and d) 2 to 4 km.

10.14 Repeat Problem 10.13 for Aircraft B, which is climbing from a) sea level to 4 km, b) sea level to 6 km, c) sea level to 12 km, and d) 6 to 12 km.

10.15 Repeat Problem 10.14 for Aircraft C.

10.16 Aircraft A is making its steepest climb. Find the variation with altitude of a) airspeed, b) climb angle, and c) rate of climb. Also find the absolute ceiling.

10.17 Repeat Problem 10.16 for Aircraft B.

10.18 Repeat Problem 10.16 for Aircraft C.

10.19 Calculate and plot the variation of the rate of climb with airspeed for Aircraft A, at a) sea level and b) 4 km, for 75% thrust rating and for 100% thrust rating. From this plot obtain the airspeed for maximum rate of climb. Compare these values with the theoretically obtained optimum values.

10.20 Repeat Problem 10.19 for Aircraft B.

10.21 Repeat Problem 10.19 for Aircraft C.

10.22 For Aircraft A, find the minimum time to climb, fuel spent, and distance traveled, while climbing from a) sea level to 2 km, b) sea level to 3 km, c) sea level to 4 km, and d) 2 to 4 km.

10.23 Repeat Problem 10.22 for Aircraft B while it is climbing from a) sea level to 4 km, b) sea level to 6 km, c) sea level to 12 km, and d) 6 to 12 km.

10.24 Solve Problem 10.23 for Aircraft C.

10.25 For Aircraft A, plot the variation of the maximum rate of climb and the associated airspeed and climb angle with altitude. From the rate of climb plot find the service and absolute ceilings. Compare the results with the theoretically obtained optimum values.

10.26 Repeat Problem 10.25 for Aircraft B.

10.27 Repeat Problem 10.25 for Aircraft C.

10.28 Consider Aircraft A, which is climbing from sea level to an altitude of 4 km at a constant Mach number of 0.25. Find a) the variation of airspeed with altitude, b) the variation of rate of climb with altitude, c) the variation in climb angle with altitude, d) time to climb, e) fuel consumed, and f) average flight path angle.

10.29 Repeat Problem 10.28 for Aircraft B, which is climbing from sea level to an altitude of 8 km at a constant Mach number of 0.4.

10.30 Repeat Problem 10.28 for Aircraft C, which is climbing from sea level to an altitude of 8 km at a constant Mach number of 0.5.

Turning Flights of Turbojet Aircraft

11.1 Introduction

This chapter is mostly devoted to coordinated turns in the horizontal plane by a turbojet aircraft. Turning is primarily performed by banking the aircraft with the help of ailerons. The sideslip during the turn is kept to zero with the help of the rudder. Since turning requires coordination between the ailerons and the rudder during the turn, this is called a *coordinated turn*. The equations of motion of the coordinated turn are derived here and turning flight parameters are deduced. Important turning parameters of an aircraft are its airspeed, rate of turn, radius of turn, bank angle, and load factor.

Turning flights involving the fastest turn and the tightest turn are of much practical interest. Turning flights of maximum load factor or maximum allowable load factor, and turning at stalling airspeed, may also assume importance in certain situations. All these flights are considered here and their flight parameters are expressed in analytic form.

Turning of aircraft in the vertical plane is also discussed in Sec. 11.8; this is quite different from the coordinated turn in the horizontal plane.

11.2 Equations of Motion of the Coordinated Turn

In a coordinated turn the aircraft turns in a circular path at constant airspeed in the horizontal plane. The aircraft turns only due to banking and the angle of side slip is kept to zero by coordinating the deflections of ailerons and rudder. The velocity vector, lift, and drag forces lie in the same plane, which is usually the plane of symmetry of the aircraft. The thrust line is considered along the tangent to the flight path at any instant during the turn. The acceleration of the aircraft is along the radius of curvature of its flight path due to centripetal force. The forces acting on the aircraft during turning are shown in Fig. 11.1.

The airspeed of the aircraft along the circular path is denoted by V , the bank angle by ϕ , and the radius of the turn by r . The turning angle is represented by χ , which is commonly known as yaw; it is the angle that the longitudinal axis of the aircraft makes with a reference line. The rate of turn (angular velocity) is designated by $\dot{\chi}$ ($= d\chi/dt$). The first three equations below are due to balance of forces along the three mutually orthogonal directions.

In a steady turn that has no acceleration along the flight path, the thrust required F is used only to overcome the drag D . This gives

$$F = D \quad (11.1)$$

The second equation is obtained by resolving forces in the vertical direction. The vertical component of lift force L balances the weight of the aircraft W , giving

$$L \cos \phi = W \quad (11.2)$$

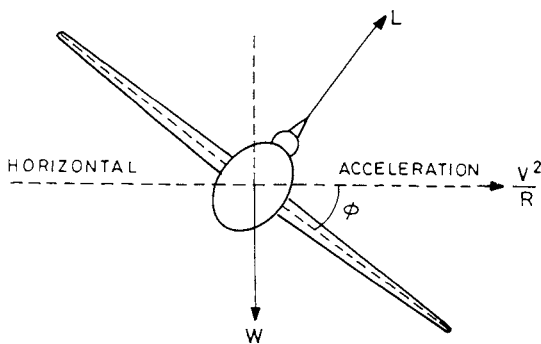


Fig. 11.1 Coordinated turn in horizontal plane (front view).

Since only the horizontal component of lift is responsible for the turn to overcome the centrifugal force, this gives rise to the third equation,

$$L \sin \phi = (W/g)V^2/r \quad (11.3)$$

where g is acceleration due to gravity.

There is also a well-known kinematic relation

$$V = r\dot{\chi} \quad (11.4)$$

which shows that the circumferential velocity V is equal to the radius times the angular velocity. The rate of fuel consumption of a turbojet engine during turning is considered to be the same as given by Eq. (8.4), but it is not used in this chapter because the turning flight is usually of short duration and the weight of the aircraft can be regarded as constant during the turn.

Since only a component of lift balances the weight of the aircraft, the lift force must be greater than the weight. The ratio L/W is commonly known as the *load factor* and is denoted by n (or n_z). From Eq. (11.2)

$$n = L/W = 1/\cos \phi = \sec \phi \quad (11.5)$$

which shows that there is direct coupling between the load factor n and the bank angle ϕ . By fixing the bank angle, the load factor is immediately fixed. The increase in bank angle also means an increase in load factor as shown in Fig. 11.2. Initially the increase in n with ϕ is very slow up to about $\phi = 60$ deg and, thereafter, it increases very rapidly. As the bank angle increases from 80 to 90 deg, the load factor increases from about 5.8 to infinity. The load factor can also be expressed as

$$n = L/W = (L/D)F/W = (F/W)E \quad (11.6)$$

which shows that the load factor is the product of the thrust/weight ratio and the aerodynamic efficiency of the aircraft during the coordinated turn.

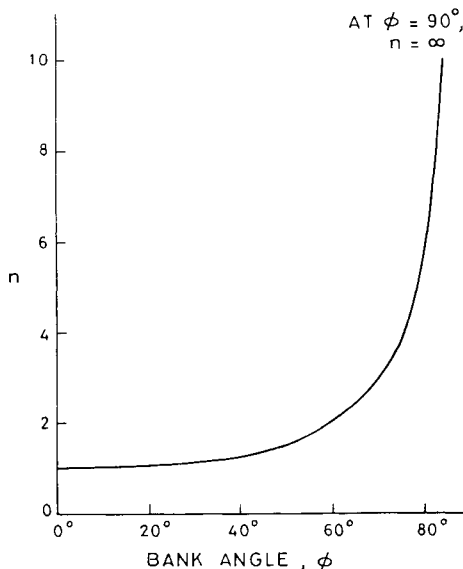


Fig. 11.2 Variation of load factor with bank angle.

11.3 Turning Flight Parameters

The important flight parameters of a turning maneuver are its airspeed, bank angle, load factor, rate of turn, and the radius of turn. These parameters will be expressed here in terms of design variables of the aircraft.

11.3.1 Airspeed and Necessary Condition for Turning

From Eq. (11.1) and the drag polar relation, it can be written that

$$F = D = qSC_D = qS(C_{D_0} + KC_L^2) \quad (11.7)$$

where S is the wing planform area, $q = \rho V^2/2$, C_L and C_D are, respectively, the lift and drag coefficients, C_{D_0} is the zero-lift drag coefficient, and K is the lift-dependent drag coefficient factor. Since the lift coefficient is defined as $C_L = 2L/\rho V^2 S$, where $L = nW$, Eq. (11.7) for the thrust can be written as

$$F = qS\{C_{D_0} + Kn^2W^2/(q^2S^2)\}$$

which after rearranging its terms becomes a quadratic equation in q as

$$(C_{D_0}S^2)q^2 - (FS)q + Kn^2W^2 = 0$$

It can be solved to give the dynamic pressure q as

$$q = \left\{ (F/S)/(2C_{D_0}) \right\} \left[1 \pm \left\{ 1 - 4KC_{D_0}n^2/(F/W)^2 \right\}^{1/2} \right] \quad (11.8)$$

Writing now $q = \rho V^2/2$, $\sigma = \rho/\rho_{SSL}$, and $E_m = 1/(2\sqrt{KC_{D_0}})$, the airspeed can be expressed as

$$V = \left[\frac{(F/W)(W/S)}{\rho_{SSL}\sigma C_{D_0}} \left\{ 1 + \left(1 - \frac{n^2}{E_m^2(F/W)^2} \right)^{1/2} \right\} \right]^{1/2} \quad (11.9)$$

where only the positive sign is retained for getting steady-equilibrium airspeed as explained in Sec. 8.6. In the case of a steady, level flight $n = 1$, the above equation becomes the same as Eq. (8.8). It follows that at a specified altitude and throttle setting, the airspeed of a given aircraft reduces in turning where $n > 1$. If a pilot desires to maintain the airspeed and wants the altitude to be the same during turning as in level flight, he must increase thrust by increasing the throttle setting.

In order to obtain real values of the airspeed, it is necessary that the quantity under the inner radical sign in Eq. (11.9) be greater than or equal to zero. This means that

$$n/E_m(F/W) \leq 1, \quad \text{i.e.,} \quad F/W \geq n/E_m \quad (11.10)$$

The above inequality provides the necessary condition for coordinated turning flight in horizontal plane.

11.3.2 Load Factor, Bank Angle, and Aerodynamic Efficiency

The load factor is obtained in terms of aircraft design parameters from Eq. (11.9) as

$$n^2 = \frac{2\rho_{SSL}\sigma(F/W)C_{D_0}E_m^2}{(W/S)} V^2 - \frac{\rho_{SSL}^2\sigma^2 C_{D_0}^2 E_m^2}{(W/S)^2} V^4 \quad (11.11)$$

which can be written as

$$n = \frac{\rho_{SSL}\sigma C_{D_0} E_m}{(W/S)} V^2 \left\{ \frac{2(F/W)(W/S) \cdot 1}{C_{D_0}\rho_{SSL}\sigma} \frac{1}{V^2} - 1 \right\}^{1/2} \quad (11.12)$$

The bank angle ϕ can be obtained from Eq. (11.5) as

$$\phi = \cos^{-1}(1/n) \quad (11.13)$$

The bank angle is also related to the turning rate $\dot{\chi}$. This can be seen from Eq. (11.3) which after using Eq. (11.4) can be written as

$$L \sin \phi - (W/g)V\dot{\chi} = 0 \quad (11.14)$$

If the bank angle ϕ is zero, the turning rate $\dot{\chi}$ must also vanish. Therefore, a steady coordinated turn is not possible without banking the aircraft. If $\phi = 90$ deg, the load factor becomes infinite. Thus, for a bank angle close to 90 deg, the coordinated turn is not possible. It can, however, be executed only by losing or gaining altitude, the latter requiring $F > W$, i.e., thrust/weight ratio greater than unity.

The lift coefficient and the aerodynamic efficiency during the turn can be found from the relations

$$C_L = \frac{2L}{\rho V^2 S} = \frac{2n(W/S)}{\rho_{SSL}\sigma V^2} \quad \text{and} \quad E = \frac{C_L}{C_D} = \frac{C_L}{C_{D_0} + K C_L^2} \quad (11.15)$$

The lift coefficient remains constant during the turn because the altitude (and thus ρ), V and n (and thus ϕ) remain constant. It follows that the drag coefficient and the aerodynamic efficiency would also remain constant during the coordinated turn.

11.3.3 Turning Rate and Turning Radius

Dividing Eq. (11.14) by the equal terms of Eq. (11.2), the turning rate is obtained as

$$\dot{\chi} = (g/V) \tan \phi = (g/V) \sqrt{n^2 - 1} = g \sqrt{n^2 - 1} / (M a^* a_{SSL}) \quad (11.16)$$

where $\dot{\chi}$ is in radians per unit of time, $a^* = a/a_{SSL}$, and a is the speed of sound in air. Using Eq. (11.11) for n^2 , the rate of turning can be expressed in terms of the aircraft design parameters as

$$\dot{\chi} = \frac{g}{V} \left\{ \frac{2\rho_{SSL}\sigma(F/W)C_{D_0}E_m^2}{(W/S)} V^2 - \frac{\rho_{SSL}^2\sigma^2 C_{D_0}^2 E_m^2}{(W/S)^2} V^4 - 1 \right\}^{1/2} \quad (11.17)$$

The turning radius is obtained directly from Eq. (11.4) as

$$r = V/\dot{\chi} = V^2 / (g \sqrt{n^2 - 1}) = M^2 a^{*2} a_{SSL}^2 / (g \sqrt{n^2 - 1}) \quad (11.18)$$

which after using Eq. (11.17) for $\dot{\chi}$ can also be expressed in terms of the aircraft design parameters as

$$r = \frac{V^2}{g} \left\{ \frac{2\rho_{SSL}\sigma(F/W)C_{D_0}E_m^2}{(W/S)} V^2 - \frac{\rho_{SSL}^2\sigma^2 C_{D_0}^2 E_m^2}{(W/S)^2} V^4 - 1 \right\}^{-1/2} \quad (11.19)$$

The load factor, turning rate, and turning radius, obtained from Eqs. (11.12), (11.17), and (11.19), respectively, can be plotted against the airspeed for a given aircraft at a fixed altitude. Typical variations of these quantities are shown in Fig. 11.3. The figure shows that n , $\dot{\chi}$, and r have optimum values. That is, there exist airspeeds at which n and $\dot{\chi}$ will be maximum and r will be minimum. In the Secs. 11.3.4–11.3.6, these optimum values and the associated flight parameters will be calculated.

Equation (11.16) shows that, for a given n , the rate of turn depends on the airspeed. The curves of $\dot{\chi}$ versus V for different specified values of n are shown by solid lines in Fig. 11.4. The corresponding values of the Mach number at sea level are also shown in the figure. Since $\dot{\chi} = V/r$, it follows that for a given radius of turn, $\dot{\chi}$ varies linearly with V . These linear variations for different values of r are shown by dashed lines.

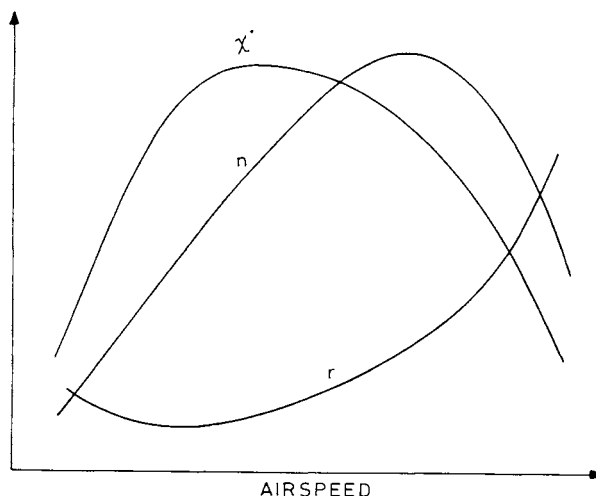


Fig. 11.3 Variations of load factor, turning rate, and turning radius with airspeed.

11.3.4 Effectiveness of Load Factor in Turning

The effectiveness of n on turning rate and turning radius will be investigated here. Noting that $V = \sqrt{2nW/\rho SC_L}$, Eqs. (11.16) and (11.18) can be, respectively, written as

$$\dot{\chi} = g\sqrt{\frac{n^2 - 1}{n}} \left\{ \frac{\rho C_L}{2(W/S)} \right\}^{1/2} \quad \text{and} \quad r = \frac{n}{g\sqrt{n^2 - 1}} \cdot \frac{2(W/S)}{\rho C_L}$$

The influence of n on $\dot{\chi}$ and r enters through the parameters

$$\sqrt{(n^2 - 1)/n} \quad \text{and} \quad n/\sqrt{n^2 - 1}$$

respectively, which are plotted in Figs. 11.5 and 11.6 against n . These figures show that the effect of load factor is mostly confined up to about $n = 3$, which corresponds to a bank angle of $\phi = 70$ deg. This suggests that an increase in the turning rate or a decrease in the turning radius will not be very effective if a pilot tries to do so by merely increasing the bank angle beyond 70 deg.

11.4 Maximum Load Factor and Maximum Bank Angle

It is not usually required to achieve the maximum load factor flight condition. Because of passenger discomfort, design limitations, or flight limitations upon the pilot, it is most undesirable to attempt to achieve the maximum load factor condition during a maneuver. The study of maximum load factor flight parameters is discussed here to give the reader an idea of the upper limit of n that can be achieved, at least theoretically, in the turning flight. In practice, the maximum allowable load factor $n_{m,\text{allowable}}$ is more important; this factor is less than the maximum load factor. The airspeed for the maximum load factor is obtained here, and the other flight parameters are deduced. The subscript nm is used to denote the condition of maximum load factor.

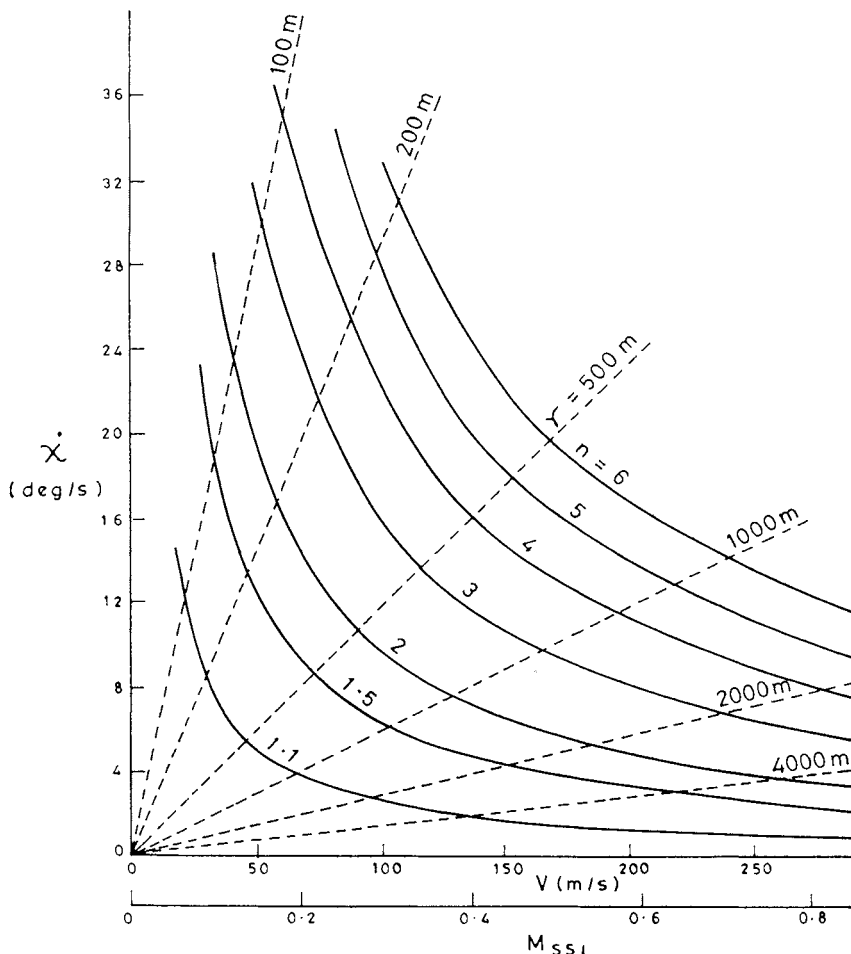


Fig. 11.4 Variation of turning rate against airspeed.

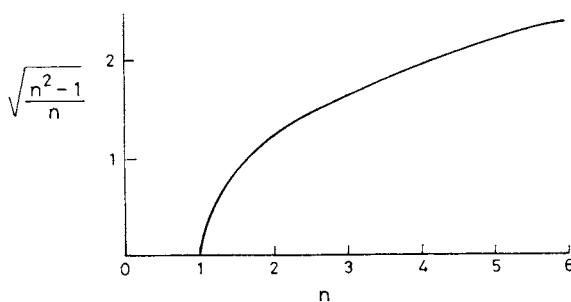


Fig. 11.5 Effect of load factor on turning rate parameter.

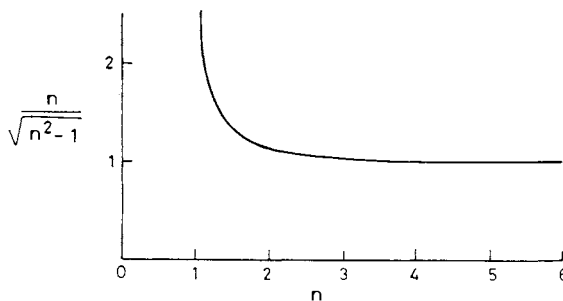


Fig. 11.6 Effect of load factor on turning radius parameter.

11.4.1 Airspeed, Load Factor, and Aerodynamic Efficiency

The airspeed V_{nm} for the maximum load factor is obtained by differentiating Eq. (11.11) or (11.12) with respect to V , putting $dn/dV = 0$, and solving the resulting algebraic equation for V . This gives

$$V_{nm} = \{(F/W)(W/S)/(\rho_{SSL}\sigma C_{D_0})\}^{1/2} \quad (11.20)$$

The airspeed for the maximum load factor increases with increase in wing loading, thrust, and altitude. The maximum load factor n_m is found from Eq. (11.12) by substituting $V = V_{nm}$. This gives

$$n_m = (F/W)E_m \quad (11.21)$$

The above relation could have been directly obtained from Eq. (11.6). For a given thrust/weight ratio, the maximum load factor is achieved by turning at maximum aerodynamic efficiency of the aircraft. The increase in the thrust of a given aircraft increases its load factor. The maximum load factor is achieved by maximizing both the thrust/weight ratio and the lift/drag ratio.

The maximum bank angle ϕ_m is obtained from Eqs. (11.5) and (11.21) as

$$\phi_m = \cos^{-1}(1/n_m) = \cos^{-1}[1/\{(F/W)E_m\}] \quad (11.22)$$

This shows that for a given aircraft, both n_m and ϕ_m can be controlled by controlling the engine thrust. In general practice, n_m is not allowed to exceed $n_{m,allowable}$. Therefore, during a maneuver the thrust/weight ratio F/W must satisfy the relation

$$(F/W)E_m \leq n_{m,allowable} \quad (11.23)$$

In the case of a transport aircraft, the $n_{m,allowable}$ is about 2.5, whereas for a fighter aircraft it may be as high as 8 for a very short duration.

The lift coefficient $C_{L,nm}$ for maximum load factor is obtained by substituting $V = V_{nm}$ in the first relation of Eq. (11.15). This gives

$$C_{L,nm} = 2n_m(W/S)/(\rho V_{nm}^2) = \sqrt{C_{D_0}/K} = C_{L,E_m} \quad (11.24)$$

which shows that the lift coefficient for the maximum load factor is the same as that required for maximum aerodynamic efficiency. Therefore,

$$E_{nm} = E_m = 1/(2\sqrt{KC_{D_0}}) \quad (11.25)$$

Equations (11.24) and (11.25) should also be obvious because the maximum load factor is obtained by keeping aerodynamic efficiency at its maximum [Eq. (11.21)].

11.4.2 Turning Rate and Turning Radius

The turning rate $\dot{\chi}_{nm}$ and the turning radius r_{nm} of the maximum load factor are obtained from Eqs. (11.16) and (11.18), respectively, as

$$\dot{\chi}_{nm} = (g/V_{nm})g\sqrt{n_m^2 - 1} \quad \text{and} \quad r_{nm} = V_{nm}^2 / (g\sqrt{n_m^2 - 1})$$

The above relations after using Eqs. (11.20) and (11.21) can be written as

$$\dot{\chi}_{nm} = g \left\{ \frac{\rho_{SSL}\sigma C_{D_0}}{(F/W)(W/S)} \right\}^{1/2} \sqrt{(F/W)^2 E_m^2 - 1} \quad (11.26)$$

and

$$r_{nm} = \frac{(F/W)(W/S)}{g\rho_{SSL}\sigma C_{D_0}} \cdot \frac{1}{\sqrt{(F/W)^2 E_m^2 - 1}} \quad (11.27)$$

The above two equations express the turning rate and the turning radius of the maximum load factor in terms of the aircraft design parameters. The design parameters that optimize the turning rate are the same as those required for optimizing the turning radius.

11.5 Fastest Turn (Maximum Turning Rate)

The *fastest turn* is the one that has the maximum rate of turning $(d\chi/dt)_m$. The fastest turn is a measure of the aircraft's maneuverability and it is regarded as a figure of merit of the aircraft. An essential requirement of a combat aircraft is that it should be able to turn as fast as possible. The fastest turn flight parameters and the maximum rate of turn would be expressed here analytically in terms of the aircraft design parameters. The fastest turn parameters will be denoted by the subscript *FT*.

11.5.1 Airspeed, Load Factor, and Aerodynamic Efficiency

It is seen from Eq. (11.17) that the turning rate depends on the airspeed. It is thus possible to find V for which $\dot{\chi}$ is maximum. This is found by differentiating Eq. (11.17) with respect to V , making $d\dot{\chi}/dV = 0$, and solving the resulting equation for V . This gives the fastest turn airspeed V_{FT} as

$$V_{FT} = \{2(W/S)/(\rho_{SSL}\sigma)\}^{1/2} (K/C_{D_0})^{1/4} = V_{E_m} \quad (11.28)$$

This shows that the fastest turn airspeed increases with the increase in wing loading and the altitude, but it is independent of the engine thrust.

Substituting $V = V_{FT}$ in Eq. (11.2), the load factor n_{FT} of the fastest turn is obtained as

$$n_{FT} = \sqrt{2(F/W)E_m - 1} = \sqrt{2n_m - 1} \quad (11.29)$$

which shows that the fastest turn load factor is less than the maximum load factor. The fastest turn bank angle ϕ_{FT} is obtained from Eq. (11.13) as

$$\phi_{FT} = \cos^{-1}(1/n_{FT}) \quad (11.30)$$

where n_{FT} is given by Eq. (11.29).

The lift coefficient $C_{L,FT}$ of the fastest turn is obtained from Eq. (11.15) by putting $V = V_{FT}$. This gives

$$C_{L,FT} = 2n_{FT}(W/S)/(\rho V_{FT}^2) = n_{FT}\sqrt{C_{D_0}/K} = n_{FT}C_{L,E_m} \quad (11.31)$$

and since $n_{FT} > 1$, it follows that the lift coefficient of the fastest turn is greater than that required for maximum aerodynamic efficiency. Making use of Eq. (11.29), the above relation can also be written as

$$C_{L,FT} = [(2(F/W)E_m - 1)C_{D_0}/K]^{1/2} \quad (11.32)$$

which shows that for a given aircraft the thrust directly involves the lift coefficient of the fastest turn. The aerodynamic efficiency E_{FT} of the fastest turn is obtained from Eqs. (11.15), (11.31), and (11.29) as

$$E_{FT} = \frac{C_{L,FT}}{C_{D_0} + K C_{L,FT}^2} = \left(\frac{2n_{FT}}{1 + n_{FT}^2} \right) E_m = \frac{1}{F/W} \sqrt{2 \cdot (F/W)E_m - 1} \quad (11.33)$$

In a coordinated turn $n_{FT} > 1$ it follows that $E_{FT} < E_m$, i.e., the aerodynamic efficiency for the fastest turn is less than the maximum aerodynamic efficiency.

11.5.2 Turning Rate and Turning Radius

The expression for the fastest turning rate $\dot{\chi}_{FT}$ ($= \dot{\chi}_m$) is obtained from Eqs. (11.16), (11.28), and (11.29) as

$$\dot{\chi}_{FT} = \frac{g}{V_{FT}} \sqrt{n_{FT}^2 - 1} = g \left\{ \frac{\rho_{SSL}\sigma}{W/S} \right\}^{1/2} \left(\frac{C_{D_0}}{K} \right)^{1/4} \left\{ \left(\frac{F}{W} \right) E_m - 1 \right\}^{1/2} \quad (11.34)$$

This shows that for increasing the fastest turn rate, it is required to have a large thrust/weight ratio, a low wing loading, and a large aspect ratio of the wings.

The expression of the turning radius r_{FT} for the fastest turn is obtained from Eqs. (11.18), (11.28), and (11.29) as

$$r_{FT} = \frac{V_{FT}^2}{g\sqrt{n_{FT}^2 - 1}} = \frac{1}{g} \cdot \frac{W/S}{\rho_{SSL}\sigma} \left(\frac{2K}{C_{D_0}} \right)^{1/2} \left\{ \left(\frac{F}{W} \right) E_m - 1 \right\}^{-1/2} \quad (11.35)$$

The design and flight variables that increase $\dot{\chi}_{FT}$ are the same as those that decrease r_{FT} , and vice versa.

11.6 Tightest Turn (Minimum Turning Radius)

A turning maneuver of minimum radius of turn r_{\min} is called the *tightest turn*. The tightest turn parameters will be subscripted by TT . An aircraft's tightest turn is a measure of its maneuverability. The design parameters of flight that minimize the turning radius of the coordinated turn are discussed here.

11.6.1 Airspeed, Load Factor, and Aerodynamic Efficiency

It is seen in Eq. (11.19) that the radius of turn depends on the airspeed such that it is possible to minimize it. Differentiate Eq. (11.19) with respect to V and put $dr/dV = 0$. The resulting equation gives the airspeed V_{TT} of the tightest turn as

$$V_{TT} = 2[K(W/S)/\{\rho_{SSL}\sigma(F/W)\}]^{1/2} \quad (11.36)$$

The tightest turn airspeed increases with the increase in altitude and wing loading. It decreases with the increase in thrust/weight ratio.

The load factor n_{TT} of the tightest turn is obtained from Eq. (11.12) by writing $V = V_{TT}$, and using Eq. (11.36) for V_{TT} . This gives

$$n_{TT} = [2 - 1/\{E_m^2(F/W)^2\}]^{1/2} = (2 - 1/n_m^2)^{1/2} \quad (11.37)$$

where the extreme right-hand-side term of the above relation is obtained by using Eq. (11.21). The above relation shows that the load factor of a tightest turn can never exceed $\sqrt{2}$ and the tightest turn is possible only when $F/W > 0.707/E_m$. The bank angle of the tightest turn is obtained from Eq. (11.13) as $\phi_{TT} = \cos^{-1}(1/n_{TT})$, where n_{TT} is given by Eq. (11.37).

The lift coefficient $C_{L,TT}$ of the tightest turn is obtained from Eqs. (11.15) and (11.36) as

$$C_{L,TT} = \frac{2n_{TT}(W/S)}{\rho_{SSL}\sigma V_{TT}^2} = \frac{1}{2KE_m} \{2(F/W)^2E_m^2 - 1\}^{1/2} = \frac{(F/W)n_{TT}}{2K} \quad (11.38)$$

and the aerodynamic efficiency E_{TT} of the tightest turn is given by Eqs. (11.15) and (11.38) as

$$E_{TT} = \frac{C_{L,TT}}{C_{D_0} + KC_{L,TT}^2} = \frac{1}{E_m(F/W)^2} \{2(F/W)^2E_m^2 - 1\}^{1/2} = \frac{n_{TT}}{(F/W)} \quad (11.39)$$

which provides E_{TT} in terms of the aircraft design parameters.

11.6.2 Turning Rate and Turning Radius

The turning rate \dot{x}_{TT} of the tightest turn is obtained from Eqs. (11.16), (11.36), and (11.37) as

$$\dot{x}_{TT} = \frac{g}{V_{TT}} \sqrt{n_{TT}^2 - 1} = \frac{g}{2} \left\{ \frac{\rho_{SSL}\sigma}{K} \cdot \frac{F/W}{W/S} \right\}^{1/2} \left\{ 1 - \frac{1}{E_m^2(F/W)^2} \right\}^{1/2} \quad (11.40)$$

This shows that the tightest turn rate can be increased by increasing the thrust/weight ratio, and by decreasing the wing loading and the altitude. The flight parameters that increase the fastest turn rate also increase the tightest turn rate.

The radius r_{TT} ($= r_{\min}$) of the tightest turn is obtained from Eqs. (11.18), (11.36), and (11.37) as

$$r_{TT} = \frac{V_{TT}^2}{g\sqrt{n_{TT}^2 - 1}} = \frac{4K}{\rho_{SSL}\sigma g} \cdot \frac{W/S}{F/W} \left\{ 1 - \frac{1}{E_m^2(F/W)^2} \right\}^{-1/2} \quad (11.41)$$

The flight parameters that increase $\dot{\chi}_{TT}$ also decrease r_{TT} , and vice versa. The flight parameters that decrease the radius of fastest turning also decrease the radius of tightest turning.

11.7 Turning at Stalling Airspeed

It is generally not desirable to fly and turn at stalling airspeed but certain eventualities such as survival in aerial combat may force the pilot to fly at stall. Certain flight tests of turning performance are also carried out near the stalling airspeed. The parameters of turning flight near stall are obtained here in terms of the aircraft design parameters. Flying at stalling airspeed is essentially flight at maximum lift coefficient.

11.7.1 Airspeed, Load Factor, and Aerodynamic Efficiency

From the definition of lift coefficient given by the first relation of Eq. (11.15), the turning airspeed V is obtained as

$$V = \{2n(W/S)/(\rho_{SSL}\sigma C_L)\}^{1/2}$$

For a given load factor at a specified altitude, the maximum lift coefficient $C_{L,m}$ during turn will yield minimum airspeed, which is called the stalling airspeed $V_{S,t}$ of the aircraft during the turn. If $n_{S,t}$ is the load factor at stall during turn, the above relation gives the stalling airspeed as

$$V_{S,t} = \{2n_{S,t}(W/S)/(\rho_{SSL}\sigma C_{L,m})\}^{1/2} \quad (11.42)$$

Since the altitude and bank angle are kept constant during the stalling turn, the airspeed $V_{S,t}$ would also remain constant. For any airspeed less than $V_{S,t}$, the aircraft will lose height during stall, because the corresponding lift component would not be sufficient to counteract the weight of the aircraft. The $V_{S,t}$ can also be expressed in a different form by noting that

$$F = D = (C_{D_0} + KC_{L,m}^2) \cdot \frac{1}{2}\rho V_{S,t}^2 S \quad \text{and} \quad E_{C_{L,m}} = \frac{C_{L,m}}{C_{D_0} + KC_{L,m}^2}$$

where $E_{C_{L,m}}$ is the aerodynamic efficiency at maximum lift coefficient. This gives

$$V_{S,t} = \left\{ \frac{2(F/W)(W/S)}{\rho_{SSL}\sigma(C_{D_0} + KC_{L,m}^2)} \right\}^{1/2} = \left\{ \frac{2(F/W)(W/S)E_{C_{L,m}}}{\rho_{SSL}\sigma C_{L,m}} \right\}^{1/2} \quad (11.43)$$

The load factor $n_{S,t}$ is obtained from Eq. (11.42), which after using the above relation can be written as

$$n_{S,t} = \rho_{SSL}\sigma V_{S,t}^2 C_{L,m} / \{2(W/S)\} = (F/W)E_{C_{L,m}} \quad (11.44)$$

The bank angle $\phi_{S,t}$ is given by $\phi_{S,t} = \cos^{-1}(1/n_{S,t})$, where $n_{S,t}$ can be obtained from Eq. (11.44).

11.7.2 Turning Rate and Turning Radius

The turning rate $\dot{\chi}_{S,t}$ at the stall is obtained from Eqs. (11.16), (11.43), and (11.44) as

$$\dot{\chi}_{S,t} = \frac{g}{V_{S,t}} \sqrt{n_{S,t}^2 - 1} = g \left\{ \frac{\rho_{SSL}\sigma C_{L,m}}{2(F/W)(W/S)E_{C_{L,m}}} \right\}^{1/2} \left\{ \left(\frac{F}{W} \right)^2 E_{C_{L,m}}^2 - 1 \right\}^{1/2} \quad (11.45)$$

The turning radius $r_{S,t}$ at the stall is found from Eqs. (11.18), (11.43), and (11.44) as

$$r_{S,t} = \frac{V_{S,t}^2}{g\sqrt{n_{S,t}^2 - 1}} = \frac{2(F/W)(W/S)E_{C_{L,m}}}{g\rho_{SSL}\sigma C_{L,m}} \left\{ \left(\frac{F}{W} \right)^2 E_{C_{L,m}}^2 - 1 \right\}^{-1/2} \quad (11.46)$$

It can be seen that the flight and design variables that increase $\dot{\chi}_{S,t}$ also help to reduce $r_{S,t}$ in the turning flight at stall.

11.8 Turning in Vertical Plane

Turning of short duration in the vertical plane is frequently required in aerobatic and combat aircraft maneuvers. It is also needed by aircraft of all types during takeoff and landing.

The basic equations of motion of turning in the vertical plane are different from those of turning in the horizontal plane. Consider that the aircraft is turning at a constant airspeed V in a circular path of radius r , as shown in Fig. 11.7. Let

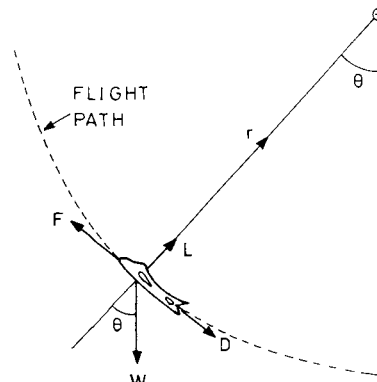


Fig. 11.7 Turning in vertical plane.

θ be the turning angle and $\dot{\theta}$ ($= d\theta/dt$) be the rate of turn in the vertical plane. Resolving the forces along the circumferential and radial directions, the following two equations of motion are, respectively, obtained:

$$F - D - W \sin \theta = 0 \quad (11.47)$$

and

$$L - W \cos \theta - (W/g)V^2/r = 0 \quad (11.48)$$

In addition, there is a kinematic relation

$$V = r\dot{\theta} \quad (11.49)$$

As the turnings are generally of short duration, the aircraft weight W can be regarded as constant during the turn.

Turning in a circular path at constant airspeed is considered here. It is, however, not simple to perform a complete circular loop with constant airspeed, because the weight of the aircraft continuously interacts with the thrust force. In most cases, loops are flown at a constant load factor with the airspeed dropping off on the climb to near-stall at the top and increasing thereafter as the aircraft descends.¹ It is reasonable to assume that V and r are constants if the turning is performed in a small portion of the arc of a circle for a very short duration. These conditions can generally be satisfied in two special cases of interest, pullup and pulldown maneuvers, which are discussed below.

11.8.1 Pullup Maneuver

In a *pullup turn* the pilot changes a horizontal level flight into the flight turning upward as shown in Fig. 11.8. This change is brought by the pilot by pulling the stick back, which deflects the elevators up, thus turning the nose of the aircraft up, causing an upward turn of the aircraft in a curved path. This curved path is regarded to be circular with constant airspeed of the aircraft for the purpose of simplifying theoretical analysis.

Using Eqs. (11.47–11.49) and applying it to the pullup case at $\theta = 0$, gives

$$F = D, \quad L - W - (W/g)V^2/r = 0, \quad \text{and} \quad V = r\dot{\theta} \quad (11.50)$$

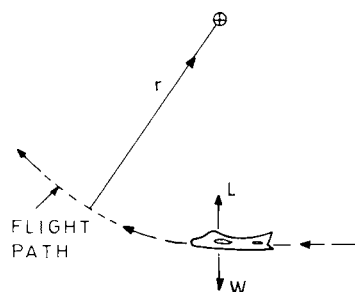


Fig. 11.8 Pullup maneuver in normal flight.

The load factor n can be obtained as

$$n = L/W = 1 + (1/g)V^2/r \quad (11.51)$$

which shows that in a pullup maneuver the load factor is greater than unity. The turning radius r and the turning rate $\dot{\theta}$ in the vertical plane are obtained from Eqs. (11.51) and (11.50), respectively, as

$$r = V^2/\{g(n - 1)\} \quad \text{and} \quad \dot{\theta} = V/r = g(n - 1)/V$$

Noting that

$$V = \sqrt{2L/(\rho SC_L)} = \sqrt{2n(W/S)/(\rho_{SSL}\sigma C_L)} \quad (11.52)$$

the turning radius and the turning rate can, respectively, be expressed as

$$r = \frac{2n(W/S)}{g(n - 1)\rho_{SSL}\sigma C_L} \quad \text{and} \quad \dot{\theta} = g(n - 1) \left\{ \frac{\rho_{SSL}\sigma C_L}{2n(W/S)} \right\}^{1/2} \quad (11.53)$$

This shows that the decrease in wing loading of a given aircraft would decrease the radius of turn and increase the rate of turn. The minimum r and maximum $\dot{\theta}$ are obtained by operating at maximum lift coefficient.

11.8.2 Pulldown Maneuver

The *pulldown maneuver* is opposite to the pullup maneuver. Here the initial horizontal level flight is changed to a descending flight along a curved path by turning downward as shown in Fig. 11.9 for inverted flight. As the pilot pushes the stick forward, the elevators deflect down, thus turning the nose of the aircraft down, causing downward turn of the aircraft in a curved path. This curved path is approximated as circular, taking the aircraft's airspeed to be constant to simplify the theoretical analysis.

Using Eqs. (11.47–11.49) and applying them to the pulldown case by putting $\theta = \pi$, gives

$$F = D, \quad L + W - (W/g)V^2/r = 0, \quad \text{and} \quad V = r\dot{\theta} \quad (11.54)$$

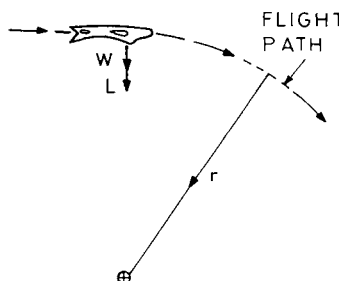


Fig. 11.9 Pulldown maneuver in inverted flight.

The load factor n is now obtained as

$$n = (L/W) = (1/g)V^2/r - 1 \quad (11.55)$$

The turning radius and the turning rate are obtained from Eqs. (11.55) and (11.54), respectively, as

$$r = V^2/\{g(n+1)\} \quad \text{and} \quad \dot{\theta} = V/r = g(n+1)/V$$

which after using Eq. (11.52) for V can be written, respectively, as

$$r = \frac{2n(W/S)}{g(n+1)\rho_{SSL}\sigma C_L} \quad \text{and} \quad \dot{\theta} = g(n+1) \left\{ \frac{\rho_{SSL}\sigma C_L}{2n(W/S)} \right\}^{1/2} \quad (11.56)$$

The above relation shows that the decrease in wing loading, with everything else remaining the same, decreases the radius of turn and increases the rate of turn. The minimum r and the maximum $\dot{\theta}$ are obtained at the maximum lift coefficient.

High-performance fighter aircraft are designed to take large load factors ranging from 3 to 10. When n is large, write $n+1 \approx n$, and $n-1 \approx n$. This makes Eqs. (11.53) and (11.56) the same, both for r and $\dot{\theta}$. This means that in maneuvers involving large load factors one does not distinguish between pullup and pulldown maneuvers when calculating the radius and rate of turns.

11.9 Application to an Aircraft

The aircraft here is the same one that has been considered in Chapters 8–10. It has $W/S = 4000 \text{ N/m}^2$, $C_{D_0} = 0.016$, and $K = 0.052$. The maximum thrust/weight ratio F_{SSL}/W of the aircraft is 0.3, and it is turning at an altitude of 6 km ($\sigma = 0.5389$). Calculate the flight parameters of the fastest and tightest turns.

The maximum aerodynamic efficiency of the aircraft is

$$E_m = 1/(2\sqrt{C_{D_0}K}) = 1/(2\sqrt{0.016 \times 0.052}) = 17.33$$

It is assumed here that the aircraft has first climbed to an altitude of 6 km under constant throttle setting with a negligible amount of fuel consumption. This gives $F/W = (F_{SSL}/W)\sigma = 0.3 \times 0.5389 = 0.1617$.

1) *Fastest turn.* The airspeed, load factor, and bank angle of the fastest turn are, respectively, obtained from Eqs. (11.28–11.30) as

$$V_{FT} = \{2(4000)/(1.225 \times 0.5389)\}^{1/2} (0.052/0.016)^{1/4} = 147.8 \text{ m/s}$$

$$n_{FT} = \sqrt{2 \times 0.1617 \times 17.33 - 1} = 2.146$$

and

$$\phi_{FT} = \cos^{-1}(1/n_{FT}) = \cos^{-1}(1/2.146) = 62.2 \text{ deg}$$

The lift coefficient and aerodynamic efficiency are obtained from Eqs. (11.32) and (11.33) as

$$C_{L,FT} = [(2(0.1617)17.33 - 1)(0.016/0.052)]^{1/2} = 1.19$$

$$E_{FT} = 1.19/\{0.016 + 0.052(1.19)^2\} = 13.3$$

The turning rate of the fastest turn is obtained from Eq. (11.34) as

$$\dot{\chi}_{FT} = (9.807/147.8)\sqrt{(2.146)^2 - 1} = 0.126 \text{ rad/s} = 7.22 \text{ deg/s}$$

and the turning radius is given by

$$r_{FT} = V_{FT}/\dot{\chi}_{FT} = (147.8/0.126) = 1173 \text{ m} = 1.173 \text{ km}$$

2) *Tightest turn.* The airspeed and load factor of the tightest turn are obtained from Eqs. (11.36) and (11.37), respectively, as

$$V_{TT} = 2 \left\{ \frac{0.052}{1.225 \times 0.5389} \cdot \frac{4000}{0.1617} \right\}^{1/2} = 88.28 \text{ m/s}$$

$$n_{TT} = \left\{ 2 - \frac{1}{(17.33)^2(0.1617)^2} \right\}^{1/2} = 1.37$$

and the bank angle ϕ_{TT} is given by

$$\phi_{TT} = \cos^{-1}(1/n_{TT}) = \cos^{-1}(1/1.37) = 43 \text{ deg}$$

The lift coefficient and aerodynamic efficiency are obtained from Eqs. (11.38) and (11.39), respectively, as

$$C_{L,TT} = \frac{(0.1617)1.37}{2 \times 0.052} = 2.13 \quad \text{and} \quad E_{TT} = \frac{n_{TT}}{F/W} = \frac{1.37}{0.1617} = 8.47$$

The turning rate of the tightest turn is given by Eq. (11.40) as

$$\dot{\chi}_{TT} = (9.807/88.28)\sqrt{(1.37)^2 - 1} = 0.104 \text{ rad/s} = 5.96 \text{ deg/s}$$

and the radius of the turn is given by

$$r_{TT} = V_{TT}/\dot{\chi}_{TT} = 88.28/0.104 = 849 \text{ m} = 0.849 \text{ km}$$

Note that the airspeed, load factor, and aerodynamic efficiency during the tightest turn are less than those for the fastest turn.

Reference

¹Layton, D., *Aircraft Performance*, Matrix Publishers, 1988.

Problems

Major specifications of Aircraft A, Aircraft B, and Aircraft C, which are required to solve these problems, are presented at the beginning of the Problems section in Chapter 8.

11.1 Aircraft A is making a level turn at sea level at an airspeed of 250 km/h. Using 80% of its maximum thrust, find the a) load factor and bank angle, b) lift coefficient and aerodynamic efficiency, and c) turning rate and turning radius.

11.2 Solve Problem 11.1 if the airspeed of Aircraft A is 350 km/h.

11.3 Solve Problem 11.1 if the airspeed of Aircraft A is increased to 350 km/h and the maximum thrust is utilized.

11.4 Solve Problem 11.1 if the turning maneuver is executed at an altitude of 4 km.

11.5 Aircraft A makes a coordinated turn in the horizontal plane at sea level. Its bank angle is 15 deg and uses maximum thrust. a) Find the load factor. b) Find two possible airspeeds for the turning, and the corresponding lift coefficients and aerodynamic efficiencies. Can these airspeeds be realized in practice? c) Find the turning rate and turning radius for each attainable airspeed.

11.6 Solve Problem 11.5 if the thrust of Aircraft A is reduced to 70%.

11.7 Solve Problem 11.5 if the turning maneuver is executed at an altitude of 4 km.

11.8 Aircraft B makes a coordinated turn at Mach 0.6 at an altitude of 4 km by using maximum available thrust. Find the a) load factor and bank angle, b) lift coefficient and aerodynamic efficiency, c) turning rate and turning radius, and d) stalling airspeed in the turn. Is this turn possible?

11.9 Solve Problem 11.8 if Aircraft B turns at an altitude of 12 km.

11.10 Solve problem 11.8 in the following two cases for Aircraft B: a) the wing loading is decreased by 10%, b) C_{D_0} is decreased by 5%.

11.11 Aircraft B is turning at sea level at the rate of 1.5 deg/s with a bank angle of 20 deg. Find the a) Mach number of turn, its lift coefficient and aerodynamic efficiency; b) load factor and the thrust required to turn; c) turning radius; and d) stalling airspeed of the turn.

11.12 Solve Problem 11.11 if Aircraft B flies at an altitude of 10 km.

11.13 Find the percentage changes incurred in the solution of Problem 11.11 for Aircraft B due to the following changes in its design parameters: a) W/S is decreased by 10%, b) C_{D_0} is decreased by 5%, c) K is decreased by 5%.

11.14 Solve Problem 11.5 if Aircraft C turns at an altitude of 6 km.

11.15 Solve Problem 11.5 if Aircraft C turns at an altitude of 12 km.

11.16 Solve Problem 11.8 for Aircraft C.

- 11.17** Solve Problem 11.8 if Aircraft C turns at an altitude of 12 km.
- 11.18** Solve Problem 11.11 if Aircraft C turns at an altitude of 4 km.
- 11.19** Solve Problem 11.11 if Aircraft C turns at an altitude of 12 km.
- 11.20** For Aircraft A performing a coordinated turn at an altitude of 3 km, plot the variations of a) load factor, b) turning rate, and c) turning radius with the increase in airspeed. Mark the optimum airspeed in each of these three cases.
- 11.21** Solve Problem 11.20 for Aircraft B turning at an altitude of 6 km.
- 11.22** Solve Problem 11.20 for Aircraft C turning at an altitude of 11 km.
- 11.23** Aircraft A is making a steady, level turn at maximum load factor at sea level. Find the a) maximum load factor and bank angle, b) airspeed and stalling airspeed, c) lift coefficient and aerodynamic efficiency, and d) rate of turn and radius of turn.
- 11.24** Solve Problem 11.23 if Aircraft A turns at an altitude of 4 km.
- 11.25** Solve Problem 11.23 if Aircraft B turns at an altitude of 6 km.
- 11.26** Solve Problem 11.23 if Aircraft B turns at an altitude of 12 km.
- 11.27** Solve Problem 11.23 if Aircraft C turns at an altitude of 11 km.
- 11.28** Aircraft A makes a steady, level turn at sea level at maximum turning rate. Find the a) maximum turning rate and the turning radius; b) airspeed, stalling airspeed, load factor, and bank angle; and c) lift coefficient and aerodynamic efficiency.
- 11.29** Solve Problem 11.28 for Aircraft A turning at an altitude of 4 km.
- 11.30** Solve Problem 11.28 for Aircraft B turning at an altitude of 6 km.
- 11.31** Aircraft B makes the fastest turn at an altitude of 6 km. Find the percentage changes made in the flight parameters for each of the following cases: a) W/S is reduced by 15%; b) C_{D_0} is reduced by 4%; c) K is reduced by 4%; and d) W/S , C_{D_0} , and K are simultaneously reduced by 15%, 4%, and 4%, respectively.
- 11.32** Solve Problem 11.28 for Aircraft C turning at an altitude of 11 km.
- 11.33** Aircraft A is executing a steady, level, tightest turn at sea level. Find the a) turning rate and turning radius; b) airspeed, stalling airspeed, load factor, and bank angle; and c) lift coefficient and the aerodynamic efficiency.
- 11.34** Solve Problem 11.33 for Aircraft A executing the tightest turn at an altitude of 4 km.

11.35 Solve Problem 11.33 for Aircraft B executing the tightest turn at an altitude of 6 km.

11.36 Aircraft B makes a steady tightest turn in the horizontal plane at an altitude of 6 km. Find the percentage changes made in the flight parameters for each of the following cases: a) W/S is reduced by 15%; b) C_{D_0} is reduced by 4%; c) K is reduced by 4%; and d) W/S , C_{D_0} , and K are simultaneously reduced by 15%, 4%, and 4%, respectively.

11.37 Solve Problem 11.36 for Aircraft C executing the tightest turn.

12

Cruising Flights of Piston-Prop Aircraft

12.1 Introduction

The performance analysis of a piston-prop aircraft begins in this chapter. Since the power characteristics of a piston-prop aircraft are quite different from those of a turbojet aircraft, the analytical expressions and the final results of the performance analysis are different in the two cases. Most of the performance parameters sought in this chapter and in Chapters 13–15 are the same as in the Chapters 8–11, respectively. The basic mathematical formulations of the performance problems of a piston-prop aircraft remain the same as in the case of a turbojet aircraft, except the expression for the rate of fuel consumption.

Terms like *cruise* or *cruising flight of a piston-prop aircraft* have the same meaning as explained in Sec. 8.2. The basic equations of motion of a cruising flight are derived here and solved for obtaining the range, endurance, and other flight parameters. Following the example of Chapter 8, in this chapter the three different types of flight programs are also analyzed. This clearly shows that any change in the flight program alters the performance of the aircraft. The presentations in this chapter and in Chapters 13–15 facilitate the comparison that can be made between the performance of piston-prop and turbojet aircraft.

12.2 Equations of Motion of a Steady Level Flight

The basic equations of motion of a piston-prop aircraft are obtained in the same way as for turbojet aircraft in Sec. 8.2. We continue to assume that the line of action of the thrust force F is along the flight path, and the aircraft weight decreases due to fuel consumption only, i.e., $dW_f = -dW$, where dW_f is the fuel consumed (a positive quantity) when the aircraft weight reduces by dW . Let L and D be the lift and drag forces acting on the aircraft whose total weight is W ; during its cruising flight the aircraft covers the range x in time t . The governing equations of motion of a steady and level flight are

$$F = D \quad (12.1)$$

$$L = W \quad (12.2)$$

$$\frac{dx}{dt} = V \quad (12.3)$$

$$- \frac{dW}{dt} = \hat{c} P_e \quad (12.4)$$

where V is the forward airspeed, and P_e is the brake power of the piston engine whose power-specific fuel consumption (PSFC) is \hat{c} .

The first two equations above are obtained by balancing the forces acting on the aircraft, along the flight path and normal to it, respectively. Equation (12.3) is the kinematic relation, and Eq. (12.4) is obtained from Eq. (5.1), which gives the rate of fuel consumption. It should be kept in mind that the airspeed V in

Eq. (12.3) is the ground airspeed of the aircraft, whereas in all the other relations V is implicit and represents the true airspeed. With the present assumption of no-wind condition, the ground airspeed and the true airspeed are identical.

A piston engine produces brake power P_e , which is converted into thrust power $P (=FV)$ to push the aircraft by using the propeller. How efficiently the engine brake power is transferred as its thrust power depends on the efficiency of the propeller. If η_p is the propeller efficiency, it can be written from Eq. (5.13) that $P = \eta_p P_e$. It is, however, convenient to introduce a conversion factor k and write this equation as

$$P = FV = k\eta_p P_e \quad (12.5)$$

because P_e is generally provided in commercial units, which are different from the standard units used for P . The value of k depends on the system of units used. If the engine power P_e is prescribed in horsepower, the value of $k = 550 \text{ ft-lb/s} \cdot \text{hp}$. On the other hand, if the engine power is in kilowatts, the value of $k = 1000 \text{ W/kW}$ where kW denotes kilowatts. In the cases P_e is given in a standard system of units, either foot/pound/second (FPS) or SI, the value of $k = 1$. Equation (12.4) can now be written as

$$-\frac{dW}{dt} = \hat{c}P/(k\eta_p) \quad (12.6)$$

where the value of η_p is about 0.85.

Equations (12.1) and (12.2) can be combined by writing them as

$$P/W = V/E \quad (12.7)$$

where E is the lift/drag ratio, commonly known as the aerodynamic efficiency of the aircraft. The above relation shows that the thrust power per unit weight is equal to V/E in a cruising flight. The inverse of the power/weight ratio is called *power loading*; this value is commonly supplied by the aircraft manufacturers.

There is yet another important relationship that occurs at several places in the performance analysis. This is an expression for the airspeed V that is obtained from the definition of lift coefficient C_L , and is written as

$$V = \sqrt{2(W/S)/(\rho C_L)} = \sqrt{2(W/S)/(\rho_{SSL}\sigma C_L)} \quad (12.8)$$

where ρ is the density of atmosphere, $\sigma = \rho/\rho_{SSL}$, and the subscript SSL represents the standard atmosphere at sea level. The above equation connects the wing loading and altitude (and thus σ) of a given aircraft with the airspeed. It shows that the airspeed increases with an increase in the wing loading W/S and altitude, and increases with a decrease in the lift coefficient.

12.3 Airspeed

The airspeed of a cruising flight is estimated here in terms of the aircraft design parameters. The lift coefficient C_L , and the drag coefficient C_D , are defined, respectively, as

$$C_L = \frac{2(W/S)}{\rho V^2} = \frac{2(W/S)}{\rho_{SSL}\sigma V^2} \quad \text{and} \quad C_D = \frac{2(D/S)}{\rho V^2} = \frac{2(D/S)}{\rho_{SSL}\sigma V^2} \quad (12.9)$$

The lift and drag coefficients are related by the parabolic drag polar

$$C_D = C_{D_0} + K C_L^2 \quad (12.10)$$

where C_{D_0} is the zero-lift drag coefficient, and K is the lift-dependent drag coefficient factor. Therefore

$$1/E = D/L = C_D/C_L = (C_{D_0} + K C_L^2)/C_L$$

which after using the first relation of Eq. (12.9) can be written as

$$\frac{1}{E} = \frac{\rho_{SSL}\sigma C_{D_0}}{2(W/S)} \cdot V^2 + \frac{2K(W/S)}{\rho_{SSL}\sigma} \cdot \frac{1}{V^2} \quad (12.11)$$

Equation (12.7) can now be expressed as

$$P/W = \rho_{SSL}\sigma C_{D_0} V^3 / \{2(W/S)\} + 2K(W/S) / (\rho_{SSL}\sigma V) \quad (12.12)$$

and for estimating the airspeed, the above relation can be written as

$$V^4 - 2k\eta_p(P_e/W)(W/S)V / (\rho_{SSL}\sigma C_{D_0}) + 4K(W/S)^2 / (\rho_{SSL}^2\sigma^2 C_{D_0}) = 0$$

The above equation does not yield an analytic expression for V and, therefore, the airspeed is obtained by solving it either graphically or by a numerical method.

12.4 Power Required

The aerodynamic drag force on an aircraft, when multiplied by its airspeed, gives the drag power, which is supplied by the engine for keeping the motion of aircraft in equilibrium. This drag power is called the *power required* for the aircraft, and it is denoted by P . Since $F = D$, it follows that $P = DV = FV$. Since a piston engine is a power-producing engine, the calculation of power required has special significance for piston-prop aircraft.

12.4.1 Power Required with Airspeed

The variation of thrust power required with airspeed of a given aircraft is directly obtained from Eq. (12.12) as

$$P = (1/2)\rho_{SSL}C_{D_0}S\sigma V^3 + 2KS(W/S)^2 / (\rho_{SSL}\sigma V) \quad (12.13)$$

The variation of thrust power required with airspeed of a piston-prop aircraft is shown in Fig. 12.1. This curve has the same characteristic features as that of the curve of F versus V of a turbojet aircraft in Fig. 8.2, except for the fact that the changes in the power required with airspeed are faster as compared to the thrust required (or drag). Starting from a low airspeed, the power required initially decreases to a certain minimum value and, thereafter, increases sharply with the airspeed. The stalling airspeed V_s and minimum power airspeed $V_{P_{min}}$ are marked in the figure. A considerable drag rise occurs in practice for airspeeds below the stall as shown by the dashed line in Fig. 12.1.

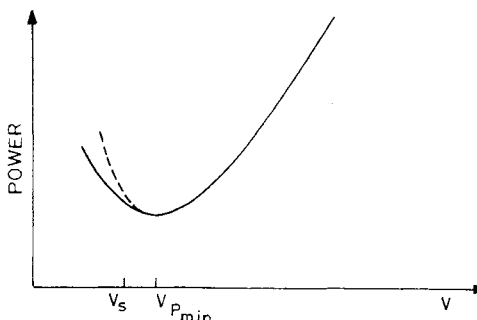


Fig. 12.1 Variation of power required with airspeed.

12.4.2 Influence of Altitude and Weight

The effect of changing altitude on the power required curve is shown in Fig. 12.2. With the increase in altitude the curve shifts upward and to the right. Since $D = P/V$, the minimum drag is the slope of the tangent, drawn from the origin to the power required curve. We have seen in Sec. 8.6.3 that the minimum drag is independent of altitude. It follows that all power required curves must have a common tangent through the origin, as shown by the dashed straight line in Fig. 12.2. These curves of different altitudes will merge into a single curve if $P/\sqrt{\sigma}$ is plotted against the equivalent airspeed $V_e (= V\sqrt{\sigma})$, as can be easily verified from Eq. (12.13).

The effect of variation of weight of a given aircraft on the power required curve is shown in Fig. 12.3. If the lift coefficient in the two curves is kept the same, it follows from the first relation of Eq. (12.9) that $V \propto \sqrt{W}$, and from Eq. (12.13) it can be reasonably concluded that $P \propto W^{3/2}$ for a cruising flight.

12.4.3 Power Required and Power Available

Typical variations in the power available (P_{av}), and power required (P), curves against the airspeed are shown in Fig. 12.4 for a piston-prop aircraft. The point

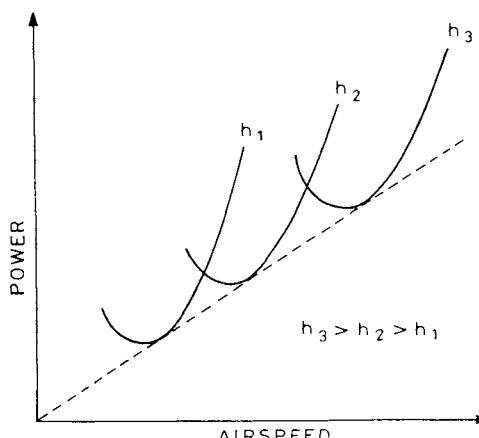


Fig. 12.2 Effect of altitude on power required.

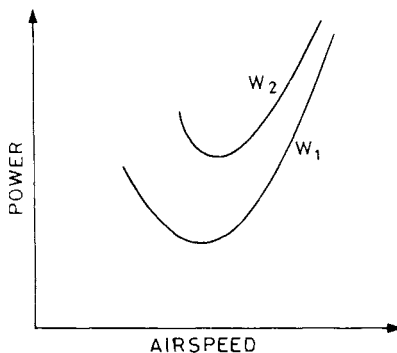


Fig. 12.3 Effect of weight on power required.

where these two curves cross signifies the stable equilibrium position of a cruising flight, as explained in Sec. 8.6.3. The power required curve P shown by a solid line is obtained from Eq. (12.13). In practice, the curve follows the dashed line at low airspeeds due to a large increase in drag after stalling. The power required curve against airspeed for a given aircraft depends on altitude and, therefore, the curve can be lowered or raised by changing the altitude. The power available curve, on the other hand, depends on both the altitude and the power setting. The power available curve can be raised or lowered either by changing the altitude or by altering the throttle setting. Therefore, the point where the two curves cross can be changed to different airspeeds.

12.5 Range and Its Flight Parameters

A basic integral relation for the range can be obtained and evaluated here for finding the ranges of three different flight programs. The flight parameters associated with each of these flight programs will also be calculated.

12.5.1 Basic Integral for Range, and for Different Flight Programs

An expression for the instantaneous range is obtained by dividing Eq. (12.3) by the equal terms of Eq. (12.6), giving

$$dx/(-dW) = k\eta_p V/(\hat{c}P)$$

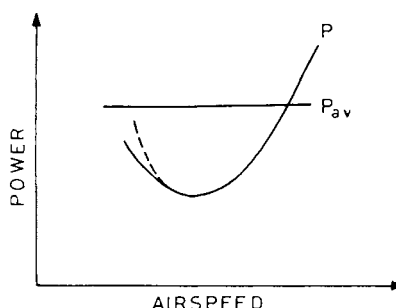


Fig. 12.4 Power required and power available curves.

which after using Eq. (12.7) can be written as

$$dx/(-dW) = k\eta_p E/(\hat{c}W) \quad (12.14)$$

The point performance (instantaneous range) $dx/(-dW)$ improves with the increase in η_p and E . It also improves with the reduction in W and \hat{c} . If x is the horizontal distance covered in flying from station 1 to station 2 during the cruise, the basic integral for the range x is obtained by integrating the above relation as

$$x = -(k\eta_p/\hat{c}) \int_1^2 E dW/W \quad (12.15)$$

where η_p and \hat{c} are assumed to be constant during the flight. The integrand in the above relation is a function of C_L , C_D , and W . The C_L and C_D of a given aircraft are functions of V , ρ , and W . It is possible to establish different flight programs depending on the variables and parameters that are being kept fixed during the flight. Three different flight programs are considered here, which are referred to as constant h - C_L , constant V - C_L , and constant h - V flights. In a constant h - C_L flight, as the name suggests, both the altitude h and the lift coefficient C_L are kept constant during the cruise. Similarly, in a constant V - C_L flight, the airspeed and lift coefficient are constant, and in a constant h - V flight, the altitude and airspeed are kept constant.

12.5.2 Range and Flight Parameters of a Constant Altitude–Constant Lift Coefficient Flight

The altitude h (and thus σ), and the lift coefficient C_L are kept constant here during the cruise. Since there is a one-to-one correspondence between C_L and C_D , constant C_L implies that C_D is also constant and, therefore, $E (= C_L/C_D)$ would also remain constant during the cruise. If x_{h-C_L} represents the range of constant h - C_L flight, Eq. (12.15) gives

$$x_{h-C_L} = -(k\eta_p E/\hat{c}) \int_1^2 dW/W \quad (12.16)$$

where the right-hand-side integral can be evaluated to give the range as

$$x_{h-C_L} = (k\eta_p E/\hat{c}) \ln(W_1/W_2) \quad (12.17)$$

where the subscript 1 represents the start of the cruise at station 1, and the subscript 2 represents the end of the cruise at station 2. Station 2 can also be regarded as variable point by dropping the subscript 2. Defining the cruise-fuel weight fraction ζ as

$$\zeta = (W_1 - W_2)/W_1 = (W_1 - W)/W = \Delta W_f/W \quad (12.18)$$

where $W \leq W_1$, the ratio W_1/W_2 can be expressed as

$$W_1/W_2 = W_1/W = 1/(1 - \zeta) \quad (12.19)$$

The expression for range given by Eq. (12.17) can now be written as

$$x_{h-C_L} = (k\eta_p E / \hat{c}) \ln \{1/(1 - \zeta)\} \quad (12.20)$$

The increase in η_p and E , and the decrease in \hat{c} , increases the range x_{h-C_L} for a given amount of fuel consumed.

The other flight parameters of the cruising flight can now also be obtained. The airspeed is given by Eq. (12.8) as

$$V = \sqrt{2(W/S)/(\rho_{SSL}\sigma C_L)} \quad (12.21)$$

where C_L and σ are constant during the flight. Therefore, from Eqs. (12.21) and (12.19),

$$V/V_1 = \sqrt{W/W_1} = \sqrt{1 - \zeta} \quad (12.22)$$

which gives the variation in the airspeed with ζ . The thrust power required is found from Eqs. (12.7) and (12.21) as

$$P = WV/E = (W/E)\sqrt{2(W/S)/(\rho_{SSL}\sigma C_L)}$$

and since σ and C_L are constant, the ratio P/P_1 can be written as

$$P/P_1 = (W/W_1)^{3/2} = (1 - \zeta)^{3/2} \quad (12.23)$$

The airspeed and power decrease nonlinearly with ζ . The reduction in weight of the aircraft with the increase in ζ is linear. The disadvantage of this flight program is that it continuously requires reduction in the airspeed by reducing the throttle setting.

12.5.3 Range and Flight Parameters of a Constant Airspeed–Constant Lift Coefficient Flight

This is a constant V - C_L flight and here also, like the previous case, C_L is constant. Consequently, both C_D and E also remain constant during the cruise. The range x_{V-C_L} of the constant V - C_L flight is given by Eq. (12.15) as

$$x_{V-C_L} = -(k\eta_p E / \hat{c}) \int_1^2 dW/W$$

The right-hand-side expression above is the same as that in Eq. (12.16). Therefore,

$$x_{V-C_L} = x_{h-C_L} = (k\eta_p E / \hat{c}) \ln \{1/(1 - \zeta)\} \quad (12.24)$$

From Eq. (12.8), it follows that for a constant V - C_L flight,

$$W/\rho = \text{const} = W_1/\rho_1 \quad (12.25)$$

Since W decreases during the flight, ρ must decrease and consequently the altitude must increase. For this reason, it is also called the *cruise-climb flight* for a piston-prop aircraft. It can be shown that the climb angle would be small and the flight path can be regarded as horizontal.

The other flight parameters of this flight can also now be obtained. From Eqs. (12.25) and (12.19),

$$\rho/\rho_1 = W/W_1 = 1 - \zeta \quad (12.26)$$

The increase in altitude during the cruise-climb can also be calculated. Using the standard atmosphere approximation, the density ratio σ can be written as

$$\sigma = \rho/\rho_{SSL} = e^{-h/\beta} \quad (12.27)$$

where $\beta = 9296$ m (30,500 ft) in the troposphere, which is the region where piston-prop aircraft usually fly. The ratio ρ/ρ_1 is given by

$$\rho/\rho_1 = (\rho/\rho_{SSL})/(\rho_1/\rho_{SSL}) = \sigma/\sigma_1 = e^{-(h-h_1)/\beta}$$

and comparing it with Eq. (12.26) gives

$$(h - h_1)/\beta = -\ln(1 - \zeta) \quad (12.28)$$

The thrust power is obtained from Eqs. (12.7) and (12.8) as

$$P = WV/E = (W/E)\sqrt{2(W/S)/(\rho_{SSL}\sigma C_L)}$$

where C_L and W/σ are constant in this flight program. This gives

$$P/P_1 = W/W_1 = 1 - \zeta \quad (12.29)$$

which shows that the weight and power decrease linearly during cruising flight.

12.5.4 Range and Flight Parameters of a Constant Altitude–Constant Airspeed Flight

This is a constant altitude–constant airspeed flight (constant h - V flight) where both h and V are constant during the flight. The lift coefficient is not constant here, and so the C_D and E would vary during the flight. The range x_{h-V} of the flight is given by Eq. (12.15) as

$$x_{h-V} = -(k\eta_p/\hat{c}) \int_1^2 (C_L/C_D) dW/W$$

The integral on the right-hand side of the above relation is the same as the integral of Eq. (8.28), which was evaluated in Chapter 8. The above expression for the range becomes

$$x_{h-V} = \frac{2k\eta_p E_m}{\hat{c}} \tan^{-1} \left\{ \frac{E_1 \zeta}{2E_m(1 - KE_1 C_{L,1} \zeta)} \right\} \quad (12.30)$$

where the subscript 1 represents the value at the start of the cruise. Note that the range does not explicitly depend on the airspeed as in the case of a turbojet aircraft [Eq. (8.35)]. The range also does not depend explicitly on the altitude and wing loading.

The other flight parameters of this flight can now also be obtained. Since the altitude and airspeed are constant, it follows from Eq. (12.8) that the ratio W/C_L is constant. This gives

$$C_L/C_{L,1} = W/W_1 = 1 - \zeta \quad (12.31)$$

The aerodynamic efficiency E of the aircraft would be given by

$$\frac{E}{E_1} = \frac{C_L/C_D}{C_{L,1}/C_{D,1}} = \frac{C_L/C_{L,1}}{C_D/C_{D,1}} = \frac{1 - \zeta}{C_D/C_{D,1}}$$

The ratio $C_D/C_{D,1}$ appearing in the above relation can be written as

$$\frac{C_D}{C_{D,1}} = \frac{C_{D_0} + KC_L^2}{C_{D_0} + KC_{L,1}^2} = 1 + \frac{KC_{L,1}^2}{C_{D,1}} \left(\frac{C_L^2}{C_{L,1}^2} - 1 \right)$$

which after using Eq. (12.31) becomes

$$C_D/C_{D,1} = 1 + KE_1 C_{L,1} \zeta (\zeta - 2) \quad (12.32)$$

Therefore,

$$E/E_1 = (1 - \zeta) / \{1 + KE_1 C_{L,1} \zeta (\zeta - 2)\} \quad (12.33)$$

The thrust power is obtained from Eqs. (12.7) and (12.8) as

$$P = WV/E = (W/E) \sqrt{2(W/S)/(\rho_{SSL} \sigma C_L)}$$

where the altitude (and thus σ) and W/C_L are constant in this flight program. The variation in the thrust power is given by

$$P/P_1 = DV/(D_1 V_1) = D/D_1 = C_D/C_{D,1}$$

which after using Eq. (12.32) becomes

$$P/P_1 = 1 + KE_1 C_{L,1} \zeta (\zeta - 2) \quad (12.34)$$

It can be seen that E/E_1 and P/P_1 depend not only on ζ but also on the factor $KE_1 C_{L,1}$. The variation with ζ for a specified value of $KE_1 C_{L,1}$ during cruising is the same as in the case of a turbojet aircraft [Eq. (8.40)] for the thrust ratio.

12.6 Endurance

The time taken by an aircraft to cover the horizontal distance between two specified stations of the cruising flight is calculated here. The basic relation of the time taken involves an integral that can be solved analytically in certain specified flight programs.

12.6.1 Basic Integral Relation

The relation for the instantaneous endurance ($-dt/dW$) on integration will yield the endurance. The instantaneous endurance is the time taken per unit weight of the fuel consumption at any instant during the cruise. It is obtained from Eqs. (12.6) and (12.7) as

$$-(dt/dW) = k\eta_p/(\hat{c}P) = (k\eta_p/\hat{c})E/(VW) \quad (12.35)$$

This shows that the instantaneous endurance is increased with the increase in η_p and E . Similarly, a decrease in the values of \hat{c} , V , P , and W , increases the endurance.

The time taken t of the cruising flight between stations 1 and 2 is given by the integration of Eq. (12.35) as

$$t = -(k\eta_p/\hat{c}) \int_1^2 E/(VW) dW \quad (12.36)$$

where η_p and \hat{c} are considered constants. The endurance depends on the specifications of a flight program. The three different flight programs discussed above for the range are also considered below for the endurance.

12.6.2 Endurance of a Constant Altitude–Constant Lift Coefficient Flight

Since the lift coefficient is kept constant during the flight, the aerodynamic efficiency E also remains constant. If t_{h-C_L} denotes endurance for a constant h - C_L flight, Eq. (12.36) can be written as

$$t_{h-C_L} = -(k\eta_p E/\hat{c}) \int_1^2 dW/(VW) \quad (12.37)$$

which after using Eq. (12.8) becomes

$$t_{h-C_L} = -(k\eta_p E/\hat{c})(\rho S C_L/2)^{1/2} \int_1^2 W^{-3/2} dW$$

After evaluating the integral on the right-hand side, the above relation becomes

$$t_{h-C_L} = \frac{2k\eta_p E}{\hat{c}} \left\{ \frac{\rho_{SSL} \sigma C_L}{2(W_1/S)} \right\}^{1/2} \left(\sqrt{\frac{W_1}{W_2}} - 1 \right) \quad (12.38)$$

and noting that $W_1/W_2 = 1/(1 - \zeta)$, the above relation is

$$t_{h-C_L} = \{2k\eta_p E/(\hat{c}V_1)\} \{1/\sqrt{1 - \zeta} - 1\} \quad (12.39)$$

For a given cruise-fuel weight fraction ζ , the endurance increases with the increase in η_p and E . Similarly, reductions in \hat{c} and V_1 increase the endurance. The other flight parameters of this flight program are presented above in Sec. 12.5.2.

12.6.3 Endurance of the Other Flight Programs

Both constant $V-C_L$ and constant $h-V$ flights are considered here; the endurance of these two flight types are represented by t_{V-C_L} and t_{h-V} , respectively. The integral in Eq. (12.36) can be analytically evaluated in both these cases. Since the airspeed is constant in both these flights, it is simpler to find the endurance by dividing the ranges of t_{V-C_L} and t_{h-V} flights by the corresponding constant airspeeds. That is,

$$t_{V-C_L} = x_{V-C_L}/V \quad \text{and} \quad t_{h-V} = x_{h-V}/V$$

which after using Eqs. (12.24) and (12.30), respectively, can be written as

$$t_{V-C_L} = \{k\eta_p E/(\hat{c}V)\} \ln\{1/(1-\zeta)\} \quad (12.40)$$

and

$$t_{h-V} = \frac{2k\eta_p E_m}{\hat{c}V} \tan^{-1} \left\{ \frac{E_1\zeta}{2E_m(1 - KE_1 C_{L,1}\zeta)} \right\} \quad (12.41)$$

The increase in η_p and the decrease in \hat{c} and V increases both the endurance t_{V-C_L} and t_{h-V} for a given ζ . An increase in ζ also increases the endurance. The other flight parameters of constant $V-C_L$ and constant $h-V$ flights were presented in Secs. 12.5.3 and 12.5.4, respectively.

12.7 Effects of Wind

It is generally assumed that the wind blows along the flight path of the aircraft. If the wind is blowing at some inclination to the path of the aircraft, the wind component along the flight path is considered. The effects of air current and of the wind component normal to the flight path in the horizontal plane are not considered here. The wind speed is considered positive for a headwind and negative for a tailwind. The true airspeed V can be expressed as $V = V_g \pm V_w$, where V_g is the ground speed, V_w is the wind speed along the flight path, the positive sign is for a headwind, and the negative sign is for a tailwind.

The ground speed can be expressed as $V_g = V \mp V_w$, where the negative sign stands for the headwind and the positive sign for the tailwind. If the airspeed V is kept constant, the presence of a headwind will decrease the ground speed and consequently the cruising endurance between two specified stations will increase; the higher the wind speed, the larger the endurance. Similarly, a tailwind causes an increase in the aircraft's ground speed and consequently the endurance will be reduced.

In the case where the airspeed V differs from the ground speed V_g due to wind, Eq. (12.3) should be written as $dx/dt = V_g$, and the specific range can be expressed as

$$\text{Specific range} = \frac{dx}{-dW} = \frac{dx/dt}{-dW/dt} = \frac{V_g}{\hat{c}P_e} = \frac{V \mp V_w}{\hat{c}P_e}$$

where the negative sign stands for the headwind and the positive sign for tailwind. If the airspeed V is kept constant during the cruise, and assuming that \hat{c} and P_e are not affected by the wind, a headwind will decrease the specific range, whereas a tailwind will increase it.

12.8 Application to an Aircraft

Consider an aircraft of weight 7350 N (1652.3 lb), wing area 11.2 m² (120.5 ft²), where the drag coefficient follows the drag polar $C_D = 0.032 + 0.142C_L^2$. It is flying at an altitude of 4 km with a piston-prop engine whose propeller efficiency is 0.85 and whose power specific fuel consumption is 0.55×10^{-6} N/s/W (0.33 lb/h/hp). The cruise-fuel weight fraction of the aircraft is 0.12. If the airspeed of the aircraft is 175 km/h, find the range and endurance during cruise in the cases of constant $h-C_L$, constant $V-C_L$, and constant $h-V$ flights.

The wing loading is $W/S = 7350/11.2 = 656.25$ N/m² and from the standard atmosphere table, $\rho_{SSL} = 1.225$ kg/m³, and $\sigma = 0.6689$ at an altitude of 4000 m. The maximum aerodynamic efficiency of the aircraft would be $E = 0.5(KC_{D_0})^{-0.5} = 0.5(0.14 \times 0.032)^{-0.5} = 7.47$. The value of $k = 1$, and $V = 175$ km/h = 48.61 m/s.

The lift coefficient of the aircraft at the start of the cruise is given by Eq. (12.8) as

$$C_L = \frac{2(W/S)}{\rho_{SSL}\sigma V^2} = \frac{2 \times 656.25}{1.225 \times 0.6689(48.61)^2} = 0.6779$$

The drag coefficient is given by the drag polar Eq. (12.10) as, $C_D = 0.032 + 0.14(0.6779)^2 = 0.0963$, and the aerodynamic efficiency at the start of the cruise is $E = C_L/C_D = 0.6779/0.0963 = 7.039$. The range of the constant $h-C_L$ flight is obtained from Eq. (12.20) as

$$x_{h-C} = \frac{1 \times 0.85 \times 7.039}{0.55 \times 10^{-6}} \ell_n\left(\frac{1}{1 - 0.12}\right) = 1.3906 \times 10^6 \text{ m} = 1390.6 \text{ km}$$

and its endurance is obtained from Eq. (12.39) as

$$t_{h-C_L} = \frac{2 \times 1 \times 0.85 \times 7.039}{0.55 \times 10^{-6} \times 48.61} \ell_n\left(\frac{1}{\sqrt{1 - 0.12}} - 1\right) = 29,542 \text{ s} = 8.21 \text{ h}$$

The range of constant $V-C_L$ flight is obtained from Eq. (12.24) as $x_{V-C_L} = x_{h-C_L} = 1390.6$ km and its endurance is obtained as $t_{h-C_L} = x_{h-C_L}/V = 1390.6/175 = 7.95$ h.

The range of the constant $h-V$ flight is given by Eq. (12.30) as

$$\begin{aligned} x_{h-V} &= \frac{2 \times 1 \times 0.85 \times 7.47}{0.55 \times 10^{-6}} \\ &\times \tan^{-1}\left(\frac{7.039 \times 0.12}{2 \times 7.47(1 - 0.14 \times 7.039 \times 0.6779 \times 0.12)}\right) \\ &= 1.4174 \times 10^6 \text{ m} = 1417.4 \text{ km} \end{aligned}$$

and its endurance would be obtained as $t_{h-V} = x_{h-V}/V = 1416.5/175 = 8.10$ h.

Therefore, the ranges of the constant $h-C_L$, constant $V-C_L$, and constant $h-V$ flights are 1390.6, 1390.6, and 1416.5 km, respectively, and their respective levels of endurance are 8.21, 7.95, and 8.10 h.

Problems

Major specifications of two different piston-prop aircraft are presented below; they are used in solving problems of this chapter and in Chapters 13–15.

Major specifications of piston-prop aircraft D and E

Specifications	Aircraft D (single engine)	Aircraft E (twin engine)
Total weight, N	12,000	35,000
Maximum fuel, N	1,600	5,000
Wing area, m ²	15	26
Maximum power, kW	200	500
C_{D_0}	0.042	0.03
K	0.074	0.048
η_p	0.83	0.85
$C_{L,m}$	1.5	1.7
\hat{c} , N/h/kW	2.45	2.5
Critical altitude, km	4.5	6

12.1 Find the wing loading, maximum power/weight ratio, fuel-weight fraction, and maximum aerodynamic efficiency of a) Aircraft D and b) Aircraft E.

12.2 Aircraft D is cruising at sea level. Find the variations in the a) thrust power required, b) instantaneous range, and c) fuel flow rate, with an increase in airspeed. Also find the stalling airspeed of the aircraft.

12.3 Solve Problem 12.2 if Aircraft D is using an aspirated engine and cruising at an altitude of 4 km.

12.4 Solve Problem 12.2 if Aircraft D is using an aspirated engine and cruising at an altitude of 6 km.

12.5 Solve Problem 12.2 if Aircraft D is using a supercharged engine and cruising at an altitude of 6 km.

12.6 Solve Problem 12.2 for Aircraft E.

12.7 Solve Problem 12.2 for Aircraft E if it is using an aspirated engine and cruising at an altitude of 4 km.

12.8 Solve Problem 12.2 for Aircraft E if it is using a supercharged engine and cruising at an altitude of 4 km.

12.9 Solve Problem 12.2 for Aircraft E if it is using a supercharged engine and cruising at an altitude of 9 km.

12.10 Solve Problem 12.2 for Aircraft D in the cases where a) the wing loading is increased by 10%, b) C_{D_0} is decreased by 5%, and c) K is decreased by 5%.

12.11 Aircraft D is cruising at sea level with an airspeed of 180 km/h at the start of the cruise and utilizes 75% of the total fuel for the cruise. The aircraft is flown with three different flight programs: a) constant $h-C_L$, b) constant $V-C_L$, and c) constant $h-V$. Find in each case i) the range covered and corresponding endurance, and ii) airspeed, altitude, lift coefficient, wing loading, and aerodynamic efficiency at the end of the cruise.

12.12 Solve Problem 12.11 if Aircraft D flies at an altitude of 3 km.

12.13 Solve Problem 12.11 if Aircraft D flies at an altitude of 6 km.

12.14 Solve Problem 12.11 if the airspeed is increased by 40%.

12.15 Solve Problem 12.11 if Aircraft D flies at an altitude of 6 km with an airspeed of 60 m/s.

12.16 Solve Problem 12.11 for Aircraft E.

12.17 Solve Problem 12.11 for Aircraft E in the cases where a) W/S is increased by 8%, b) C_{D_0} is reduced by 4%, c) K is reduced by 4%, and d) if these changes in W/S , C_{D_0} , and K are carried out simultaneously. Compare the results obtained with those in Problem 12.16 and find the percentage changes in the flight variables in each case.

12.18 Solve Problem 12.11 for Aircraft E if it is flying at an altitude of 6 km with an airspeed of 280 km/h.

12.19 Aircraft E starts cruising at an altitude of 5 km with an airspeed of 250 km/h. Find the percentage changes made in the range and its endurance in the constant $h-V$ flight when a) wing loading is increased by 10%, b) C_{D_0} is decreased by 2%, and c) if these changes in wing loading and C_{D_0} are simultaneously carried out.

12.20 Aircraft D is using an aspirated engine to cruise at an altitude of 5 km, utilizing 85% of the maximum thrust power available. If the aircraft consumes a cruise-fuel weight fraction of 0.12, find the cruising range and the time taken to cover the distance in the cases of a) constant $V-C_L$ flight, and b) constant $h-V$ flight.

12.21 Solve Problem 12.20 for Aircraft D if it is using a supercharged engine.

12.22 Solve Problem 12.20 for Aircraft E.

12.23 Solve Problem 12.20 for Aircraft E if it is using a turbocharged engine.

12.24 Solve Problem 12.20 for Aircraft D if it is using a supercharged engine and is cruising at an altitude of 7 km.

12.25 Aircraft D has an aspirated engine and cruises at an altitude of 5 km, covering a range of 1000 km. It uses only 80% of the available thrust power at that altitude. For a) constant $V-C_L$ and b) constant $h-V$ flight programs, find the following: i) the amount of fuel consumed during the cruise, and ii) the time spent in the cruise.

12.26 Solve Problem 12.25 for Aircraft D if it is using a turbocharged engine.

12.27 Solve Problem 12.25 for Aircraft E.

12.28 Do Problem 12.25 for Aircraft E if it is using a supercharged engine.

12.29 Aircraft D cruises at an altitude of 6 km using an aspirated engine. Calculate the range covered, fuel consumed, lift coefficient, and aerodynamic efficiency in the cases of a) constant $V-C_L$ and b) constant $h-V$ flight programs, if the aircraft cruises at an initial airspeed of 80% of the maximum airspeed.

12.30 Solve Problem 12.29 for Aircraft D if it is using a supercharged engine.

12.31 Solve Problem 12.29 for Aircraft E if it is using an aspirated engine.

12.32 Solve Problem 12.29 for Aircraft E if it is using a supercharged engine.

This page intentionally left blank

13

Optimization of Cruising Flights of Piston-Prop Aircraft

13.1 Introduction

Optimization of cruising flight is an essential activity of aircraft performance. The optimization can be carried out for minimum-thrust flight, maximum-range flight, and for maximum-endurance flight. All these cases are considered here for piston-prop aircraft. Three different flight programs, namely, constant $h-C_L$, constant $V-C_L$, and constant $h-V$ are considered here, both for maximum range and maximum endurance, similar to the flight programs for turbojet aircraft discussed in Chapter 9. In all these cases, generally the airspeed for optimum flight is established first and then the other flight parameters are obtained.

13.2 Minimum-Power Flight

The rate of fuel consumption is least for flight at minimum power. The minimum power/weight ratio P_{\min}/W is an important performance parameter. Since power varies as the cube of airspeed, the use of piston-prop aircraft at higher speed becomes prohibitive. First, the airspeed for minimum power is obtained here, and then the other flight parameters are deduced.

13.2.1 Airspeed

The airspeed for minimum power $V_{P_{\min}}$ can be obtained by differentiating Eq. (12.13) with respect to V , and setting $dP/dV = 0$. This gives

$$3\rho_{SSL}\sigma C_{D_0}SV^2/2 - 2K(W/S)^2/(\rho_{SSL}\sigma V^2) = 0$$

for $V = V_{P_{\min}}$. The solution of the above equation yields

$$V_{P_{\min}} = \left\{ \frac{2(W/S)}{\rho_{SSL}\sigma} \right\}^{1/2} \left(\frac{K}{3C_{D_0}} \right)^{1/4} = \frac{V_{P_{\min},SSL}}{\sqrt{\sigma}} = \frac{V_{E_m}}{3^{1/4}} \quad (13.1)$$

The airspeed for minimum power increases with the increase in wing loading (W/S) and altitude, and with the decrease in zero-lift drag coefficient C_{D_0} . The $V_{P_{\min}}$ is 24% less than V_{E_m} . If the altitude (and thus σ) is kept constant during minimum-power flight, the airspeed decreases during cruising due to reduction in the weight of the aircraft caused by fuel consumption. On the other hand, if the airspeed is kept constant during minimum-power flight, Eq. (13.1) gives $W/\rho = \text{constant} = W_1/\rho_1$, where subscript 1 represents the value at the start of the cruise. Since W decreases during the cruise, it follows that ρ must decrease, and thus altitude must increase during the flight. Therefore, the flight in which W/ρ is constant is called the cruise-climb flight. Since the climb angle of the cruise

is very small, the flight is regarded as horizontal for the purpose of theoretical analysis.

13.2.2 Lift Coefficient, Aerodynamic Efficiency, and Power

The lift and drag coefficients for minimum power, $C_{L,P_{\min}}$ and $C_{D,P_{\min}}$, respectively, are obtained from the two relations of Eq. (12.9) by substituting $V_{P_{\min}}$ for V . This gives

$$C_{L,P_{\min}} = (3C_{D_0}/K)^{1/2} = \sqrt{3}C_{L,E_m} \quad (13.2)$$

and

$$C_{D,P_{\min}} = 4C_{D_0} = 2C_{D,E_m}$$

where C_{L,E_m} and C_{D,E_m} are the lift and drag coefficients, respectively, for maximum aerodynamic efficiency. The aerodynamic efficiency for maximum power, $E_{P_{\min}}$, is then given by

$$E_{P_{\min}} = \frac{C_{L,P_{\min}}}{C_{D,P_{\min}}} = \frac{\sqrt{3}}{2} \cdot \frac{C_{L,E_m}}{C_{D,E_m}} = 0.866E_m \quad (13.3)$$

The minimum power required is obtained from Eq. (12.7) as $P_{\min}/W = V_{P_{\min}}/E_{P_{\min}}$, which after using Eqs. (13.1) and (13.3) can be written as

$$\frac{P_{\min}}{W} = \left\{ \frac{2(W/S)}{\rho_{SSL}\sigma} \right\}^{1/2} \left(\frac{K}{3C_{D_0}} \right)^{1/4} \frac{1}{0.866E_m} = \frac{V_{P_{\min}}}{0.866E_m} = \frac{V_{P_{\min},SSL}}{0.866\sqrt{\sigma}E_m} \quad (13.4)$$

The minimum-thrust power required increases with the increase in wing loading and altitude, but decreases with the increase in the maximum aerodynamic efficiency of the aircraft.

13.3 Maximum-Range Flights

The maximum ranges and their associated flight parameters for the three different flight programs discussed in Chapter 12 are provided here. The knowledge of the maximum-range flight parameters helps a pilot to cover larger distance for a given amount of fuel during the cruise. For each maximum-range flight, the associated parameters including the maximum range and its endurance are provided.

13.3.1 Maximum Range and Flight Parameters of a Constant Altitude–Constant Lift Coefficient Flight

The range of a constant h - C_L flight is obtained from Eq. (12.20) as

$$x_{h-C_L} = (k\eta_p E/\hat{c}) \ln \{1/(1 - \xi)\}$$

where η_p and \hat{c} are regarded as constants, and k is the conversion factor, depending on the system of unit chosen. For a given ξ , the range is maximum if $E = E_m$. The maximum range $x_{mr;h-C_L}$ is then given by the above relation as

$$x_{mr;h-C_L} = (k\eta_p E_m/\hat{c}) \ln \{1/(1 - \xi)\} \quad (13.5)$$

The maximum range can be increased by increasing the propeller efficiency and maximum aerodynamic efficiency, and by decreasing the power-specific fuel consumption.

It is seen above that the maximum range is obtained by flying at maximum aerodynamic efficiency of the aircraft. This gives the maximum-range airspeed $V_{\text{mr};h-C_L}$ of the constant $h\text{-}C_L$ flight as

$$V_{\text{mr};h-C_L} = V_{E_m} = \{2(W/S)/(\rho_{\text{SSL}}\sigma)\}^{1/2} \left(K/C_{D_0} \right)^{1/4} \quad (13.6)$$

and the ratio of airspeeds as

$$V_{\text{mr};h-C_L}/V_{1\text{mr};h-C_L} = \sqrt{W/W_1} = \sqrt{1-\zeta} \quad (13.7)$$

where the subscript 1 represents the value at station 1, which is the start of the cruise. The maximum-range airspeed varies nonlinearly with the cruise-fuel weight fraction.

The lift and drag coefficients, $C_{L;\text{mr};h-C_L}$ and $C_{D;\text{mr};h-C_L}$, respectively, of the constant $h\text{-}C_L$ flight are given by

$$C_{L,\text{mr};h-C_L} = C_{L,E_m} = \sqrt{C_{D_0}/K} \quad \text{and} \quad C_{D,\text{mr};h-C_L} = C_{D,E_m} = 2C_{D_0} \quad (13.8)$$

The aerodynamic efficiency $E_{\text{mr};h-C_L}$ for the maximum range is

$$E_{\text{mr};h-C_L} = E_m = 1(2\sqrt{C_{D_0}K})$$

The power/weight ratio $P_{\text{mr};h-C_L}/W$ of the flight program is found from Eq. (12.7) as

$$\frac{P_{\text{mr};h-C_L}}{W} = \frac{V_{\text{mr};h-C_L}}{E_{\text{mr};h-C_L}} = \frac{V_{E_m}}{E_m} = \frac{1}{E_m} \left\{ \frac{2(W/S)}{\rho_{\text{SSL}}\sigma} \right\}^{1/2} \left(\frac{K}{C_{D_0}} \right)^{1/4}$$

which gives the ratio of thrust powers

$$P_{\text{mr};h-C_L}/P_{1\text{mr};h-C_L} = (W/W_1)\sqrt{W/W_1} = (W/W_1)^{3/2} = (1-\zeta)^{3/2}$$

The power varies nonlinearly with ζ during the cruise.

13.3.2 Maximum Range and Flight Parameters of a Constant Airspeed–Constant Lift Coefficient Flight

It was seen in Chapter 12 that constant $V\text{-}C_L$ and constant $h\text{-}C_L$ flights have the same range. That is,

$$x_{V-C_L} = x_{h-C_L} = (k\eta_p E/\hat{c}) \ln \{1/(1-\zeta)\}$$

It follows that their maximum ranges would also be the same as given by

$$x_{\text{mr};V-C_L} = x_{\text{mr};h-C_L} = (k\eta_p E_m/\hat{c}) \ln \{1/(1-\zeta)\} \quad (13.9)$$

Here also the maximum range of constant $V \cdot C_L$ flight is achieved by flying at the aircraft's maximum aerodynamic efficiency. The lift coefficient, drag coefficient, and aerodynamic efficiency of the maximum-range flight, denoted by $C_{L,\text{mr};V-C_L}$, $C_{D,\text{mr};V-C_L}$, and $E_{\text{mr};V-C_L}$, respectively, are given by

$$C_{L,\text{mr};V-C_L} = C_{L,\text{mr};h-C_L} = C_{L,E_m} = \sqrt{C_{D_0}/K}$$

$$C_{D,\text{mr};V-C_L} = C_{D,\text{mr};h-C_L} = C_{D,E_m} = 2C_{D_0}$$

and

$$E_{\text{mr};V-C_L} = E_{\text{mr};h-C_L} = E_m = 1/(2\sqrt{C_{D_0}K})$$

The maximum-range airspeed $V_{\text{mr};V-C_L}$ of the flight is given by

$$V_{\text{mr};V-C_L} = V_{E_m} = \{2(W/S)/(\rho_{SSL}\sigma)\}^{1/2} (K/C_{D_0})^{1/4} \quad (13.10)$$

and since the airspeed is constant, it follows from the above equation that $W/\sigma = \text{constant} = W_1/\sigma_1$, which pertains to cruise-climb flight, as mentioned above.

The thrust power variation for maximum range of the constant $V \cdot C_L$ flight is obtained from Eq. (12.7) as

$$\frac{P_{\text{mr};V-C_L}}{W} = \frac{V_{\text{mr};V-C_L}}{E_{\text{mr};V-C_L}} = \frac{V_{E_m}}{E_m} = \frac{1}{E_m} \left\{ \frac{2(W/S)}{\rho_{SSL}\sigma} \right\}^{1/2} \left(\frac{K}{C_{D_0}} \right)^{1/4}$$

which gives the ratio of thrust powers,

$$P_{\text{mr};V-C_L}/P_{1\text{mr};V-C_L} = W/W_1 = 1 - \zeta$$

The thrust power for maximum range of constant $V \cdot C_L$ flight varies linearly with the cruise-fuel weight fraction.

The endurance $t_{\text{mr};V-C_L}$ of constant $V \cdot C_L$ flight is obtained by dividing the range by the airspeed. That is,

$$t_{\text{mr};V-C_L} = \frac{x_{\text{mr};V-C_L}}{V_{\text{mr};V-C_L}} = \frac{k\eta_p E_m}{\hat{c}V_{E_m}} l_v \left(\frac{1}{1 - \zeta} \right) \quad (13.11)$$

which in terms of the aircraft design parameters can be written as

$$t_{\text{mr};V-C_L} = \left\{ \frac{\rho_{SSL}\sigma}{2(W/S)} \right\}^{1/2} \left(\frac{C_{D_0}}{K} \right)^{1/4} \frac{k\eta_p E_m}{\hat{c}} l_v \left(\frac{1}{1 - \zeta} \right)$$

The endurance of the maximum range for a given ζ increases with the decrease in wing loading, K , and \hat{c} .

13.3.3 Maximum Range and Flight Parameters of a Constant Altitude—Constant Airspeed Flight

An expression for the range x_{h-V} of constant $h \cdot V$ flight is given by Eq. (12.30) as

$$x_{h-V} = \frac{2k\eta_p E_m}{\hat{c}} \tan^{-1} \left\{ \frac{E_1 \zeta}{2E_m(1 - K E_1 C_{L,1} \zeta)} \right\} \quad (13.12)$$

where subscript 1 represents the value at Station 1, which is the starting station of the cruising flight, and

$$C_{L,1} = \frac{2(W_1/S)}{\rho V^2}, \quad E_m = \frac{1}{2\sqrt{C_{D_0}K}}, \quad \zeta = \frac{\Delta W_f}{W_1} \quad (13.13)$$

and

$$E_1 = \frac{C_{L,1}}{C_{D,1}} = \frac{C_{L,1}}{C_{D_0} + KC_{L,1}^2} = \frac{2(W_1/S)/\rho V^2}{C_{D_0} + 4K(W_1/S)/\rho^2 V^4} \quad (13.14)$$

It was pointed out in Sec. 9.3.3 that the presence of arc tan function in the expression for range prohibits us from obtaining analytic expressions for the flight parameters of maximum-range flight.

The analytic expressions for the maximum range and its associated flight parameters can be obtained if it is noted that in practice the function involving arc tan is much less than unity.¹ This allows for the approximation of the arc tan function as

$$\tan^{-1} \left\{ \frac{E_1 \zeta}{2E_m(1 - KE_1 C_{L,1} \zeta)} \right\} \approx \frac{E_1 \zeta}{2E_m(1 - KE_1 C_{L,1} \zeta)} \quad (13.15)$$

which simplifies Eq. (13.12) as

$$x_{h-V} = \frac{k\eta_p E_1 \zeta}{\hat{c}(1 - KE_1 C_{L,1} \zeta)} = \frac{k\eta_p}{\hat{c}} \cdot \frac{C_{L,1} \zeta}{C_{D_0} + K(1 - \zeta)C_{L,1}^2}$$

Using the value of $C_{L,1}$ from Eq. (13.13), the above relation becomes

$$x_{h-V} = \frac{k\eta_p}{\hat{c}} \cdot \frac{2(W_1/S)\rho\zeta V^2}{C_{D_0}\rho^2V^4 + 4K(1 - \zeta)(W_1/S)^2} \quad (13.16)$$

If $\zeta = \zeta^*$ is the cruise-fuel weight fraction consumed during the cruising flight that is intended to be optimized, the above equation is written as

$$x_{h-V} = \frac{k\eta_p}{\hat{c}} \cdot \frac{2(W_1/S)\rho\zeta^* V^2}{C_{D_0}\rho^2V^4 + 4K(1 - \zeta^*)(W_1/S)^2} \quad (13.17)$$

To optimize x_{h-V} with respect to V for a given aircraft when all the other variables on the right-hand side of Eq. (13.17) are constant, we differentiate it with respect to V and put $dx_{h-V}/dV = 0$. The resulting algebraic equation can be solved, giving the maximum-range airspeed $V_{mr;h-V}$ as

$$V_{mr;h-V} = \{2(W_1/S)/(\rho_{SSL}\sigma)\}^{1/2} \left\{ K(1 - \zeta^*)/C_{D_0} \right\}^{1/4} \quad (13.18)$$

The maximum-range airspeed increases with the increase in wing loading and altitude. It also increases with the decrease in zero-lift drag coefficient.

It is now easier to find the other maximum-range flight parameters of the flight program. The lift coefficient $C_{L,mr;h-V}$ for the maximum-range is obtained as

$$C_{L,mr;h-V} = 2(W/S)/(\rho V_{mr;h-V}^2) = (W/W_1) \left[C_{D_0}/\{K(1 - \zeta^*)\} \right]^{1/2}$$

but, with $W/W_1 = 1 - \zeta$, the above equation becomes

$$C_{L,\text{mr};h-V} = (1 - \zeta) [C_{D_0}/\{K(1 - \zeta^*)\}]^{1/2} \quad (13.19)$$

The aerodynamic efficiency $E_{\text{mr};h-V}$ for the maximum range is given by

$$E_{\text{mr};h-V} = C_{L,\text{mr};h-V}/C_{D,\text{mr};h-V} = C_{L,\text{mr};h-V}/(C_{D_0} + KC_{L,\text{mr};h-V}^2)$$

where $C_{D,\text{mr};h-V}$ is the drag coefficient of the aircraft during flight. Using Eq. (13.19) in the above relation, it becomes

$$E_{\text{mr};h-V} = 2E_m(1 - \zeta)\sqrt{(1 - \zeta^*)}/\{(1 - \zeta^*) + (1 - \zeta)^2\} \quad (13.20)$$

The thrust power required $P_{\text{mr};h-V}$ for maximum-range flight is obtained from Eqs. (12.7), (13.18), and (13.20) as

$$\frac{P_{\text{mr};h-V}}{W} = \frac{V_{\text{mr};h-V}}{E_{\text{mr};h-V}} = \left\{ \frac{2(W_1/S)}{\rho_{\text{SSL}}\sigma} \right\}^{1/2} \left\{ \frac{K(1 - \zeta^*)}{C_{D_0}} \right\}^{1/4} \cdot \frac{(1 - \zeta^*) + (1 - \zeta)^2}{2E_m(1 - \zeta)\sqrt{(1 - \zeta^*)}} \quad (13.21)$$

It may be noted that the airspeed, lift coefficient, aerodynamic efficiency, and the thrust power required, for the maximum range of a constant h - V flight also depend on ζ^* , in addition to the aircraft design variables. To set these parameters for the maximum range of the constant h - V flight, a pilot must know, a priori, the amount of cruise-fuel weight fraction ζ^* that will be consumed during the cruise.

The maximum range of constant h - V flight is found from Eq. (13.12) as

$$x_{\text{mr};h-V} = \frac{2k\eta_p E_m}{\hat{c}} \tan^{-1} \left\{ \frac{E_{1\text{mr};h-V}\zeta}{2E_m(1 - KE_{1\text{mr};h-V}C_{L,1\text{mr};h-V}\zeta)} \right\} \quad (13.22)$$

where

$$C_{L,1\text{mr};h-V} = (C_{L,\text{mr};h-V})_{\zeta=0} = \left\{ \frac{C_{D_0}}{K(1 - \zeta^*)} \right\}^{1/2} \quad (13.23)$$

and

$$E_{1\text{mr};h-V} = (E_{\text{mr};h-V})_{\zeta=0} = 2E_m\sqrt{(1 - \zeta^*)}/\{1 + (1 - \zeta^*)\} \quad (13.24)$$

Using Eqs. (13.23) and (13.24), the maximum range given by Eq. (13.22) can be expressed as

$$x_{\text{mr};h-V} = (2k\eta_p E_m/\hat{c}) \tan^{-1} [\zeta\sqrt{(1 - \zeta^*)}/\{(1 - \zeta) + (1 - \zeta^*)\}] \quad (13.25)$$

where ζ has the value ζ^* at the end of the cruise. The maximum range can be increased by increasing E_m and η_p , and by decreasing \hat{c} . The range is not affected by changes in the altitude and wing loading. Since the airspeed is

kept constant, the endurance $t_{\text{mr};h-V}$ of the maximum range can be obtained as $t_{\text{mr};h-V} = x_{\text{mr};h-V} / V_{\text{mr};h-V}$, which gives

$$t_{\text{mr};h-V} = \left\{ \frac{\rho_{\text{SSL}}\sigma}{2(W_1/S)} \right\}^{1/2} \left\{ \frac{C_{D_0}}{K(1-\zeta^*)} \right\}^{1/4} \frac{2k\eta_p E_m}{\hat{c}} \times \tan^{-1} \left\{ \frac{\zeta\sqrt{(1-\zeta^*)}}{(1-\zeta)+(1-\zeta^*)} \right\} \quad (13.26)$$

The endurance of maximum-range flight like the maximum range itself, can also be increased by increasing E_m and η_p , and by decreasing \hat{c} . The endurance of the maximum-range flight decreases with an increase in altitude and wing loading.

The different flight parameters given by Eqs. (13.19–13.26) vary with ζ for a flight that is optimized for $\zeta = \zeta^*$. These equations do not predict the maximum-range flight parameters for any other ζ except for $\zeta = \zeta^*$.

The effectiveness of ζ^* in expressions for the range [Eq. (13.25)] and endurance [Eq. (13.26)] can be investigated by defining the functions f_x and f_t as

$$f_x = \tan^{-1} \left\{ \frac{\zeta\sqrt{1-\zeta^*}}{(1-\zeta)+(1-\zeta^*)} \right\} \quad \text{and} \quad f_t = (1-\zeta^*)^{-1/4} f_x$$

These two functions do not depend on aircraft design parameters. The functions f_x and f_t can be plotted against ζ for different values of ζ^* . It can be seen (similar to Fig. 9.1) that the changes in ζ^* appreciably influence endurance but not range.

It may be desired to obtain the maximum-range flight parameters for all values of ζ . This is done by putting $\zeta^* = \zeta$ in Eqs. (13.18–13.21) which, respectively, give

$$V_{\text{mr};h-V} = \{2(W_1/S)/(\rho_{\text{SSL}}\sigma)\}^{1/2} \left\{ K(1-\zeta)/C_{D_0} \right\}^{1/4} \quad (13.27)$$

$$C_{L,\text{mr};h-V} = \left\{ C_{D_0}(1-\zeta)/K \right\}^{1/2} \quad (13.28)$$

$$E_{\text{mr};h-V} = 2E_m\sqrt{(1-\zeta)/(2-\zeta)} \quad (13.29)$$

and

$$\frac{P_{\text{mr};h-V}}{W} = \left\{ \frac{2(W_1/S)}{\rho_{\text{SSL}}\sigma} \right\}^{1/2} \left\{ \frac{K(1-\zeta)}{C_{D_0}} \right\}^{1/4} \frac{(2-\zeta)}{2E_m\sqrt{(1-\zeta)}} \quad (13.30)$$

Similarly, the maximum range and its endurance, of the constant h - V flight program, for all values of ζ are obtained by putting $\zeta^* = \zeta$ in Eqs. (13.25) and (13.26), giving, respectively,

$$x_{\text{mr};h-V} = (2k\eta_p E_m/\hat{c}) \tan^{-1} \left\{ \zeta/(2\sqrt{1-\zeta}) \right\} \quad (13.31)$$

and

$$t_{\text{mr};h-V} = \left\{ \frac{\rho_{\text{SSL}}\sigma}{2(W_1/S)} \right\}^{1/2} \left\{ \frac{C_{D_0}}{K(1-\zeta)} \right\}^{1/4} \frac{2k\eta_p E_m}{\hat{c}} \tan^{-1} \left\{ \frac{\zeta}{2\sqrt{1-\zeta}} \right\} \quad (13.32)$$

Equations (13.27–13.32) give the corresponding values for any ζ , but for each ζ a different maximum-range flight would result.

13.4 Maximum-Endurance Flights

For certain flight missions the endurance of the aircraft is more important than its range. The maximum endurance and its flight parameters would be obtained here. The endurance depends on the type of flight program. The maximum endurance of the constant $h-C_L$, constant $V-C_L$, and constant $h-V$ flight programs are discussed below.

13.4.1 Maximum Endurance and Flight Parameters of a Constant Altitude–Constant Lift Coefficient Flight

The endurance of a constant $h-C_L$ flight is given by Eq. (12.39) as

$$t_{h-C_L} = \{(2k\eta_p E / (\hat{c}V_1))\} \left\{ 1/\sqrt{1-\zeta} - 1 \right\} \quad (13.33)$$

where η_p and \hat{c} are considered constant, $E (=E_1)$ is also constant because C_L is kept constant during the flight.

For a given cruise-fuel weight fraction ζ , the endurance t_{h-C_L} of a given aircraft would be maximum if E/V_1 is maximum. The ratio E/V_1 can be expressed as

$$\frac{E}{V_1} = \frac{1}{V_1} \cdot \frac{C_L}{C_{D_0} + KC_L^2} = \frac{2(W_1/S)\rho V_1}{\rho^2 C_{D_0} V_1^4 + 4K(W_1/S)^2}$$

Differentiate the above relation with respect to V_1 and put $d(E/V_1)/dV_1 = 0$. The resulting algebraic relation yields the maximum-endurance airspeed $V_{1me;h-C_L}$ at the start of the cruise as

$$V_{1me;h-C_L} = \{2(W_1/S)/(\rho_{SSL}\sigma)\}^{1/2} \left\{ K / (3C_{D_0}) \right\}^{1/4} \quad (13.34)$$

The maximum-endurance airspeed at the start of the cruise increases with the increase in wing loading and altitude. It can be seen that it is less than the maximum-range airspeed. The variation of airspeed during cruise is obtained from Eq. (12.22) as

$$V_{me;h-C_L} / V_{1me;h-C_L} = \sqrt{W/W_1} = \sqrt{1-\zeta}$$

Putting the value of $V_{1me;h-C_L}$ from Eq. (13.34) in the above relation gives

$$V_{me;h-C_L} = \{2(W/S)/(\rho_{SSL}\sigma)\}^{1/2} \left\{ K / (3C_{D_0}) \right\}^{1/4} \quad (13.35)$$

The airspeed increases with the increase in wing loading and altitude. The airspeed decreases linearly with the increase in ζ .

The other flight parameters of the maximum endurance can also be deduced. The lift coefficient $C_{L,me;h-C_L}$ that is kept constant is given by

$$C_{L,me;h-C_L} = 2(W/S) / (\rho V_{me;h-C_L}^2) = (3C_{D_0}/K)^{1/2} = \sqrt{3} C_{L,E_m} \quad (13.36)$$

The corresponding drag coefficient $C_{D,\text{me};h-C_L}$ of the flight is given by

$$C_{D,\text{me};h-C_L} = C_{D_0} + K C_{L,\text{me};h-C_L}^2 = 4C_{D_0}$$

The aerodynamic efficiency $E_{\text{me};h-C_L}$ of the flight would be obtained as

$$E_{\text{me};h-C_L} = \frac{C_{L,\text{me};h-C_L}}{C_{D,\text{me};h-C_L}} = \frac{\sqrt{3}}{4\sqrt{KC_{D_0}}} = \frac{\sqrt{3}}{2} E_m \quad (13.37)$$

The aerodynamic efficiency for maximum endurance is less than the maximum aerodynamic efficiency of the aircraft.

The thrust power $P_{\text{me};h-C_L}$ is obtained from Eqs. (12.7), (13.35), and (13.37) as

$$P_{\text{me};h-C_L} = \frac{W V_{\text{me};h-C_L}}{E_{\text{me};h-C_L}} = \frac{2W}{\sqrt{3}E_m} \left\{ \frac{2(W/S)}{\rho_{SSL}\sigma} \right\}^{1/2} \left(\frac{K}{3C_{D_0}} \right)^{1/4}$$

The power requirement for maximum endurance increases with the increase in wing loading and altitude, but decreases with the increase in maximum aerodynamic efficiency.

The maximum endurance $t_{m;h-C_L}$ is obtained from Eq. (13.33) as

$$t_{m;h-C_L} = 2k\eta_p E_{\text{me};h-C_L} / (\hat{c}V_{\text{me};h-C_L}) (1/\sqrt{1-\zeta} - 1)$$

which after using Eqs. (13.35) and (13.37) becomes

$$t_{m;h-C_L} = \frac{\sqrt{3}k\eta_p E_m}{\hat{c}} \left\{ \frac{\rho_{SSL}\sigma}{2(W/S)} \right\}^{1/2} \left\{ \frac{3C_{D_0}}{K} \right\}^{1/4} \left(\frac{1}{\sqrt{1-\zeta}} - 1 \right) \quad (13.38)$$

For a given ζ , the maximum endurance increases with the increase in altitude and E_m , but decreases with the increase in power-specific fuel consumption \hat{c} and wing loading.

13.4.2 Maximum Endurance and Flight Parameters of a Constant Airspeed–Constant Lift Coefficient Flight

The endurance of constant $V-C_L$ flight is given by Eq. (12.40) as

$$t_{V-C_L} = \{k\eta_p E / (\hat{c}V)\} \ln\{1/(1-\zeta)\} \quad (13.39)$$

where η_p and \hat{c} are considered constant, and k is the conversion factor depending on the system of units chosen. For a given ζ , the endurance would be maximum if the ratio E/V is maximum. This situation is exactly the same as in Sec. 13.4.1 for the maximum endurance of constant $h-C_L$ flight, where the optimum V was sought at the start of the cruise. This means that the maximum-endurance airspeed $V_{\text{me};V-C_L}$ of constant $V-C_L$ flight would be the same as the maximum endurance airspeed $V_{\text{me};h-C_L}$ of constant $h-C_L$ flight at the start of the cruise. This gives

$$V_{\text{me};V-C_L} = V_{\text{me};h-C_L} = \{2(W_1/S)/(\rho_{SSL}\sigma_1)\}^{1/2} \left\{ K / (3C_{D_0}) \right\}^{1/4} \quad (13.40)$$

The lift coefficient $C_{L,\text{me};V-C_L}$, drag coefficient $C_{D,\text{me};V-C_L}$, and $E_{\text{me};V-C_L}$ of constant $V-C_L$ flight would also be the same values as those given for the maximum endurance of the constant $h-C_L$ flight in the Sec. 13.4.1. This gives

$$C_{L,\text{me};V-C_L} = C_{L,\text{me};h-C_L} = (3C_{D_0}/K)^{1/2}\sqrt{3} C_{L,E_m} \quad (13.41)$$

$$C_{D,\text{me};V-C_L} = C_{D,\text{me};h-C_L} = 4C_{D_0}$$

and

$$E_{\text{me};V-C_L} = E_{\text{me};h-C_L} = \sqrt{3}/(4\sqrt{KC_{D_0}}) = \sqrt{3} E_m/2 \quad (13.42)$$

It may also be recalled that since a constant $V-C_L$ flight is a cruise-climb flight, $W/\rho = \text{constant}$, and the magnitude of climb during the cruise can be calculated from Eq. (12.28).

The power required $P_{\text{me};V-C_L}$ is obtained from Eq. (12.7) as

$$P_{\text{me};V-C_L} = \frac{W V_{\text{me};V-C_L}}{E_{\text{me};V-C_L}} = \frac{2W}{\sqrt{3} E_m} \left\{ \frac{2(W_1/S)}{\rho_{\text{SSL}}\sigma} \right\}^{1/2} \left(\frac{K}{3C_{D_0}} \right)^{1/4}$$

which shows that the power required changes during the cruise because the aircraft weight varies due to fuel consumption.

The maximum endurance $t_{m;V-C_L}$ of constant $V-C_L$ flight is found from Eq. (13.39) as

$$t_{m;V-C_L} = \{k\eta_p E_{\text{me};V-C_L}/(\hat{c}V_{\text{me};V-C_L})\} \ln\{1/(1-\zeta)\}$$

which after using Eqs. (13.40) and (13.42) can be written as

$$t_{m;V-C_L} = \frac{\sqrt{3}k\eta_p E_m}{2\hat{c}} \left\{ \frac{\rho_{\text{SSL}}\sigma_1}{2(W_1/S)} \right\}^{1/2} \left\{ \frac{3C_{D_0}}{K} \right\}^{1/4} \ln \left(\frac{1}{1-\zeta} \right) \quad (13.43)$$

Parameters like wing loading, maximum aerodynamic efficiency, and altitude that affect the maximum endurance of constant $h-C_L$ flight also similarly affect the maximum endurance of constant $V-C_L$ flight. Note that constant $h-C_L$ and constant $V-C_L$ flights have the same maximum range but different maximum endurance.

13.4.3 Maximum Endurance and Flight Parameters of a Constant Altitude–Constant Airspeed Flight

The endurance of a constant $h-V$ flight is given by Eq. (12.41) as

$$t_{h-V} = \frac{2k\eta_p E_m}{\hat{c}V} \tan^{-1} \left\{ \frac{E_1\zeta}{2E_m(1 - KE_1 C_{L,1}\zeta)} \right\} \quad (13.44)$$

where η_p and \hat{c} are considered constant. It is convenient to introduce the approximation of Eq. (13.15), which simplifies Eq. (13.44) as

$$t_{h-V} = k\eta_p E_1\zeta / \{\hat{c}V(1 - KE_1 C_{L,1}\zeta)\}$$

which, after using the values of $C_{L,1}$ and E_1 , can be written as

$$t_{h-V} = \{(k\eta_p/\hat{c})2(W_1/S)\rho V \zeta\}/\{\rho^2 V^4 C_{D_0} + 4K(1 - \zeta)(W_1/S)^2\}$$

In order to optimize t_{h-V} with respect to airspeed, all the quantities on the right-hand side of the above equation, except the airspeed V , must be constant. Therefore, let $\zeta = \zeta^*$ be the cruise-fuel weight fraction that has been fixed for the optimization of the endurance. The above equation can be written as

$$t_{h-V} = \{(k\eta_p/\hat{c})2(W_1/S)\rho V \zeta^*\}/\{\rho^2 V^4 C_{D_0} + 4K(1 - \zeta^*)(W_1/S)^2\}$$

Differentiate the above relation with respect to V and put $dt_{h-V}/dV = 0$. The resulting algebraic equation can be solved for V , giving the maximum endurance airspeed $V_{me:h-V}$ as

$$V_{me:h-V} = \{2(W_1/S)/(\rho_{SSL}\sigma)\}^{1/2} \left\{ K(1 - \zeta^*)/(3C_{D_0}) \right\}^{1/4} \quad (13.45)$$

The maximum-endurance airspeed increases with the increase in wing loading and altitude, and with the decrease in zero-lift drag coefficient. Unlike the other two flight programs of maximum endurance, the airspeed here also depends on ζ^* .

The other flight parameters of maximum endurance of the constant h - V flight can now also be obtained. The lift coefficient $C_{L,me:h-V}$ for maximum endurance is given by

$$C_{L,me:h-V} = \frac{2(W/S)}{\rho V_{me:h-V}^2} = \frac{W}{W_1} \sqrt{\frac{3C_{D_0}}{K(1 - \zeta^*)}} = (1 - \zeta) \sqrt{\frac{3C_{D_0}}{K(1 - \zeta^*)}} \quad (13.46)$$

and the drag coefficient $C_{D,me:h-V}$ is obtained as

$$C_{D,me:h-V} = C_{D_0} + KC_{L,me:h-V}^2 = C_{D_0} \left\{ \frac{(1 - \zeta^*) + 3(1 - \zeta)^2}{(1 - \zeta^*)} \right\} \quad (13.47)$$

The aerodynamic efficiency $E_{me:h-V}$ of the aircraft for maximum endurance is given by

$$E_{me:h-V} = \frac{C_{L,me:h-V}}{C_{D,me:h-V}} = \frac{2E_m(1 - \zeta)\sqrt{3(1 - \zeta^*)}}{(1 - \zeta^*) + 3(1 - \zeta)^2} \quad (13.48)$$

The thrust power $P_{me:h-V}$ for maximum endurance is obtained from Eq. (12.7) as $P_{me:h-V}/W = V_{me:h-V}/E_{me:h-V}$, which after using Eqs. (13.45) and (13.48) can be expressed as

$$\frac{P_{me:h-V}}{W} = \left\{ \frac{2(W_1/S)}{\rho_{SSL}\sigma} \right\}^{1/2} \left\{ \frac{K(1 - \zeta^*)}{3C_{D_0}} \right\}^{1/4} \frac{(1 - \zeta^*) + 3(1 - \zeta)^2}{2E_m(1 - \zeta)\sqrt{3(1 - \zeta^*)}} \quad (13.49)$$

Thus, it can be seen that, like the maximum-endurance airspeed, all other flight parameters for maximum endurance value of constant h - V flight also depend on ζ^* .

The maximum endurance is obtained from Eq. (13.44) as

$$t_{m:h-V} = \frac{2k\eta_p E_m}{\hat{c} V_{me:h-V}} \tan^{-1} \left\{ \frac{E_{1me:h-V}\zeta}{2E_m(1 - KE_{1me:h-V}C_{L,1me:h-V}\zeta)} \right\} \quad (13.50)$$

where

$$C_{L,1\text{me};h-V} = (C_{L,\text{me};h-V})_{\zeta=0} = \sqrt{3C_{D_0}/\{K(1-\zeta^*)\}} \quad (13.51)$$

and

$$E_{1\text{me};h-V} = (E_{\text{me};h-V})_{\zeta=0} = 2E_m\sqrt{3(1-\zeta^*)}/\{3 + (1-\zeta^*)\} \quad (13.52)$$

Using Eqs. (13.45), (13.51), and (13.52), Eq. (13.50) for maximum endurance becomes

$$t_{m;h-V} = \frac{2k\eta_p E_m}{\hat{c}} \left\{ \frac{\rho_{SSL}\sigma}{2(W_1/S)} \right\}^{1/2} \left\{ \frac{3C_{D_0}}{K(1-\zeta^*)} \right\}^{1/4} \tan^{-1} \left\{ \frac{\zeta\sqrt{3(1-\zeta^*)}}{(1-\zeta^*) + 3(1-\zeta)} \right\} \quad (13.53)$$

This expresses maximum endurance in terms of aircraft design parameters. Once ζ^* is fixed, the value of the constant airspeed is fixed by Eq. (13.45). Equations (13.46–13.49), respectively, give the variations of lift coefficient, drag coefficient, aerodynamic efficiency, and thrust power against ζ for the flight that is optimized for $\zeta = \zeta^*$. Similarly, Eq. (13.53) gives the variation of maximum endurance against ζ for the flight that is optimized for $\zeta = \zeta^*$. Each change in ζ^* corresponds to an altogether different flight for the constant h - V flight program. These relations do not yield maximum-endurance flight parameters for any other value of ζ except for $\zeta = \zeta^*$.

To obtain the maximum-endurance flight parameters and the maximum endurance for each ζ , put $\zeta^* = \zeta$ in Eqs. (13.45–13.49) and Eq. (13.53), which, respectively, give

$$V_{\text{me};h-V} = \{2(W_1/S)/(\rho_{SSL}\sigma)\}^{1/2} \{K(1-\zeta)/(3C_{D_0})\}^{1/4} \quad (13.54)$$

$$C_{L,\text{me};h-V} = \sqrt{3C_{D_0}(1-\zeta)/K} \quad (13.55)$$

$$C_{D,\text{me};h-V} = \{1 + 3(1-\zeta)\}C_{D_0} \quad (13.56)$$

$$E_{\text{me};h-V} = 2E_m\sqrt{3(1-\zeta)}/\{1 + 3(1-\zeta)\} \quad (13.57)$$

$$\frac{P_{\text{me};h-V}}{W} = \left\{ \frac{2(W_1/S)}{\rho_{SSL}\sigma} \right\}^{1/2} \left\{ \frac{K(1-\zeta)}{3C_{D_0}} \right\}^{1/4} \cdot \frac{1 + 3(1-\zeta)}{2E_m\sqrt{3(1-\zeta)}} \quad (13.58)$$

and

$$t_{m;h-V} = \frac{2k\eta_p E_m}{\hat{c}} \left\{ \frac{\rho_{SSL}\sigma}{2(W_1/S)} \right\}^{1/2} \left\{ \frac{3C_{D_0}}{K(1-\zeta)} \right\}^{1/4} \tan^{-1} \left\{ \frac{0.433\zeta}{\sqrt{1-\zeta}} \right\} \quad (13.59)$$

Equations (13.54–13.58) give the values of the maximum-endurance flight parameters, and Eq. (13.59) gives the maximum endurance for each ζ . Any change in ζ would correspond to a different maximum-endurance flight of the constant h - V flight program.

13.5 Application to an Aircraft

Consider the aircraft of Sec. 12.8 (Chapter 12). If the aircraft is cruising at an altitude of 4 km, find the maximum-range airspeed, the maximum range, and its endurance for constant V - C_L and constant h - V flights.

The maximum-range airspeed and the maximum range of constant $V \cdot C_L$ flight are obtained from Eqs. (13.10) and (13.9), respectively, as

$$V_{\text{mr}; V \cdot C_L} = \left(\frac{2 \times 656.25}{1.225 \times 0.6689} \right)^{1/2} \left(\frac{0.14}{0.032} \right)^{1/4} = 57.88 \text{ m/s} = 208.4 \text{ km/h}$$

and

$$x_{\text{mr}; V \cdot C_L} = \frac{1 \times 0.85 \times 7.47}{0.55 \times 10^{-6}} \ln \left(\frac{1}{1 - 0.12} \right) = 1.4758 \times 10^6 \text{ m} = 1475.8 \text{ km}$$

The corresponding endurance is given by

$$t_{\text{mr}; V \cdot C_L} = x_{\text{mr}; V \cdot C_L} / V_{\text{mr}; V \cdot C_L} = 1475.8 / 208.4 = 7.08 \text{ h}$$

The airspeed for maximum range and the maximum range of the constant $h \cdot V$ flight are obtained from Eqs. (13.27) and (13.31), respectively, as

$$\begin{aligned} V_{\text{mr}; h \cdot V} &= \left(\frac{2 \times 656.25}{1.225 \times 0.6689} \right)^{1/2} \left\{ \frac{0.14(1 - 0.12)}{0.032} \right\}^{1/4} \\ &= 56.06 \text{ m/s} = 201.8 \text{ km/h} \end{aligned}$$

and

$$\begin{aligned} x_{\text{mr}; h \cdot V} &= \frac{2 \times 1 \times 0.85 \times 7.47}{0.55 \times 10^{-6}} \tan^{-1} \left(\frac{0.12}{2\sqrt{1 - 0.12}} \right) \\ &= 1.4748 \times 10^6 \text{ m} = 1474.8 \text{ km} \end{aligned}$$

and the corresponding endurance is given by

$$t_{\text{mr}; h \cdot V} = x_{\text{mr}; h \cdot V} / V_{\text{mr}; h \cdot V} = 1474.8 / 201.8 = 7.31 \text{ h}$$

Therefore, the maximum-range airspeed, maximum range, and the endurance of constant $V \cdot C_L$ flight are 208.4 km/h, 1475.8 km, and 7.08 h, respectively. Similarly, the corresponding quantities of constant $h \cdot V$ flight are 201.8 km/h, 1474.8 km, and 7.31 h, respectively.

Reference

¹Ojha, S. K., "Optimization of Constant Altitude-Constant Airspeed Flight for Piston-Prop Aircraft," *The Aeronautical Journal*, The Royal Aeronautical Society, April 1993, pp. 145–148.

Problems

Major specifications of Aircraft D and Aircraft E, which are required to solve these problems, are presented at the beginning of the Problems Section in Chapter 12.

13.1 Aircraft D is cruising with minimum required thrust power at sea level. Find the a) minimum power airspeed, b) lift and drag coefficients, and the aerodynamic efficiency of the aircraft, and c) minimum power/weight ratio.

13.2 Solve Problem 13.1 for Aircraft D flying at an altitude of a) 3 km and b) 6 km.

13.3 Solve Problem 13.1 for Aircraft E.

13.4 Solve Problem 13.1 for Aircraft E flying at an altitude of a) 4 km and b) 8 km.

13.5 Find the percentage changes made in the solutions of Problem 13.1 for each of the following changes in the design variables: a) W/S is increased by 20%, b) C_{D_0} is decreased by 10%, and c) K is decreased by 10%.

13.6 Find the percentage changes made in the solutions of Problem 13.3 for Aircraft E due to the following changes in the design variables: a) W/S is increased by 15%, b) C_{D_0} is decreased by 5%, and c) K is decreased by 6%.

13.7 Aircraft D cruises at an altitude of 6 km. What percentage of the maximum available power would be required to fly at the minimum possible power in the cases of a) an aspirated engine and b) a supercharged engine.

13.8 Solve Problem 13.7 for Aircraft E flying at an altitude of 4 km.

13.9 Aircraft D cruises for maximum range at sea level and utilizes $\zeta = 0.12$ for the purpose. In the cases of a) constant $h-C_L$, b) constant $V-C_L$, and c) constant $h-V$ flight programs, obtain the following: i) the maximum-range airspeed, ii) the range covered and the associated endurance, iii) the required power/weight ratio, and iv) the airspeed, lift coefficient, aerodynamic efficiency, altitude, wing loading, and power loading at the end of the cruise.

13.10 Solve Problem 13.9 if Aircraft D cruises at an altitude of 4 km.

13.11 Find the percentage of maximum available power required at the beginning and at the end of the cruise in each case of Problem 13.9 when the aircraft has a) an aspirated engine and b) a turbocharged engine.

13.12 Solve Problem 13.9 for Aircraft E.

13.13 Solve Problem 13.9 if Aircraft E cruises at an altitude of 5 km.

13.14 Solve Problem 13.9 if Aircraft E cruises at an altitude of 7 km using a) an aspirated engine, and b) a supercharged engine. Is the best-range airspeed realizable in both the cases? If not, solve the problem using the maximum airspeed.

13.15 Aircraft D is scheduled to cover a range of 950 km at an altitude of 4 km under maximum-range flight condition. What is the cruise-fuel weight fraction consumed in the cases of a) constant $h-V$, b) constant $h-C_L$, and c) constant $V-C_L$ flight programs.

13.16 What percentage change would occur in each case in the required fuel-weight fractions of Problem 13.15 for each of the following changes in the design variables: a) W/S is increased by 10%, b) C_{D_0} is decreased by 5%, and c) K is decreased by 5%.

13.17 Solve Problem 13.15 if Aircraft D flies at an altitude of 6 km.

13.18 Find the percentage changes in the solutions of Problem 13.17 for the following changes in the design variables: a) W/S is increased by 10%, b) C_{D_0} is decreased by 5%, and c) K is decreased by 5%.

13.19 Solve Problem 13.15 for Aircraft E.

13.20 Solve Problem 13.15 for Aircraft E if the weight of the aircraft is decreased by 10%.

13.21 Solve Problem 13.15 for Aircraft E.

13.22 Find the percentage changes in the solutions of Problem 13.21 for the following changes in the design variables: a) W/S is increased by 10%, b) C_{D_0} is decreased by 5%, and c) K is decreased by 5%.

13.23 Aircraft D is going to start cruising at an altitude of 4 km and consumes $\zeta = 0.1$ during the cruise. It is scheduled to undertake the following three flight programs: a) constant $h-C_L$, b) constant $V-C_L$, and c) constant $h-V$. In each of these cases of flight find i) the airspeed for maximum endurance and ii) the maximum endurance and its range.

13.24 Solve Problem 13.23 if Aircraft D cruises at an altitude of 6 km.

13.25 Solve Problem 13.23 for Aircraft E.

13.26 Solve Problem 13.23 if Aircraft E cruises at an altitude of 6 km.

13.27 Find the percentage changes that would occur in the solutions of Problem 13.23 for Aircraft D due to each of the following changes in the design variables of the aircraft: a) W/S is increased by 20%, b) C_{D_0} is reduced by 5%, c) K is reduced by 5%, and d) these changes in W/S , C_{D_0} , and K are made simultaneously.

13.28 Find the percentage changes that would occur in the solutions of Problem 13.25 if the weight of Aircraft E is decreased by 5%.

13.29 Find the weight of the fuel consumed in the maximum-endurance flight lasting 2 h of Aircraft D at an altitude of 4 km in the cases of a) constant $V-C_L$ flight and b) constant $h-V$ flight.

13.30 Solve Problem 13.29 for Aircraft E.

This page intentionally left blank

Climbing Flights of Piston-Prop Aircraft

14.1 Introduction

The basic equations of motion of steady climb of a piston-prop aircraft are provided here. Analytic relations are established that express important performance parameters in terms of the aircraft design parameters. The important performance parameters of the climbing flight of an aircraft are its climb angle, rate of climb, range, time taken, and fuel consumed during the climb.

The cases of steepest and fastest climbs are of special interest in climb performance. The steepest climb and its flight parameters are obtained here by optimizing the angle of climb. Similarly, the fastest climb and its flight parameters are obtained by optimizing the rate of climb.

14.2 Basic Equations of Climb Performance

The basic equations of motion do not depend on the type of engine used by the aircraft. They are obtained by the balance of forces, as in the case of a turbojet aircraft described in Chapter 10. Consider an aircraft of weight W climbing at an angle γ , as shown in Fig. 10.1. Let L , D , and F , respectively, denote the lift, drag, and thrust forces acting on the aircraft. Balancing the forces along the flight path and normal to it gives, respectively, the following two equations of motion:

$$F - D - W \sin \gamma = 0 \quad (14.1)$$

and

$$L - W \cos \gamma = 0 \quad (14.2)$$

The two kinematic relations giving the horizontal and vertical components of airspeed V are

$$dx/dt = V \cos \gamma \quad (14.3)$$

and

$$dh/dt = V \sin \gamma \quad (14.4)$$

where x is the horizontal distance and h is the altitude. The term dh/dt is the rate of climb, which can be denoted as \dot{h} or R/C. These two equations are useful in finding the range covered and time taken in performing the climb. It may be recalled here that the airspeed V appearing in Eqs. (14.3) and (14.4) is the ground airspeed but it is regarded as the true airspeed because a no-wind condition is considered to be the case during the climb.

In case one desires to obtain the weight of fuel consumed during the climb, which may be small, the relation

$$-\frac{dW}{dt} = \hat{c} P_e \quad (14.5)$$

as in Eq. (12.4), can be used. The quantity P_e is the brake power of the piston engine and \hat{c} is its power-specific fuel consumption (PSFC). The thrust power P ($=FV$) is related to the engine power, P_e , as

$$P = k \eta_p P_e \quad (14.6)$$

where η_p is the propeller efficiency, and k is the conversion factor whose value depends on the units used as explained in Sec. 12.2.

14.3 Climbing Flight Parameters

The climb angle, rate of climb, time taken, and the horizontal distance covered in the climb are important parameters of climb performance. These parameters will be expressed here in terms of the aircraft design parameters.

14.3.1 Climb Angle

The climb angle is obtained from Eq. (14.1) as

$$\sin \gamma = F/W - D/W = P/(VV) - D/W \quad (14.7)$$

which after using Eq. (14.6) can be written as

$$\sin \gamma = k \eta_p (P_e/W)/V - D/W \quad (14.8)$$

In practice, γ (radian) is small such that $\sin \gamma \approx \gamma$ and $\cos \gamma \approx 1$. This implies that the aircraft is close to level flight. Equation (14.8) can now be written as

$$\gamma = k \eta_p (P_e/W)/V - D/W \quad (14.9)$$

where γ is in radians. The ratio D/W can be written as

$$D/W = D \cos \gamma / L = D/L = 1/E \quad (14.10)$$

so that

$$\gamma = k \eta_p (P_e/W)/V - 1/E \quad (14.11)$$

Using the level-flight drag approximation, the ratio D/W can also be expressed as

$$D/W = \rho V^2 C_{D_0}/\{2(W/S)\} + 2K(W/S)/(\rho V^2) \quad (14.12)$$

and, therefore,

$$\gamma = k \eta_p (P_e/W)/V - [\rho_{SSL} \sigma V^2 C_{D_0}/\{2(W/S)\} + 2K(W/S)/(\rho_{SSL} \sigma V^2)] \quad (14.13)$$

where $\sigma = \rho/\rho_{SSL}$, and the subscript SSL represents standard atmosphere at sea level. The above relation expresses the climb angle in terms of its aircraft design and flight parameters. If γ is known for a given aircraft, the above relation provides the climb airspeed V .

14.3.2 Rate of Climb

The rate of climb is given by Eqs. (14.4) and (14.1) as

$$\dot{h} = dh/dt = V \sin \gamma = V \gamma = (FV - DV)/W \quad (14.14)$$

The difference $FV - DV$ between the thrust and drag powers is called the *excess power*. Thus, the excess power per unit weight directly gives the rate of climb. Substituting the value of γ from Eq. (14.9), the rate of climb can be written as

$$\dot{h} = k\eta_p(P_e/W) - DV/W \quad (14.15)$$

which after using Eq. (14.10) for D/W becomes

$$\dot{h} = k\eta_p(P_e/W) - V/E \quad (14.16)$$

and if Eq. (14.12) is used for D/W , Eq. (14.15) becomes

$$\dot{h} = k\eta_p(P_e/W) - [\rho_{SSL}\sigma V^3 C_{D_0}/\{2(W/S)\} + 2K(W/S)/(\rho_{SSL}\sigma V)] \quad (14.17)$$

The above relation expresses the rate of climb in terms of the aircraft design and flight parameters.

14.3.3 Range and Time Taken in Climb

The horizontal distance covered x , and the time taken t , during the climb from an altitude h_1 to altitude h_2 ($h_2 > h_1$), will be calculated here. The quantity x is called the *range of the climbing flight*.

The climb angle is considered small, as mentioned above. Using Eqs. (14.3) and (14.4), the ratio dx/dh can be written as

$$dx/dh = (dx/dt)/(dh/dt) = 1/\gamma$$

which on integration gives the range as

$$x = \int_{h_1}^{h_2} dh/\gamma \quad (14.18)$$

where γ is given by Eq. (14.11) or Eq. (14.13).

The time taken in climb is obtained by writing $dt/dh = 1/\dot{h}$, which on integration gives

$$t = \int_{h_1}^{h_2} dh/\dot{h} \quad (14.19)$$

where \dot{h} is obtained from Eq. (14.16) or Eq. (14.17). The evaluation of integrals in Eqs. (14.18) and (14.19) would depend on the functional form of their integrands. In general, it would not be possible to integrate them in analytic form except in some specific cases.

14.3.4 Fuel Consumption in Climb

The fuel consumption during climb is usually small but can be calculated. The fuel-altitude exchange ratio dW/dh can be expressed as

$$dW/dh = (dW/dt)/(dh/dt) = -\hat{c} P_e / \dot{h}$$

which in a differential form becomes

$$dW/W = -\hat{c}(P_e/W)dh/\dot{h}$$

If W_1 and W_2 are the weights of fuel at the altitudes h_1 and h_2 , respectively, during the climb, the above relation can be integrated to yield

$$W_2/W_1 = \exp \left\{ -\hat{c} \int_{h_1}^{h_2} (P_e/W)dh/\dot{h} \right\}$$

where \hat{c} is considered constant. Writing $\Delta W_f = W_1 - W_2$, the above relation can be expressed as

$$\zeta = \Delta W_f / W_1 = 1 - \exp \left\{ -\hat{c} \int_{h_1}^{h_2} (P_e/W)dh/\dot{h} \right\} \quad (14.20)$$

where ζ is the climb-fuel weight fraction.

14.4 Steepest Climb

The steepest and fastest climb parameters are important in the climb performance of an aircraft. The steepest climb parameters are obtained in this section whereas the fastest climb is dealt with in Sec. 14.5. The subscript SC is used here to represent the condition of the steepest climb γ_m . The steepest climb may be preferred for safely clearing the obstacles around an airport, such as mountains, trees, or buildings at the end of the runway. The steepest climb establishes the upper limit of the climb angle.

14.4.1 Airspeed and Climb Angle of Steepest Climb

The airspeed V_{SC} of the steepest climb is obtained by maximizing γ of Eq. (14.13) with respect to V . Differentiating Eq. (14.13) with respect to V and putting $d\gamma/dV = 0$, gives

$$V^4 + \frac{k\eta_p(P_e/W)(W/S)}{\rho_{SSL}\sigma C_{D_0}} V - \frac{4K(W/S)^2}{\rho_{SSL}^2\sigma^2 C_{D_0}} = 0 \quad (14.21)$$

for $V = V_{SC}$. The above relation does not yield an analytic solution for V . However, in some cases involving piston-prop aircraft the first term (V^4) may be much

less than the other two terms on the left-hand side of the above equation. In such cases, neglecting the first term of the above relation and solving the resulting equation, gives¹

$$V_{SC} = 4K(W/S)/\{\rho_{SSL}\sigma k\eta_p(P_e/W)\} \quad (14.22)$$

The airspeed of the steepest climb increases with an increase in wing loading and altitude, but decreases with the decrease in K (increase in aspect ratio). The airspeed also increases with the decrease in P_e/W and the propeller efficiency of the aircraft.

The maximum climb angle γ_m is obtained by substituting $V = V_{SC}$ in Eq. (14.13), which gives

$$\gamma_m = \frac{\rho_{SSL}\sigma\{k\eta_p(P_e/W)\}^2}{8K(W/S)} - \frac{8C_{D_0}K^2(W/S)}{\rho_{SSL}\sigma\{k\eta_p(P_e/W)\}^2} \quad (14.23)$$

The first term on the right-hand side of the above relation is generally much bigger¹ than the second term, especially at lower altitudes. This gives

$$\gamma_m = \rho_{SSL}\sigma\{k\eta_p(P_e/W)\}^2/\{8K(W/S)\} \quad (14.24)$$

The design parameters that help to increase γ_m in the above relation decrease the steepest climb airspeed of Eq. (14.22). It has been pointed by Hale¹ that the steepest climb airspeed given by Eq. (14.22) may be less than the stalling airspeed. Therefore, in practice one may often have to choose V_{SC} , which is slightly higher than the stalling airspeed of the aircraft.

14.4.2 Steepest Climb Rate

The rate of climb of the steepest climb is obtained from Eq. (14.14) as

$$\dot{h}_{SC} = V_{SC} \cdot \gamma_{SC} = V_{SC}\gamma_m \quad (14.25)$$

which after using Eqs. (14.22) and (14.24) can be written as

$$\dot{h}_{SC} = (1/2)k\eta_p(P_e/W) \quad (14.26)$$

The steepest climb rate increases with the increase in propeller efficiency and engine power/weight ratio of the aircraft.

14.4.3 Range of Steepest Climb

The horizontal distance x_{SC} covered during the steepest climb from an altitude h_1 to altitude h_2 is given by Eq. (14.18) as

$$x_{SC} = \int_{h_1}^{h_2} dh/\gamma_m \quad (14.27)$$

which after using Eq. (14.24) for γ_m can be written as

$$x_{SC} = \int_{h_1}^{h_2} \{8K(W/S)\} dh / [\rho_{SSL}\sigma\{k\eta_p(P_e/W)\}^2]$$

Since the weight of fuel consumed in the climb is generally small, the weight of the aircraft is considered to remain constant during the climb. The propeller efficiency is also regarded as constant. The above relation can be written as

$$x_{SC} = [8K(W/S)/\{\rho_{SSL}(k\eta_p)^2\}] \int_{h_1}^{h_2} dh / \{\sigma(P_e/W)^2\} \quad (14.28)$$

We will now consider that the throttle setting is kept constant during the climb. In the case of aspirated piston-prop aircraft, for constant throttle setting, the variation of engine power with altitude (and thus σ) can be expressed as [Eq. (5.2)]

$$P_e = \sigma P_{e,SSL} \quad (14.29)$$

so that the range of steepest climb given by Eq. (14.28) becomes

$$x_{SC} = \frac{8K(W/S)}{\rho_{SSL}\{k\eta_p(P_{e,SSL}/W)\}^2} \int_{h_1}^{h_2} \frac{dh}{\sigma^3}$$

Using Eq. (12.27) for σ , the right-hand side integral can be evaluated and the above relation for the range becomes

$$x_{SC} = \frac{8\beta K(W/S)}{3\rho_{SSL}\{k\eta_p(P_{e,SSL}/W)\}^2} (e^{3h_2/\beta} - e^{3h_1/\beta}) \quad (14.30)$$

In the case of a supercharged (turbocharged) piston-prop aircraft, if the altitudes h_1 and h_2 are below the critical altitude, the engine power remains constant [Eq. (5.3)], giving

$$P_e = P_{e,SSL} \quad (14.31)$$

Equation (14.28) in this case becomes

$$x_{SC} = \frac{8K(W/S)}{\rho_{SSL}\{k\eta_p(P_{e,SSL}/W)\}^2} \int_{h_1}^{h_2} \frac{dh}{\sigma}$$

and, after using Eq. (12.27) for σ , the integral on the right-hand side can be evaluated, giving the range as

$$x_{SC} = \frac{8\beta K(W/S)}{\rho_{SSL}\{k\eta_p(P_{e,SSL}/W)\}^2} (e^{h_2/\beta} - e^{h_1/\beta}) \quad (14.32)$$

Again, in the case of supercharged piston-prop aircraft, if the altitudes h_1 and h_2 are above the critical altitude, the engine power varies as [Eq. (5.4)]

$$P_e = (\sigma/\sigma_{cr}) P_{e,SSL} \quad (14.33)$$

where σ_{cr} is the density ratio ρ/ρ_{SSL} at a critical altitude whose value is supposed to be known. Equation (14.28) can be written as

$$x_{\text{SC}} = \left[8K(W/S)\sigma_{\text{cr}}^2 / \{\rho_{\text{SSL}}(k\eta_p P_{e,\text{SSL}}/W)^2\} \right] \int_{h_1}^{h_2} (dh/\sigma^3)$$

and, after using Eq. (12.27) for σ , the integral on the right-hand side can be evaluated, giving the range as

$$x_{\text{SC}} = \frac{8\beta K(W/S)\sigma_{\text{cr}}^2}{3\rho_{\text{SSL}}\{k\eta_p(P_{e,\text{SSL}}/W)\}^2} (e^{3h_2/\beta} - e^{3h_1/\beta}) \quad (14.34)$$

Equations (14.30), (14.32), and (14.34) predict the horizontal distances covered (ranges) in terms of the aircraft design parameters. Equation (14.30) pertains to aspirated engine aircraft. Equations (14.32) and (14.33) pertain to supercharged engines, depending on whether the aircraft is flying below or above the critical altitude, respectively.

14.4.4 Time Taken in Steepest Climb

The time taken t_{SC} during the steepest climb from an altitude h_1 to h_2 is given by Eq. (14.19) as

$$t_{\text{SC}} = \int_{h_1}^{h_2} dh / \dot{h}_{\text{SC}} \quad (14.35)$$

which after using Eq. (14.26) for \dot{h}_{SC} can be written as

$$t_{\text{SC}} = \int_{h_1}^{h_2} 2 dh / \{k\eta_p(P_e/W)\} \quad (14.36)$$

Here also the throttle setting is considered to remain constant. In the case of an aspirated piston-prop engine aircraft, using Eqs. (14.29) and (12.27), the above integral can be evaluated, giving the time

$$t_{\text{SC}} = \frac{2\beta}{k\eta_p(P_{e,\text{SSL}}/W)} (e^{h_2/\beta} - e^{h_1/\beta}) \quad (14.37)$$

In the case of supercharged piston-prop aircraft, if the altitudes h_1 and h_2 are below the critical altitude, using Eqs. (14.31) and (12.27), the integral in Eq. (14.36) can be evaluated, giving the time

$$t_{\text{SC}} = 2(h_2 - h_1) / \{k\eta_p(P_{e,\text{SSL}}/W)\} \quad (14.38)$$

Again if the supercharged piston-prop aircraft is flying at altitudes where both h_1 and h_2 are above the critical altitude, Eqs. (14.33) and (12.27) are used to evaluate the integral in Eq. (14.36), giving the time

$$t_{\text{SC}} = \frac{2\beta\sigma_{\text{cr}}}{k\eta_p(P_{e,\text{SSL}}/W)} (e^{h_2/\beta} - e^{h_1/\beta}) \quad (14.39)$$

Equations (14.37–14.39) above express the steepest climb times in terms of the aircraft design parameters, where Eq. (14.37) is for aspirated engine aircraft. Equations (14.38) and (14.39) are for supercharged engines, depending on whether the aircraft is flying below or above the critical altitude, respectively.

14.5 Fastest Climb

The maximum rate of climb is called the *fastest climb*. The subscript FC is used to represent the condition of the fastest climb \dot{h}_m . The fastest climb represents the minimum time taken by an aircraft to climb to a specified altitude, and consequently reduces fuel consumption. The fastest climb is also preferred by air traffic control at a busy airport. The fastest climb performance parameters are described here in terms of aircraft design parameters.²

14.5.1 Airspeed and Climb Angle of the Fastest Climb

The airspeed V_{FC} of the fastest climb of a given aircraft is obtained by optimizing its rate of climb with respect to airspeed. Differentiate Eq. (14.17) with respect to V and put $d\dot{h}/dV = 0$. The solution of the resulting algebraic equation gives the fastest climb airspeed as

$$V_{FC} = \{2(W/S)/(\rho_{SSL}\sigma)\}^{1/2} \left\{ K / (3C_{D_0}) \right\}^{1/4} = V_{P_{min}} = V_{P_{min},SSL} / \sqrt{\sigma} \quad (14.40)$$

where the subscript P_{min} represents minimum power. The above result can also be obtained from Eq. (14.15), which shows that the maximum rate of climb can be achieved by minimizing drag power P ($=DV$). Note that the fastest climb airspeed is independent of the power of the piston-prop engine.

The other flight parameters of the fastest climb can now be obtained. The lift coefficient $C_{L,FC}$ of the climb is given by

$$C_{L,FC} = C_{L,P_{min}} = \sqrt{3}C_{L,E_m} = (3C_{D_0}/K)^{1/2}$$

and the corresponding aerodynamic efficiency E_{FC} of the fastest climb is obtained as

$$E_{FC} = E_{P_{min}} = 0.866E_m \quad (14.41)$$

The angle of climb of the fastest climb is obtained from Eq. (14.11) as

$$\gamma_{FC} = k\eta_p(P_e/W)/V_{FC} - 1/E_{FC}$$

which after using Eqs. (14.40) and (14.41) can be written as

$$\gamma_{FC} = k\eta_p(P_e/W)\sqrt{\sigma}/V_{P_{min},SSL} - 1/(0.866E_m) \quad (14.42)$$

where

$$V_{P_{min},SSL} = \left\{ \frac{2(W/S)}{\rho_{SSL}} \right\}^{1/2} \left(\frac{K}{3C_{D_0}} \right)^{1/4} \quad \text{and} \quad E_m = \frac{1}{2\sqrt{KC_{D_0}}} \quad (14.43)$$

The quantity γ_{FC} increases with the increase in maximum aerodynamic efficiency E_m of the aircraft and its propeller efficiency η_p . The increase in wing loading W/S decreases γ_{FC} . The effect of altitude on γ_{FC} depends on how the engine power P_e varies with altitude, i.e., it depends on the type of piston engine installed to the aircraft. The variation of γ_{FC} with altitude for a supercharged (turbocharged) engine is different from that of an aspirated engine.

For an aspirated engine $P_e = \sigma P_{e,SSL}$, and Eq. (14.42) becomes

$$\gamma_{FC} = k\eta_p(P_{e,SSL}/W)\sigma^{3/2}/V_{P_{min},SSL} - 1/(0.866E_m) \quad (14.44)$$

If we are dealing with a supercharged piston-prop engine and the aircraft is flying below the critical altitude, then $P_e = P_{e,SSL}$, and Eq. (14.42) becomes

$$\gamma_{FC} = k\eta_p(P_{e,SSL}/W)\sqrt{\sigma}/V_{P_{min},SSL} - 1/(0.866E_m) \quad (14.45)$$

On the other hand, if the altitude is above the critical altitude of the supercharged piston-prop engine, then $P_e = (\sigma/\sigma_{cr})P_{e,SSL}$, and Eq. (14.42) becomes

$$\gamma_{FC} = k\eta_p(P_{e,SSL}/W)(\sigma^{3/2}/\sigma_{cr})/V_{P_{min},SSL} - 1/(0.866E_m) \quad (14.46)$$

The above three relations express the fastest climb angles in terms of the aircraft design parameters, where Eq. (14.44) is for an aspirated engine. Equations (14.45) and (14.46) apply to supercharged (turbocharged) engines, depending on whether the aircraft is flying below or above the critical altitude, respectively.

14.5.2 Maximum Rate of Climb

The fastest climb is synonymous with the maximum rate of climb. The maximum climb rate is obtained from Eq. (14.16) as

$$\dot{h}_{FC} = \dot{h}_m = k\eta_p(P_e/W) - V_{FC}/E_{FC}$$

which after using Eqs. (14.40) and (14.41) becomes

$$\dot{h}_m = k\eta_p(P_e/W) - V_{P_{min},SSL}/(0.866E_m\sqrt{\sigma}) \quad (14.47)$$

where $V_{P_{min},SSL}$ and E_m are obtained from the relations of Eq. (14.43). The maximum rate of climb increases with the increase in engine power P_e and with the decrease in wing loading (W/S). The variation of \dot{h}_m with altitude depends on the type of piston engine being used.

For an aspirated engine aircraft, the maximum climb rate is given by

$$\dot{h}_m = k\eta_p(P_{e,SSL}/W)\sigma - V_{P_{min},SSL}/(0.866E_m\sqrt{\sigma}) \quad (14.48)$$

For a supercharged (turbocharged) engine below its critical altitude

$$\dot{h}_m = k\eta_p(P_{e,SSL}/W) - V_{P_{min},SSL}/(0.866E_m\sqrt{\sigma}) \quad (14.49)$$

and if the supercharged engine is above its critical altitude

$$\dot{h}_m = k\eta_p(P_{e,SSL}/W)(\sigma/\sigma_{cr}) - V_{P_{min},SSL}/(0.866E_m\sqrt{\sigma}) \quad (14.50)$$

It can be noted that for standard atmosphere at sea level where $\sigma = 1$, the maximum rates of climbs for both the aspirated and the supercharged engines are the same.

14.5.3 Range of Fastest Climb

The horizontal distance x_{FC} covered during the fastest climb from an altitude h_1 to h_2 will be calculated here. This horizontal distance is called the *range of the climb*.

The range of the fastest climb is obtained from Eq. (14.20) as

$$x_{FC} = \int_{h_1}^{h_2} dh / \gamma_{FC} \quad (14.51)$$

For a constant throttle setting, the variation of γ_{FC} with altitude is given by Eqs. (14.44–14.46) depending on the type of piston engine being used on the aircraft.

In the case of aspirated piston engine aircraft, the γ_{FC} given by Eq. (14.44) is

$$\gamma_{FC} = \frac{1}{V_{P_{min},SSL}} \left\{ k, \eta_p (P_{e,SSL}/W) \sigma^{3/2} - \frac{V_{P_{min},SSL}}{0.866 E_m} \right\} \quad (14.52)$$

For the sake of brevity the notations a and b are introduced as

$$a = k \eta_p (P_{e,SSL}/W), \quad \text{and} \quad b = V_{P_{min},SSL}/(0.866 E_m) \quad (14.53)$$

where a and b are constant quantities for a given aircraft. Equation (14.52) can now be written as

$$\gamma_{FC} = (a \sigma^{3/2} - b) / V_{P_{min},SSL}$$

and the range x_{FC} given by Eq. (14.51) becomes

$$x_{FC} = V_{P_{min},SSL} \int_{h_1}^{h_2} dh / (a \sigma^{3/2} - b) \quad (14.54)$$

Using Eq. (12.27) for σ , the right-hand-side integral of the above relation can be evaluated, and the range is obtained as

$$x_{FC} = V_{P_{min},SSL} \{2\beta/(3b)\} \ln \{(be^{3h_1/2\beta} - a)/(be^{3h_2/2\beta} - a)\} \quad (14.55)$$

In the case of a supercharged (turbocharged) piston engine aircraft flying below its critical altitude, the γ_{FC} given by Eq. (14.45) is

$$\gamma_{FC} = (a \sqrt{\sigma} - b) / V_{P_{min},SSL}$$

and Eq. (14.51) for the range can be written as

$$x_{FC} = V_{P_{min},SSL} \int_{h_1}^{h_2} dh / (a \sqrt{\sigma} - b)$$

Using Eq. (12.27) for σ , the right-hand-side integral of the above relation can be evaluated, and the range can be expressed as

$$x_{FC} = V_{P_{min},SSL} \cdot (2\beta/b) \ln \{(be^{h_1/2\beta} - a)/(be^{h_2/2\beta} - a)\} \quad (14.56)$$

In the case of a supercharged piston-engine aircraft if both h_1 and h_2 are above the critical altitude, the γ_{FC} of Eq. (14.46) can be written as

$$\gamma_{FC} = \{(a/\sigma_{cr})\sigma^{3/2} - b\}/V_{P_{min},SSL}$$

and Eq. (14.51) for the range becomes

$$x_{FC} = V_{P_{min},SSL} \int_{h_1}^{h_2} dh / \{(a/\sigma_{cr})\sigma^{3/2} - b\}$$

where a , b , and σ_{cr} are constant quantities. Noting that the above integral has the same form as in Eq. (14.54), it can be evaluated in the same way and the range can be expressed as

$$x_{FC} = V_{P_{min},SSL} \cdot \frac{2\beta}{3b} \ln \frac{be^{3h_1/2\beta} - (a/\sigma_{cr})}{be^{3h_2/2\beta} - (a/\sigma_{cr})} \quad (14.57)$$

In Eqs. (14.55–14.57), a and b are given by the relations of Eq. (14.53), $\beta = 9296$ m in the troposphere, $V_{P_{min},SSL}$ is given by Eq. (14.40), and σ_{cr} is supposed to be a known quantity for a given aircraft.

14.5.4 Time Taken in Fastest Climb

The time taken during the fastest climb of a piston-prop aircraft is given by Eq. (14.19) as

$$t_{FC} = \int_{h_1}^{h_2} dh / \dot{h}_m \quad (14.58)$$

For a constant throttle setting during climb, the variation of \dot{h}_m with altitude is given by Eqs. (14.48–14.50) depending on the type of piston engine of the aircraft.

In the case of aspirated piston-engine aircraft, Eqs. (14.48) and (14.58) for \dot{h}_m and t_{FC} , respectively, can be written as

$$\dot{h}_m = a\sigma - b/\sqrt{\sigma} \quad \text{and} \quad t_{FC} = \int_{h_1}^{h_2} \sqrt{\sigma} dh / (a\sigma^{3/2} - b)$$

Using Eq. (12.27) for σ , the above integral can be evaluated and t_{FC} can be expressed as

$$t_{FC} = \frac{2\beta A}{3b} \left[\sqrt{3} \left\{ \tan^{-1} \frac{2e^{-h_2/2\beta} + A}{A\sqrt{3}} - \tan^{-1} \frac{2e^{-h_1/2\beta} + A}{A\sqrt{3}} \right\} \right. \\ \left. + \frac{1}{2} \ln \frac{e^{-h_2/\beta} + Ae^{-h_2/2\beta} + A^2}{e^{-h_1/\beta} + Ae^{-h_1/2\beta} + A^2} - \ln \frac{e^{-h_2/2\beta} - A}{e^{-h_1/2\beta} - A} \right] \quad (14.59)$$

where $A = (b/a)^{1/3}$, a and b are given by the relations of Eq. (14.53), and $\beta = 9296$ m in the troposphere.

In the case of a supercharged piston-engine aircraft climbing below the critical altitude, Eqs. (14.49) and (14.58) for \dot{h}_m and t_{FC} , respectively, can be written as

$$\dot{h}_m = a - b/\sqrt{\sigma} \quad \text{and} \quad t_{FC} = \int_{h_1}^{h_2} \sqrt{\sigma} dh / (a\sqrt{\sigma} - b)$$

Using Eq. (12.27) for σ , the above integral can be evaluated and t_{FC} can be expressed as

$$t_{FC} = (2\beta/a) \ln \{(ae^{-h_1/2\beta} - b)/(ae^{-h_2/2\beta} - b)\} \quad (14.60)$$

If the supercharged piston-engine aircraft is climbing where both h_1 and h_2 are above the critical altitude, Eqs. (14.50) and (14.58) for \dot{h}_m and t_{FC} , respectively, can be written as

$$\dot{h}_m = (a/\sigma_{cr})\sigma - b/\sqrt{\sigma} \quad \text{and} \quad t_{FC} = \int_{h_1}^{h_2} \sqrt{\sigma} dh / \{(a/\sigma_{cr})\sigma^{3/2} - b\}$$

where a , b , and σ_{cr} are known constant quantities for a given aircraft. Using Eq. (12.27) for σ , the above integral can be evaluated and t_{FC} can be expressed as

$$t_{FC} = \frac{2\beta B}{3b} \left[\sqrt{3} \left\{ \tan^{-1} \frac{2e^{-h_2/2\beta} + A}{A\sqrt{3}} - \tan^{-1} \frac{2e^{-h_1/2\beta} + A}{A\sqrt{3}} \right\} \right. \\ \left. + \frac{1}{2} \ln \frac{e^{-h_2/2\beta} + Ae^{-h_2/2\beta} + A^2}{e^{-h_1/2\beta} + Ae^{-h_1/2\beta} + A^2} - \ln \frac{e^{-h_2/2\beta} - A}{e^{-h_1/2\beta} - A} \right] \quad (14.61)$$

where $B = (b\sigma_{cr}/a)^{1/3}$, a and b are given by the relations of Eq. (14.53), and σ_{cr} is supposed to be a known quantity for a given aircraft.

14.5.5 Fuel Consumption in Fastest Climb

The climb fuel weight fraction ξ_{FC} of the fastest climb is obtained from Eq. (14.20) as

$$\xi_{FC} = 1 - \exp \left\{ -\hat{c} \int_{h_1}^{h_2} \frac{P_e/W}{\dot{h}_m} dh \right\} \quad (14.62)$$

where the variations in P_e and \dot{h}_m with altitude depend on the type of piston engine of the aircraft.

In the case of an aspirated piston-engine aircraft, $P_e = \sigma P_{e,SSL}$, and $\dot{h}_m = a\sigma - b/\sqrt{\sigma}$, and Eq. (14.62) can be written as

$$\xi_{FC} = 1 - \exp \left\{ -\hat{c} \cdot \frac{P_{e,SSL}}{W} \int_{h_1}^{h_2} \frac{\sigma^{3/2}}{a\sigma^{3/2} - b} dh \right\}$$

Using Eq. (12.27) for σ , the above integral can be evaluated and ξ_{FC} can be expressed as

$$\xi_{FC} = 1 - \exp \left\{ \frac{2\beta \hat{c}(P_{e,SSL}/W)}{3a} \ln \frac{ae^{-3h_2/2\beta} - b}{ae^{-3h_1/2\beta} - b} \right\} \quad (14.63)$$

In the case of a supercharged piston-engine aircraft flying below the critical altitude, $P_e = P_{e,SSL}$, and $\dot{h}_m = a - b/\sqrt{\sigma}$, and Eq. (14.62) can be written as

$$\zeta_{FC} = 1 - \exp \left\{ -\hat{c} \cdot \frac{P_{e,SSL}}{W} \int_{h_1}^{h_2} \frac{\sqrt{\sigma}}{a\sqrt{\sigma} - b} dh \right\}$$

Using Eq. (12.27) for σ , the above integral can be evaluated and ζ_{FC} can be expressed as

$$\zeta_{FC} = 1 - \exp \left\{ \frac{2\beta\hat{c}(P_{e,SSL}/W)}{a} \ln \frac{ae^{-h_2/2\beta} - b}{ae^{-h_1/2\beta} - b} \right\} \quad (14.64)$$

If the supercharged piston-engine aircraft is climbing, where both h_1 and h_2 are above the critical altitude, $P_e = (\sigma/\sigma_{cr})P_{e,SSL}$, and $\dot{h}_m = (a/\sigma_{cr})\sigma - b/\sqrt{\sigma}$, and Eq. (14.62) can be written as

$$\zeta_{FC} = 1 - \exp \left\{ -\hat{c} \cdot \frac{(P_{e,SSL}/W)}{\sigma_{cr}} \int_{h_1}^{h_2} \frac{\sigma^{3/2}}{\frac{a}{\sigma_{cr}}\sigma^{3/2} - b} dh \right\}$$

Using Eq. (12.27) for σ , the above integral can be evaluated and ζ_{FC} can be expressed as

$$\zeta_{FC} = 1 - \exp \left\{ \frac{2\beta\hat{c}(P_{e,SSL}/W)}{3a} \ln \frac{ae^{-3h_2/2\beta} - b\sigma_{cr}}{ae^{-3h_1/2\beta} - b\sigma_{cr}} \right\} \quad (14.65)$$

In Eqs. (14.63–14.65), a and b are given by the relations of Eq. (14.53), $\beta = 9296$ m in the troposphere, and σ_{cr} is supposed to be a known quantity for a given aircraft.

14.5.6 Ceilings

The maximum altitude attainable in steady, level flight is known as the *absolute ceiling*. The maximum rate of climb of an aircraft at its absolute ceiling is zero. The absolute ceilings of both aspirated and supercharged piston-prop aircraft are obtained in this section. The subscript c is used to represent the condition at the absolute ceiling.

In the case of an aspirated piston-prop aircraft, put $\dot{h}_m = 0$ in Eq. (14.48), giving

$$\sigma_C = [V_{P_{min},SSL}/\{0.866E_m k \eta_p (P_{e,SSL}/W_C)\}]^{2/3} \quad (14.66)$$

and similarly, for supercharged piston-prop aircraft, the density ratio σ_C at the absolute ceiling is obtained from Eq. (14.50) as

$$\sigma_C = [V_{P_{min},SSL}\sigma_{cr}/\{0.866E_m k \eta_p (P_{e,SSL}/W_C)\}]^{2/3} \quad (14.67)$$

where $P_{e,SSL}$ is the maximum engine power at sea level in the standard atmosphere. The weight of the aircraft during its climb can be considered constant, i.e., $W_C = W = \text{const}$. Having obtained σ_C from the above relations (14.66) or

(14.67), as the case may be, the ceiling altitude h_C in the standard atmosphere can be obtained by the relation $\sigma_C = e^{-h_C/\beta}$, or more accurately, by using the standard atmosphere table. It can be noted that, due to fuel consumption, W decreases continuously and, therefore, h_C would ideally go on increasing asymptotically.

The concepts of service and operational ceilings can be explained similarly to their use in the case of turbojet aircraft.

14.6 Application to an Aircraft

Consider the same aircraft whose cruising flight was calculated in Sec. 12.8. The aircraft has a critical altitude of 6 km and a maximum engine brake power of 75 kW (100.6 hp) at sea level. Calculate for both aspirated and supercharged engines a) the ceiling altitude; b) the variations in V_{FC} , γ_{FC} , and \dot{h}_m with altitude; and c) the variations in x_{FC} and ζ_{FC} with altitude. Assume that the aircraft's climb started from sea level.

The value of $V_{P_{min},SSL}$ of the aircraft is obtained from Eq. (14.43) as

$$V_{P_{min},SSL} = \left\{ \frac{2(656.25)}{1.225} \right\}^{1/2} \left(\frac{0.14}{3 \times 0.032} \right)^{1/4} = 35.96 \text{ m/s}$$

1) *Calculations of ceiling altitudes.* In the case of an aspirated engine, the absolute ceiling is obtained from Eq. (14.66) as

$$\sigma_C = \left\{ \frac{35.97}{0.866 \times 7.47 \times 1 \times 0.85(75000/7350)} \right\}^{2/3} = 0.7434$$

which on using the standard atmosphere table gives $h_C = 2987 \text{ m}$.

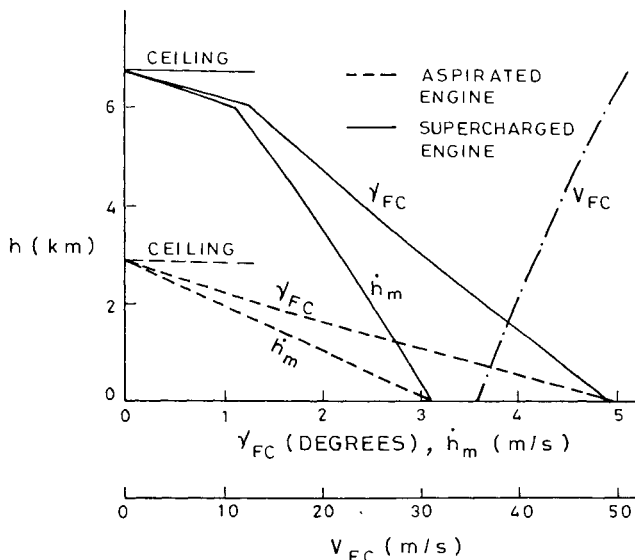


Fig. 14.1 Variations of γ_{FC} , \dot{h} , and V_{FC} with altitude for aspirated and supercharged engines.

In the case of a supercharged engine, the absolute ceiling is obtained from Eq. (14.67) as

$$\sigma_c = \left\{ \frac{35.97 \times 0.5389}{0.866 \times 7.47 \times 1 \times 0.85(75000/7350)} \right\}^{2/3} = 0.4923$$

which on using the standard atmosphere table gives $h_c = 6807$ m.

2) *Calculations of V_{FC} , γ_{FC} , and \dot{h}_m .* The fastest climb airspeed is obtained from Eq. (14.40) as $V_{FC} = 35.97/\sqrt{\sigma}$, which has been plotted in Fig. 14.1 by using the standard atmosphere table.

The variations of γ_{FC} for an aspirated engine, a supercharged engine below critical altitude, and a supercharged engine above critical altitude are obtained from Eqs. (14.44), (14.45), and (14.46), respectively, as

$$\gamma_{FC} = 0.241\sigma^{3/2} - 0.155, \quad \gamma_{FC} = 0.241\sqrt{\sigma} - 0.155$$

and

$$\gamma_{FC} = 0.448\sigma^{3/2} - 0.155$$

The above curves are plotted in Fig. 14.1 by using the standard atmosphere table. The curve for aspirated engine is shown by a dashed line, whereas for a supercharged engine it is shown by a solid line.

The variations of \dot{h}_m for an aspirated engine, a supercharged engine below critical altitude, and a supercharged engine above the critical altitude, are obtained

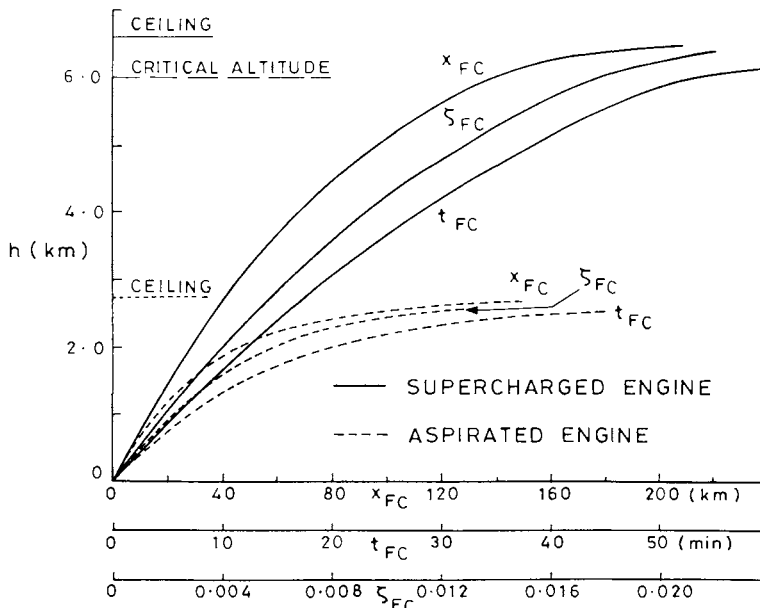


Fig. 14.2 Variations of x_{FC} , t_{FC} , and ζ_{FC} with altitude for aspirated and supercharged engines.

from Eqs. (14.48), (14.49), and (14.50), respectively, as $\dot{h}_m = 8.67\sigma - 5.56/\sqrt{\sigma}$, $\dot{h}_m = 8.67 - 5.56/\sqrt{\sigma}$, and $\dot{h}_m = 16.12\sigma - 5.56/\sqrt{\sigma}$.

These curves have been plotted in Fig. 14.1 by using the standard atmosphere table.

3) Calculations of t_{FC} , x_{FC} , and ζ_{FC} . Here, $a = k\eta_p(P_{e,SSL}/W) = 1 \times 0.85$ ($75,000/7350$) = 8.673 m/s, and

$$b = V_{P_{min},SSL}/(0.866E_m) = \frac{35.97}{0.866 \times 7.47} = 5.560 \text{ m/s}$$

$$A = (b/a)^{1/3} = (5.560/8.673)^{1/3} = 0.862$$

$$B = \left(\frac{b}{a}\sigma_{cr}\right)^{1/3} = \left(\frac{5.560 \times 0.5389}{8.673}\right)^{1/3} = 0.702$$

$$\beta = 9296 \text{ m}, \quad h_2 = h, \quad \text{and} \quad h_1 = 0$$

In the case of aspirated engines, supercharged engines below the critical altitude, and supercharged engines above the critical altitude, the values of x_{FC} for different h can be obtained from Eqs. (14.55), (14.56), and (14.57), respectively. Similarly, t_{FC} is given by Eqs. (14.59–14.61), and ζ_{FC} is given by Eqs. (14.63–14.65). The values of x_{FC} , t_{FC} , and ζ_{FC} against altitude are plotted in Fig. 14.2 and the ceiling altitudes are marked, both for aspirated and supercharged engines.

References

¹Hale, F. J., *Aircraft Performance, Selection, and Design*, Wiley, New York, 1984.

²Ojha, S. K., Fastest Climb of a Piston-Prop Aircraft, *Journal of Aircraft*, Vol. 30, No. 1, 1993, pp. 146–148.

Problems

The major specifications of Aircraft D and Aircraft E, which are required to solve the problems below, are presented at the beginning of the Problems section in Chapter 12.

14.1 Aircraft D has an aspirated engine and makes a steady climb from sea level to ceiling at an airspeed of 160 km/h. Find the variations in the a) climb angle, b) rate of climb, c) range covered, d) time taken, and e) climb-fuel weight fraction, with the increase in altitude.

14.2 Solve Problem 14.1 if Aircraft D climbs at an airspeed of 180 km/h.

14.3 Solve Problem 14.1 if Aircraft D has a supercharged engine. Can it climb up to its ceiling altitude?

14.4 Solve Problem 14.1 for Aircraft E.

14.5 Solve Problem 14.1 if Aircraft E climbs at an airspeed of 200 km/h.

14.6 Solve Problem 14.1 for Aircraft E if it uses a supercharged engine and climbs at a constant airspeed of 270 km/h.

14.7 Aircraft D uses an aspirated engine and climbs at an airspeed of 200 km/h. Find the percentage changes made in the climb angle and the rate of climb at a) sea level and b) an altitude of 6 km, for each of the following changes in the design parameters of the aircraft: i) W/S is increased by 20%, ii) C_{D_0} is increased by 10%, and iii) K is increased by 10%.

Also find the percentage variation in the range covered and time taken to climb from sea level to an altitude of 6 km due to each of the above changes.

14.8 Solve Problem 14.7 if Aircraft D has a turbocharged engine.

14.9 Solve Problem 14.7 for Aircraft E if it is climbing at a constant airspeed of 250 km/h.

14.10 Solve Problem 14.7 for Aircraft E if it is using a supercharged engine and climbing at a constant airspeed of 250 km/h.

14.11 Aircraft D is fitted with an aspirated engine. Plot the variations of a) the climb angle, and b) the rate of climb, with airspeed at i) sea level and ii) an altitude of 5 km. From the above plots, find the airspeeds of the steepest and fastest climbs. Compare these values with the theoretically obtained values.

14.12 Solve Problem 14.11 if Aircraft D has a turbocharged engine.

14.13 Solve Problem 14.11 for Aircraft E.

14.14 Solve Problem 14.11 for Aircraft E with a turbocharged engine.

14.15 Aircraft D, which is fitted with an aspirated engine, makes the steepest possible steady climb from sea level. Using the approximate analytical results obtained in this chapter, find the a) airspeed, b) rate of climb, and c) climb angle, at the altitudes of i) sea level, ii) 4 km, and iii) 7 km. Also find the range and the time taken to climb a) from sea level to an altitude of 4 km and b) from an altitude of 4 to 8 km.

14.16 Solve Problem 14.15 for Aircraft D by using the numerical method and compare the results with those obtained from the approximate method used in Problem 14.15.

14.17 Solve Problem 14.15 if Aircraft D has a supercharged engine.

14.18 Solve Problem 14.15 for Aircraft D if it is fitted with a supercharged engine, using a numerical method and compare the results with those obtained by the approximate method used in Problem 14.17.

14.19 Solve Problem 14.15 for Aircraft E.

- 14.20** Solve Problem 14.15 for Aircraft E by using a numerical method and compare the results with those obtained using the approximate method as in Problem 14.19.
- 14.21** Solve Problem 14.15 for Aircraft E, which is using a turbocharged engine.
- 14.22** Solve Problem 14.15 for Aircraft E, with a turbocharged engine, by using a numerical method, and compare the results with those obtained from the approximate method used in Problem 14.21.
- 14.23** Aircraft D has an aspirated engine and makes the fastest steady climb from sea level. Plot the variation of the a) airspeed, b) climb angle, c) rate of climb, d) range covered, e) time taken, and f) fuel consumed, with the increase in altitude.
- 14.24** Solve Problem 14.23 for Aircraft D if it is using a turbocharged engine.
- 14.25** Solve Problem 14.23 for Aircraft E.
- 14.26** Solve Problem 14.23 for Aircraft E if it is fitted with a supercharged engine.
- 14.27** Aircraft D is fitted with an aspirated engine and is scheduled to make the fastest climb at an altitude of 5 km. The aircraft has the capacity to undergo the following changes in its design parameters: a) W/S can be increased by 20%, b) C_{D_0} can be decreased by 10%, c) K can be decreased by 10%, and d) η_p can be increased by 5%. For each of these individual changes, find the percentage changes made in the a) airspeed, b) climb angle, and c) rate of climb.
- 14.28** Solve Problem 14.27 if Aircraft D has a turbocharged engine.
- 14.29** Solve Problem 14.27 for Aircraft E.
- 14.30** Solve Problem 14.27 if Aircraft E has a supercharged engine.

15

Coordinated Turning Flights of Piston-Prop Aircraft

15.1 Introduction

The meaning of a coordinated turn in the horizontal plane was already explained at the beginning of Chapter 11. The equations of motion of a coordinated turn are obtained here for piston-prop aircraft and the applicable turning flight parameters are deduced. The important flight parameters are airspeed, rate of turn, radius of turn, load factor, and bank angle.

The cases of interest in a turning flight are those that produce the fastest turn, tightest turn, maximum load factor, and stall. All these cases are analyzed here, and their flight parameters are obtained in terms of the aircraft design parameters. Attempts are made to present the results of turning performance in analytic form.

15.2 Equations of Motion of a Coordinated Turn

A coordinated turn in horizontal plane along a circular path is considered here. Turning is accomplished by banking the aircraft, whose angle of sideslip is kept at zero. The thrust line is considered along the flight path. The lines of actions of forces of thrust F , drag D , and lift L are in the same plane, which is the plane of symmetry of the aircraft. A steady turn is considered where there is no acceleration along the flight path. The only acceleration is due to centripetal force acting along the radius of curvature r of the flight path. The forces acting on the aircraft are the same as shown in Fig. 11.1. Resolving the forces in the three orthogonal directions and proceeding in the same manner as in Sec.11.2, the following equations of motion are obtained:

$$F = D \quad (15.1)$$

$$L \cos \phi = W \quad (15.2)$$

$$L \sin \phi = (W/g)V^2/r \quad (15.3)$$

and

$$V = r\dot{\chi} \quad (15.4)$$

where ϕ is bank angle, χ is the turning angle (angle of yaw), $\dot{\chi}$ ($= d\chi/dt$) is the rate of turn (angular velocity), W is the weight of aircraft, and g is the acceleration due to gravity.

The rate of fuel consumption during the turn is given by

$$-dW/dt = \hat{c}P_e \quad (15.5)$$

where \hat{c} is the power-specific fuel consumption (PSFC) of the piston-prop aircraft, and P_e is the engine brake power. The thrust power P ($= FV$) of an aircraft is related to its engine power by the propeller efficiency η_p as follows:

$$P = k\eta_p P_e \quad (15.6)$$

where k is the conversion factor whose value depends on the system of units used, as explained in Eq. (12.5). Equation (15.5), however, will not be used here because a turning flight is usually of short duration, where the weight of aircraft can be regarded as constant during the turn due to insignificant fuel consumption during the period of turning.

The lift/weight ratio L/W is called the load factor and is denoted by n . Knowledge of the load factor during a turn or maneuver is important because the aircraft structure, pilot, and passengers cannot withstand high load factors. Equation (15.2) shows that the load factor is directly connected to the bank angle ϕ thus

$$n = L/W = 1/\cos \phi = \sec \phi \quad (15.7)$$

Increase in the load factor with ϕ is shown in Fig. 11.2. Using Eq. (15.1), the load factor can also be expressed as

$$n = L/W = (F/W)L/D = (F/W)E \quad (15.8)$$

where E ($= L/D$) is the aerodynamic efficiency of the aircraft.

15.3 Turning Flight Parameters

The turning flight parameters are the airspeed of the turn, bank angle, load factor, aerodynamic efficiency, rate of the turn, and the radius of the turn. These parameters are expressed here in terms of the aircraft design parameters.

15.3.1 Airspeed, Load Factor, and Bank Angle

From Eq. (15.1), using the parabolic drag polar for the drag coefficient, the thrust force F can be expressed as

$$F = D = (1/2)\rho V^2 S C_D = (1/2)\rho V^2 S (C_{D_0} + K C_L^2) \quad (15.9)$$

where

$$C_L = 2L/(\rho V^2 S) = 2n(W/S)/(\rho V^2) \quad (15.10)$$

Substituting the above value of C_L in Eq. (15.9) and rearranging it gives

$$V^4 - 2(FV)V/(\rho S C_{D_0}) + 4Kn^2(W/S)^2/(\rho^2 C_{D_0}) = 0$$

Writing $FV = P = k\eta_p P_e$, and $\rho = \rho_{SSL}\sigma$, the above equation can be written

$$V^4 - 2k\eta_p(P_e/S)V/(\rho_{SSL}\sigma C_{D_0}) + 4Kn^2(W/S)^2/(\rho_{SSL}^2\sigma^2 C_{D_0}) = 0 \quad (15.11)$$

Unlike the case of a turbojet aircraft in Sec. 11.3, the above equation for a piston-prop aircraft cannot be solved for the airspeed V in analytic form. However, it is

possible to obtain V by a numerical or graphical method of solution of Eq. (15.11) in a specific problem.

The load factor is obtained by rearranging Eq. (15.11) as

$$n = \left[\frac{1}{4K(W/S)} \{ 2k\eta_p(P_e/W)\rho_{SSL}\sigma V - C_{D_0}\rho_{SSL}^2\sigma^2 V^4/(W/S) \} \right]^{1/2} \quad (15.12)$$

The bank angle ϕ would then be obtained as $\phi = \cos^{-1}(1/n)$, where ϕ is in radians.

15.3.2 Lift Coefficient and Aerodynamic Efficiency

The lift coefficient is obtained from its definition, which [using Eq. (15.7)] can be written as

$$C_L = 2L/(\rho V^2 S) = 2n(W/S)/(\rho V^2) = 2n(W/S)/(\rho_{SSL}\sigma V^2) \quad (15.13)$$

Since $n > 1$, the lift coefficient of an aircraft during turning is more than during cruising flight ($n = 1$) for a given altitude and airspeed.

The drag coefficient C_D is obtained from the parabolic drag polar

$$C_D = C_{D_0} + K C_L^2 \quad (15.14)$$

and the aerodynamic efficiency, E , of the aircraft is obtained as

$$E = C_L/C_D = C_L/(C_{D_0} + K C_L^2) \quad (15.15)$$

where C_{D_0} is the zero-lift drag coefficient and K is the lift-dependent drag coefficient factor. Both C_{D_0} and K are design parameters, which are supposed to be known quantities for a given aircraft.

15.3.3 Turning Rate and Turning Radius

The turning rate is obtained by dividing Eq. (15.3) by the equal terms of Eq. (15.2) and using Eq. (15.4) as

$$\tan \phi = V^2/(gr) = (V/g)\dot{\chi}$$

Using Eq. (15.7) in the above relation, the turning rate can be written as

$$\dot{\chi} = (g/V) \tan \phi = (g/V) \sqrt{n^2 - 1} \quad (15.16)$$

Similarly, from Eqs. (15.4) and (15.16), the turning radius can be written as

$$r = V/\dot{\chi} = V^2/(g\sqrt{n^2 - 1}) \quad (15.17)$$

In the above two Eqs. (15.16) and (15.17), n is given by Eq. (15.12) and V is the solution of Eq. (15.11). Thus, both $\dot{\chi}$ and r can be expressed in terms of the aircraft design parameters.

15.4 Turning Flight at Maximum Load Factor

The maximum load factor gives an upper limit to n that can be achieved, at least theoretically. The flight condition with the maximum load factor is usually avoided because of design or flight limitations. The maximum allowable load factor $n_{m,\text{allowable}}$, which is generally less than the maximum load factor n_m , is more important in practice. The airspeed for the maximum load factor is established here, and the other turning flight parameters are deduced. The subscript nm is used to denote the condition of the maximum load factor.

15.4.1 Airspeed, Load Factor, and Bank Angle

The variation of load factor with airspeed is given by Eq. (15.12). The maximum load factor airspeed V_{nm} is obtained by differentiating Eq. (15.12) with respect to V , putting $dn/dV = 0$, and solving the resulting algebraic equation for V . This gives

$$V_{nm} = \left\{ k\eta_p(P_e/S)/(2\rho_{SSL}\sigma C_{D_0}) \right\}^{1/3} \quad (15.18)$$

The airspeed for the maximum load factor increases with the increase in propeller efficiency, engine power, and altitude. Substituting the above relation for airspeed in Eq. (15.12), the maximum load factor is obtained as

$$n_m = 0.687 \left[\frac{1}{K(W/S)} \{k\eta_p(P_e/W)\}^2 E_m \rho_{SSL} \sigma \right]^{1/3} \quad (15.19)$$

The maximum load factor increases with the increase in engine power/weight ratio, propeller efficiency, and maximum aerodynamic efficiency. It decreases with an increase in wing loading and altitude.

The maximum bank angle ϕ_m can now be obtained as $\phi_m = \cos^{-1}(1/n_m)$. An increase in the maximum load factor also means an increase in the maximum bank angle.

15.4.2 Lift Coefficient and Aerodynamic Efficiency

The lift coefficient $C_{L,nm}$ of maximum load factor flight is obtained from Eq. (15.13), which after using Eqs. (15.18) and (15.19) becomes

$$C_{L,nm} = 2n_m(W/S)/(\rho_{SSL}\sigma V_{nm}^2) = \sqrt{3C_{D_0}/K} = \sqrt{3}C_{L,E_m}$$

The lift coefficient of the maximum load factor flight is greater than that required for maximum aerodynamic efficiency. The drag coefficient $C_{D,nm}$ of the maximum load factor flight can be obtained as

$$C_{D,nm} = C_{D_0} + K C_{L,nm}^2 = 4C_{D_0} = 2C_{D,E_m}$$

The aerodynamic efficiency E_{nm} for the maximum load factor is given by

$$E_{nm} = C_{L,nm}/C_{D,nm} = (1/4)\sqrt{3/(K C_{D_0})} = (\sqrt{3}/2)E_m$$

The aerodynamic efficiency for the maximum load factor is less than that required for the maximum aerodynamic efficiency for piston-prop aircraft.

15.4.3 Turning Rate and Turning Radius

The turning rate $\dot{\chi}_{nm}$ and the turning radius r_{nm} for the maximum load factor are obtained from Eqs. (15.16) and (15.17), respectively, as

$$\dot{\chi}_{nm} = (g/V_{nm})\sqrt{n_m^2 - 1} \quad \text{and} \quad r_{nm} = V_{nm}^2 / (g\sqrt{n_m^2 - 1})$$

where the analytic expressions for V_{nm} and n_m in terms of the aircraft design variables are found in Eqs. (15.18) and (15.19), respectively.

15.5 Fastest Turn

The maximum rate of turning is called the *fastest turn*. It is denoted by $\dot{\chi}_m$ which stands for $(d\chi/dt)_m$. The fastest turn is a figure of merit representing the aircraft's maneuverability, and it is especially important for aerobatic and combat aircraft. The airspeed for the maximum turning rate can be calculated and expressions for the other flight parameters of the fastest turn can be obtained. The subscript FT is used to denote the condition of the fastest turn.

15.5.1 Airspeed, Load Factor, and Bank Angle

It is seen from Eqs. (15.16) and (15.12) that the rate of turn of a given aircraft depends on its airspeed. The airspeed of the fastest turn, V_{FT} , can be obtained by differentiating Eq. (15.16) with respect to V , and putting $d\dot{\chi}/dV = 0$. This gives

$$\frac{d\dot{\chi}}{dV} = \frac{\partial \dot{\chi}}{\partial V} + \frac{\partial \dot{\chi}}{\partial n} \frac{dn}{dV} = -(g/V^2)\sqrt{n^2 - 1} + \{gn/(V\sqrt{n^2 - 1})\}dn/dV = 0$$

which after rearrangement becomes $n^2 - 1 - (V/2)dn^2/dV = 0$ for $V = V_{FT}$. From Eq. (15.12), we obtain n^2 and dn^2/dV , and substitute them in the above relation, giving

$$V^4 + \left\{ \frac{k\eta_p(P_e/W)(W/S)}{\rho_{SSL}\sigma C_{D_0}} \right\} V - \frac{4K(W/S)^2}{\rho_{SSL}^2\sigma^2 C_{D_0}} = 0 \quad (15.20)$$

for $V = V_{FT}$. It is not possible to solve the above equation for V in analytic form. In any specific problem, the airspeed V can be obtained by solving Eq. (15.20) by a numerical or graphical method.

It is, however, possible to solve Eq. (15.20) analytically after making an approximation¹ that in certain problems the V^4 term may be much smaller than the other two terms. Thus, ignoring the first term of Eq. (15.20), the fastest turn airspeed is given by

$$V_{FT} = 4K(W/S)/\{k\eta_p(P_e/W)\rho_{SSL}\sigma\} \quad (15.21)$$

The airspeed of the fastest turn is found to increase with an increase in wing loading and altitude.

The load factor n_{FT} of the fastest turn is obtained from Eq. (15.12) by putting $V = V_{FT}$, which gives

$$n_{FT} = \left[2 - \frac{4K(W/S)}{\rho_{SSL}\sigma E_m} \{k\eta_p(P_e/W)\}^{-2} \right]^{1/2} \quad (15.22)$$

The negative term on the right-hand side of the above equation is generally sufficiently small¹ as compared to 2; this is especially true at low altitudes. Therefore, the fastest turn load factor can be approximated as

$$n_{FT} = \sqrt{2} = 1.414 \quad (15.23)$$

The bank angle ϕ_{FT} of the fastest turn is given by $\phi_{FT} = \cos^{-1}(1/n_{FT})$ which after using the approximation of Eq. (15.23) can be written as

$$\phi_{FT} = \cos^{-1}(1/\sqrt{2}) = 0.785 \text{ rad} = 45 \text{ deg}$$

This shows that the load factor and the bank angle of the fastest turn for a piston-prop aircraft can be considered to be approximately constant quantities.

15.5.2 Lift Coefficient and Aerodynamic Efficiency

The lift and drag coefficients, $C_{L,FT}$ and $C_{D,FT}$, of the fastest turn are obtained from Eqs. (15.13) and (15.14), respectively, as

$$C_{L,FT} = 2n_{FT}(W/S)/(\rho_{SSL}\sigma V_{FT}^2) \quad (15.24)$$

and

$$C_{D,FT} = C_{D_0} + KC_{L,FT}^2 \quad (15.25)$$

where V_{FT} is the solution of Eq. (15.20), and n_{FT} can be obtained from Eq. (15.12). The aerodynamic efficiency, E_{FT} , of the fastest turn is given by

$$E_{FT} = C_{L,FT}/(C_{D_0} + KC_{L,FT}^2) \quad (15.26)$$

If the approximations given by Eqs. (15.21) and (15.23) are used, the $C_{L,FT}$ of Eq. (15.24) can be expressed as

$$C_{L,FT} = \{2\sqrt{2}\rho_{SSL}\sigma/(W/S)\}\{k\eta_p(P_e/W)/4K\}^2 \quad (15.27)$$

and by substituting this value of $C_{L,FT}$ in Eqs. (15.25) and (15.26), the approximate analytic expressions for the drag coefficient and aerodynamic efficiency of the aircraft can be obtained for the fastest turning flight.

15.5.3 Turning Rate and Turning Radius

The turning rate $\dot{\chi}_{FT}$, and the turning radius r_{FT} , of the fastest turn are found from Eqs. (15.16) and (15.17), respectively, as

$$\dot{\chi}_{FT} = (g/V_{FT})\sqrt{n_{FT}^2 - 1} \quad (15.28)$$

and

$$r_{FT} = V_{FT}/\dot{\chi}_{FT} = V_{FT}^2/(g\sqrt{n_{FT}^2 - 1}) \quad (15.29)$$

where V_{FT} is the solution of Eq. (15.20), and n_{FT} is obtained by substituting $V = V_{FT}$ in Eq. (15.12).

If the approximations given by Eqs. (15.21) and (15.23) are used, the turning rate and turning radius of the fastest turn given by Eqs. (15.28) and (15.29), respectively, become

$$\dot{\chi}_{FT} = g\rho_{SSL}\sigma k\eta_p(P_e/W)/\{4K(W/S)\} \quad (15.30)$$

and

$$r_{FT} = 4K(W/S)/\{g\rho_{SSL}\sigma k\eta_p(P_e/W)\} \quad (15.31)$$

The rate of the fastest turn increases with an increase in propeller efficiency and power/weight ratio of the aircraft. However, it decreases with an increase in altitude and wing loading. The aircraft design variables that increase $\dot{\chi}_{FT}$ decrease r_{FT} , and vice versa.

15.6 Tightest Turn

In a tightest turn the radius of turn is at a minimum. The tightest turn is a measure of the aircraft's maneuverability and is also a figure of merit of the aircraft. The subscript TT is used here to denote the tightest turn condition.

15.6.1 Airspeed, Load Factor, and Bank Angle

From Eqs. (15.17) and (15.12) it can be seen that the radius of turn is a function of the airspeed. It is possible to obtain the airspeed V_{TT} of the tightest turn by differentiating Eq. (15.17) with respect to V , and putting $dr/dV = 0$. This gives

$$\frac{dr}{dV} = \frac{\partial r}{\partial V} + \frac{\partial r}{\partial n} \frac{dn}{dV} = \frac{2V}{g(n^2 - 1)^{1/2}} - \frac{nV^2}{g(n^2 - 1)^{3/2}} \cdot \frac{dn}{dV} = 0$$

which after rearrangement becomes $n^2 - 1 - (V/4)dn^2/dV = 0$, for $V = V_{TT}$. Obtaining n^2 and dn^2/dV from Eq. (15.12) and substituting them in the above relation gives

$$V_{TT} = 8K(W/S)/\{3k\eta_p(P_e/W)\rho_{SSL}\sigma\} \quad (15.32)$$

The tightest turn airspeed increases with an increase in wing loading and altitude. Since the lift-dependent drag coefficient factor K is inversely proportional to the aspect ratio of the wing, a decrease in aspect ratio would increase the tightest turn airspeed.

The load factor n_{TT} of the fastest turn is obtained by putting $V = V_{TT}$ in Eq. (15.12), giving

$$n_{TT} = \left[\frac{4}{3} - \left\{ \frac{1.78K(W/S)}{\rho_{SSL}\sigma E_m} \cdot \{k\eta_p(P_e/W)\}^{-2} \right\}^2 \right]^{1/2} \quad (15.33)$$

The negative term on the right-hand side of the above equation is generally much smaller than unity in practice,¹ especially at lower altitudes. Therefore, the above equation can be approximated as

$$n_{TT} = \sqrt{4/3} = 2/\sqrt{3} = 1.155 \quad (15.34)$$

The bank angle ϕ_{TT} of the tightest turn is obtained as $\phi_{TT} = \cos^{-1}(1/n_{TT})$, where n_{TT} is given by Eq. (15.33). If the approximation given by Eq. (15.34) is used,

$$\phi_{TT} = \cos^{-1}(1/1.155) = 0.523 \text{ rad} = 30 \text{ deg}$$

Thus, the load factor and bank angle of the tightest turn of a piston-prop aircraft can be regarded as approximately constant quantities that do not depend on the flight or design parameters.

15.6.2 Lift Coefficient and Aerodynamic Efficiency

The lift coefficient $C_{L,TT}$, drag coefficient $C_{D,TT}$, and aerodynamic efficiency E_{TT} of the tightest turn are obtained from Eqs. (15.13), (15.14), and (15.15), respectively, as

$$C_{L,TT} = 2n_{TT}(W/S)/(ρ_{SSL}σ V_{TT}^2) \quad (15.35)$$

$$C_{D,TT} = C_{D_0} + K C_{L,TT}^2 \quad (15.36)$$

and

$$E_{TT} = C_{L,TT}/C_{D,TT} = C_{L,TT}/(C_{D_0} + K C_{L,TT}^2) \quad (15.37)$$

where V_{TT} and n_{TT} are obtained from Eqs. (15.32) and (15.33), respectively.

If the approximate value of n_{TT} , given by Eq. (15.34), is used and V_{TT} is obtained from Eq. (15.32), the lift coefficient in Eq. (15.35) can be written as

$$C_{L,TT} = \{3\sqrt{3}ρ_{SSL}σ/(W/S)\}\{kη_p(P_e/W)/(4K)\}^2$$

The values of $C_{D,TT}$ and E_{TT} are then obtained by using the above value of $C_{L,TT}$ in Eqs. (15.36) and (15.37), respectively.

15.6.3 Turning Rate and Turning Radius

The turning rate \dot{x}_{TT} , and the turning radius r_{TT} , of the tightest turn are obtained from Eqs. (15.16) and (15.17), respectively, as

$$\dot{x}_{TT} = (g/V_{TT})\sqrt{n_{TT}^2 - 1} \quad (15.38)$$

and

$$r_{TT} = V_{TT}/\dot{x}_{TT} = V_{TT}^2/\{g\sqrt{n_{TT}^2 - 1}\} \quad (15.39)$$

where V_{TT} and n_{TT} are given by Eqs. (15.32) and (15.33), respectively.

If the approximate value of n_{TT} given by Eq. (15.34) is used, and V_{TT} is obtained from Eq. (15.32), Eqs. (15.38) and (15.39), respectively, can be written as

$$\dot{\chi}_{TT} = \sqrt{3}g\rho_{SSL}\sigma k\eta_p(P_e/W)/\{8K(W/S)\} \quad (15.40)$$

and

$$r_{TT} = \{64/(3\sqrt{3}g)\}[K(W/S)/\{\rho_{SSL}\sigma k\eta_p(P_e/W)\}]^2 \quad (15.41)$$

The turning rate of the tightest turn increases with an increase in η_p , P_e/W , and altitude. The turning rate decreases with an increase in K and wing loading. The aircraft design parameters that increase $\dot{\chi}_{TT}$ decrease r_{TT} , and vice versa.

15.7 Turning Flight at Stalling Airspeed

The turning flight parameters near stalling airspeed in a coordinated turn are obtained here in terms of the aircraft design parameters. It should also be remembered that it is generally not desirable to fly near stall. At the stalling airspeed, the lift coefficient is at a maximum which is denoted by $C_{L,m}$, and the corresponding drag coefficient is $C_{D,m}$. During combat, aerobatic maneuvers, or flight tests it may become necessary to fly at the stalling airspeed.

15.7.1 Airspeed, Load Factor, and Bank Angle

From Eq. (15.13) of the lift coefficient, the stalling airspeed $V_{S,t}$ in a turning flight is given by

$$V_{S,t} = \{2n_{S,t}(W/S)/(\rho_{SSL}\sigma C_{L,m})\}^{1/2} \quad (15.42)$$

where $n_{S,t}$ is the load factor at stall in turning. Then $n_{S,t}$ is given by Eq. (15.12) as

$$n_{S,t} = \left[\frac{1}{4K(W/S)} \left\{ 2k\eta_p(P_e/W)\rho_{SSL}\sigma V_{S,t} - \frac{C_{D_0}\rho_{SSL}^2\sigma^2}{(W/S)} V_{S,t}^4 \right\} \right]^{1/2} \quad (15.43)$$

The above expression contains $V_{S,t}$ on the right-hand side, which can also be eliminated as shown below.

To express $V_{S,t}$ in terms of the aircraft design variables, write Eq. (15.42) as

$$V_{S,t}^4 = 4n_{S,t}^2(W/S)^2 / (\rho_{SSL}^2\sigma^2 C_{L,m}^2) \quad (15.44)$$

and the substitution of the value of $n_{S,t}$, given by Eq. (15.43), in the Eq. (15.44) gives

$$V_{S,t} = [2k\eta_p(P_e/W)(W/S)/\{(\rho_{SSL}\sigma)(C_{D_0} + KC_{L,m}^2)\}]^{1/3} \quad (15.45)$$

It is possible to write

$$C_{D_0} + KC_{L,m}^2 = C_{D,m} = C_{L,m}/E_m$$

where $C_{D,m}$ is the drag coefficient at $C_{L,m}$; in other words, $C_{D,m}$ is the drag coefficient at stall in turning. This is based on the assumption that the parabolic

drag polar is valid down to stall speed, which is not strictly true. In view of this, Eq. (15.45) can also be written as

$$V_{S,t} = \{2k\eta_p(P_e/W)(W/S)E_m/(\rho_{SSL}\sigma C_{L,m})\}^{1/3} \quad (15.46)$$

The above relation could also have been obtained from Eqs. (15.6) and (15.9) by writing these equations for stall in turning as

$$k\eta_p P_e = P = D_m V_{S,t} = \frac{1}{2}\rho V_{S,t}^3 S C_{D,m} = \frac{1}{2}\rho_{SSL}\sigma V_{S,t}^3 S \frac{C_{L,m}}{E_m}$$

where D_m is the maximum drag at stall in turning. Equation (15.46) immediately follows from the above relation.

The load factor at stall in turning is obtained from Eq. (15.42) as

$$n_{S,t} = \rho_{SSL}\sigma V_{S,t}^2 C_{L,m}/\{2(W/S)\}$$

which after using Eq. (15.46) can be written as

$$n_{S,t} = \frac{\rho_{SSL}\sigma C_{L,m}}{2(W/S)} \left\{ \frac{2k\eta_p(P_e/W)(W/S)E_m}{\rho_{SSL}\sigma C_{L,m}} \right\}^{2/3} \quad (15.47)$$

The bank angle $\phi_{S,t}$ at the stall in turning is obtained as $\phi_{S,t} = \cos^{-1}(1/n_{S,t})$, where $n_{S,t}$ is given by Eq. (15.47).

15.7.2 Turning Rate and Turning Radius

The turning rate $\dot{\chi}_{S,t}$ and the turning radius $r_{S,t}$ at stall are obtained from Eqs. (15.16) and (15.17), respectively, as

$$\dot{\chi}_{S,t} = \frac{g}{V_{S,t}} \sqrt{n_{S,t}^2 - 1} \quad \text{and} \quad r_{S,t} = \frac{V_{S,t}}{\dot{\chi}_{S,t}} = \frac{V_{S,t}^2}{g\sqrt{n_{S,t}^2 - 1}}$$

where $V_{S,t}$ and $n_{S,t}$ are given by Eqs. (15.46) and (15.47), respectively.

15.8 Application to an Aircraft

Consider the same aircraft as presented in comparable sections in Chapters 12–14. It has $W = 7350$ N (1652.3 lb), $S = 11.2$ m 2 (120.5 ft 2), $P_e = 7500$ W (100.6 hp), $C_{D_0} = 0.032$, and $K = 0.14$. Find the values of the flight parameters for the fastest turn at an altitude of 2 km ($\sigma = 0.8217$) for an aspirated piston-prop aircraft.

The aircraft has $W/S = 7350/11.2 = 656.25$ N/m 2 , $P_e/SSL/W = 75,000/7350 = 10.2$ m/s. The power/weight ratio P_e/W of the aspirated piston-prop engine aircraft at an altitude of 2 km is $P_e/W = (P_e/SSL/W)\sigma = 10.2 \times 0.8217 = 8.38$ m/s.

The airspeed of the fastest turn is obtained by solving Eq. (15.20) numerically, which gives $V_{FT} = 37.54$ m/s. The load factor n is obtained from Eq. (15.12) by

putting $V = V_{FT} = 37.54$ m/s, giving

$$n = \left[\frac{1}{4 \times 0.14(656.25)} \left\{ 2 \times 1 \times 0.85(8.38)1.225 \times 0.8217 \times 37.54 - \frac{0.032(1.225)^2}{656.25} \times (0.8217)^2 \times (37.54)^4 \right\} \right]^{1/2} = 1.094$$

The lift coefficient and aerodynamic efficiency are obtained from Eqs. (15.24) and (15.26), respectively, as

$$C_{L,FT} = 2 \times 1.094(656.25) / \{1.225 \times 0.8217(37.54)^2\} = 1.012$$

and

$$E_{FT} = 1.012 / \{0.032 + 0.14(1.012)^2\} = 5.77$$

The turning rate is obtained from Eq. (15.28) as

$$\dot{\chi}_{FT} = \frac{9.807}{37.54} \sqrt{(1.094)^2 - 1} = 0.116 \text{ rad/s} = 6.65 \text{ deg/s}$$

and the turning radius is given by

$$r_{FT} = V_{FT} / \dot{\chi}_{FT} = 37.54 / 0.116 = 324 \text{ m}$$

Hence the values of the flight parameters of this aircraft for the fastest turn are airspeed = 37.54 m/s, load factor = 1.094, lift coefficient = 1.012, aerodynamic efficiency = 5.77, turning rate = 6.65 deg/s, and turning radius = 324 m.

Reference

¹Hale, F. J., *Aircraft Performance, Selection, and Design*, Wiley, New York, 1984.

Problems

The major specifications of Aircraft D and Aircraft E, which are required to solve the problems here, are presented at the beginning of the Problems section in Chapter 12.

15.1 Aircraft D executes a level turn at sea level at an airspeed of 200 km/h, using 80% of its maximum thrust power. Find the load factor, bank angle, lift coefficient, aerodynamic efficiency, turning rate, and turning radius.

15.2 Solve Problem 15.1 if the airspeed of Aircraft D is increased by 10%.

15.3 Solve Problem 15.1 if Aircraft D utilizes maximum thrust.

15.4 Solve Problem 15.1 for Aircraft D if the turning maneuver is executed at an altitude of 4 km using a) an aspirated engine and b) a turbocharged engine.

15.5 Aircraft D makes a coordinated turn in the horizontal plane at sea level. Its bank angle is 10 deg and maximum thrust power is used. Find the load factor, airspeed, turning rate, and turning radius.

15.6 Aircraft E makes a coordinated turn at Mach number 0.2 at an altitude of 6 km, using maximum available thrust power with an aspirated engine. Find the load factor, bank angle, lift coefficient, aerodynamic efficiency, turning rate, and turning radius. What is the stalling speed in this turn? Is this turn possible?

15.7 Solve Problem 15.6 if Aircraft E uses a supercharged engine.

15.8 Find the percentage changes made in the load factor, bank angle, turning rate, and turning radius of Problem 15.6 for the following three cases of Aircraft E: a) wing loading is decreased by 10%, b) C_{D_0} is decreased by 5%, and c) K is decreased by 5%.

15.9 Aircraft E is turning at sea level at the rate of 1.5 deg/s with a bank angle of 15 deg, using maximum power. Find the a) Mach number of the turn, its lift coefficient, and aerodynamic efficiency; b) load factor and the power required to turn; c) turning radius; and d) stalling speed in this turn.

15.10 Find the percentage changes incurred in the solutions of Problem 15.9 for Aircraft E due to each of the following changes in its parameters: a) W/S is decreased by 10%, b) C_{D_0} decreased by 5%, and c) K is decreased by 5%.

15.11 For Aircraft D performing a coordinated turn at an altitude of 2 km, plot the following curves and mark the optimum airspeed for each case, and compare these values with the theoretically obtained optimum values: a) variation of load factor with airspeed, b) variation of rate of turn with airspeed, c) variation of turning radius with airspeed.

15.12 Solve Problem 15.11 for Aircraft D if it uses a turbocharged engine.

15.13 Solve Problem 15.11 for Aircraft E turning at an altitude of 6 km, using an aspirated engine.

15.14 Solve Problem 15.13 for Aircraft E turning at an altitude of 6 km, using a turbocharged engine.

15.15 Aircraft D is to make a steady, level turn, at maximum load factor, at an altitude of 3 km using an aspirated engine. Find the a) airspeed, load factor, and bank angle; b) lift coefficient and aerodynamic efficiency; and c) rate of turn and radius of turn.

15.16 Solve Problem 15.15 if Aircraft D uses a turbocharged engine.

15.17 Solve Problem 15.15 if Aircraft E turns at an altitude of 7 km, and is using an aspirated engine.

15.18 Solve Problem 15.15 if Aircraft E turns at an altitude of 7 km, using a turbocharged engine.

15.19 Aircraft D makes a steady, level turn at sea level at the fastest turning rate. Find the a) airspeed, load factor, and bank angle; b) lift coefficient and aerodynamic efficiency; and c) turning rate and turning radius. Do you think it is possible to turn at this airspeed?

15.20 Solve Problem 15.19 for Aircraft D turning at an altitude of 4 km if it uses an aspirated engine.

15.21 Solve Problem 15.19 for Aircraft D turning at an altitude of 4 km if it uses a turbocharged engine.

15.22 Solve Problem 15.19 for Aircraft E turning at an altitude of 6 km if it uses an aspirated engine.

15.23 Solve Problem 15.19 for Aircraft E turning at an altitude of 6 km, if it uses a turbocharged engine.

15.24 Aircraft E makes the fastest turning rate at an altitude of 6 km and is using an aspirated engine. Find the percentage changes made in the airspeed, load factor, bank angle, turning rate, and turning radius for the following changes in its design parameters: a) W/S is reduced by 15%; b) C_{D_0} is reduced by 4%; c) K is reduced by 4%; d) W/S , C_{D_0} , and K are simultaneously reduced by 15%, 4%, and 4%, respectively.

15.25 Solve Problem 15.24 for Aircraft E if it uses a turbocharged engine.

15.26 Aircraft D makes the tightest steady level turn at sea level. Find the a) airspeed, load factor, and bank angle, b) lift coefficient and aerodynamic efficiency, and c) turning radius and turning rate.

15.27 Solve Problem 15.26 for Aircraft D turning at an altitude of 3 km if it uses an aspirated engine.

15.28 Solve Problem 15.26 for Aircraft D turning at an altitude of 3 km if it uses a turbocharged engine.

15.29 Solve Problem 15.26 for Aircraft E turning at an altitude of 7 km if it uses an aspirated engine.

15.30 Solve Problem 15.26 for Aircraft E turning at an altitude of 7 km if it uses a turbocharged engine.

15.31 Aircraft D is making coordinated turn at stalling airspeed by using full power. Find the airspeed, load factor, bank angle, turning rate, and turning radius when it is a) at sea level; b) at an altitude of 4 km, using an aspirated engine; and c) at an altitude of 4 km, using a turbocharged engine.

15.32 Solve Problem 15.31 for Aircraft E.

This page intentionally left blank

Takeoff and Landing Performance

16.1 Introduction

The takeoff is the starting phase of an aircraft's flight, which after completion of the aircraft's mission, or due to some other reasons, generally ends with a smooth landing as the last phase of the flight. The takeoff and landing are the most significant for aircraft operation because the majority of aircraft accidents occur during these two phases. The analysis developed here is primarily aimed at calculating takeoff and landing distances and their times. Both these phases, as defined, include only a very small portion of the airborne flight distance.

Certain characteristic distances and airspeeds connected with the landing and takeoff phases of flight are first explained. The additional friction force during ground roll, existing between the wheels and the ground, requires special attention. For convenience in calculation, both the takeoff and landing phases are each subdivided into four segments. Based on the theoretical analysis developed for calculation, methods for reducing takeoff and landing distances are presented. A general discussion is included on the various retarding devices that are commonly used during the landing phase of an aircraft.

The possibility of engine failure can never be completely eliminated. The possibility of engine failure is taken into account when designing modern aircraft as well as in deciding the length of runway required for safety considerations.

The takeoff and landing distances and time are considerably influenced by the altitude, ambient temperature, runway slope, and the wind. A proper consideration of these factors is essential for avoiding undesirable consequences. For safety reasons, the Federal Aviation Regulation (FAR)¹ has laid down certain operational procedures during climb up to the height of 460 m (1500 ft), but these are not discussed here.

16.2 Characteristic Distances Along Runway

The characteristic lengths or distances along the runway strip of an airport during takeoff and landing flights are explained below.

16.2.1 Liftoff Distance

The distance from the start of the ground roll until the aircraft has become airborne is called the *liftoff* distance and is denoted by x_{Lo} . The length OB in Fig. 16.1 is equal to x_{Lo} . The liftoff distance consists of the ground roll distance x_g , plus the rotation distance x_R . During the ground roll, from the position 0 to A, both the rear and front wheels of the aircraft are rolling on the ground. At Station A the front wheels are lifted by aerodynamic forces, and only the rear wheels continue to roll on the ground until position B is reached. At position B the rear wheels are also lifted up as the aircraft becomes airborne.

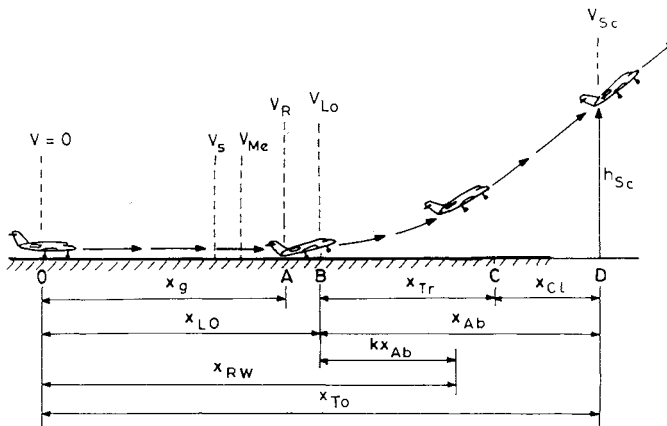


Fig. 16.1 Characteristic distances and airspeeds for the takeoff phase.

16.2.2 Length of Runway (Takeoff Run Length)

The length of runway x_{RW} of an aircraft is the liftoff distance x_{Lo} plus a portion kx_{Ab} of the airborne distance x_{Ab} up to the screen height, as shown in Fig. 16.1. That is,

$$x_{RW} = x_{Lo} + kx_{Ab} \quad (16.1)$$

If the screen height is taken as 10.7 m (35 ft) for a commercial aircraft, the value of k is 1/2 according to FAR.¹

In the case of an aircraft engine failure (or inoperative engine), the length of runway $x_{RW,EF}$ is defined in the same way as given by Eq. (16.1). That is,

$$x_{RW,EF} = x_{Lo,EF} + kx_{Ab,EF} \quad (16.2)$$

where $x_{Lo,EF}$ is the liftoff distance and $x_{Ab,EF}$ is the length of airborne distance, in the event of the engine failure or the engine becoming inoperative.

For practical reasons the *runway length required* is the greater of the two distances, $1.15x_{RW}$ and $x_{RW,EF}$, if the screen height is taken as 10.7 m (35 ft). The runway required has a hard concrete surface compatible with the aircraft weight and the undercarriage design.

The ordinary level ground after the end of the runway that can be used to stop an aborted takeoff is called the *stopway*. The distance extending beyond the stopway until the first obstacle appears on the ground is called the *clearway*.

16.2.3 Takeoff Distance and Screen Height

The takeoff distance x_{To} is the straight horizontal distance from the start of takeoff on the runway until the lowest portion of the aircraft has reached the screen height of 15.24 m (50 ft) or 10.7 m (35 ft), as specified by the aviation regulations. The takeoff length is shown in Fig. 16.1. It is composed of the ground roll distance x_g , the rotation distance x_R , the transition distance x_{Tr} from the position B to C in which the aircraft flies in a curved flight path, and finally the

climb distance x_{Cl} from the position C to D where the aircraft climbs along a straight path. That is,

$$x_{To} = x_g + x_R + x_{Tr} + x_{Cl} = x_{Lo} + x_{Ab} \quad (16.3)$$

In the case of engine failure, the takeoff distance $x_{To,EF}$ is defined in the same way as above. That is,

$$x_{To,EF} = x_{Lo,EF} + x_{Ab,EF} \quad (16.4)$$

For practical considerations, the *takeoff length required* is taken to be the greater of the two distances, $1.15x_{To}$ and $x_{To,EF}$, if the screen height is taken as 10.7 m (35 ft).

It is seen above that the takeoff distance extends until the aircraft has reached the screen height. The *screen height* (imaginary erect screen) is also called *obstacle height* where the obstruction may be imaginary. The screen height ensures that the aircraft clears all obstacles such as trees, houses, and other civil structures before commencing unhampered climb. The screen height is fixed by aviation regulations of the country or the airlines concerned. Usually one follows FAR¹ of the United States, which fixes the screen height at either 10.7 m (35 ft) or 15.4 m (50 ft) depending on the type of aircraft and its performance.

16.2.4 Landing Distance

The landing distance x_{La} is the horizontal distance, starting from the point where the lowest portion of the airborne aircraft is at the screen height to the point where the aircraft comes to a standstill on the runway. The screen height may be 10.7 m (35 ft) or 15.24 m (50 ft) as specified by the aviation regulations. The landing distance is shown in Fig. 16.2. It comprises the airborne distance $x_{Ab,La}$ during landing and the distance $x_{Td,La}$ after touchdown. That is,

$$x_{La} = x_{Ab,La} + x_{Td,La} \quad (16.5)$$

The landing distance is the total horizontal distance of the landing phase.

16.2.5 Accelerate-and-Stop Distance (Emergency Distance)

The accelerate-and-stop distance assumes importance if one of the engines of an aircraft fails at an airspeed that is less than the critical engine failure speed that

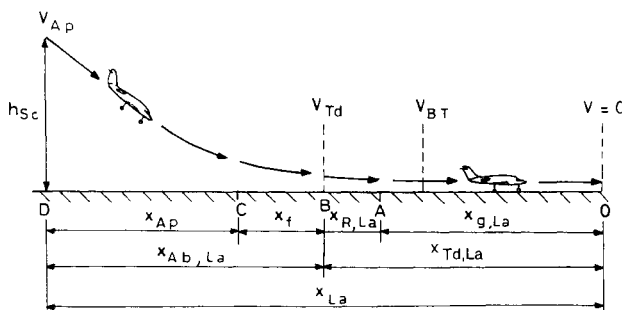


Fig. 16.2 Characteristic distances and airspeeds for the landing phase.

is defined in Sec. 16.3.3. In this case the pilot has no other option but to abort the takeoff and decelerate the aircraft quickly by applying the brakes until the aircraft stops. If x_{EF} is the distance of the position, measured from the start of takeoff, at which the engine has failed, and x_{STOP} is the distance, measured from the position of engine failure, until the aircraft has come to rest, the accelerate-and-stop distance x_{AS} is given by

$$x_{AS} = x_{EF} + x_{STOP} \quad (16.6)$$

The accelerate-and-stop distance is also called the *emergency distance*. The different segments of x_{AS} and their calculations are discussed below in Sec. 16.8.4. If the length x_{AS} is equal to the length $x_{To,EF}$, it is called the *balanced field length* as discussed in Sec. 16.8.5 below.

16.2.6 Takeoff Field Length

The takeoff distance x_{To} of the aircraft (all engines operative), the takeoff distance $x_{To,EF}$ of an aircraft with engine failure, and the emergency distance x_{AS} have been defined already. The greater of the distances, $1.15x_{To}$, $x_{To,EF}$, and x_{AS} is called the *takeoff field length*.

16.3 Characteristic Airspeeds During Takeoff and Landing

In the takeoff phase, the speed of the aircraft increases continuously from zero at the start of the takeoff until the aircraft reaches a certain height above the runway. While the speed is increasing the aircraft is passing through certain important characteristic airspeeds which in the ascending order of magnitude are the stalling airspeed V_S , minimum control airspeed V_{MC} , critical engine failure recognition airspeed V_{CEFR} , takeoff rotation airspeed V_R , liftoff airspeed V_{Lo} , and the climb airspeed V_{Cl} . Many of these airspeeds are shown in Fig. 16.1. Similarly, at the time of landing the characteristic airspeeds are the approach airspeed V_{Ap} , touchdown airspeed V_{Td} , and braking airspeed V_{Br} , as shown in Fig. 16.2. The important features of these airspeeds are presented below; a more comprehensive list and account of the characteristic airspeeds during takeoff and landing is given by Grover² and Williams.³

16.3.1 Stalling Airspeed (Minimum Flight Airspeed)

The minimum airspeed at which an aircraft can become airborne is the *stalling airspeed* at which level flight can be maintained with zero acceleration. It is also called the *minimum flight airspeed* in the takeoff configuration. It is rare for an aircraft to fly at its stalling airspeed because doing so may be unsafe and unstable. Certain control surfaces become less effective at stall due to flow separation over them. The stalling airspeed occurs at the maximum lift coefficient of the wings for a given flap deflection. It will be seen below that the stalling airspeed V_S is often regarded as the reference airspeed when specifying the other characteristic airspeeds.

16.3.2 Minimum-Control Airspeed

The minimum-control airspeed can be applied for the ground roll and for the airborne aircraft, and these two airspeeds are denoted by $V_{MC,g}$ and $V_{MC,Ab}$, respectively, where the latter is the more important airspeed. Both of these airspeeds are related to the ability of the pilot to maintain directional control of the aircraft in case of a sudden disturbance created by an engine failure. The minimum control airspeed $V_{MC,Ab}$, as the name suggests, is the lowest airspeed at which it is possible to fly the aircraft, as demonstrated by a test pilot, after an engine fails, with zero yaw or with a bank angle less than 5 deg. A broad requirement is that $V_{MC,Ab}$ should not exceed $1.2V_S$ with maximum takeoff weight. It is easier to achieve ground control of an aircraft than to control it once it is airborne, and the value of $V_{MC,g}$ is less than $V_{MC,Ab}$.

16.3.3 Critical Engine Failure Recognition Airspeed (Decision Airspeed)

It is usually accepted that an average pilot takes about 1 s to recognize that an engine has failed. The engine failure recognition airspeed is, therefore, the airspeed that is measured 1 s after the engine failure airspeed. The critical engine failure recognition airspeed V_{CEFR} is, therefore, also considered to be the airspeed 1 s after the critical engine failure airspeed V_{CEF} . The *critical engine failure recognition airspeed* is defined as the airspeed at which the pilot has both options—to abort or to continue the takeoff—such that in both these cases the field lengths would be the same. This is called *balanced field length*, and is explained in Sec. 16.8.5. If engine failure is recognized at an airspeed less than V_{CEFR} , the takeoff has to be aborted. If the engine failure is recognized at an airspeed greater than V_{CEFR} , the takeoff has to be continued, at least until the screen height has been reached. In the event of some rare coincidence, if engine failure is recognized just at V_{CEFR} , the pilot has both options. The V_{CEFR} is also called *decision airspeed*, which is commonly denoted by V_1 . Clearly, V_{CEFR} must be greater than $V_{MC,g}$, and also less than the corresponding liftoff airspeed V_{Lo} .

16.3.4 Takeoff Rotation Airspeed

In a takeoff flight when the aircraft is close to becoming airborne, the front portion of the aircraft is generally lifted first, and soon after the rear portion is also lifted. This means that both the nose and the rear wheels are not lifted simultaneously to make the aircraft airborne. The nose wheels are lifted (not retracted) first above the ground by rotating the aircraft about the rear wheels which continue to roll on the ground. The airspeed at which the aircraft is rotating during the takeoff is called the *takeoff rotation airspeed* V_R which is generally equal to about $1.1V_S$. The minimum value of V_R can be equal to V_{CEFR} . The aircraft continues to accelerate horizontally during rotation, although with a lesser magnitude. The V_R must be such that the aircraft reaches the screen height within the airspeed range specified by the FAR.

16.3.5 Liftoff Airspeed (Unstick Airspeed)

The *liftoff airspeed* is the airspeed at which the rear wheels are also lifted above the ground and the aircraft becomes airborne. The liftoff airspeed V_{Lo} is generally equal to about $1.15V_S$. This means that V_{Lo} is about 5% more than the rotation

airspeed. The liftoff airspeed is also called the *unstick airspeed* of the aircraft, because the aircraft no longer continues to stick to the ground during the rest of the takeoff phase.

16.3.6 Climb Airspeed (Takeoff Safety Airspeed)

The airspeed of the aircraft at the screen height above the ground is called the *climb airspeed*. It is the most important target airspeed in the takeoff flight for the reasons of aircraft safety during climb. It is also called the *takeoff safety airspeed*. The rotation airspeed and the subsequent acceleration of the aircraft are regulated to achieve the specified climb airspeed V_{C1} at the screen height. The climb airspeed ranges from $1.2V_S$ to $1.3V_S$. In the case of an engine failure, or a single-engine aircraft, it is close to $1.25V_S$ and commonly denoted as V_2 . In the case of all-engines-operative aircraft, it is close to $1.3V_S$ and is commonly denoted as V_3 , which is only moderately greater than V_2 .

16.3.7 Approach Airspeed at Screen Height (Threshold Airspeed)

The approach airspeed V_{Ap} is the airspeed of the aircraft descent at the screen height, as shown in Fig. 16.2; the screen height is usually taken as 50 ft (15.24 m) above the ground. This is also called the *threshold airspeed* of the aircraft. Its value is about $1.3V_{S,Ap}$, where $V_{S,Ap}$ is the stalling airspeed of the approach configuration of the aircraft.

16.3.8 Touchdown Airspeed

The airspeed at which the wheels of the aircraft touch the ground at the time of landing is called the *touchdown airspeed* and is denoted by V_{Td} . The touchdown airspeed is usually about $1.15V_{S,Ap}$. The vertical component of velocity at touchdown is generally kept quite close to zero.

16.4 Braking Friction During Takeoff and Landing

Relative motion between two surfaces that are in contact with each other gives rise to a force called the mechanical friction or simply the *friction* that opposes the motion. This can be rolling friction or sliding friction, the latter being comparatively of much larger magnitude. The friction force is directly proportional to the force acting normal to the surface of contact. The constant of proportionality is called the *coefficient of friction* which is a nondimensional quantity. The coefficient of rolling friction is much less than the coefficient of sliding friction, and the magnitudes of both these coefficients depend on the surface roughness and the conditions at the place of contact.

The action of the brakes during the ground roll of an aircraft causes its wheels to partly roll and to partly slide. The friction force so developed is termed the *braking friction*; its value lies between the values for sliding and rolling frictions. The coefficient of braking friction is denoted here by μ ; it depends on several factors such as the runway surface material, runway contamination, tire material and its condition, and the amount of sliding due to braking. Some typical variations for μ against the percentage of slip for different runway surface conditions are shown⁴ in Fig. 16.3. Each curve exhibits an optimum value of μ .

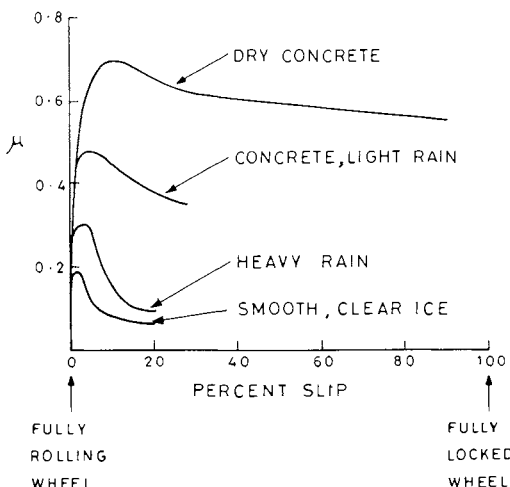


Fig. 16.3 Coefficient of braking friction for various surface conditions.

An aircraft generally has two sets of wheels. One set of wheels, located at the front near the nose, is called the *front* or *nose wheels*. The other set of wheels is at the rear, under the carriage, and is called the *rear* or *undercarriage wheels*. The weight of the aircraft is supported more by the rear wheels than by the front wheels. Let W_{fr} and W_r denote the portions of the aircraft weight W that are supported by the front and rear wheels, respectively. Similarly, let L_{fr} and L_r be the portions of the aircraft lift force L that are balanced at the front and rear wheels, respectively, during the ground roll, as shown in Fig. 16.4. The braking friction force F_{Br} acting opposite to the direction of motion of the aircraft is given by $F_{Br} = \mu(W_{fr} - L_{fr}) + \mu(W_r - L_r)$, and since $W_{fr} + W_r = W$, and $L_{fr} + L_r = L$, the braking force can be expressed as

$$F_{Br} = \mu(W - L) \quad (16.7)$$

This shows that as L increases during the passage of ground roll, F_{Br} decreases continuously until it vanishes at the liftoff point.

16.5 Analysis of the Takeoff Phase of an Aircraft

The performance analysis of takeoff consists of calculating the distance and time covered during the takeoff phase. The takeoff phase is subdivided into four segments for developing a simplified analysis to obtain the horizontal distance and time covered in each segment.

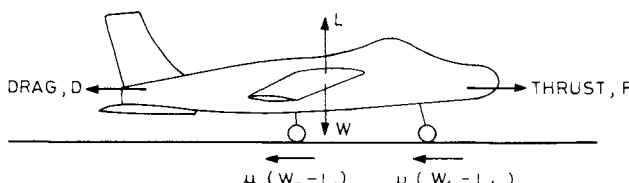


Fig. 16.4 Forces acting on the aircraft during the ground roll.

16.5.1 Segments of Takeoff Phase

The takeoff phase of an aircraft begins when the aircraft has started rolling on the ground for the takeoff run from the position 0, as shown in Fig. 16.1. The takeoff phase is completed when the aircraft has reached the screen height h_{Sc} at Station D. The aircraft continues to accelerate throughout the ground roll, and even further, until a steady climb is achieved. The amount of acceleration throughout the run is such (about 2 m/s^2) that the passengers' comfort is not disrupted.

The total takeoff phase is divided into four different segments for the convenience of calculations, because the attitude of the aircraft is different in each segment. The main actions of the aircraft in these segments are, respectively, the ground roll, the rotation of the aircraft, the transition, and the climb. These segments are defined here, and performance analysis of aircraft in these segments is carried out.

16.5.2 Calculation of Takeoff Distance and Time

The horizontal distance covered and time taken during each segment of the takeoff will be calculated. The sum of the horizontal distances and the sum of the times of these individual segments give the total horizontal distance and total time covered, respectively, during the takeoff phase.

16.5.2.1 Ground roll distance and time. The ground roll segment begins from its starting position 0 on the runway (Fig 16.1) and ends at position A where the rotation airspeed of the aircraft has reached. In this segment all the landing wheels of aircraft are rolling on the ground and the airspeed has increased from 0 to V_R . The distance 0A is denoted by x_g and the time taken to travel this distance is denoted by t_g .

The forces acting on the aircraft during the takeoff ground roll are shown in Fig. 16.4. The forward force is the thrust F which is provided by the jet engine or piston-prop engine. The forces of aerodynamic drag and mechanical friction oppose the forward motion of the aircraft. Balancing the forces along the direction of motion of the aircraft and using Eq. (16.7), the equation of motion for the ground roll can be written as

$$(W/g) dV/dt = F - D - \mu(W - L) \quad (16.8)$$

The lift and drag forces during the ground roll are influenced by the ground effect, which must be taken into account; the lift is increased and drag is reduced due to ground effect as explained in Chapter 3. If a denotes the acceleration of the aircraft during the ground run, $a = dV/dt = (dV/dx) dx/dt = V dV/dx = (1/2) dV^2/dx$ and, therefore,

$$dx = dV^2/2a \quad \text{and} \quad dt = dV/a \quad (16.9)$$

where a is obtained from Eq. (16.8) as

$$a = (g/W)\{F - D - \mu(W - L)\} \quad (16.10)$$

Considering the rotation airspeed V_R to be approximately the same as the liftoff airspeed V_{L_0} , the integration of the equations of relation (16.9) gives, respectively,

$$x_g = (1/2) \int_0^{V_{L_0}} dV^2/a \quad \text{and} \quad t_g = \int_0^{V_{L_0}} dV/a \quad (16.11)$$

where a is given by Eq. (16.10). It has been found convenient for the purpose of integration to approximate the thrust variation F with airspeed as parabolic. Since μ and W can be regarded as constants during the ground roll, and L and D are mostly proportional to V^2 , the variation of acceleration a with airspeed is also parabolic. This parabolic expression helps in evaluating the above two integrals analytically, but the parabolic expression itself contains two constants whose determinations are not simple. The analysis presented below is, however, considerably simplified by having recourse to certain empirical results.

The right-hand-side integrals in relation (16.11) can be easily evaluated if the acceleration a can be regarded as constant. It can be seen that if the acceleration is constant, the distance of the aircraft from the starting station is proportional to the square of the ground speed and the corresponding time taken is proportional to ground speed. The integrals of relation (16.11) can be evaluated numerically if V and a are known at different points of the ground roll.

The typical behaviors of F , D , and $\mu(W - L)$, during the takeoff of an aircraft are presented in Fig. 16.5. The resultant horizontal force $\{F - D - \mu(W - L)\}$ is a measure of the acceleration a . It is not an uncommon practice for the sake of simplicity to regard the acceleration as a constant and take it as equal to \bar{a} , which is the value of a where the airspeed is $V = 0.7V_{L_0}$. Therefore, the equations of relation (16.11) can be written as

$$x_g = V_{L_0}^2/2\bar{a} = \{WV_{L_0}^2/2g\}\{F - D - \mu(W - L)\}_{V=0.7V_{L_0}}^{-1} \quad (16.12)$$

and

$$t_g = V_{L_0}/\bar{a} = \{WV_{L_0}/g\}\{F - D - \mu(W - L)\}_{V=0.7V_{L_0}}^{-1} \quad (16.13)$$

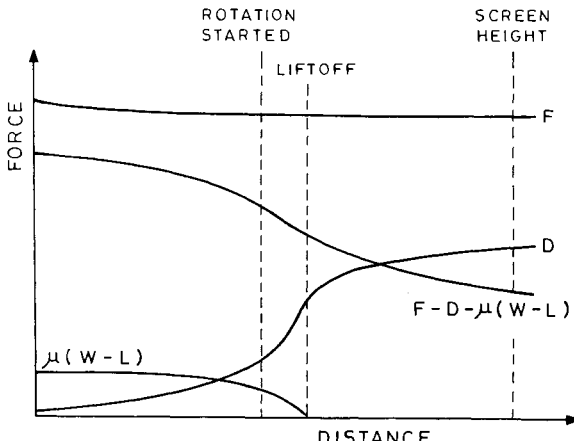


Fig. 16.5 Changes in forces during takeoff phase.

The aircraft weight W in the above two equations is considered to be a constant because only an insignificant fraction of the fuel is consumed during the ground run. The thrust F of a jet engine aircraft can also be regarded as known constant during the ground run. If it is a piston-prop aircraft, its thrust force F decreases during the takeoff ground run and its value at $V = 0.7V_{L_0}$ is supposed to be known. The lift and drag forces are also estimated at an airspeed of $V = 0.7V_{L_0}$. Once the values of F , D , and L have been obtained, Eqs. (16.12) and (16.13) predict the ground roll distance and time, respectively.

16.5.2.2 Rotation distance and time. When the rotation airspeed V_R is reached at Station A, the aircraft is rotated by using elevator control that causes the nose-up, and consequently the front wheels are lifted above the ground. Between positions A and B, the front wheels are up, the rear wheels are rolling on the ground and the aircraft is rotating about them as shown in Fig. 16.1. The rotation of a big transport aircraft may be at the rate of about 3 deg/s whereas that of a small aircraft or military aircraft may be greater. During rotation the angle of attack and the lift and drag coefficients increase; the lift coefficient may reach about $0.8c_{L,m}$. As soon as the lift exceeds the aircraft weight at Station B where the airspeed has reached the liftoff airspeed V_{L_0} , the rear wheels also leave the ground and the aircraft becomes airborne. It is now required to calculate the horizontal distance AB and the time taken to cover this distance.

The rotation time of the aircraft is very small in practice, about 3 s, and it can be assumed that the horizontal airspeed of the aircraft remains constant during this period. These assumptions considerably simplify the calculations of time and distance because the theoretical formulation and solution of the equations of motion can be avoided. Taking the rotation time t_R as only 3 s, and the known constant horizontal airspeed as V_{L_0} during the rotation segment, immediately gives

$$t_R = 3 \text{ s} \quad \text{and} \quad x_R = 3V_{L_0} \quad (16.14)$$

During the rotation of aircraft about its rear wheels the pilot must ensure that the tail of the aircraft does not touch the ground.

16.5.2.3 Transition distance and time. Soon after the aircraft has become airborne at Station B, it initially moves in a curved flight path up to the Station C before settling into the straight climb path from C onward. The distance BC is called the *transition segment* of takeoff flight. The horizontal distance BC covered during the curved flight path is called the transition distance and is denoted by x_{Tr} . For the convenience of calculation it is assumed that the curved flight path is a circular arc that is performed at the constant airspeed V_{L_0} as shown in Fig. 16.6. At the end of the transition segment the aircraft climbs at an angle of γ which is assumed to be a known small quantity.

During the transition phase the lift force is more than the aircraft weight because the lift force has also to overcome the centrifugal force $(W/g)V_{L_0}^2/R_{Tr}$, where R_{Tr} is the radius of curvature of the flight path during the transition segment. Therefore,

$$L = W + (W/g)V_{L_0}^2/R_{Tr}, \quad \text{i.e.,} \quad L/W = 1 + V_{L_0}^2/(gR_{Tr}) \quad (16.15)$$

which shows that the load factor exceeds unity by an amount $(V_{L_0}^2/gR_{Tr})$ during the transition phase. Strictly speaking, Eq. (16.15) is true only at Station B, but

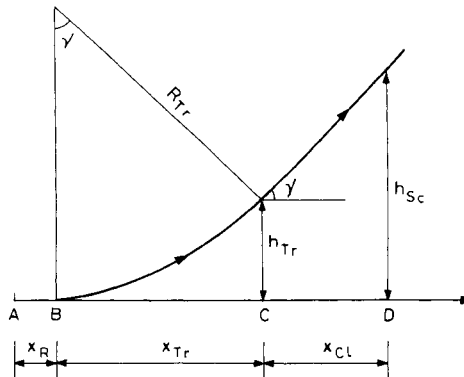


Fig. 16.6 Rotation, transition, and climb segments.

it is considered to remain valid in the region BC because the climb angle is very small in practice. The lift and weight can be expressed as

$$L = (1/2)\rho V_{Lo}^2 SC_{L,Lo} \quad \text{and} \quad W = (1/2)\rho V_S^2 SC_{L,m}$$

where $C_{L,Lo}$ is the lift coefficient of the aircraft at the time of liftoff. These two relations give

$$L/W = (C_{L,Lo}/C_{L,m})(V_{Lo}/V_S)^2 \quad (16.16)$$

The values of $C_{L,Lo}$ and V_{Lo} are supposed to be known for the particular aircraft under consideration. In the absence of this information we can assume their typical empirical values to be $C_{L,Lo} = 0.8C_{L,m}$, and $V_{Lo} = 1.2V_S$. The lift/weight ratio given by Eq. (16.16) can be written as $L/W = 0.8 \times (1.2)^2 = 1.15$, and the radius of curvature of the transition flight path is obtained from Eq. (16.15) as $R_{Tr} = V_{Lo}^2/(0.15g)$. The transition length x_{Tr} as shown in Fig. 16.6 would be given by

$$x_{Tr} = R_{Tr} \sin \gamma = \{V_{Lo}^2/(0.15g)\} \sin \gamma \quad (16.17)$$

and the time taken t_{Tr} during the transition segment would be given as

$$t_{Tr} = R_{Tr} \gamma / V_{Lo} = V_{Lo} \gamma / (0.15g) \quad (16.18)$$

where γ is in radians.

Before proceeding further for calculating the climb distance and the corresponding time taken in Sec. 16.5.2.4, we first estimate the height h_{Tr} at the end of transition phase. Since the transition flight path is considered to be a circular arc the transition height would be obtained as

$$h_{Tr} = R_{Tr} - R_{Tr} \cos \gamma = (1 - \cos \gamma)R_{Tr}$$

and if h_{Tr} is less than the screen height h_{Sc} , one proceeds further to calculate the climb segment as presented below.

16.5.2.4 Climb distance and time. The climb segment starts at Station C (Fig. 16.6) where the aircraft starts climbing along a straight flight path at constant airspeed V_{Cl} . The climb segment is completed as soon as the lowest part of the aircraft has reached the screen height h_{Sc} above the ground. If the aircraft has reached the screen height at Station D on the runway, the horizontal distance CD is the climb segment, which is denoted by x_{Cl} . From the geometry of Fig. 16.6 it is clear that

$$x_{Cl} = (h_{Sc} - h_{Tr}) / \tan \gamma \quad (16.19)$$

and, therefore, the time taken t_{Cl} to complete this climb distance will be given by

$$t_{Cl} = x_{Cl} / (V_{Cl} \cos \gamma) \quad (16.20)$$

It would be worth considering here the example of an actual aircraft that would indicate the kinds of magnitudes involved in the distances and times of these various segments of takeoff phase. A Boeing 747-100 aircraft weighing 332,490 kg_f (733,000 lb_f) requires a liftoff time of 43 s, takeoff time of 54 s, liftoff distance of 1900 m, and takeoff distance of 2900 m, to reach the screen height of 15.24 m, and it has an average acceleration of about 1.8 m/s². The variations of the aircraft speed and the height of its wheels above the ground along the runway are shown in Fig. 16.7; this figure is obtained from the presentation made by McCormick.⁵

16.5.3 Shortening of Takeoff Length

The difficulty in the availability of sufficient runway length at many places and the increased cost of its construction has led to the devising of methods to shorten the takeoff length. The takeoff distance can be shortened if the ground roll and airborne distances are minimized.

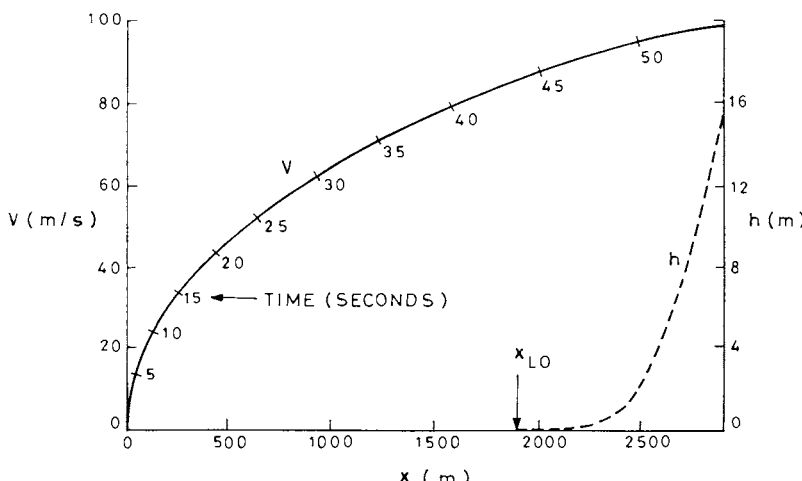


Fig. 16.7 Airspeed and height variations against distance in takeoff phase of a Boeing 747-100 aircraft.

Equations (16.12) and (16.14), respectively, show that the ground roll and rotation distances can be very effectively shortened by minimizing the liftoff airspeed. This amounts to initiating the liftoff at maximum lift coefficient, which in turn increases the drag and reduces the excess thrust. The runway length can be made smaller by reducing the coefficient of braking friction, which requires that the runway surface be hard and dry.

Another method of reducing x_g is by increasing thrust by keeping the thrust augmentation at its maximum throughout the ground roll, but this is sometimes not permitted. In case thrust augmentation is limited to a shorter time than that required for the takeoff ground roll, it is pertinent to enquire whether to use it early or late in the ground roll. Thrust augmentation is more effective if more work is done by it. If ΔF is the additional thrust produced by the augmentation being used for a small distance ΔS and for a short time Δt , the additional work done by augmentation $\Delta(\text{WDA})$ is given by $\Delta(\text{WDA}) = \Delta F \cdot \Delta S = \Delta F \cdot V \Delta t$, where WDA is the abbreviation used for work done by augmentation. This shows that the work done by thrust augmentation is greater if V is greater. This suggests that the thrust augmentation should be utilized late in the takeoff so that its time limit is completed just before the aircraft becomes airborne.

16.6 Analysis of Landing Phase of Aircraft

A semiempirical method of calculating the horizontal distance traveled and time taken in completing the landing phase of an aircraft is explained here. The method is similar to that used for the takeoff phase of the aircraft.

16.6.1 Segments of Landing Phase

After completing its mission, or due to some other reason, an aircraft finally descends and approaches for landing. When the aircraft is about 300 m above the ground level of the runway, the undercarriage is lowered and the flaps are set to the landing configuration. The aircraft descends along a straight flight path which is sometimes referred to as the *glide path* and is usually at an angle of about 3 deg to the horizontal. As the aircraft's height falls below about 60 m, the speed of the aircraft is gradually decreasing. At the screen height the approach airspeed V_{Ap} is generally not less than $1.3V_{S,Ap}$.

By definition, the landing phase starts when the aircraft is at the screen height (also called the *threshold point*), and ends when it has come to a standstill on the straight runway.

The performance analysis of the landing phase requires the calculation of its horizontal distance and time, and the method of calculation is similar to that used for takeoff but in the reverse order. The significant features here are that the thrust is nearly zero during landing and the braking friction is severe. For the convenience of calculation, the landing phase is also divided into four segments, DC, CB, BA, and AO, as shown in Fig. 16.8. The main actions of aircraft in these segments are, respectively, approach, flare (transition), rotation, and landing roll on the ground.

16.6.2 Calculation of Landing Phase Distance and Time

The horizontal distance covered and the time taken during each of the four segments of the landing phase will be calculated. The sum of these horizontal

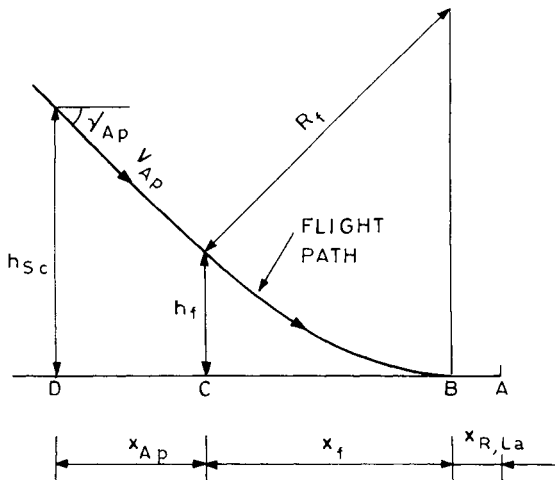


Fig. 16.8 Approach, flare, and rotation segments.

distances and times yields the total distance and the total time covered, respectively, during the landing phase.

16.6.2.1 Approach distance and time. The approach, the flare (transition), and the rotation segments are shown in Fig. 16.8 which is very similar to Fig. 16.6 but in the reverse order, because the aircraft is now descending. The segment DC is the approach segment where the aircraft is descending along a straight flight path at an angle γ_{Ap} at constant airspeed. At position C, the flare segment starts where the aircraft is initiated to move along a curved flight path. If h_f is the height of the aircraft at position C, it is clear from the geometry of Fig. 16.8 that the length of the approach segment x_{Ap} is given by

$$x_{Ap} = (h_{Sc} - h_f) / \tan \gamma_{Ap} \quad (16.21)$$

and since the approach airspeed V_{Ap} is constant during the segment, the time taken t_{Ap} is obtained as

$$t_{Ap} = x_{Ap} / (V_{Ap} \cos \gamma_{Ap}) \quad (16.22)$$

For a passenger transport aircraft V_{Ap} is about $1.3 V_{S,Ap}$, where $V_{S,Ap}$ is given by

$$V_{S,Ap} = \sqrt{2(W_{Ap}/S)/(\rho C_{L,m;Ap})}$$

and the quantities W_{Ap} and $C_{L,m;Ap}$ are the aircraft weight and maximum lift coefficient, respectively, in the approach configuration. Due to fuel consumption enroute, the weight of an aircraft in approach configuration is generally considerably less as compared to the takeoff weight.

16.6.2.2 Flare distance and time. The segment CB in Fig. 16.8 is the transition segment which is also called the *flare segment*, where the aircraft flies in a curved path. The angle of descent continuously decreases from about 3 deg at

Station C to nearly 0 deg at Station B, which is the touchdown point of the main or rear wheels, while the nose-wheels may be still above the ground. The purpose of the flare is to make the glide path less steep for minimizing the vertical component of velocity at the touchdown point. The ground effect, which increases C_L and reduces C_D , automatically induces flare on some aircraft, so that little or no action by the pilot is required. The undercarriage is usually designed to withstand impact load due to the vertical component of velocity of about 3 m/s, but the pilot aims at much lower values of about 0.5 m/s at the touchdown. In the transition segment, the aircraft is assumed to be moving at a constant airspeed of V_{Ap} along a circular arc of radius R_f . The declination of the aircraft changes from γ_{Ap} at Station C to zero at Station B. It is required here to calculate the distance CB, which is denoted by x_f , and the time taken to complete the distance, which is denoted by t_f .

Proceeding in a similar fashion to the case of the transition segment during takeoff, the lift L_f at the time of flare can be written as

$$L_f = W_{Ap} + (W_{Ap}/g)V_{Ap}^2/R_f, \quad \text{i.e.,} \quad L_f/W_{Ap} = 1 + V_{Ap}^2/(gR_f) \quad (16.23)$$

Since

$$L_f = (1/2)C_{L,Ap}\rho V_{Ap}^2 S \quad \text{and} \quad W_{Ap} = (1/2)C_{L,m:Ap}\rho V_{S,Ap}^2 S$$

the ratio

$$L_f/W_{Ap} = (C_{L,Ap}/C_{L,m:Ap})(V_{Ap}/V_{S,Ap})^2 \quad (16.24)$$

The values of $C_{L,Ap}$ and V_{Ap} are supposed to be known for the particular aircraft under consideration. In the absence of this information, we can assume their typical empirical values to be

$$C_{L,Ap} = 0.64C_{L,m:Ap} \quad \text{and} \quad V_{Ap} = 1.3V_{S,Ap}$$

From Eq. (16.24), this gives $L_f/W_{Ap} = 0.64(1.3)^2 = 1.08$, and the radius of curvature of the transition path is given by Eq. (16.23) as $R_f = V_{Ap}^2/(0.08g)$.

From the geometry of Fig. 16.8, it is clear that

$$x_f = R_f \sin \gamma_{Ap} = \{V_{Ap}^2/(0.08g)\} \sin \gamma_{Ap} \quad (16.25)$$

and the time taken t_f to complete the flare segment would be

$$t_f = R_f \gamma_{Ap} / V_{Ap} = V_{Ap} \gamma_{Ap} / (0.08g) \quad (16.26)$$

where γ_{Ap} is in radians. In practice, for a passenger aircraft γ_{Ap} is about 0.05 rad (3 deg), and at the point of touchdown it may be about half a degree.

16.6.2.3 Rotation distance and time. The rear wheels of the aircraft touch the ground at Station B while the front wheels are still in the air. Immediately after touching the rear wheels at Station B the aircraft is rotated down and at Station A the front wheels also touch the ground. The airspeed $V_{R,La}$ at the time of rotation while landing at Station B can be taken to be approximately equal to the touchdown airspeed V_{Td} at the position B on the ground. It is then required to calculate the

distance BA (Fig. 16.8) and the time taken during the rotation segment. Similar to the case during takeoff, here also the rotation time is taken to be 3 s with a constant airspeed of V_{Td} . Therefore, the rotation distance $x_{R,La}$ of the landing run and the corresponding time $t_{R,La}$ are, respectively, given by

$$x_{R,La} = 3V_{Td} \quad \text{and} \quad t_{R,La} = 3 \text{ s} \quad (16.27)$$

16.6.2.4 Landing roll distance and time. The landing roll starts from Station A, where all the wheels are on the ground, and ends at Station O where the aircraft comes to rest (Fig. 16.2). The ground roll distance AO during the landing is denoted by $x_{g,La}$ and the corresponding time by $t_{g,La}$. The airspeed of the aircraft at A is assumed to be the same as the touchdown airspeed V_{Td} at B, and the aircraft is slowing down with a constant average deceleration of \bar{d} . This gives

$$x_{g,La} = V_{Td}^2 / 2\bar{d} \quad \text{and} \quad t_{g,La} = V_{Td} / \bar{d} \quad (16.28)$$

where \bar{d} can be taken to be equal to 0.55 g for maximum braking, 0.35 g for medium braking, and 0.15 g for simple braking.⁶

16.6.3 Shortening the Landing Phase

The landing distance consists of the airborne and ground roll distances. The ground roll distance, as seen from Eq. (16.28), increases as the square of the touchdown speed. Therefore, for the ground roll distance, V_{Td} should be kept low by operating at the highest possible lift coefficient which has the additional advantage of increasing the drag. The thrust should be kept as low as possible. The air brakes and reverse thrust, if available, should be employed at the earliest time, soon after touchdown, because they are more effective at higher airspeeds.

The airborne distance until touchdown can be shortened if high drag and low thrust are maintained throughout the descent.

16.7 Aircraft Retardation Devices

After touchdown the pilot brings the aircraft at rest as soon as possible, within a specified region on the runway. Aircraft retardation is an important phase which should be made smoothly, causing no discomfort to passengers and the crew. In the early days of aviation, retardation was accomplished using only mechanical devices such as wheel brakes or arresting gears. A modern aircraft is much heavier, requiring large touchdown airspeed. The dissipation of large amounts of kinetic energy after touchdown by entirely mechanical means becomes prohibitive because of the requirement of large weight for the brakes assembly component.

It thus becomes essential to employ some other means of energy dissipation for supplementing the mechanical device. The most common other means of aircraft retardation are propulsive and aerodynamic devices. The propulsive device for retarding a turbojet aircraft consists essentially in the reversal of jet thrust by a mechanical arrangement at the exhaust of the jet engine. The drag due to jet reversal for braking purposes could be about 40% of the rated takeoff thrust. In the case of a propeller-driven aircraft, negative pitch of the propeller blades reverses the thrust, which can be about 50% of the static thrust. Moreover, the

reversible-pitch propeller blade device is inexpensive and carries no extra weight penalty.

Aerodynamic retardation devices use air brakes, spoilers on wing surfaces, and drag chutes. These aerodynamic devices create excessive drag force opposing the forward motion of the aircraft and are used immediately after touchdown.

16.8 Performance with Engine Failure

The possibility of engine failure during flight can never be ruled out. For the reasons of safety, all modern aircraft are designed to take into consideration possible engine failure. Aircraft performance analysis in the engine-inoperative case is discussed below.

16.8.1 Engine Failure Probability and Its Effects

Modern turbine engines are very reliable with a very low probability of failure. The probability of failure of an engine increases with the increase in the total number of aircraft engines. For example, the probability that one engine will fail in a four-engine aircraft is double that for a twin-engine aircraft. Engine failures during takeoff are more common than during cruise. The failure of two engines out of a total of three or four engines during takeoff is extremely unlikely and, therefore, is not considered here in the takeoff performance. For safety reasons, a transport aircraft should have a sufficient reserve of thrust and must be equipped with at least two engines. Engine failure brings considerable decrease in thrust, gives rise to yawing and rolling moments, generates asymmetrical flight conditions, and produces additional drag forces due to the dead engine and its airframe. Engine failure is a very serious matter and, therefore, airworthiness safety requirements have been laid down by FAR and BCAR (British Civil Airworthiness Requirements) for engine-inoperative aircraft. The takeoff of a multiple-engine aircraft with one engine inoperative is permitted to continue only when the engine failure is recognized after the attainment of a certain minimum airspeed that is specified by the designer, otherwise the takeoff run has to be aborted.

16.8.2 Forces During Takeoff with Engine Failure

Soon after an engine fails, the forces along the flight path undergo certain rapid changes as shown in Fig. 16.9. The thrust reduces considerably, either to zero or to idling thrust within about 4 s time after the engine failure. The failure of an engine increases the drag of aircraft due to asymmetric flight and windmilling of the propeller or its compressor blades. The extra drag is also created in takeoff rotation due to an increase in angle of attack of the aircraft. There is also an increase in induced drag during rotation and after, due to 1) download on the tail by extra wing lift and 2) reduction in ground effect after liftoff. The retraction of the undercarriage, which starts about 3 s after liftoff, also varies the drag. The braking friction force on the wheels continuously reduces and finally vanishes at the liftoff point. The changes in the resultant force $\{F - D - \mu(W - L)\}$ during the takeoff run are also shown in Fig. 16.9.

16.8.3 Airspeeds in Takeoff and Abort

The characteristic airspeeds in the cases of all-engines-operative takeoff, engine failure takeoff, and aborted flight are shown in Fig. 16.10. The airspeeds V_{EF} and

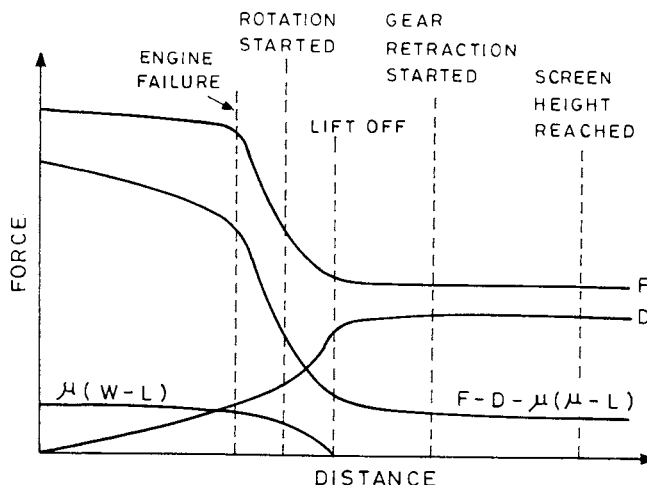


Fig. 16.9 Changes in forces during the takeoff phase in case of engine failure.

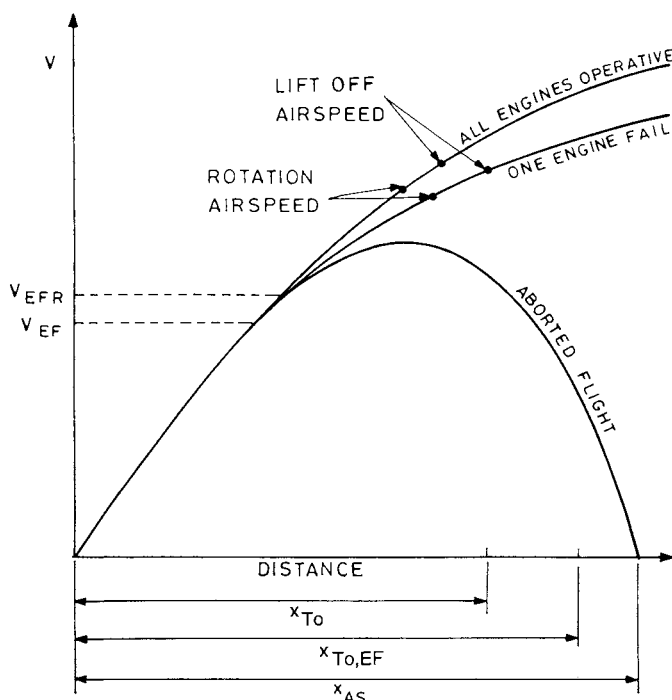


Fig. 16.10 All-engines-operative, one-engine-fail, and aborted flights.

V_{EFR} , respectively, represent the engine failure and engine failure recognition airspeeds. In the case of engine failure, as can be expected, the takeoff rotation and liftoff airspeeds are slightly delayed as compared to the case for all-engines-operative aircraft. The engine failure also reduces the acceleration. It can be seen that in the case of aborted flight the aircraft also continues to accelerate after engine failure, but for a very short duration because there may still be some appreciable thrust in the failed engine for a short time. Moreover, due to the inertia of the aircraft, the positive acceleration takes some time to become zero before the deceleration starts. The pilot takes some time, generally assumed to be 1 s, to recognize that engine failure has occurred. More delay also occurs by the time the pilot decides to close the throttle, and to lift dampers, air brakes, and wheel-brakes; this delay usually amounts to 3–4 s after engine failure has occurred.

16.8.4 Analysis of Accelerate-and-Stop Distance

The distance and time covered by an aircraft whose flight has been aborted due to an engine failure are calculated here. Throughout its motion the aircraft is rolling on the ground because it has not become airborne. Initially the aircraft accelerates, and soon after engine failure the acceleration decreases quickly, rapidly changing to deceleration due to the application of the aircraft's brakes, until the aircraft stops. The distance covered by the aircraft from the start of ground roll on the straight runway until the aircraft finally stops is called the *accelerate-and-stop distance*, denoted by x_{AS} , while the corresponding time is denoted by t_{AS} .

For the purposes of calculation, the accelerate-and-stop distance is divided into three segments, as shown in Fig. 16.11. The first segment OA is the *acceleration segment* of length x_{EF} and time t_{EF} . At the end of this segment at point A the engine fails. The next segment AB, of length x_I and time t_I , is the *inertia segment* during which the acceleration initially decreases and finally changes to deceleration. The last segment BC, of length x_{Br} and time t_{Br} , is the *braking segment* where the aircraft is continuously decelerating until it stops at the end of the segment. The

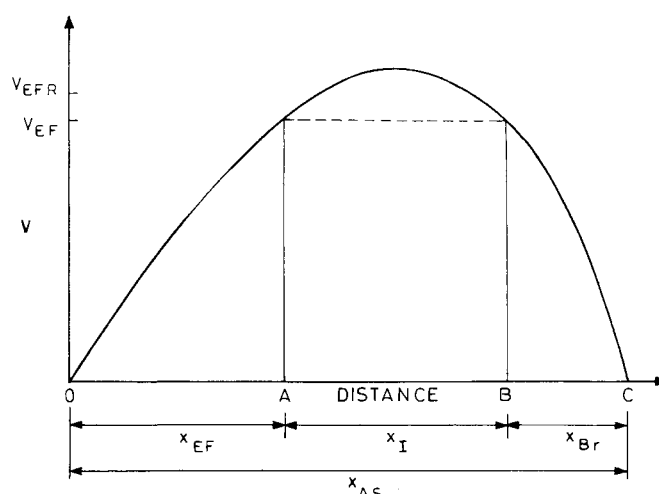


Fig. 16.11 Segments of accelerate-and-stop distance.

accelerate-and-stop distance x_{AS} and time t_{AS} are given by $x_{AS} = x_{EF} + x_I + x_{Br}$, and $t_{AS} = t_{EF} + t_I + t_{Br}$. The distance and time of each segment are calculated below.

16.8.4.1 Acceleration distance and time. The aircraft is accelerating throughout this segment just like all-engines-operative aircraft. The procedures for calculating distance and time are the same as those used in obtaining Eqs. (16.12) and (16.13). Therefore,

$$x_{EF} = V_{EF}^2 / 2\bar{a} \quad \text{and} \quad t_{EF} = V_{EF} / \bar{a} \quad (16.29)$$

where \bar{a} is the average acceleration in the segment.

16.8.4.2 Inertia distance and time. The *inertia distance* is the segment AB of length x_I , and time taken to cover the distance is t_I . The aircraft here initially accelerates and then decelerates. The duration of t_I is small; it is assumed to be 3.5 s with constant average airspeed of V_{EFR} , which is supposed to be a known quantity. This gives

$$x_I = 3.5V_{EFR} \quad \text{and} \quad t_I = 3.5 \text{ s} \quad (16.30)$$

16.8.4.3 Braking distance and time. The *braking segment* starts from B and ends at C where the aircraft stops. Since Station B is quite close to the place where the pilot applies brakes, the aircraft is continuously decelerating in this segment. If \bar{d} is the average deceleration, the braking distance and time are given by

$$x_{Br} = V_{EF}^2 / (2\bar{d}) \quad \text{and} \quad t_{Br} = V_{EF} / \bar{d} \quad (16.31)$$

where \bar{d} may have the same values as in Eq. (16.28).

16.8.5 Critical or Balanced Field Length

The concept of *balanced field length* is of concern when one of the engines of a twin-engine (or multiple-engine) aircraft fails during the ground run of a takeoff. It is shown in Fig. 16.10 that the engine failure takeoff distance $x_{To,EF}$ is generally not equal to the acceleration-and-stop distance x_{AS} . If V_{EFR} reduces due to reduction in engine failure airspeed V_{EF} , the $x_{To,EF}$ would increase due to reduction in the rate of climb, and x_{AS} would decrease because it is easier to stop a slower-moving aircraft. Therefore, it is possible to obtain V_{EFR} at which $x_{To,EF} = x_{AS}$, and this length is called the *critical (or balanced) field length* which is denoted by x_{CFL} , as shown in Fig. 16.12. The corresponding value of the V_{EFR} is called the *critical engine failure recognition airspeed* which is denoted by V_{CEFR} . The x_{CFL} is generally about 15% in excess of the takeoff distance x_{To} of the all engines-operative aircraft.

In case V_{EFR} is less than V_{CEFR} , the flight has to be aborted, otherwise for the case $V_{EFR} > V_{CEFR}$ the flight has to be continued. If $V_{EFR} = V_{CEFR}$, the pilot has both options, either to continue or abort the flight.

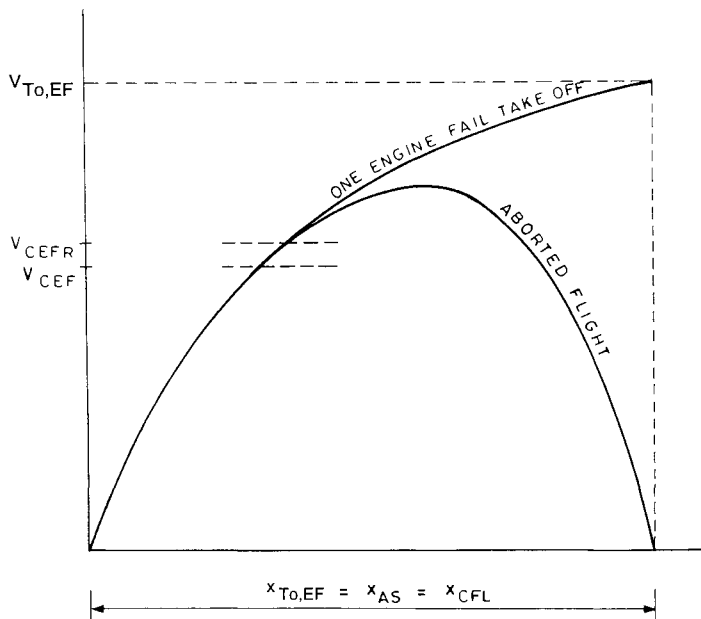


Fig. 16.12 Critical (or balanced) field length, x_{CFL} .

16.9 Effects of Wind, Runway Slope, Temperature, and Altitude

The atmospheric changes and runway slope have appreciable influence on the distance and duration of ground roll. These effects are taken into account during takeoff and landing.

16.9.1 Effect of Wind

The effect of wind on the ground roll distance of takeoff flight can be calculated by noting that the airspeed V_{Lo} appearing in Eqs. (16.12) and (16.13) is strictly the ground speed $V_{g,Lo}$ of the aircraft at the liftoff position when there is no wind. Equations (16.12) and (16.13), respectively, are written as

$$x_g = V_{g,Lo}^2 / (2\bar{a}) \quad \text{and} \quad t_g = V_{g,Lo} / \bar{a} \quad (16.32)$$

Let $x_{g,w}$ and $t_{g,w}$ denote the takeoff ground roll distance and time, respectively, in the presence of wind that is moving parallel to the runway with velocity V_w . The above two relations in the presence of wind are written, respectively, as

$$x_{g,w} = (V_{Lo} \mp V_w)^2 / (2\bar{a}) \quad \text{and} \quad t_{g,w} = (V_{Lo} \mp V_w) / \bar{a} \quad (16.33)$$

where negative and positive signs denote headwinds and tailwinds, respectively, and the average acceleration \bar{a} remains the same as in the case of no wind. From Eqs. (16.32) and (16.33), it can be written that

$$\frac{x_{g,w}}{x_g} = \frac{V_{Lo}^2}{V_{g,Lo}^2} \left(1 \mp \frac{V_w}{V_{Lo}} \right)^2 \quad \text{and} \quad \frac{t_{g,w}}{t_g} = \frac{V_{Lo}}{V_{g,Lo}} \left(1 \mp \frac{V_w}{V_{Lo}} \right)$$

Since the liftoff airspeed is a specified constant for a given temperature and pressure, it follows that $V_{Lo} = V_{g,Lo}$, and the above equations become, respectively,

$$x_{g,W}/x_g = (1 \mp V_W/V_{Lo})^2 \quad \text{and} \quad t_{g,W}/t_g = (1 \mp V_W/V_{Lo})$$

Assuming that V_W is much less than V_{Lo} , the first relation above can be written as

$$x_{g,W}/x_g = 1 \mp 2V_W/V_{Lo}$$

This shows that a headwind reduces both the distance $x_{g,W}$ and the duration $t_{g,W}$ of the takeoff as compared to the no-wind case, and vice versa in the case of a tailwind.

Now using relation (16.28) and proceeding in the same way as above, the distance $x_{g,La,W}$ and the time $t_{g,La,W}$ of the ground roll during the landing phase in the presence of wind can be calculated by the following two relations, respectively,

$$x_{g,La,W}/x_{g,La} = 1 \mp V_W/V_{Td} \quad \text{and} \quad t_{g,La,W}/t_{g,La} = 1 \mp V_W/V_{Td}$$

where the negative sign is for the headwind and the positive sign is for the tailwind. It must be recalled that the wind is assumed to be moving parallel to the straight flight path. If the wind velocity is slightly inclined to the flight path, V_W will be the component of the wind velocity along the flight path. If the wind velocity vector is considerably inclined to the flight path, the corresponding treatment of the wind effect is not considered here.

16.9.2 Effect of Runway Slope

Considering the downward slope θ as positive, it will increase the acceleration by $g \sin \theta$ and the forward force by $W \sin \theta$. The ground roll distance and time are denoted by $x_{g,slope}$ and $t_{g,slope}$, respectively, when a runway slope is present. They are obtained from Eq. (16.32) as

$$x_{g,slope} = \frac{V_{g,Lo}^2}{2(\bar{a} + g \sin \theta)} \quad \text{and} \quad t_{g,slope} = \frac{V_{g,Lo}}{\bar{a} + g \sin \theta} \quad (16.34)$$

From Eqs. (16.32) and (16.34), we can write

$$x_{g,slope}/x_g = \{1 + (g/\bar{a}) \sin \theta\}^{-1} \quad \text{and} \quad t_{g,slope}/t_g = \{1 + (g/\bar{a}) \sin \theta\}^{-1} \quad (16.35)$$

which shows that both the ground roll and its time are decreased by a positive slope (downhill) and increased by a negative slope (uphill). If \bar{a} is obtained from Eq. (16.32) and is substituted in the corresponding relation of Eq. (16.35), the ratios of the ground runs and their times can also be written as

$$\frac{x_{g,slope}}{x_g} = \left(1 + \frac{2gx_g \sin \theta}{V_{g,Lo}^2}\right)^{-1} \quad \text{and} \quad \frac{t_{g,slope}}{t_g} = \left(1 + \frac{gt_g \sin \theta}{V_{g,Lo}}\right)^{-1}$$

16.9.3 Effect of Temperature and Altitude

The effects of temperature and altitude on the takeoff run distance are felt because these factors change the air density. The increase in ambient temperature, or altitude, decreases the ambient air density and increases the value of the liftoff airspeed. The decrease in air density causes a reduction in the thrust force of the engine, which decreases the acceleration, and consequently the takeoff ground roll distance of the aircraft is increased. The increase in liftoff airspeed also increases the takeoff ground roll distance. The lift force on the aircraft is directly proportional to the air density.

A rule of thumb can be obtained for density altitude below 1600 m, which gives the percentage increase of climb distance for each 100 m rise in altitude. There is approximately a 1% increase in climb distance for reciprocating engine aircraft, a 2.3% increase for a turbojet engine aircraft with high thrust/weight ratio, and a 3.4% increase for a turbojet engine aircraft with low thrust/weight ratio. A turbojet aircraft is more sensitive to density change as compared to a reciprocating engine aircraft.

The aircraft manufacturer is required to supply data on the effects of aircraft weight, airfield altitude, and ambient temperature on the performance of the aircraft during takeoff, climb, and landing. This information is generally provided for airfield altitude up to 3000 m and temperature up to 50°C by means of standard curves called the WAT curves; the abbreviation WAT stands for weight, altitude, and temperature. These curves help the pilot to determine the payload for safe operation of the aircraft.

References

¹Federal Aviation Regulations; Part 25—Airworthiness Standards: Normal, Utility, and Aerobatic Category Airplanes, U.S. Federal Aviation Administration.

²Grover, J. H. H., *Handbook of Aircraft Performance*, Blackwell Science, Osney Mead, England, UK, 1989.

³Williams, J., “Airfield Performance Prediction Methods for Transport and Combat Aircraft,” *Aircraft Performance-Prediction Methods and Optimization*, Advisory Group for Aeronautical Research and Development (AGARD) Lecture Ser. 56, 1972.

⁴Dole, C. E., *Flight Theory and Aerodynamics*, Wiley, New York, 1981.

⁵McCormick, B. W., *Aerodynamics, Aeronautics, and Flight Mechanics*, Wiley, New York, 1979.

⁶Torenbeek, E., *Synthesis of Subsonic Airplane Design*, Delft Univ., Delft, The Netherlands, 1976.

Problems

In the multiple choice problems below, mark the correct answer.

- 16.1** The liftoff distance of an aircraft is a) the same as the takeoff distance, b) the distance at which the front wheel is lifted from the ground, c) the distance at which both the front and rear wheels are lifted from the ground.

16.2 The length of runway required is a) the takeoff length, b) the liftoff length, c) the liftoff length plus a part of the airborne distance.

16.3 The length of runway required for a screen height of 10.7 m is the greater of the two distances: a) x_{RW} and $x_{RW,EF}$, b) x_{RW} and $1.15x_{RW,EF}$, c) $1.15x_{RW}$ and $x_{RW,EF}$.

16.4 The clearway a) extends beyond the stopway, b) is situated before the stopway, c) is the same as the stopway.

16.5 The takeoff length required is a) the same as the takeoff length, b) the same as the takeoff length with engine failure, c) none of these two answers is correct.

16.6 The takeoff length required for a screen height of 10.7 m is the greater of the two distances a) x_{To} and $1.15x_{To,EF}$, b) $1.15x_{To}$ and $x_{To,EF}$, c) x_{To} and $x_{To,EF}$.

16.7 The takeoff field length is a) the same as the takeoff distance required, b) the greater of the distances $x_{To,EF}$ and x_{AS} , c) the greatest of the distances $1.15x_{To}$, $x_{To,EF}$, and x_{AS} .

16.8 The landing distance is the same as the a) ground roll distance during landing, b) ground roll distance plus a part of the airborne distance from screen height, c) ground roll distance plus the airborne distance from screen height.

16.9 Minimum control airspeed of an aircraft is a) the same as the stalling airspeed, b) the same as the liftoff airspeed, c) none of these two airspeeds.

16.10 The decision airspeed is the same airspeed at which a) the pilot decides to liftoff, b) the pilot decides to liftoff after an engine failure, c) the critical engine failure airspeed is recognized.

16.11 The takeoff rotation airspeed is generally equal to about a) $1.1V_S$, b) $1.2V_S$, c) $1.3V_S$.

16.12 The takeoff safety airspeed in the case of engine failure, as compared to the case of all-engine operative, is a) greater, b) less, c) equal.

16.13 The unstick airspeed is the same as the a) rotation airspeed, b) liftoff airspeed, c) minimum-control airspeed.

16.14 The threshold airspeed is the same as the a) touchdown airspeed, b) airspeed at the screen height during landing, c) liftoff airspeed.

16.15 Which of the following statements is correct? a) $V_{MC,Ab} > 1.3V_S$, b) $V_{MC,g} < V_{CEFR}$, c) $V_2 > V_3$.

16.16 The coefficient of braking friction a) is the same as the coefficient of rolling friction, b) is the same as the coefficient of sliding friction, c) lies between sliding and rolling frictions.

16.17 For a given aircraft rolling on the ground, the braking friction will a) be more if lift is more, b) be more if lift is less, c) have no effect on lift.

16.18 During the rotation segment, the aircraft rotates about the a) center of gravity of the aircraft, b) rear wheels of the aircraft, c) center of pressure of the aircraft.

16.19 For an aircraft rolling on the ground with a specified thrust, the acceleration a) will be more if lift is more, b) will be more if lift is less, c) is not affected by lift.

16.20 For a given aircraft, the increase in gravitational force will a) increase the rolling distance, b) decrease the rolling distance, c) have no effect on rolling distance.

16.21 The takeoff time of a large modern transport aircraft is generally about a) 1 min, b) 3 min, c) 5 min.

16.22 The average acceleration of a large transport aircraft is generally about a) 2 m/s^2 , b) 4 m/s^2 , c) 8 m/s^2 .

16.23 Give a brief summary of the various retardation devices that are commonly employed.

16.24 As soon as an engine fails during takeoff ground roll, a) the aircraft starts decelerating, b) the aircraft first accelerates and then decelerates, c) the airspeed is first constant and then decreases.

16.25 In a balanced field length a) the takeoff distance is equal to the landing distance, b) the takeoff distance is equal to the acceleration-and-stop distance, c) the takeoff distance with engine failure is equal to the acceleration-and-stop distance.

16.26 Headwinds a) increase the takeoff distance, b) decrease the takeoff distance, c) have no effect on the takeoff distance.

16.27 Headwinds a) increase the landing distance, b) decrease the landing distance, c) have no effect on the landing distance.

16.28 A downhill slope a) increases the landing distance, b) decreases the landing distance, c) has no effect on the landing distance.

16.29 On cooler days the takeoff distance is a) reduced, b) increased, c) not affected.

16.30 The takeoff distance of an aircraft at higher altitudes, as compared to that at sea level a) is reduced, b) increases, c) is unchanged.

16.31 An aircraft is accelerated uniformly during ground roll with an acceleration of $0.2g$ until the rotation airspeed of 250 km/h is reached. Find the ground roll

distance. Find the percentage increase in the ground roll distance if the rotation airspeed is increased by 10%.

16.32 Write the equations of motion of an aircraft during its ground roll in takeoff when the thrust vector is inclined at an angle ϵ with the flight path and the runway has a downhill slope of θ deg.

16.33 For Aircraft A, whose specifications are given at the beginning of the Problems section in Chapter 8, the $V_R = V_{Lo} = 1.2V_S$, $C_{L,Lo} = 0.8C_{L,m}$, and the coefficient of braking friction during ground roll in the takeoff is $\mu = 0.02$. Assuming that the lift-dependent drag coefficient is reduced by 20% due to ground effect, calculate the ground roll distance and the takeoff time of the aircraft in the standard atmosphere at sea level.

16.34 Find the percentage change in the ground roll distance and takeoff time for the aircraft in Problem 16.33 if the location is at an altitude where the ambient pressure and temperature are 7900 N/m² and 1°C, respectively.

16.35 For the aircraft in Problem 16.33 whose x_g and t_g are calculated at sea level, also find the distances and times of the other segments of the takeoff phase. Assume that the aircraft reaches the climb angle of 5 deg with the airspeed $V_{Cl} = 1.3V_S$. Hence, calculate the total distance and time of the takeoff phase of the flight.

Aerobic Maneuvers and Flight Boundaries

17.1 Introduction

Acceleration or turning of an aircraft can be termed a *maneuver*. Maneuvers are an essential part of flying because no flight is possible without them. Coordinated turning in the horizontal plane, and turning in the vertical plane, as discussed in Chapters 11 and 15, are also maneuvers. There are several other types of maneuvers which constitute the subject matter of this chapter. Mathematical discussions of the various maneuvers explained in this chapter are difficult to comprehend and are beyond the scope of this book. Although many of these maneuvers are confidently performed by pilots, it appears that complete mathematical discussions of them may not be available in the literature.

Aerobatics refers to the spectacular flying and maneuvering of aircraft. Not all aircraft can perform all types of maneuvers. Aerobic and combat aircraft are specially designed to undertake many more maneuvers than are possible with other types of aircraft. All pilots are trained to make certain maneuvers, but this training is more intense for test and aerobatic pilots. Through aerobatics the pilots learn to obtain maximum performance from the aircraft while ensuring smoothness and coordination.

The airspeed and load factor are the two most important quantities in maneuvers. The load factor depends on the airspeed, and the curve of the load factor against airspeed defines the flight envelope. The boundaries of a flight envelope are limited by lift, structural strength, and maximum dynamic pressure. The upper limit of the load factor depends not only on the airframe but also on the pilot and other passengers of the aircraft. Whether the load factor is first limited by the physical limitation of the pilot, or by the structural limitation of the aircraft, depends on the pilot's capability of withstanding high g loads and the structural strength of the aircraft.

Safety has always been of paramount importance in flying. Prior to the start of flying for aerobic maneuvers, the pilot must ensure that there are no loose articles inside the cockpit or cabin. It is not uncommon for articles like pencils, clipboards, tools, etc. to be left in the cockpit or cabin by the last person who flew the aircraft or the maintenance engineers who worked on the aircraft. The region in which aerobic maneuvers are to be performed and the neighboring air space must be free of any other aircraft or birds. Aerobic maneuvers should not be performed over a city, town, or other area of human habitation. Safety reasons also demand that aerobatics should be performed at a safe altitude, say about 1000 m above the ground, for the pilot to have sufficient altitude to regain normal flight after any adverse occurrence. The pilot should be fully aware of all the instructions in the flight manual pertaining to the aircraft that he intends to fly.

The proper alignment for aerobatics requires the selection of a suitable reference line or reference point in space. Such a reference point can be a visible tall building, tall tree, road, river, or even a cloud. The horizon also makes a good reference

line. If such a reference point is not selected the correct shape of an aerobatic maneuver is likely to be missed. For example, a vertical loop might be performed in an inclined plane. Before conducting basic flight maneuvers a pilot is given training in air exercises by means of which he becomes proficient in performing the basic flight maneuvers.

17.2 Proficiency Flight Maneuvers

The flight training maneuvers and the related factors that are useful in developing a high degree of pilot skill are described here. These exercises are low-speed flying, steep turning, stalling, spinning, and recovery from unusual attitudes. The chandelle and the lazy 8 formations are also regarded as flight exercises because they provide training in coordinating the activities of control surfaces. Only a few of these exercises are briefly explained here. Although these maneuvers are not performed in everyday flying, the elements and principles involved in them are applicable to the pilot's performance of customary flight operations. They aid the pilot in developing a fine control touch, coordination, orientation, and division of attention between the inside and outside of the cockpit for accurate and safe maneuvering of the aircraft. They also help the pilot to analyze the effect of wind and other forces acting on the aircraft.

17.2.1 Flight Near Critically Low Airspeeds

A pilot is required to practice low-speed flying because the aircraft is controlled at very low airspeeds in many aerobatic maneuvers. Low-speed flying develops the pilot's confidence and ability to fly behind the power curve (region of reverse command) and to use sight, sound, and feel to recognize a hazardous situation from a close quarter. Since low-speed flying is performed close to stalling airspeed, the experience of low-speed flying helps the pilot to recognize when the aircraft is approaching stall. In low-speed flying the pilot assesses the margin of safety above the stalling speed by the diminishing response of the controls. The exercises of slow flights are conducted not only in level flights, but also in turning, climbing, and descending flights.

Low-speed flying has certain characteristic features. At low airspeeds the angle of attack is high, bringing the center of pressure (CP) and the center of gravity (CG, ahead of CP) closer, which weakens the normal nose-down tendency brought by the lift-weight couple. The high angle of attack obscures the view ahead, and increases the drag which in turn demands more power, of which an excess is generally not available at low speeds. The effectiveness of the control surfaces is reduced at low speeds and coarse (large) movements of these surfaces become necessary. In a piston-prop aircraft the slipstream effect of the propeller becomes more pronounced which produces yaw, which in turn is controlled by rudder deflection. This results in the aircraft being flown in a "crossed controls" condition to achieve balanced flight. Approaching toward stalling airspeed with crossed controls makes the aircraft vulnerable to a pronounced *emphatic* wing drop and possible entry into a spin.

Climbing at low airspeeds requires a higher lift coefficient and, therefore, higher drag and more engine power. A lesser amount of excess power is available at low airspeeds as can also be seen from the power required and power available curves of the aircraft. Power must be used when making turns at low airspeeds to prevent losing altitude.

Descent at low airspeeds can be made with or without power. In a power-on condition the descent at selected airspeed can be made by reducing the power and lowering attitude of the nose. Power-off condition or glide is only possible by adjusting the nose attitude.

17.2.2 Recoveries from Unusual Attitudes

In aerobatic maneuvers the aircraft may assume unusual attitudes, either intentionally or inadvertently. Pilots are trained to recover from such unusual situations. Attitudes involving unusually high or low pitch, with steep bank angles, are considered here.

When the aircraft nose is high and there is a steep bank angle, it is recommended to lower the nose by moving the control column forward, and increase the power smoothly. At the same time the wings should be rolled level by using the aileron and rudder. It is likely that the aircraft may be in the region of stall and so the application of the controls must be smooth, positive and prompt.

In the event that the aircraft has reached a vertical or near-vertical nose-up position with the airspeed being extremely low, *tail slide* may occur. In this situation, hold the control column and wait for the nose to drop of its own accord, or apply the rudder to encourage the nose to drop sideways. This will lead to diving from which recovery can be made in the usual way. In case the aircraft has inadvertently become inverted with insufficient airspeed for the ailerons to be effective, move the control column backward to lower the nose, and when sufficient airspeed has been attained a roll out to the upright position can be made.

The case where nose is low with a steep bank angle corresponds to a situation similar to spiral dive. In such cases, reduce the power to prevent excessive altitude loss or exceeding the speed limitation of the aircraft, and use the aileron and rudder to roll the wings level and then recover from the dive in the normal way.

17.2.3 Chandelle

The *chandelle* is a maximum-performance climbing turn commencing from straight and level flight and finishing when the aircraft has climbed to a certain altitude and turned through 180 deg as shown in Fig. 17.1. On the completion of the maneuver the wings of the aircraft should be level but the nose should be

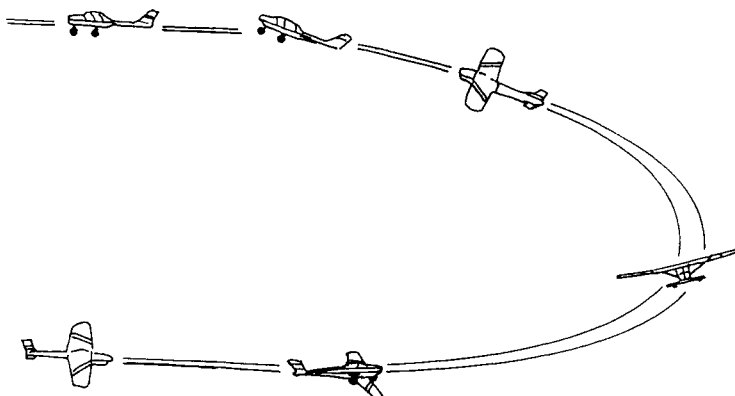


Fig. 17.1 Chandelle.

in a high-pitch attitude at the minimum controllable airspeed. It is not essential to use full power, but the power once selected, must not be adjusted. Generally, maximum continuous power (MCP) is initially selected, which is not changed during the maneuver.

The maneuver is started from level flight at the recommended entry airspeed when the bank is steadily applied and at the same time a steady climb is initiated. As an example, when the aircraft has turned through about 30 deg from the original heading, the bank angle has reached 30 deg, and the nose has acquired some positive attitude above the horizon. The bank angle continues to increase at the same steady rate, and also the pitch is increasing because of the smooth application of the back elevator pressure. When the aircraft has turned through 90 deg, the bank angle is at a maximum of about 60 deg; some books refer to a different bank angle at a 90 deg point turn. Soon afterward the bank is decreased at the same steady rate, until the aircraft completes the 180 deg turn, with the wings reaching the level position. All this time the nose is pitching up steadily so that when the wings are once again level, the nose is at the highest point, and the aircraft is flying at the minimum possible airspeed (about 5 kn above stall). The rate of turning at which the maneuver is flown is entirely up to the pilot, but the pitch and bank rates must correspond exactly with each other, with respect to the power selected initially. Coordinated flight is maintained throughout the maneuver.

17.2.4 Lazy 8

The flight path of a lazy 8 does not look like a figure 8, but when viewed from the top it traces the shape of an S over the ground; the end points of the S when extended appropriately would look like a figure 8. It is a precision coordination maneuver. It basically consists of two 180 deg turns in opposite directions while making a climb and descent in symmetric pattern during each of the 180 deg turns, as shown in Fig. 17.2. The wings will be in the horizontal plane only on the completion of each 180 deg change in the heading.

The maneuver is commenced from level flight at the recommended airspeed; any airspeed in excess of normal cruising speed is suitable for beginning the

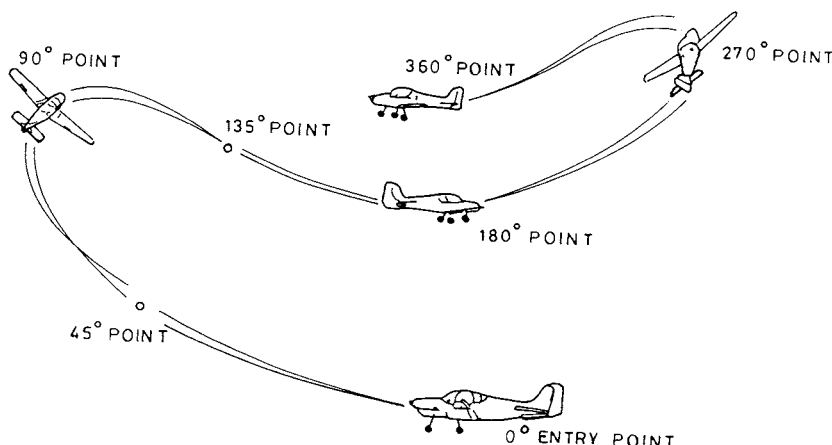


Fig. 17.2 Lazy 8.

maneuver. It starts as a coordinated climb turn where the wings are gradually banked and the climb is initiated. By the time the aircraft reaches the 45 deg point, the bank is reaching 15 deg and simultaneously the pitch is attaining its maximum, while the airspeed is decreasing. From the 45 deg point to the 90 deg point of the turn, the bank angle continues to increase, the pitch decreases, and the airspeed continues to decrease. At the 90 deg point of the turn, the bank angle is about 30 deg, pitch is level (zero), and the airspeed is at a minimum while the altitude is at a maximum. After reaching 90 deg point the aircraft makes a descending turn with a decreasing bank angle, the nose pitch lessening, and the airspeed increasing. When the aircraft has reached the 135 deg turn, the nose is at a maximum pitch down and the bank angle is about 15 deg. From the 135 deg point of the turn, the changes in the bank angle and the pitch attitude continue to be coordinated so that the aircraft arrives at the 180 deg point of the turn in level flight and at the airspeed that was used at the commencement of the lazy 8 maneuver. This completes half of the maneuver; when it is repeated in the opposite direction, the full maneuver has been performed. Throughout the maneuver, it may be necessary to control the rudder deflections so the aircraft is maintained in balance.

17.3 Basic Aerobatics

Rolls, loops, and turns constitute basic aerobatic maneuvers, and there can be different types in each category. Only some are described here in detail. Individual aircraft may have different flight characteristics, especially in relation to the effect of the rate and amount of control movements. This gives rise to subtle differences in the techniques that are generally acceptable to achieve the same result. Therefore, it becomes difficult to specify in detail exactly how an aerobatic maneuver can best be performed when speaking about all aircraft types.

17.3.1 *The Slow Roll*

In a slow roll maneuver, the aircraft turns around its longitudinal axis through 360 deg while in level flight, as shown in Fig. 17.3. The rolling is carried out at a speed that is a good margin above the stalling airspeed, and at a safe height. The higher the speed, the easier it is to control the roll and the less height is lost. The rate of roll depends on the amount of aileron control used, the speed at which the roll is started, and the type of aircraft.

At the recommended airspeed, apply the ailerons to commence roll in the required direction. In order to maintain a constant rate of roll and to keep the nose of the aircraft on the datum point, the use of the elevators and rudder is also required. The nose of the aircraft is held close to the reference axis. During one complete rotation, the wings are in the vertical position twice, and the aircraft is in the inverted position once.

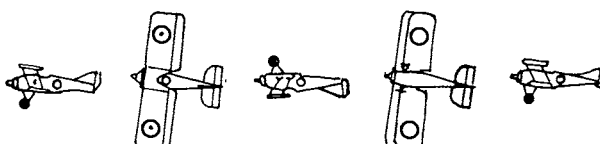


Fig. 17.3 Slow roll.

As the wings approach the vertical position, there is a tendency for the nose to drop, so the rudder movement is required to retard the downward movement of the nose; any fore or aft movement of the control column will only take the nose away from the datum point. As the aircraft approaches the inverted position, the rudder becomes ineffective in reducing the tendency of the nose to drop, and so the elevators are deployed to keep the nose up in the correct position. During the inverted position, the pilot feels negative g and his weight is transferred to the shoulder straps. In order to reduce the loss of height in inverted flight due to lesser lift, the angle of attack has to be higher, i.e., the nose has to be higher in relation to the horizon.

A shallow dive may be necessary to obtain the recommended entry, following which the nose of the aircraft is raised to the rotation point. With practice the roll can be done without raising the nose, and constant height and direction can be maintained throughout the maneuver.

17.3.2 Loop

In the loop the aircraft starts from a straight and level attitude, and returns to it after having flown through 360 deg turn in a circular path in the vertical plane as shown in Fig. 17.4. Throughout the loop the wings are kept laterally level, the aircraft remains in balance, and a positive load factor is maintained which varies in amount depending on the position at the loop. The minimum airspeed necessary at the start of the loop depends on the airspeed lost in the first half of the maneuver and that required to maintain maximum control at the top of the loop.

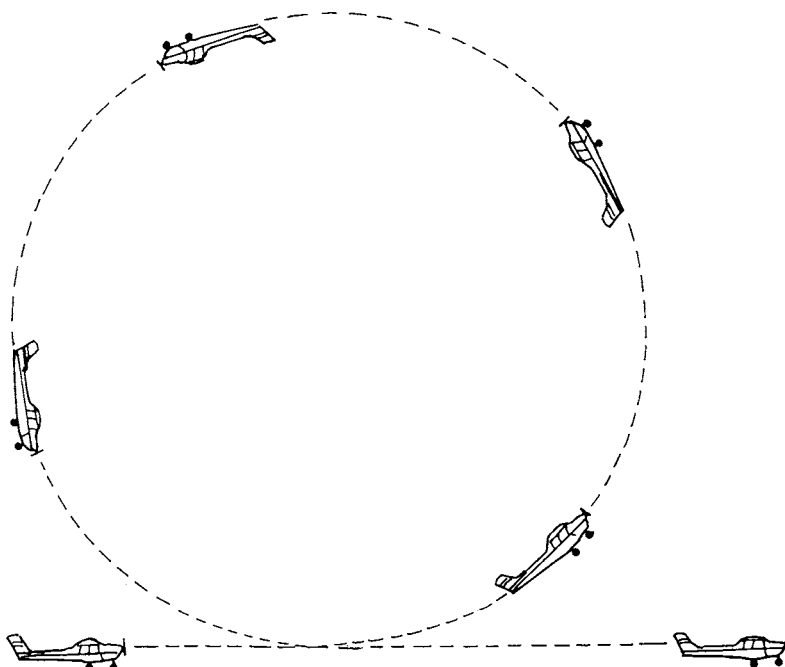


Fig. 17.4 Loop.

The loop formation is started at the recommended airspeed of straight and level flight by gently raising the nose of the aircraft by the movement of the control column, and maintaining a constant rate of pitch throughout the loop. Coordination of all control movements, including the throttle, is an essential part of the maneuver. During the whole of the maneuver the rudder is used to prevent any yaw. At the top of the loop the aircraft will be in an inverted position at low speed, so the care should be taken that the aircraft does not stall.

A positive load factor is maintained throughout the loop, which varies in amount depending on the position at the loop. The accelerometer will also read differently at different positions of the loop, although the centripetal force remains constant. As an example, consider that $3g$ centripetal acceleration is maintained throughout the loop as shown in Fig. 17.4. The accelerometer will read $3g$ on the sides of the loop, $2g$ at the top of the loop, and $4g$ at the bottom of the loop because in level flight the wings must produce an extra $1g$ lift to balance the weight. At the top of the loop, the gravitational force acting vertically down supplies the additional g unit to make up for the total acceleration, while the accelerometer reading of $2g$ shows only the loading on the wings.

A circular loop where the pilot always remains inside the loop is explained above. There can, however, be loops of different shapes, such as nearly square, rectangular, octagonal, etc. It is also possible to form a loop where the pilot remains outside the loop throughout.

17.3.3 Stall Turn

The stall turn consists of bringing the aircraft to a vertical attitude, then using the rudder to yaw through 180 deg about the normal axis, as shown in Fig. 17.5. When the aircraft is climbing vertically up it is cartwheeled sideways until it is pointing vertically downward, following which it is eased out of the dive and returns to straight level flight.

The maneuver is started at the recommended airspeed by making a firm and positive pullup for the vertical climb attitude, and full power is applied while climbing. As the aircraft approaches the vertical, the airspeed will have become very low, the use of rudder is required to maintain a balanced condition, and the aileron is required to keep the wings literally level. After the aircraft attains the vertical altitude, the rudder is applied to cartwheel the aircraft (to the right in Fig. 17.5) through 180 deg turn. In a good turn the aircraft should not get into a partially inverted attitude during the cartwheel stage.

As the nose drops down toward the vertical, start applying the opposite rudder to check the swing and to ensure that the aircraft points straight down. When the vertically down attitude is achieved, raise the nose up in pitching plane toward the horizon. When the nose passes through the horizon, gradually increase the power and return to level flight.

17.3.4 The Roll-Off-the-Top of a Loop

The maneuver of the roll-off-the-top of a loop consists of a half roll-off-the-top of a half loop as shown in Fig. 17.6. That is, the aircraft in the first half makes a semiloop which inverts the aircraft, and during the second half it rolls-off from the inverted section of the loop into the erect flight attitude. The maneuver involves a gain in altitude from the point of entry and reverses the direction of aircraft by turning it 180 deg. In order to maintain the best possible aileron effectiveness

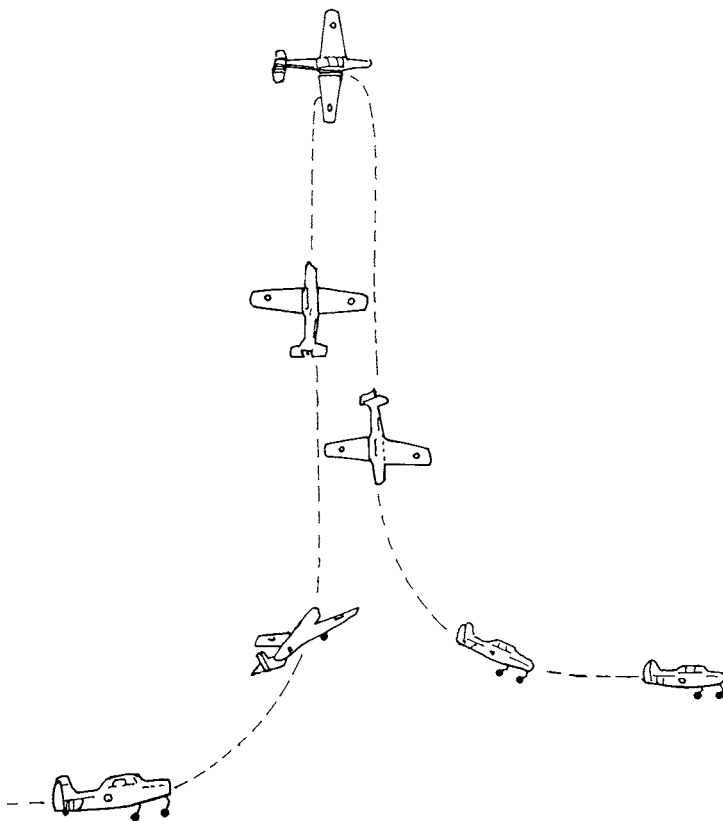


Fig. 17.5 Stall turn.

throughout the period of roll, it is necessary to use a higher entry speed than that required for the complete circular loop.

Once the entry speed has been achieved, which is about 15–20 kn (28–37 km/h) higher than that used for the complete loop, a positive pullup is initiated and the throttle is opened to the maximum allowable limit. A fairly tight looping must be attempted so that the airspeed at the top of the loop is sufficient to allow a good aileron effectiveness for the rolling section. When the aircraft approaches the inverted attitude and the nose is close to about 30 deg above the horizon, any further loop formation is arrested by suitably moving the elevators with the help of the control column. After arresting the loop, commence the rolling either to the left or to the right, as desired.

The airspeed during the rolling section is generally very low, and full aileron deflection may be required to maintain the rate of roll that at best will be rather slow. Throughout the rolling stage the controls should be used in the same manner as required for the second half of a slow roll.

17.3.5 Snap Roll

In the *snap roll* the aircraft rotates very quickly about its longitudinal axis. It is also known as a *flick roll*. In a one-turn snap roll (Fig. 17.7), the aircraft rotates

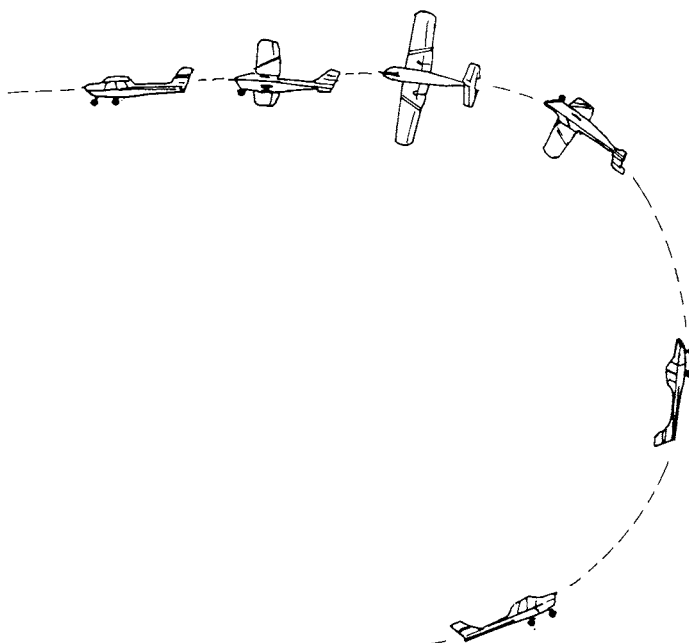


Fig. 17.6 Roll-off-the-top of a loop.

360 deg in about 3–4 s from the start to the finish. It can be regarded as a one-turn spin in horizontal flight. The snap roll generates autorotation over which the pilot has a certain degree of control. Having initiated the snap roll by rapid application of the rudder, it will normally continue of its own accord until the pilot stops it, or it falls into a spin.

The rate of rotation depends on the type of aircraft and the airspeed of entry into the maneuver. Due to high stresses being imposed during the maneuver, it is necessary not to exceed the recommended entry airspeed. The recommended entry airspeed in this case is lower than the maneuver airspeed because the maneuver is initiated with the aircraft in a nose-high attitude of about 15 deg above the horizon; this initial positive pitch attitude helps to reduce the tendency of the nose of the aircraft to drop too low during the recovery stage.

At the recommended entry airspeed the aircraft is stalled at higher than the normal stalling airspeed, i.e., it is an accelerated stall achieved by pulling the nose above the horizon. An imbalance of lift is created when the rudder is fully deflected

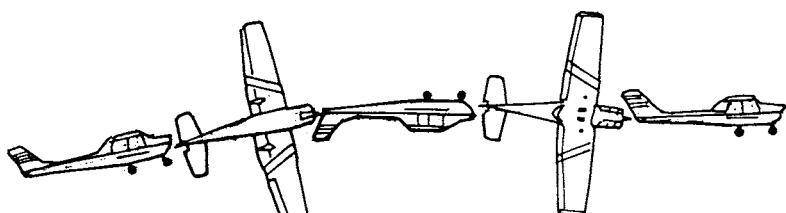


Fig. 17.7 Snap roll.

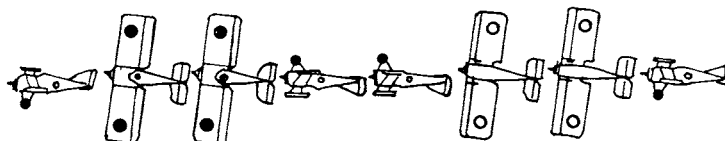


Fig. 17.8 Hesitation rolls.

in the desired direction as the stall is introduced. The result is rapid rotation in the direction of the application of the rudder. In some aircraft, however, the ailerons may be used to assist the rolling caused by the action of rudder. When the aircraft has passed the inverted position and is approaching about three-quarters of the roll (about 270 deg), recovery is initiated by applying full opposite rudder and moving the control column sharply forward. The roll is stopped and all three controls can be used in the normal way to reestablish straight and level flight.

17.3.6 *Hesitation Rolls*

The different hesitation rolls are a variation of the basic slow roll where the roll is temporarily halted at different points during the roll. In four-point roll, the aircraft pauses after every 90 deg of turn during the roll as shown in Fig. 17.8. In an eight-point roll, the aircraft pauses after every 45 deg of turn during the roll. Similarly, there can be 3-, 6-, 12-, 16-, and 32-point rolls. The rolls up to 12-point are quite common, and the rolls belonging to the 32-point hesitation roll can be confused with a shaky roll. The technique of performing a hesitation roll is the same as with the slow roll, except that the aircraft pauses at different intervals. Because of these pauses, the overall roll takes longer to complete and more airspeed is needed to start the roll.

17.3.7 *Several Other Maneuvers*

There are several other basic maneuvers, such as cuban 8, half cuban 8, reverse half cuban 8, barrel roll, aileron roll, etc. as discussed by Campbell and Tempest.¹ The *cuban 8* consists of the figure 8 extended horizontally in the vertical plane, as shown in Fig. 17.9. In a *barrel roll*, the aircraft describes a helical flight path

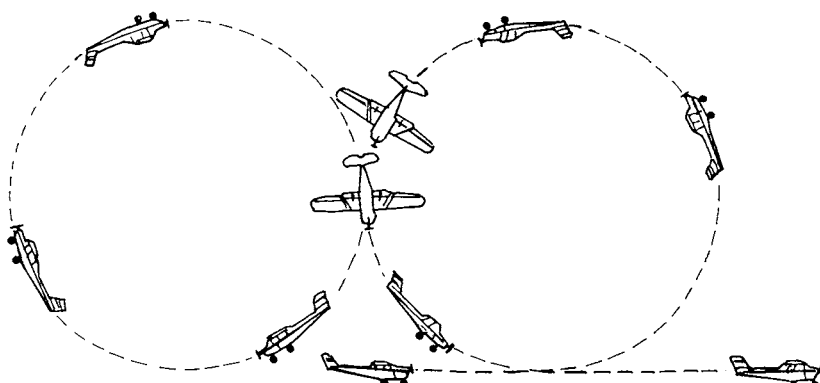


Fig. 17.9 Cuban 8.

around the outside of an imaginary barrel, and the aircraft rolls through 360 deg about an axis that is on one side of the aircraft. The *aileron roll* consists of a 360 deg roll about the longitudinal axis and is performed by using all three controls with the ailerons being the primary control throughout.

Certain maneuvers such as snaking, Dutch roll, phugoid, short-period oscillations, etc. are usually associated with the stability characteristics of an aircraft.

Several advanced aerobaticssuch as fractions of flicks, lomcovaks, tail slide, torque rolls, knife flight, bridges, advanced spinning, falling leaf, etc. are described by Williams.² The number of different aerobatics is very large, and about 100,000 different maneuvers have been reported. There exist endless possibilities for combining different maneuvers.

17.4 Flight Boundaries

A maneuvering flight may be limited by the aerodynamic lift, structural strength of the aircraft, or by the physical considerations of the pilot. These cases are specified by the load factor, which also depends on the airspeed of the aircraft.

17.4.1 Airspeed-Load Factor Boundaries

The airspeed is generally limited by the stalling or buffeting of the aircraft. The airspeed V depends on the load factor n , hence the limits of airspeeds are commonly expressed by V - n diagram, which is also called V - g diagram, where g is acceleration due to gravity. It is worth mentioning here that n is often stated in terms of g ; e.g., $n = 2$ is often stated as $2g$. A typical V - n diagram is shown in Fig. 17.10. Such a diagram is valid for a specified weight and configuration of the aircraft. It is also assumed that the loading is symmetric, because when asymmetric loading exists, as in rolling, the structural strength limitations are considerably reduced. Figure 17.10 also depends on altitude, but the dependence can be eliminated by representing the horizontal axis by the equivalent airspeed, rather than by its true airspeed. The V - n diagram, however, does not contain the thrust capability of the aircraft.

The curves in Fig. 17.10 can be classified as due to lift boundary limitation, structural limitation, and the never-exceed airspeed limitation or maximum dynamic pressure limitation, as explained below.

17.4.1.1 Lift boundary limitation. The lift boundaries of the V - n diagram shown in Fig. 17.10 are the curves DE, EF, and FA. The flights below the curve DE, left to the curve EF, and above the curve FA are not possible because of stall where the maximum lift coefficient is achieved. If the stall is at higher airspeeds, usually buffeting sets in much before the stalling angle is reached, and the flight is limited by buffeting. In Fig. 17.10 the point F is at $n = 1$, the corresponding airspeed $V_S = 240$ km/h is the stalling airspeed below which straight level flight is not possible. The stalling airspeed increases with the increase in load factor which is represented by the curves FA and ED for positive and negative load factors, respectively. Every point along the lift boundary represents the condition of maximum lift coefficient $C_{L,m}$, or the maximum angle of attack; if the lift boundary is due to buffeting, the usable maximum lift coefficient is less than $C_{L,m}$. The stalling angle and the maximum lift coefficient in accelerated flight, in an aircraft of specified configuration, are the same as in unaccelerated flight.

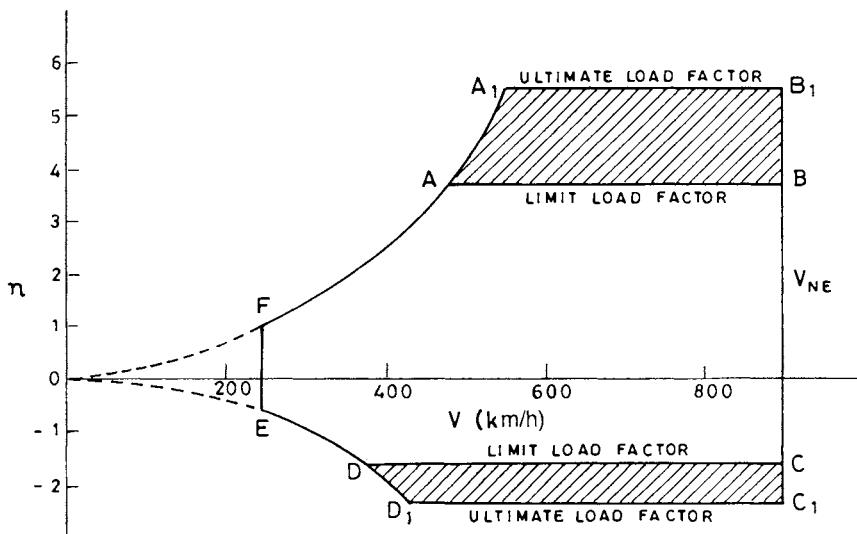


Fig. 17.10 *V-n* Diagram.

17.4.1.2 Structural limitation. The load on an aircraft of specified weight increases with the increase in load factor. An aircraft structure can withstand only a certain maximum load. This maximum load can be based either on the permanent damage (deformation) to the structure, or the structural failure of the aircraft. The *limit load factor* is defined as the load factor that, if exceeded, may result in permanent structural deformation; it is shown in Fig. 17.10 by the lines AB and DC for positive and negative load factors, respectively. The *ultimate load factor* is defined as the load factor that, if exceeded, may lead to structural failure; it is shown in the figure by the lines A₁B₁ and D₁C₁ for positive and negative load factors, respectively. The ultimate load factor is about 1.5 times the limit load factor. Defining the ultimate load factor should not be considered as an invitation to exceed the limit load factor during maneuvers.

In practice, high negative loadings are generally rare due to pilot discomfort in the abnormal attitudes required to achieve them, and because of this, the aircraft need not be designed to withstand negative load factors to the same extent as is necessary with positive load factors.

For the positive load factors, the structural limit line AB and the lift boundary FA meet at the corner point A. The airspeed at the corner point is called the *maneuver speed* or the *corner speed*, which is usually represented by the symbol V_A . This is the maximum airspeed at which the pilot can perform extreme control movements involving the full deflection of the control surfaces without causing structural overloads. At airspeeds higher than V_A , maximum control deflections in excess of the structural limitations should not be used. Similarly, the airspeed V_D , at the other corner point D, is the maneuver speed for the negative load factor.

17.4.1.3 Never-exceed airspeed limitation (maximum dynamic pressure). The airspeed at which the vertical line BC is drawn is called the *never-exceed airspeed* which is commonly denoted by the symbol V_{NE} . It is also called the *red line airspeed* because the airspeed indicator is marked with a red line at the never-exceed airspeed. Increasing the airspeed beyond V_{NE} may result into

structural failure or aerodynamic instability. Since it is actually the dynamic pressure that determines the structural loading, V_{NE} for high-speed aircraft is often specified as a function of altitude, or is expressed as calibrated airspeed rather than as true airspeed. For the same reason, the V_{NE} often replaced by the corresponding maximum dynamic pressure that the aircraft can withstand.

There are both advantages and disadvantages to increase the dynamic pressure limit of an aircraft. An aircraft having high dynamic pressure can penetrate an enemy's defences at low altitudes and high airspeeds and avoid early radar detection; this means that the aircraft has more survivability. Also the aircraft that can withstand high dynamic pressure can operate in regions (altitude and airspeed) that may not be possible for an aircraft with low-dynamic pressure. The main disadvantage is that increasing the dynamic pressure limit of the aircraft at the design stage significantly increases the structural and propulsion weights of the aircraft, and thus reduce its performance by increasing the takeoff weight.

17.4.2 *Human Limitation*

An increase in the load factor, due to acceleration in maneuvering flights, causes stresses in the nervous systems of the pilot and other passengers. This has adverse effects on blood circulation that can be tolerated up to certain limits for short duration. It can cause disorientation, head pains, respiratory distress, "greyout" or "spots before the eyes," blackout (loss of vision), and even unconsciousness, if the maneuver is prolonged for a longer time. Positive g maneuvers cause flow of blood away from the brain to the lower parts of the body, resulting in the loss of oxygen from the brain, and consequently in "blacking out" and eventually in unconsciousness; blackout normally occurs when n is between 4.5 and 5. Negative g maneuvers force blood in the head, resulting in "reddish" visual indications and eventually in unconsciousness, if the maneuver is prolonged for a few seconds; this may occur when n is about -4.

The bank angle of civil transport aircraft in normal service does not usually exceed 30 deg, for which $n = 1.15$, and thus passengers do not feel lateral acceleration, except in emergencies. Military pilots are generally more tolerant of g stresses than the passengers or pilots of a civil aircraft. Military pilots flying combat aircraft wear anti- g suits (also referred to as g suits) so that they can sustain load factors up to about 8 without blacking out. Centrifuge studies have revealed that the human body can withstand accelerations up to 12 g for 2–3 s, primarily due to the natural flexibility of the body organs and the inertial delay in the movement of blood away from the brain.

It may happen that the pilot can withstand greater g loads than his aircraft, or vice versa. If the pilot can withstand greater g loads than his aircraft, he must always be aware not to exceed the aircraft limitations. On the other hand, if the aircraft can withstand greater g loads than the pilot, the pilot must be conscious of the possibility of greyout or blackout while moving the aircraft closer to flight boundaries. It should also be kept in mind that although the pilot can withstand very high g loads for a brief interval of time, the aircraft structure cannot, and if more than limiting load factor is applied even for a shortest moment of time, the airframe would have been exposed to the damaging load factor.

17.5 *Sustained Turn Performance and Agility*

Sustained turn and agility are two quite different terms of significance in judging the capability of a combat aircraft.

17.5.1 *Sustained Turn Performance*

A combat aircraft in air-to-air battle must remain within its maximum airspeed and altitude limits; i.e., the maneuvering must be conducted within the maximum energy levels attainable and preferably without a loss of energy during the maneuver. It is here that the sustained turn performance assumes importance.

The *sustained turn* is the performance at the point where the thrust is equal to drag in a level turn at a specified power setting (usually military or maximum power). In another words, it is a stabilized turn at constant airspeed and constant altitude without loss of energy ($P_S = 0$). The sustained turning performance may be lift limited, structurally limited, or thrust limited, depending on the aerodynamic design, structural strength, and thrust capability of the aircraft. Unlike the $V-n$ diagram, the sustained turning performance includes the thrust capability of the aircraft.

17.5.2 *Agility*

The concept of agility is of recent origin. It is derived from the word *agile* whose dictionary meanings are swift, active, light, and quick in motion. Attempts have been made to clearly define the agility of an aircraft so that it can be quantified for the purposes of design, testing, and operation.

Agility is considered different from maneuverability. *Maneuverability* is the ability of an aircraft to change altitude, airspeed, or direction in any combination, whereas *agility* is the aircraft's ability to shift from one maneuver to another. Agility is inversely proportional to the time required for transition from one maneuver to another.

In measuring agility, the emphasis is on time. By means of agility, one seeks to minimize the time required to achieve some desired outcome. It is said that agility is the ability to shift from one unfolding pattern of actions and ideas to another by being able to transition from one orientation to another. These definitions of agility broaden the concept of agility that can be applied not only to the airframe but also to the pilot, weapon, or to any other element. Thus, there can be airframe agility, pilot agility, weapon agility, etc. Airframe agility depends on the airframe's ability to change from one maneuver to another. Pilot agility depends on the pilot's ability to observe, orient, decide, and act. Weapon agility depends on the weapon's ability to orient, launch, and adopt a right course toward the target.

References

¹Campbell, R. D., and Tempest, B., *Basic Aerobatics*, Granada, England, UK, 1984.

²Williams, N., *Aerobatics*, Airlife, Shrewsbury, England, UK, 1989.

Problems

In the multiple choice problems below, mark the correct answer.

17.1 What are the precautions necessary before starting a maneuver?

17.2 Why it is important to select a reference line or reference point before starting a maneuver?

17.3 The tendency for nose drop in inverted flight as compared to normal flight is a) less, b) the same, c) more.

17.4 In aerobatic maneuvers the rudder is used for a) yaw only, b) yaw and pitch only, c) yaw, pitch, and roll.

17.5 Discuss the problems associated with low-speed flying.

17.6 The chandelle is a 180 deg turn where the altitude of the aircraft is a) the same at the entry as at the exit, b) less at the entry than at the exit, c) more at the entry than at the exit.

17.7 The power during turn in the chandelle a) increases, b) remains constant, c) decreases.

17.8 During the lazy 8 maneuver the pitch is zero only a) once, b) three times, c) five times.

17.9 During the lazy 8 maneuver the airspeed a) first decreases up to the 45 deg turn, then increases up to 90 deg turn; b) first decreases up to the 90 deg turn, then increases up to 180 deg turn; c) first decreases up to 180 deg turn, then increases up to the completion of the turn at 360 deg.

17.10 An aircraft rolls due to the action of ailerons; why then in a slow roll is the rudder used?

17.11 During a circular loop formation, the load factor is a) always positive, b) positive only in certain sections of the loop, c) always negative.

17.12 To enter into the maneuver for roll-off-the-top of a loop, the airspeed, as compared to that required for entering into the complete circular loop, should be a) the same, b) lower, c) higher.

17.13 The snap roll is started by using a) ailerons only, b) rudder only, c) both ailerons and rudder.

17.14 The entry airspeed of a hesitation roll as compared to that of slow roll is a) less, b) more, c) equal.

17.15 What is the stall turn?

17.16 What are the dangers associated with the tail slide when the nose is vertically up?

17.17 Describe how to come out of a maneuver if the nose is too low with a steep bank angle.

17.18 Describe how to know if the wings are level when the aircraft is climbing vertically up.

17.19 Why does the angle of attack in the slow roll have to be higher during the inverted section of the flight?

17.20 During the lazy 8 maneuver the bank angle is zero only a) once, b) twice, c) three times.

17.21 The airspeed in the chandelle a) first increases and then decreases, b) decreases continuously throughout, c) remains constant.

17.22 The maximum pitch in the chandelle occurs at the a) 90 deg point of the turn, b) 135 deg point of the turn, c) 180 deg point of the turn.

17.23 Since circular loop formation in the vertical plane is primarily due to ailerons, why the rudder is also used?

17.24 In the roll-off-the-top of a loop, the rolling is arrested a) before the top of the loop, b) at the top of the loop, c) after the top of the loop.

17.25 In a snap roll the aircraft a) only rotates, b) moves in two dimensions only, c) moves in all three dimensions.

17.26 It is more stressful for the pilot to encounter an acceleration of a) $2g$, b) $-1g$, c) both $2g$ and $-1g$ are equally stressing.

17.27 What is the difference between spiral and spin of an aircraft?

17.28 What is the difference between power-on and power-off stalls?

17.29 Draw freehand the cuban 8, showing the attitudes of the aircraft at different sections from the start to the finish.

17.30 How do the forces on control surfaces during aerobatics performed by a piston-prop aircraft generally differ from those of a turbojet aircraft?

17.31 What differences will it make, as compared to powered flight, if a glider performs a loop in the vertical plane?

17.32 In inverted level flight, as compared to normal level flight, the position of the tail is a) well up, b) well down, c) the same in both cases.

17.33 Pushing the control column forward produces a) positive g , b) negative g , c) no change in g .

Performance Evaluation by Flight Tests

18.1 Introduction

The proof of the performance of an aircraft and its handling qualities finally rests with testing and estimating them by actually flying the aircraft. This is called *flight testing* and is carried out both for testing performance as well as for evaluating stability and control. The handling qualities of an aircraft form a part of its stability and control testing. The flight tests decide the success of the enormous efforts lasting several years that go into the design and production of an aircraft, starting from the conceptual stage. The computed and predicted characteristics during the design and production stages finally have to be evaluated by flight tests. These tests provide data on the actual characteristics of the aircraft, provide information for development, and supply data for further research. Flight testing is a necessary and integral part of aeronautical development. This chapter is limited to the performance testing of a given aircraft.

Flight tests are tailored so that the results can be obtained in minimum time and space with the least cost and effort. There may be further constraints for human resources and equipment. This leads to the designing of certain special flight test techniques and to developing the methods in which they are presented. The test aircraft and its flight crew are sufficient to collect all performance data by recording the basic flight parameters and engine parameters during the flight test maneuvers. However, they may use theory for establishing the correct parameters, for making instrument corrections, or for carrying out data reductions to standard forms. Existing performance theories help in grouping the performance variables for minimizing the flight tests and their presentation.

Performance testing is also not devoid of certain major problems. The measurement of actual flight parameters during the test may become difficult. This is because they depend on the nature of instruments (their accuracy, sensitivity, reliability, size, etc.), the atmosphere and weather conditions, and the effects of disturbances produced by the aircraft or the instrument on the quantity to be measured. It is also not always possible to fly exactly the same way as required for the test; e.g., near the stall or in the reverse command region. This calls for special piloting techniques.

Flight tests require the presentation of test data to some standard set of conditions. Every flight, even of the same aircraft with the same mission, may be different because of changing atmospheric and weather conditions. Flight tests can be used and compared provided the results are reduced to some commonly agreed-on standard conditions. This may require the use of differential methods that are made more reliable by scheduling the test values closer to the standard values so that the size of corrections can be kept at a minimum.

Among the different performance variables there are some, like rpm and pressure altitude, over which full control is possible during flight, to any predetermined value in the working range. There are certain variables, like airspeed and weight,

that can be adjusted in flight, but not exactly to any predetermined values. The atmospheric conditions, like temperature, density, and winds, are yet another class of variables over which there is hardly any control. This has required the need for the standard atmosphere. The weight of the aircraft is also often standardized, e.g., 95% of the takeoff weight of the test aircraft.

A flight test involves preflight preparation, in-flight techniques, and data reduction. A full discussion of these factors and the problems associated with them for each and every flight would require a separate book. This information presently exists in the form of reports and manuals.¹⁻³ This chapter very briefly explains some commonly used flight tests, the various quantities measured, and the methods of presentation of the results. The emphasis is on the performance testing of a jet aircraft unless otherwise stated. Readers are advised to review Chapter 6 and Secs. 3.8.1 and 4.3.6 before reading this chapter.

It should be kept in mind that flight tests are conducted for a given type of aircraft and the results are not generalized and then used for another type of aircraft. Each aircraft series is treated separately for the purpose of flight tests. For example, if a Boeing 747 is tested, the data and results obtained from the test are valid for all Boeing 747 aircraft if no modification is carried out.

18.2 Airspeed, Temperature, and Angle of Attack Calibrations

The *airspeed calibration* involves the calibration of the pitot-static tube, and the *temperature calibration* is the determination of the temperature probe recovery factor. Improper readings of airspeed and outside air temperature will render all performance data and most of the stability and control data worthless. Accurate temperature determination is required for true airspeed measurement, test data reduction, and measurement of engine control systems, fire control systems, etc. The importance of these calibrations should not be underestimated and, for this reason, calibration tests of the pitot-static and temperature systems comprise the first flights in any test program. The temperature probe calibration is generally done simultaneously with pitot-static calibration.

18.2.1 Pitot-Static Calibration Tests

The airspeed errors emerging from pitot-static system were explained in Sec. 6.6. A suitable location of the pitot-static system in the vicinity of the aircraft is important. Many different types of pitot-static systems exist which are classified primarily by the location of their mounting. Thus, there are fuselage-mounted systems, aircraft noseboom systems, and wingboom systems. A test aircraft usually uses the aircraft noseboom system.

Several different methods of pitot-static calibration tests exist.⁴ These can be listed as 1) the tower fly-by test, 2) the pacer test, 3) the speed course test, 4) the radar method, 5) the smoke trail method, 6) the trailing bomb method, and 7) the trailing cone method. Limited space prohibits elaborating on each of these methods here. The tower fly-by test is quite common because it is simple and requires no sophisticated equipment.⁵ The aircraft in the fly-by test is sighted through a theodolite from an elevated area such as the roof of a hangar, building, or a tower. In the pacer calibration method, the test aircraft is flown in formation with another aircraft whose instrument and position error calibrations are known. In the trailing bomb method, the static pressure of the pitot-static system of the

test aircraft is compared with the static pressure measured by a bomb-shaped body (trailing bomb) suspended on a long length of pressure tubing below the aircraft; the static pressure error of the trailing bomb itself, if it exists, can be calibrated in a wind tunnel.

18.2.2 Determination of Temperature Probe Recovery Factor

The theory that defines the temperature recovery factor is explained here first before describing the determination of temperature recovery factor. For an adiabatic flow process, the ratio of the total temperature to the static temperature is given by

$$T_0/T = 1 + (\gamma - 1)M^2/2$$

If the flow process is not adiabatic, the temperature recovery factor K_t can be introduced to modify the kinetic term so that the above relation becomes

$$T_0/T = 1 + K_t(\gamma - 1)M^2/2$$

In the case of an aircraft cruising at Mach number M in the air, $\gamma = 1.4$, the total temperature T_0 is the indicated temperature T_i of the temperature indicator which has been corrected for the instrument error, and T is the ambient air temperature. Therefore, the above relation for flight test can be written as

$$T_i/T = 1 + K_t M^2/5 \quad (18.1)$$

To find K_t it is necessary to know T , T_i , and M . The value of the ambient air temperature T can be obtained from a pacer aircraft, weather balloon, or tower thermometer. The quantities M and T_i are obtained from the flight test. The aircraft is cruised for a short duration at different Mach numbers and the results are plotted in the form of $(T_i/T - 1)$ versus $M^2/5$. The typical experimental points are shown in Fig. 18.1 and they all lie along the straight line passing through the origin. The slope of this line with the horizontal axis is the value of K_t . For a well-designed temperature probe the value of K_t lies between 0.95 and 1.

Having obtained K_t as above, if M and T_i are measured during any other flight that uses the same temperature probe system, T can be obtained from Eq. (18.1).

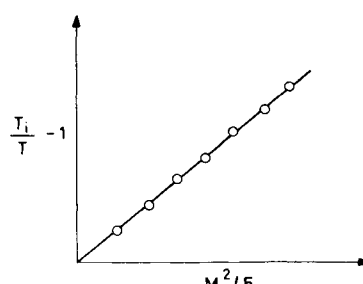


Fig. 18.1 Temperature probe calibration.

18.2.3 Angle of Attack Calibration

The indicated angle of attack includes some error due to positioning of the angle of attack vanes or the differential pressure sensors. This error varies as the forward airspeed varies due to variation in the flow field. This error is calibrated by using the relation between angle of attack and accelerations, as given by $\alpha_{\text{True}} = \tan^{-1}(-a_x/a_z)$, where α_{True} is the true angle of attack, and a_x and a_z are accelerations along the longitudinal and normal axes, respectively.

The aircraft is flown in stabilized level flights at various airspeeds to note α_i , a_x , and a_z , where α_i is the indicated angle of attack. A graph between α_{True} and α_i can be drawn which is the calibration graph to find α_{True} when α_i is known from the flight test.

18.3 Lift Coefficient Curve and Drag Polar by Flight Tests

Lift and drag coefficients and the drag polar can be determined from cruising flights of very short intervals.

18.3.1 Lift Coefficient Curve Determination

In a steady, straight level flight, the lift coefficient C_L is given by

$$C_L = 2W / (\rho_{\text{SSL}} V_e^2 S) \quad (18.2)$$

The test aircraft is first stabilized in straight level flight. At any instant of time during the cruise, V_e is obtained from the indicated airspeed, W is calculated by subtracting the fuel used from the gross weight, and the angle of attack α is noted. The value of C_L can be calculated from Eq. (18.2). This will give one test point of the C_L versus α curve. Continue the test for different values of α and thus accumulate more test points to draw a smooth curve, as shown in Fig. 18.2. Equation (18.2) has the advantage of being independent of the altitude and can be used both for incompressible and compressible flow airspeeds. The method can also be used to obtain trim curves of longitudinal stability if the elevator deflection is also measured.

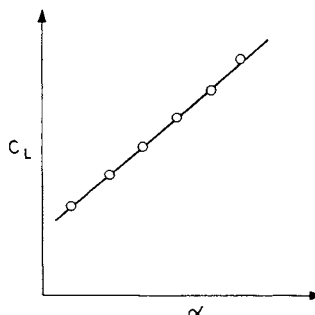


Fig. 18.2 Lift coefficient curve.

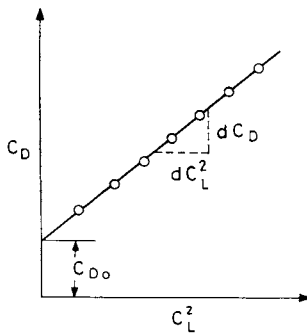


Fig. 18.3 Straight line form of drag polar.

18.3.2 Drag Polar Determination

The test requires the determination of both C_L and C_D simultaneously for different α . The aircraft is flown in the cruising flight and the C_L is obtained as in Sec. 18.3.1. Since $D = F$, the drag coefficient is obtained from the relation, $C_D = 2F/(\rho_{SSL} V_e^2 S)$. The indicated airspeed yields V_e and the thrust F can be calculated from the in-flight measurements of engine parameters like Mach number, ambient temperature, engine speed, exhaust area, etc. Thus, both C_L and C_D can be obtained for a given α . The test is repeated for different values of α to obtain the corresponding values of C_L and C_D . It is not necessary to measure α unless the plot of C_L or C_D versus α is desired.

C_D is plotted against C_L^2 as shown in Fig. 18.3, and a straight line is drawn passing through them as closely as possible. The equation of this straight line represents the drag polar, $C_D = C_{D_0} + KC_L^2$, where C_{D_0} is the height of the intercept of the straight line with the C_D axis, and K is the slope dC_D/dC_L^2 of the straight line with the C_L^2 axis as shown in the figure. If required, Oswald's span efficiency factor e can be found from the relation, $e = 1/\pi(AR)K$, where AR is the aspect ratio of the wing.

The drag polars for different configurations or flap positions of the aircraft are found in the same way as described above.

18.4 Stall Tests

The stalling airspeed and the stalling characteristics of an aircraft are important performance parameters that are determined by flight tests. These tests are required for safety reasons and form the baseline characteristics of an aircraft upon which its handling qualities and performance evaluation are based. The characteristic airspeeds during takeoff and landing phases are defined in terms of stalling airspeed of the aircraft; e.g., the liftoff airspeed may be stated as $1.15V_S$, indicating that it should be 15% more than the stalling airspeed. Aircraft are also flown to the stall limit in instantaneous turns. Stall warning and stall prevention systems, if they exist, are assessed by the stall tests. Stall tests are also conducted to check for compliance with stall specifications laid down by the concerned regulatory agency like the Federal Aviation Regulations (FAR) or British Civil Airworthiness Requirements (BCAR).

18.4.1 Stalling Behavior of an Aircraft

Stall of an aircraft is due to large regions of flow separation over the upper surface of its wing. This produces loss of lift and increase in drag. Stall changes pitching, rolling, and yawing moments characteristics of the aircraft. The unsteady flow separation from the wing, when passing over the fuselage and tail unit may cause buffeting. Control surfaces affected by the stall tend to lose their effectiveness. The resulting effects of the stall may be gentle or severe. In severe stall the aircraft may exhibit violent and random pitching, rolling, and yawing motions. If the stalling behavior is not controlled, it may lead to the aircraft entering into a spin.

The stalling characteristics of a given aircraft depend on the nature of flow separation, separation-bubble formation, and the location of the first flow separation and how it spreads over the wings. Various design techniques are used to improve the stalling behavior of the aircraft.

18.4.2 Three Phases of Stall Tests

The stall tests are divided into three distinct phases—approach to stall, the stall, and recovery after stall.

18.4.2.1 Approach to stall. The symptoms and the behavior of an aircraft, prior to the stall itself, constitute the “approach to stall” phase. The recognition and the knowledge of this phase is of utmost importance to avoid the occurrence of stall. A pilot generally avoids inadvertent stall while maneuvering at low airspeeds.

As the stall approaches, the pilot is required to assess the aircraft attitudes, tendency for pitch or yaw off, adverse dynamic characteristics like Dutch roll, and the engine behavior. He should examine the effectiveness of high-lift devices and their effect on the controllability of the aircraft. He should also note whether there is any deterioration in handling qualities, like the reduction in control power or the reduction in control forces. The pilot also assesses the adequacy of stall warning, ability to avoid stall once the warning is perceived, and the efficacy of stall prevention devices, like the stick pusher, if it exists.

The test is mainly qualitative. The aircraft is initially trimmed to $1.4V_S$, then its speed is reduced. After a gap of every 5 or 10 kn, the speed is stabilized and the various items mentioned in the above paragraph are assessed.

18.4.2.2 Stall. Flight tests are required to identify and define the stall. For practical considerations, *stall* may be defined as one of the following: 1) The moment the aircraft reaches its maximum lift coefficient, $C_{L,m}$, which can be recognized as the first *g-break*. If the aircraft has more than one peak in the lift coefficient curve, the first of these peaks would be defined as the stall. This is the conventional method of defining the stall. 2) The period during which the aircraft exhibits uncommanded roll, yaw, or pitch; this is the most probable feature in a modern fighter aircraft. 3) The occurrence of intolerable buffeting of the aircraft. 4) The period when the aircraft is flying at minimum airspeed with the pitch control column fully back; if $C_{L,m}$ is not attained even with the pitch control fully back, maneuverability may be impaired.

Different types of aircraft exhibit stalling behavoir of different types. For example, some aircraft may exhibit only wing rock, others may have both yaw-off and wing rock, some have conventional stall, and some others may exhibit activation of the stick-pusher.

The airspeeds and incidences achieved at stall depend on the weight of aircraft, its altitude, and the load factor. They also depend on the position of center of gravity, amount of aft stick available, rate of deceleration (called the *bleed rate*), power, Mach number, and sideslip β . The aircraft configuration, like the position of flaps, undercarriage, and external stores, also affects the airspeeds and incidences.

The stall test is both qualitative and quantitative. Having defined the stall for a given aircraft, the test crew must assess its stall behavior and handling qualities. They should note the indicated airspeed (IAS), incidence, and control deflections. The aircraft's stability, controllability, and tendency toward spin or divergence should be assessed. The behavior of the power plant and subsystem operations should also be noted.

18.4.2.3 Recovery after stall. The effectiveness of recovery controls, the aircraft, and its engine behavior, and the handling qualities of the aircraft are assessed during recovery after stall. The altitude, loss of altitude, and time taken during recovery are noted. The rapidity with which the aircraft unstalls, and the effectiveness of high-lift devices and stabilization systems are assessed. The effect of possible mishandling and proneness to restalling are also looked into. The recovery after the stall test is mainly qualitative.

18.4.3 Test Techniques

Stalls are usually tested in both straight and turning flights. In straight flight, the rate of deceleration of the aircraft can be either slow or fast. Thus, the three different cases of stalls are considered here—straight slow stall, straight fast stall, and stall in turning flight.

18.4.3.1 Straight slow stall. The aircraft is first set at the required configuration, altitude, and power setting for the test. It is then trimmed at a speed of about $1.4V_S$. Altitude, airspeed, fuel counts, control positions, and trim settings are recorded. A slight increase in pitch is then made to start deceleration toward the stall at the rate of 1 kn (1.85 km/h or 0.51 m/s) per second or slower. The desired deceleration rate is achieved by adjusting the pitch. During this speed reduction it is important to have no sideslip. Control response is checked at intervals by making small control movements, deflecting each control surface in turn. At each significant stage, the airspeed, rate of descent, control positions, and forces should be recorded. It may often be necessary to make several such speed reduction tests to obtain full information.

18.4.3.2 Straight fast stall. The straight fast stall test is carried out in the same way as the straight slow stall test mentioned above, except that the bleed rate here should be reduced to 3 or 4 kn/s instead of 1 kn/s. This is also near 1 g stall which should be maintained throughout the phase of approach to stall.

Both slow and fast stalls are conducted at straight and level flights with $n = 1$. From the data of fuel counts, airspeed, and altitude accumulated during the slow and fast stalls, the maximum lift coefficient and the bleed rate can be calculated. A plot of $C_{L,m}$ against the bleed rate can be drawn as shown in Fig. 18.4. From this graph, the value of $C_{L,m}$ at the bleed rate of exactly 1 kn/s can be found. This value of $C_{L,m}$ is used to plot a graph of weight W versus equivalent airspeed $V_{e,s}$ at stall by using the relation $V_{e,s} = \sqrt{2(W/S)/(\rho_{SSL}C_{L,m})}$ which is valid for

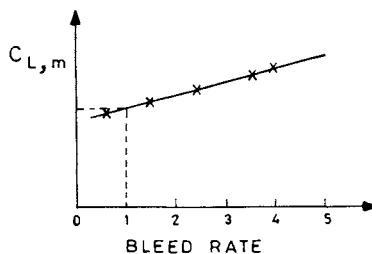


Fig. 18.4 Maximum lift coefficient with bleed rate.

different altitudes because the equivalent airspeed is used. A typical shape of the curve is shown in Fig. ?? for clean configuration, and similar curves for various other configurations can be drawn.

The fast stall mentioned above is not the dynamic stall, which is discussed below.

18.4.3.3 Stall in turning flight (dynamic stall). The stall in turning flight is called an *accelerated* or *dynamic stall*. The aircraft is first trimmed in straight flight at required configuration, altitude, airspeed, and power setting. It is then gradually rolled in a tightening turn of constant airspeed. The nose is lowered to keep the airspeed constant as the load factor increases, until the aircraft stalls. The same observations are required as mentioned in the straight slow stall.

It may happen that the load factor cannot be increased up to stall because of certain limiting factors. These limits can be either of maximum allowable load factor or the elevator movement may have reached its limit before the stall. In such cases, the airspeed should be reduced by holding a steady value of the load factor, just below the maximum allowable, until the stall is reached. A full turning stall test is carried out in one direction, but a comparative check can be made by turning the aircraft in the other direction.

18.5 Takeoff and Landing Tests

The takeoff and landing tests are important phases of the flight test program of an aircraft. A number of takeoff and landing tests are conducted in the various configurations and gross weights that may possibly exist in the operation of the aircraft, including the cases of refused takeoff and emergency landing. The takeoff and landing tests and their method of data presentation are briefly described below.

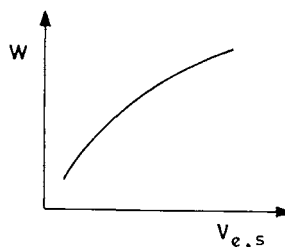


Fig. 18.5 Effect of weight on $V_{e,s}$.

18.5.1 High-Speed Taxi Tests

The possibility of refused takeoff is always present. This suggests that high-speed taxi tests should be conducted first before actual takeoff or landing tests. The parameters that are usually determined from high-speed taxi tests are thrust transients, drag, and braking coefficient of friction. These tests are conducted on different types of surfaces, including both dry and contaminated surfaces. The aircraft is tested for several gross weights and in different configurations that are likely to exist during the ground roll of takeoff or landing. Some braking tests are also conducted as part of the high-speed taxi tests. Full braking effectiveness is generally evaluated during refused takeoff or actual landing tests.

18.5.2 Takeoff Performance Tests

The important quantities determined in takeoff tests are the ground roll and the airborne distances and times the aircraft requires to clear the screen height of 10.7 m (35 ft) or 15.24 m (50 ft) above the ground. Other recordings are made externally by people on the ground; these include ground speed and acceleration, runway temperature, ambient pressure, wind speed, and wind direction. The data that are recorded internally by the cabin crew of the aircraft may include certain power parameters, such as indicated airspeed, altitude, ambient temperature, exhaust gas temperature, and other items that may be considered desirable. If the aircraft is instrumented to measure longitudinal acceleration a_x , its first integration will give velocity and the second integration will give the distance. Accordingly, the personnel in the cockpit note the takeoff distance accurately. Also, if the aircraft wheel is fitted with a counter, the rpm of the wheel can be measured and by knowing its diameter the ground roll distance can be calculated.

The external data can be recorded by ground observers standing along the runway length. The aircraft is first operated at full throttle with full brakes. As soon as the brakes are released slowly, the aircraft starts moving and gaining speed. By noting the times when the aircraft passes through various known distances along the length of the runway, the velocity and acceleration can be calculated. Efforts are made to visually locate the exact distance the aircraft has taken to become airborne. The external data are usually recorded by a theodolite, which is a surveying instrument with a rotating telescope to measure the angular displacement of the aircraft both in the horizontal and vertical planes. Several theodolites may be placed along the length of the runway for observation. Figure 18.6 shows

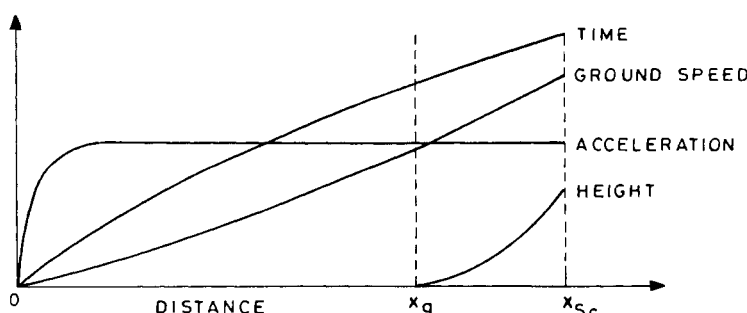


Fig. 18.6 Takeoff performance data.

typical variations in the time, ground speed, acceleration, and height of the aircraft during takeoff along the runway length until the aircraft has reached the screen height.

Improved versions of the theodolite, such as the phototheodolite, are also available. The theodolite data can also be in the form of printed digital readouts which can be used to develop plots similar to those shown in Fig. 16.1. The takeoff data is also recorded by cinematography.

All takeoff performance data are corrected to sea level standard atmosphere conditions, with zero wind, unless specified otherwise.

18.5.3 Landing Performance Tests

Landing performance tests require the determination of airborne distance from the screen height (50 or 35 ft) above the ground to the touchdown, then ground roll distance up to until the aircraft achieves a complete halt. The measurement and presentation of the airborne and ground roll distances are accomplished in the same manner as described for the takeoff tests. The landing performance data are also corrected to the standard atmosphere conditions at sea level, unless specified otherwise. The average of the best two of at least four landings is reported.

Evaluation of the brake effectiveness during ground roll is a special feature of the landing tests. After the aircraft has touched down, maximum braking power is applied without allowing the aircraft to skid. Stopping distance is a function of the brake effectiveness, type of runway, and the condition of its surface. Brake effectiveness depends on the brake energy, temperature, and the aircraft weight. The effects of aerodynamic braking and the other methods of reducing ground roll distance, such as thrust reversing and drag chute, are also tested.

18.5.4 Data Scatter and Its Minimization

Takeoff and landing performance tests are subject to a considerable amount of data scatter and have a low degree of repeatability. Certain factors cannot be quantified, which makes mathematical corrections inapplicable. Individual pilot technique is also greatly responsible for the variation in takeoff data as well as in landing data. Some of the factors that significantly influence takeoff performance are 1) the speed and sequence of brake release and power application, 2) the positions of the controls during acceleration, 3) the airspeed at rotation and pitch rate during rotation, and 4) the angle of attack at liftoff. Similarly, the reasons for landing data scatter are 1) the variations in power handling during the approach, flare, and touchdown, 2) the altitude of flare initiation and the rate of rotation in flare, 3) the length of holdoff time and the touchdown speed, and 4) the rapidity of initiation of aerodynamic or mechanical braking.

It appears that it is possible to minimize the takeoff data scatter by standardizing certain techniques that may be possible for the pilots. Items that can be standardized are 1) throttle setting prior to brake release, and throttle technique at and immediately after the brake release; 2) the control positions during acceleration; 3) the airspeed at rotation and rate of rotation; and 4) the attitude of aircraft at liftoff, and the gear and flap retraction points. Other items can also be considered. Similarly, the landing procedure for an aircraft can also be standardized. The standardization techniques, either for takeoff or landing, are different for different types of aircraft.

18.6 Climb Performance Tests

The methods of partial climbs and level flight accelerations are quite common for testing the climb performance of aircraft. These two methods and their relative advantages are discussed here. The method of level flight acceleration is more suitable to a high-performance aircraft. The climb test data are finally reduced (modified) to standard atmosphere conditions. Both experimental and analytical methods are used for data reduction.

18.6.1 Sawtooth Climb Tests (Partial Climbs)

The *sawtooth climb test* determines airspeed for maximum rate of climb at different altitudes. Thus, this method provides a climb schedule for the maximum rate of climb.

In a narrow band of altitude, comprising small regions above and below the fixed altitude (test altitude), the aircraft climbs and descends alternately, to carry out the tests at different airspeeds. A series of timed climbs are made from a point below the test (fixed) altitude to a point above it. The airspeeds are chosen to bracket the expected best climb airspeed of the aircraft. The climbs are performed at the same power setting and configuration of the aircraft as used in practice, and are designed to obtain the minimum time to climb. After completing the tests for a given test altitude, the aircraft returns to the ground and is prepared to undertake similar tests at the next test altitude.

The sawtooth climb test mentioned above can be explained by Fig. 18.7 for a test altitude, say $h = h_1$. The succeeding ascents and descents produce a wavy flight path resembling a sawtooth pattern, hence the name is sawtooth climb test; the barograph trace of the flight would also resemble a sawtooth pattern. It is also called the method of *partial climbs* because the tests are carried out only in the partial bands of the actual climb in practice. The band thickness $2\Delta h$ is chosen with the test altitude in the middle of this band, as shown by a dash-dot horizontal line in the figure. The altitude increment $2\Delta h$ should be such that the aircraft would traverse it in about 1 min; any smaller time increments may introduce excessive scatter in the data. The two dashed horizontal lines A_1A_4 and C_1C_4 are, respectively, the lower and upper limits of the altitude band of the test altitude at h_1 .

The aircraft is first trimmed in the climb configuration while still well below the point A_1 as shown in Fig. 18.7. The final trim and power adjustments are made

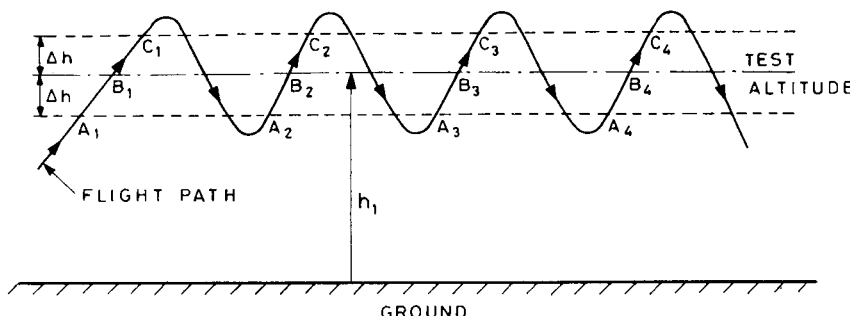


Fig. 18.7 Sawtooth climb test.

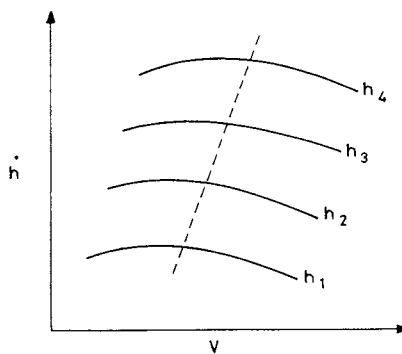


Fig. 18.8 Variation of rate of climb with airspeed at different altitudes.

before reaching A_1 . During the climb from A_1 to C_1 , the aircraft configuration, indicated airspeed V_i , and N (engine rpm), are kept constant. Since the altitude band $2\Delta h$ is small, the true airspeed V of the aircraft can also be considered constant during the partial climb, otherwise V can be taken as the mean value of the climb in the band. The quantities V_i , N , T_i (indicated temperature), h_p (pressure altitude), fuel count, and the time t , are recorded both at the time of entering at A_1 and leaving at C_1 of the altitude band; the records are made by stopwatch and photo-trace or magnetic tape recorders. The average of these readings in each case would be their values for the test altitude at B_1 . For example, the value of T_i at the test altitude would be given by $T_i = \{(T_i)_{A_1} + (T_i)_{C_1}\}/2$, and similarly for the other quantities.

After emerging from the upper limit at C_1 of the test band, the aircraft soon descends to reach below the altitude band for another climb run. The trim setting is not changed during the descent, so that only a small trim adjustment will be required for the next climb run from A_2 to C_2 with different airspeed. As in the case of climb from A_1 to C_1 , similar readings are taken while the aircraft is climbing from A_2 to C_2 , A_3 to C_3 , A_4 to C_4 , and so on, until the sufficient data are acquired at different airspeeds for bracketing the best (fastest) climb airspeed at the altitude h_1 . Equation (10.58) for a turbojet aircraft and Eq. (14.40) for a piston-prop aircraft can be good theoretical guides for saving time in locating the fastest climb airspeed V_{FC} . If V_m represents the maximum airspeed, the relation $V_{FC} = V_S + (V_m - V_S)/3$ is suggested³ for a piston-prop aircraft for quickly locating the V_{FC} through flight tests.

Before leaving the test altitude, it should be examined for the points that might need repeating. Similarly, the sawtooth climb test can be carried out for the other test altitudes h_2 , h_3 , h_4 , etc. The plot of the rate of climb \dot{h} against V is shown in Fig. 18.8 for different test altitudes; the best climb schedule is shown by a dashed line.

18.6.2 Level Flight Acceleration Tests

It is only the excess power, or more precisely the specific excess power, that is used in climb, acceleration, turning, and their combinations. If the climbing is confined along a straight flight path, the performance of an aircraft is governed by the relation

$$\dot{h}_e = (F - D)V/W = dh/dt + (V/g)dV/dt \quad (18.3)$$

showing that the specific excess power is used both in the climb and acceleration. If it has no acceleration, $dV/dt = 0$, and the excess power is used in the climb only. Similarly, if the climb is zero, $dh/dt = 0$, and the excess power is used in the level acceleration only. Therefore, the excess power can be used purely in climb or purely in level acceleration, and by measuring either the climb performance or level acceleration performance, the other can be estimated. This forms the genesis of the level acceleration technique, according to which, by measuring level acceleration performance, the rate of climb performance can be estimated.

Level flight accelerations from near-minimum to maximum airspeeds are flown at different altitudes. The aircraft configuration is kept the same as used in practice during the climb. The values of indicated airspeed, time, fuel flow, ambient air temperature, and indicated altitude are recorded. The airspeed and time are the most important quantities. The fuel flow is recorded to obtain the weight of the aircraft, which can generally be considered constant during an acceleration run of short duration. The ambient air temperature is recorded to make certain corrections and for the reduction of data to standard conditions. The altitude is measured to make altitude correction, if it exists. Since at any fixed altitude the duration of the acceleration run is short, the recording of data must be mechanical, usually by photo-trace or magnetic tape recorders.

The aircraft is first stabilized at some medium airspeed at the desired altitude. It is then slowed to just above the minimum level-flight airspeed without adjusting the trim. Acceleration is now started by smoothly increasing the throttle to the desired value. The acceleration first increases and then recedes. The readings are recorded at short intervals until the acceleration is quite small. Similarly, level acceleration runs are conducted at different test altitudes.

The two curves shown in Fig. 18.9 are drawn from the measurements carried out during the level flight acceleration run of the aircraft at a fixed altitude. Differentiating h_e numerically from the values taken from the h_e versus t curve of Fig. 18.9, the \dot{h}_e versus V curve shown in Fig. 18.10 can be plotted. The topmost point A of the curve in Fig. 18.10 would correspond to the point of inflexion of the h_e versus t curve in Fig. 18.9. The curve shown in Fig. 18.10 is for a fixed altitude, and different other curves can be obtained by carrying out the level flight acceleration runs at different altitudes in the same manner. This system of curves is shown in Fig. 10.10, and by cross-plotting it, Fig. 10.11 can be obtained. The line joining the peaks of these curves represents the airspeed for maximum \dot{h}_e at each altitude; in other words, it gives the climb schedule for maximum \dot{h}_e at each altitude. If acceleration during the climb is zero, $\dot{h}_e = \dot{h}$, and in such cases the line joining the peaks of the curves in Fig. 10.10 also gives the airspeed for maximum

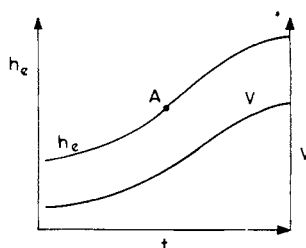


Fig. 18.9 Variations of h_e and V with time.

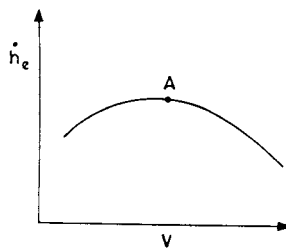


Fig. 18.10 Variation of \dot{h}_e with V at fixed altitude.

\dot{h}_e (rate of climb) at each altitude; in other words, it gives the climb schedule for maximum rate of climb at each altitude.

18.6.3 Relative Merits of Sawtooth Climb and Level Acceleration Tests

The sawtooth climb test is the oldest method of determining the airspeeds for the best climb rates at different altitudes. It is still used for reciprocating engine aircraft or for other low-performance aircraft. It is also used for high-performance aircraft at higher altitudes where its performance is weakened sufficiently. At low altitudes, high-performance aircraft have high rates of climb and it becomes difficult to apply the sawtooth climb test. This is because the aircraft remains in the test band for a very short time, making it difficult to measure various quantities. It is also not easy for a high-performance aircraft to achieve stabilized climb airspeed because it usually accelerates during the climb. The sawtooth climb test can also be used for determining the optimum climb schedule at different energy heights, by carrying out partial climbs at different airspeeds throughout the range at varying heights, selected such that the energy height remains constant.

The level flight acceleration test is used for finding the climb schedule of high-performance aircraft. The test is of very short duration, and is thus quite economical in flying hours as compared with the time spent in performing sawtooth climb tests. In principle, at a specified altitude, only one level acceleration flight run is required, whereas the sawtooth climb test requires several runs. However, in practice the single-level acceleration may have high data scatter and it may require two or more level acceleration runs at a given altitude. Nevertheless, the level acceleration flight test technique requires much less flying time than the sawtooth climb test technique; it may usually require one-half the time or less to cover the same airspeed and altitude range.

In the level flight acceleration test, the data for acceleration are also obtained in conjunction with the climb data. The method is also applicable to obtain supersonic climb schedules, and wind gradient errors are small. The level flight acceleration test can be used at any desired altitude compatible with clearing ground obstructions.

The level flight acceleration test has, however, the disadvantage that the measurement of rate of climb is replaced by the measurement of acceleration, which is inherently less accurate. It would thus be advantageous to mix the two techniques in the case of high-performance aircraft. That is, one would use the sawtooth climb

test method at higher altitudes where its performance is considerably reduced, and use the method of level acceleration at lower altitudes.

It should be kept in mind that one assumption, which is inherent in replacing the rate of climb by the level acceleration, is that the excess power will be the same in level acceleration as in climb, at the same forward airspeed. This is not strictly true because the attitude of the aircraft during climb is different from that in level flight; the drag of the aircraft is less in the climb than in the level flight at the same forward airspeed. On a jet aircraft, the error in rate of climb resulting from this assumption is usually less than 2%.³

18.6.4 *Climb to Ceiling for a Jet Aircraft*

Climb to near-ceiling altitude is flown in accordance with a given climb schedule. This climb schedule may be provided by flight tests, either by sawtooth climb test or level flight acceleration test discussed above; both these tests must provide the same climb schedule. It can be a best-climb schedule obtained by flight tests, a schedule recommended by the manufacturer, maximum energy climb schedule, or some other climb schedule of interest. The ceiling altitude may be operational ceiling, service ceiling, or some other ceiling of interest.

The main purpose of the climb to ceiling altitude is to check or evaluate the standard day climb performance of an aircraft in a specific configuration. The three main parameters of investigation are time to climb, distance traveled, and fuel consumed. In addition, data may be obtained on various other parameters, such as engine speed, exhaust gas temperature, engine pressure ratio, net thrust, outside air temperature, indicated airspeed, pressure altitude, etc. These other parameters are useful in analysis, but are secondary to the three main parameters.

A difficult step for obtaining good climb data is finding an area of satisfactory meteorological conditions. A survey balloon may be sent up before the test flight, to determine wind and temperature data of the atmosphere. Atmospheric conditions of smooth air, light or no winds, and stable temperature gradients from the ground to the ceiling are desirable. Data should be recorded at approximately equal intervals of altitude. For a jet aircraft, recordings by automatic mechanical means may be necessary to obtain simultaneous readings of the several quantities of interest.

18.6.5 *Experimental Method of Data Presentation*

The reduction of flight test data to standard conditions is an important component of flight tests. Both experimental and analytical methods are used for data reduction. This sub-section describes the experimental method, whereas the analytical approach is discussed in Sec. 18.6.6. In the experimental method, performance under standard conditions is deduced directly from the data of flight tests on the aircraft with no other numerical data being called upon from other sources. Therefore, it is also called the experimental method of data reduction. This is possible because the performance of both the engine and aircraft configuration can be expressed by certain parameters. This reduces the number of variables to a reasonable number that can be handled. The exact relationships of these functional forms are obtained by plotting the flight test results as graphs or carpet plots. The performance at standard conditions or at any other specified conditions of weight, height, rpm, temperature, etc. can be determined from these graphs or carpet plots.

The experimental method requires correctly choosing variables and grouping them to form generalized parameters for the particular aircraft. Birmingham's π -theorem, or the theoretical formulation of the performance problem and its solution, considerably helps in forming these generalized parameters. The experimental method has the disadvantage that many more flight tests are required to cover a full range of these parameters. The results are frequently plotted in the form of carpet plots which are not so easy to understand as the more straightforward types of graphs.

The climb performance presented here serves the purpose of illustrating the remarks made above for the experimental method.

From the engine characteristics [Eq. (4.12)] it is seen that

$$F/\delta = f(V/\sqrt{\theta}, N/\sqrt{\theta}) \quad (18.4)$$

and from the aircraft configuration characteristics

$$D/\delta = f(V/\sqrt{\theta}, W/\delta) \quad (18.5)$$

Equation (18.3), exhibiting the specific excess power \dot{h}_e , can be written as

$$F/\delta - D/\delta = (W/\delta)(\dot{h}_e/\sqrt{\theta})/(V/\sqrt{\theta})$$

which in view of Eqs. (18.4) and (18.5) can be written in functional form

$$\dot{h}_e/\sqrt{\theta} = f(V/\sqrt{\theta}, N/\sqrt{\theta}, W/\delta) \quad (18.6)$$

From the climb test conducted, which is not necessarily for optimum climb schedule or for any other fixed schedule, the parameter $\dot{h}_e/\sqrt{\theta}$ can be plotted graphically or by means of a number of carpet charts as shown in Fig. 18.11. Each of the three carpet charts of Fig. 18.11 corresponds to a different value of $N/\sqrt{\theta}$, showing the variation of $\dot{h}_e/\sqrt{\theta}$ for different constant values of $V/\sqrt{\theta}$ (or M) and

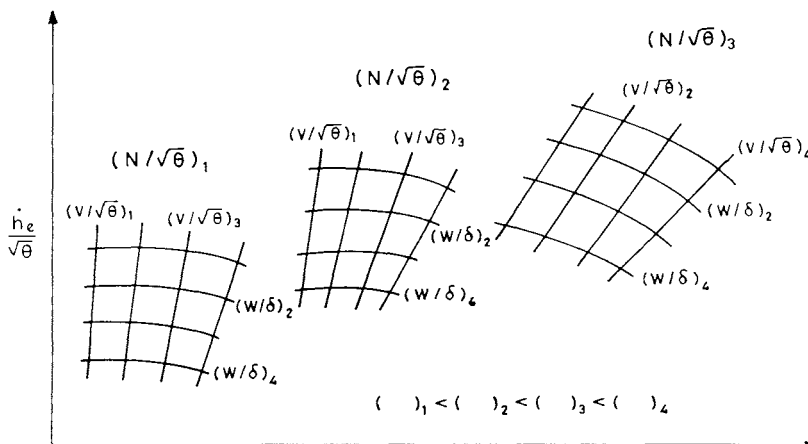


Fig. 18.11 Climb carpet plot.

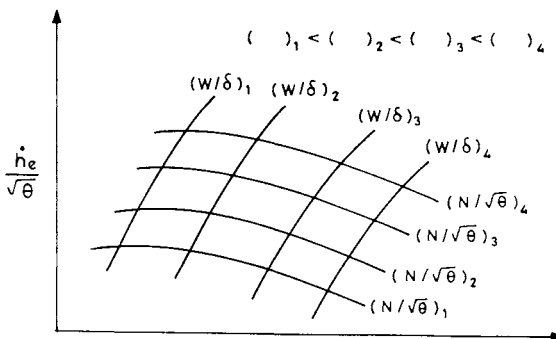


Fig. 18.12 Specified climb schedule carpet.

W/δ ; the aircraft performance corresponding to the standard conditions can be read from this chart.

If the optimum climb schedule, or any other fixed climb schedule is used, assuming consistent fuel consumption during climb, there is one-to-one relation between $V/\sqrt{\theta}$ and W/δ , i.e., $V/\sqrt{\theta} = f(W/\delta)$. Therefore, in such fixed (specified) climb schedules, Eq. (18.6) is simplified to $\dot{h}_e/\sqrt{\theta} = f(N/\sqrt{\theta}, W/\delta)$, and its typical carpet plot would be the same as that shown in Fig. 18.12. A different carpet plot is required for each different specified climb schedule.

18.6.6 Analytical (Differential) Method of Data Reduction

The analytical method of data reduction utilizes numerical data from other sources for deduction of the performance under standard conditions from the flight tests carried out under nonstandard conditions. The simplest relationship, usually linear, is generally used between the variables to derive the results for the standard conditions from the data accumulated from the other sources. For example, the differential relationship of a performance variable F depending on T can be written as $dF = (dF/dT)dT$, where dF and dT are considered small, $dF = F_{\text{std}} - F$, $dT = T_{\text{std}} - T$, the quantities F and T represent the test values, and the subscript std denotes standard condition. The above relation can be written as

$$F_{\text{std}} - F = (dF/dT)(T_{\text{std}} - T) \quad (18.7)$$

where T_{std} is the known quantity. Therefore, by obtaining F and T from flight tests, the value F_{std} can be determined if dF/dT is known from the earlier accumulated results of the other sources.

The correction method employing an equation such as Eq. (18.7) is valid only for small variations (differentials), and so it is commonly referred to as the *differential method*. Flight tests are conducted close to the standard conditions and corrections are applied to adjust for the relatively small discrepancies between the test and the standard conditions. The correction for each variable to the standard conditions is applied one-by-one, hence the method is also called the *step-by-step method of data reduction*. The various corrections applied to each variable are discussed below.

18.6.6.1 Tapeline altitude correction. An altimeter set to 76 cm (29.92 in.) of mercury level measures correctly the pressure altitude h_p on the test day, but this may not be the true or tapeline altitude h . This is because the pressure and the lapse rate on a test day are generally different from that of the standard atmosphere. Therefore, the change in the ambient pressure dp , sensed by the altimeter, would yield dh_p , which is different from the change in true altitude dh . This is illustrated in Fig. 18.13, where both the standard and nonstandard pressure distributions are plotted against the altitude. The climb test of the aircraft measures dh_p/dt whereas it is required to obtain dh/dt , the true rate of climb.

The change in true altitude is given by Eq. (2.2) as

$$dh = -dp/(\rho g) \quad (18.8)$$

This shows that for the same pressure change dp , the altitude change dh will be greater on hotter days due to reduction in ρ ; this can also be seen in Fig. 18.13. Since the pressure altitudes are flown,

$$p = p_{\text{std}}, \quad \text{i.e.,} \quad dp = dp_{\text{std}} \quad (18.9)$$

and from the equation of state,

$$\rho RT = \rho_{\text{std}} RT_{\text{std}}, \quad \text{i.e.,} \quad \rho/\rho_{\text{std}} = T_{\text{std}}/T \quad (18.10)$$

From Eqs. (18.8) and (18.9), it can be written that

$$dh_p (= dh_{\text{std}}) = -dp_{\text{std}}/(\rho_{\text{std}} g) = -dp/(\rho_{\text{std}} g) \quad (18.11)$$

Dividing Eq. (18.8) by the equal terms of Eq. (18.11), and using Eq. (18.10), leads to

$$dh/dh_p = \rho_{\text{std}}/\rho = T/T_{\text{std}}$$

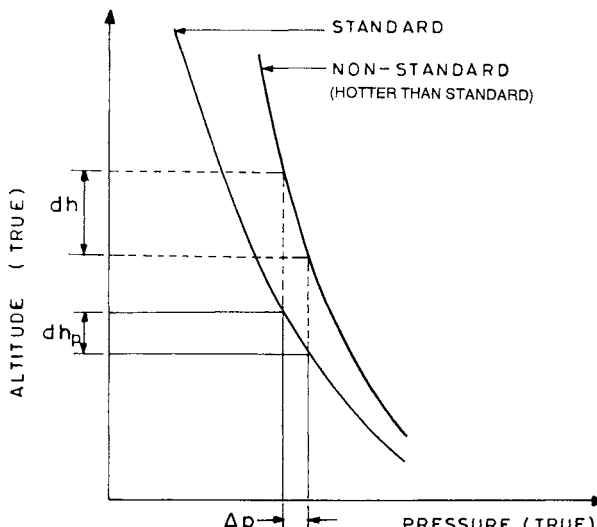


Fig. 18.13 Tapeline altitude correction.

which in a differential form can be written as

$$dh = (T/T_{\text{std}})dh_p \quad (18.12)$$

In case it is desired to obtain the true altitude from the pressure altitude, the above equation can be integrated to yield

$$h = \int_0^{h_p} (T/T_{\text{std}})dh_p \quad (18.13)$$

where the variation of T with h_p is supposed to be known.

The true rate of climb dh/dt is obtained from Eq. (18.12) by dividing it by dt , thus

$$dh/dt = (T/T_{\text{std}})dh_p/dt \quad (18.14)$$

where T and T_{std} are the absolute temperatures of the test day and the standard atmosphere, respectively, and dh_p/dt is the rate of climb of the pressure altitude as measured by the altimeter during flight test.

18.6.6.2 True airspeed and thrust corrections. The nonstandard temperature affects the true airspeed and the thrust. These effects are so intimately connected that it is difficult to separate them. A change in temperature changes true airspeed and thrust, and this change in the true airspeed produces a secondary change in the thrust or thrust power. The two effects are, therefore, analyzed simultaneously.

Consider that V is the true airspeed of the test and V_{std} is the standard or desired true airspeed. Denoting their difference by dV , so that

$$dV = V_{\text{std}} - V, \quad \text{i.e.,} \quad V + dV = V_{\text{std}} \quad (18.15)$$

Since $V = V_e/\sqrt{\sigma}$, and $V_{\text{std}} = V_e/\sqrt{\sigma_{\text{std}}}$, this gives

$$V_{\text{std}}/V = \sqrt{\sigma}/\sqrt{\sigma_{\text{std}}} = \sqrt{\rho}/\sqrt{\rho_{\text{std}}} = \sqrt{p T_{\text{std}}/p_{\text{std}} T}$$

As the aircraft is flown according to the pressure altitude, $p = p_{\text{std}}$, and the above relation becomes

$$V_{\text{std}}/V = \sqrt{T_{\text{std}}/T} \quad (18.16)$$

The thrust force during test will be denoted by F , the standard thrust by F_{std} , and their difference by dF , so that

$$F + dF = F_{\text{std}} \quad (18.17)$$

If thrust measuring equipment is available, F can be determined. The standard thrust F_{std} can be obtained from the engine charts supplied by the aircraft manufacturer if the standard conditions of the nozzle pressure ratio and total temperature are specified. Hence dF can be obtained from the above relation.

If thrust measuring equipment is not available, dF can be obtained from the relation

$$dF = \{\partial F/\partial(N/\sqrt{\theta})\}d(N/\sqrt{\theta}) \quad (18.18)$$

where $d(N/\sqrt{\theta}) = (N/\sqrt{\theta})_{\text{std}} - (N/\sqrt{\theta})$ is found by computing the change in $(N/\sqrt{\theta})$ between the standard and test conditions. The quantity $\partial F/\partial(N/\sqrt{\theta})$ is obtained from the engine charts for the test values of $(N/\sqrt{\theta})$, p , and M . If the charts are in the form of $F/\delta = f(N/\sqrt{\theta}, M)$, the value of dF can be found from the relation

$$dF = [\{\partial(F/\delta)/\partial(N/\sqrt{\theta})\}d(N/\sqrt{\theta})]\delta \quad (18.19)$$

where δ has its test value. The quantities dV and dF will now be considered as known quantities.

The rates of climb, \dot{h}_{std} and \dot{h} , representing the rates of climb of the standard and test conditions, respectively, can be written as

$$\dot{h}_{\text{std}} = V_{\text{std}}(F_{\text{std}} - D)/W_{\text{std}} \quad (18.20)$$

and

$$\dot{h} = V(F - D)/W \quad (18.21)$$

where it is assumed that the drag D of the aircraft during the test is the same as for the standard conditions; this is true if the climb is taking place at constant equivalent airspeed because C_D is then not affected by the change in airspeed or atmospheric conditions. Making use of Eqs. (18.15) and (18.17), Eq. (18.20) can be written as

$$\dot{h}_{\text{std}} = [(V + dV)\{(F + dF) - D\}]/W_{\text{std}}$$

Neglecting the smaller product $dV \cdot dF$, the above relation can be written as

$$\dot{h}_{\text{std}} = (F - D)(V + dV)/W_{\text{std}} + VdF/W_{\text{std}}$$

which after using Eq. (18.21) becomes

$$\dot{h}_{\text{std}} = (\dot{h}W/W_{\text{std}})(1 + dV/V) + VdF/W_{\text{std}} \quad (18.22)$$

Using Eqs. (18.15) and (18.16), the factor $(1 + dV/V)$ can be written as

$$(1 + dV/V) = V_{\text{std}}/V = \sqrt{T_{\text{std}}/T}$$

and Eq. (18.22) becomes

$$\dot{h}_{\text{std}} = \dot{h}(W/W_{\text{std}})\sqrt{T_{\text{std}}/T} + VdF/W_{\text{std}}$$

where \dot{h} , W , T , and V are the test values during flight test, dF is known from Eq. (18.18) or Eq. (18.19), and W_{std} and T_{std} are the known standard values. Hence the \dot{h}_{std} can be obtained from the above relation.

18.6.6.3 Wind correction. A wind of constant velocity, having no wind gradient, will not affect the rate of climb of an aircraft, regardless of its magnitude and direction. The existence of wind gradient (windshear) during climb, however, affects the climb performance of the aircraft. The wind correction, like most other corrections, is less valid if the error is large. Attempts should be made to minimize the wind error by flying in light, constant winds, or preferably in no-wind condition. The effect of wind is also minimized by flying the aircraft at 90 deg to the wind direction. A theoretical approach to the wind correction is presented in Chapter 14.

A good estimate of wind effects can also be obtained by flying successive climbs in opposite directions. This is shown in Fig. 18.14 where the positive wind gradient means the aircraft is climbing into an increasing headwind, and vice versa for the negative wind gradient. This also serves to locate the magnitude of wind error because the vertical displacement of the rate of climb from the median line will be a direct measure of the wind gradient as shown in the figure. The increase in headwind during climb will be sensed by the pitot-static tube as an increase in the airspeed of the aircraft. This will be corrected by the pilot by raising the nose of the aircraft, and the rate of climb will increase. The increase in headwind during a positive wind gradient increases the airspeed of the aircraft which in turn increases the rate of climb.

18.6.6.4 Weight correction. A departure from the standard weight of the aircraft affects its climb performance. The correction to standard weight can be made either by making partial climb tests, or level acceleration tests, for different weights and deducing the weight correction from these tests. In the following discussion the weight correction is obtained theoretically by a differential method.

It can be shown that a nonstandard weight of an aircraft affects its climb performance in two ways. First, a heavier-than-normal aircraft would require more energy from the engine due to increase in potential energy Wh for the same h ; this is called the *inertia effect*. Second, the heavier aircraft has higher wing loading and, therefore, for maintaining the same airspeed it must fly at higher angle of attack, this results in more induced drag. This is called the *induced drag effect* due to change in weight, and this additional drag must also be overcome by the engine.

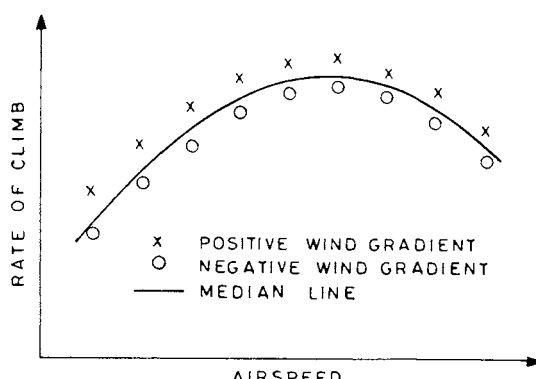


Fig. 18.14 Wind-gradient effect on rate of climb.

The inertia and induced drag effects will be evaluated here by assuming that the excess power $FV - DV$ is spent only in generating the rate of climb, and the energy spent in acceleration is negligible. The rate of climb is given by $(FV - DV)/W$. The variation of rate of climb with weight would be obtained by differentiating the above relation with respect to weight. This gives

$$d\dot{h}/dW = -(FV - DV)/W^2 - (V/W)dD/dW$$

which is based on the assumption that $dF/dW = 0$; this implies that the change in angle of attack due to weight will not affect the thrust. The above relation can be written as

$$d\dot{h} = -\dot{h}dW/W - (V/W)dD \quad (18.23)$$

Since $D = (1/2)\rho V^2 S C_{D_0} + (2K W^2 \cos^2 \gamma)/(\rho V^2 S)$, and considering that C_{D_0} is not affected by the change in weight,

$$dD = 2K \cos^2 \gamma dW^2 / (\rho V^2 S)$$

which represents the change in induced drag due to change in weight. Using the above relation, Eq. (18.23) becomes

$$d\dot{h} = -\dot{h}dW/W - 2K \cos^2 \gamma dW^2 / (W\rho V S)$$

Writing $d\dot{h} = \dot{h}_{std} - \dot{h}$, $dW = W_{std} - W$, and $dW^2 = W_{std}^2 - W^2$, the above equation becomes

$$\dot{h}_{std} = \dot{h}(2 - W_{std}/W) - 2K \cos^2 \gamma (W_{std}^2 - W^2) / (W\rho_{SSL}\sigma V S)$$

The first term on the right-hand side of the above relation is the inertia effect and the second term is the induced drag effect, due to change in weight from the standard weight of the aircraft.

18.6.6.5 Summary. The corrections are generally applied in the same order in which they are discussed in this section, starting from the tapeline altitude correction in Sec. 18.6.1 to the weight correction in Sec. 18.6.6.4. The attempt should always be to keep the test variables close to the standard values because the differential method of correction discussed in this section is valid only for small differences.

The reasons for various corrections can be summarized as follows: the tapeline altitude correction is due to nonstandard temperature, the true airspeed and thrust corrections are also due to nonstandard temperature, the wind correction is due to wind gradient (windshear) in the vertical direction, and the weight correction involving both inertia and induced drag effects is due to nonstandard weight.

18.7 Descent Performance Tests

Descending flight tests are usually carried out at idling power, or at no-power (engine inoperative), or for the gliders. An important purpose of these flights is to obtain airspeeds for maximum endurance and maximum range. The results are corrected for the standard conditions. The data collected from the descent flight tests also enable one to calculate lift curve slope and drag polar of the aircraft.

Descent performance tests are carried out by the method of partial descents which is similar to the method of partial climbs, except for the fact that the tests and measurements are conducted during the time of partial descent of the aircraft. This consists of a series of partial descents (Fig. 18.7) carried out in a test band of thickness $2\Delta h$ at different airspeeds. The tests are usually conducted at a constant IAS during each descending flight. This constant IAS is different in each succeeding descent. Since the band thickness $2\Delta h$ is small the true airspeed V can also be considered as constant, otherwise V can be taken as the mean value in the band.

From the measurements, the rate of descent \dot{h} , equivalent airspeed V_e , and the true airspeed V , can be determined. The angle of descent γ can be calculated from the measurements of \dot{h} and V , because $\gamma = \sin^{-1}(\dot{h}/V)$. The drag force can be calculated from Eq. (10.77) which can be written as, $D = F - W \sin \gamma - (W/g)dV/dt$, where F is estimated from the manufacturer's engine data. The lift force L can also be calculated because $L = W \cos \gamma$.

The variation of rate of descent against airspeed is shown in Fig. 18.15. The airspeed for maximum endurance V_{me} would be the one that gives the minimum rate of descent as shown in Fig. 18.15. The airspeed for minimum angle of descent $V_{\gamma_{min}}$ will be the one that exists at the point of tangent to the curve from the origin, as shown in the figure.

The variation of drag with airspeed is shown in Fig. 18.16 where the airspeed for minimum drag $V_{D_{min}}$ is also marked. In the case of gliding flight of a given aircraft, the airspeed for minimum drag is equal to the airspeed of minimum gliding angle (flattest glide).

From the data of L , D , and V_e for each succeeding descent flight test, the lift coefficient $C_L = 2(W/S)/(\rho_{SSL} V_e^2)$, and the drag coefficient $C_D = 2(D/S)/(\rho_{SSL} V_e^2)$ can be obtained. Since each partial descent test corresponds to a different α , and thus a different C_L and C_D , the plot of C_D against C_L^2 would give the drag polar in the form of a straight line.

It should be remembered that D and α are function of the weight of the aircraft which is continuously changing during flight due to fuel consumption. Therefore, D and α of each succeeding descent would correspond to a different weight. Also the repetition of a particular airspeed at different weights will result in a different rate of descent, a different angle of attack, and consequently a different drag. This, therefore, requires that the results of all succeeding partial descents be related (corrected) to a representative standard weight. However, the experimental scatter is usually such that a weight difference of about 2% of the standard weight can be

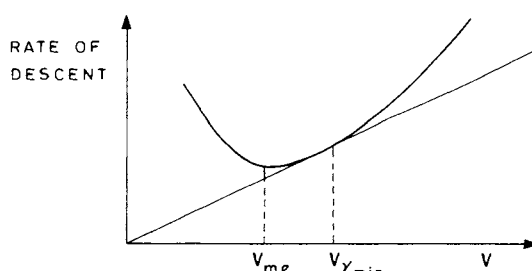


Fig. 18.15 Variation of rate of descent with airspeed.

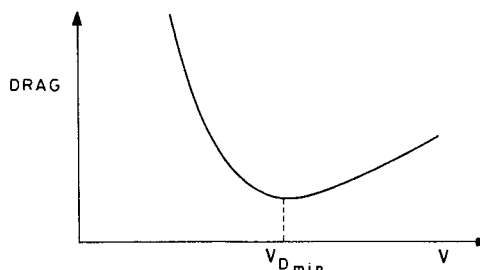


Fig. 18.16 Variation of drag with airspeed.

ignored. This mean that the weights of 10,200 kg_f and 9800 kg_f at the first and last test points, respectively, should have a standard weight of 10,000 kg_f, and the results may be treated as a mean within the error band.

The descent data reduction process for turbojets is the same as that for climb data reduction discussed above.

18.8 Cruise Performance Tests

Cruise performance tests for both turbojet and reciprocating engine aircraft are explained here. The cruise performance of turbojet engine aircraft is discussed first followed by the reciprocating engine aircraft.

18.8.1 Constant Weight to Pressure Ratio Method

Performance curves of cruising flight of a turbojet aircraft are obtained here in parametric form. These curves can be cross-plotted and presented in a form that can quickly yield maximum range and maximum endurance if the fuel consumed during the cruise is known.

18.8.1.1 Aircraft configuration–engine combination characteristics. It was seen in Chapter 8 on cruising flight that the thrust required F by the aircraft configuration can be expressed in functional form as

$$F/\delta = f(W/\delta, M) \quad (18.24)$$

where $\delta = p/p_{SSL}$, p is the ambient atmospheric pressure at the test altitude, W is the all-up weight of the aircraft. Similarly, in Chapter 4 it is seen that certain characteristics of a turbojet engine can be expressed in functional form as

$$N/\sqrt{\theta} = f(F/\delta, M) \quad (18.25)$$

and

$$\dot{W}_f / (\delta \sqrt{\theta}) = f(N/\sqrt{\theta}, M) \quad (18.26)$$

where $\theta = T/T_{SSL}$, T is the absolute temperature of ambient atmosphere, N is the engine rpm, and \dot{W}_f is the fuel flow rate.

It is possible to combine Eqs. (18.24–18.26) by writing the aircraft configuration–engine combination characteristics as

$$N/\sqrt{\theta} = f(W/\delta, M) \quad (18.27)$$

and

$$\dot{W}_f / (\delta \sqrt{\theta}) = f(N/\sqrt{\theta}, W/\delta) \quad (18.28)$$

The solutions represented by Eqs. (18.27) and (18.28) can be obtained from flight tests.

The aircraft is flown at the required altitude at a constant Mach number. If the aircraft has stabilized within 2% of the desired W/δ , it is flown for at least 1 min such that its airspeed does not change more than 3.7 km/h (2 kn). The values of W , p , T_i , V_i , N and \dot{W}_f are recorded at the beginning and end of the constant W/δ flight of short duration. The mean values of these values are taken for the purpose of calculations or drawing graphs. Similarly, the flight tests are carried out at the other desired altitudes corresponding to different values of W/δ . Typical sets of graphs obtained from these flight tests are shown in Figs. 18.17 and 18.18, representing the solutions of Eqs. (18.27) and (18.28). As the values of W/δ and $N/\sqrt{\theta}$ are known at a particular altitude, Figs. 18.17 and 18.18 can predict the Mach number and the fuel flow rate, respectively, during the cruising flight. The range and endurance can also be deduced if the total fuel consumed during the cruise is known.

18.8.1.2 Maximum range and maximum endurance. The curves of Figs. 18.17 and 18.18 do not directly give the maximum range and maximum endurance of the cruising flight. These curves can be cross-plotted in a form that considerably facilitate the process of obtaining the maximum range and maximum endurance of the cruising flight. The subscripts mrf and brf will be used to denote the conditions of maximum and best range factors, respectively. The conditions of maximum and best endurance will be denoted by the subscripts me and be, respectively.

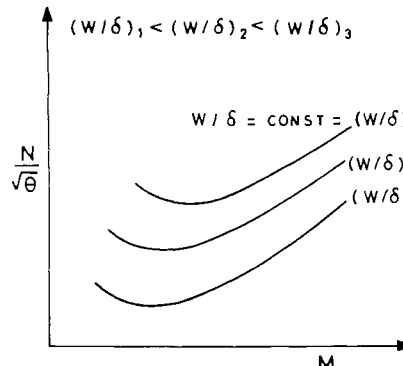


Fig. 18.17 $N\sqrt{\theta}$ versus M .

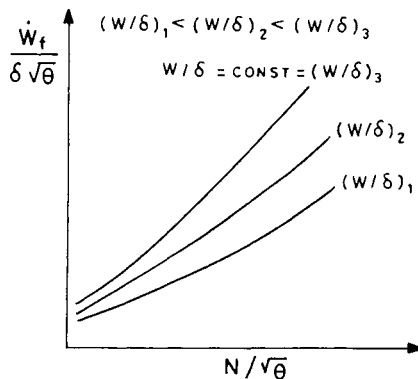


Fig. 18.18 $\dot{W}_f/\delta\sqrt{\theta}$ versus $N/\sqrt{\theta}$.

From Figs. 18.17 and 18.18, or from the data accumulated during flight tests, it is possible to obtain Figs. 18.19 and 18.20. Figure 18.19 is the plot of the range factor WV/\dot{W}_f against M for different fixed values of W/δ . The peaks of these curves in Fig. 18.19 show the maximum range factors and their Mach numbers, and the locus of these peaks is shown by a dashed line in the figure. Similarly, Fig. 18.20 is the plot of a measure of fuel flow rate $\dot{W}_f/\delta\sqrt{\theta}$ against the Mach number for different values of W/δ . Each curve exhibits an optimum value (minimum) of $\dot{W}_f/\delta\sqrt{\theta}$ and the corresponding Mach number. The locus of these optimum values is shown by a dashed line in the figure.

Figure 18.19 can be cross-plotted to produce Figs. 18.21a and 18.21b. Figure 18.21a is obtained by noting the values of maximum range factor (RF_m) and the corresponding W/δ along the dashed line of Fig. 18.19. Similarly, Fig. 18.21b is obtained by noting the values of the Mach number (M_{mrf}) for the maximum range factor, and the corresponding W/δ along the dashed line in Fig. 18.19. Figures 18.21a and 18.21b give the values of the maximum range factor and its Mach number, respectively, for different values of W/δ . The best (largest) range factor (RF_{br}) is marked by the horizontal dashed line in Fig. 18.21a, and the corresponding values of W/δ and M are shown in Figs. 18.21a and 18.21b, respectively, by

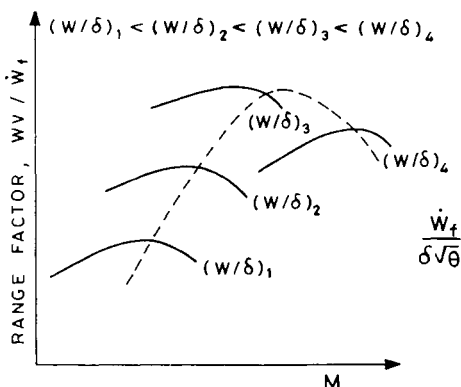


Fig. 18.19 WV/\dot{W}_f versus M .

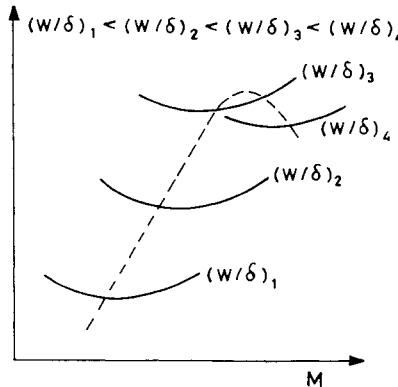


Fig. 18.20 $\dot{W}_f/\delta\sqrt{\theta}$ versus M .

dashed lines. This helps in finding the maximum range and the best (largest) range if the total fuel consumed W_f , δ , and θ are known during the cruise.

Figure 18.20 can also be similarly cross-plotted, by reading the values along its dashed line, and the two curves, $(\dot{W}_f/\delta\sqrt{\theta})_{me}$ versus W/δ , and M_{me} versus W/δ , can be obtained as shown in Figs. 18.22a and 18.22b, respectively. These two curves predict the values of W/δ and M for minimum $\dot{W}_f/\delta\sqrt{\theta}$. The fuel flow rate $(\dot{W}_f/\delta\sqrt{\theta})_{be}$ for best endurance is marked by the horizontal dashed line in Fig. 18.22a, and the corresponding values of $(W/\delta)_{be}$ and M_{be} are shown in Figs. 18.22a and 18.22b, respectively, by dashed lines. This helps to obtain the maximum endurance and the best (longest) endurance if the total fuel consumed W_f , δ , and θ are known during the cruise.

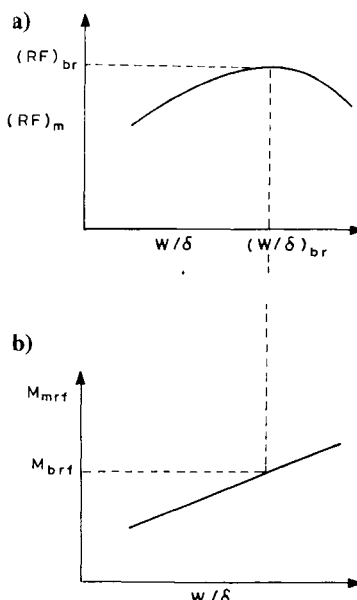


Fig. 18.21 Maximum range parameters: a) range factor and b) Mach number.

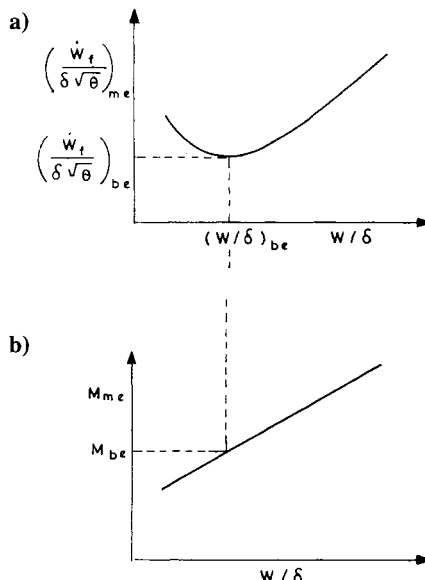


Fig. 18.22 Maximum endurance parameters: a) fuel flow rate parameter and b) Mach number.

18.8.2 Constant Altitude Method for Piston-Prop Aircraft

The cruise performance testing of a piston-prop aircraft is explained here. A commonly used speed-power test is considered that can yield the drag polar, maximum range, and maximum endurance.

18.8.2.1 Speed-power test. The variation of power with airspeed can be expressed in the form of a parametric relationship that can be presented graphically by flight tests. The theory behind this relationship is presented here first before describing the tests.

The expression for thrust power can be written as

$$P = TV = DV = (1/2)C_{D_0}\rho_{SSL}\sigma V^3 S + 2K W^2 / (\rho_{SSL}\sigma V S)$$

which gives

$$P \sqrt{\sigma} = (1/2)C_{D_0}\rho_{SSL}(V \sqrt{\sigma})^3 S + 2K W^2 / (\rho_{SSL} V \sqrt{\sigma} S)$$

On introducing the equivalent airspeed $V_e = V \sqrt{\sigma}$, the above relation becomes

$$P \sqrt{\sigma} = (1/2)C_{D_0}\rho_{SSL}V_e^3 S + 2K W^2 / (\rho_{SSL} V_e S)$$

The thrust power $P = k\eta_p P_e$, where P_e is the engine power, η_p is the propeller efficiency, and k is the conversion factor as explained in Chapter 5.

Let W_{std} be the standard weight of the aircraft which is suitably chosen. Dividing the above relation throughout by $(W/W_{std})^{3/2}$ and rearranging it, gives

$$\frac{k\eta_p P_e \sqrt{\sigma}}{(W/W_{std})^{3/2}} = \frac{1}{2}\rho_{SSL}C_{D_0}S\left(\frac{V_e}{\sqrt{W/W_{std}}}\right)^3 + \frac{2K W_{std}^2}{\rho_{SSL}S(V_e/\sqrt{W/W_{std}})} \quad (18.29)$$

Introducing the four quantities P_{iw} , V_{iw} , K_1 , and K_2 as

$$P_{iw} = (k\eta_p P_e \sqrt{\sigma}) / (W/W_{std})^{3/2}, \quad V_{iw} = V_e / \sqrt{W/W_{std}} \quad (18.30)$$

$$K_1 = (1/2)\rho_{SSL} C_{D_0} S, \quad \text{and} \quad K_2 = 2K / (\rho_{SSL} S) \quad (18.31)$$

Equation (18.29) can be written as

$$P_{iw} = K_1(V_{iw})^3 + K_2 W_{std}^2 / V_{iw} \quad (18.32)$$

If the design parameters C_{D_0} and K are known for a given aircraft, the constants K_1 and K_2 become known quantities. Equation (18.32) gives the exact relationship between P_{iw} and V_{iw} , and the values of P_{iw} can be plotted against V_{iw} .

The curve of P_{iw} versus V_{iw} is, however, obtained through flight tests, and the speed-power test method is called the *Piw-Viw* method.

The flight tests are conducted at different altitudes with different airspeeds so that they cover the complete flight envelope of altitudes and airspeeds. The speed-power test is conducted for at least four different altitudes ranging from near sea level to the near-maximum altitude of the aircraft. At each altitude, the test should be conducted for five different constant (stabilized) airspeeds, and at least two of these should be in the low-speed range belonging to the back side of the power required curve. The items that need be recorded are h_i , V_i , rpm, ambient atmospheric temperature, manifold pressure, carburetor air temperature, fuel flow rate, and any other quantity that may be desirable. From these data records, the values of V_{iw} and P_{iw} can be obtained from the relations of Eq. (18.30), where P_e is found from the available engine performance charts. Therefore, the values of P_{iw} can be plotted against V_{iw} .

The data scatter can be more appropriately accounted for by plotting the product $P_{iw} \cdot V_{iw}$ against $(V_{iw})^4$, which according to Eq. (18.32) is a straight line. Thus, a straight line can be drawn through the data points shown in Fig. 18.23. From this straight line the plot of P_{iw} vs V_{iw} can be obtained as shown in Fig. 18.24.

18.8.2.2 Drag polar from *Piw-Viw* method. The P_{iw} vs V_{iw} curve obtained by flight tests in the Sec. 18.8.2.1 is quite convenient for establishing the drag polar of the aircraft. The lift coefficient of the aircraft can be written as

$$C_L = \frac{2W}{\rho V^2 S} = \frac{2(W/W_{std}) W_{std}}{\rho_{SSL} V_e^2 S} = \frac{2W_{std}}{\rho_{SSL} S (V_e / \sqrt{W/W_{std}})^2}$$

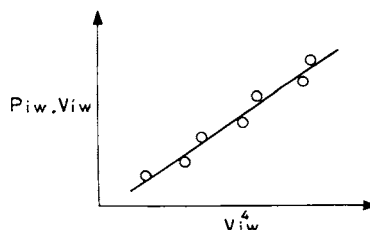
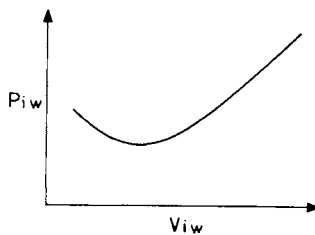


Fig. 18.23 $P_{iw} \cdot V_{iw}$ versus $(V_{iw})^4$.

Fig. 18.24 P_{iw} versus V_{iw} .

which gives

$$C_L = 2W_{std}/\{\rho_{SSL}(V_{iw})^2 S\} \quad (18.33)$$

Similarly the drag coefficient of the aircraft can be written as

$$C_D = \frac{2D}{\rho V^2 S} = \frac{2P}{\rho_{SSL}\sigma V^3 S} = \frac{2k\eta_p P_e}{\rho_{SSL}\sigma V^3 S} = \frac{2Piw}{\rho_{SSL}S(V_e/\sqrt{W/W_{std}})^3}$$

which gives

$$C_D = 2Piw/\{\rho_{SSL}(V_{iw})^3 S\} \quad (18.34)$$

In Eqs. (18.33) and (18.34), the W_{std} , ρ_{SSL} , and S are known quantities, the values of P_{iw} and V_{iw} can be read from the curve of Fig. 18.24, which is obtained from flight tests. When these values are substituted in Eqs. (18.33) and (18.34), they establish the curve of C_D versus C_L , which is the required drag polar curve of the aircraft. On plotting this curve in the form of C_D versus C_L^2 , it can yield the values of C_{D_0} and K .

18.8.2.3 Maximum range and maximum endurance. The speed-power flight tests collect data for the fuel flow rates at various altitudes, gross (total) weights, and airspeeds, that sufficiently cover the operating envelope of the aircraft. The fuel flow rate against the Mach number can be presented by Fig. 18.25. Each curve of this figure represents one altitude and one gross weight; this means that W/δ of each curve is different. The optimum point on each curve gives the

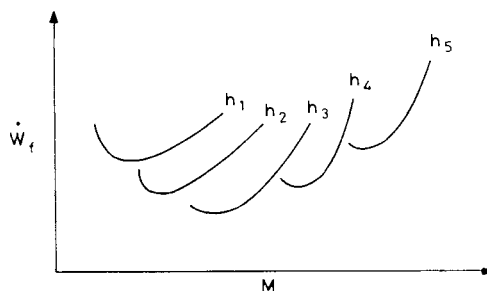
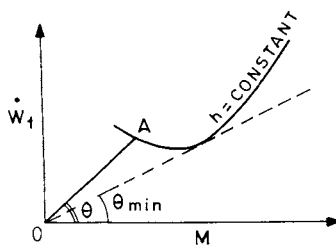


Fig. 18.25 Fuel flow rate versus Mach number at different altitudes.

Fig. 18.26 \dot{W}_f versus M at fixed altitude.

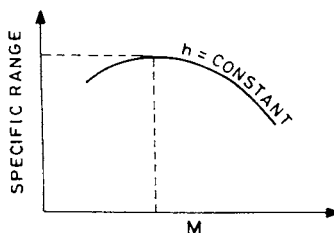
minimum \dot{W}_f (and thus corresponds to maximum endurance) and the corresponding Mach number.

Each curve of Fig. 18.25 can yield the specific range against Mach number. As an example, consider a curve of Fig. 18.25 which is drawn in Fig. 18.26. At point A on the curve, the specific range (SR) would be given by

$$SR = V/\dot{W}_f = Ma/\dot{W}_f = a/\tan\theta$$

where a is the speed of sound at the fixed altitude, and θ is the angle made by the line OA with the Mach number line; the tangent drawn from the origin to the curve gives θ_{min} , which is the minimum value of θ that corresponds to the maximum SR at the altitude under consideration. Therefore, from Fig. 18.26 another Fig. 18.27 can be drawn for specific range versus Mach number; the dashed horizontal and vertical lines in Fig. 18.27 mark, respectively, the maximum SR and its Mach number for the altitude under consideration. Thus, the specific range versus Mach number curves for different altitudes, shown in Fig. 18.28, can be constructed from the corresponding curves of Fig. 18.25. These different curves of Fig. 18.28 can, however, also be obtained directly from the data accumulated from the speed-power test.

Each flight test of the cruise being of short duration, the constant altitude flight can also be regarded as a constant W/δ flight. From Fig. 18.25, the two Figs. 18.29a and 18.29b can be drawn by knowing the values of \dot{W}_f and M at the optimum point of each constant h (or constant W/δ) curve. These two curves give the fuel flow rate and Mach number for maximum endurance at different W/δ ; their values for the best endurance can also be selected as shown by the dashed lines in the figure. Similarly, from Fig. 18.28, the two Figs. 18.30a and 18.30b can be drawn that give the specific range and Mach number for the maximum range at different W/δ ; their values for the best range can also be selected as shown by the dashed lines in the figure.

Fig. 18.27 Specific range versus M at fixed altitude.

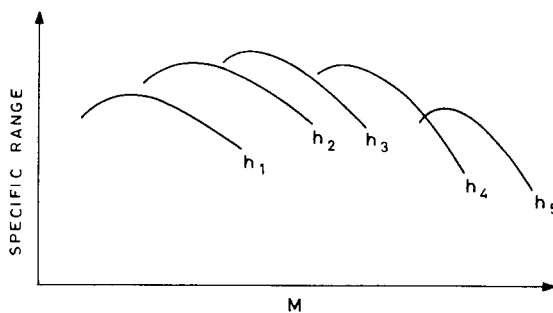


Fig. 18.28 Specific range versus Mach number at different altitudes.

18.9 Turning Performance Tests

The higher maneuverability requires more lift and more thrust. The maximum lift is limited by the aerodynamic reasons and the maximum thrust is limited by the engine thrust considerations. These give rise to lift and thrust boundaries of maneuvering flight which will be obtained here through flight tests. The results will be presented graphically in the form of maneuver boundaries, showing the effect of three important variables—load factor, airspeed, and altitude.

18.9.1 Lift Boundary Tests

The lift boundary tests are conducted at or near the stall. The lift boundary is caused by aerodynamic limitation of usable lift. The lift is given by

$$L = (1/2)C_L \rho V^2 S = (0.5\gamma p_{SSL} S) C_L M^2 \delta$$

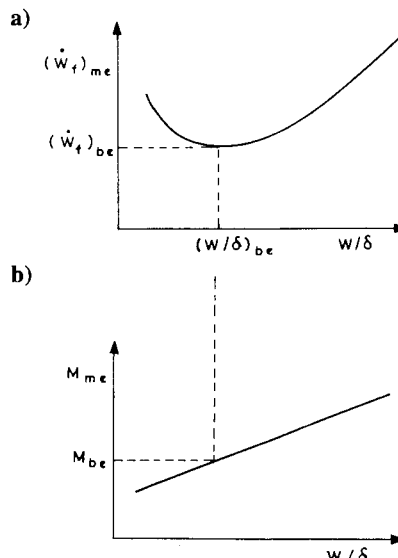


Fig. 18.29 Maximum endurance parameters for piston-prop aircraft: a) \dot{W}_f with w/δ and b) Mach number with w/δ .

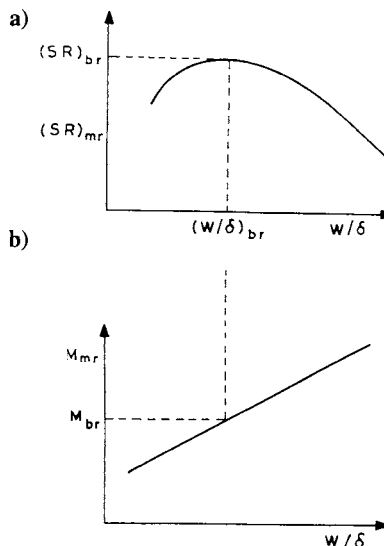


Fig. 18.30 Maximum range parameters for piston-prop aircraft: a) maximum specific range with W/δ and b) Mach number with W/δ .

Writing $L = nW$, the above relation can be written as

$$nW = (0.5\gamma p_{SSL}S)C_L M^2 \delta \quad (18.35)$$

For maneuvering a given aircraft, additional lift (and thus additional n) is required, which is obtained by increasing the angle of attack of the wing. With the increase in angle of attack, the wing will eventually stall so that the lift coefficient cannot be increased beyond its maximum value $C_{L,m}$, which is obtained at the stalling angle. Consequently, this also sets an upper limit to the load factor n that can be used for the maneuvering flight. Therefore, Eq. (18.35) at the lift boundary becomes

$$(nW/\delta)_m = (0.5\gamma p_{SSL}S)C_{L,m} M^2 \delta$$

where the subscript m refers to maximum value for a given aircraft. The above relation in functional form can be expressed as

$$(nW/\delta)_m = f(C_{L,m}, M) \quad (18.36)$$

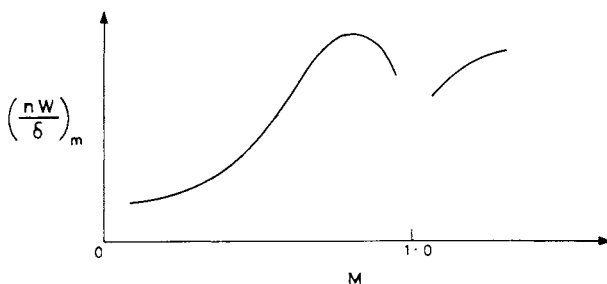


Fig. 18.31 $(nW/\delta)_m$ versus Mach number for lift boundary.

The maximum lift coefficient $C_{L,m}$ is a constant quantity at low speeds or at incompressible flow Mach numbers, otherwise it would depend on Mach number.

In the case of aircraft operating at $C_{L,m}$ during the maneuver, Eq. (18.36) becomes

$$(nW/\delta)_m = f(M)$$

The $(nW/\delta)_m$ versus M curve is obtained from flight tests. The lift boundary in a flight test can be easily achieved if the thrust boundary of the aircraft is higher than the lift boundary. The aircraft is first flown in straight level flight, then n (and thus ϕ) is increased such that its airspeed slows at the rate of 1 kn per second, and the altitude is kept constant. The moment the aircraft shows stalling behavior, the readings of n , airspeed, fuel count, and ambient temperature, are noted. The test is repeated at different airspeeds and altitudes to obtain the curve shown in Fig. 18.31. It becomes difficult to fly and take reliable measurements in the transonic region, which leads to some gap in the curve. From this $(nW/\delta)_m$ versus M plot, different curves of n versus M can be drawn for reference weight at different altitudes. These are the lift boundary curves that are finally used by the pilots.

The lift boundary is generally applicable to combat aircraft requiring higher instantaneous rates of turns. The design of a military combat aircraft caters to a lift boundary higher than the thrust boundary. In such a case, the aircraft cannot be stabilized at a particular speed and altitude to reach the lift boundary. The lift boundary can, however, be reached in a dive turn for a particular speed by utilizing the potential energy. The aircraft is first stabilized at the required speed at a higher altitude above the test altitude. Then the aircraft is put in a diving turn to maintain the speed, and increase n until stall condition is reached at the test altitude; such a maneuver is called a windup turn.

In the above, the maximum lift coefficient $C_{L,m}$ is considered as the limiting boundary. However, the maximum lift coefficient is not always the usable boundary. Because of buffeting, wing rock, yaw divergence, etc. the usable C_L may be lower than the maximum lift coefficient. This gives rise to buffet boundary, wing rock boundary, or yaw divergence boundary, and these boundaries can be similarly obtained as the $C_{L,m}$ boundary discussed above. These boundaries do not limit the aircraft to level flight and presupposes a dynamic situation in which g -levels may be changing quite rapidly. The lift boundary test, therefore, becomes subjective, depending on how the pilot defines the stall.

18.9.2 Thrust Boundary Tests

An aircraft in turning flight has higher drag than in level flight for the same constant airspeed and so more thrust is required in turning. An increase in n for turning requires an increase in thrust, and eventually a condition may be reached when all available thrust is being used for sustaining the aircraft in level flight. Any further increase in n (or bank angle) will be achieved only by losing altitude of the aircraft. The thrust boundary shows the maximum value of n that can be maintained at a given power setting in turning flight, without changing the airspeed and altitude. There are both direct and indirect methods of determining the thrust boundary by flight tests that are discussed below.

18.9.2.1 Thrust limited stabilized turn test (direct method). The excess power required to change height and airspeed in a maneuver is given by Eq. (18.3) as

$$(F - D)V/W = dh/dt + (V/g)dV/dt$$

In a stabilized turn the altitude and airspeed are constant, consequently both the terms on the right hand side of the above relation would be zero. Therefore, in a stabilized turn,

$$F = D \quad (18.37)$$

In a thrust limited stabilized turn, the thrust (=drag) is kept constant; this constant thrust is usually either military thrust or maximum thrust in the case of a combat aircraft. This is also called *sustained turn*.

From Eqs. (18.37) and (11.7) it follows that

$$F/\delta = (1/2)C_{D_0}\gamma p_{SSL}M^2S + 2K(nW/\delta)^2/(\gamma p_{SSL}M^2S)$$

For a given aircraft the above relation in functional form can be written as

$$(nW/\delta) = f(F/\delta, M) \quad (18.38)$$

which shows that if the thrust and altitude (and thus δ) are fixed, the load factor is a function of Mach number only. Also from Eq. (18.25)

$$F/\delta = f(N/\sqrt{\theta}, M) \quad (18.39)$$

which implies that if the aircraft is flying at constant values of N , M , and altitude (and thus δ and θ), the thrust force also gets fixed. Equation (18.38) after using Eq. (18.39) becomes

$$(nW/\delta) = f(N/\sqrt{\theta}, M) \quad (18.40)$$

It shows that if the N and altitude are fixed, the load factor for a given aircraft is function of Mach number only.

The variation of N with M , for a limited (fixed) thrust at constant altitude, is called thrust boundary. This can be directly obtained at any fixed altitude by making stabilized turns at different airspeeds (Mach numbers), hence it is called *direct method*. In the stabilized turns, the load factor, airspeed, and altitude, are kept constant. It is far more important to maintain a constant airspeed (Mach number) than to be exactly on the aim airspeed (Mach number). A constant airspeed anywhere within 18.5 km/h (10 kn) of the desired (aim) airspeed is satisfactory, except when the desired airspeed happens to be maximum or minimum airspeed.

The aircraft is first stabilized in straight level flight at the desired airspeed. The aircraft is then rolled smoothly into the turn with power advanced (i.e., rpm increased) as the load factor increases, to maintain the same constant airspeed. Once stabilized in the turn, maintain the load factor constant if it can be measured accurately, and hold the airspeed and altitude constant with small bank angle adjustments. If the bank angle can be measured accurately, ϕ is held constant.

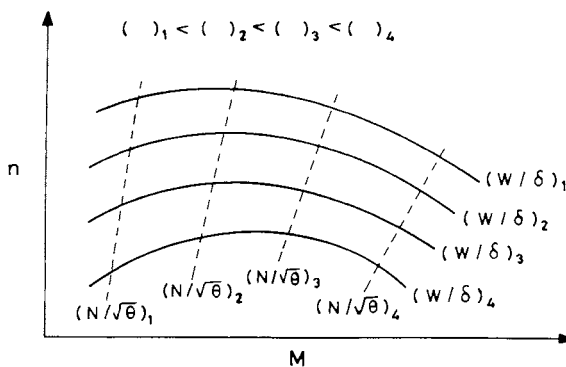


Fig. 18.32 Thrust boundary curves.

The object during the turn is to keep the following quantities constant which in the order of importance can be written as, load factor, airspeed, altitude, and bank angle. The stabilized turn of 360 deg is made, and the average values of these quantities are taken if they change during the full turn.

The flight tests are carried out at constant W/δ (i.e., at constant altitude, if W has the same value each time) for different Mach numbers, covering the entire range between the minimum and maximum Mach numbers. Repeating the tests for different constant values of W/δ , the curves in the form shown in Fig. 18.32 can be obtained. The lines of constant $N/\sqrt{\theta}$ are also shown in the figure by dashed lines. Along the lines of constant $N/\sqrt{\theta}$, the value of M can be read and nW/δ can be calculated. This will yield the curves of nW/δ versus M for different constant values of $N/\sqrt{\theta}$, as shown in Fig. 18.33. This is the graphical representation of the thrust boundary parameters given by Eq. (18.40). For the given values of aircraft weight W , atmospheric pressure (and thus δ), atmospheric temperature (and thus θ), and engine rpm (denoted by N), the corresponding curves of n against M can be obtained as shown in Fig. 18.34; these are the curves used by pilots.

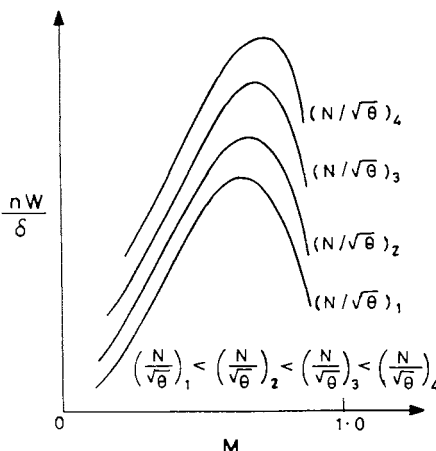


Fig. 18.33 Parametric representation of thrust boundary.

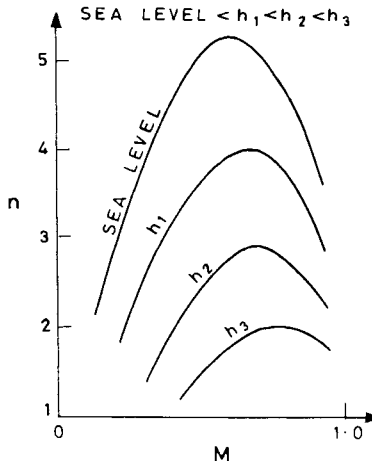


Fig. 18.34 Thrust boundary at different altitudes.

18.9.2.2 Accelerated-level decelerated-turn test (indirect method).

The aircraft during the test is first accelerated in straight level flight which is followed by a controlled level deceleration in turn by increasing n (and thus bank angle). This is called the *indirect method* because the aircraft does not fly on the thrust boundary as in the direct method discussed above. The indirect method is based on the fact that the excess thrust can be used in different ways, and having measured it in one way, it is possible to calculate the aircraft's performance in another way; this philosophy is the same one that was used earlier in one of the climb performance tests.

The theoretical basis of the indirect method is first explained here by writing the expression of the specific excess power \dot{h}_e (or P_s) as

$$\dot{h}_e = (F - D)V/W = dh/dt + (V/g)dV/dt \quad (18.41)$$

Making use of the expression for drag $D = (C_{D_0} + KC_L^2)\rho V^2 S/2$, the first relation above becomes

$$F = (1/2)C_{D_0}\rho V^2 S + 2K(nW)^2/(\rho V^2 S) + Wh_e/V$$

which can also be written as

$$F/\delta = (C_{D_0}\gamma p_{SSL}S/2)M^2 + \{2K/(\gamma p_{SSL}S)\}(n^2 W^2/\delta^2)(1/M^2) + Wh_e/(V\delta) \quad (18.42)$$

This shows that for a given aircraft

$$Wh_e/(V\delta) = f(F/\delta, M, n^2 W^2/\delta^2) \quad (18.43)$$

If the thrust, altitude, and Mach number are kept constant during the maneuver, the above functional relationship simplifies to

$$Wh_e/(V\delta) = f(n^2 W^2/\delta^2) \quad (18.44)$$

and Eq. (18.42) shows that this functional relationship would be linear.

The existence of linear relationship mentioned above provides considerable simplification to the flight test, because by obtaining the values of $W\dot{h}_e/(V\delta)$ for two different values of $(nW/\delta)^2$ at a constant Mach number, the straight line can be drawn. This straight line would give the value of $(nW/\delta)^2$ for $W\dot{h}_e/(V\delta) = 0$, i.e., for $\dot{h}_e = 0$, which corresponds to $F = D$. Since W and δ are known quantities, the value of n for the corresponding M can be obtained. Similarly, from different straight lines, the values of n for different M can be obtained which form the thrust boundary. If the test is conducted well, and with good luck, the thrust boundary for all the Mach numbers lying between the minimum and maximum airspeeds, can be obtained in a single run for the test altitude—the significance of the indirect method lies in the fact that a considerable time is saved. The method of obtaining the thrust boundary through flight test is explained below.

The test is performed by initially stabilizing the aircraft near minimum airspeed at the test altitude, then opening the throttle quickly and smoothly. The aircraft is allowed to accelerate but the altitude is maintained constant. When the aircraft has stabilized at its maximum level airspeed, it is rolled for a smooth level turn, maintaining the same altitude and engine rpm. The aircraft is rolled slowly so that the airspeed falls slowly and steadily, at a rate that does not exceed 1 kn/s, or preferably even more slowly.

The overall time of the above test, consisting of straight level acceleration followed by controlled level deceleration in turning, is divided into a convenient number of time intervals, say about 20 s each. The airspeed, altitude, time, ambient air temperature, and fuel counts are recorded at these intervals. The values of the acceleration and the rate of change of height can be estimated for the mid-points of the selected intervals. The acceleration is calculated from the measurement of velocity at the neighboring intervals. The altitude is supposed to be kept constant during the test, but if it changes, the correction must be applied by invoking the right-hand-side term $d\dot{h}/dt$ of Eq. (18.41) for \dot{h}_e .

From the above test, $W\dot{h}_e/V\delta$ and $(nW/\delta)^2$ can be obtained for different Mach numbers, which are plotted separately in Figs. 18.35a and 18.35b, respectively. The curve AB in Fig. 18.35a, and $A'B'$ in Fig. 18.35b, correspond to the level acceleration part of the test flight. Similarly, the curves BC in Fig. 18.35a, and $B'C'$ in Fig. 18.35b, belong to the decelerated turning part of the test flight. At any fixed Mach number, say $M = M_1$, the values of $\dot{h}_e/V\delta$ at A_1 , and $(nW/\delta)^2$ at A'_1 , belonging to level acceleration, are noted and marked with a cross (X) on the positive side of the graph in Fig. 18.36. Similarly, for the same Mach number M_1 , the values of $\dot{h}/V\delta$ at C_1 and $(nW/\delta)^2$ at C'_1 are read, belonging to the decelerated turn, and are marked with a cross (X) on the negative side of the graph in Fig. 18.36 because in the decelerated turn, \dot{h}_e would be negative. These two cross marks belonging to the Mach number M_1 are joined by a straight line, because it was shown above that the curve of $\dot{h}_e/V\delta$ versus $(nW/\delta)^2$ would be linear. Therefore, for different Mach numbers, the different straight lines shown in Fig. 18.36 can be obtained. Along the horizontal axis of Fig. 18.36, $\dot{h}_e = 0$ (i.e., $F = D$), the values of $(nW/\delta)^2$ and M can be read to produce the graph of (nW/δ) versus M as shown in Fig. 18.37. Since the aircraft weight W (or reference weight) and the atmospheric pressure ratio δ are known quantities, the curves of n versus M for the fixed weight can be generated from 18.37 for different altitudes, and one such curve for a fixed altitude is shown in Fig. 18.38.

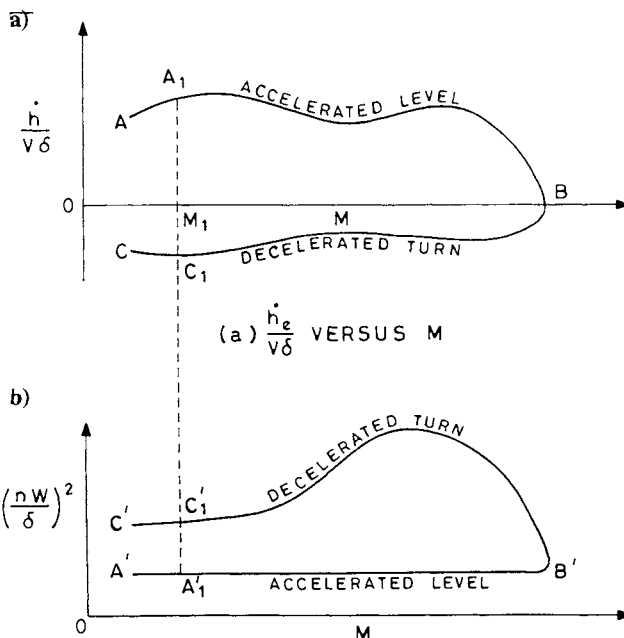


Fig. 18.35 Flight test curves for thrust boundary: a) $\dot{h}_e / V\delta$ versus M and b) $(nW/\delta)^2$ versus M .

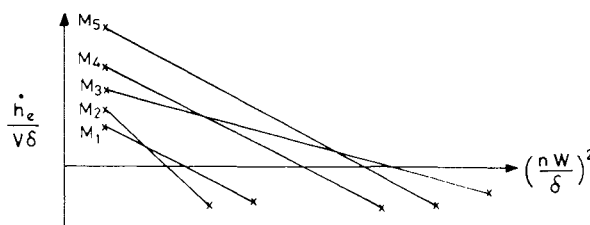


Fig. 18.36 Linear variation of $\dot{h}_e / V\delta$ with $(nW/\delta)^2$.

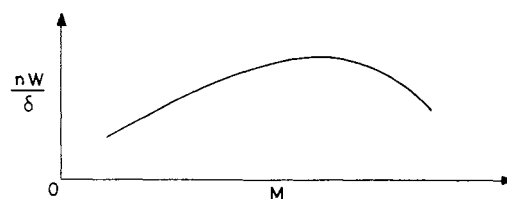


Fig. 18.37 Variation of nW/δ with Mach number.

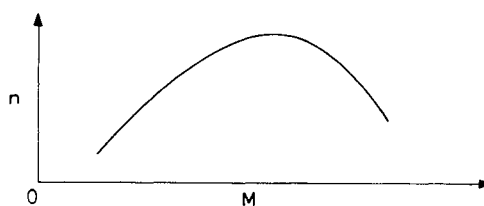


Fig. 18.38 Thrust boundary curve at fixed altitude and fixed weight.

It can be remarked here that it is not essential that a decelerated turn be made after level acceleration to obtain a straight line in Fig. 18.36. The straight line can also be obtained by making, instead, another level acceleration at different altitude but having the same engine setting ($N/\sqrt{\theta}$) as in the first level acceleration. The underlying idea is that the other cross point need not necessarily be on the negative side of the graph, as in Fig. 18.36, for obtaining a straight line. It can also be on the positive side of the graph but this would require another accelerated flight at a different altitude, and the accuracy of the inclination of the straight line may also decrease.

Once the n versus M plot is found, the rate of turn and radius of turn can be calculated at various altitudes. This gives rise to the curves of rate of turn versus Mach number, each curve belonging to a different altitude. Similarly, curves showing the radius of turn versus Mach number can be drawn for different altitudes.

References

¹Herrington, R. M., et al., *Flight Test Engineering Hand Book*, Rev. ed., Air Force TR 6273, Jan. 1966.

²Durbin, E. J., et al. (eds.), *Flight Test Manual, Vol. 1—Performance*, Rev. ed., AGARD, Pergamon, New York, 1962.

³Performance Testing (notes), Empire Test Pilot School, England, UK.

⁴Performance Phase Textbook Vol. 1, AF-TPS-CUR-86-01, U.S. Air Force Test Pilot School, Edwards, AFB, CA, 1986.

⁵Layton, D., *Aircraft Performance*, Matrix, 1988.

Problems

In the multiple choice problems below, mark the correct answer.

18.1 What is the necessity of flight testing?

18.2 The temperature recovery factor is introduced to modify the kinetic term in the ratio of total temperature to static temperature if the flow process is a) nonadiabatic, b) nonisothermal, c) nonisentropic.

18.3 In a straight and level stabilized flight of an aircraft at 400 and 100 kn, the longitudinal accelerations recorded along the wind axis were 0.45 and 0.177 kn/s, respectively, and the vertical accelerations recorded were 1.01 and 0.99 kn/s, respectively. Find the angles of attack at these speeds.

18.4 Is it possible to determine Oswald's span efficiency factor e from flight tests? Justify your answer.

18.5 How is stalling speed defined by the aviation regulations?

18.6 Why is the measurement of stall speed done at a bleed rate of 1 kn/s or slower?

18.7 From flight tests the stalling speed in level flight of an aircraft is found to be 60 kn (111.12 km/h) in clean configuration. If the test crew plans to find out the stalling speed of the aircraft in the clean configuration in turning flight, at what speeds they may expect the aircraft to stall in the banked turns of 45 and 60 deg.

18.8 What kinds of equipment used to collect external data during the takeoff flight tests? What information do they yield?

18.9 Why is there generally more data scatter in landing flight tests?

18.10 The total weight of a two-seater aircraft is 1700 kg_f and the corresponding minimum landing speed is 83.34 km/h (45 kn). A test pilot was required to fly this aircraft as a single seater. The reduction in weight due to the absence of the second member is 80 kg_f . What minimum landing speed can be expected at this weight of the aircraft?

18.11 At sea level test flights the landing speed of a light aircraft is found to be 92.6 km/h (50 kn). If the test crew has to do landing tests at an airfield with 1524 m (5000 ft) elevation, what landing speed can be expected? Assume the weight of the aircraft to be the same in the two cases.

18.12 By measuring level acceleration performance, the climb performance can be estimated because a) the specific excess power can be used purely in climb or purely in level acceleration, b) the specific excess power is the sum of climb and acceleration performance, c) both the above items (a and b) exist.

18.13 What assumption is made in using the level acceleration performance of the aircraft for the purpose of estimating its climb performance.

18.14 What are the advantages of the level acceleration test as compared to the sawtooth climb test?

18.15 Explain why the test of climb to ceiling is carried out.

18.16 Enumerate the various corrections applied to the climb schedule and briefly state the reasons for these corrections.

18.17 An aircraft is flying level at 5 km pressure altitude and its speed is 257.2 m/s (500 kn). Calculate its energy height and state any of the assumptions made.

18.18 Which of the following statements is not correct: a) The energy height of an aircraft is always higher than its geometric height. b) The energy rate of climb

dh_e/dt , can be positive even if the aircraft is in a descent. c) The energy height is the total energy (potential and kinetic) per unit mass of the aircraft.

18.19 To find the climb performance of a supersonic aircraft a level acceleration was carried out at 4 km altitude. The maximum value of the rate of change of velocity at this altitude was measured to be 1.28 m/s^2 and it occurred at 231.5 m/s (450 kn). What will be the maximum rate of climb of this aircraft at 4 km altitude and at what speed should it be flown to achieve this rate of climb? Explain the assumption made to exchange the level acceleration performance to climb performance.

18.20 From the flight test it was found that the rate of climb of an aircraft at a speed of 400 km/h is 1200 m/min . From these data find out the time required to accelerate the aircraft from 350 to 450 km/h in a level flight, assuming that its acceleration during this period is constant.

18.21 What does one generally aims to find in the descent performance tests?

18.22 Is it possible to obtain the drag polar from descent flight tests? If your reply is yes, explain how this is accomplished.

18.23 From flight tests the maximum value of lift/drag ratio of an aircraft is found to be 5.5 . Find the flattest possible gliding angle in the engine failed condition.

18.24 The endurance of an aircraft is a) proportional to the fuel flow rate, b) proportional to the drag, c) inversely proportional to the fuel flow rate.

18.25 What is the test technique used to find the level performance data?

18.26 From level flight performance testing a plot between $\dot{W}_f/\delta\sqrt{\theta}$ and the Mach number was obtained for a constant W/δ of $13,000 \text{ kg}_f$. The minimum value of $\dot{W}_f/\delta\sqrt{\theta}$ was found to be $1550 \text{ kg}_f/\text{h}$. Find the aircraft weight and the rate of fuel consumption for this minimum value of $\dot{W}_f/\delta\sqrt{\theta}$ that corresponds to the maximum endurance at the altitude of a) 3048 m ($= 10,000 \text{ ft}$, $\delta = 0.6878$, $\theta = 0.9313$), and b) 6096 m ($20,000 \text{ ft}$, $\delta = 0.4599$, $\theta = 0.8626$).

18.27 What is the meaning of lift and thrust boundaries?

18.28 Explain the flight test technique used to establish the lift boundary.

18.29 What are the test techniques used in finding the thrust boundary of an aircraft and explain them.

18.30 From the maneuver boundary (lift boundary) flight testing, a graph of nW/δ versus the Mach number was obtained. It was found that the maximum value, $(nW/\delta)_m = 180 \times 10^3 \text{ kg}_f$ occurred at $M = 0.78$. Find the maximum value of n that can be pulled at the lift boundary at this Mach number at a) sea level ($\delta = 1.0$), b) $10,000 \text{ ft}$ ($\delta = 0.6878$), and c) $20,000 \text{ ft}$ ($\delta = 0.4599$). Find the corresponding

airspeeds at these altitudes in the standard atmosphere, and also calculate the ceiling altitude. Assume the weight of the aircraft is $12,000 \text{ kg}_f$.

18.31 At a pressure altitude of 280 millibars the maximum load factor obtained at the lift boundary is 2.2 for a subsonic aircraft. For the same aircraft of the same weight, find the maximum load factor during the lift boundary test at a pressure altitude of 500 millibars.

18.32 The maximum load factor of an aircraft, considering that it can sustain it without any structural failure, is given by the designer as 8. What should be the maximum angle of bank that the test crew can fly in a correctly banked turn?

18.33 The stalling speed of an aircraft in straight and level flight is 203.72 km/h (110 kn). While executing a steady banked turn in the horizontal plane the pilot encounters stall at 455.6 km/h (246 kn). What would be the load factor at that time?

This page intentionally left blank

Weather Hazards and Flying

19.1 Introduction

Weather can be quite hazardous and it is relevant for a performance calculator to be aware of the difficulties in quantifying the performance of an aircraft when it is flying through hazardous weather. It is certainly a cherished goal to calculate the aircraft's performance under hazardous weather conditions, but this still appears to be too far in the future even in the present age of high-speed computers and more sophisticated measuring instruments. An important reason for this is that meteorological science has yet to progress sufficiently to quantify some weather conditions accurately. Moreover, even if we take for granted that this goal of meteorology has been achieved, it is still not a simple task to quantify the performance of the aircraft under hazardous weather conditions because of the difficulties in the theoretical formulation of the problem and its solution.

This chapter is devoted to the qualitative understanding of hazardous weather conditions and to providing a brief account of the measures to be taken by a pilot when encountering hazardous weather. A lucid account of flying under different weather conditions is given by Buck.¹

Weather hazards can be due to fog, turbulence, thunderstorm clouds, icing, high-altitude jet streams, and windshear; this list is not in the order of priority. These weather hazards and flying through them are discussed in this chapter. Lastly, the hazard created by flying birds is also included; although birds do not generate weather conditions, their movements are intensified in certain weather patterns.

19.2 Fog and Flying

Loss of visibility makes flying difficult in fog. Different methods of fog formation are explained here.

19.2.1 Fog Formation

Fog is formed due to the condensation of water vapor as explained in Sec. 2.8. The presence of condensation nuclei in the atmosphere considerably helps condensation so that tiny water droplets can be formed when the relative humidity is about 80% or sometimes even less than 70%. The ideal conditions for the formation of fog are high relative humidity, close proximity of the dew point temperature, sufficient number of condensation nuclei, and the existence of a cooling process for initiating condensation. In addition, high surface winds are required for setting in motion mixing action which spreads and increases the thickness of the fog. In very still air dew may be deposited but fog is unlikely to form. Fog is white in color when composed solely of water droplets but the presence of carbon and dust particles may cause fog to look darker.

Fog is most likely to occur where moisture is abundant, such as above the ocean, lakes, rivers, and water-logged areas. Fog is also common over and near industrial

areas because of heavy concentrations of pollutant gases that act as condensation nuclei. Fog is more common during the cold months of the year than during the warm months, because on colder days the atmospheric temperature is closer to the dew point temperature. Fog is usually dissipated by sunlight filtering down through it, which results in heating the fog from below.

19.2.2 Different Methods of Fog Formation

There are five different methods of producing fog in the atmosphere. The classification of fog is based on these methods. Thus, there is 1) radiation or ground fog, 2) advection fog, 3) upslope or hill fog, 4) steam fog, and 5) precipitation-induced fog or frontal fog. This classification gives importance to the processes that cool the air, adding water vapor to it to form fog. In ground and advection fogs, the air is cooled from below by conduction. In upslope or hill fog, the air is cooled by adiabatic expansion. In steam and precipitation-induced fogs, the existing cold air is saturated by the addition of water vapor from evaporation to form fog. These different types of fog are explained below.

19.2.2.1 Radiation fog (ground fog). Radiation fog is formed by initial cooling of the Earth below the fog by the radiation process, hence it is called the radiation fog. Thereafter, the air particles in close contact with the Earth are cooled by conduction. If the air is moist, it becomes saturated, and further nocturnal cooling produces excess water vapor which condenses. If there is no wind, or calm prevails, the condensation will be deposited on the ground as dew. The temperature variation above the surface is shown in Fig. 19.1a. If light surface winds of 4–15 km/h prevail over the Earth, the cooling process extends upward from the Earth's surface due to mixing, and an isothermal layer of fog droplets is formed as shown in Fig. 19.1b. The sky can be discernible if the thickness of the fog is less than about 80–90 m. If the wind speed exceeds 15 km/h or so, turbulence is set up, causing adiabatic lapse rate (Fig. 19.1c) through the surface layer and a sheet of stratus or stratocumulus cloud would be formed aloft as described in Chapter 2. The inversions shown in Fig. 19.1 for each case result from the cooling process and are not prerequisites for the fog to form.

Radiation fog is most likely to form just after sunrise than at dawn, because the calm night is followed by light surface winds soon after sunrise. A cloudless sky, high humidity, and light winds encourage the formation of fog. Radiation fog is also commonly called *ground fog* since it forms only over the land and not over the sea.

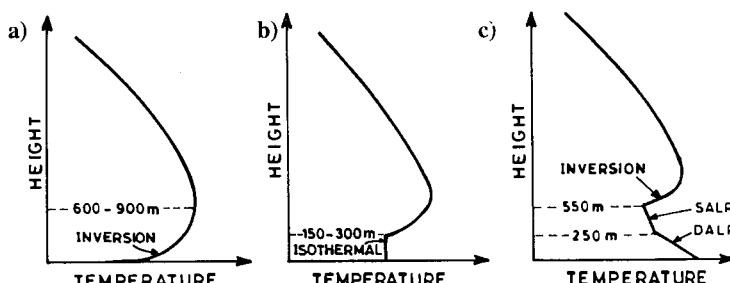


Fig. 19.1 Effects of surface cooling: a) heavy dew, b) fog, and c) stratiform cloud.

19.2.2.2 Advection fog. Advection fog forms when warm and moist air blows over colder land or sea surface. The cold surface cools the moist air to its dew point by conduction from below. Wind speed of about 10–30 km/h is necessary for the formation of advection fog. It occurs frequently in coastal regions. In winter the land is colder than the adjacent sea. The warmer moist air of the sea breeze, flowing over the cold land, produces the *sea-breeze fog*, which is an advection fog. Similarly, fog can also be formed over the surface of the sea.

19.2.2.3 Upslope or hill fog. Upslope fog is caused by cooling of air due to adiabatic expansion when it moves up a slope. A light upslope wind is necessary for its formation. Gradually rising land near coastal areas is a most favorable terrain for upslope fog. Upslope fog is also called *hill fog*. Upslope or hill fog is essentially an orographic cloud whose base is obscuring high ground or a hilltop. To an observer on the high ground or hilltop, the orographic cloud appears as hill fog.

19.2.2.4 Steam fog. Steam fog is formed when cold air passes over a warm water surface. The evaporation of warm water saturates the cold air and the excess of water vapor condenses as fog. Steam fog occurs over sea, rivers, and lakes, especially during the autumn. Arctic smoke is nothing but steam fog.

19.2.2.5 Precipitation-induced fog (frontal fog). The evaporation of rain or drizzle in the cold air causes precipitation-induced fog. The water vapor of evaporation saturates the cold air and the excess water vapor condenses as fog. This type of fog is associated with warm fronts because the rain from the warm air evaporates and saturates the cooler air below, resulting in the formation of fog. It is therefore also called frontal fog.

19.2.3 Flying in Fog

Visibility is the major problem faced by pilots in the presence of fog. A pilot should be well versed in flying in atmospheric conditions that increase the probability of fog formation. It should be kept in mind that fog can form quickly and at times unexpectedly. It is possible that the pilot may enter into the airport flight planning room and when he leaves after discussing the flight plan, less than an hour later, he may find the visibility too poor for immediate departure.

Although fog is normally not a problem enroute, it can present a problem at takeoff or landing. It is not considered prudent to wait to land, hoping the fog will disappear soon. A pilot should be ready with other alternates if preflight planning indicates any possibility of fog forming in the terminal area. Otherwise the takeoff time should be changed so that the pilot will arrive at his destination after the fog has lifted or dissipated.

19.3 Turbulence and Flying

Intense turbulent winds pose hazardous conditions for flying. Turbulence is classified and different sources of turbulence are explained here.

19.3.1 **Turbulence and Its Classification**

Atmospheric winds often get transformed into high-frequency irregular winds of changing velocity; this is called turbulent flow or simply *turbulence* of the atmosphere. Such turbulence causes irregular vibrations in an aircraft flying through it. These vibrations of the aircraft cause anxiety and sometimes fear among its passengers. The intensity of these vibrations may vary considerably. Many times these vibrations exert no appreciable effect on passengers' comfort except that the passengers feel them and are required to put on seat belts. Sometimes turbulence may throw occupants against their seat belts and back into their seats. Turbulence has been classified into four categories: light, moderate, severe, and extreme. This classification is based on the influence it creates on passengers' comfort and the magnitude of the aircraft vibrations.

19.3.2 **Sources of Turbulence**

Winds become turbulent when vertical air currents are superimposed on the horizontal motion of winds. Rough terrain, separated flows, vortices, and wind-shear are the most important causes of turbulent flows in the atmosphere. The regions where most of the atmospheric turbulence is found are identified here and the causes of its presence are explained.

19.3.2.1 Turbulence in vertical air currents. Thermals arising from the surfaces of large concrete structures, metallic structures, and chimneys give rise to bumps and jolts to aircraft flying through them. This is caused by a sudden increase in lift force due to an increase in effective incidence provided by the rising thermals. Flow inside clouds, especially unstable clouds, is also turbulent due to vertical air currents.

19.3.2.2 Turbulence in rough terrain. Farms, trees, small and large buildings, and other civil structures are all good sources of turbulence due to flow separation, vortices, and shear flows near the ground which may be effective up to an altitude of about 300 m (984 ft) above the ground. If there is a covering of dust on the land below, turbulence may cause a massive rising cloud of dust particles, thus hampering the pilot's visibility during takeoff or landing.

19.3.2.3 Orographic turbulence. Ground irregularities are plentiful in the vicinity of hills and mountains due to uneven and discontinuous slopes, cuts, twisted ranges, and passages. All these irregularities create wind-shear and vortices causing turbulence. Even the prediction of average wind speed and its direction becomes difficult. On the windward side of a hill, winds are moving up along the slopes, but they are turbulent due to uneven and broken terrain. On the downward side (lee side) of the hill, winds are moving downward, resulting in mountain winds of wavelike motion which may persist for a considerable distance. Below these winds with wavelike motion are found winds with rotary or vortex motion, carrying rotary clouds above them. The region around rotary clouds is very turbulent.

19.3.2.4 Clear air turbulence. Turbulence called *clear air turbulence* (CAT) also exists at high altitudes where the air is very clear with no signs of cloud. CAT is found outside the core regions of jet streams near the tropopause as discussed below in Sec. 19.6. Wind-shear is generally the cause of CAT, and it has

been statistically determined that CAT occurs where the wind gradients exceed 14.8 km/h (8 kn) per 305 m (1000 ft). CAT does not occur in the core regions of the jet streams. Sometimes CAT also occurs in the wavelike motion formed in the mountain winds.

19.3.3 Flying in Turbulence

An aircraft frequently encounters turbulence and in most cases it is not unsafe to fly through it. When an aircraft vibrates in turbulent flow, the vibrations are felt as pitch, roll, yaw, and their combinations. It is not humanly possible for the pilot to correct each of these high-frequency vibrations. Instead, he is advised to simply correct the attitude of the aircraft by bringing it back to its original position if on average it is drifting to either side.

In mountainous regions it is advisable to fly at an altitude about 50% higher than the height of the mountain range. The pilot should avoid strong downdrafts on the lee-side, and also avoid rolling clouds. Pressure altimeter readings near mountain peaks should not be relied on, since they may indicate altitudes in excess of 300 m higher than the actual ones.

19.4 Thunderstorm Clouds and Flying

A tremendous amount of thunderstorm activity surrounds the Earth. About 1800 storms are in progress at any given moment, producing 44,000 thunderstorms and generating nearly nine million lightning flashes throughout the world each day.²

19.4.1 Thunderstorms and Their Power

Thunderstorm clouds are cumulonimbus clouds that store enormous amount of wind energy and electrical energy which is released in the forms of thunder and other storm manifestations. Thunderstorm clouds are “weather factories,” producing rain, hail, snow, turbulence, gusts of wind, and lightning, in addition to thunder and stormy conditions, as dictated by the nature of the clouds. It can be said¹ that thunderstorms are Cb clouds gone wild to become devils of the atmosphere. Thunderstorms constitute the most severe weather hazards faced by pilots. The rain, hail, and lightning accompanying a thunderstorm cause less trouble than the storm itself. Thunderstorms may contain extreme turbulence, strong updrafts and downdrafts, sidedrafts, gusts, and squalls, which may violently toss an aircraft so that its controls become ineffective. The yearly occurrence of thunderstorms is not uniformly distributed over the Earth.

A typical 5-km-wide thunderstorm has 10 times the power of the Hiroshima atomic bomb. A thunderstorm cloud may rise to a height of about 18 km and may contain hailstones the size of baseballs, traveling at about 190 km/h. Such a storm can precipitate heavy rains and may give birth to tornadoes.

19.4.2 Structure of Thunderstorm Clouds

A thunderstorm cloud may be embedded in cumulus cloud. Thunderstorm bases are generally found between 1.2 km (4000 ft) and 1.8 km (6000 ft), although very rarely they have also been seen at an altitude of 4.9 km (16,000 ft). The tops of thunderstorm clouds may vary from an attitude of about 7.6 km (25,000 ft) to as high as 24.4 km (80,000 ft) and may protrude into the stratosphere. The

tops of thunderstorms are generally lower in the northern latitudes, but so is the stratosphere.

A thunderstorm cloud may have one or more cells with fairly well-defined air circulation and life histories. Each cell may have a diameter ranging from 1 to 10 km with a lifespan of 2–3 h during which it grows, matures, and finally decays. Thus, a large thunderstorm cloud has three different types of cells: growing cells, mature cells, and old and decaying cells.

A growing thunderstorm cell contains only rising air currents which form cumulus clouds at the top. The release of heat in condensation gives rise to warm air that rises, cools, and condenses, releasing more heat which causes up-currents; the rising air is supplemented by the entrainment of the surrounding air. These updrafts have nonuniform velocity distributions across the cell. The airspeed of these updrafts may reach about 150 km/h, but 40–60 km/h is quite common. This means that the vertical development of a thunderstorm can be greater than the rate of climb of an airplane of average performance.

During a mature stage of the cell development, hail is formed, and the cell contains both up-currents and down-currents. The downdraft speeds are usually smaller as compared to the updraft speeds. The down currents are partly due to falling rain and hail which exist in the upper portion of the cell. In the final stage when the cell has become old, the anvil of ice appears at the top, the up-currents cease, and only down-currents exist, which also decay. As the heavy rain and hail stop, the cell dies out. The life of a thunderstorm is about 1 or 2 h.

19.4.3 *Lightning, Hail, Turbulence, and Downburst*

Lightning, hail, turbulence, and downburst are important constituents of a thunderstorm that affect the performance of an aircraft. Turbulence is the most important factor since it may violently toss the whole aircraft. The more streamlined the shape of an aircraft, the worse it behaves in turbulence.

19.4.3.1 *Lightning.* Lightning is a phenomenon resulting from the weather conditions that surround the Earth. The most common weather condition producing lightning is the thunderstorm. Lightning is due to the separation of positive and negative charges in a cloud, and the flash is the discharge between them. Lightning flashes can travel from one point to another in the same cloud, from one cloud to another cloud, from a cloud to the ground, and also from the ground to a cloud. The current in a single flash of lightning may vary between 10,000 and 100,000 A, and lasts for a very small fraction of a second.

A typical single lightning flash may measure 10 km from one end to the other. A single lightning flash may consist of a number of strokes in quick succession, so that one continues to see the light in many branches, with the total flash lasting for about a second. The sound of the complete flash is, however, heard for about half a minute in the form of bangs, rumbles (high-frequency sound), and crackles (low-frequency sound). This is because lightning produces high temperature causing sudden expansion of the air along the path of the flash. The sound so produced from different parts of the flash reaches the observer quickly at the speed of sound. From many parts, equidistant from us, the sound reaches us at the same time causing big bangs, and from other locations it reaches us in quick successions, causing rumbles and crackles.

Lightning that strikes aircraft poses special hazards. Structural damage is possible, especially for an aircraft with a wooden frame. Lightning is not dangerous to occupants of metal-frame aircraft because metal, being a good conductor of electricity, allows the lightning current to pass smoothly without heating the metal. The static electricity buildup in the airframe may spoil the smooth functioning of radio equipment and magnetic compasses, but not much interruption to VHF. The lightning may cause *lightning blindness*, which makes instrument reading impossible for the crew during a brief period ranging from 30 to 50 s. The electrical circuits may be disrupted. The solid-state electricity of modern avionics is particularly vulnerable to lightning strikes. Lightning also brings the possibility that the fuel vapor in the fuel cells of the aircraft may be set on fire.

The aircraft itself may pick up positive charges while passing through clouds containing an excess of positive charge. If an aircraft flies through a cloud having a negative charge concentration, the positive charge of the aircraft may discharge into the cloud; the aircraft here is the origin of the lightning. Weird flames may appear along the wings and around the propeller tips, these are called *St. Elmo's lights*.³

19.4.3.2 Hail. Hail exists at the top of the cloud in the anvil and where the temperature may be below -10 or -15°C . Most hail in a thunderstorm does not reach the ground since it may be suspended at the top, moving within the cloud due to rising air currents, or may get converted into water droplets before reaching the ground. Hailstones of about 1–2 cm in diameter occur most frequently. On striking an aircraft, hailstones can damage the wings, tail, radome, and glass windows. Radar cannot easily detect hail or other ice regions.

19.4.3.3 Turbulence. Turbulence is found in most parts of a thunderstorm cloud and in its surrounding neighbors. The essential problem is how to locate the regions of minimum turbulence in a thunderstorm. Rain generally dampens turbulence to some extent. Therefore, the most severe turbulence is not in the middle of a rainstorm, but near by. If a pilot misses the rain by a good margin, he will probably miss the severe turbulence. Severe turbulence is present not only within the cloud but also in the clear air in the proximity of the cloud and above it. Rapid changes in barometric pressure, vertical drafts past the pitot-static tube, and the clogging of holes of the pitot-static tube by rain cause erratic and unreliable readings of altimeter and airspeed indicators. More has been said earlier in this chapter about turbulence and flying through it.

19.4.3.4 Downburst. A thunderstorm cloud produces several downburst clusters of intense downdrafts with airspeeds of about 100 km/h. At about 30 m above the ground the downdraft begins to spread, until at ground level it is entirely horizontal. A single cluster may contain several much smaller downdrafts hitting ground. The size (diameter) of these small downdrafts is about 2–4 km, and to emphasize the smallness of this weather phenomenon, it is often called a *microburst*. A microburst can produce an airspeed of about 120 km/h just about 15 to 30 m above the ground. An aircraft facing a microburst ahead at low levels first encounters headwinds, then vertically downward air currents of the downdraft (microburst), followed rather abruptly by tailwinds. Encounters with microbursts should be avoided because flying through them can be very dangerous.

19.4.4 Flying in Thunderstorm Clouds

Flying through a thunderstorm should always be avoided; in particular, pilots of light aircraft should never attempt to fly through a thunderstorm. If a thunderstorm is starting to occur at the time of takeoff, it is better to wait, since it will not last for more than an hour or two. In the case of a transport aircraft pilot facing thunderstorm clouds enroute, it is better to bypass them from the top, bottom, or side by never coming close to the thunderstorm. The tops of thunderstorm clouds are generally so high that even most modern jet aircraft cannot fly over them. Flying under the base of thunderstorm clouds is possible only for low-flying aircraft provided the visibility is good. The peaks of mountains may protrude into the base of a thunderstorm cloud so that flying under their base may not be possible. It is often possible to circumnavigate a thunderstorm cloud without encountering special flight problems. If thunderstorm clouds are aligned horizontally one after another, it may be possible to fly between two thunderstorm clouds with the help of radar. A pilot must be proficient in operating and understanding radar signals since they help to locate the dangerous cells of a thunderstorm cloud. If an aircraft is passing through a cumulus cloud it is sometimes possible to avoid a thunderstorm cloud.

In case a pilot must fly through a thunderstorm cloud, certain instructions are recommended in the operator's manual for the particular aircraft and these must be followed. Some of these instructions to pilots can easily be understood, such as the following:

- 1) Fasten the seat belt, wear dark glasses even at night, lower the seat, and put cockpit lights to full bright. All these measures are to guard a pilot against blindness from the bright flashes of lightning.
- 2) Shut off all radios and other equipment that are not necessary and likely to be damaged by lightning or severe vibrations. Secure loose objects in the cabin.
- 3) For piston-prop aircraft, the carburetor mixture should be set to full rich.
- 4) Put on the heat for the pitot-static tube, carburetor, or jet inlets.
- 5) The autopilot should not be used. Since this device ensures constant altitude, it will make the aircraft dive to compensate for updrafts, causing excessive airspeed. Similarly, it will make the aircraft climb in a downdraft, creating the risk of a stall.
- 6) Fly at the recommended turbulence-penetration airspeed, power setting, trim, and attitude before entering the turbulent region. The penetration airspeed is about 50% higher than the stalling airspeed, but sufficiently lower than the cruising airspeed. The higher the speed of the aircraft, the greater will be the jolt to the aircraft given by an updraft or downdraft in the thunderstorm cloud.
- 7) Avoid areas with temperatures of -10 to $+10^{\circ}\text{C}$, because most lightning discharges occur in these regions and carburetor icing will be at its maximum. The majority of discharges occur where rain is mixed with snow.
- 8) Enter the thunderstorm through the area that looks dark like rain, rather than whitish like hail. This may avoid the chance of encountering hail.
- 9) To minimize time in the turbulent area, cross the thunderstorm at right angles by keeping a constant altitude.
- 10) Once inside the thunderstorm, do not attempt to turn back, and avoid all unnecessary maneuvers. The reason for this is to minimize any excessive loads to those already imposed by turbulence on the aircraft.
- 11) If the pilot decides to fly around a thunderstorm, try to fly around the right side of it. The wind circulates anticlockwise and, therefore, the pilot will get more favorable winds. Do not attempt to penetrate between two thunderstorm clouds if the space between them is narrow. The apparently clear narrow space may have more severe turbulence than the clouds themselves. However, if the clear space has a width of

about 1.6 km (1 mile) or more, it is safe to fly through the center. Always try to go through such a space at the highest possible altitude.

19.5 Ice and Flying

The hazard of icing in cold weather starts when an aircraft parked outside is brought to the runway. It may be there all the time during climbs, enroute, and even after landing. A brief historical account of research conducted on icing as a hazard to flying is provided by Lloyd.⁴

19.5.1 Hazards of Icing

The atmospheric moisture in the form of ice may deposit on the exposed surfaces of an aircraft or inside its power plant. Ice deposits destroy streamlined shapes and reduce the air flow in the nozzles of airbreathing engines. Ice deposits on aircraft affect its flying qualities. The weight of accumulated ice is generally of secondary importance as compared to the disruption of flow around the wings and tail surfaces. The higher the speed of an aircraft in icing zones, the faster will be the ice accumulation. Ice can be deposited as slowly as 0.5 in./h or as rapidly as 1 in./min, depending on the nature of the icing zone in the atmosphere. The pilot generally first notices ice deposits at the corners of the windshield, and it spreads, forming on most other areas of the windshield to completely destroy the pilot's visibility.

The ice deposits on wings or tailplanes spoil their streamline shapes, produce roughness or waviness on the surfaces, reduce lift, increase drag, and raise the stalling speed. This reduction in lift can be as much as 50% and the increase in drag can be as high as 35%. The pilot immediately senses this by a drop in the airspeed. If ice is building up on the propellers, it is almost certain that the same thing is happening on the wings, tail surfaces, and other projecting surfaces. If the loss of airspeed occurs in clouds without any visible sign of ice on the wings, it is an indication that the ice may be forming on propellers. Icing on propellers slowly causes loss of power and gradual onset of engine roughness. The ice first forms on the spinner or propeller dome and then spreads to the blades of the propeller. Ice on the propeller blades may reduce their efficiency by about 20%. Ice generally accumulates unevenly on the propeller blades. The unequal amount of deposit on the different blades of a propeller disturbs the balance of the propeller mount, causing terrific vibrations of the propeller blades. These vibrations lead to undue stresses on the blades and engine mounts, leading to their possible failure. Broken pieces of ice from the propeller hit the sides of the fuselage next to the propellers, with loud whacks that cause dents in the surface of the fuselage. Ice deposits may spoil the smooth functioning of control surfaces, linkages, brakes, and landing gears.

Ice formation affects not only the surfaces directly exposed to the atmosphere but also the engines that are embodied in the body of the aircraft. In the case of piston-engine aircraft, ice deposits may be formed in the carburetor due to sudden expansion of moist air inside it, although the atmospheric temperature may be as high as 25°C. Carburetor icing is usually indicated by a loss of power (drop in manifold pressure or in rpm) and, if severe enough, it may cause complete engine failure because the inductive flow may be closed completely due to the icing. Many aviation accidents have occurred due to carburetor icing because pilots did not sufficiently appreciate the ever-present dangers of icing when the atmospheric temperature was well above freezing and no chances of ice deposit yet existed on the exposed surface of the aircraft. Gas turbine engines are also much more

vulnerable to the hazard of icing. Ice forming on the intake cooling constricts the air intake. Chunks of ice at the inlet phase may be sucked into the engine, causing engine failure. Ice on rotor or stator blades affects their performance and efficiency, and may result in flameout.

Icing also affects the aircraft's flight instruments. Ice deposits on the pitot and static holes produce unreliable reading (or even no reading) of the altimeter, airspeed indicator, rate of climb indicator, and turn and bank indicators. Icing on the radio antennas can degrade radio reception and destroy all communications with the ground.

19.5.2 Types and Characteristics of Ice Formation

Ice crystals may differ in shape, size, appearance, and quality, depending on the method of sublimation, condensation, freezing, and the size of water drops. Generally ice exists in the forms of frost, rime, clear ice, snow, and hail.

19.5.2.1 Frost. *Frost* is white, semicrystalline ice that is formed due to sublimation of water vapor on cold surfaces. It can form on the surfaces of an automobile or aircraft when parked outside in open air during the night in cold weather. Frost on the surface of an aircraft must be removed before takeoff because it causes considerable surface roughness which increases drag and thereby increases stalling airspeed by about 10%. Consequently, the takeoff airspeed is also accordingly increased. Frost is generally not formed during flight.

19.5.2.2 Rime ice. *Rime ice* is the most common form of ice formation (it constitutes about 72% of the cases of ice formation) and is due to instantaneous freezing of supercooled small water droplets when they strike an aircraft. They maintain their spherical shape as they freeze and the air particles get trapped between them. Rime ice is rough, porous, milky-white, opaque, and quite brittle. It is formed near the leading edges of wings, on the tailplane, pitot-static tubes, and on the antennas and other aircraft parts during flight. Figure 19.2 gives a schematic view of typical rime formation around the leading edge of a wing section. Formation of rime ice takes place in the range of 0 to -40°C temperature, but is most common between -10 and -20°C . The weight of rime deposits is often immaterial as compared to its danger in altering the leading-edge shapes of wings, and choking the orifices of the carburetor and instruments.

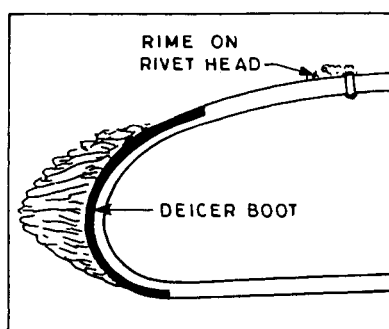


Fig. 19.2 Rime ice formation around leading edge.

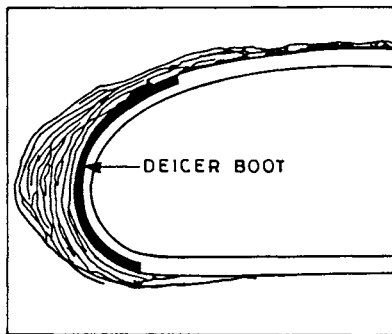


Fig. 19.3 Clear ice formation around leading edge.

19.5.2.3 Clear ice. A heavy coating of glassy ice formed during flight in a dense cloud or freezing rain is known as *clear ice*. It is formed by the relatively slow freezing of supercooled large water droplets striking the surfaces of the wings and other parts of the aircraft. The slow freezing rate and the large drops of water allow the water to spread on the surface before cooling with hardly any trapping of air bubbles. This makes the ice spread over the surface, giving it a smooth and glazed look. The bigger the water drop, the larger the distance it will spread back over the wing before freezing. A typical pattern of clear ice formation around the front portion of a wing section is schematically shown in Fig. 19.3. Clear ice is hard to break, transparent, smooth, glazed, and adheres tenaciously to the surface. It is primarily formed between 0 and -10°C , although it can also form at -25°C . Clear ice formations are to be expected in clouds carrying vertical upcurrents which sustain large drops of water. Clear ice produces all the hazards of icing that are mentioned in the beginning of this article.

19.5.2.4 Snow. *Snow* is due to water vapor changing directly into ice crystals which join and form a single snowflake. These ice crystals are formed at below the freezing temperatures of moist air. When millions of these flakes fall on the ground, like rain showers, we refer to this as a snowfall. Dry snow does not stick to the surface of the aircraft whereas this is not so for wet snow.

19.5.2.5 Hail. *Hail* is another important form of ice that does not stick to an aircraft's surface and grow. It exists in certain clouds as small solid pieces that may hit the aircraft, and cause danger, as discussed above in Sec. 19.4.

19.5.3 Intensity of Icing

The intensity of icing is classified into four categories: trace, light, moderate, and heavy. This classification is based on the rate at which ice forms on a small probe or projection protruding into the atmosphere from the aircraft surface, and gives an indication of how much the pilot can depend on deicing or anti-icing facilities during flight.

19.5.3.1 Trace. In *trace icing*, the accumulation of ice on the small probe is half an inch per 129 km (80 miles) of flight. The rate of ice formation on the

surface is just slightly greater than the rate of its sublimation. Ice is not a hazard in this case even if deicing or an anti-icing facility is not used for an hour.

19.5.3.2 Light. In *light icing*, the accumulation of ice on the small probe is half an inch per 64 km (40 miles) of flight. In this case the rate of accumulation may create problems if the flight is prolonged in this environment for more than an hour. Light icing does not create a hazard if deicing or an anti-icing facility is occasionally used.

19.5.3.3 Moderate. In *moderate icing*, the accumulation of ice on the small probe is half an inch per 32 km (20 miles) of flight. Here the rate of ice buildup is excessive and even short encounters may be hazardous. The use of deicing or anti-icing equipment is very necessary here, and sometimes diversion of the flight path may even become necessary.

19.5.3.4 Severe. If the accumulation of ice is half an inch per 16 km (10 miles) of flight, it is rated as *severe icing*. In this case, the icing on the aircraft surface is extremely severe and deicing or anti-icing equipment cannot combat the icing hazard. Diversion of the flight path becomes immediately necessary.

19.5.4 Methods to Combat Icing

An aircraft is generally equipped with facilities to combat ice formation up to a certain extent. The methods of *deicing* and *anti-icing* have been most common on the wings, tailplanes, and propellers, and recently the method of *hot wings* has also been introduced. For icing inside the carburetor the method of *preheating* is used.

19.5.4.1 Deicing method. The process of removing ice after it has formed is called the *deicing method*. In this method structural ice is first allowed to form to about a quarter of an inch thick and then deicing equipment is operated to remove it. This procedure must be used again and again at certain intervals. In a deicing facility the surfaces around the leading edge of the wing and the tailplane have rubber skins, or boots (Figs. 19.2 and 19.3), that can be pulsated by compressed air flow underneath the boots. These pulsations crack the ice, which is carried downstream by the winds. Certain models of deicing equipment use an automatic on and off scheduling device so that the pilot need not keep track of these schedules. The deicing device, however, is not 100% efficient because many times certain pieces of ice fail to be removed and continue to stick and move up and down with the pulsating boot.

19.5.4.2 Anti-icing method. The process of preventing ice formation is called the *anti-icing method*. This procedure does not allow any ice formation even at the beginning of ice formation. Here an active fluid is allowed to spread over the surface, and it prevents ice from adhering to the surface. This device is commonly used on propellers where the centrifugal force helps to spread the anti-icing fluid evenly.

19.5.4.3 Method of hot wings. The wings, tailplanes, and propellers of most new aircraft can be heated either electrically or by the flow of hot air brought from the engine. This procedure is commonly referred to as the *method of hot wings*. This method can be used either as a deicing device or as an anti-icing device, but is commonly used as an anti-icing device. When used as a deicer, the device is turned on after some ice has formed. This melts the ice, the water flows back on the wing and refreezes to act as a spoiler on the wing surface. For this reason, the method of hot wings is commonly used as an anti-icing device, and the wing is heated even before the airplane flies into an ice-forming region so that ice is not formed on the vulnerable surfaces. Electrical heating is commonly used to heat pitot-static tubes and the windshields of the canopy.

19.5.4.4 Preheating method. The preheating method is used to avoid ice formation inside the carburetor. The principle is to sufficiently preheat the cool and moist air entering the carburetor so that its moisture content is minimized and ice formation is avoided. Sometimes it becomes difficult to recognize when preheating is required. In the case of a fixed-pitch propeller, a drop in rpm may be a good indication for using preheating, but the pilot must be sure that the aircraft is not climbing because even then the rpm may drop. In the case of a constant-speed propeller, a drop in the manifold pressure gauge may be a good indication for using preheating.

19.5.5 Flying in Icing Conditions

The basic principle should be to avoid icing zones, if possible. Otherwise a pilot must take the positive step of flying into safer zones as soon as ice formation is noticed anywhere on the aircraft. The various devices to combat icing are not sufficient to allow flying for several hours in the icing zones. They only give the pilot some time to work his or her way out of the icing situation. Moreover, the ice combating facility is not provided for the entire aircraft and may not be extremely efficient.

Icing may first start on the ground itself. Frost or ice coatings, if noticed on the aircraft on the ground, have to be cleaned off, otherwise the runway length may not be sufficient for takeoff. There should not be any ice on controls and linkages to obstruct their smooth movement. The windshield of the cockpit must be maintained clean, especially at the time of landing and takeoff. An initial check must be made of the equipment that combats icing. The pilot should turn the heating for the pitot-static tube on icing zones. Special care is required for the carburetor of a piston-engine aircraft, by keeping the carburetor heat on, even when the outside air temperature may be well above freezing.

The pilot should choose the altitude of least icing if flying through an icing zone cannot be avoided. The chances of ice formation on the aircraft are more if it flies through wet snow or rain showers at freezing levels. Ice clouds are generally not hazards because the ice will not adhere to the surface of the aircraft. Fuel consumption is greater when an aircraft is flying through icing conditions, due to increase in drag. The larger the duration of the flight, the greater is the accumulation of ice. Similarly, the faster the airspeed, the more quickly the ice deposit will form. Therefore, in icing regions the pilot should not attempt to make prolonged flights and, similarly, the rates of climb or descent should be fast but the airspeeds should be slower. The decision whether to continue or return should be made rapidly by the

pilot because once ice has commenced forming, the condition may become critical in a matter of about 5–6 min. If the accumulation of ice has already become serious, the pilot should attempt a forced landing immediately. Maneuvers and steep turns should be avoided in icing conditions because the stalling airspeed is higher than normal. The braking mechanism should be checked before landing. Landing on a runway with icing requires special care due to reduced braking friction. After landing successfully, the pilot and passengers should be careful not to slip when putting their feet on the icy ground.

19.6 High-Altitude Jet Stream and Flying

Jet streams of wind moving from west to east are found in the upper atmosphere near the tropopause. This is one of the most important discoveries of this century in the field of atmospheric science, and was made about 50 years ago. The high-altitude flights of the last few decades have significantly augmented our knowledge of these jet streams. We now have better knowledge about the structure, location, and frequency of occurrence of jet streams in the atmosphere. However, like many other weather phenomena, it is still not possible to forecast them exactly.

19.6.1 Structure of the Jet Stream

The jet stream frequently appears in a series of broken, disconnected, well-defined long segments of noncircular cross section, running from west to east. Two or more jet streams may also exist at the same time. A continuous jet stream may also appear as shown in Fig. 19.4, running from west to east in a serpentine manner around the Earth in the temperate zone. Jet streams grow, intensify, decline, and finally die out.

Jet streams are generally 1909–4827 km (1000–3000 miles) long, their vertical thickness is 914–2134 m (3000–7000 ft), and they can be about 161–644 km (100–400 miles) wide in the lateral direction. To be designated as a jet stream, the wind speed must be at least 90 km/h (50 kn). The wind speed in the core region is generally between 180 and 270 km/h (100 and 150 kn) but it can be as high as 541 km/h (300 kn). The magnitude of the wind speed in the core region determines the strength of the jet stream.

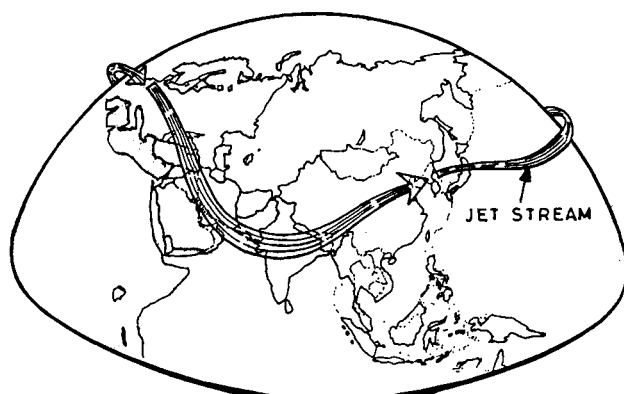


Fig. 19.4 Jet stream circling the Earth.

19.6.2 Location and Frequency of Occurrence

Jet streams are usually found in the mid-latitudes between 30° and 60°N but in some cases they are also found as close as 20°N of the equator in winter. They are usually found between the altitudes of 6 km (20,000 ft) and 12 km (40,000 ft). Jet streams can shift toward the north or south and do not remain fixed at the same place. From day to day the strength of the jet stream, its size, and its length change, and jet streams tend to migrate to other places. The wind speeds in jet streams are greater in the winter than in the summer.

19.6.3 Flying in the Jet Stream

The speed and range of an aircraft are greatly increased if it flies within the jet stream along the direction of the wind, and the reverse is the case of flying against the winds of the jet stream. Pilots flying at high altitudes try to take advantage of this fact. It is reported that one airline on the Tokyo to Honolulu route saved half a million dollars in fuel cost alone, apart from saving time, during a series of 220 flights by utilizing the jet stream flow for eastward journey and avoiding it for the westward journey. While flying in the CAT of the jet stream, the pilot faces the same problems as mentioned in the Section 19.3 above.

19.7 Windshear and Flying

Shear of winds in any direction is called *windshear*. Windshear is a change in wind speed and its direction over a short distance. Some amount of windshear is present almost all the time in the atmosphere. Fortunately, strong windshears dangerously affecting the aircraft performance are rare; an aircraft must not be in the wrong place at a wrong time. Each generation of aircraft has brought advances in performance as signaled by speed, range, payload, and specific fuel consumption. It does not necessarily follow, however, that the pilot of a modern high-performance aircraft can cope with an encounter with windshear any better than the pilot of a straight-wing, propeller-driven aircraft. A continual scan of airspeed, altitude, rate of climb (or descent), and engine instruments is required for timely recognition of windshear. In a strong windshear during landing, the first instrument indications to a pilot are the changes in airspeed and rate of descent, followed by the changes in pitch attitude and glide slope.

19.7.1 Types of Windshear

The wind speed at a point can be resolved into three components along the orthogonal directions of x , y , and z , where z is along the vertical, x and y are in the horizontal plane, and y is along the spanwise direction. The shear in the vertical component of velocity can be called the *air current shear* as shown in Fig. 19.5, both for an updraft and downdraft. The shear in the horizontal component of

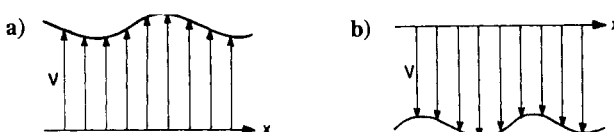


Fig. 19.5 Air current shear: a) shear in updraft and b) shear in downdraft.

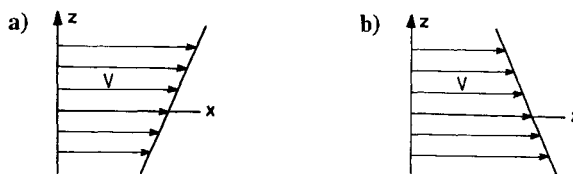


Fig. 19.6 Constant windshear in vertical direction: a) positive windshear $dV/dz > 0$ and b) negative windshear $dV/dz < 0$.

velocity along x is commonly called the windshear. Usually the windshear is the most dominant type of shear.

The amount of windshear (dV/dz) may be constant or changing in the vertical direction. Constant windshear in the vertical direction is shown in Fig. 19.6. If the wind speed increases in the z -direction, this constitutes a positive windshear as shown in Fig. 19.6a. Similarly, in a negative windshear the wind speed decreases in the z direction as shown in Fig. 19.6b. The amount of windshear (dV/dy) can also be constant or changing in the spanwise direction. Constant windshear in the spanwise direction is shown in Fig. 19.7, and will be positive or negative depending on whether dV/dy is positive or negative as shown in Figs. 19.7a and 19.7b, respectively.

Headwind shear is a rapidly increasing headwind component or a decreasing tailwind component. *Tailwind shear* is a rapidly increasing tailwind component or a decreasing headwind component. During the climbing flight of an aircraft, Fig. 16.6a corresponds to the headwind shear and Fig. 16.6b corresponds to the tailwind shear. A crosswind shear is a change in the crosswind component over a short distance. Intense vertical air current shear can occur simultaneously with windshears. These types of shear can vary with the horizontal distance, vertical distance, or both.

19.7.2 Sources of Windshear Formation

Every takeoff and landing in windy conditions is subject to windshear caused by the ground boundary layer, and windshear is more pronounced when close to the ground. High ground, hilly terrains, and large buildings near the runway can also cause cross-windshears. Severe head or tail windshears, cross-windshears, and vertical air current shears are caused by meteorological conditions. The presence of a cold or warm air front near an airfield produces windshear both in the horizontal and vertical planes. The directions of these windshears depend on the orientation of the front with respect to the runway used. Most severe windshear

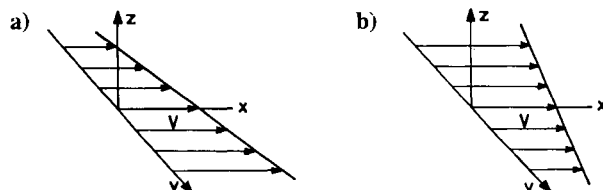


Fig. 19.7 Constant windshear in spanwise direction: a) positive windshear $dV/dy > 0$ and b) negative windshear $dV/dy < 0$.

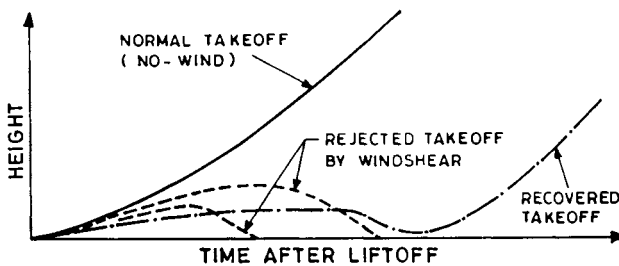


Fig. 19.8 Takeoff windshear incidents.

occurs in thunderstorm areas. The strong updrafts and downdrafts of a thunderstorm produce strong shears in air currents and winds. Microbursts emerging from a thunderstorm produce intense windshear at low levels near the ground due to powerful downdrafts.

19.7.3 Flying in the Windshear

Windshears are most threatening below 150 m (500 ft); these belong to the class of low-level windshears. At such low heights there is very little time and altitude available to respond to and recover from an inadvertent encounter. The knowledge of how a windshear affects aircraft performance can be essential for the proper control of flight path in takeoff and landing during an inadvertent low-altitude windshear. Primarily the windshear affects lift and side forces, depending on the type of windshear. This in turn changes pitch and yaw of the aircraft. A positive headwind shear (or a negative tailwind shear) increases airspeed on the upper surface of the wing and decreases on the lower surface, consequently the pressure on the upper surface is decreased and that on the lower surface is increased, producing more lift. The opposite is the effect of negative headwind shear (or positive tailwind shear). A headwind or tailwind shear alters the pitch of aircraft, whereas crosswind shear changes the yaw of the aircraft.

Windshear changes the normal flight path as shown in Figs. 19.8 and 19.9. During takeoff the normal flight path for the no-wind case is shown in Fig. 19.8 by a solid line. A windshear encounter soon after takeoff can force the aircraft to return back to the ground as shown in two such cases drawn by dashed lines in Fig. 19.8. It is also possible that the aircraft could recover and resume climb as shown by the dashed-and-dotted line in the figure. At the time of landing

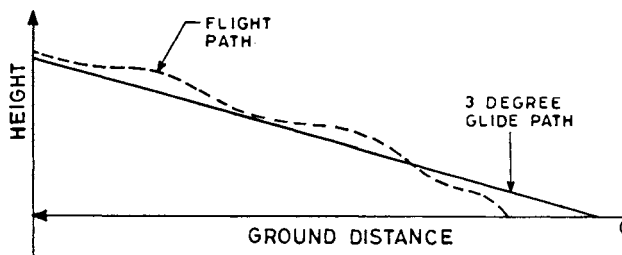


Fig. 19.9 Deviation from glide path due to windshear.

the windshear can change the 3 deg glide angle path of the aircraft as shown in Fig. 19.9; the flight path shown by the dashed line would depend on the type of windshear.

There is so little time and altitude available during low-altitude windshear encounters that controlling airspeed without regard to pitch may increase the possibility of contact with the terrain. The most effective tools available to a pilot for controlling the flight path are pitch attitude and thrust. Increasing pitch will produce the necessary lift force that is required for changing the direction of the flight path. Increasing thrust, combined with pitch attitude control, can ensure the best flight path control that may be available during the encounter of the windshear and within the capability of the aircraft. Higgins and Roosme⁵ have mentioned certain precautionary measures for pilots to take during takeoff as well as during landing, if windshear conditions are anticipated.

Modern pilots are given proper training on the flight simulator for coping with the rare, anxious moments that may arise due to low-level windshear. Without effective windshear training, the pilot may acquire flying habits that can momentarily inhibit or preclude an appropriate response to windshear situations that occur infrequently and permit only a limited time for resolution.

19.8 Bird-Strike Hazard and Flying

Birds of different size, weight, and habits live in our environment. A heavy bird suddenly striking a flying aircraft can be dangerous. During the last two decades the bird-strike hazard has received much attention by governments, airlines, the military, and airport administrators. Minimizing bird-strokes has become a designated responsibility of the highest levels of airport management.

19.8.1 Birds and Bird-Strikes

The consequences of bird-strokes when an aircraft during flight encounters birds (Fig. 19.10) may range from no or minor damage to engine flameouts and in some rare cases total destruction of the aircraft. The airlines or other aviation institutions have to spend an appreciable amount of money every year for repairing the damages.

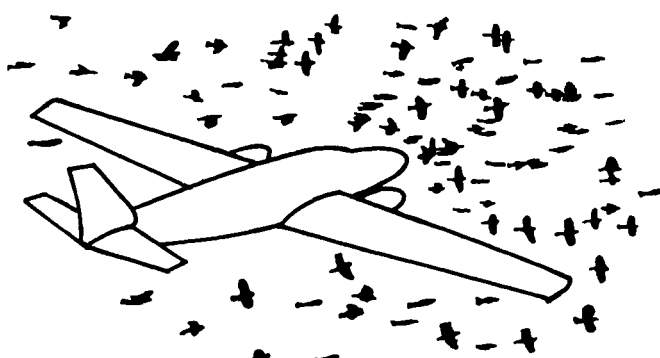


Fig. 19.10 Bird-strike problem.

Studies have been made by various governmental and private organizations to obtain pertinent statistical information about birds and bird-strikes. Many concerned institutions have made studies⁶ on 1) identification of species of birds frequenting the airport; 2) observation of each species regarding its likes and dislikes, and determination of bird characteristics like feeding, nesting, roosting, and migration habits; and 3) identification of areas on the airport that are attractive to birds, and determination of the type of their activity.

The majority of bird-strokes occur during daylight hours, but significant numbers occur at night. In certain seasons, which depend on the region of the airport, bird-strokes are at a peak. About 75% of recorded bird-strokes occurred within 61 m (200 ft) above ground level and in the vicinity of airports. About 20% of bird-strokes occurred between 61 m (200 ft) and 1524 m (5000 ft) above ground level and no bird-strike have been recorded above 3658 m (12,000 ft). This shows that the bird-strike problem exists in the low-flying areas such as near airports, or in some other areas where low-flying activities of aircraft are conducted.

19.8.2 Factors Attracting Birds to the Vicinity of Airports

Although birds may not like aircraft noise, nevertheless they are attracted to the vicinity of airports for various reasons. Birds often congregate at airports in large numbers because the very large open area of the airport is by itself a strong attraction for soaring and loitering. Certain birds nest in airport buildings and hangars, sometimes opening doors by themselves.⁶ Birds may also nest in any suitable opening in an immobile aircraft, sometimes within half an hour of parking. Small or big shady areas, dense vegetation, uneven terrain, bodies of water, poor drainage, and large grassy areas surrounding an airport become attractive nesting and roosting areas for birds. Often the major areas of roosting are on nearby parks and private properties surrounding the airport. An airfield's large area, and the food and water supply around it, may cause the airfield to become a stopover of migratory birds. The proliferation of potential problem birds, such as vultures and kites, is mostly due to primitive slaughterhouses, and primitive carcass and garbage disposal systems, resulting from unplanned development of towns and cities in the vicinity of airfields.

19.8.3 Remedial Activities

The birds menace can be minimized by adopting methods that discourage birds from coming to airports or to places where low-flying activities occur. Antibird operations on or near the airport fall into the following three categories: 1) Dispersal of birds on the airport, 2) frightening birds so that they do not return, and 3) topographic and environmental changes around the airport.

Dispersal of birds present on the airport runways and infield reduces their immediate danger to aircraft. The dispersal of birds is carried out by various devices ranging from using old-fashioned scarecrows to the killing of birds. Temporary measures for removing birds, or keeping them away from the runway, include making distress calls, setting off firecrackers, flying model airplanes, and employing falcons. Noisy dispersal methods should be undertaken with caution because the resulting continuous noise may become more objectionable to airport neighbors than jet engine noise. Leaving dead birds around, for others to see, is not effective, because while it may frighten off birds of the same breed temporarily, it may also

quickly attract other species of scavenger birds like crows and buzzards, thereby compounding the problem.

Scaring birds out of established roosting and nesting areas can be a more durable solution of antibird operation near an airport. Getting the birds out of their nesting and roosting areas permanently requires more time. Harassment to birds should start before dark, as the birds come to roost, and should continue well into the hours of darkness with noise, lights, distress calls, and firecrackers. Placing stuffed owls, the natural enemy of most small birds, near nests in buildings and trees is an old trick, which is still effective to some extent.

Topographic and environmental changes around the airport are the most effective methods of alleviating the bird-strike problem. This requires planned development of towns and cities with no such activity within about 15 km surrounding the major airport that would encourage the presence of potential problem birds. Airport buildings and hangars should have pigeon-proof designs. It also requires controlling airfield vegetation, improving drainage, and installing a hard and smooth ground surface for the infield area. Low areas that fill briefly with rainwater should also be filled because the water brings earthworms to the surface in great numbers and this attracts birds, particularly gulls.

References

- ¹Buck, R. N., *Weather Flying*, Macmillan, New York, 1978.
- ²Bogard, J. K., "Lightning and How It Affects Jet Aircraft," *Boeing Airliner Magazine*, April–June, 1984.
- ³Mac Donalds, S. A. F., *From the Ground Up*, 3rd reprint, Himalayan Books, New Delhi, 1989.
- ⁴Lloyd, A. T., "Ice Research in History," *Boeing Airliner Magazine*, Jan.–March 1990.
- ⁵Higgins, P. R., and Roosme, A., "Hazards of Landing Approaches and Takeoffs in a Windshear Environment," *Boeing Airliner Magazine*, Jan. 1977.
- ⁶Bowers, P. M., "Airports and the Bird-Strike Problem," *Boeing Airliner Magazine*, April–June 1981.

Problems

In the multiple choice problems below, mark the correct answer.

19.1 Radiation fog may form in a) clear sky, winds calm to 3 km/h, and high humidity; b) light winds up to 15 km/h, instability, and high humidity; c) cloudless inland night, winds 4–12 km/h, and high humidity.

19.2 Radiation fog forms most frequently in a) troughs of low pressure, b) anti-cyclones, ridges, and cols, c) depressions and cols.

19.3 Fog over melting snow is a) evaporation fog, b) advection fog, c) radiation fog.

19.4 Advection fog is not formed when a) the wind remains calm, b) the sky is nearly overcast, c) wind speeds exceed 15–20 km/h.

19.5 Advection fog forms a) both over land and sea, b) over land only, c) over the sea only.

19.6 While flying through heavy rain beneath cumulonimbus cloud, the pilot should expect to a) gain height, b) lose height, c) maintain height.

19.7 Ice formation on the wings of an aircraft leads to a) decrease in drag, increase in lift, and perhaps to buffeting of the tail, b) increase in drag and decrease in lift with no effect on the tail, c) increase in drag and increase in lift with no effect on the tail.

19.8 The height of cumulonimbus cloud is greatest in the a) tropical region, b) temperate region, c) polar region.

19.9 If a thunderstorm is located in the approach area, the pilot should a) not attempt to land until the storm passes, b) undertake diversion from the airfield, c) circumnavigate the storm.

19.10 Clear air turbulence is generally encountered when the aircraft is flying through a) thunderstorm, b) layer-type clouds, c) high-altitude, high-speed jet stream.

19.11 Thunderstorms are caused by a) high humidity, instability, and voltage difference, b) thunder and lightning, c) the anvil of a cumulonimbus cloud.

19.12 Large anvil of a cumulonimbus cloud indicates that the cloud cell a) has reached the dissipating stage, b) is at the mature stage, c) will now produce thunder and storm.

19.13 Flying at the maximum speed V_{NE} through turbulent thunderstorm may cause a) the aircraft to suffer high-speed stall, b) an increase in the risk of structural failure, c) the aircraft to safely cross the thunderstorm in minimum time.

19.14 Orographic thunderstorms occur a) almost exclusively during the daylight, b) mostly during the night hours, c) at any time during 24 h.

19.15 The effect of bright flashes of lightning strike can be minimized if the pilot a) turns off all radios and unnecessary electronic items, b) engages the autopilot, c) wears dark glasses and turns the cockpit lighting to maximum.

19.16 If a maturing thunderstorm is noticed at about 15 km ahead by the pilot of a light aircraft, he a) has enough visibility and terrain clearance to pass beneath the storm, b) must alter heading to circumnavigate the storm, c) has time to climb above the storm.

19.17 When fog freezes on a parked aircraft, it is called a) rime, b) hoar frost, c) glazed frost.

19.18 If carburetor icing is suspected during cruise, the pilot should a) operate at full power using a fully rich mixture, b) operate at full carburetor heat, c) first operate at partial carburetor heat to see if this is enough to clear the ice.

19.19 The frost point temperature is a) 0°C , b) the temperature at which fog freezes, c) the subzero temperature at which the air becomes saturated at the surface.

19.20 If you are flying a little below the aircraft's ceiling altitude and encounter clear ice in freezing rain, you should a) climb or descend for about 15 min to see if the icing stops, b) fly as fast as possible to clear the icing zone at the earliest possible time, c) change your heading and seek air traffic control clearance for a change of route.

19.21 The significant low-level windshear during the final phases of landing of a modern jet aircraft a) is not a hazard, b) poses a great danger because the resolution time is too short, c) is not a hazard because the aircraft is designed to withstand it.

19.22 A microburst is a) windshear of small size, b) updraft of small size, c) downdraft of small size.

19.23 A microburst changes the aircraft's a) attitude only, b) both attitude and airspeed, c) attitude, airspeed, and altitude.

19.24 A windshear is a) shear of air currents only, b) shear of winds only, c) shear of both winds and air currents.

19.25 Severe windshear is caused by a) updrafts, b) uniform gusts, c) downdrafts near the ground.

19.26 The term CAT refers to a) clean air turbulence, b) clear air turbulence, c) contaminated air turbulence.

19.27 When flying through turbulence, the flight controls should a) respond to each turbulent fluctuation, b) respond to average turbulent fluctuations taking place each minute, c) try to bring back the attitude of the aircraft.

19.28 The basic cause of turbulence is a) viscosity, b) windshear, c) temperature gradient.

19.29 Turbulence is found in a) winds only, b) air currents only, c) both in winds and air currents.

19.30 The majority of bird-strikes occur in a) daylight, b) night, c) early morning and late evening.

19.31 Bird-strikes mostly occur a) above 100 m, b) above 60 m, c) below 60 m.

20

Weather Observations, Reports, and Forecasts to Flying

20.1 Introduction

Weather information and forecasts are generally helpful to the public because the life of every human being is influenced by the weather. In certain areas over the Earth, the severe weather changes are rapid. Others can wait for favorable weather conditions, but the pilot cannot always choose to avoid weather conditions. A pilot learns to live with the weather. The ability to fly in any type of weather is often vital to mission success, especially during military operations. It is prudent to keep the pilot well informed of weather conditions during flight. A pilot needs meteorological information and the forecast for the following reasons.

1) Such information enables the pilot to understand the expected meteorological conditions, perhaps a day in advance, so that he can plan to take advantage of them. He or she can also determine whether the flight would be under visual flight rules (VFR) or instrument flight rules (IFR).

2) This information helps the pilot to understand the prevailing atmosphere and weather during takeoff at the starting airfield. He or she should also know the forecast for the airfield of departure of the expected weather for about half an hour or 1 h after takeoff in case he decides to return, because the weather may deteriorate rapidly after takeoff.

3) This information enables the pilot to recognize and properly interpret dynamic changes in the meteorological conditions during the flight. These changes can refer to the types of clouds with their bases and tops, temperatures and winds at flight level, freezing level, visibility at flight level, and areas of severe weather like thunderstorms, turbulence, icing, and hail.

4) The pilot needs the meteorological forecast for the terminal airfield and alternative airfields. Such information refers to cloud conditions, surface winds including windshear, freezing level, precipitation, visibility, and altimeter setting. The pilot should also know the runway conditions to enable him or her to estimate the length of the landing distance, and to warn of any necessary braking action in case of ice, snow, or any other type of contamination.

It is likely that the departure may be delayed longer than one and one half hours. In such cases it is again the responsibility of the pilot to recheck the weather. Unfortunately, a large number of air accidents are attributable to weather conditions. Pilots need not be trained meteorologists but they must know certain meteorological principles that affect the safety of flying. They should develop a “weather sense”—the ability to use the weather to their best advantage for flying.

The importance of weather in aviation has led to the tremendous expansion of national and international weather services. Meteorological changes occur on a large scale. Any change of weather in one region has its repercussions elsewhere on our globe. The interdependence of meteorological conditions on the Earth has led to the evolution of coordinated efforts among weather services throughout

the world. There is a worldwide organization that observes, collects, analyzes, forecasts, and distributes, weather information. There are several special meteorological services meant for pilots only.

Weather information is distributed through modern electronic devices such as teletypewriter networks, weather facsimile networks, telephones, and closed circuit television. The vast amount of information is presented in the form of maps, charts, and reports, and by using symbols, abbreviations, and coded words.

A brief description of the various instruments and facilities used for collecting data on weather elements is first presented here. The symbols, abbreviations, and coded words used in meteorology are described here, but this list is not complete due to limited space in this book. The different types of weather reports are briefly explained. In Sec. 20.4, different types of forecasts are explained.

20.2 Means for Measuring Weather Elements

Weather conditions are measured by different instruments, equipment, and other means, which are very briefly enumerated here.

20.2.1 Thermometers

Standard mercury thermometers, one of the oldest well-known devices, are still commonly used at meteorological stations. There are also some special-purpose thermometers used for obtaining maximum and minimum temperatures, recordings, and upper air measurements. The instrument used for making a continuous record of temperature is called a *thermograph*, and the continuous record produced thereby is called a *thermogram*.

20.2.2 Barometers

Instruments measuring atmospheric pressure are called *barometers*. Fortein's mercury barometer is commonly used for measuring atmospheric pressure at meteorological stations. It is regarded as standard equipment for calibrating other types of barometers.

Measurements of atmospheric pressure are also now commonly made by the aneroid barometer, which does not use gauging fluid; the word *aneroid* means "without liquid." It has a metallic bellows containing a partial vacuum. The bellows expands or contracts depending on the atmospheric pressure changes. The movement of the bellows is transferred to an indicator on a dial by means of mechanical linkages. An aircraft altimeter is generally an aneroid barometer that is calibrated to read the altitude directly in feet or meters rather than in units of pressure. A *barograph* is an aneroid barometer that gives a continuous record of atmospheric pressure, and the record is called a *barogram*.

20.2.3 Anemometers

An instrument measuring wind speed is called an *anemometer*. Some anemometers measure only wind speed while some others measure both wind speed and direction. The most common type of anemometer is the cup anemometer used by all meteorological stations. In a cup anemometer three or four cups in the horizontal plane are rotated about the vertical axis by wind force. There are some other types of anemometers¹ such as windmill, gust, hot-wire, and pressure anemometers.

20.2.4 *Hygrometers*

The word *hygro* means wet or moist, and hygrometers measure relative humidity. The hygrometer consists of two thermometers: one is a dry bulb and the other a wet bulb. The wet-bulb thermometer is kept wet by a damp muslin bag wrapped around it. The two thermometers read the same if the relative humidity is 100%. In unsaturated air the wet-bulb thermometer would cool due to evaporation of water vapor over it. The temperature of the wet-bulb thermometer and, therefore, the difference between the temperatures of the dry-bulb and wet-bulb thermometers, depends on the relative humidity, which can be calibrated.

Relative humidity is also measured by hair hygrometers. The oil-free human hair stretches on being humid, the amount of stretch being proportional to the relative humidity of the air. This property is exploited in designing hygrometers by mounting the hair under tension. Hair hygrometers are also used for obtaining a continuous record of the relative humidity; the instrument is then called a *hygrograph*. An instrument that makes a continuous record of both the humidity and temperature is called a *hygrothermograph*.

20.2.5 *Transmissometer*

The *transmissometer* records automatically and continuously the transparency of the atmosphere both during the day and night. A photocell is used to detect the brightness of the light received from a horizontal searchlight beam whose original brightness is known.

20.2.6 *Visibility Meter*

This visibility meter measures the visibility at night by means of the *Gold visibility meter*. The word "Gold" refers to the name of the inventor. The meter uses a photometer consisting of a glass slide of increasing capacity.

Visibility is also often assessed visually by noting the distance of a known object that can be clearly recognized.

20.2.7 *Cloud-Base Recorder (Ceilometer)*

The cloud-base recorder records continuously and automatically the base of clouds. It has a transmitter, a receiver (photoelectric cell), and a recording unit. A beam of light is transmitted upward, and is then scattered and reflected by the cloud that is detected by the receiver. It is also called a *ceilometer*. It can be used during the daylight hours as well as at night.

20.2.8 *Pilot Balloon (Pibal)*

A pilot balloon, known as a *pibal* for short, is a balloon of 76.2-cm (30-in.) diameter filled with hydrogen or helium gas. It ascends as soon as it is released from the ground, and carries no weather instrument. By observing its motion with a theodolite and assuming its standard rate of ascent, it is possible to find the speed and direction of the wind at different altitudes. The height of a cloud can also be determined. Pilot balloons are launched at 6-h intervals, and are usable only in daylight and good weather.

20.2.9 Radiosonde

The *radiosonde* is a large hydrogen- or helium-gas-filled balloon which carries a box and a parachute. The box weighs 0.907 kg, (2 lb) and carries temperature, pressure, and humidity measuring instruments, and a miniature radio transmitter. The parachute helps in returning the box safely to the Earth after the balloon has burst at altitudes of about 24–32 km (15–20 miles). The transmission of the three weather elements is made periodically via coded signals. The word *sonde* refers to a device sent up for obtaining information about the atmospheric conditions. To facilitate the recovery of the box, a reward is offered to the person who returns the radiosonde to a neighboring weather office after it has fallen to the ground.

20.2.10 Rawinsonde

The word *rawin* is the contraction of the words “radar radio” and “wind.” Unlike the pilot balloon, the rawinsonde can be used during night and cloudy weather.

20.2.11 Weather Reconnaissance Aircraft

Some organizations use special-purpose aircraft which are called *weather reconnaissance* aircraft. These aircraft are specially equipped with weather measuring instruments and are flown by a special team. These aircraft act as flying weather stations. They are generally used in areas where the weather information is missing, and for locating and tracking hurricanes and typhoons.

20.2.12 Meteorological Rockets

Certain rockets called *meteorological rockets* have the special mission of collecting weather and atmospheric information from higher altitudes. The nose of these rockets carries a radiosonde that can be ejected along with a parachute as soon as the rocket has reached its maximum altitude. As the radiosonde floats back to the Earth, it sends coded signals to the mother station on the Earth, like a normal radiosonde.

20.2.13 Weather Satellites

Weather satellites have recently boosted the quality of weather information reporting tremendously. They are capable of encircling the Earth for many months at altitudes of 1000 km or more. They can continuously take weather photographs and weather records, analyze them, and send them back to various stations on our Earth. The weather satellites can also now provide sophisticated information on clouds, amount of water vapor, snow, ice, mountain waves, squall lines, jet streams, hurricanes, and storms, and can take pictures of many of them.

20.2.14 Radar

Radar is an extremely useful facility of a meteorological station for detecting and tracking weather conditions such as rains, thunderstorms, squall lines, tornadoes, and hurricanes. Radar is also installed on many aircraft today. Radar is based on the principle that electromagnetic waves, after being reflected back by solid objects (including water droplets), provide information about the distance and direction of the objects. Certain objects, like water droplets, reflect more electromagnetic waves than others, like ice crystals. The reflected waves produce “echoes” that can

be seen on the radar screen. The strength of these echoes depends on the nature of the reflecting object. A weather radar is adjusted to the wave length that gives the best signal returns. All important weather stations use radar facility and bring out *radar reports*, called *rareps* for short. Weather radar is different from the radar used by the air traffic control (ATC) office because it is designed to pick up the movements of aircraft and not weather conditions.

20.2.15 Automatic Meteorological Observation Stations

An automatic meteorological observation station (AMOS) is now increasingly becoming a very standard, versatile, and desirable facility at many standard weather stations. It can measure runway visibility, amount of precipitation, altimeter setting, temperature, dew-point, wind speed, and wind direction. The AMOS can even transmit these reports automatically and provide printed copies of them.

20.2.16 Pilot Observations

Thousands of pilots are flying every hour, who have directly seen and faced different weather conditions. These pilots have become an important source of weather information, which is being exploited. A pilot generally informs the ground weather station about any unusual weather conditions encountered during the flight. This information is communicated to all the weather stations in contact with the pilot.

20.3 Weather Symbols, Abbreviations, and Codes

Weather information must be clearly understood, digested, and used by pilots. The intelligible presentation and communication of a huge amount of weather information in the minimum space and time has resulted in the evolution of weather symbols, abbreviations, and codes, which are very briefly described here.

20.3.1 Symbols for Wind Speed and Direction

Wind speed is indicated to the nearest multiple of 5 kn. For example, if the wind speeds are 7, 12, 23, and 36 kn, they will be indicated as 10, 10, 25, and 40 kn, respectively. Wind speed symbols are explained in Fig. 20.1. The magnitudes of wind speeds are represented by barbs, semibarbs, and pennants, which make obtuse angles with the common line as shown in Figs. 20.1a and 20.1b. The line shows the direction of wind from the side of the barb (or pennant) to the opposite side. One full barb is equivalent to 10 kn, the semibarb is equal to 5 kn, and one pennant represent 50 kn of wind speed. The no-wind case is represented in Fig. 20.1c by

SYMBOLS							
WIND-SPEEDS	25 KNOTS	50 KNOTS	CALM, LESS THAN 1 Km/hr	ABOUT 1 KNOT	20 KNOTS	WIND DIRECTION GIVEN, BUT SPEED MISSING	WIND DIRECTION VARIABLE

Fig. 20.1 Different types of symbols for wind speed.

SYMBOLS							
WIND-SPEEDS	0 KNOT (CALM)	5 KNOTS	20 KNOTS	35 KNOTS	50 KNOTS	100 KNOTS	115 KNOTS

Fig. 20.2 Illustrations of wind speed symbols.

two small concentric circles. If the wind speed is extremely low, about 1 kn, it is shown by a single line, as in Fig. 20.1d. If the measurements are not taken at the specified pressure altitude, but near to it, the full barbs are shown broken, as in Fig. 20.1e for 20 kn of wind speed. The situation when the wind direction is given but its speed is missing, is indicated by a "cross and line" as shown in Fig. 20.1f. If the wind direction is quite variable it is indicated by a circle and concentric dashed circle, as shown in Fig. 20.1g. Some illustrative symbols of wind speeds are shown in Fig. 20.2, where the wind direction in each case is kept constant, from west to east.

The direction of the wind is specified to the nearest multiples of 10 deg, and is measured in a clockwise direction from the north. For example, if the wind directions are 12, 94, 176, 276, and 284 deg, they will be specified as 10, 90, 180, 280, and 280 deg, respectively. The wind direction can be any value between 0 and 360 deg, and it is written near the barbs by the middle digit of the three-digit number. With the help of this single digit and the direction of the line, it is possible to decode the wind direction without any confusion. This is illustrated in Fig. 20.3, where the wind speed is kept constant but the wind direction is changing.

20.3.2 Notations for Barometric Pressure

The barometric pressure is denoted by three digits which are decoded in millibars as follows: First, place a decimal point after the second digit, i.e., before the last digit. If the first two digits of the three-digit group represent any number between 00 and 50, place the number 10 before the first digit. If the first two digits lie between 51 and 90, place the number 9 before the first digit. For example, if the three-digit number is 162, first read it as 16.2 and since 16 lies between 00 and 50, put 10 before 16.2, so that the decoded barometric pressure is 1016.2 mb. Similarly, take another example of a three-digit number 814 which should be read first as 81.4, and since 81 lies between 51 and 99, put 9 before 81.4, so that the decoded number reads 981.4 mb of the barometric pressure.

SYMBOLS							
WIND DIRECTIONS	040° FROM NORTH EAST TO SOUTH WEST	090° FROM EAST TO WEST	160° FROM SOUTH EAST TO NORTH WEST	180° FROM SOUTH TO NORTH	210° FROM SOUTH WEST TO NORTH EAST	270° FROM WEST TO EAST	340° FROM NORTH WEST TO SOUTH EAST

Fig. 20.3 Illustrations of wind direction.

Fig. 20.4 Barometric (pressure) tendency.

20.3.3 Symbols for Barometric Change and Tendency

Barometric pressure change and its tendency during the past 3 h at any weather station is indicated by certain symbols. The change in barometric pressure is designated by a series of three symbols. The first symbol is either a positive or negative sign indicating the increase or decrease in barometric pressure in the past 3 h. The second and third symbols are the integers expressing the magnitude of the pressure change in millibars in the past 3 h. For example, +16 indicates that the barometric pressure has increased by 16 mb in the past 3 h.

The barometric tendency indicates the behavior of the barometric pressure in the past 3 h. It informs whether the barometer pressure was fully or partly rising, steady, or decreasing during the period of the past 3 h. This information is given by simple lines as symbols which are easy to understand, as explained in Fig. 20.4.

20.3.4 Symbols for the Past State and the Present State of the Weather

The past state of the weather can be shown with the help of the symbols shown in Fig. 20.5. These are eight different symbols whose meanings are also explained in the figure.

The present state of the weather is shown by symbols. Cagle and Halpine² explain one hundred of these symbols.

20.3.5 Symbols for Clouds

There is an international code for representing 27 types of clouds by different symbols. Of these, the 15 most common cloud symbols that pilots should know are

Fig. 20.5 Symbols for past states of the weather.

presented in Fig. 20.6 in three different columns. The first column is for low clouds, and the second and third columns show middle and high clouds, respectively. Each of these columns has two parts, the first part depicting the symbol and the second part explaining the type of cloud it represents. The notations used for clouds are included near the bottom of the figure for ready reference.

20.3.6 Symbols for Sky Coverage

The sky may be completely clear or some clouds at low, medium, or high levels may exist. A weather station is required to inform pilots as to how much of the sky is covered by these clouds. What is important here is not the type or the

LOW CLOUDS		MIDDLE CLOUDS		HIGH CLOUDS	
SYMBOL	DESCRIPTION	SYMBOL	DESCRIPTION	SYMBOL	DESCRIPTION
	Cu with little vertical development and seemingly flattened		Thin As (entire cloud layer semitransparent)		Filaments of Ci, scattered and not increasing
	Cu of considerable development, generally towering, with or without other Cu or Sc bases, all at same level		Thin Ac; cloud elements not changing much and at a single level		Ci, often anvil-shaped, derived from or associated with Cb
	Cb with tops lacking clear-cut outlines, but distinctly not cirriform or anvil-shaped; with or without Cu, Sc, or St		Thin Ac in bands or in a layer gradually spreading over sky and usually thickening as a whole		Cs covering the entire sky
	Sc not formed by spreading out of Cu		Double-layered Ac or a thick layer of Ac, not increasing; or As and Ac both present at same or different levels		Cc alone or Cc with some Ci or Cs, but the Cc being the main cirriform cloud present
	St, but not Fs of bad weather	CLOUD ABBREVIATIONS			
	Cb having a clearly fibrous (cirriform) top often anvil-shaped, with or without Cu, Sc, St, or Scud	Ac — Altocumulus	Sc — Stratocumulus	As — Altostratus	St — Stratus
		Cb — Cumulonimbus		Cc — Cirrocumulus	
		Ci — Cirrus		Cs — Cirrostratus	
		Cu — Cumulus		Fc — Fractocumulus	
		Fs — Fractostratus		Ns — Nimbostratus	

Fig. 20.6 Cloud symbols.

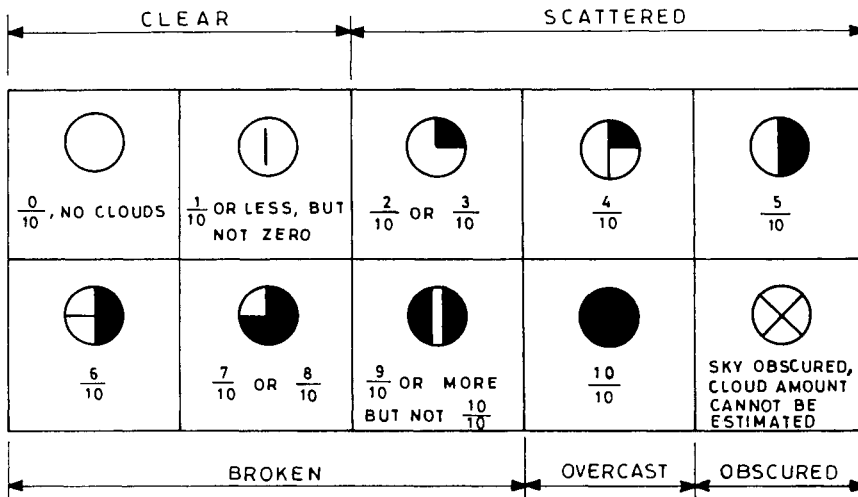


Fig. 20.7 Sky coverage symbols.

height of clouds but the extent to which these clouds cover the plane parallel to the Earth, as can be observed from a weather station. This information is presented by symbols that approximately quantify the amount of sky coverage. The numerical figure is provided by the fraction of 10. For example, if half the sky is covered by clouds, sky coverage is quantified as 5/10 (five-tenths). A complete list of symbols and the amount of sky cover they indicate is shown in Fig. 20.7.

The sky coverage is also often expressed for simplicity by using the terms clear, scattered, broken, and overcast, when more precise quantification is not necessary, as in the above paragraph. These terms are easy to remember. The amounts of coverage they indicate are also shown in Fig. 20.7. If the sky is less than one-tenth covered with clouds it is called *clear*, while if one-tenth to five-tenths of the sky is covered by clouds, this is called *scattered*. If sky coverage is six-tenths to nine-tenths, it is called *broken*, and the sky coverage above this fraction is called *overcast*. When the cloud amount cannot be estimated, this is called *obscured*. Figure 20.8 shows the symbols that are used to briefly denote sky coverage.

20.3.7 Symbols for Fronts

A surface weather map shows symbols of different fronts by different types of lines, as shown in Fig. 20.9. If it is a color map, the figure also indicates the color by which these lines should be shown.

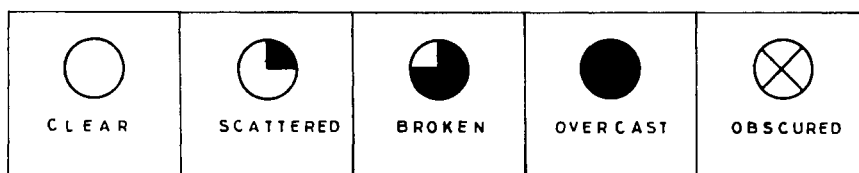


Fig. 20.8 Sky coverage symbols in brief.

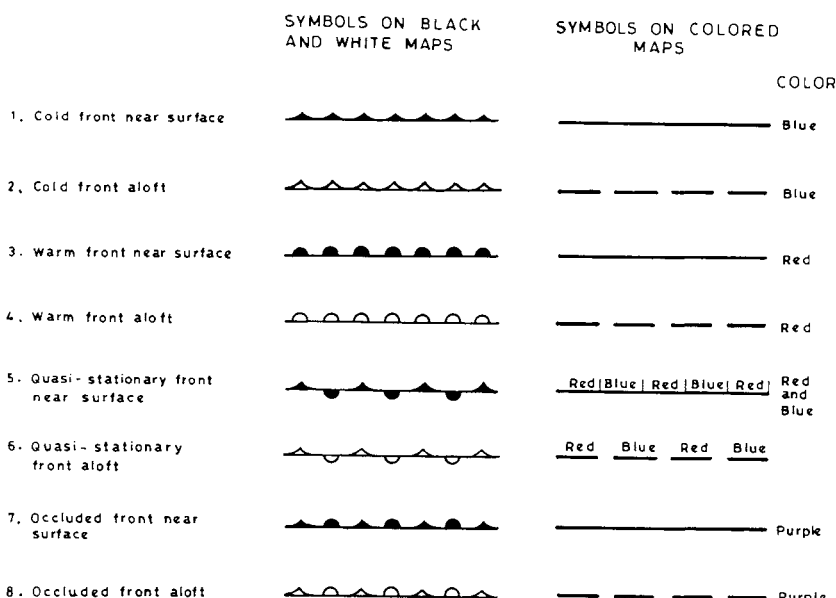


Fig. 20.9 Symbols for fronts.

20.3.8 Abbreviations and Codes

The use of abbreviated words is very common in weather reports and forecasts. This allows more information to be conveyed in less space and time. Weather depiction charts use a number of abbreviations for significant weather conditions; see Table 20.1.

A sequence report of weather has its own abbreviations whose detailed list can be found in Ref. 2. A few words and their codes are illustrated in Table 20.2.

20.4 Weather Reports

A meteorological or weather report is the statement of the weather conditions that are prevailing, or have prevailed, at a particular place and time. The weather report is distinctly different from a weather forecast, which is defined in Sec. 20.5. This distinction must be clear because some fatal accidents have occurred when some pilots assumed that a report has been a forecast. The report is also called *actual* and a standardized code is given to the report for brevity.

Table 20.1 Abbreviations for weather conditions

Words	Abbreviation	Words	Abbreviation
Thunderstorm	T	Drizzle	L
Freezing rain	E	Shower	W
Freezing drizzle	ZL	Haze	H
Rain	R	Smoke	K
Snow	S	Fog	F
Sleet	E	Ground fog	GF

Table 20.2 Sequence report abbreviations

Words	Codes	Words	Codes
Aircraft	ACFT	Horizon	HRZN
Aloft	ALF	Icing	ICG
Between	BTN	Lightning	LTNG
Broken	BRKN	Mountain	MTN
Ceiling	CIG	Occluded front	OCFNT
Cloud	CLD	Overcast	OVC
Cumulus	CU	Precipitation	PCPN
Dewpoint	DWPNT	Pressure	PRES
Drizzle	DRZL	Runway	RNWY
Extreme	XTRM	Snow	SNW
Falling	FLG	Squall lines	SQLNS
Forecast	FCST	Temperature	TMP
Freeze	FRZ	Turbulence	TURBC
Front	FNT	Visibility	VSBY
Ground fog	GNDFG	Weather	WX
Hailstone	HLSTO	Wind	WND

The weather report is prepared in the form of maps, charts, and reports. It is made available to all weather offices, to which it is transmitted by facsimile (fax) machines from a central meteorological analysis office. Different types of weather reports are explained here briefly.

20.4.1 Surface Weather Maps (*Synoptic Charts*)

A surface weather map contains isobars, regions of high and low barometric pressures, fronts, and station models. All these are presented at sea level so that a pilot gets an overall picture of the weather near the ground, but these conditions can be regarded as approximately valid up to an altitude of about 1524 m (5000 ft). Surface weather maps may be either color or black and white. The color map is hand-drawn by weather forecasters. The black-and-white (sometimes brown-and-white) map is produced by a fax machine. Some surface weather maps also indicate the regions of precipitation, areas of fog, haze, or smoke, and the places of dust or sand storms.

These surface weather maps are commonly called *synoptic charts* because they present a synopsis of meteorological conditions over a large area at a given time. The word *synoptic* is a combination of two Greek words, meaning a general view. Synoptic charts are issued eight times a day at 3-h intervals. The charts are always several hours late when received at a weather office, because it takes several hours to analyze, prepare, and distribute them, after the information is received from weather stations all over the continent.

20.4.2 Station Models

A station model contains symbolic presentation of certain important weather conditions in the proximity of the weather station. There are three types of station

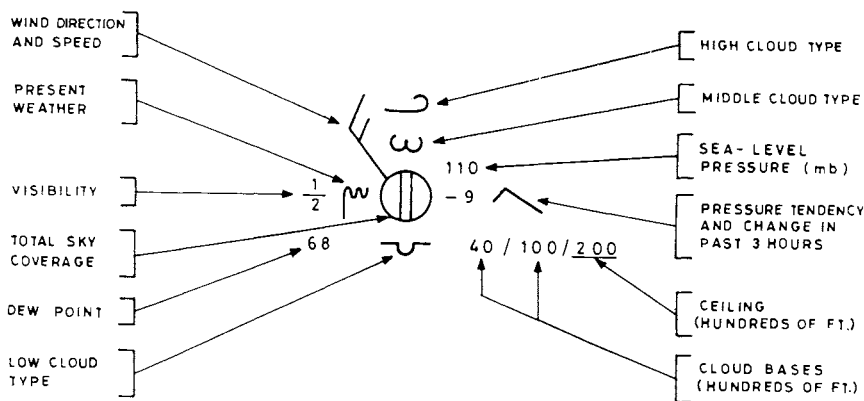


Fig. 20.10 Sectional station model.

models: a) sectional station model, b) the facsimile station model, and c) the international station model. The sectional station model is shown in Fig. 20.10 and for the sake of convenience we have explained the various notations and symbols. The three models are basically the same except that the international station model gives more information and facsimile station model contains a little less weather information as compared to that given by the sectional station model.

20.4.3 Weather Depiction Map

The map gives the regions of precipitation or any other important weather phenomena. The map also depicts the sky coverage, visibility (when 6 miles, i.e., 9656 m, or less), and cloud base [up to 6096 m (20,000 ft) above the ground]. Facsimile maps are prepared every 3 h and sent to the various stations over facsimile lines.

20.4.4 Airway or Aviation Weather Reports (Sequence Reports)

An aviation weather report is a statement of weather conditions actually existing at a particular place at a given time. Aviation weather reports are taken hourly at several stations. The weather data are transmitted by teletype circuit by means of abbreviated English-language words that can be easily decoded. The weather data are transmitted in a particular sequence, hence these are also called *sequence reports* or simply *sequences*.

This is the most rapid method of obtaining and relaying weather information by teletype circuits and they are transmitted hourly. It is also used in making amendments in forecasts. A sequence report is a very useful document that is used by pilots before flying. There are also sequence reports called SCAN, meaning *significant changes and notices to airmen*. These special sequence reports are transmitted only when any significant weather change has occurred that may appreciably influence aircraft safety or performance.

The sequence report does not provide a complete weather picture because between two weather stations the weather can be drastically different from that reported at either station, and also weather conditions can change very rapidly.

20.4.5 Radar Summary Charts

The type of radar echo is indicative of the type of weather that is prevailing. Thus, radar is able to indicate regions of rain, ice, snow showers, and drizzle. It can also track thunderstorms, tornadoes, and provide weather warning (WW). The radar information from various radar stations is collected and analyzed. The results are presented with the help of symbols and notations in the form of a map which is called a *radar summary chart*.

20.4.6 Freezing Level Charts

This is a map denoting altitudes of freezing level. That is, the altitudes where the temperature is 0 deg are indicated. The reporting station is shown by a thick dot, and a three-digit number is written by its side. If two zeros are put on the right-hand side of the three-digit number, it will give the freezing altitude in feet at the reporting station. The map also contains continuous lines showing the freezing temperature at different altitudes in steps of 1219 m (4000 ft). The places of freezing temperature at sea level are shown by a dotted line.

20.4.7 Wind Aloft Charts

The knowledge of wind speeds and directions at different altitudes helps a pilot to calculate the correct headings, ground speed, range, and endurance. A pilot, however, is not generally allowed to fly at the “best wind” altitude by air traffic control regulations. Therefore, it is important for a pilot to know wind speeds and directions at other possible flight altitudes. This is provided by *wind aloft charts* which can be categorized into three levels: low, intermediate, and upper. These are essentially maps, with each map giving information about wind speeds and directions at a fixed altitude above different reporting stations. Thus, for each altitude there is one different map.

The low-level chart contains maps of wind speeds and directions at the altitudes of 610 m (2000 ft), 1524 m (5000 ft), 2438 m (8000 ft), and 3048 m (10,000 ft) above the sea level. The intermediate-level wind chart contains similar maps for the altitudes of 6096 m (20,000 ft), 7620 m (25,000 ft), and 9144 m (30,000 ft), above sea level. The upper-level wind charts are maps of wind speed and its direction at the altitudes of 10,668 m (35,000 ft), 12,192 m (40,000 ft), and 15,240 m (50,000 ft) above sea level, and are useful to pilots of high-altitude commercial jet aircraft, military aircraft, and for research purposes. Wind aloft charts are transmitted four times daily over facsimile circuits.

20.4.8 Upper-Level Charts (*Constant Pressure Charts*)

Above 1524 m (5000 ft) the pressure patterns, the positions of high and low pressure, and the frontal positions start to change from sea level conditions. At higher altitudes, different weather maps are required for giving information similar to that of a surface weather map. The upper-level charts are actually weather maps, each map giving weather information at a fixed-pressure altitude. They are also called *constant pressure charts*. At the bottom of the map the pressure is given in terms of millibars, and the corresponding pressure altitude (in meters or feet) above sea level can be obtained from the table of standard atmosphere. For example, the 850-mb chart corresponds to an altitude of 1457 m (4781 ft), as obtained from the table of standard atmosphere; this chart is useful in planning

flights at an altitude of about 1524 m (5000 ft) above sea level. Thus, there are 850-, 700-, 500-, 300-, 200-, and 100-mb charts. Each of these maps exhibits isobars, station models depicting wind speed and its direction, temperature, dew-point, and altitude above the reporting stations, in the forms of symbols and notations. The 300- and 200-mb maps are useful for flights at altitudes around 9144 m (30,000 ft) and 12,192 m (40,000 ft), respectively; these heights are used by the present generation of subsonic jet aircraft.

20.4.9 Pilot's Reports (Pireps)

The reports are made by pilots during flight. These are transmitted by pilots to all those airway stations that are found enroute. The pilot generally reports unusual weather conditions such as thunderstorms, turbulence, icing, hail, cloud bases, and cloud tops. The pilot also relays information about the strong winds, funnels, strong echoes of airborne radar, temperature altitudes, places of marked change, and weather conditions near the peaks and ridges of mountain ranges.

20.5 Weather Forecasts to Aviation

The meteorological or weather forecast is a statement of weather conditions that are expected to prevail at a particular place and time. Some important types of forecasts are briefly explained here.

20.5.1 Terminal Forecasts

The *terminal forecast* describes expected weather at a specific airfield. The forecast states in specific terms the ceiling and cloud heights above the station, cloud layers in ascending order of height, visibility in statute miles (omitted if over 8 miles), and surface winds (omitted if less than 10 kn). The internationally sponsored TAFOR (*Terminal Aviation FORcast*) is transmitted in the form of coded words that can be easily decoded. Terminal forecasts are transmitted four times daily, and their validity period is indicated in the forecasts.

20.5.2 Area Forecasts

The area forecast states the weather conditions to be expected over a particular region. The area forecast includes the regional forecast for each region in the area. The forecast identifies the area covered by the forecast. Area forecasts are intended primarily for short- and medium-range flights. These forecasts are made on the teletype circuit by coded words in a particular sequence that can be decoded at the receiving station. They are prepared every 6 h and are valid for a 12-h period.

20.5.3 Upper Winds and Temperature Forecasts

The upper winds and temperature forecasts provide an estimate of upper wind speed and direction at selected levels (altitudes). Temperature forecasts are also added to all wind forecasts. These forecasts are transmitted every 6 h and are valid for a period of 12 h or as indicated on the forecast itself. The winds and temperatures at the heights not forecasted can be obtained by linear interpolation.

20.5.4 Prognostic Weather Charts (*Progs*)

Prognostic weather charts, referred to simply as *progs*, are issued to show what the surface weather map is expected to look like after a specified number of hours. These are graphic maps of the movements of the high- and low-pressure areas, surface fronts, wind patterns, low and middle clouds, and precipitation areas that can be expected in the next 24-h period. The Weather Bureau also issues 36- and 48-h progs. Surface progs are transmitted over facsimile circuit to local weather stations. Prognostic weather charts are useful to the pilot in predicting the changes that may occur before the actual time of departure or during the progress of the flight.

20.5.5 Upper-Level Prognostic Charts (Constant-Pressure Prog Charts)

The upper-level prognostic charts indicate weather conditions that may be expected to exist at some later specified time at higher altitudes. Like upper-level charts, they are prepared for the various pressure altitudes and are therefore also called *constant pressure prog charts*. The 36-h, 700-mb prog chart is used for flight planning near 3048 m (10,000 ft) altitude. Since the wind flows parallel to the contour lines at a speed directly proportional to the distance between the contours, the values of wind direction and speed may be computed from the constant-pressure prog charts. The charts drawn for high altitudes corresponding to less than 300 mb also include the data for jet stream axes and wind speed, found by drawing isotachs, which are lines of constant wind speed.

20.5.6 Severe Weather Forecasts

Certain weather stations also issue *severe weather forecasts* on teletype service. These forecasts are also reflected in terminal and area forecasts and in in-flight weather advisories. The severe weather forecast describes storms, hail, turbulence, and surface winds that are expected to arrive. These forecasts include the area for which they are made and the time period for which they are valid. Severe weather forecasts also describe the weather system that is expected to cause the severe weather conditions. The forecast states whether it is meant for the general public or for aviation use only.

20.5.7 In-Flight Weather Advisories

In-flight weather advisories serve the needs of airborne pilots and give warnings of the weather expected in the next 2–4 h. These are of two types: 1) SIGMET (significant meteorological information) and 2) AIRMET (airmen's meteorological information). SIGMETs are applicable to all aircraft and concern hazardous weather such as tornadoes, squall lines, hail (size 3/4 in. or more), severe and extreme turbulence, heavy icing, dust, and sandstorms. SIGMETs are issued, preferably, 2 h in advance. AIRMETs are advisories to light aircraft and are applicable to all those aircraft that have limited facilities with regard to equipment or pilots' qualifications. SIGMETs provide information even when the weather is less severe. In-flight weather advisories are issued on request to aircrews over the normal air-ground communication channel.

20.5.8 Nowcasting

Nowcasting is a new term that is now increasingly being used in the international meteorology community to define very short-range and very short-duration forecasts. The short range of the forecast refers to the immediate neighborhood of the airfield, and it is of short duration—2 h or less. Nowcasting serves the purpose of providing immediate necessary weather information that may be required by pilots. The term *nowcasting*, as used by the Air Force, is synonymous with two terms currently in use, namely, *trend forecast* and *weather warnings* (WW). A trend forecast in the Air Force is valid for 2 h after the time it is issued, while a WW informs pilots of the anticipated deterioration of weather elements to certain specified limits, or below these limits, in the immediate neighborhood of the airfield.

References

- ¹Peter, S., *Wind Forces in Engineering*, Pergamon, New York, 1972.
²Malcolm, W. C., and Halpine., C. G., *A Pilot's Meteorology*, Van Nostrand Reinhold, New York, 1970.
-

Problems

In the multiple choice problems below, mark the correct answer.

- 20.1** Why do pilots need a weather forecast?
- 20.2** What is the difference between the weather report and weather forecast?
- 20.3** What is a meteorological rocket?
- 20.4** What speeds do the wind symbols indicate if the actual wind speeds are 5, 18, 25, and 27 kn?
- 20.5** What is the barometric tendency?
- 20.6** Find the symbols for the past state of the weather in the cases of a) snow, b) sandstorm, and c) thunderstorm.
- 20.7** Explain the term “ceiling” in the case of clouds.
- 20.8** How are hot and cold fronts near the surface represented in the cases of a) a black-and-white map and b) a color map.
- 20.9** What is a sequence report?
- 20.10** What are synoptic charts?
- 20.11** Trend forecasts issued at major aerodromes are valid for a) the next hour, b) the next half-hour, c) the next 2 h.

20.12 To receive the conditions expected at your flight destination at expected time of arrival (ETA), you should request a) a report for that aerodrome, b) an actual for that aerodrome, c) a forecast for that aerodrome.

20.13 What are constant-pressure charts?

20.14 Write the full forms of the following abbreviations used in meteorology: Pireps, AIRMET, SIGMET, TAFOR, and WW.

20.15 What are the radiosonde and the rawinsonde?

20.16 What directions will the wind symbols, respectively, indicate if the actual wind directions are 7, 86, 104, 215, and 314 deg?

20.17 Decode the barometric pressures if they are coded as a) 154, b) 100, c) 984, and d) 990.

20.18 What do you understand by the barometric changes represented by a) +10, b) +16, c) -4, and d) -11?

20.19 Draw the symbols for a) stratus clouds, b) cumulus clouds, and c) cumulonimbus clouds. Mention the level of cloud in each case.

20.20 What do the ceilometer and pibal measure?

20.21 Draw the wind symbols in the cases of wind blowing at the speeds of a) 17 kn, blowing from south to north at 184 deg; b) 23 kn, from west to east at 266 deg; and c) 47 kn, blowing from southeast to northwest at 156 deg.

20.22 Some commonly used terms for indicating sky coverage are: scattered, broken, and overcast. Explain their meanings.

20.23 What is a sectional station model?

20.24 Decode the following codes of a sequence report: ACFT, FNT, ICG, MTN, and WX.

20.25 What are the abbreviations used in the case of significant weather for a) thunderstorm, b) snow, c) smoke, and d) freezing rain.

20.26 What are transmissometers and AMOS?

20.27 The actual barometric pressures are a) 890 mb, b) 940 mb, c) 1010 mb, and d) 1030 mb. Find their respective three-digit code numbers.

20.28 Draw the symbols of barometric tendency in the cases of a) pressure first decreases then rises, b) pressure remains steady, c) pressure rising then steady, and d) pressure rising.

- 20.29** What is meant by the sky coverage numerical figures a) $\frac{2}{10}$, b) $\frac{6}{10}$, and c) $\frac{10}{10}$.
- 20.30** What are the symbols for fog, drizzle, and rain, in the case of the past state of the weather?
- 20.31** What are the differences among forecasts, advisories, and prognoses?
- 20.32** What is the difference between forecasting and nowcasting?

Appendix A

Basic Conversion Factors

Temperature

$$^{\circ}\text{C} = (5/9)(^{\circ}\text{F} - 32) \quad \text{and} \quad ^{\circ}\text{F} = (9/5)^{\circ}\text{C} + 32$$

$$\text{K} = ^{\circ}\text{C} + 273.16 \quad \text{and} \quad ^{\circ}\text{R} = ^{\circ}\text{F} + 459.69$$

where $^{\circ}\text{R}$ = degree Rankine, and K = degree Kelvin

Plane Angle

$$1 \text{ deg} = 1.745 \times 10^{-2} \text{ rad} = 60 \text{ min} = 3600 \text{ s}$$

$$1 \text{ rad} = 57.296 \text{ deg} = 3438 \text{ min} = 2.063 \times 10^{-5} \text{ s}$$

Length

	Kilometer	Meter	Feet	Mile
1 km	1	1000	3281	0.6214
1 m	10^{-3}	1	3.281	6.214×10^{-4}
1 ft	3.048×10^{-4}	0.3048	1	1.894×10^{-4}
1 mile	1.609	1609	5280	1

Mass

	kg	slug	g
1 kg	1	0.06852	1,000
1 slug	14.59	1	14,590
1 g	0.001	6.852×10^{-5}	1

Speed

	m/s	km/h	ft/s	mile/h	kn
1 m/s	1	3.6	3.281	2.237	1.944
1 km/h	0.2778	1	0.9113	0.6214	0.5400
1 ft/s	0.3048	1.097	1	0.6818	0.5925
1 mile/h	0.4470	1.609	1.467	1	0.8689
1 kn	0.5144	1.852	1.688	1.151	1

Force

	N	lb	kg_f
1 N	1	0.2248	0.1020
1 lb	4.448	1	0.4536
1 kg_f	9.807	2.205	1

Pressure

	N/m ²	lb/ft ²	atm	cm Hg
1 N/m ²	1	0.02089	9.869×10^{-6}	7.501×10^{-4}
1 lb/ft ²	47.88	1	4.725×10^{-4}	0.03591
1 atm	1.013×10^5	2116	1	76
1 cm Hg at 0°C	1333	27.85	0.01316	1

Power

	kW	W	ft-lb/s	ft-lb/min	hp
1 kW	1	1000	737.6	4.425×10^4	1.341
1 W	0.001	1	0.7376	44.25	1.341×10^{-3}
1 ft-lb/s	1.356×10^{-3}	1.356	1	60	1.818×10^{-3}
1 ft-lb/min	2.260×10^{-5}	2.260×10^{-2}	1.667×10^{-2}	1	3.030×10^{-5}
1 hp	0.7457	745.7	550	3.3×10^4	1

Appendix B

Useful Data for Solving Numerical Problems

Standard atmosphere property ratios, SI units

Altitude <i>h</i> , m	Temperature ratio θ	Density ratio σ	Pressure ratio δ	Sound speed ratio a^*
0	1.0000	1.0000	1.0000	1.0000
1,000	0.9774	0.9075	0.8870	0.9886
2,000	0.9549	0.8217	0.7846	0.9772
3,000	0.9324	0.7422	0.6920	0.9656
4,000	0.9098	0.6689	0.6085	0.9538
5,000	0.8873	0.6012	0.5334	0.9419
6,000	0.8648	0.5389	0.4660	0.9299
7,000	0.8423	0.4816	0.4057	0.9177
8,000	0.8198	0.4292	0.3518	0.9054
9,000	0.7973	0.3813	0.3040	0.8929
10,000	0.7748	0.3376	0.2615	0.8802
11,000	0.7523	0.2978	0.2240	0.8673
12,000	0.7519	0.2546	0.1914	0.8671
13,000	0.7519	0.2176	0.1636	0.8671
14,000	0.7519	0.1860	0.1398	0.8671
15,000	0.7519	0.1590	0.1195	0.8671
16,000	0.7519	0.1359	0.1022	0.8671
17,000	0.7519	0.1162	0.0873	0.8671
18,000	0.7519	0.0993	0.0747	0.8671
19,000	0.7519	0.0849	0.0638	0.8671
20,000	0.7519	0.0726	0.0546	0.8671
21,000	0.7551	0.0618	0.0467	0.8690
22,000	0.7585	0.0527	0.0399	0.8709
23,000	0.7620	0.0449	0.0342	0.8729
24,000	0.7654	0.0383	0.0293	0.8749
25,000	0.7689	0.0327	0.0252	0.8769

$$\theta = T/T_{SSL}, \quad \sigma = \rho/\rho_{SSL}, \quad \delta = p/p_{SSL}, \quad \text{and} \quad a^* = a/a_{SSL}$$

Standard atmosphere sea level (SSL) values:

$$T_{SSL} = 288.15 \text{ K} = 15^\circ \text{ C} \quad R = 287 \text{ m}^2/(\text{s}^2\text{K})$$

$$\rho_{SSL} = 1.225 \text{ kg/m}^3 \quad \gamma = 1.4$$

$$p_{SSL} = 1.01325 \times 10^5 \text{ N/m}^2 \quad g_{SL} = 9.8067 \text{ m/s}^2$$

$$a_{SSL} = 340.3 \text{ m/s}$$

Major specifications of aircraft 1 and 2

Specifications	Aircraft 1 (glider)	Aircraft 2 (unpowered aircraft)
Total weight, N	3920	12,470
Wing area, m ²	15	16.20
C_{D_0}	0.015	0.020
K	0.03	0.059
$C_{L,m}$	1.20	1.45

Major specifications of turbojet aircraft A, B, and C

Specifications	Aircraft A (jet trainer)	Aircraft B (executive)	Aircraft C (long-range)
Total weight, N	12,500	66,750	2,700,000
Maximum fuel, N	3,200	24,500	1,000,000
Wing area, m ²	6.12	21.5	475
Maximum thrust, N	2,600	26,250	800,000
C_{D_0}	0.032	0.026	0.017
K	0.10	0.084	0.042
M_{dr}	0.72	0.82	0.85
$C_{L,m}$	1.22	1.32	2.2
c , N/h/N	1.18	0.95	0.8

Major specifications of piston-prop aircraft D and E

Specifications	Aircraft D (single engine)	Aircraft E (twin engine)
Total weight, N	12,000	35,000
Maximum fuel, N	1,600	5,000
Wing area, m ²	15	26
Maximum power, kW	200	500
C_{D_0}	0.042	0.03
K	0.074	0.048
η_p	0.83	0.85
$C_{L,m}$	1.5	1.7
\hat{c} , N/h/kW	2.45	2.5
Critical altitude, km	4.5	6

Index

- Abbott, I. H., 120
Abbreviated words, 494
Absolute altitude, 175
Absolute ceiling, 264, 265
Absolute humidity, 47
Accelerate-and-stop distance, 379, 395
Accelerated-level decelerated-turn, 455
Acceleration
 correction factor, 279
 distance, 396
 segment, 395
Accelerometer, 12
Acid rain, 63
Actual, 494
Adjustable-pitch propeller, 170
Advance ratio of the propeller, 162
Advanced aerobatics, 413
Advection, 30
Advection fog, 465
Aerobatics, 403, 407
Aerodynamic efficiency, 19, 104, 108
Aerodynamic efficiency of the aircraft, 217
Aerodynamic interference effect, 111
Aerodynamics, 19
Aerosols, 48
Aerothermodynamic duct, 146
Afterburner, 136
Agility, 416
Aileron roll, 413
Ailerons, 3, 7
Air
 current, 40, 186
 current shear, 477
 front, 58
 inlet duct, 128
 intake, 4
 mass, 58
 traffic control, 489
Air-cooled engines, 153
Airborne distance, 378
Aircraft, 1
 configuration, 5, 104
 retardation devices, 392
Airfoil(s), 87, 88
Airframe, 1
Airplane, 1
Airscrew, 160
Airspeed, 87, 178–184, 196, 200, 217, 296, 304, 314, 315, 329, 348, 364, 371, 380–382, 385, 393, 414, 437
 calibration, 420
 for minimum thrust, 237
 indicator, 10, 178, 179
 measurement, 178
Albedo, 31
All-up weight, 15
Altimeter, 11
Altitude 175–177, 221, 264
Altitude measurements, 177
Analytical method of data reduction, 435
Ananthasayanam, M. R., 76
Anderson, J. D., Jr., 121, 147, 171
Anemogram, 189
Anemograph, 189
Anemometer, 189, 486
Angle of attack, 88, 162
Angle of attack calibration, 422
Anti-icing
 device, 154
 method, 474
Anti-g suits, 415
Anticyclones, 37
Approach
 light contact height, 65
 segment, 390
 to stall, 424
Area forecast, 498
Artificial horizon, 12
Aspect ratio, 93
Aspirated engine, 155, 157
Atmosphere, 29, 67, 68, 70, 73, 74, 177
Atmospheric density, 38
Atmospheric pollution, 60, 63
Atmospheric turbulence, 466
Attitude
 director indicator, 12
 indicator, 12
Augmentor wing, 103
Automatic direction finder, 13
Automatic meteorological observation station, 489
Aviation weather reports, 496
Axial flow compressor, 129
Backing, 188
Balanced field length, 380, 381, 396
Bank angle, 296, 365
Barbs, 489
Barogram, 486
Barograph, 486
Barometers, 486
Barometric pressure, 35, 490
Barometric tendency, 37, 491
Barrel roll, 412

- Barry, R. G., 75
 Base drag, 106
 Basic operational weight, 16
 Beaufort
 numbers, 188
 scale, 188
 Bennett, D. C. T., 75
 Bent, R. D., 171
 Bernard, R. H., 25
 Bernoulli's equation, 117
 Best endurance, 204, 205
 Best-endurance glide(s), 203, 207
 Best (maximum) range, 198, 200
 Best-range airspeed, 200
 Best-range glide, 198
 Bird-strikes, 480
 Birdsall, D. L., 290
 Blackout, 415
 Bleed rate, 425
 Bogard, J. K., 482
 Bordan gauges, 116
 Boundary-layer
 fences, 103
 flow, 83
 injection, 101
 suction, 102
 Bowers, P. M., 482
 Brake
 horsepower, 156
 power, 141
 state, 171
 Braking friction, 382
 Braking segment, 396
 Breguet's range formula, 225
 British Civil Airworthiness Requirements, 423
 Buck, R. N., 482
 Bursting of the short bubble, 89
 Buzz, 21
 Bypass ratio, 142
 Cagle, M. W., 75, 211
 Calibrated airspeed, 178, 183
 Camber line, 88
 Campbell, R. D., 120, 416
 Carburetor
 air inlet temperature gauge, 154
 air temperature gauge, 160
 icing, 154
 mixture temperature gauge, 154
 Carruthers, N. B., 119, 290
 Cat's whiskers, 52
 Ceiling, 56, 264–266
 altitude, 221, 264
 of clouds, 56
 Ceilometer, 487
 Center
 of gravity, 6
 of pressure, 17
 Centrifugal compressor, 129
 Champion, K. S. W., 76
 Chandelle, 405
 Chord of the airfoil, 87
 Chorley, R. J.,
 Chow, C.-Y., 120
 Clancy, L. J., 120
 Clear air turbulence, 466
 Clear ice, 473
 Clearway, 378
 Climb, 259–264, 266, 267, 271, 273, 279, 345,
 347–349, 352, 429
 airspeed, 382
 angle, 259, 261, 346
 performance tests, 429
 schedule, 286–288
 segment, 388
 to near-ceiling, 433
 Cloud-base recorder, 487
 Cloud(s), 51–54, 56, 210, 470, 491
 Coanda effect, 103
 Coarse-pitch propeller, 163
 Cockpit, 2
 Cockpit controls, 8
 Coefficient
 of rolling friction, 382
 of sliding friction, 382
 of viscosity, 82
 Cohen, E., 147
 Col, 37
 Cold, 37
 Cold air waterfall, 44
 Cold front, 59
 Combined controls, 110
 Compressibility correction, 184
 Compressible flow, 85, 118
 Compressor, 129
 Compressor stall, 130
 Condensation, 48
 Conditional stability, 55
 Conduction, 30
 Connolly, T. F., 171
 Constant
 airspeed glide, 196
 EAS climb, 279
 lift coefficient glide, 196, 197
 Mach number climb, 280
 pressure charts, 497
 pressure prog charts, 499
 Constant-airspeed guide, 198
 Constant-pitch propeller, 169
 Constant-speed propeller, 169
 Control
 column, 8
 surfaces, 7, 109
 Control wheel, 8
 Convection, 30
 Convergence, 46
 Convergent-divergent nozzle, 128
 Cooling drag, 106, 153
 Coordinated turn, 293, 363
 Coriolis force, 40
 Corner speed, 414
 Counter-rotating propellers, 171

- Course-pitch propeller, 163
 Critical altitude, 156
 Critical engine failure recognition airspeed, 381, 396
 Critical field length, 396
 Critical Mach number, 91
 Cruise, 215, 313
 Cruise performance tests, 442
 Cruise-climb flight, 225, 238, 248, 319, 329, 332, 338
 Cruising
 endurance, 215
 flight, 313
 range, 215
 Cuban 8, 412
 Cumuliform cloud, 53
 Cumulus clouds, 53
 Cup anemometer, 189
 Cyclones, 36
 Cyclostrophic force, 40
 Cylinder head temperature gauge, 159
- Daily, J. W., 120
 Data scatter, 428
 Davies, D. P., 25
 Decision airspeed, 381
 Deicing
 device, 154
 method, 474
 Delta wing, 94
 Density
 altitude, 177
 ratio variation, 72
 Derating, 141
 Descent performance tests, 440
 Design parameters, 23
 Dew, 50
 Dew point, 47
 Dhawan, S., 210
 Different flight programs, 222, 317
 Differential heating of terrains, 31
 Differential method, 435
 Diffusers, 129
 Dihedral, 93
 Direction indicator, 14
 Directional gyro, 14
 Directional stability, 20
 Distance
 measuring equipment, 13
 traveled in climb, 263
 Dobson, G. M. B., 76
 Doebelein, E. O., 120
 Doldrums, 42
 Dole, C. E., 120, 399
 Dommasch, D. O., 171
 Downburst, 469
 Downwash, 89
 Drag, 106, 107, 128, 153, 439
 coefficient, 105
 polar, 91, 97
 polar determination, 423
 rise Mach number, 93
 Drizzle, 57
 Drooped leading edge, 99
 Dry air adiabatic lapse rate, 34
 Dry fog, 51
 Dual flow, 140, 142
 Durbin, E. J., 190, 458
 Dutch roll, 7, 112, 413
 Dynamic, 7
 pressure, 119
 pressure limit, 415
 stall, 426
- Effect
 of pollution, 61
 of runway slope, 398
 of temperature, 398
 of wind, 323, 397
 Effectiveness of load factor, 298
 Elevator(s), 4, 7
 Elevon, 110
 Elsom, D., 75
 Emergency distance, 380
 Empty weight, 16
 End-plates, 4
 Endurance, 197, 215, 321–323
 Energy
 height, 281
 optimization, 286
 Engine
 failure probability, 393
 failure recognition airspeed(s), 381, 393
 instruments, 158
 parameters, 137
 power, 156
 ratings, 127, 157
 test stand, 134
 Engine-inoperative cruise, 230
 Environmental lapse rate, 55
 Eppler, R., 120
 Equations
 of climb, 259, 345
 of motion, 18, 193, 216, 293, 313, 363
 Equivalent airspeed, 178, 181
 Equivalent power-specific fuel consumption, 141
 Equivalent shaft horsepower, 141
 Equivalent shaft power, 140
 Equivalent thrust, 143
 Etages of clouds, 54
 Euler's equations, 117
 Evaporation, 48
 Excess power, 262, 347
 Exhaust nozzle, 131
 Exosphere, 67
 Expansion wave, 86
 Experimental method of data reduction, 433
 Experimental methods, 115
 Externally blown flap, 103
 Eye of the typhoon, 44

- Fall wind, 43
- Fastest climb, 271, 352
- Fastest turn, 301, 367
- Feathering axis, 170
- Feathering state, 171
- Federal Aviation Regulations, 377, 399, 423
- Field length, 396
- Figure(s) of merit, 23, 137
- Fin, 4
- Fine-pitch propeller, 163
- Fineness ratio, 104
- Fish rain, 45
- Fixed-pitch propeller, 169
- Flame speed, 131
- Flameout, 131
- Flaperon, 110
- Flap(s), 3, 99–101, 103
- Flare segment, 390
- Flattest glide, 198, 199
- Flight, 194, 218, 237, 249, 329
 - boundaries, 413
 - control, 109
 - display, 12
 - of birds, 209
 - speed, 180
 - testing, 419
 - visibility, 65
- Flight Test Manual, 181
- Flow
 - parameters, 86
 - visualization, 116
- Flow(s), 82–86, 117, 118, 140, 142, 466
- Flutter, 21
- Fly-by-wire, 10
- Flying
 - in fog, 465
 - in icing conditions, 475
 - in the jet stream, 477
 - in the windshear, 479
 - in thunderstorm clouds, 470
 - in turbulence, 467
 - stove, 146
- Fog, 51, 463–465
- Forces during takeoff with engine failure, 393
- Form drag, 106
- Fowler flap, 101
- Fractions of flicks, 413
- Freezing, 49
 - Freezing level charts, 497
- Friction, 382
- Frog rain, 45
- Frontal breakdown, 59
- Frontal development, 59
- Frontal zone, 58
- Frontogenesis, 59
- Frontolysis, 59
- Front(s), 58–60
- Frost, 50, 472
- Froude momentum theory, 165
- Fuel
 - consumption in climb, 263
 - ice, 154
 - injection systems, 155
- Fuel/air ratio, 153
- Fundamental thrust equation, 133
- Funnel effect, 44
- Fuselage, 2, 104
- Gas
 - turbine, 126, 131
 - turbine engine, 131
- Gault, D. E., 120
- Geometric altitude, 175
- Geopotential altitude, 176
- Geostrophic deflection, 40
- Geostrophic force, 40
- Glauert similarity rule, 90
- Glider, 1
- Glide, 193, 196–199, 203, 207
- Gliding
 - angle, 194, 199, 201, 204, 206
 - flight parameters, 194
- Global wind circulation, 41
- Goin, K. L., 120
- Gold visibility meter, 487
- Goldsmith, E. L., 147
- Goodmanson, L. T., 120
- Grain rain, 45
- Graphical method of solution, 287
- Gratzer, L. B., 120
- Grennfelt, P., 75
- Greyout, 415
- Gross thrust, 133
- Gross weight, 15
- Ground
 - fog, 464
 - interference, 114
 - roll distance, 378
 - roll segment, 384
 - speed, 180
- Grover, J. H. H., 399
- Guide vanes, 129
- Gust
 - anemometer, 189
 - factor, 188
 - speed, 187
- Gust-load factor, 188
- Gustiness factor, 187
- Gyro horizon, 12
- Hage, R. E., 25, 120
- Hail, 57, 469, 473
- Hale, F. J., 76, 147, 233, 256, 290, 360, 373
- Halo(s), 30, 46, 53
- Halo effect, 53
- Halpine, C. G., 75, 211, 500
- Harper, J. J., 120
- Hazard of icing, 471
- Heading indicator, 14
- Headwind, 180

- Headwind shear, 478
 Heaslet, M. A., 120
 Helicopter, 1
 Herrington, R. M., 458
 Hesitation rolls, 412
 Higgins, P. R., 482
 High-lift devices, 98
 High-pressure (HP) compressor, 130
 High-pressure regions, 37
 High-speed solution, 218
 High-speed taxi tests, 427
 High-subsonic airfoils, 88
 High-subsonic wings, 94
 Highs, 37
 Hills of air, 37
 Hinge moment, 109
 Holder, D. W., 120
 Horizontal buoyancy, 113
 Horizontal situation indicator, 14
 Horizontal stabilizer, 4
 Horley, R. J., 75
 Houghton, E. L., 119, 290
 Human limitation, 415
 Humidity, 47, 48
 Hygrograph, 487
 Hygrometers, 487
 Hygrothermograph, 487
 Hypersonic airspeed, 87
 Icing, 154, 471, 473, 474
 Ideal efficiency, 165
 Impact ice, 154
 In-flight weather advisories, 499
 Incidence, 88
 Incompressible flow, 85, 117
 Indicated airspeed, 178, 180
 Indicated horsepower, 156
 Indirect method, 455
 Induced drag, 106
 Induced drag effect, 439
 Inertia
 distance, 396
 effect, 439
 segment, 395
 Inertial navigation system, 14
 Instantaneous endurance, 322
 Instantaneous range, 222
 Instrument flight rules, 485
 Instrumental landing system, 13
 Instrumented runway visual range, 65
 Interference drag, 106
 Internally blown flap, 103
International Cloud Atlas, 52, 75
 Inversion, 34
 Inviscid fluid, 82
 Ionosphere, 67
 Irrotational flow, 84
 Isobar, 35
 Isosteric, 38
 Isothermal layer, 34
 Jet streams, 45, 476, 477
 Karamcheti, K., 120
 Karman vortex street, 84
 Katabatic wind, 43
 Knife flight, 413
 Kruger, 101
 Kruger flap, 99
 Kruger-Fowler flap, 101
 Kuchemann, D., 120
 Kuethe, A. M., 120
 Lambert, M., 25
 Laminar flow, 82
 Laminar separation bubble, 84, 89
 Land breeze, 43
 Landing
 distance, 379
 performance tests, 428
 phase, 389
 roll distance, 392
 Laplace equation, 117
 Lapse rate, 33, 34
 Latent heat of vaporization, 34, 48
 Lateral stability, 20
 Law of Buys-Ballot, 40
 Layton, D., 190, 309, 458
 Lazy 8, 406
 Leading-edge flaps, 100
 Leading-edge slat, 99
 Leakage drag, 106
 Lean limit of flammability, 130
 Least-time track, 38
 Length of runway, 378
 Level flight acceleration tests, 430
 Levels of clouds, 54
 Liepmann, H. W., 120
 Lift, 90
 boundary, 413
 boundary tests, 450
 coefficient, 105
 coefficient curve, 96
 coefficient curve determination, 422
 coefficient glide, 196, 197
 Lift and drag coefficients, 90, 95
 Lift-dependent drag coefficient factor, 97, 107
 Liftoff, 377
 airspeed, 381, 385
 distance, 377
 Light icing, 474
 Lightning, 468
 Limit load factor, 414
 Liquid-cooled engine, 153
 Lloyd, A. T., 482
 Load factor, 296, 365
 Local winds, 42
 Lomax, H., 120
 Lomcovaks, 413
 Loney, S. L., 26
 Long bubble, 89
 Longitudinal stability, 20

- Loop, 408
 Low-pressure (LP) compressor, 130
 Low-pressure region, 36
 Low-speed airfoils, 88
 Low-speed solution, 218
 Low-speed wings, 94
 Lows, 36
 Ludlam, F. H., 75
 Lull, 187
 Lush, K. J., 290
- MacDonalds, S. A. F., 25, 190, 482
 Mach number, 5, 87, 91, 93, 280
 Machmeter, 11
 Mackerel sky, 53
 Magnetic compass, 14
 Mair, W. A., 290
 Malcolm, W. C., 500
 Maneuver speed, 414
 Manifold
 absolute pressure, 158
 pressure, 152
 pressure gauge, 159
 Mares' tails, 52
 Maskell, E. C., 119
 Mason, B. J., 75
 Maximum
 aerodynamic efficiency, 108
 allowable thrust, 127
 continuous power, 406
 endurance, 443, 448
 except takeoff (METO) power, 157
 load factor, 298, 366
 range, 247, 443, 448
 range factor, 444
 rate of climb, 353
 Maximum-endurance flights, 251, 336
 Maximum-energy climb, 287
 Maximum-range flight(s), 239, 330
 McConnell, K. G., 120
 McCormick, B. W., 120, 399
 McCullough, G. B., 120
 McKinley, J. L., 171
 Mean line, 88
 Mean wind speed, 186
 Mechanical convection, 46
 Mechanical high-lift devices, 98
 Mechanical horizon, 12
 Merzkirch, W., 120
 Mesopause, 66
 Mesosphere, 66
 Meteorological rockets, 488
 Method
 of hot wings, 475
 of partial climbs, 429
 Microburst, 469
 Middleton, D. H., 26
 Miele, A., 76, 120
 Military power, 136
 Minimal flight path, 38
 Minimum
 flight airspeed, 380
 power airspeed, 315
 Minimum-control airspeed, 381
 Minimum-power flight, 329
 Minimum-thrust flight, 237
 Minzner, R. A., 76
 Mist, 51
 Mixer blades, 130
 Moderate icing, 474
 Moist air, 39
 Moist air adiabatic lapse rate, 34
 Moisture, 50
 Monsoon, 42
 Moran, J., 121
 Most economical climb, 278
 Mountain breezes, 43
 Multiple flow, 140, 142
- Narasimha, R., 76, 119
 Navier, 116
 Navier-Stokes equation, 116, 117
 Navigational display, 15
 Necessary condition
 for turning, 295
 of flight, 218
 Nelson, R. C., 25
 Net thrust, 133
 Never-exceed airspeed, 414
 Newton's
 law of gravitation, 176
 second law, 260
 third law of motion, 125
 Newtonian fluid, 82
 Nicolai, L. M., 120
 Nomenclature of clouds, 52
 Nominal best climb schedule, 288
 Nondirectional radio beacon, 13
 Normal shock, 85
 Nose wheels, 383
 Notations for barometric pressure, 490
 Nowcasting, 500
 Nozzles, 131
 Numerical Method, 276
- Oblique shocks, 85
 Obstacle height, 379
 Occluded fronts, 60
 Oil
 pressure gauge, 159
 temperature gauge, 159
 Ojha, S. K., 119, 120, 256, 290, 341, 360
 Operating weight, 16
 Operational ceiling, 266
 Operational empty weight, 16
 Optimal Climb, 280
 Ordway, F. I., 147
 Orographic clouds, 54
 Oswald's span efficiency factor, 107,
 195
 Outside air temperature gauge, 160
 Overcast, 493

- Pallet, E. H. J., 26, 120
 Panel method, 117
 Pankhurst, R. C., 120
 Parasite drag, 107
 Payload, 16
 Peery, D. J., 190
 Pennants, 489
 Performance
 ceiling, 265
 with engine failure, 393
 Perkins, C. D., 25, 120
 Peter, S., 500
 Philpott, D. R., 25
 Phototheodolite, 428
 Phugoid motions, 7
 Pibal, 487
 Piggott, D., 211
 Pilot
 balloon, 487
 observations, 489
 Pireps, 498
 Piston engine(s), 151, 156
 Piston-prop, 151
 Pitch, 6, 7, 161
 Pitch angle, 161
 Pitot
 pressure, 118
 tube, 118
 Pitot-static calibration, 420
Piw-Viw, 447
 Plain flap, 101
 Polar
 easterlies, 42
 front, 59
 Pollution, 60–64
 Pollution control, 64
 Pond, H. L., 76
 Pope, A., 120
 Port, 3
 Port wing, 3
 Position errors, 183
 Potential, 55
 Power, 157
 available, 316
 loading, 314
 plant, 5
 required, 315, 316
 variations, 157
 Power-specific fuel, 364
 Power-specific fuel consumption, 157, 364
 Powered flight control, 10
 Powered high-lift devices, 103
 Prandtl–Glauert similarity rule, 90
 Precipitation, 50
 Precipitation-induced fog (frontal fog), 465
 Preheating method, 475
 Pressure, 17, 35, 38, 39, 89, 117–119, 130, 152,
 158, 159, 415, 497, 499
 aloft, 38
 altitude, 177
 anemometer, 189
 charts, 497, 499
 coefficient, 89
 drag, 106
 pattern flying, 38
 systems, 35
 tendency, 37
 Prevailing visibility, 64
 Prevailing westerlies, 42
 Primary control surfaces, 109
 Primary flight controls, 109
 Primary flight display, 12
 Primary flow, 140, 142
 Principle of soaring, 209
 Profile drag, 107
 Prognostic weather charts (Progs), 499
 Propeller, 160, 162, 163, 169–171
 efficiency, 167, 168
 geometry, 160
 parameters, 166
 reversing, 171
 state, 170
 Propulsive efficiency of the aircraft, 224
 Pulldown maneuver, 307
 Pullup turn, 306
 Pushers, 160
 Quarter-chord line, 93
 Quasi-steady climb, 279
 Radar, 488
 method, 420
 reports, 489
 summary chart, 497
 Radiation, 30, 31
 Radiation fog, 464
 Radio
 magnetic indicator, 13
 navigation aids, 13
 Rain, 45, 57, 63
 Ram recovery, 128
 Ramjet, 145
 Ramp weight, 15
 Range, 196, 215, 221, 317
 Range factor, 224
 Rankine–Froude momentum theory, 165
 Rareps, 489
 Rate
 of climb, 260, 262, 267, 273, 347, 349
 of descent, 195, 199, 201, 204, 206
 Rated power, 157
 Rawinsonde, 488
 Rawin, 488
 Reattachment, 83
 Recovery after the stall test, 425
 Red line airspeed, 414
 Reddish visual indications, 415
 Relative humidity, 47
 Reynolds number, 87
 Rich limit of flammability, 130
 Richel, H., 75
 Ridge, 37

- Riegels, F. W., 120
- Riley, W. F., 120
- Rime ice, 472
- Rocket, 147
- Rogers, G. F. C., 147
- Roll-off-the-top of a loop, 409
- Rolling friction, 382
- Roll(s), 6, 7, 112, 378, 384, 392, 407, 410, 413
- Roosme, A., 482
- Root-chord, 93
- Roshko, A., 120
- Rotation
 - airspeed, 385
 - distance, 378, 386, 391
- Rotational flows, 85
- Rotors, 129
- Rudder, 4, 7
- Rudder pedals, 9
- Ruddervators, 110
- Runway, 64
 - length required, 378
 - visual range, 65
- Rutowski, E. S., 290
- Sachs, P., 120, 190
- Sandborn, V. A., 120
- Saturated-air adiabatic lapse rate, 34
- Saturation ratio, 47
- Sawtooth climb test, 429
- Scale-altitude correction, 183
- Schjoldager, J., 75
- Schlichting, H., 119
- Scorer, R. S., 75
- Screen height, 379
- Sea breeze, 43
- Seasonal winds, 42
- Secondary flow, 140, 142
- Seddon, J., 147
- Separation, 83
- Sequence reports, 496
- Sequences, 496
- Service ceiling, 265
- Severe icing, 474
- Severe weather forecasts, 499
- Shaft
 - horsepower, 156
 - power, 126
 - turbine, 140
- Shear, 45, 440, 477, 478
- Sherby, S. S., 171
- Shevare, G. R., 120
- Shock
 - stall, 91
 - wave, 85
- Short bubble, 89
- Shrimp rain, 45
- Sidestick, 9
- Significant changes and notices to airmen, 496
- Skin friction drags, 107
- Slat, 99
- Sliding friction, 382
- Slotted flap, 101
- Slotted wings, 99
- Slow roll, 407
- Smith, J. T. M., 75
- Smog, 51
- Smoke trail method, 420
- Snaking, 7, 413
- Snap roll, 410
- Snow, 57, 473
- Soaring, 209
- Soaring in clouds, 210
- Soaring in thermals, 209
- Soaring in upslope winds, 210
- Solar radiation, 31
- Span, 93
- Specific energy, 281
- Specific excess power, 282
- Specific humidity, 47
- Specific impulse, 137
- Specific range, 222, 323, 449
- Specific thrust, 261
- Speed, 186, 414
 - course test, 420
 - of sound, 5
- Speed-power test, 446
- Split flap, 101
- Spoilers, 8
- Spray region, 67
- Squall, 188
- Squall line, 59
- St. Elmo's lights, 469
- Stabilator, 110
- Stability, 20, 54, 55
- Stage pressure ratio, 130
- Stagnation pressure, 117
- Stall
 - in turning flight, 426
 - prevention systems, 423
 - tests, 423, 425
 - turn, 409
 - warning, 423
- Stalling airspeed, 315, 371, 380
- Stalling angle, 90
- Stalling behavior of an aircraft, 424
- Standard
 - altitude, 177
 - atmosphere property ratios, 73
 - atmosphere, 67, 177
 - / engine rating, 157
- Starboard, 3
- Starboard wing, 3
- Static pressure, 117
- Static pressure distribution, 89
- Station
 - models, 495
 - pressure, 38
- Stationary fronts, 60
- Stator blades, 131
- Stators, 129
- Steady equilibrium positions, 220

- Steam fog, 465
 Steepest climb, 266, 348
 Step-by-step method, 435
 Stepped-altitude flight, 249
 Stewart, S., 26
 Stinton, D., 120, 190, 290
 Stokes equations, 116
 Stopway, 378
 Straight fast stall, 425
 Straight slow stall, 425
 Straighteners, 129
 Stratiform cloud, 53
 Stratopause, 66
 Stratosphere, 66
 Stratus clouds, 52
 Structural limit, 414
 Sublimation, 49
 Subsonic airspeed, 87
 Subsonic diffuser, 128
 Supercharged engine, 155
 Supercharger, 155
 Supercritical airfoils, 88
 Supersonic airfoils, 88
 Supersonic airspeed, 87
 Supersonic diffuser, 128
 Supersonic wings, 94
 Surface
 inversion, 34
 singularities, 117
 Surge, 130
 Sustained turn, 416
 Sweep angle, 93
 Swept-back propeller blades, 171
 Swept-back wing, 94
 Symbols
 for barometric change, 491
 for clouds, 491
 for fronts, 493
 for sky coverage, 492
 Synoptic, 495
 Synoptic charts, 495
 Tab, 110
 Tachometer, 158
 Tail
 slide, 405
 unit, 4
 Tailwind, 180
 Tailwind shear, 478
 Takeoff
 distance, 378
 field length, 380
 length required, 379
 rotation airspeed, 381
 safety airspeed, 382
 tests, 427
 Tapeline
 altitude, 175
 altitude correction, 436
 Taper ratio, 93
 Taxiing weight, 15
 Temperature
 altitude, 177
 calibration, 420
 forecasts, 498
 inversion, 34
 lapse rate, 33
 recovery factor, 421
 Tempest, B., 416
 Terminal forecast, 498
 Theodolite, 428
 Thermal convection, 46
 Thermals, 46, 209, 210
 Thermogram, 486
 Thermograph, 486
 Thermometers, 486
 Three Ts of combustion, 130
 Threshold
 airspeed, 382
 point, 389
 Throttle ice, 154
 Thrust, 134, 143
 augmentation, 135
 available, 133, 218
 boundary tests, 452
 determination, 134
 limited stabilized turn, 453
 required, 218
 Thrust-specific fuel consumption, 136, 216
 Thunderstorms, 467
 Thwaites, B., 120
 Tightest turn, 303, 369
 Time taken in climb, 262
 Tip vortices, 84
 Tip-chord, 93
 Toe brakes, 9
 Torenbeek, E., 25, 120, 290, 399
 Tornado, 44
 Torque rolls, 413
 Total
 energy, 281
 pressure, 117
 pressure ratio, 130
 weight, 15
 Touchdown, 379
 Touchdown airspeed, 382
 Trace icing, 473
 Tractors, 160
 Trade winds, 42
 Trailing bomb method, 420
 Trailing cone method, 420
 Trailing vortices, 85
 Trailing-edge flaps, 99
 Transition
 distance, 378
 segment, 386
 Transonic airfoils, 88
 Transonic airspeed, 87
 Transonic area rule, 112
 Trend forecast, 500
 Trim
 controller, 9

- drag, 106
- tabs, 110
- Trimming, 110
- Tropic of cancer, 41
- Tropic of capricorn, 41
- Tropopause, 66
- Troposphere, 66
- Trough, 37
- True airspeed, 178, 180, 437
- True altitude, 175
- True thrust corrections, 437
- Turbine, 126
- Turbocharged piston engines, 156
- Turbofan engine, 141
- Turbojet engines, 128
- Turboprop engine, 139
- Turboshaft engine, 140
- Turbosupercharged piston engines, 156
- Turbulence, 466, 469
- Turbulent flow, 82, 466
- Turn coordinator, 12
- Turn-and-slip indicator, 11
- Turning at stalling airspeed, 304, 380
- Turning flight, 295, 364, 371
- Turning in vertical plane, 305
- Turning performance tests, 450
- Turning radius, 297, 302, 303, 365
- Turning rate, 297, 302, 303, 365
- Turn(s), 293, 301, 303, 304, 306, 363, 367, 369, 416
- Twin-spool compressor, 130
- Twisted wing, 93
- Two-dimensional flows, 83
- Two-spool turbofan, 142
- Types of propellers, 169
- Typhoon, 44
- Ultimate load factor, 414
- Undercarriage wheels, 383
- Underdown, R. B., 75
- Unsteady flow, 82
- Unstick airspeed, 382
- Upper surface blowing, 103
- Upper-level charts, 497
- Upslope fog, 465
- Upwash, 89
- Useful load, 16
- V-n* diagram, 413
- Valley
 - breezes, 43
 - of air, 36
- Vapor pressure, 39
- Variable-pitch propeller, 170
- Vaughan, W. W., 76
- Vectored thrust, 103
- Veering, 188
- Vertical speed indicator, 11
- Vertical stabilizer, 4
- Virga, 50
- Visibility, 64, 65
- Visibility meter, 487
- Visual approach slope indicator, 14
- Visual flight rules, 485
- Von Braun, W., 147
- Von Doenhoff, A. E., 120
- Vortex generator(s), 4, 103
- Vortices, 84
- Wake, 84
- Warm fronts, 59
- Water
 - injection, 136
 - vapor, 46
- Wave drag, 106, 128
- Weather
 - charts, 499
 - depiction map, 496
 - factories, 467
 - forecast, 498
 - reconnaissance, 488
 - report, 494
 - satellites, 488
 - symbols, 489
 - warnings, 500
- Weight, 16
 - correction, 439
 - fractions, 16
- Westerlies, 42
- Wet-bulb thermometer, 487
- Whitten, R. C., 76
- Williams, J., 399
- Williams, N., 416
- Wind
 - aloft charts, 497
 - correction, 439
 - direction, 188
 - forecasts, 498
 - shadow thermals, 210
 - speed measurement, 188
 - speed symbols, 489
 - tunnel, 115
 - tunnel walls interference, 113
 - velocity, 180
- Wind(s), 40–43, 180, 186, 210
- Windmill anemometer, 189
- Windmill state, 171
- Windshear, 45, 440, 477
- Wing planform, 93
- Winglets, 4
- Wings(s), 3, 93–95, 99, 103
- Yaw, 6, 7
- Yaw-roll coupling, 112
- Yuan, S. V., 121
- Zero
 - fuel weight, 16
 - payload, 16
- Zero-lift drag coefficient, 97, 107
- Zhongjia, Y., 75

Errata	Fundamentals of Aircraft		
Page no.	Location of error	Error	Correction to be made
1	Third paragraph, 5 th Line	whcih	which
3	Fig1.2, Left Hand Side and near bottom of the figure	Star Sign(·) missing	Put star sign (·) just above the following block Leading Edge Slat
118	Equation (3.17)	Factor 2 is missing just after radical sign	$V=\sqrt{2(p_0-p)/\rho}$
138	The equation which is just above equation (4.12)	Factor p_{SSL} is missing between δ and D^2 on the left hand side.	$\delta p_{SSL} D^2$
173	Question 5.30, second line, item b)	The word "not" between the words "are" and "twisted" should not be there	blades are twisted
217	Equation (8.8)	The first S on the Right Hand Side should be W.	F/S should be written as F/W
223	The line just above equation (8.17)	Slash should be replaced by hyphen	cruise/fuel should be written as cruise-fuel.
224	Fig 8.7	All the three inclined lines of the figure appear as broken lines	All these three lines should be smooth lines

228	Sixth line from bottom, second word	"having" should be replaced	Replace it by "that keeps"
268	Equation (10.44)	After ℓ_0 , the four β 's under radical sign	All these four β 's should be written as B
272	The second line below equation (10.55)	the first plus(+) sign just after the number 2	this + sign should be replaced by = sign
276	Fig 10.5, right hand side	"T" is wrongly entered in notation $T_{m,SSL}$	"T" should be replaced by "F", keeping the same subscripts
277	Fig 10.6, right hand side	"T" is wrongly entered in notation $T_{m,SSL}$	"T" should be replaced by "F", keeping the same subscripts
279	The equation which is on the third line from bottom	The exponent 2 β which is just before the = sign	It should be just β , i.e. remove the number 2
301	Third line from bottom	Eq.(11.2)	Eq. (11.12)
331	The equation which is below equation (13.8)	Slash sign after the number 1 on the right hand side is missing	$1/(2 \sqrt{C_{D0}} K)$

345	Left Hand Side of equation(14.4)	n	h
378	Fig 16.1, just below th hatched line having letters A and B	The symbol x_R is missing	Put x_R between the arrows just below A and B.
379	Eleventh line from top	Symbol h_{Sc} is missing after the words "screen height"	Write as screen height h_{Sc}
386	16 th line from top, last symbol	It should be capital C in the symbol	Put capital C in the symbol $C_{\ell,m}$
387	6 th line from bottom	The word "transition" is missing	Write it as "transition height"
395	Article 16.8.4, last line of its first paragraph	there should be a capital S in the notation t_{As}	t_{AS}
426	Second line below fig 18.4	Fig.??	Fig. 18.5
444	Fig 18.19, on the right hand side	Notation $W_f/\delta\sqrt{\theta}$ is wrongly entered here	Remove this notation completely
445	Fig.18.20, on the left hand side of vertical line	Notation $W_f/\delta\sqrt{\theta}$ is missing	Put that missing notation on the left hand side of the vertical line of the figure.

	451	Third line above equation (18.36)	Last symbol δ on the right hand side wrongly entered	Remove symbol δ
	453	15 th line from bottom	N	η
	456	13 th line from bottom	$\dot{h}/V\delta$	$\dot{Whe}/V\delta$
	456	9 th line from bottom	$\dot{h}e/V\delta$	$\dot{Whe}/V\delta$
	457	Fig 18.35, part (a), left hand side of vertical line	$\dot{h}/V\delta$	$\dot{Whe}/V\delta$
	457	Fig 18.35, title of part (a) of the figure	$\dot{h}e/V\delta$	$\dot{Whe}/V\delta$
	457	Title of Fig 18.35	$\dot{h}e/V\delta$	$\dot{Whe}/V\delta$
	457	Fig 18.36, on the left hand side of vertical line	$\dot{h}e/V\delta$	$\dot{Whe}/V\delta$
	457	Title of Fig 18.36	$\dot{h}e/V\delta$	$\dot{Whe}/V\delta$
	489	Article 20.3.1, second line	as 10	as 5
	489	Article 20.3.1, second line	and 40 kn	and 35 kn
	491	Second line above article 20.3.5	is shown	is also shown